



CD-ROM
Included

INTRODUCTION TO FINITE ELEMENTS IN ENGINEERING

THIRD EDITION

Tirupathi R. Chandrupatla
Ashok D. Belegundu

Programs Included in the CD-ROM

| | | | | | |
|--|---|------------------------------------|---|---|--|
| CH-1 | CH-2 GAUSS CGSOL SKYLINE | CH-3 FEM1D | CH-4 TRUSS2D TRUSSKY | CH-5 CST | CH-6 AXISYM |
| CH-7 QUAD QUADCG AXIQUAD | CH-8 BEAM FRAME2D FRAME3D | CH-9 TETRA3D HEXAFRON | CH-10 HEAT1D HEAT2D TORSION | CH-11 INVITR JACOBI BEAMKM CSTKM GENEIGEN | CH-12 MESHGEN PLOT2D, BESTFIT BESTFITQ CONTOURA CONTOURB |

CD-ROM Contents

| Directory | Description |
|-----------|-------------------------------------|
| \QBASIC | Programs in QBASIC |
| \FORTRAN | Programs in Fortran Language |
| \C | Programs in C |
| \VB | Programs in Visual Basic |
| \EXCELVB | Programs in Excel Visual Basic |
| \MATLAB | Programs in MATLAB |
| \EXAMPLES | Example Data Files (.inp extension) |

List of Key Symbols Used in the Text

| Symbol | Description |
|---|---|
| $\mathbf{u}(x, y, z) = [u(x, y, z), v(x, y, z), w(x, y, z)]^T$ | displacements along coordinate directions at point (x, y, z) |
| $\mathbf{f} = [f_x, f_y, f_z]^T$ | components of body force per unit volume, at point (x, y, z) |
| $\mathbf{T} = [T_x, T_y, T_z]^T$ | components of traction force per unit area, at point (x, y, z) on the surface |
| $\boldsymbol{\epsilon} = [\epsilon_x, \epsilon_y, \epsilon_z, \gamma_{yz}, \gamma_{zx}, \gamma_{xy}]^T$ | strain components; ϵ are normal strains and γ are engineering shear strains |
| $\boldsymbol{\sigma} = [\sigma_x, \sigma_y, \sigma_z, \tau_{yz}, \tau_{zx}, \tau_{xy}]^T$ | stress components; σ are normal stresses and τ are engineering shear stresses |
| Π | Potential energy = $U + WP$, where U = strain energy, WP = work potential |
| \mathbf{q} | vector of displacements of the nodes (degrees of freedom or DOF) of an element, dimension $(NDN * NEN, 1)$ —see next Table for explanation of NDN and NEN |
| \mathbf{Q} | vector of displacements of ALL the nodes of an element, dimension $(NN * NDN, 1)$ —see next Table for explanation of NN and NDN |
| \mathbf{k} | element stiffness matrix; strain energy in element, $U_e = \frac{1}{2} \mathbf{q}^T \mathbf{k} \mathbf{q}$ |
| \mathbf{K} | global stiffness matrix for entire structure: $\Pi = \frac{1}{2} \mathbf{Q}^T \mathbf{K} \mathbf{Q} - \mathbf{Q}^T \mathbf{F}$ |
| \mathbf{f}^e | body force in element e distributed to the nodes of the element |
| \mathbf{T}^e | traction force in element e distributed to the nodes of the element |
| $\Phi(x, y, z)$ | virtual displacement variable; counterpart of the real displacement $\mathbf{u}(x, y, z)$ |
| $\boldsymbol{\psi}$ | vector of virtual displacements of the nodes in an element; counterpart of \mathbf{q} |
| \mathbf{N}, \mathbf{D} , and \mathbf{B} | shape functions in $\xi\eta\zeta$ coordinates, material matrix, strain-displacement matrix, respectively. $\mathbf{u} = \mathbf{N}\mathbf{q}$, $\boldsymbol{\epsilon} = \mathbf{B}\mathbf{q}$ and $\boldsymbol{\sigma} = \mathbf{D}\mathbf{B}\mathbf{q}$ |

Structure of Input Files†

```

TITLE      (*)
PROBLEM DESCRIPTION  (*)
NN NE NM NDIM NEN NDN      (*)
4 2 2 2 3 2      --- 1 Line of data, 6 entries per line
ND NL NMPC      (*)
5 2 0      --- 1 Line of data, 3 entries
Node#  Coordinate#1 ... Coordinate#NDIM  (*)
1      3      0
2      3      2
3      0      2
4      0      0      } ---NN Lines of data, (NDIM+1)entries
Elem#  Node#1 ... Node#NEN  Mat#  Element Characteristics†† (*)
1      4      1      2      1      0.5      0. } ---NE Lines of data,
2      3      4      2      2      0.5      0. } (NEN+2+ #of Char.)entries
DOF#  Specified Displacement  (*)
2      0
5      0
6      0
7      0
8      0      } ---ND Lines of data, 2 entries
DOF#  Load  (*)
4      -7500
3      3000      } ---NL Lines of data, 2 entries
MAT#  Material  Properties†† (*)
1      30e6      0.25 12e-6 } ---NM Lines of data, (1+ # of prop.)entries
2      20e6      0.3  0.
B1 i  B2  j  B3 (Multipoint constraint: B1*Qi+B2*Qj=B3)  (*)
} ---NMPC Lines of data, 5 entries

```

†HEAT1D and HEAT2D Programs need extra boundary data about flux and convection. (See Chapter 10.)

(*) = DUMMY LINE - necessary

Note: No Blank Lines must be present in the input file

††See below for description of element characteristics and material properties

Main Program Variables

NN = Number of Nodes; NE = Number of Elements; NM = Number of Different Materials

NDIM = Number of Coordinates per Node (e.g., NDIM = 2 for 2-D, or = 3 for 3-D); NEN = Number of Nodes per Element (e.g., NEN = 3 for 3-noded triangular element, or = 4 for a 4-noded quadrilateral)

NDN = Number of Degrees of Freedom per Node (e.g., NDN = 2 for a CST element, or = 6 for 3-D beam element)

ND = Number of Degrees of Freedom along which Displacement is Specified = No. of Boundary Conditions

NL = Number of Applied Component Loads (along Degrees of Freedom)

NMPC = Number of Multipoint Constraints; NQ = Total Number of Degrees of Freedom = NN * NDN

| Program | Element Characteristics | Material Properties |
|-----------------------|----------------------------------|---------------------------|
| FEM1D, TRUSS, TRUSSKY | Area, Temperature Rise | E |
| CST, QUAD | Thickness, Temperature Rise | E, ν, α |
| AXISYM | Temperature Rise | E, ν, α |
| FRAME2D | Area, Inertia, Distributed Load | E |
| FRAME3D | Area, 3-inertias, 2-Distr. Loads | E |
| TETRA, HEXAFNT | Temperature Rise | E, ν, α |
| HEAT2D | Element Heat Source | Thermal Conductivity, k |
| BEAMKM | Inertia, Area | E, ρ |
| CSTKM | Thickness | E, ν, α, ρ |

Introduction to Finite Elements in Engineering

Introduction to Finite Elements in Engineering

T H I R D E D I T I O N

TIRUPATHI R. CHANDRUPATLA

*Rowan University
Glassboro, New Jersey*

ASHOK D. BELEGUNDU

*The Pennsylvania State University
University Park, Pennsylvania*



Prentice Hall, Upper Saddle River, New Jersey 07458

Library of Congress Cataloging-in-Publication Data

Chandrupatla, Tirupathi R.,

Introduction to finite elements in engineering / Tirupathi R. Chandrupatla, Ashok D. Belegundu.-- 3rd ed.

p. cm.

Includes bibliographical references and index.

ISBN 0-13-061591-9

1. Finite element method. 2. Engineering mathematics. I. Belegundu, Ashok D.,

II. Title

TA347.F5 C463 2001

620'.001'51535--dc21

Vice President and Editorial Director, ECS: *Marcia J. Horton*

Acquisitions Editor: *Laura Fischer*

Editorial Assistant: *Erin Katchmar*

Vice President and Director of Production and Manufacturing, ESM: *David W. Riccardi*

Executive Managing Editor: *Vince O'Brien*

Managing Editor: *David A. George*

Production Services/Composition: *Preparé, Inc.*

Director of Creative Services: *Paul Belfanti*

Creative Director: *Carole Anson*

Art Director: *Jayne Conte*

Art Editor: *Greg Dulles*

Cover Designer: *Bruce Kenselaar*

Manufacturing Manager: *Trudy Pisciotti*

Manufacturing Buyer: *Lynda Castillo*

Marketing Manager: *Holly Stark*



© 2002 by Prentice-Hall, Inc.
Upper Saddle River, New Jersey 07458

All rights reserved. No part of this book may be reproduced in any form or by any means, without permission in writing from the publisher.

The author and publisher of this book have used their best efforts in preparing this book. These efforts include the development, research, and testing of the theories and programs to determine their effectiveness. The author and publisher make no warranty of any kind, expressed or implied, with regard to these programs or the documentation contained in this book. The author and publisher shall not be liable in any event for incidental or consequential damages in connection with, or arising out of, the furnishing, performance, or use of these programs.

"Visual Basic" and "Excel" are registered trademarks of the Microsoft Corporation, Redmond, WA.

"MATLAB" is a registered trademark of The MathWorks, Inc., 3 Apple Hill Drive, Natick, MA 01760-2098.

Printed in the United States of America

10 9 8 7 6

ISBN 0-13-061591-9

Pearson Education Ltd., *London*

Pearson Education Australia Pty. Ltd., *Sydney*

Pearson Education Singapore, Pte. Ltd.

Pearson Education North Asia Ltd., *Hong Kong*

Pearson Education Canada, Inc., *Toronto*

Pearson Educación de México, S.A. de C.V.

Pearson Education—Japan, *Tokyo*

Pearson Education Malaysia, Pte. Ltd.

Pearson Education, *Upper Saddle River, New Jersey*

To our parents

Contents

| | |
|---|-----------|
| PREFACE | xv |
| 1 FUNDAMENTAL CONCEPTS | 1 |
| 1.1 Introduction | 1 |
| 1.2 Historical Background | 1 |
| 1.3 Outline of Presentation | 2 |
| 1.4 Stresses and Equilibrium | 2 |
| 1.5 Boundary Conditions | 4 |
| 1.6 Strain–Displacement Relations | 4 |
| 1.7 Stress–Strain Relations | 6 |
| <i>Special Cases, 7</i> | |
| 1.8 Temperature Effects | 8 |
| 1.9 Potential Energy and Equilibrium; The Rayleigh–Ritz Method | 9 |
| <i>Potential Energy II, 9</i> | |
| <i>Rayleigh–Ritz Method, 11</i> | |
| 1.10 Galerkin’s Method | 13 |
| 1.11 Saint Venant’s Principle | 16 |
| 1.12 Von Mises Stress | 17 |
| 1.13 Computer Programs | 17 |
| 1.14 Conclusion | 18 |
| Historical References | 18 |
| Problems | 18 |
| 2 MATRIX ALGEBRA AND GAUSSIAN ELIMINATION | 22 |
| 2.1 Matrix Algebra | 22 |
| <i>Row and Column Vectors, 23</i> | |
| <i>Addition and Subtraction, 23</i> | |
| <i>Multiplication by a Scalar, 23</i> | |

- Matrix Multiplication, 23*
- Transposition, 24*
- Differentiation and Integration, 24*
- Square Matrix, 25*
- Diagonal Matrix, 25*
- Identity Matrix, 25*
- Symmetric Matrix, 25*
- Upper Triangular Matrix, 26*
- Determinant of a Matrix, 26*
- Matrix Inversion, 26*
- Eigenvalues and Eigenvectors, 27*
- Positive Definite Matrix, 28*
- Cholesky Decomposition, 29*
- 2.2 Gaussian Elimination 29
 - General Algorithm for Gaussian Elimination, 30*
 - Symmetric Matrix, 33*
 - Symmetric Banded Matrices, 33*
 - Solution with Multiple Right Sides, 35*
 - Gaussian Elimination with Column Reduction, 36*
 - Skyline Solution, 38*
 - Frontal Solution, 39*
- 2.3 Conjugate Gradient Method for Equation Solving 39
 - Conjugate Gradient Algorithm, 40*
 - Problems 41
 - Program Listings, 43*

3 ONE-DIMENSIONAL PROBLEMS

45

- 3.1 Introduction 45
- 3.2 Finite Element Modeling 46
 - Element Division, 46*
 - Numbering Scheme, 47*
- 3.3 Coordinates and Shape Functions 48
- 3.4 The Potential-Energy Approach 52
 - Element Stiffness Matrix, 53*
 - Force Terms, 54*
- 3.5 The Galerkin Approach 56
 - Element Stiffness, 56*
 - Force Terms, 57*
- 3.6 Assembly of the Global Stiffness Matrix and Load Vector 58
- 3.7 Properties of K 61
- 3.8 The Finite Element Equations; Treatment of Boundary Conditions 62
 - Types of Boundary Conditions, 62*
 - Elimination Approach, 63*
 - Penalty Approach, 69*
 - Multipoint Constraints, 74*

- 3.9 Quadratic Shape Functions 78
- 3.10 Temperature Effects 84
 - Input Data File, 88*
 - Problems 88
 - Program Listing, 98*

4 TRUSSES

103

- 4.1 Introduction 103
- 4.2 Plane Trusses 104
 - Local and Global Coordinate Systems, 104*
 - Formulas for Calculating ℓ and m , 105*
 - Element Stiffness Matrix, 106*
 - Stress Calculations, 107*
 - Temperature Effects, 111*
- 4.3 Three-Dimensional Trusses 114
- 4.4 Assembly of Global Stiffness Matrix for the Banded and Skyline Solutions 116
 - Assembly for Banded Solution, 116*
 - Input Data File, 119*
 - Problems 120
 - Program Listing, 128*

5 TWO-DIMENSIONAL PROBLEMS USING CONSTANT STRAIN TRIANGLES

130

- 5.1 Introduction 130
- 5.2 Finite Element Modeling 131
- 5.3 Constant-Strain Triangle (CST) 133
 - Isoparametric Representation, 135*
 - Potential-Energy Approach, 139*
 - Element Stiffness, 140*
 - Force Terms, 141*
 - Galerkin Approach, 146*
 - Stress Calculations, 148*
 - Temperature Effects, 150*
- 5.4 Problem Modeling and Boundary Conditions 152
 - Some General Comments on Dividing into Elements, 154*
- 5.5 Orthotropic Materials 154
 - Temperature Effects, 157*
 - Input Data File, 160*
 - Problems 162
 - Program Listing, 174*

6 AXISYMMETRIC SOLIDS SUBJECTED TO AXISYMMETRIC LOADING

178

- 6.1 Introduction 178
- 6.2 Axisymmetric Formulation 179
- 6.3 Finite Element Modeling: Triangular Element 181
 - Potential-Energy Approach, 183*
 - Body Force Term, 184*
 - Rotating Flywheel, 185*
 - Surface Traction, 185*
 - Galerkin Approach, 187*
 - Stress Calculations, 190*
 - Temperature Effects, 191*
- 6.4 Problem Modeling and Boundary Conditions 191
 - Cylinder Subjected to Internal Pressure, 191*
 - Infinite Cylinder, 192*
 - Press Fit on a Rigid Shaft, 192*
 - Press Fit on an Elastic Shaft, 193*
 - Belleville Spring, 194*
 - Thermal Stress Problem, 195*
 - Input Data File, 197*
- Problems 198
 - Program Listing, 205*

7 TWO-DIMENSIONAL ISOPARAMETRIC ELEMENTS AND NUMERICAL INTEGRATION

208

- 7.1 Introduction 208
- 7.2 The Four-Node Quadrilateral 208
 - Shape Functions, 208*
 - Element Stiffness Matrix, 211*
 - Element Force Vectors, 213*
- 7.3 Numerical Integration 214
 - Two-Dimensional Integrals, 217*
 - Stiffness Integration, 217*
 - Stress Calculations, 218*
- 7.4 Higher Order Elements 220
 - Nine-Node Quadrilateral, 220*
 - Eight-Node Quadrilateral, 222*
 - Six-Node Triangle, 223*
- 7.5 Four-Node Quadrilateral for Axisymmetric Problems 225
- 7.6 Conjugate Gradient Implementation of the Quadrilateral Element 226
 - Concluding Note, 227*
 - Input Data File, 228*
- Problems 230
 - Program Listings, 233*

| | |
|---|------------|
| 8 BEAMS AND FRAMES | 237 |
| 8.1 Introduction 237 | |
| <i>Potential-Energy Approach, 238</i> | |
| <i>Galerkin Approach, 239</i> | |
| 8.2 Finite Element Formulation 240 | |
| 8.3 Load Vector 243 | |
| 8.4 Boundary Considerations 244 | |
| 8.5 Shear Force and Bending Moment 245 | |
| 8.6 Beams on Elastic Supports 247 | |
| 8.7 Plane Frames 248 | |
| 8.8 Three-Dimensional Frames 253 | |
| 8.9 Some Comments 257 | |
| <i>Input Data File, 258</i> | |
| Problems 261 | |
| <i>Program Listings, 267</i> | |
| 9 THREE-DIMENSIONAL PROBLEMS IN STRESS ANALYSIS | 275 |
| 9.1 Introduction 275 | |
| 9.2 Finite Element Formulation 276 | |
| <i>Element Stiffness, 279</i> | |
| <i>Force Terms, 280</i> | |
| 9.3 Stress Calculations 280 | |
| 9.4 Mesh Preparation 281 | |
| 9.5 Hexahedral Elements and Higher Order Elements 285 | |
| 9.6 Problem Modeling 287 | |
| 9.7 Frontal Method for Finite Element Matrices 289 | |
| <i>Connectivity and Prefront Routine, 290</i> | |
| <i>Element Assembly and Consideration of Specified dof, 290</i> | |
| <i>Elimination of Completed dof, 291</i> | |
| <i>Backsubstitution, 291</i> | |
| <i>Consideration of Multipoint Constraints, 291</i> | |
| <i>Input Data File, 292</i> | |
| Problems 293 | |
| <i>Program Listings, 297</i> | |
| 10 SCALAR FIELD PROBLEMS | 306 |
| 10.1 Introduction 306 | |
| 10.2 Steady State Heat Transfer 308 | |
| <i>One-Dimensional Heat Conduction, 309</i> | |
| <i>One-Dimensional Heat Transfer in Thin Fins, 316</i> | |
| <i>Two-Dimensional Steady-State Heat Conduction, 320</i> | |
| <i>Two-Dimensional Fins, 329</i> | |
| <i>Preprocessing for Program Heat2D, 330</i> | |

- 10.3 Torsion 331
 - Triangular Element, 332*
 - Galerkin Approach, 333*
- 10.4 Potential Flow, Seepage, Electric and Magnetic Fields, and Fluid Flow in Ducts 336
 - Potential Flow, 336*
 - Seepage, 338*
 - Electrical and Magnetic Field Problems, 339*
 - Fluid Flow in Ducts, 341*
 - Acoustics, 343*
 - Boundary Conditions, 344*
 - One-Dimensional Acoustics, 344*
 - 1-D Axial Vibrations, 345*
 - Two-Dimensional Acoustics, 348*
- 10.5 Conclusion 348
 - Input Data File, 349*
 - Problems 350
 - Program Listings, 361*

11 DYNAMIC CONSIDERATIONS

- 11.1 Introduction 367
- 11.2 Formulation 367
 - Solid Body with Distributed Mass, 368*
- 11.3 Element Mass Matrices 370
- 11.4 Evaluation of Eigenvalues and Eigenvectors 375
 - Properties of Eigenvectors, 376*
 - Eigenvalue-Eigenvector Evaluation, 376*
 - Generalized Jacobi Method, 382*
 - Tridiagonalization and Implicit Shift Approach, 386*
 - Bringing Generalized Problem to Standard Form, 386*
 - Tridiagonalization, 387*
 - Implicit Symmetric QR Step with Wilkinson Shift for Diagonalization, 390*
- 11.5 Interfacing with Previous Finite Element Programs and a Program for Determining Critical Speeds of Shafts 391
- 11.6 Guyan Reduction 392
- 11.7 Rigid Body Modes 394
- 11.8 Conclusion 396
 - Input Data File, 397*
 - Problems 399
 - Program Listings, 404*

| | |
|--|------------|
| 12 PREPROCESSING AND POSTPROCESSING | 411 |
| 12.1 Introduction | 411 |
| 12.2 Mesh Generation | 411 |
| <i>Region and Block Representation, 411</i> | |
| <i>Block Corner Nodes, Sides, and Subdivisions, 412</i> | |
| 12.3 Postprocessing | 419 |
| <i>Deformed Configuration and Mode Shape, 419</i> | |
| <i>Contour Plotting, 420</i> | |
| <i>Nodal Values from Known Constant Element Values</i> <i>for a Triangle, 421</i> | |
| <i>Least Squares Fit for a Four-Noded Quadrilateral, 423</i> | |
| 12.4 Conclusion | 424 |
| <i>Input Data File, 425</i> | |
| Problems | 425 |
| <i>Program Listings, 427</i> | |
| APPENDIX Proof of $dA = \det \mathbf{J} d\xi d\eta$ | 440 |
| BIBLIOGRAPHY | 443 |
| ANSWERS TO SELECTED PROBLEMS | 447 |
| INDEX | 449 |

Preface

The first edition of this book appeared over 10 years ago and the second edition followed a few years later. We received positive feedback from professors who taught from the book and from students and practicing engineers who used the book. We also benefited from the feedback received from the students in our courses for the past 20 years. We have incorporated several suggestions in this edition. The underlying philosophy of the book is to provide a clear presentation of theory, modeling, and implementation into computer programs. The pedagogy of earlier editions has been retained in this edition.

New material has been introduced in several chapters. Worked examples and exercise problems have been added to supplement the learning process. Exercise problems stress both fundamental understanding and practical considerations. Theory and computer programs have been added to cover acoustics, axisymmetric quadrilateral elements, conjugate gradient approach, and eigenvalue evaluation. Three additional programs have now been introduced in this edition. All the programs have been developed to work in the Windows environment. The programs have a common structure that should enable the users to follow the development easily. The programs have been provided in Visual Basic, Microsoft *Excel/Visual Basic*, MATLAB, together with those provided earlier in QBASIC, FORTRAN and C. The Solutions Manual has also been updated.

Chapter 1 gives a brief historical background and develops the fundamental concepts. Equations of equilibrium, stress-strain relations, strain-displacement relations, and the principles of potential energy are reviewed. The concept of Galerkin's method is introduced.

Properties of matrices and determinants are reviewed in Chapter 2. The Gaussian elimination method is presented, and its relationship to the solution of symmetric banded matrix equations and the skyline solution is discussed. Cholesky decomposition and conjugate gradient method are discussed.

Chapter 3 develops the key concepts of finite element formulation by considering one-dimensional problems. The steps include development of shape functions, derivation of element stiffness, formation of global stiffness, treatment of boundary conditions, solution of equations, and stress calculations. Both the potential energy approach and Galerkin's formulations are presented. Consideration of temperature effects is included.

Finite element formulation for plane and three-dimensional trusses is developed in Chapter 4. The assembly of global stiffness in banded and skyline forms is explained. Computer programs for both banded and skyline solutions are given.

Chapter 5 introduces the finite element formulation for two-dimensional plane stress and plane strain problems using constant strain triangle (CST) elements. Problem modeling and treatment of boundary conditions are presented in detail. Formulation for orthotropic materials is provided. Chapter 6 treats the modeling aspects of axisymmetric solids subjected to axisymmetric loading. Formulation using triangular elements is presented. Several real-world problems are included in this chapter.

Chapter 7 introduces the concepts of isoparametric quadrilateral and higher order elements and numerical integration using Gaussian quadrature. Formulation for axisymmetric quadrilateral element and implementation of conjugate gradient method for quadrilateral element are given.

Beams and application of Hermite shape functions are presented in Chapter 8. The chapter covers two-dimensional and three-dimensional frames.

Chapter 9 presents three-dimensional stress analysis. Tetrahedral and hexahedral elements are presented. The frontal method and its implementation aspects are discussed.

Scalar field problems are treated in detail in Chapter 10. While Galerkin as well as energy approaches have been used in every chapter, with equal importance, only Galerkin's approach is used in this chapter. This approach directly applies to the given differential equation without the need of identifying an equivalent functional to minimize. Galerkin formulation for steady-state heat transfer, torsion, potential flow, seepage flow, electric and magnetic fields, fluid flow in ducts, and acoustics are presented.

Chapter 11 introduces dynamic considerations. Element mass matrices are given. Techniques for evaluation of eigenvalues (natural frequencies) and eigenvectors (mode shapes) of the generalized eigenvalue problem are discussed. Methods of inverse iteration, Jacobi, tridiagonalization and implicit shift approaches are presented.

Preprocessing and postprocessing concepts are developed in Chapter 12. Theory and implementation aspects of two-dimensional mesh generation, least-squares approach to obtain nodal stresses from element values for triangles and quadrilaterals, and contour plotting are presented.

At the undergraduate level some topics may be dropped or delivered in a different order without breaking the continuity of presentation. We encourage the introduction of the Chapter 12 programs at the end of Chapter 5. This helps the students to prepare the data in an efficient manner.

We thank Nels Madsen, Auburn University; Arif Masud, University of Illinois, Chicago; Robert L. Rankin, Arizona State University; John S. Strenkowski, NC State University; and Hormoz Zareh, Portland State University, who reviewed our second edition and gave many constructive suggestions that helped us improve the book.

Tirupathi Chandrupatla expresses his gratitude to J. Tinsley Oden, whose teaching and encouragement have been a source of inspiration to him throughout his career. He also expresses his thanks to many students at Rowan University and Kettering University who took his courses. He expresses his thanks to his colleague Paris vonLockette, who gave valuable feedback after teaching a course from the second edition. We thank

our production editor Fran Daniele for her meticulous approach in the final production of the book.

Ashok Belegundu thanks his students at Penn State for their feedback on the course material and programs. He expresses his gratitude to Richard C. Benson, chairman of mechanical and nuclear engineering, for his encouragement and appreciation. He also expresses his thanks to Professor Victor W. Sparrow in the acoustics department and to Dongjai Lee, doctoral student, for discussions and help with some of the material in the book. His late father's encouragement with the first two editions of this book are an ever present inspiration.

We thank our acquisitions editor at Prentice Hall, Laura Fischer, who has made this a pleasant project for us.

TIRUPATHI R. CHANDRUPATLA
ASHOK D. BELEGUNDU

About the Authors

Tirupathi R. Chandrupatla is Professor and Chair of Mechanical Engineering at Rowan University, Glassboro, New Jersey. He received the B.S. degree from the Regional Engineering College, Warangal, which was affiliated with Osmania University, India. He received the M.S. degree in design and manufacturing from the Indian Institute of Technology, Bombay. He started his career as a design engineer with Hindustan Machine Tools, Bangalore. He then taught in the Department of Mechanical Engineering at I.I.T., Bombay. He pursued his graduate studies in the Department of Aerospace Engineering and Engineering Mechanics at the University of Texas at Austin and received his Ph.D. in 1977. He subsequently taught at the University of Kentucky. Prior to joining Rowan, he was a Professor of Mechanical Engineering and Manufacturing Systems Engineering at GMI Engineering & Management Institute (formerly General Motors Institute), where he taught for 16 years.

Dr. Chandrupatla has broad research interests, which include finite element analysis, design, optimization, and manufacturing engineering. He has published widely in these areas and serves as a consultant to industry. Dr. Chandrupatla is a registered Professional Engineer and also a Certified Manufacturing Engineer. He is a member of ASEE, ASME, NSPE, SAE, and SME.

Ashok D. Belegundu is a Professor of Mechanical Engineering at The Pennsylvania State University, University Park. He was on the faculty at GMI from 1982 through 1986. He received the Ph.D. degree in 1982 from the University of Iowa and the B.S. degree from the Indian Institute of Technology, Madras. He was awarded a fellowship to spend a summer in 1993 at the NASA Lewis Research Center. During 1994–1995, he obtained a grant from the UK Science and Engineering Research Council to spend his sabbatical leave at Cranfield University, Cranfield, UK.

Dr. Belegundu's teaching and research interests include linear, nonlinear, and dynamic finite elements and optimization. He has worked on several sponsored projects for government and industry. He is an associate editor of *Mechanics of Structures and Machines*. He is also a member of ASME and an Associate fellow of AIAA.

Introduction to Finite Elements in Engineering

CHAPTER 1

Fundamental Concepts

1.1 INTRODUCTION

The finite element method has become a powerful tool for the numerical solution of a wide range of engineering problems. Applications range from deformation and stress analysis of automotive, aircraft, building, and bridge structures to field analysis of heat flux, fluid flow, magnetic flux, seepage, and other flow problems. With the advances in computer technology and CAD systems, complex problems can be modeled with relative ease. Several alternative configurations can be tested on a computer before the first prototype is built. All of this suggests that we need to keep pace with these developments by understanding the basic theory, modeling techniques, and computational aspects of the finite element method. In this method of analysis, a complex region defining a continuum is discretized into simple geometric shapes called finite elements. The material properties and the governing relationships are considered over these elements and expressed in terms of unknown values at element corners. An assembly process, duly considering the loading and constraints, results in a set of equations. Solution of these equations gives us the approximate behavior of the continuum.

1.2 HISTORICAL BACKGROUND

Basic ideas of the finite element method originated from advances in aircraft structural analysis. In 1941, Hrenikoff presented a solution of elasticity problems using the "frame work method." Courant's paper, which used piecewise polynomial interpolation over triangular subregions to model torsion problems, appeared in 1943. Turner, et al. derived stiffness matrices for truss, beam, and other elements and presented their findings in 1956. The term *finite element* was first coined and used by Clough in 1960.

In the early 1960s, engineers used the method for approximate solution of problems in stress analysis, fluid flow, heat transfer, and other areas. A book by Argyris in 1955 on energy theorems and matrix methods laid a foundation for further developments in finite element studies. The first book on finite elements by Zienkiewicz and Cheung was published in 1967. In the late 1960s and early 1970s, finite element analysis was applied to nonlinear problems and large deformations. Oden's book on nonlinear continua appeared in 1972.

Mathematical foundations were laid in the 1970s. New element development, convergence studies, and other related areas fall in this category.

Today, the developments in mainframe computers and availability of powerful microcomputers has brought this method within reach of students and engineers working in small industries.

1.3 OUTLINE OF PRESENTATION

In this book, we adopt the potential energy and the Galerkin approaches for the presentation of the finite element method. The area of solids and structures is where the method originated, and we start our study with these ideas to solidify understanding. For this reason, several early chapters deal with rods, beams, and elastic deformation problems. The same steps are used in the development of material throughout the book, so that the similarity of approach is retained in every chapter. The finite element ideas are then extended to field problems in Chapter 10. Every chapter includes a set of problems and computer programs for interaction.

We now recall some fundamental concepts needed in the development of the finite element method.

1.4 STRESSES AND EQUILIBRIUM

A three-dimensional body occupying a volume V and having a surface S is shown in Fig. 1.1. Points in the body are located by x, y, z coordinates. The boundary is constrained on some region, where displacement is specified. On part of the boundary, dis-

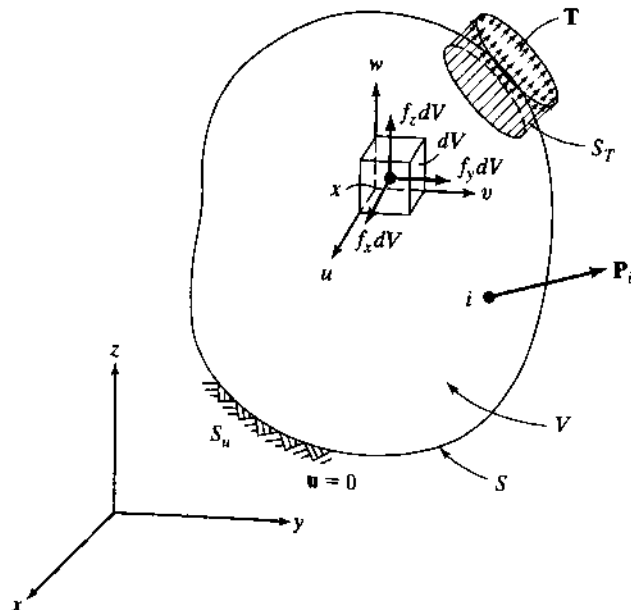


FIGURE 1.1 Three-dimensional body.

tributed force per unit area \mathbf{T} , also called traction, is applied. Under the force, the body deforms. The deformation of a point \mathbf{x} ($= [x, y, z]^T$) is given by the three components of its displacement:

$$\mathbf{u} = [u, v, w]^T \quad (1.1)$$

The distributed force per unit volume, for example, the weight per unit volume, is the vector \mathbf{f} given by

$$\mathbf{f} = [f_x, f_y, f_z]^T \quad (1.2)$$

The body force acting on the elemental volume dV is shown in Fig. 1.1. The surface traction \mathbf{T} may be given by its component values at points on the surface:

$$\mathbf{T} = [T_x, T_y, T_z]^T \quad (1.3)$$

Examples of traction are distributed contact force and action of pressure. A load \mathbf{P} acting at a point i is represented by its three components:

$$\mathbf{P}_i = [P_x, P_y, P_z]^T \quad (1.4)$$

The stresses acting on the elemental volume dV are shown in Fig. 1.2. When the volume dV shrinks to a point, the stress tensor is represented by placing its components in a

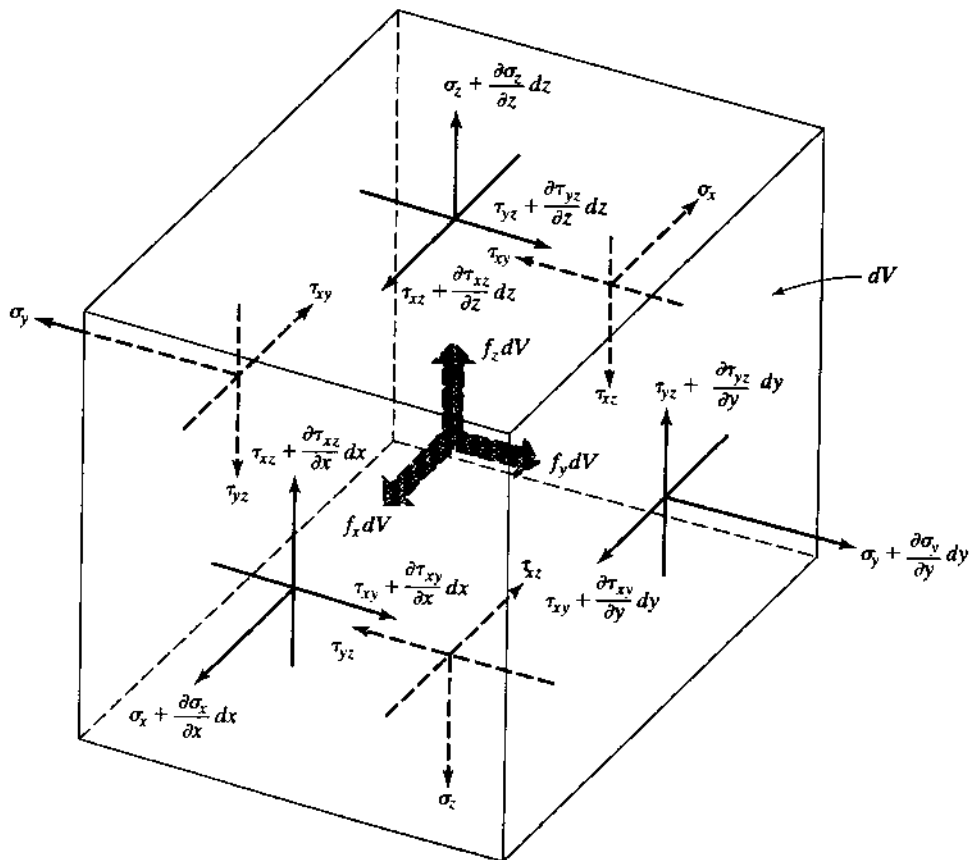


FIGURE 1.2 Equilibrium of elemental volume.

(3 × 3) symmetric matrix. However, we represent stress by the six independent components as in

$$\boldsymbol{\sigma} = [\sigma_x, \sigma_y, \sigma_z, \tau_{yz}, \tau_{xz}, \tau_{xy}]^T \quad (1.5)$$

where $\sigma_x, \sigma_y, \sigma_z$ are normal stresses and $\tau_{yz}, \tau_{xz}, \tau_{xy}$ are shear stresses. Let us consider equilibrium of the elemental volume shown in Fig. 1.2. First we get forces on faces by multiplying the stresses by the corresponding areas. Writing $\Sigma F_x = 0$, $\Sigma F_y = 0$, and $\Sigma F_z = 0$ and recognizing $dV = dx dy dz$, we get the equilibrium equations

$$\begin{aligned} \frac{\partial \sigma_x}{\partial x} + \frac{\partial \tau_{xy}}{\partial y} + \frac{\partial \tau_{xz}}{\partial z} + f_x &= 0 \\ \frac{\partial \tau_{xy}}{\partial x} + \frac{\partial \sigma_y}{\partial y} + \frac{\partial \tau_{yz}}{\partial z} + f_y &= 0 \\ \frac{\partial \tau_{xz}}{\partial x} + \frac{\partial \tau_{yz}}{\partial y} + \frac{\partial \sigma_z}{\partial z} + f_z &= 0 \end{aligned} \quad (1.6)$$

1.5 BOUNDARY CONDITIONS

Referring to Fig. 1.1, we find that there are displacement boundary conditions and surface-loading conditions. If \mathbf{u} is specified on part of the boundary denoted by S_u , we have

$$\mathbf{u} = \mathbf{0} \text{ on } S_u \quad (1.7)$$

We can also consider boundary conditions such as $\mathbf{u} = \mathbf{a}$, where \mathbf{a} is a given displacement.

We now consider the equilibrium of an elemental tetrahedron $ABCD$, shown in Fig. 1.3, where DA, DB , and DC are parallel to the x -, y -, and z -axes, respectively, and area ABC , denoted by dA , lies on the surface. If $\mathbf{n} = [n_x, n_y, n_z]^T$ is the unit normal to dA , then area $BDC = n_x dA$, area $ADC = n_y dA$, and area $ADB = n_z dA$. Consideration of equilibrium along the three axes directions gives

$$\begin{aligned} \sigma_x n_x + \tau_{xy} n_y + \tau_{xz} n_z &= T_x \\ \tau_{xy} n_x + \sigma_y n_y + \tau_{yz} n_z &= T_y \\ \tau_{xz} n_x + \tau_{yz} n_y + \sigma_z n_z &= T_z \end{aligned} \quad (1.8)$$

These conditions must be satisfied on the boundary, S_T , where the tractions are applied. In this description, the point loads must be treated as loads distributed over small, but finite areas.

1.6 STRAIN-DISPLACEMENT RELATIONS

We represent the strains in a vector form that corresponds to the stresses in Eq. 1.5,

$$\boldsymbol{\epsilon} = [\epsilon_x, \epsilon_y, \epsilon_z, \gamma_{yz}, \gamma_{xz}, \gamma_{xy}]^T \quad (1.9)$$

where ϵ_x, ϵ_y , and ϵ_z are normal strains and γ_{yz}, γ_{xz} , and γ_{xy} are the engineering shear strains.

Figure 1.4 gives the deformation of the dx - dy face for small deformations, which we consider here. Also considering other faces, we can write

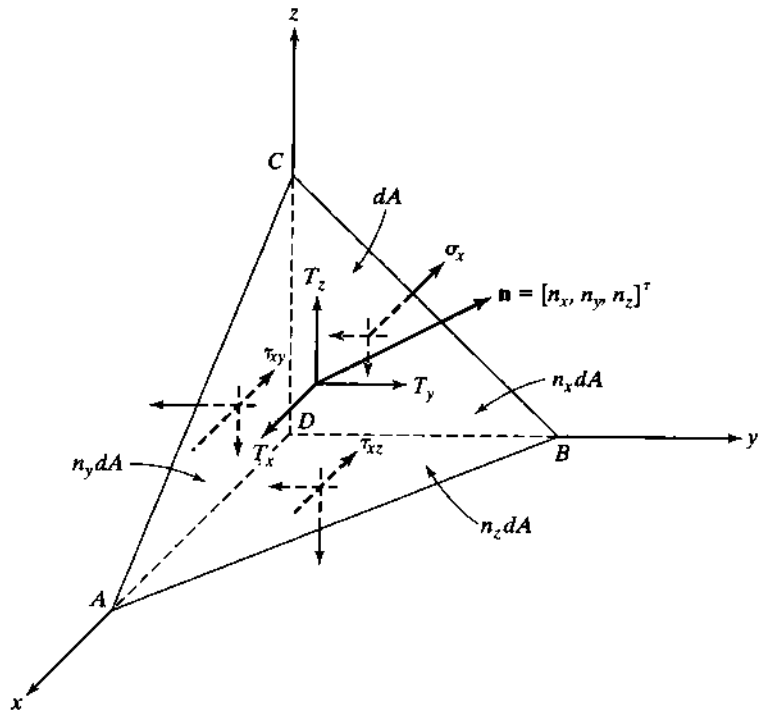


FIGURE 1.3 An elemental volume at surface.

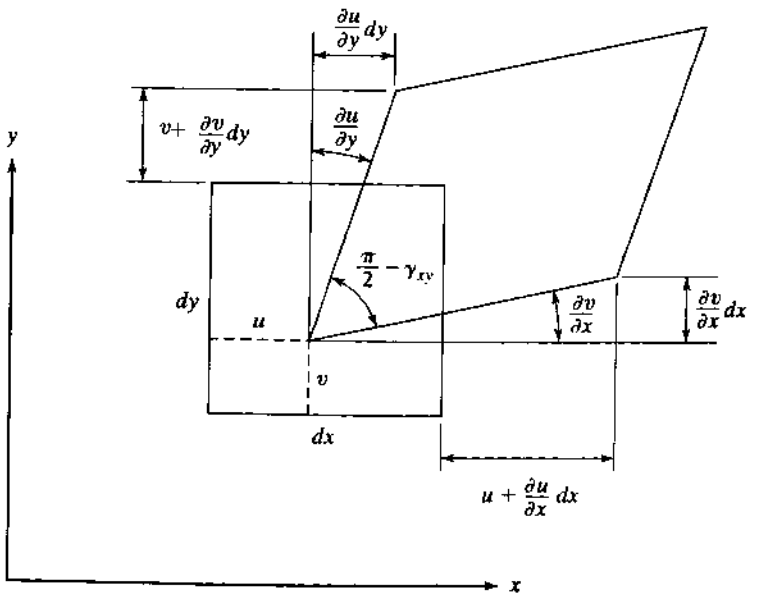


FIGURE 1.4 Deformed elemental surface.

$$\boldsymbol{\epsilon} = \left[\frac{\partial u}{\partial x}, \frac{\partial v}{\partial y}, \frac{\partial w}{\partial z}, \frac{\partial v}{\partial z} + \frac{\partial w}{\partial y}, \frac{\partial u}{\partial z} + \frac{\partial w}{\partial x}, \frac{\partial u}{\partial y} + \frac{\partial v}{\partial x} \right]^T \quad (1.10)$$

These strain relations hold for small deformations.

1.7 STRESS-STRAIN RELATIONS

For linear elastic materials, the stress-strain relations come from the generalized Hooke's law. For isotropic materials, the two material properties are Young's modulus (or modulus of elasticity) E and Poisson's ratio ν . Considering an elemental cube inside the body, Hooke's law gives

$$\begin{aligned} \epsilon_x &= \frac{\sigma_x}{E} - \nu \frac{\sigma_y}{E} - \nu \frac{\sigma_z}{E} \\ \epsilon_y &= -\nu \frac{\sigma_x}{E} + \frac{\sigma_y}{E} - \nu \frac{\sigma_z}{E} \\ \epsilon_z &= -\nu \frac{\sigma_x}{E} - \nu \frac{\sigma_y}{E} + \frac{\sigma_z}{E} \end{aligned} \quad (1.11)$$

$$\gamma_{yz} = \frac{\tau_{yz}}{G}$$

$$\gamma_{xz} = \frac{\tau_{xz}}{G}$$

$$\gamma_{xy} = \frac{\tau_{xy}}{G}$$

The shear modulus (or modulus of rigidity), G , is given by

$$G = \frac{E}{2(1 + \nu)} \quad (1.12)$$

From Hooke's law relationships (Eq. 1.11), note that

$$\epsilon_x + \epsilon_y + \epsilon_z = \frac{(1 - 2\nu)}{E} (\sigma_x + \sigma_y + \sigma_z) \quad (1.13)$$

Substituting for $(\sigma_y + \sigma_z)$ and so on into Eq. 1.11, we get the inverse relations

$$\boldsymbol{\sigma} = \mathbf{D}\boldsymbol{\epsilon} \quad (1.14)$$

\mathbf{D} is the symmetric (6×6) material matrix given by

$$\mathbf{D} = \frac{E}{(1 + \nu)(1 - 2\nu)} \begin{bmatrix} 1 - \nu & \nu & \nu & 0 & 0 & 0 \\ \nu & 1 - \nu & \nu & 0 & 0 & 0 \\ \nu & \nu & 1 - \nu & 0 & 0 & 0 \\ 0 & 0 & 0 & 0.5 - \nu & 0 & 0 \\ 0 & 0 & 0 & 0 & 0.5 - \nu & 0 \\ 0 & 0 & 0 & 0 & 0 & 0.5 - \nu \end{bmatrix} \quad (1.15)$$

Special Cases

One dimension. In one dimension, we have normal stress σ along x and the corresponding normal strain ϵ . Stress-strain relations (Eq. 1.14) are simply

$$\sigma = E\epsilon \quad (1.16)$$

Two dimensions. In two dimensions, the problems are modeled as plane stress and plane strain.

Plane Stress. A thin planar body subjected to in-plane loading on its edge surface is said to be in plane stress. A ring press fitted on a shaft, Fig. 1.5a, is an example. Here stresses σ_z , τ_{xz} , and τ_{yz} are set as zero. The Hooke's law relations (Eq. 1.11) then give us

$$\begin{aligned} \epsilon_x &= \frac{\sigma_x}{E} - \nu \frac{\sigma_y}{E} \\ \epsilon_y &= -\nu \frac{\sigma_x}{E} + \frac{\sigma_y}{E} \\ \gamma_{xy} &= \frac{2(1+\nu)}{E} \tau_{xy} \\ \epsilon_z &= -\frac{\nu}{E} (\sigma_x + \sigma_y) \end{aligned} \quad (1.17)$$

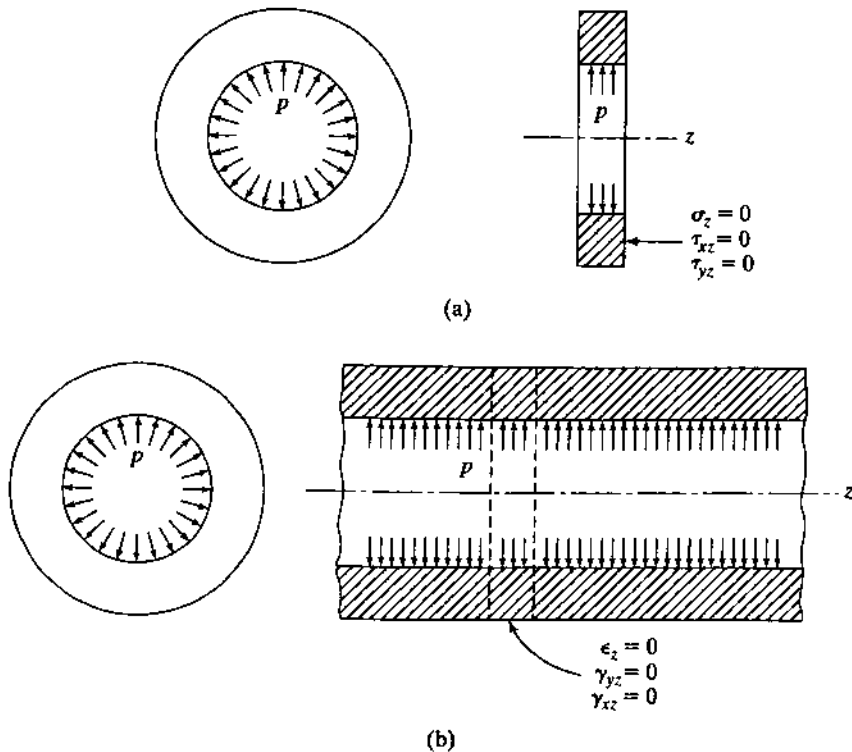


FIGURE 1.5 (a) Plane stress and (b) plane strain.

The inverse relations are given by

$$\begin{Bmatrix} \sigma_x \\ \sigma_y \\ \tau_{xy} \end{Bmatrix} = \frac{E}{1-\nu^2} \begin{bmatrix} 1 & \nu & 0 \\ \nu & 1 & 0 \\ 0 & 0 & \frac{1-\nu}{2} \end{bmatrix} \begin{Bmatrix} \epsilon_x \\ \epsilon_y \\ \gamma_{xy} \end{Bmatrix} \quad (1.18)$$

which is used as $\boldsymbol{\sigma} = \mathbf{D}\boldsymbol{\epsilon}$.

Plane Strain. If a long body of uniform cross section is subjected to transverse loading along its length, a small thickness in the loaded area, as shown in Fig. 1.5b, can be treated as subjected to plane strain. Here $\epsilon_z, \gamma_{zx}, \gamma_{yz}$ are taken as zero. Stress σ_z may not be zero in this case. The stress-strain relations can be obtained directly from Eqs. 1.14 and 1.15:

$$\begin{Bmatrix} \sigma_x \\ \sigma_y \\ \tau_{xy} \end{Bmatrix} = \frac{E}{(1+\nu)(1-2\nu)} \begin{bmatrix} 1-\nu & \nu & 0 \\ \nu & 1-\nu & 0 \\ 0 & 0 & \frac{1}{2}-\nu \end{bmatrix} \begin{Bmatrix} \epsilon_x \\ \epsilon_y \\ \gamma_{xy} \end{Bmatrix} \quad (1.19)$$

\mathbf{D} here is a (3×3) matrix, which relates three stresses and three strains.

Anisotropic bodies, with uniform orientation, can be considered by using the appropriate \mathbf{D} matrix for the material.

1.8 TEMPERATURE EFFECTS

If the temperature rise $\Delta T(x, y, z)$ with respect to the original state is known, then the associated deformation can be considered easily. For isotropic materials, the temperature rise ΔT results in a uniform strain, which depends on the coefficient of linear expansion α of the material. α , which represents the change in length per unit temperature rise, is assumed to be a constant within the range of variation of the temperature. Also, this strain does not cause any stresses when the body is free to deform. The temperature strain is represented as an initial strain:

$$\boldsymbol{\epsilon}_0 = [\alpha\Delta T, \alpha\Delta T, \alpha\Delta T, 0, 0, 0]^T \quad (1.20)$$

The stress-strain relations then become

$$\boldsymbol{\sigma} = \mathbf{D}(\boldsymbol{\epsilon} - \boldsymbol{\epsilon}_0) \quad (1.21)$$

In plane stress, we have

$$\boldsymbol{\epsilon}_0 = [\alpha\Delta T, \alpha\Delta T, 0]^T \quad (1.22)$$

In plane strain, the constraint that $\epsilon_z = 0$ results in a different $\boldsymbol{\epsilon}_0$,

$$\boldsymbol{\epsilon}_0 = (1+\nu)[\alpha\Delta T, \alpha\Delta T, 0]^T \quad (1.23)$$

For plane stress and plane strain, note that $\boldsymbol{\sigma} = [\sigma_x, \sigma_y, \tau_{xy}]^T$ and $\boldsymbol{\epsilon} = [\epsilon_x, \epsilon_y, \gamma_{xy}]^T$, and that \mathbf{D} matrices are as given in Eqs. 1.18 and 1.19, respectively.

1.9 POTENTIAL ENERGY AND EQUILIBRIUM; THE RAYLEIGH-RITZ METHOD

In mechanics of solids, our problem is to determine the displacement \mathbf{u} of the body shown in Fig. 1.1, satisfying the equilibrium equations 1.6. Note that stresses are related to strains, which, in turn, are related to displacements. This leads to requiring solution of second-order partial differential equations. Solution of this set of equations is generally referred to as an *exact* solution. Such exact solutions are available for simple geometries and loading conditions, and one may refer to publications in theory of elasticity. For problems of complex geometries and general boundary and loading conditions, obtaining such solutions is an almost impossible task. Approximate solution methods usually employ potential energy or variational methods, which place less stringent conditions on the functions.

Potential Energy, Π

The total potential energy Π of an elastic body, is defined as the sum of total strain energy (U) and the work potential:

$$\Pi = \underset{(U)}{\text{Strain energy}} + \underset{(\text{WP})}{\text{Work potential}} \quad (1.24)$$

For linear elastic materials, the strain energy per unit volume in the body is $\frac{1}{2}\boldsymbol{\sigma}^T\boldsymbol{\epsilon}$. For the elastic body shown in Fig. 1.1, the total strain energy U is given by

$$U = \frac{1}{2} \int_V \boldsymbol{\sigma}^T \boldsymbol{\epsilon} dV \quad (1.25)$$

The work potential WP is given by

$$\text{WP} = - \int_V \mathbf{u}^T \mathbf{f} dV - \int_S \mathbf{u}^T \mathbf{T} dS - \sum_i \mathbf{u}_i^T \mathbf{P}_i \quad (1.26)$$

The total potential for the general elastic body shown in Fig. 1.1 is

$$\Pi = \frac{1}{2} \int_V \boldsymbol{\sigma}^T \boldsymbol{\epsilon} dV - \int_V \mathbf{u}^T \mathbf{f} dV - \int_S \mathbf{u}^T \mathbf{T} dS - \sum_i \mathbf{u}_i^T \mathbf{P}_i \quad (1.27)$$

We consider conservative systems here, where the work potential is independent of the path taken. In other words, if the system is displaced from a given configuration and brought back to this state, the forces do zero work regardless of the path. The potential energy principle is now stated as follows:

Principle of Minimum Potential Energy

For conservative systems, of all the kinematically admissible displacement fields, those corresponding to equilibrium extremize the total potential energy. If the extremum condition is a minimum, the equilibrium state is stable.

Kinematically admissible displacements are those that satisfy the single-valued nature of displacements (compatibility) and the boundary conditions. In problems where displacements are the unknowns, which is the approach in this book, compatibility is automatically satisfied.

To illustrate the ideas, let us consider an example of a discrete connected system.

Example 1.1

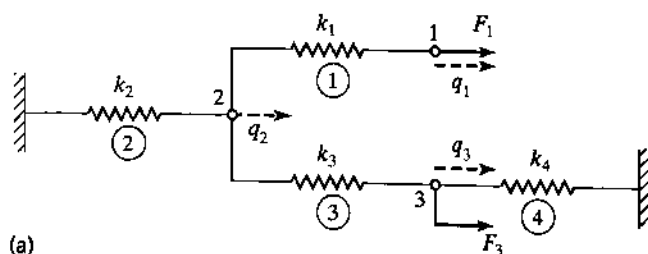
Figure E1.1a shows a system of springs. The total potential energy is given by

$$\Pi = \frac{1}{2}k_1\delta_1^2 + \frac{1}{2}k_2\delta_2^2 + \frac{1}{2}k_3\delta_3^2 + \frac{1}{2}k_4\delta_4^2 - F_1q_1 - F_3q_3$$

where δ_1 , δ_2 , δ_3 , and δ_4 are extensions of the four springs. Since $\delta_1 = q_1 - q_2$, $\delta_2 = q_2$, $\delta_3 = q_3 - q_2$, and $\delta_4 = -q_3$, we have

$$\Pi = \frac{1}{2}k_1(q_1 - q_2)^2 + \frac{1}{2}k_2q_2^2 + \frac{1}{2}k_3(q_3 - q_2)^2 + \frac{1}{2}k_4q_3^2 - F_1q_1 - F_3q_3$$

where q_1 , q_2 , and q_3 are the displacements of nodes 1, 2, and 3, respectively.



(a)

FIGURE E1.1a

For equilibrium of this three degrees of freedom system, we need to minimize Π with respect to q_1 , q_2 , and q_3 . The three equations are given by

$$\frac{\partial \Pi}{\partial q_i} = 0 \quad i = 1, 2, 3 \quad (1.28)$$

which are

$$\frac{\partial \Pi}{\partial q_1} = k_1(q_1 - q_2) - F_1 = 0$$

$$\frac{\partial \Pi}{\partial q_2} = -k_1(q_1 - q_2) + k_2q_2 - k_3(q_3 - q_2) = 0$$

$$\frac{\partial \Pi}{\partial q_3} = k_3(q_3 - q_2) + k_4q_3 - F_3 = 0$$

These equilibrium equations can be put in the form of $\mathbf{Kq} = \mathbf{F}$ as follows:

$$\begin{bmatrix} k_1 & -k_1 & 0 \\ -k_1 & k_1 + k_2 + k_3 & -k_3 \\ 0 & -k_3 & k_3 + k_4 \end{bmatrix} \begin{Bmatrix} q_1 \\ q_2 \\ q_3 \end{Bmatrix} = \begin{Bmatrix} F_1 \\ 0 \\ F_3 \end{Bmatrix} \quad (1.29)$$

If, on the other hand, we proceed to write the equilibrium equations of the system by considering the equilibrium of each separate node, as shown in Fig. E1.1b, we can write

$$\begin{aligned} k_1\delta_1 &= F_1 \\ k_2\delta_2 - k_1\delta_1 - k_3\delta_3 &= 0 \\ k_3\delta_3 - k_4\delta_4 &= F_3 \end{aligned}$$

which is precisely the set of equations represented in Eq. 1.29.

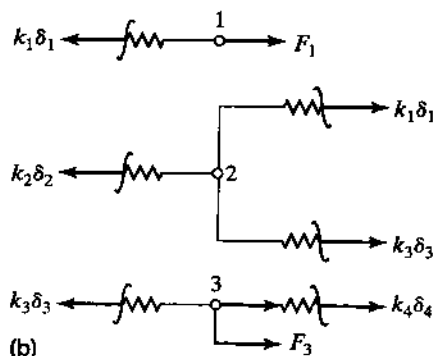


FIGURE E1.1b

We see clearly that the set of equations 1.29 is obtained in a routine manner using the potential energy approach, without any reference to the free-body diagrams. This makes the potential energy approach attractive for large and complex problems. ■

Rayleigh–Ritz Method

For continua, the total potential energy Π in Eq. 1.27 can be used for finding an approximate solution. The Rayleigh–Ritz method involves the construction of an assumed displacement field, say,

$$\begin{aligned} u &= \sum a_i \phi_i(x, y, z) & i &= 1 \text{ to } \ell \\ v &= \sum a_j \phi_j(x, y, z) & j &= \ell + 1 \text{ to } m \\ w &= \sum a_k \phi_k(x, y, z) & k &= m + 1 \text{ to } n \\ & & n &> m > \ell \end{aligned} \quad (1.30)$$

The functions ϕ_i are usually taken as polynomials. Displacements u, v, w must be **kinematically admissible**. That is, u, v, w must satisfy specified boundary conditions. Introducing stress–strain and strain–displacement relations, and substituting Eq. 1.30 into Eq. 1.27 gives

$$\Pi = \Pi(a_1, a_2, \dots, a_r) \quad (1.31)$$

where r = number of independent unknowns. Now, the extremum with respect to a_i , ($i = 1$ to r) yields the set of r equations

$$\frac{\partial \Pi}{\partial a_i} = 0 \quad i = 1, 2, \dots, r \quad (1.32)$$

Example 1.2

The potential energy for the linear elastic one-dimensional rod (Fig. E1.2), with body force neglected, is

$$\Pi = \frac{1}{2} \int_0^L EA \left(\frac{du}{dx} \right)^2 dx - 2u_1$$

where $u_1 = u(x = 1)$.

Let us consider a polynomial function

$$u = a_1 + a_2x + a_3x^2$$

This must satisfy $u = 0$ at $x = 0$ and $u = 0$ at $x = 2$. Thus,

$$0 = a_1$$

$$0 = a_1 + 2a_2 + 4a_3$$

Hence,

$$a_2 = -2a_3$$

$$u = a_3(-2x + x^2) \quad u_1 = -a_3$$

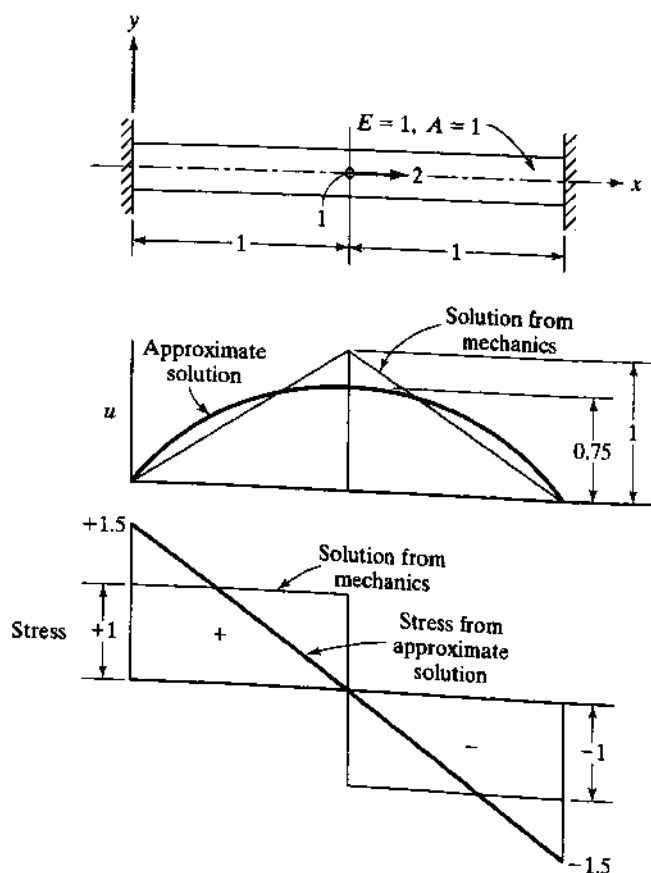


FIGURE E1.2

Then $du/dx = 2a_3(-1 + x)$ and

$$\begin{aligned}\Pi &= \frac{1}{2} \int_0^2 4a_3^2(-1 + x)^2 dx - 2(-a_3) \\ &= 2a_3^2 \int_0^2 (1 - 2x + x^2) dx + 2a_3 \\ &= 2a_3^2\left(\frac{2}{3}\right) + 2a_3\end{aligned}$$

We set $\partial\Pi/\partial a_3 = 4a_3\left(\frac{2}{3}\right) + 2 = 0$, resulting in

$$a_3 = -0.75 \quad u_1 = -a_3 = 0.75$$

The stress in the bar is given by

$$\sigma = E \frac{du}{dx} = 1.5(1 - x) \quad \blacksquare$$

We note here that an exact solution is obtained if piecewise polynomial interpolation is used in the construction of u .

The finite element method provides a systematic way of constructing the basis functions ϕ_i used in Eq. 1.30.

1.10 GALERKIN'S METHOD

Galerkin's method uses the set of governing equations in the development of an integral form. It is usually presented as one of the weighted residual methods. For our discussion, let us consider a general representation of a governing equation on a region V :

$$Lu = P \quad (1.33)$$

For the one-dimensional rod considered in Example 1.2, the governing equation is the differential equation

$$\frac{d}{dx} \left(EA \frac{du}{dx} \right) = 0$$

We may consider L as the operator

$$\frac{d}{dx} EA \frac{d}{dx} (\quad)$$

operating on u .

The exact solution needs to satisfy (1.33) at every point x . If we seek an approximate solution \tilde{u} , it introduces an error $\epsilon(x)$, called the *residual*:

$$\epsilon(x) = L\tilde{u} - P \quad (1.34)$$

The approximate methods revolve around setting the residual relative to a weighting function W_i , to zero:

$$\int_V W_i(L\tilde{u} - P) dV = 0 \quad i = 1 \text{ to } n \quad (1.35)$$

The choice of the weighting function W_i leads to various approximation methods. In the Galerkin method, the weighting functions W_i are chosen from the basis functions used for constructing \tilde{u} . Let \tilde{u} be represented by

$$\tilde{u} = \sum_{i=1}^n Q_i G_i \quad (1.36)$$

where $G_i, i = 1$ to n , are basis functions (usually polynomials of x, y, z). Here, we choose the weighting functions to be a linear combination of the basis functions G_i . Specifically, consider an arbitrary function ϕ given by

$$\phi = \sum_{i=1}^n \phi_i G_i \quad (1.37)$$

where the coefficients ϕ_i are arbitrary, except for requiring that ϕ satisfy homogeneous (zero) boundary conditions where \tilde{u} is prescribed. The fact that ϕ in Eq. 1.37 is constructed in a similar manner as \tilde{u} in Eq. 1.36 leads to simplified derivations in later chapters.

Galerkin's method can be stated as follows:

Choose basis functions G_i . Determine the coefficients Q_i in $\tilde{u} = \sum_{i=1}^n Q_i G_i$ such that

$$\int_V \phi(L\tilde{u} - P) dV = 0 \quad (1.38)$$

for every ϕ of the type $\phi = \sum_{i=1}^n \phi_i G_i$, where coefficients ϕ_i are arbitrary except for requiring that ϕ satisfy homogeneous (zero) boundary conditions. The solution of the resulting equations for Q_i then yields the approximate solution \tilde{u} .

Usually, in the treatment of Eq. 1.38 an integration by parts is involved. The order of the derivatives is reduced and the natural boundary conditions, such as surface-force conditions, are introduced.

Galerkin's method in elasticity. Let us turn our attention to the equilibrium equations 1.6 in elasticity. Galerkin's method requires

$$\int_V \left[\left(\frac{\partial \sigma_x}{\partial x} + \frac{\partial \tau_{xy}}{\partial y} + \frac{\partial \tau_{xz}}{\partial z} + f_x \right) \phi_x + \left(\frac{\partial \tau_{xy}}{\partial x} + \frac{\partial \sigma_y}{\partial y} + \frac{\partial \tau_{yz}}{\partial z} + f_y \right) \phi_y + \left(\frac{\partial \tau_{xz}}{\partial x} + \frac{\partial \tau_{yz}}{\partial y} + \frac{\partial \sigma_z}{\partial z} + f_z \right) \phi_z \right] dV = 0 \quad (1.39)$$

where

$$\phi = [\phi_x, \phi_y, \phi_z]^T$$

is an arbitrary displacement consistent with the boundary conditions of \mathbf{u} . If $\mathbf{n} = [n_x, n_y, n_z]^T$ is a unit normal at a point \mathbf{x} on the surface, the integration by parts formula is

$$\int_V \frac{\partial \alpha}{\partial x} \theta dV = - \int_V \alpha \frac{\partial \theta}{\partial x} dV + \int_S n_x \theta ds \quad (1.40)$$

where α and θ are functions of (x, y, z) . For multidimensional problems, Eq. 1.40 is usually referred to as the Green-Gauss theorem or the divergence theorem. Using this formula, integrating Eq. 1.39 by parts, and rearranging terms, we get

$$\begin{aligned} - \int_V \boldsymbol{\sigma}^T \boldsymbol{\epsilon}(\phi) dV + \int_V \boldsymbol{\phi}^T \mathbf{f} dV + \int_S [(n_x \sigma_x + n_y \tau_{xy} + n_z \tau_{xz}) \phi_x \\ + (n_x \tau_{xy} + n_y \sigma_y + n_z \tau_{yz}) \phi_y + (n_x \tau_{xz} + n_y \tau_{yz} + n_z \sigma_z) \phi_z] dS = 0 \end{aligned} \quad (1.41)$$

where

$$\boldsymbol{\epsilon}(\phi) = \left[\frac{\partial \phi_x}{\partial x}, \frac{\partial \phi_y}{\partial y}, \frac{\partial \phi_z}{\partial z}, \frac{\partial \phi_y}{\partial z} + \frac{\partial \phi_z}{\partial y}, \frac{\partial \phi_x}{\partial z} + \frac{\partial \phi_z}{\partial x}, \frac{\partial \phi_x}{\partial y} + \frac{\partial \phi_y}{\partial x} \right]^T \quad (1.42)$$

is the strain corresponding to the arbitrary displacement field ϕ .

On the boundary, from Eq. 1.8, we have $(n_x \sigma_x + n_y \tau_{xy} + n_z \tau_{xz}) = T_x$, and so on. At point loads $(n_x \sigma_x + n_y \tau_{xy} + n_z \tau_{xz}) dS$ is equivalent to P_x , and so on. These are the natural boundary conditions in the problem. Thus, Eq. 1.41 yields the Galerkin's "variational form" or "weak form" for three-dimensional stress analysis:

$$\int_V \boldsymbol{\sigma}^T \boldsymbol{\epsilon}(\phi) dV - \int_V \boldsymbol{\phi}^T \mathbf{f} dV - \int_S \boldsymbol{\phi}^T \mathbf{T} dS - \sum_i \boldsymbol{\phi}^T \mathbf{P} = 0 \quad (1.43)$$

where ϕ is an arbitrary displacement consistent with the specified boundary conditions of \mathbf{u} . We may now use Eq. 1.43 to provide us with an approximate solution.

For problems of linear elasticity, Eq. 1.43 is precisely the **principle of virtual work**. ϕ is the kinematically admissible virtual displacement. The principle of virtual work may be stated as follows:

Principle of Virtual Work

A body is in equilibrium if the internal virtual work equals the external virtual work for every kinematically admissible displacement field $(\phi, \boldsymbol{\epsilon}(\phi))$.

We note that Galerkin's method and the principle of virtual work result in the same set of equations for problems of elasticity when same basis or coordinate functions are used. Galerkin's method is more general since the variational form of the type Eq. 1.43 can be developed for other governing equations defining boundary-value problems. Galerkin's method works directly from the differential equation and is preferred to the Rayleigh-Ritz method for problems where a corresponding function to be minimized is not obtainable.

Example 1.3

Let us consider the problem of Example 1.2 and solve it by Galerkin's approach. The equilibrium equation is

$$\frac{d}{dx} EA \frac{du}{dx} = 0 \quad \begin{array}{l} u = 0 \text{ at } x = 0 \\ u = 0 \text{ at } x = 2 \end{array}$$

Multiplying this differential equation by ϕ , and integrating by parts, we get

$$\int_0^2 -EA \frac{du}{dx} \frac{d\phi}{dx} dx + \left(\phi EA \frac{du}{dx} \right)_0^1 + \left(\phi EA \frac{du}{dx} \right)_1^2 = 0$$

where ϕ is zero at $x = 0$ and $x = 2$. $EA (du/dx)$ is the tension in the rod, which takes a jump of magnitude 2 at $x = 1$ (Fig. E1.2). Thus,

$$\int_0^2 -EA \frac{du}{dx} \frac{d\phi}{dx} dx + 2\phi_1 = 0$$

Now we use the same polynomial (basis) for u and ϕ . If u_1 and ϕ_1 are the values at $x = 1$, we have

$$u = (2x - x^2)u_1$$

$$\phi = (2x - x^2)\phi_1$$

Substituting these and $E = 1$, $A = 1$ in the previous integral yields

$$\phi_1 \left[-u_1 \int_0^2 (2 - 2x)^2 dx + 2 \right] = 0$$

$$\phi_1 \left(-\frac{8}{3}u_1 + 2 \right) = 0$$

This is to be satisfied for every ϕ_1 . We get

$$u_1 = 0.75$$

1.11 SAINT VENANT'S PRINCIPLE

We often have to make approximations in defining boundary conditions to represent a support-structure interface. For instance, consider a cantilever beam, free at one end and attached to a column with rivets at the other end. Questions arise as to whether the riveted joint is totally rigid or partially rigid, and as to whether each point on the cross section at the fixed end is specified to have the same boundary conditions. Saint Venant considered the effect of different approximations on the solution to the total problem. Saint Venant's principle states that as long as the different approximations are statically equivalent, the resulting solutions will be valid provided we focus on regions sufficiently far away from the support. That is, the solutions may significantly differ only within the immediate vicinity of the support.

1.12 VON MISES STRESS

Von Mises stress is used as a criterion in determining the onset of failure in ductile materials. The failure criterion states that the von Mises stress σ_{VM} should be less than the yield stress σ_Y of the material. In the inequality form, the criterion may be put as

$$\sigma_{VM} \leq \sigma_Y \quad (1.44)$$

The von Mises stress σ_{VM} is given by

$$\sigma_{VM} = \sqrt{I_1^2 - 3I_2} \quad (1.45)$$

where I_1 and I_2 are the first two invariants of the stress tensor. For the general state of stress given by Eq. 1.5, I_1 and I_2 are given by

$$\begin{aligned} I_1 &= \sigma_x + \sigma_y + \sigma_z \\ I_2 &= \sigma_x\sigma_y + \sigma_y\sigma_z + \sigma_z\sigma_x - \tau_{yz}^2 - \tau_{xz}^2 - \tau_{xy}^2 \end{aligned} \quad (1.46)$$

In terms of the principal stresses σ_1 , σ_2 , and σ_3 , the two invariants can be written as

$$\begin{aligned} I_1 &= \sigma_1 + \sigma_2 + \sigma_3 \\ I_2 &= \sigma_1\sigma_2 + \sigma_2\sigma_3 + \sigma_3\sigma_1 \end{aligned}$$

It is easy to check that von Mises stress given in Eq. 1.45 can be expressed in the form

$$\sigma_{VM} = \frac{1}{\sqrt{2}} \sqrt{(\sigma_1 - \sigma_2)^2 + (\sigma_2 - \sigma_3)^2 + (\sigma_3 - \sigma_1)^2} \quad (1.47)$$

For the state of plane stress, we have

$$\begin{aligned} I_1 &= \sigma_x + \sigma_y \\ I_2 &= \sigma_x\sigma_y - \tau_{xy}^2 \end{aligned} \quad (1.48)$$

and for plane strain

$$\begin{aligned} I_1 &= \sigma_x + \sigma_y + \sigma_z \\ I_2 &= \sigma_x\sigma_y + \sigma_y\sigma_z + \sigma_z\sigma_x - \tau_{xy}^2 \end{aligned} \quad (1.49)$$

where $\sigma_z = \nu(\sigma_x + \sigma_y)$.

1.13 COMPUTER PROGRAMS

Computer use is an essential part of the finite element analysis. Well-developed, well-maintained, and well-supported computer programs are necessary in solving engineering problems and interpreting results. Many available commercial finite element packages fulfill these needs. It is also the trend in industry that the results are acceptable only when solved using certain standard computer program packages. The commercial packages provide user-friendly data-input platforms and elegant and easy to follow display formats. However, the packages do not provide an insight into the formulations and solution methods. Specially developed computer programs with available source codes enhance the learning process. We follow this philosophy in the development of this

book. Every chapter is provided with computer programs that parallel the theory. The curious student should make an effort to see how the steps given in the theoretical development are implemented in the programs. Source codes are provided in QBASIC, FORTRAN, C, VISUALBASIC, Excel Visual Basic, and MATLAB. Example input and output files are provided at the end of every chapter. We encourage the use of commercial packages to supplement the learning process.

1.14 CONCLUSION

In this chapter, we have discussed the necessary background for the finite element method. We devote the next chapter to discussing matrix algebra and techniques for solving a set of linear algebraic equations.

HISTORICAL REFERENCES

1. Hrenikoff, A., "Solution of problems in elasticity by the frame work method." *Journal of Applied Mechanics, Transactions of the ASME* 8: 169–175 (1941).
2. Courant, R., "Variational methods for the solution of problems of equilibrium and vibrations." *Bulletin of the American Mathematical Society* 49: 1–23 (1943).
3. Turner, M. J., R. W. Clough, H. C. Martin, and L. J. Topp, "Stiffness and deflection analysis of complex structures." *Journal of Aeronautical Science* 23(9): 805–824 (1956).
4. Clough, R. W., "The finite element method in plane stress analysis." *Proceedings American Society of Civil Engineers*, 2d Conference on Electronic Computation, Pittsburgh, Pennsylvania, 23: 345–378 (1960).
5. Argyris, J. H., "Energy theorems and structural analysis." *Aircraft Engineering*, 26: Oct.–Nov., 1954; 27: Feb.–May, 1955.
6. Zienkiewicz, O. C., and Y. K. Cheung, *The Finite Element Method in Structural and Continuum Mechanics*. (London: McGraw-Hill, 1967).
7. Oden, J. T., *Finite Elements of Nonlinear Continua*. (New York: McGraw-Hill, 1972).

PROBLEMS

- 1.1. Obtain the **D** matrix given by Eq. 1.15 using the generalized Hooke's law relations (Eq. 1.11).
- 1.2. In a plane strain problem, we have

$$\begin{aligned}\sigma_x &= 20\,000 \text{ psi}, \sigma_y = -10\,000 \text{ psi} \\ E &= 30 \times 10^6 \text{ psi}, \nu = 0.3\end{aligned}$$

Determine the value of the stress σ_z .

- 1.3. If a displacement field is described by

$$\begin{aligned}u &= (-x^2 + 2y^2 + 6xy)10^{-4} \\ v &= (3x + 6y - y^2)10^{-4}\end{aligned}$$

determine ϵ_x , ϵ_y , γ_{xy} at the point $x = 1$, $y = 0$.

- 1.4. Develop a deformation field $u(x, y)$, $v(x, y)$ that describes the deformation of the finite element shown. From this determine ϵ_x , ϵ_y , γ_{xy} . Interpret your answer.

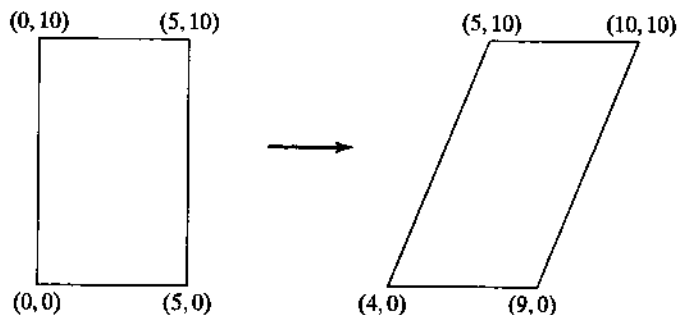


FIGURE P1.4

1.5. A displacement field

$$u = 1 + 3x + 4x^3 + 6xy^2$$

$$v = xy - 7x^2$$

is imposed on the square element shown in Fig. P1.5.

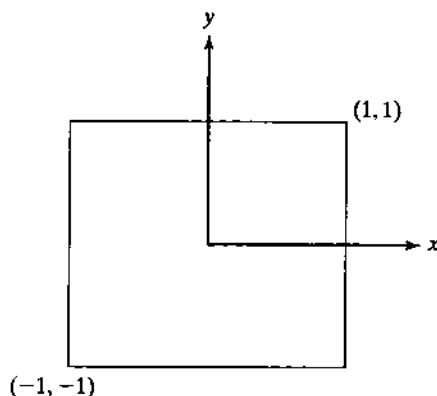


FIGURE P1.5

- (a) Write down the expressions for ϵ_x , ϵ_y and γ_{xy} .
- (b) Plot contours of ϵ_x , ϵ_y , and γ_{xy} using, say, MATLAB software.
- (c) Find where ϵ_x is a maximum within the square.
- 1.6.** In a solid body, the six components of the stress at a point are given by $\sigma_x = 40$ MPa, $\sigma_y = 20$ MPa, $\sigma_z = 30$ MPa, $\tau_{yz} = -30$ MPa, $\tau_{xz} = 15$ MPa, and $\tau_{xy} = 10$ MPa. Determine the normal stress at the point, on a plane for which the normal is $(n_x, n_y, n_z) = (\frac{1}{2}, \frac{1}{2}, 1/\sqrt{2})$. (Hint: Note that normal stress $\sigma_n = T_x n_x + T_y n_y + T_z n_z$.)
- 1.7.** For isotropic materials, the stress-strain relations can also be expressed using Lamé's constants λ and μ , as follows:

$$\sigma_x = \lambda \epsilon_v + 2\mu \epsilon_x$$

$$\sigma_y = \lambda \epsilon_v + 2\mu \epsilon_y$$

$$\sigma_z = \lambda \epsilon_v + 2\mu \epsilon_z$$

$$\tau_{yz} = \mu \gamma_{yz}, \tau_{xz} = \mu \gamma_{xz}, \tau_{xy} = \mu \gamma_{xy}$$

Here $\epsilon_v = \epsilon_x + \epsilon_y + \epsilon_z$. Find expressions for λ and μ in terms of E and ν .

- 1.8. A long rod is subjected to loading and a temperature increase of 30°C . The total strain at a point is measured to be 1.2×10^{-5} . If $E = 200 \text{ GPa}$ and $\alpha = 12 \times 10^{-6}/^\circ\text{C}$, determine the stress at the point.
- 1.9. Consider the rod shown in Fig. P1.9, where the strain at any point x is given by $\epsilon_x = 1 + 2x^2$. Find the tip displacement δ .

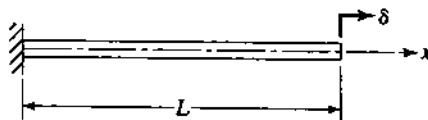


FIGURE P1.9

- 1.10. Determine the displacements of nodes of the spring system shown in Fig. P1.10.

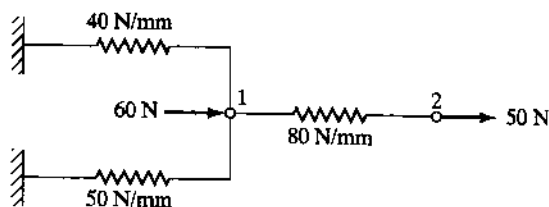


FIGURE P1.10

- 1.11. Use the Rayleigh–Ritz method to find the displacement of the midpoint of the rod shown in Fig. P1.11.

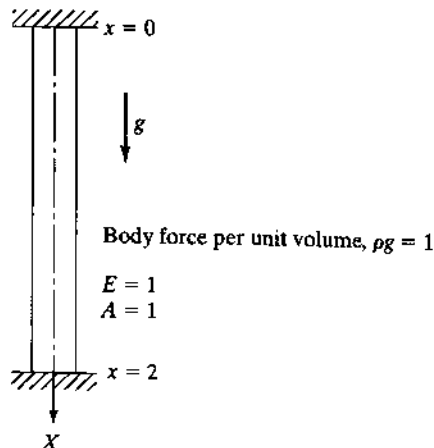


FIGURE P1.11

- 1.12. A rod fixed at its ends is subjected to a varying body force as shown. Use the Rayleigh–Ritz method with an assumed displacement field $u = a_0 + a_1x + a_2x^2$ to determine displacement $u(x)$ and stress $\sigma(x)$.
- 1.13. Use the Rayleigh–Ritz method to find the displacement field $u(x)$ of the rod in Fig. P1.13. Element 1 is made of aluminum, and element 2 is made of steel. The properties are

$$E_{al} = 70 \text{ GPa}, A_1 = 900 \text{ mm}^2, L_1 = 200 \text{ mm}$$

$$E_{st} = 200 \text{ GPa}, A_2 = 1200 \text{ mm}^2, L_2 = 300 \text{ mm}$$

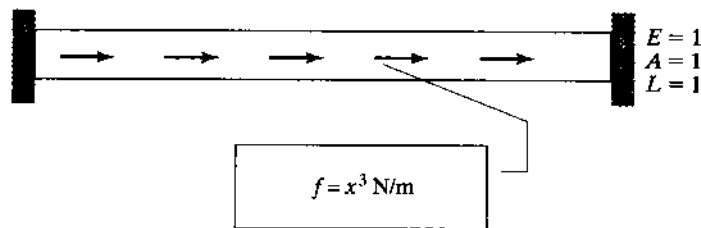


FIGURE P1.12

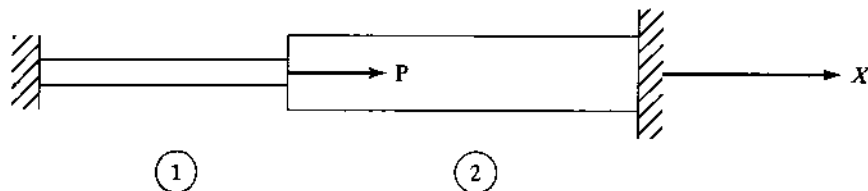


FIGURE P1.13

Load $P = 10,000$ N. Assume a piecewise linear displacement field $u = a_1 + a_2x$ for $0 \leq x \leq 200$ mm and $u = a_3 + a_4x$ for $200 \leq x \leq 500$ mm. Compare the Rayleigh-Ritz solution with the analytical strength-of-materials solution.

- 1.14. Use Galerkin's method to find the displacement at the midpoint of the rod (Figure P1.11).
- 1.15. Solve Example 1.2 using the potential energy approach with the polynomial $u = a_1 + a_2x + a_3x^2 + a_4x^3$.
- 1.16. A steel rod is attached to rigid walls at each end and is subjected to a distributed load $T(x)$ as shown in Fig. P1.16.
- (a) Write the expression for the potential energy, Π .

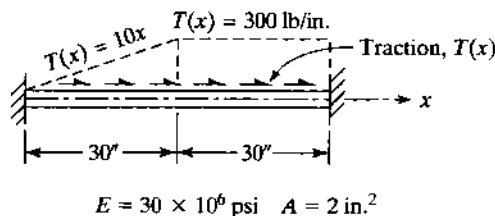


FIGURE P1.16

- (b) Determine the displacement $u(x)$ using the Rayleigh-Ritz method. Assume a displacement field $u(x) = a_0 + a_1x + a_2x^2$. Plot u versus x .
- (c) Plot σ versus x .
- 1.17. Consider the functional I for minimization given by

$$I = \int_0^L \frac{1}{2} k \left(\frac{dy}{dx} \right)^2 dx + \frac{1}{2} h (a_0 - 800)^2$$

with $y = 20$ at $x = 60$. Given $k = 20$, $h = 25$, and $L = 60$, determine a_0 , a_1 , and a_2 using the polynomial approximation $y(x) = a_0 + a_1x + a_2x^2$ in the Rayleigh-Ritz method.

CHAPTER 2

Matrix Algebra and Gaussian Elimination

2.1 MATRIX ALGEBRA

The study of matrices here is largely motivated from the need to solve systems of simultaneous equations of the form

$$\begin{aligned} a_{11}x_1 + a_{12}x_2 + \cdots + a_{1n}x_n &= b_1 \\ a_{21}x_1 + a_{22}x_2 + \cdots + a_{2n}x_n &= b_2 \end{aligned} \quad (2.1a)$$

$$a_{n1}x_1 + a_{n2}x_2 + \cdots + a_{nn}x_n = b_n$$

where x_1, x_2, \dots, x_n are the unknowns. Equations 2.1 can be conveniently expressed in matrix form as

$$\mathbf{Ax} = \mathbf{b} \quad (2.1b)$$

where \mathbf{A} is a square matrix of dimensions $(n \times n)$, and \mathbf{x} and \mathbf{b} are vectors of dimension $(n \times 1)$, given as

$$\mathbf{A} = \begin{bmatrix} a_{11} & a_{12} & \cdots & a_{1n} \\ a_{21} & a_{22} & \cdots & a_{2n} \\ \cdots & \cdots & \cdots & \cdots \\ a_{n1} & a_{n2} & \cdots & a_{nn} \end{bmatrix} \quad \mathbf{x} = \begin{Bmatrix} x_1 \\ x_2 \\ \vdots \\ x_n \end{Bmatrix} \quad \mathbf{b} = \begin{Bmatrix} b_1 \\ b_2 \\ \vdots \\ b_n \end{Bmatrix}$$

From this information, we see that a matrix is simply an array of elements. The matrix \mathbf{A} is also denoted as $[A]$. An element located at the i th row and j th column of \mathbf{A} is denoted by a_{ij} .

The multiplication of two matrices, \mathbf{A} and \mathbf{x} , is also implicitly defined: The dot product of the i th row of \mathbf{A} with the vector \mathbf{x} is equated to b_i , resulting in the i th equation of Eq. 2.1a. The multiplication operation and other operations will be discussed in detail in this chapter.

The analysis of engineering problems by the finite element method involves a sequence of matrix operations. This fact allows us to solve large-scale problems because computers are ideally suited for matrix operations. In this chapter, basic matrix operations are given as needed later in the text. The Gaussian elimination method for solv-

ing linear simultaneous equations is also discussed, and a variant of the Gaussian elimination approach, the skyline approach, is presented.

Row and Column Vectors

A matrix of dimension $(1 \times n)$ is called a **row vector**, while a matrix of dimension $(m \times 1)$ is called a **column vector**. For example,

$$\mathbf{d} = [1 \quad -1 \quad 2]$$

is a (1×3) row vector, and

$$\mathbf{e} = \begin{Bmatrix} 2 \\ 2 \\ -6 \\ 0 \end{Bmatrix}$$

is a (4×1) column vector.

Addition and Subtraction

Consider two matrices \mathbf{A} and \mathbf{B} , both of dimension $(m \times n)$. Then, the sum $\mathbf{C} = \mathbf{A} + \mathbf{B}$ is defined as

$$c_{ij} = a_{ij} + b_{ij} \quad (2.2)$$

That is, the (ij) th component of \mathbf{C} is obtained by adding the (ij) th component of \mathbf{A} to the (ij) th component of \mathbf{B} . For example,

$$\begin{bmatrix} 2 & -3 \\ -3 & 5 \end{bmatrix} + \begin{bmatrix} 2 & 1 \\ 0 & 4 \end{bmatrix} = \begin{bmatrix} 4 & -2 \\ -3 & 9 \end{bmatrix}$$

Subtraction is similarly defined.

Multiplication by a Scalar

The multiplication of a matrix \mathbf{A} by a scalar c is defined as

$$c\mathbf{A} = [ca_{ij}] \quad (2.3)$$

For example, we can write

$$\begin{bmatrix} 10\,000 & 4500 \\ 4500 & -6000 \end{bmatrix} = 10^3 \begin{bmatrix} 10 & 4.5 \\ 4.5 & -6 \end{bmatrix}$$

Matrix Multiplication

The product of an $(m \times n)$ matrix \mathbf{A} and an $(n \times p)$ matrix \mathbf{B} results in an $(m \times p)$ matrix \mathbf{C} . That is,

$$\begin{matrix} \mathbf{A} & \mathbf{B} & = & \mathbf{C} \\ (m \times n) & (n \times p) & & (m \times p) \end{matrix} \quad (2.4)$$

The (ij) th component of \mathbf{C} is obtained by taking the dot product

$$c_{ij} = (\textit{i} \text{th row of } \mathbf{A}) \cdot (\textit{j} \text{th column of } \mathbf{B}) \quad (2.5)$$

For example,

$$\begin{matrix} \begin{bmatrix} 2 & 1 & 3 \\ 0 & -2 & 1 \end{bmatrix} & \begin{bmatrix} 1 & 4 \\ 5 & -2 \\ 0 & 3 \end{bmatrix} & = & \begin{bmatrix} 7 & 15 \\ -10 & 7 \end{bmatrix} \\ (2 \times 3) & (3 \times 2) & & (2 \times 2) \end{matrix}$$

It should be noted that $\mathbf{AB} \neq \mathbf{BA}$; in fact, \mathbf{BA} may not even be defined, since the number of columns of \mathbf{B} may not equal the number of rows of \mathbf{A} .

Transposition

If $\mathbf{A} = [a_{ij}]$, then the transpose of \mathbf{A} , denoted as \mathbf{A}^T , is given by $\mathbf{A}^T = [a_{ji}]$. Thus, the rows of \mathbf{A} are the columns of \mathbf{A}^T . For example, if

$$\mathbf{A} = \begin{bmatrix} 1 & -5 \\ 0 & 6 \\ -2 & 3 \\ 4 & 2 \end{bmatrix}$$

then

$$\mathbf{A}^T = \begin{bmatrix} 1 & 0 & -2 & 4 \\ -5 & 6 & 3 & 2 \end{bmatrix}$$

In general, if \mathbf{A} is of dimension $(m \times n)$, then \mathbf{A}^T is of dimension $(n \times m)$.

The transpose of a product is given as the product of the transposes in reverse order:

$$(\mathbf{ABC})^T = \mathbf{C}^T \mathbf{B}^T \mathbf{A}^T \quad (2.6)$$

Differentiation and Integration

The components of a matrix do not have to be scalars; they may also be functions. For example,

$$\mathbf{B} = \begin{bmatrix} x + y & x^2 - xy \\ 6 + x & y \end{bmatrix}$$

In this regard, matrices may be differentiated and integrated. The derivative (or integral) of a matrix is simply the derivative (or integral) of each component of the matrix. Thus,

$$\frac{d}{dx} \mathbf{B}(x) = \left[\frac{db_{ij}(x)}{dx} \right] \quad (2.7)$$

$$\int \mathbf{B} dx dy = \left[\int b_{ij} dx dy \right] \quad (2.8)$$

The formula in Eq. 2.7 will now be specialized to an important case. Let \mathbf{A} be an $(n \times n)$ matrix of constants, and $\mathbf{x} = [x_1, x_2, \dots, x_n]^T$ be a column vector of n variables. Then, the derivative of \mathbf{Ax} with respect to variable x_p is given by

$$\frac{d}{dx_p}(\mathbf{Ax}) = \mathbf{a}^p \quad (2.9)$$

where \mathbf{a}^p is the p th column of \mathbf{A} . This result follows from the fact that the vector (\mathbf{Ax}) can be written out in full as

$$\mathbf{Ax} = \left\{ \begin{array}{l} a_{11}x_1 + a_{12}x_2 + \cdots + a_{1p}x_p + \cdots + a_{1n}x_n \\ a_{21}x_1 + a_{22}x_2 + \cdots + a_{2p}x_p + \cdots + a_{2n}x_n \\ \cdots \\ a_{n1}x_1 + a_{n2}x_2 + \cdots + a_{np}x_p + \cdots + a_{nn}x_n \end{array} \right\} \quad (2.10)$$

Now, we see clearly that the derivative of \mathbf{Ax} with respect to x_p yields the p th column of \mathbf{A} as stated in Eq. 2.9.

Square Matrix

A matrix whose number of rows equals the number of columns is called a square matrix.

Diagonal Matrix

A diagonal matrix is a square matrix with nonzero elements only along the principal diagonal. For example,

$$\mathbf{A} = \begin{bmatrix} 2 & 0 & 0 \\ 0 & 6 & 0 \\ 0 & 0 & -3 \end{bmatrix}$$

Identity Matrix

The identity (or unit) matrix is a diagonal matrix with 1's along the principal diagonal. For example,

$$\mathbf{I} = \begin{bmatrix} 1 & 0 & 0 & 0 \\ 0 & 1 & 0 & 0 \\ 0 & 0 & 1 & 0 \\ 0 & 0 & 0 & 1 \end{bmatrix}$$

If \mathbf{I} is of dimension $(n \times n)$ and \mathbf{x} is an $(n \times 1)$ vector, then

$$\mathbf{Ix} = \mathbf{x}$$

Symmetric Matrix

A symmetric matrix is a square matrix whose elements satisfy

$$a_{ij} = a_{ji} \quad (2.11a)$$

or equivalently,

$$\mathbf{A} = \mathbf{A}^T \quad (2.11b)$$

That is, elements located symmetrically with respect to the principal diagonal are equal. For example,

$$\mathbf{A} = \begin{bmatrix} 2 & 1 & 0 \\ 1 & 6 & -2 \\ 0 & -2 & 8 \end{bmatrix}$$

Upper Triangular Matrix

An upper triangular matrix is one whose elements below the principal diagonal are all zero. For example,

$$\mathbf{U} = \begin{bmatrix} 2 & -1 & 6 & 3 \\ 0 & 14 & 8 & 0 \\ 0 & 0 & 5 & 1 \\ 0 & 0 & 0 & 3 \end{bmatrix}$$

Determinant of a Matrix

The determinant of a square matrix \mathbf{A} is a scalar quantity denoted as $\det \mathbf{A}$. The determinants of a (2×2) and a (3×3) matrix are given by the **method of cofactors** as follows:

$$\det \begin{bmatrix} a_{11} & a_{12} \\ a_{21} & a_{22} \end{bmatrix} = a_{11}a_{22} - a_{21}a_{12} \quad (2.12)$$

$$\det \begin{bmatrix} a_{11} & a_{12} & a_{13} \\ a_{21} & a_{22} & a_{23} \\ a_{31} & a_{32} & a_{33} \end{bmatrix} = a_{11}(a_{22}a_{33} - a_{32}a_{23}) \\ - a_{12}(a_{21}a_{33} - a_{31}a_{23}) \\ + a_{13}(a_{21}a_{32} - a_{31}a_{22}) \quad (2.13)$$

Matrix Inversion

Consider a square matrix \mathbf{A} . If $\det \mathbf{A} \neq 0$, then \mathbf{A} has an inverse, denoted by \mathbf{A}^{-1} . The inverse satisfies the relations

$$\mathbf{A}^{-1}\mathbf{A} = \mathbf{A}\mathbf{A}^{-1} = \mathbf{I} \quad (2.14)$$

If $\det \mathbf{A} \neq 0$, then we say that \mathbf{A} is **nonsingular**. If $\det \mathbf{A} = 0$, then we say that \mathbf{A} is **singular**, for which the inverse is not defined. The minor M_{ij} of a square matrix \mathbf{A} is the determinant of the $(n - 1 \times n - 1)$ matrix obtained by eliminating the i th row and the j th column of \mathbf{A} . The cofactor C_{ij} of matrix \mathbf{A} is given by

$$C_{ij} = (-1)^{i+j}M_{ij}$$

Matrix \mathbf{C} with elements C_{ij} is called the cofactor matrix. The adjoint of matrix \mathbf{A} is defined as

$$\text{Adj } \mathbf{A} = \mathbf{C}^T$$

The inverse of a square matrix \mathbf{A} is given as

$$\mathbf{A}^{-1} = \frac{\text{adj } \mathbf{A}}{\det \mathbf{A}}$$

For example, the inverse of a (2×2) matrix \mathbf{A} is given by

$$\begin{bmatrix} a_{11} & a_{12} \\ a_{21} & a_{22} \end{bmatrix}^{-1} = \frac{1}{\det \mathbf{A}} \begin{bmatrix} a_{22} & -a_{12} \\ -a_{21} & a_{11} \end{bmatrix}$$

Quadratic Forms Let \mathbf{A} be an $(n \times n)$ matrix and \mathbf{x} be an $(n \times 1)$ vector. Then, the scalar quantity

$$\mathbf{x}^T \mathbf{A} \mathbf{x} \quad (2.15)$$

is called a quadratic form, since upon expansion we obtain the quadratic expression

$$\begin{aligned} \mathbf{x}^T \mathbf{A} \mathbf{x} = & x_1 a_{11} x_1 + x_1 a_{12} x_2 + \cdots + x_1 a_{1n} x_n \\ & + x_2 a_{21} x_1 + x_2 a_{22} x_2 + \cdots + x_2 a_{2n} x_n \\ & + x_n a_{n1} x_1 + x_n a_{n2} x_2 + \cdots + x_n a_{nn} x_n \end{aligned} \quad (2.16)$$

As an example, the quantity

$$u = 3x_1^2 - 4x_1x_2 + 6x_1x_3 - x_2^2 + 5x_3^2$$

can be expressed in matrix form as

$$\begin{aligned} u &= [x_1 \quad x_2 \quad x_3] \begin{bmatrix} 3 & -2 & 3 \\ -2 & -1 & 0 \\ 3 & 0 & 5 \end{bmatrix} \begin{Bmatrix} x_1 \\ x_2 \\ x_3 \end{Bmatrix} \\ &= \mathbf{x}^T \mathbf{A} \mathbf{x} \end{aligned}$$

Eigenvalues and Eigenvectors

Consider the eigenvalue problem

$$\mathbf{A} \mathbf{y} = \lambda \mathbf{y} \quad (2.17a)$$

where \mathbf{A} is a square matrix, $(n \times n)$. We wish to find a nontrivial solution. That is, we wish to find a nonzero eigenvector \mathbf{y} and the corresponding eigenvalue λ that satisfy Eq. 2.17a. If we rewrite Eq. 2.17a as

$$(\mathbf{A} - \lambda \mathbf{I}) \mathbf{y} = \mathbf{0} \quad (2.17b)$$

we see that a nonzero solution for \mathbf{y} will occur when $\mathbf{A} - \lambda \mathbf{I}$ is a singular matrix or

$$\det(\mathbf{A} - \lambda \mathbf{I}) = 0 \quad (2.18)$$

Equation 2.18 is called the *characteristic equation*. We can solve Eq. 2.18 for the n roots or eigenvalues $\lambda_1, \lambda_2, \dots, \lambda_n$. For each eigenvalue λ_i , the associated eigenvector \mathbf{y}^i is then obtained from Eq. 2.17b:

$$(\mathbf{A} - \lambda_i \mathbf{I}) \mathbf{y}^i = \mathbf{0} \quad (2.19)$$

Note that the eigenvector \mathbf{y}^i is determined only to within a multiplicative constant since $(\mathbf{A} - \lambda_i \mathbf{I})$ is a singular matrix.

Example 2.1

Consider the matrix

$$\mathbf{A} = \begin{bmatrix} 4 & -2.236 \\ -2.236 & 8 \end{bmatrix}$$

The characteristic equation is

$$\det \begin{bmatrix} 4 - \lambda & -2.236 \\ -2.236 & 8 - \lambda \end{bmatrix} = 0$$

which yields

$$(4 - \lambda)(8 - \lambda) - 5 = 0$$

Solving this above equation, we get

$$\lambda_1 = 3 \quad \lambda_2 = 9$$

To get the eigenvector $\mathbf{y}^1 = [y_1^1, y_2^1]^T$ corresponding to the eigenvalue λ_1 , we substitute $\lambda_1 = 3$ into Eq. 2.19:

$$\begin{bmatrix} (4 - 3) & -2.236 \\ -2.236 & (8 - 3) \end{bmatrix} \begin{Bmatrix} y_1^1 \\ y_2^1 \end{Bmatrix} = \begin{Bmatrix} 0 \\ 0 \end{Bmatrix}$$

Thus, the components of \mathbf{y}^1 satisfy the equation

$$y_1^1 - 2.236y_2^1 = 0$$

We may now *normalize* the eigenvector, say, by making \mathbf{y}^1 a unit vector. This is done by setting $y_2^1 = 1$, resulting in $\mathbf{y}^1 = [2.236, 1]^T$. Dividing \mathbf{y}^1 by its length yields

$$\mathbf{y}^1 = [0.913, 0.408]^T$$

Now, \mathbf{y}^2 is obtained in a similar manner by substituting λ_2 into Eq. 2.19. After normalization

$$\mathbf{y}^2 = [-0.408, 0.913]^T \quad \blacksquare$$

Eigenvalue problems in finite element analysis are of the type $\mathbf{A}\mathbf{y} = \lambda\mathbf{B}\mathbf{y}$. Solution techniques for these problems are discussed in Chapter 11.

Positive Definite Matrix

A symmetric matrix is said to be **positive definite** if all its eigenvalues are strictly positive (greater than zero). In the previous example, the symmetric matrix

$$\mathbf{A} = \begin{bmatrix} 4 & -2.236 \\ -2.236 & 8 \end{bmatrix}$$

had eigenvalues $\lambda_1 = 3 > 0$ and $\lambda_2 = 9 > 0$ and, hence, is positive definite. An alternative definition of a positive definite matrix is as follows:

A symmetric matrix \mathbf{A} of dimension $(n \times n)$ is positive definite if, for *any* nonzero vector $\mathbf{x} = [x_1, x_2, \dots, x_n]^T$,

$$\mathbf{x}^T \mathbf{A} \mathbf{x} > 0 \quad (2.20)$$

Cholesky Decomposition

A positive definite symmetric matrix \mathbf{A} can be decomposed into the form

$$\mathbf{A} = \mathbf{L}\mathbf{L}^T \quad (2.21)$$

where \mathbf{L} is a lower triangular matrix, and its transpose \mathbf{L}^T is upper triangular. This is *Cholesky decomposition*. The elements of \mathbf{L} are calculated using the following steps: The evaluation of elements in row k does not affect the elements in the previously evaluated $k - 1$ rows. The decomposition is performed by evaluating rows from $k = 1$ to n as follows:

$$l_{kj} = \frac{\left(a_{kj} - \sum_{i=1}^{j-1} l_{ki}l_{ji} \right)}{l_{jj}} \quad j = 1 \text{ to } k - 1 \quad (2.22)$$

$$l_{kk} = \sqrt{a_{kk} - \sum_{i=1}^{k-1} l_{ki}^2}$$

In this evaluation, the summation is not carried out when the upper limit is less than the lower limit.

The inverse of a lower triangular matrix is a lower triangular matrix. The diagonal elements of the inverse \mathbf{L}^{-1} are inverse of the diagonal elements of \mathbf{L} . Noting this, for a given \mathbf{A} , its decomposition \mathbf{L} can be stored in the lower triangular part of \mathbf{A} and the elements below the diagonal of \mathbf{L}^{-1} can be stored above the diagonal in \mathbf{A} . This is implemented in the program CHOLESKY.

2.2 GAUSSIAN ELIMINATION

Consider a linear system of simultaneous equations in matrix form as

$$\mathbf{A}\mathbf{x} = \mathbf{b}$$

where \mathbf{A} is $(n \times n)$ and \mathbf{b} and \mathbf{x} are $(n \times 1)$. If $\det \mathbf{A} \neq 0$, then we can premultiply both sides of the equation by \mathbf{A}^{-1} to write the unique solution for \mathbf{x} as $\mathbf{x} = \mathbf{A}^{-1}\mathbf{b}$. However, the explicit construction of \mathbf{A}^{-1} , say, by the cofactor approach, is computationally expensive and prone to round-off errors. Instead, an elimination scheme is better. The powerful Gaussian elimination approach for solving $\mathbf{A}\mathbf{x} = \mathbf{b}$ is discussed in the following pages.

Gaussian elimination is the name given to a well-known method of solving simultaneous equations by successively eliminating unknowns. We will first present the method by means of an example, followed by a general solution and algorithm. Consider the simultaneous equations

$$\begin{aligned} x_1 - 2x_2 + 6x_3 &= 0 & \text{(I)} \\ 2x_1 + 2x_2 + 3x_3 &= 3 & \text{(II)} \\ -x_1 + 3x_2 &= 2 & \text{(III)} \end{aligned} \quad (2.23)$$

The equations are labeled as I, II, and III. Now, we wish to eliminate x_1 from II and III. We have, from Eq. I, $x_1 = +2x_2 - 6x_3$. Substituting for x_1 into Eqs. II and III yields

$$\begin{aligned}
 x_1 - 2x_2 + 6x_3 &= 0 & \text{(I)} \\
 0 + 6x_2 - 9x_3 &= 3 & \text{(II}^{(1)}) \\
 0 + x_2 + 6x_3 &= 2 & \text{(III}^{(1)})
 \end{aligned}
 \tag{2.24}$$

It is important to realize that Eq. 2.24 can also be obtained from Eq. 2.23 by **row operations**. Specifically, in Eq. 2.23, to eliminate x_1 from II, we subtract 2 times I from II, and to eliminate x_1 from III we subtract -1 times I from III. The result is Eq. 2.24. Notice the zeroes below the main diagonal in column 1, representing the fact that x_1 has been eliminated from Eqs. II and III. The superscript (1) on the labels in Eqs. 2.24 denotes the fact that the equations have been modified once.

We now proceed to eliminate x_2 from III in Eqs. 2.24. For this, we subtract $\frac{1}{6}$ times II from III. The resulting system is

$$\begin{bmatrix}
 x_1 - 2x_2 + 6x_3 = 0 \\
 0 + 6x_2 - 9x_3 = 3 \\
 0 \quad 0 \quad \frac{15}{2}x_3 = \frac{3}{2}
 \end{bmatrix}
 \begin{matrix}
 \text{(I)} \\
 \text{(II}^{(1)}) \\
 \text{(III}^{(2)})
 \end{matrix}
 \tag{2.25}$$

The coefficient matrix on the left side of Eqs. 2.25 is upper triangular. The solution now is virtually complete, since the last equation yields $x_3 = \frac{1}{5}$, which, upon substitution into the second equation, yields $x_2 = \frac{4}{5}$, and then $x_1 = \frac{2}{5}$ from the first equation. This process of obtaining the unknowns in reverse order is called **back-substitution**.

These operations can be expressed more concisely in matrix form as follows: Working with the augmented matrix $[\mathbf{A}, \mathbf{b}]$, the Gaussian elimination process is

$$\begin{bmatrix}
 1 & -2 & 6 & 0 \\
 2 & 2 & 3 & 3 \\
 -1 & 3 & 0 & 2
 \end{bmatrix}
 \rightarrow
 \begin{bmatrix}
 1 & -2 & 6 & 0 \\
 0 & 6 & -9 & 3 \\
 0 & 1 & 6 & 2
 \end{bmatrix}
 \rightarrow
 \begin{bmatrix}
 1 & -2 & 6 & 0 \\
 0 & 6 & -9 & 3 \\
 0 & 0 & 15/2 & 3/2
 \end{bmatrix}
 \tag{2.26}$$

which, upon back-substitution, yields

$$x_3 = \frac{1}{5} \quad x_2 = \frac{4}{5} \quad x_1 = \frac{2}{5}
 \tag{2.27}$$

General Algorithm for Gaussian Elimination

We just discussed the Gaussian elimination process by means of an example. This process will now be stated as an algorithm, suitable for computer implementation.

Let the original system of equations be as given in Eqs. 2.1, which can be restated as

$$\begin{matrix}
 \text{Row } i \\
 \begin{bmatrix}
 a_{11} & a_{12} & a_{13} & \cdots & a_{1j} & \cdots & a_{1n} \\
 a_{21} & a_{22} & a_{23} & \cdots & a_{2j} & \cdots & a_{2n} \\
 a_{31} & a_{32} & a_{33} & \cdots & a_{3j} & \cdots & a_{3n} \\
 \cdots & \cdots & \cdots & \cdots & \cdots & \cdots & \cdots \\
 a_{i1} & a_{i2} & a_{i3} & \cdots & a_{ij} & \cdots & a_{in} \\
 \cdots & \cdots & \cdots & \cdots & \cdots & \cdots & \cdots \\
 a_{n1} & a_{n2} & a_{n3} & \cdots & a_{nj} & \cdots & a_{nn}
 \end{bmatrix}
 \end{matrix}
 \begin{Bmatrix}
 x_1 \\
 x_2 \\
 x_3 \\
 \vdots \\
 x_i \\
 \vdots \\
 x_n
 \end{Bmatrix}
 =
 \begin{Bmatrix}
 b_1 \\
 b_2 \\
 b_3 \\
 \vdots \\
 b_i \\
 \vdots \\
 b_n
 \end{Bmatrix}
 \tag{2.28}$$

Column
 j

Gaussian elimination is a systematic approach to successively eliminate variables $x_1, x_2, x_3, \dots, x_{n-1}$ until only one variable, x_n , is left. This results in an upper triangular matrix with reduced coefficients and reduced right side. This process is called forward elimination. It is then easy to determine $x_n, x_{n-1}, \dots, x_3, x_2, x_1$ successively by the process of back-substitution. Let us consider the start of step 1, with \mathbf{A} and \mathbf{b} written as follows:

$$\left[\begin{array}{ccccccc} a_{11} & a_{12} & a_{13} & \cdots & a_{1j} & \cdots & a_{1n} \\ a_{21} & a_{22} & a_{23} & \cdots & a_{2j} & \cdots & a_{2n} \\ \vdots & \vdots & \vdots & \cdots & \vdots & \cdots & \vdots \\ a_{i1} & a_{i2} & a_{i3} & \cdots & a_{ij} & \cdots & a_{in} \\ \cdots & \cdots & \cdots & \cdots & \cdots & \cdots & \cdots \\ a_{n1} & a_{n2} & a_{n3} & \cdots & a_{nj} & \cdots & a_{nn} \end{array} \right] \quad \text{Start} \quad \left\{ \begin{array}{c} b_1 \\ b_2 \\ \vdots \\ b_i \\ \vdots \\ b_n \end{array} \right\} \quad (2.29)$$

of step
 $k = 1$

The idea at step 1 is to use equation 1 (the first row) in eliminating x_1 from remaining equations. We denote the step number as a superscript set in parentheses. The reduction process at step 1 is

$$a_{ij}^{(1)} = a_{ij} - \frac{a_{i1}}{a_{11}} \cdot a_{1j}$$

and (2.30)

$$b_i^{(1)} = b_i - \frac{a_{i1}}{a_{11}} \cdot b_1$$

We note that the ratios a_{i1}/a_{11} are simply the row multipliers that were referred to in the example discussed previously. Also, a_{11} is referred to as a *pivot*. The reduction is carried out for all the elements in the shaded area in Eq. (2.29) for which i and j range from 2 to n . The elements in rows 2 to n of the first column are zeroes since x_1 is eliminated. In the computer implementation, we need not set them to zero, but they are zeroes for our consideration. At the start of step 2, we thus have

$$\left[\begin{array}{ccccccc} a_{11} & a_{12} & a_{13} & \cdots & a_{1j} & \cdots & a_{1n} \\ 0 & a_{22}^{(1)} & a_{23}^{(1)} & \cdots & a_{2j}^{(1)} & \cdots & a_{2n}^{(1)} \\ 0 & a_{32}^{(1)} & a_{33}^{(1)} & \cdots & a_{3j}^{(1)} & \cdots & a_{3n}^{(1)} \\ \vdots & \vdots & \vdots & \cdots & \vdots & \cdots & \vdots \\ 0 & a_{i2}^{(1)} & a_{i3}^{(1)} & \cdots & a_{ij}^{(1)} & \cdots & a_{in}^{(1)} \\ \vdots & \vdots & \vdots & \cdots & \vdots & \cdots & \vdots \\ 0 & a_{n2}^{(1)} & a_{n3}^{(1)} & \cdots & a_{nj}^{(1)} & \cdots & a_{nn}^{(1)} \end{array} \right] \quad \text{Start of} \quad \left\{ \begin{array}{c} b_1 \\ b_2^{(1)} \\ b_3^{(1)} \\ \vdots \\ b_i^{(1)} \\ \vdots \\ b_n^{(1)} \end{array} \right\} \quad (2.31)$$

step $k = 2$

The elements in the shaded area in Eq. 2.31 are reduced at step 2. We now show the start of step k and the operations at step k in

$$\begin{array}{c}
 \left[\begin{array}{cccccccc}
 a_{11} & a_{12} & a_{13} & \cdots & \cdots & \cdots & a_{1j} & \cdots & a_{1n} \\
 0 & a_{22}^{(1)} & a_{23}^{(1)} & \cdots & \cdots & \cdots & a_{2j}^{(1)} & \cdots & a_{2n}^{(1)} \\
 0 & 0 & a_{33}^{(1)} & \cdots & \cdots & \cdots & a_{3j}^{(2)} & \cdots & a_{3n}^{(2)} \\
 \hline
 0 & 0 & 0 & \cdots & a_{k+1,k+1}^{(k-1)} & \cdots & a_{k+1,j}^{(k-1)} & \cdots & a_{k+1,n}^{(k-1)} \\
 \vdots & \vdots & \vdots & \ddots & \vdots & \vdots & \vdots & \vdots & \vdots \\
 \text{Row } i & 0 & 0 & 0 & \cdots & a_{i,k+1}^{(k-1)} & \cdots & a_{ij}^{(k-1)} & \cdots & a_{in}^{(k-1)} \\
 \hline
 0 & 0 & 0 & \cdots & a_{n,k+1}^{(k-1)} & \cdots & a_{nj}^{(k-1)} & \cdots & a_{nn}^{(k-1)}
 \end{array} \right]
 \end{array}
 \begin{array}{c}
 \left. \begin{array}{c}
 b_1 \\
 b_2^{(1)} \\
 b_3^{(2)} \\
 \vdots \\
 b_{k+1}^{(k-1)} \\
 \vdots \\
 b_i^{(k-1)} \\
 \vdots \\
 b_n^{(k-1)}
 \end{array} \right\} \text{Start of} \\
 \text{step } k
 \end{array}
 \quad (2.32)$$

At step k , elements in the shaded area are reduced. The general reduction scheme with limits on indices may be put as follows:

In step k ,

$$\begin{aligned}
 a_{ij}^{(k)} &= a_{ij}^{(k-1)} - \frac{a_{ik}^{(k-1)}}{a_{kk}^{(k-1)}} a_{kj}^{(k-1)} & i, j &= k+1, \dots, n \\
 b_i^{(k)} &= b_i^{(k-1)} - \frac{a_{ik}^{(k-1)}}{a_{kk}^{(k-1)}} b_k^{(k-1)} & i &= k+1, \dots, n
 \end{aligned}
 \quad (2.33)$$

After $(n-1)$ steps, we get

$$\left[\begin{array}{cccccccc}
 a_{11} & a_{12} & a_{13} & a_{14} & \cdots & a_{1n} \\
 & a_{22}^{(1)} & a_{23}^{(1)} & a_{24}^{(1)} & \cdots & a_{2n}^{(1)} \\
 & & a_{33}^{(2)} & a_{34}^{(2)} & \cdots & a_{3n}^{(2)} \\
 & & & a_{44}^{(3)} & \cdots & a_{4n}^{(3)} \\
 & & & & & \vdots \\
 & & & & & a_{nn}^{(n-1)}
 \end{array} \right]
 \begin{array}{c}
 \left\{ \begin{array}{c}
 x_1 \\
 x_2 \\
 x_3 \\
 x_4 \\
 \vdots \\
 x_n
 \end{array} \right\} = \left\{ \begin{array}{c}
 b_1 \\
 b_2^{(1)} \\
 b_3^{(2)} \\
 b_4^{(3)} \\
 \vdots \\
 b_n^{(n-1)}
 \end{array} \right\}
 \end{array}
 \quad (2.34)$$

The superscripts are for the convenience of presentation. In the computer implementation, these superscripts can be avoided. We now drop the superscripts for convenience, and the back-substitution process is given by

$$x_n = \frac{b_n}{a_{nn}}
 \quad (2.35)$$

and then

$$x_i = \frac{b_i - \sum_{j=i+1}^n a_{ij} x_j}{a_{ii}} \quad i = n-1, n-2, \dots, 1
 \quad (2.36)$$

This completes the Gauss elimination algorithm.

The algorithm discussed earlier is given next in the form of computer logic.

Algorithm 1: General Matrix**Forward elimination (reduction of A , b)**

```

DO  k = 1, n - 1
DO  i = k + 1, n
    c = aik / akk
DO  j = k + 1, n
    aij = aij - c akj
    bi = bi - c bk

```

Back-substitution

$$b_n = \frac{b_n}{a_{nn}}$$

```

DO  ii = 1, n - 1
    i = n - ii
    sum = 0
DO  j = i + 1, n
    sum = sum + aij bj
    bi = (bi - sum) / aii

```

[Note: \mathbf{b} contains the solution to $\mathbf{Ax} = \mathbf{b}$.]

Symmetric Matrix

If \mathbf{A} is symmetric, then the previous algorithm needs two modifications. One is that the multiplier is defined as

$$c = \frac{a_{ki}}{a_{kk}} \quad (2.37)$$

The other modification is related to the DO LOOP index (the third DO LOOP in the previous algorithm):

$$\text{DO } j = i, n \quad (2.38)$$

Symmetric Banded Matrices

In a **banded** matrix, all of the nonzero elements are contained within a band; outside of the band all elements are zero. The stiffness matrix that we will come across in subsequent chapters is a symmetric and banded matrix.

Algorithm 2: Symmetric Banded Matrix**Forward elimination**

```

DO k = 1, n - 1
  nbk = min(n - k + 1, nbw)
  DO i = k + 1, nbk + k - 1
    i1 = i - k + 1
    c = ak,i1/ak,1
    DO j = i, nbk + k - 1
      j1 = j - i + 1
      j2 = j - k + 1
      ai,j1 = ai,j1 - cak,j2
    bi = bi - cbk
  
```

Back-substitution

$$b_n = \frac{b_n}{a_{n,1}}$$

```

DO ii = 1, n - 1
  i = n - ii
  nbi = min(n - i + 1, nbw)
  sum = 0
  DO j = 2, nbi
    sum = sum + ai,jbi+j-1
  bi =  $\frac{b_i - \text{sum}}{a_{i,1}}$ 

```

[Note: The DO LOOP indices are based on the original matrix as in Eq. 2.39; the correspondence in Eq. 2.41 is then used while referring to elements of the banded matrix \mathbf{A} . Alternatively, it is possible to express the DO LOOP indices directly as they refer to the banded \mathbf{A} matrix. Both approaches are used in the computer programs.]

Solution with Multiple Right Sides

Often, we need to solve $\mathbf{Ax} = \mathbf{b}$ with the same \mathbf{A} , but with different \mathbf{b} 's. This happens in the finite element method when we wish to analyze the same structure for different loading conditions. In this situation, it is computationally more economical to separate the calculations associated with \mathbf{A} from those associated with \mathbf{b} . The reason for this is that the number of operations in reduction of an $(n \times n)$ matrix \mathbf{A} to its triangular form is proportional to n^3 , while the number of operations for reduction of \mathbf{b} and back-substitution is proportional only to n^2 . For large n , this difference is significant.

The previous algorithm for a symmetric banded matrix is modified accordingly as follows:

Algorithm 3: Symmetric Banded, Multiple Right Sides

Forward elimination for A

```

DO k = 1, n - 1
  nbk = min(n - k + 1, nbw)
  DO i = k + 1, nbk + k - 1
    i1 = i - k + 1
    c = ak,i1/ak,1
    DO j = i, nbk + k - 1
      j1 = j - i + 1
      j2 = j - k + 1
      ai,j1 = ai,j1 - cak,j2
    
```

Forward elimination of each b

```

DO k = 1, n - 1
  nbk = min(n - k + 1, nbw)
  DO i = k + 1, nbk + k - 1
    i1 = i - k + 1
    c = ak,i1/ak,1
    bi = bi - cbk
  
```

Back-substitution This algorithm is the same as in Algorithm 2.

Gaussian Elimination with Column Reduction

A careful observation of the Gaussian elimination process shows us a way to reduce the coefficients column after column. This process leads to the simplest procedure for **skyline solution**, which we present later. We consider the column-reduction procedure for symmetric matrices. Let the coefficients in the upper triangular matrix and the vector **b** be stored.

We can understand the motivation behind the column approach by referring back to Eq. 2.41, which is

$$\begin{bmatrix} a_{11} & a_{12} & a_{13} & a_{14} & \cdots & a_{1n} \\ & a_{22}^{(1)} & a_{23}^{(1)} & a_{24}^{(1)} & \cdots & a_{2n}^{(1)} \\ & & a_{33}^{(2)} & a_{34}^{(2)} & \cdots & a_{3n}^{(2)} \\ & & & a_{44}^{(3)} & \cdots & a_{4n}^{(3)} \\ & & & & \vdots & \vdots \\ & & & & & a_{nn}^{(n-1)} \end{bmatrix} \begin{Bmatrix} x_1 \\ x_2 \\ x_3 \\ x_4 \\ \vdots \\ x_n \end{Bmatrix} = \begin{Bmatrix} b_1 \\ b_2^{(1)} \\ b_3^{(2)} \\ b_4^{(3)} \\ \vdots \\ b_n^{(n-1)} \end{Bmatrix}$$

Let us focus our attention on, say, column 3 of the reduced matrix. The first element in this column is unmodified, the second element is modified once, and the third element is modified twice. Further, from Eq. 2.33, and using the fact that $a_{ij} = a_{ji}$ since \mathbf{A} is assumed to be symmetric, we have

$$\begin{aligned} a_{23}^{(1)} &= a_{23} - \frac{a_{12}}{a_{11}} a_{13} \\ a_{33}^{(1)} &= a_{33} - \frac{a_{13}}{a_{11}} a_{13} \\ a_{33}^{(2)} &= a_{33}^{(1)} - \frac{a_{23}^{(1)}}{a_{22}^{(1)}} a_{23}^{(1)} \end{aligned} \quad (2.42)$$

From these equations, we make the critical observation that *the reduction of column 3 can be done using only the elements in columns 1 and 2 and the already reduced elements in column 3*. This idea whereby column 3 is obtained using only elements in previous columns that have already been reduced is shown schematically:

$$\begin{bmatrix} a_{11} & a_{12} & a_{13} \\ & a_{22}^{(1)} & a_{23}^{(1)} \\ & & a_{33}^{(2)} \end{bmatrix} \rightarrow \begin{bmatrix} a_{11} & a_{12} & a_{13} \\ & a_{22}^{(1)} & a_{23}^{(1)} \\ & & a_{33}^{(1)} \end{bmatrix} \rightarrow \begin{bmatrix} a_{11} & a_{12} & a_{13} \\ & a_{22}^{(1)} & a_{23}^{(1)} \\ & & a_{33}^{(2)} \end{bmatrix} \quad (2.43)$$

The reduction of other columns is similarly completed. For instance, the reduction of column 4 can be done in three steps as shown schematically in

$$\begin{Bmatrix} a_{14} \\ a_{24} \\ a_{34} \\ a_{44} \end{Bmatrix} \rightarrow \begin{Bmatrix} a_{14} \\ a_{24}^{(1)} \\ a_{34}^{(1)} \\ a_{44}^{(1)} \end{Bmatrix} \rightarrow \begin{Bmatrix} a_{14} \\ a_{24}^{(1)} \\ a_{34}^{(2)} \\ a_{44}^{(2)} \end{Bmatrix} \rightarrow \begin{Bmatrix} a_{14} \\ a_{24}^{(1)} \\ a_{34}^{(2)} \\ a_{44}^{(3)} \end{Bmatrix} \quad (2.44)$$

We now discuss the reduction of column $j, 2 \leq j \leq n$, assuming that columns to the left of j have been fully reduced. The coefficients can be represented in the following form:

$$\begin{array}{cccccccc}
 & & & & & \text{Column} & & \\
 & & & & & j & & \\
 \left[\begin{array}{cccccc}
 a_{11} & a_{12} & a_{13} & \cdots & a_{1j-1} & a_{1j} & \cdots & \cdots \\
 & a_{22}^{(1)} & a_{23}^{(1)} & \cdots & a_{2j-1}^{(1)} & a_{2j} & \cdots & \cdots \\
 & & a_{33}^{(2)} & \cdots & a_{3j-1}^{(2)} & a_{3j} & \cdots & \cdots \\
 & & & \ddots & & \vdots & & \vdots \\
 & & & & a_{j-1j-1}^{(j-2)} & \vdots & & \vdots \\
 & & & & & \vdots & & \vdots \\
 & & & & & & & a_{jj}
 \end{array} \right] \begin{array}{l}
 \text{Step } k = 1 \\
 \text{Step } k = 2 \\
 \vdots \\
 \text{Step } k \\
 \vdots \\
 \text{Step } k + 1 \\
 \vdots
 \end{array}
 \end{array}
 \quad (2.45)$$

$i = 3 \text{ to } j$ $i = 2 \text{ to } j$
 $i = k + 1$ to j

The reduction of column j requires only elements from columns to the left of j and appropriately reduced elements from column j . We note that for column j , the number of steps needed are $j - 1$. Also, since a_{11} is not reduced, we need to reduce columns 2 to n only. The logic is now given as

$$\begin{array}{l}
 \text{DO } j = 2 \text{ to } n \\
 \quad \text{DO } k = 1 \text{ to } j - 1 \\
 \quad \quad \text{DO } i = k + 1 \text{ to } j \\
 \quad \quad \quad a_{ij}^{(k)} = a_{ij}^{(k-1)} - \frac{a_{ki}^{(k-1)}}{a_{kk}^{(k-1)}} a_{kj}^{(k-1)}
 \end{array}
 \quad (2.46)$$

Interestingly, the reduction of the right side \mathbf{b} can be considered as the reduction of one more column. Thus, we have

$$\begin{array}{l}
 \text{DO } k = 1 \text{ to } n - 1 \\
 \quad \text{DO } i = k + 1 \text{ to } n \\
 \quad \quad b_i^{(k)} = b_i^{(k-1)} - \frac{a_{ki}^{(k-1)}}{a_{kk}^{(k-1)}} b_k^{(k-1)}
 \end{array}
 \quad (2.47)$$

From Eq. 2.46, we observe that if there are a set of zeroes at the top of a column, the operations need to be carried out only on the elements ranging from the first nonzero element to the diagonal. This leads naturally to the skyline solution.

Skyline Solution

If there are zeroes at the top of a column, only the elements starting from the first nonzero value need be stored. The line separating the top zeroes from the first nonzero element is called the *skyline*. Consider the example

$$\begin{array}{c}
 \text{Column height} \rightarrow \\
 \begin{array}{|c|c|c|c|c|c|c|c|}
 \hline
 1 & 2 & 2 & 4 & 4 & 4 & 3 & 5 \\
 \hline
 a_{11} & a_{12} & 0 & a_{14} & 0 & 0 & 0 & 0 \\
 a_{22} & a_{23} & a_{24} & a_{25} & 0 & 0 & 0 & 0 \\
 a_{33} & a_{34} & 0 & a_{36} & 0 & 0 & 0 & 0 \\
 a_{44} & 0 & a_{46} & 0 & a_{48} & 0 & 0 & 0 \\
 a_{55} & a_{56} & a_{57} & 0 & 0 & 0 & 0 & 0 \\
 a_{66} & a_{67} & a_{68} & 0 & 0 & 0 & 0 & 0 \\
 a_{77} & a_{78} & 0 & 0 & 0 & 0 & 0 & 0 \\
 a_{88} & 0 & 0 & 0 & 0 & 0 & 0 & 0 \\
 \hline
 \end{array}
 \end{array}
 \quad \text{Skyline} \quad (2.48)$$

For efficiency, only the active columns need be stored. These can be stored in a column vector \mathbf{A} and a diagonal pointer vector \mathbf{ID} as

$$\begin{array}{c}
 \mathbf{A} = \begin{array}{|c|}
 \hline
 a_{11} \\
 a_{12} \\
 a_{22} \\
 a_{23} \\
 a_{33} \\
 a_{14} \\
 a_{24} \\
 a_{34} \\
 a_{44} \\
 \vdots \\
 a_{88} \\
 \hline
 \end{array}
 \quad \begin{array}{l}
 \text{Diagonal pointer (ID)} \\
 \leftarrow 1 \\
 \leftarrow 3 \\
 \leftarrow 5 \\
 \leftarrow 9 \\
 \leftarrow 9 \\
 \leftarrow 25
 \end{array}
 \quad \mathbf{ID} = \begin{array}{|c|}
 \hline
 1 \\
 3 \\
 5 \\
 9 \\
 13 \\
 17 \\
 20 \\
 25 \\
 \hline
 \end{array}
 \end{array}
 \quad (2.49)$$

The height of column I is given by $\text{ID}(I) - \text{ID}(I - 1)$. The right side, \mathbf{b} , is stored in a separate column. The column reduction scheme of the Gauss elimination method can be applied for solution of a set of equations. A skyline solver program is given.

Frontal Solution

Frontal method is a variation of the Gaussian elimination method that uses the structure of the finite element problem. The elimination process is handled by writing the eliminated equation to the computer hard disk, thus reducing the need for a large amount of memory. Large finite element problems can thus be solved using small computers. The frontal method is presented in Chapter 9 and implemented for the hexahedral element.

2.3 CONJUGATE GRADIENT METHOD FOR EQUATION SOLVING

The conjugate gradient method is an iterative method for the solution of equations. This method is becoming increasingly popular and is implemented in several computer codes. We present here the Fletcher-Reeves version of the algorithm for symmetric matrices.

Consider the solution of the set of equations

$$\mathbf{Ax} = \mathbf{b}$$

where \mathbf{A} is a symmetric positive definite ($n \times n$) matrix and \mathbf{b} and \mathbf{x} are ($n \times 1$). The conjugate gradient method uses the following steps for symmetric \mathbf{A} .

Conjugate Gradient Algorithm

Start at point \mathbf{x}_0 :

$$\begin{aligned} \mathbf{g}_0 &= \mathbf{Ax}_0 - \mathbf{b}, & \mathbf{d}_0 &= -\mathbf{g}_0 \\ \alpha_k &= \frac{\mathbf{g}_k^T \mathbf{g}_k}{\mathbf{d}_k^T \mathbf{A} \mathbf{d}_k} \\ \mathbf{x}_{k+1} &= \mathbf{x}_k + \alpha_k \mathbf{d}_k \\ \mathbf{g}_{k+1} &= \mathbf{g}_k + \alpha_k \mathbf{A} \mathbf{d}_k \\ \beta_k &= \frac{\mathbf{g}_{k+1}^T \mathbf{g}_{k+1}}{\mathbf{g}_k^T \mathbf{g}_k} \\ \mathbf{d}_{k+1} &= -\mathbf{g}_{k+1} + \beta_k \mathbf{d}_k \end{aligned} \quad (2.50)$$

Here $k = 0, 1, 2, \dots$. The iterations are continued until $\mathbf{g}_k^T \mathbf{g}_k$ reaches a small value. This method is robust and converges in n iterations. This procedure is implemented in the program CGSOLVE, which is included on the disk. This procedure is adaptable to parallel processing in finite element applications and can be accelerated by using preconditioning strategies. The program input and output are as follows:

INPUT FOR GAUSS, CGSOLVE

```

EIGHT EQUATIONS
'---- Number of Equations ---
8
'---- Matrix A() in Ax = B ---
6 0 1 2 0 0 2 1
0 5 1 1 0 0 3 0
1 1 6 1 2 0 1 2
2 1 1 7 1 2 1 1
0 0 2 1 6 0 2 1
0 0 0 2 0 4 1 0
2 3 1 1 2 1 5 1
1 0 2 1 1 0 1 3
'---- Right hand side B() in Ax = B ---
1 1 1 1 1 1 1 1

```

OUTPUT

```

Program Gauss - CHANDRUPATLA & BELEGUNDU
EIGHT EQUATIONS
X( 1 )= 3.9255E-01
X( 2 )= 6.3974E-01
X( 3 )= -1.4303E-01
X( 4 )= -2.1723E-01
X( 5 )= 3.8019E-01
X( 6 )= 5.1182E-01
X( 7 )= -6.1281E-01
X( 8 )= 4.4779E-01

```

PROBLEMS

2.1. Given that

$$\mathbf{A} = \begin{bmatrix} 8 & -2 & 0 \\ -2 & 4 & -3 \\ 0 & -3 & 3 \end{bmatrix} \quad \mathbf{d} = \begin{Bmatrix} 2 \\ -1 \\ 3 \end{Bmatrix}$$

determine the following:

(a) $\mathbf{I} - \mathbf{d}\mathbf{d}^T$

(b) $\det \mathbf{A}$

(c) the eigenvalues and eigenvectors of \mathbf{A} . Is \mathbf{A} positive definite?(d) the solution to $\mathbf{A}\mathbf{x} = \mathbf{d}$ using Algorithms 1 and 2, by hand calculation.

2.2. Given that

$$\mathbf{N} = [\xi, 1 - \xi^2]$$

find

(a) $\int_{-1}^1 \mathbf{N} d\xi$

(b) $\int_{-1}^1 \mathbf{N}^T \mathbf{N} d\xi$

2.3. Express $q = x_1 - 6x_2 + 3x_1^2 + 5x_1x_2$ in the matrix form $\frac{1}{2} \mathbf{x}^T \mathbf{Q}\mathbf{x} + \mathbf{c}^T \mathbf{x}$.2.4. Implement Algorithm 3 in BASIC. Hence, solve $\mathbf{A}\mathbf{x} = \mathbf{b}$ with \mathbf{A} as in Problem 2.1, and each of the following \mathbf{b} s:

$$\mathbf{b} = [5, -10, 3]^T$$

$$\mathbf{b} = [2.2, -1, 3]^T$$

2.5. Using the cofactor approach, determine the inverse of the matrix

$$\begin{bmatrix} 2 & 1 & 1 \\ 1 & 2 & 1 \\ 1 & 1 & 2 \end{bmatrix}$$

2.6. Given that the area of a triangle with corners at (x_1, y_1) , (x_2, y_2) , and (x_3, y_3) can be written in the form

$$\text{Area} = \frac{1}{2} \det \begin{bmatrix} 1 & x_1 & y_1 \\ 1 & x_2 & y_2 \\ 1 & x_3 & y_3 \end{bmatrix}$$

determine the area of the triangle with corners at $(1, 1)$, $(4, 2)$, and $(2, 4)$.

- 2.7. For the triangle in Fig. P2.7, the interior point P at $(2, 2)$ divides it into three areas, A_1 , A_2 , and A_3 , as shown. Determine A_1/A , A_2/A , and A_3/A .

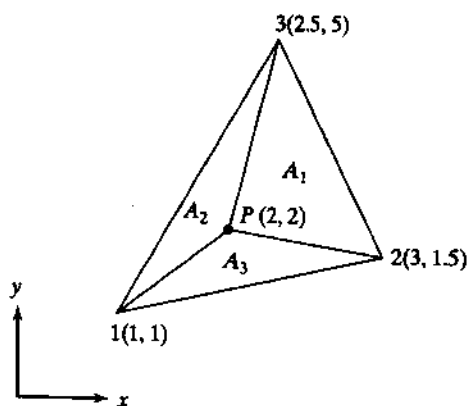


FIGURE P2.7

- 2.8. A symmetric matrix $[A]_{n \times n}$ has a bandwidth nbw and is stored in the matrix $[B]_{n \times nbw}$.
- Find the location in B that corresponds to $A_{11,14}$.
 - Find the location in A that corresponds to $B_{6,1}$.
- 2.9. For a symmetric (10×10) matrix with all nonzero elements, determine the number of locations needed for banded and skyline storage methods.
- 2.10. Perform the Cholesky decomposition of the positive definite matrix

$$\begin{bmatrix} 4 & 3 & 1 \\ 3 & 6 & 2 \\ 1 & 2 & 3 \end{bmatrix}$$

- 2.11. A square matrix A can be decomposed into $A = LU$ where L is lower triangular and U is upper triangular. Let

$$\begin{bmatrix} 5 & 3 & 1 \\ 2 & 4 & 2 \\ 2 & 1 & 6 \end{bmatrix} = \begin{bmatrix} 1 & 0 & 0 \\ l_{21} & 1 & 0 \\ l_{31} & l_{32} & 1 \end{bmatrix} \begin{bmatrix} u_{11} & u_{12} & u_{13} \\ 0 & u_{22} & u_{23} \\ 0 & 0 & u_{33} \end{bmatrix} \\ = LU$$

Determine L and U .

Program Listings

```

***** PROGRAM GAUSS *****
*      GAUSS ELIMINATION METHOD      *
*      GENERAL MATRIX               *
* T.R.Chandrupatla and A.D.Belegundu *
*****
\===== MAIN PROGRAM =====
Private Sub cmdStart_Click()
    Call InputData
    Call GaussRow
    Call Output
    cmdView.Enabled = True
    cmdStart.Enabled = False
End Sub

```

```

\===== INPUT DATA =====
Private Sub InputData()
    File1 = InputBox("Input File d:\dir\fileName.ext", "Name of File")
    Open File1 For Input As #1
    Line Input #1, Title: Line Input #1, Dummy
    Input #1, N
    Line Input #1, Dummy
    ReDim A(N, N), B(N)
    '===== READ DATA =====
    For I = 1 To N
        For J = 1 To N: Input #1, A(I, J): Next J
    Next I
    Line Input #1, Dummy
    For I = 1 To N: Input #1, B(I): Next I
    Close #1
End Sub

```

```

\===== GAUSSIAN ELIMINATION =====
Private Sub GaussRow()
    '----- Forward Elimination -----
    For K = 1 To N - 1
        For I = K + 1 To N
            C = A(I, K) / A(K, K)
            For J = K + 1 To N
                A(I, J) = A(I, J) - C * A(K, J)
            Next J
            B(I) = B(I) - C * B(K)
        Next I
    Next K
    '----- Back-substitution -----
    B(N) = B(N) / A(N, N)
    For II = 1 To N - 1
        I = N - II
        C = 1 / A(I, I): B(I) = C * B(I)
        For K = I + 1 To N
            B(I) = B(I) - C * A(I, K) * B(K)
        Next K
    Next II
End Sub

```

```

***** PROGRAM CGSOL *****
'* CONJUGATE GRADIENT METHOD *
'* FOR SOLVING AX=B, A Symmetric *
'* T.R.Chandrupatla and A.D.Belegundu *
*****

```

```

===== MAIN PROGRAM =====
Private Sub cmdStart_Click()
    Call InputData
    Call CgSol
    Call Output
    cmdView.Enabled = True
    cmdStart.Enabled = False
End Sub

```

```

===== CONJUGATE GRADIENT METHOD =====
===== FOR SOLVING EQUATIONS =====
Private Sub CgSol()
    DIM G(N), D(N), AD(N)
    FOR I = 1 TO N
        X(I) = 0
        G(I) = -B(I)
        D(I) = B(I)
    NEXT I
    GG1 = 0
    FOR I = 1 TO N
        GG1 = GG1 + G(I) * G(I)
    NEXT I
    DO WHILE GG1 > .000001
        ITER = ITER + 1
        DAD = 0
        FOR I = 1 TO N
            C = 0
            FOR J = 1 TO N
                C = C + A(I, J) * D(J)
            NEXT J
            AD(I) = C
            DAD = DAD + C * D(I)
        NEXT I
        AL = GG1 / DAD
        GG2 = 0
        FOR I = 1 TO N
            X(I) = X(I) + AL * D(I)
            G(I) = G(I) + AL * AD(I)
            GG2 = GG2 + G(I) * G(I)
        NEXT I
        BT = GG2 / GG1
        FOR I = 1 TO N
            D(I) = -G(I) + BT * D(I)
        NEXT I
        GG1 = GG2
    LOOP
    ERASE G, D, AD
End Sub

```

One-Dimensional Problems

3.1 INTRODUCTION

The total potential energy and the stress-strain and strain-displacement relationships are now used in developing the finite element method for a one-dimensional problem. The basic procedure is the same for two- and three-dimensional problems discussed later in the book. For the one-dimensional problem, the stress, strain, displacement, and loading depend only on the variable x . That is, the vectors \mathbf{u} , $\boldsymbol{\sigma}$, $\boldsymbol{\epsilon}$, \mathbf{T} , and \mathbf{f} in Chapter 1 now reduce to

$$\begin{aligned} \mathbf{u} &= u(x) & \boldsymbol{\sigma} &= \sigma(x) & \boldsymbol{\epsilon} &= \epsilon(x) \\ \mathbf{T} &= T(x) & \mathbf{f} &= f(x) \end{aligned} \quad (3.1)$$

Furthermore, the stress-strain and strain-displacement relations are

$$\sigma = E\epsilon \quad \epsilon = \frac{du}{dx} \quad (3.2)$$

For one-dimensional problems, the differential volume dV can be written as

$$dV = A dx \quad (3.3)$$

The loading consists of three types: the **body force** f , the **traction force** T , and the **point load** P_i . These forces are shown acting on a body in Fig. 3.1. A body force is a distributed force acting on every elemental volume of the body and has the units of force per unit volume. The self-weight due to gravity is an example of a body force. A traction force is a distributed load acting on the surface of the body. In Chapter 1, the traction force is defined as force per unit area. For the one-dimensional problem considered here, however, the traction force is defined as force per unit length. This is done by taking the traction force to be the product of the force per unit area with the perimeter of the cross section. Frictional resistance, viscous drag, and surface shear are examples of traction forces in one-dimensional problems. Finally, P_i is a force acting at a point i and u_i is the x displacement at that point.

The finite element modeling of a one-dimensional body is considered in Section 3.2. The basic idea is to discretize the region and express the displacement field in terms

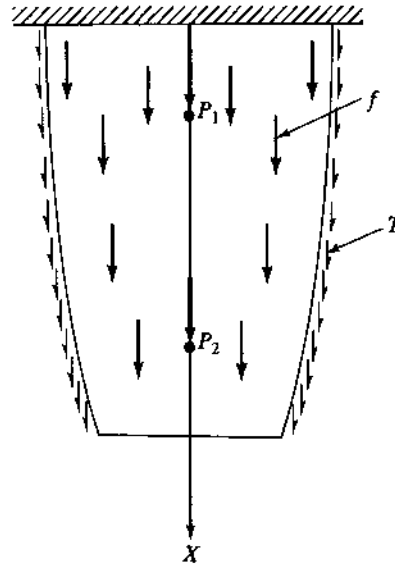


FIGURE 3.1 One-dimensional bar loaded by traction, body, and point loads.

of values at discrete points. Linear elements are introduced first. Stiffness and load concepts are developed using potential energy and Galerkin approaches. Boundary conditions are then considered. Temperature effects and quadratic elements are discussed later in this chapter.

3.2 FINITE ELEMENT MODELING

The steps of element division and node numbering are discussed here.

Element Division

Consider the bar in Fig. 3.1. The first step is to **model** the bar as a *stepped shaft*, consisting of a discrete number of elements, each having a uniform cross section. Specifically, let us model the bar using four finite elements. A simple scheme for doing this is to divide the bar into four regions, as shown in Fig. 3.2a. The average cross-sectional area within each region is evaluated and then used to define an element with uniform cross section. The resulting four-element, five-node finite element model is shown in Fig. 3.2b. In the finite element model, every element connects to two nodes. In Fig. 3.2b, the element numbers are circled to distinguish them from node numbers. In addition to the cross section, traction and body forces are also (normally) treated as constant within each element. However, cross-sectional area, traction, and body forces can differ in magnitude from element to element. Better approximations are obtained by increasing the number of elements. It is convenient to define a node at each location where a point load is applied.

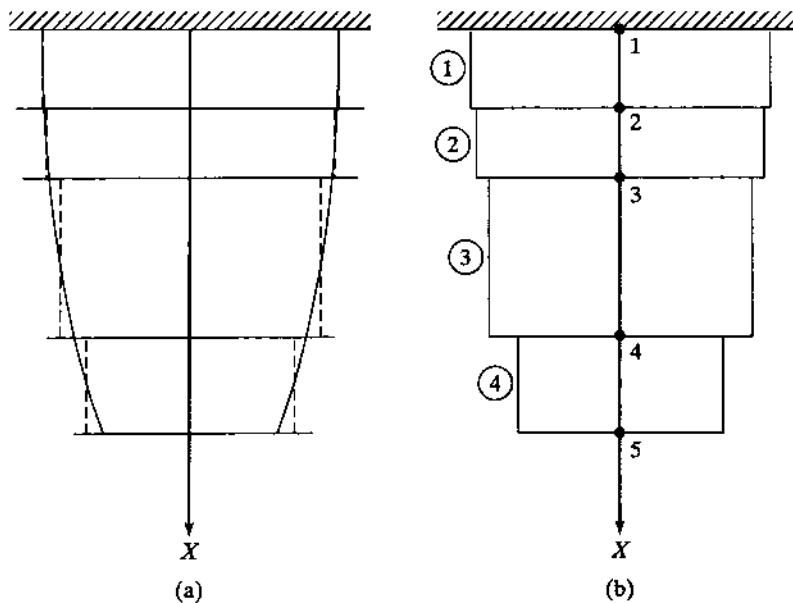


FIGURE 3.2 Finite element modeling of a bar.

Numbering Scheme

We have shown how a rather complicated looking bar has been modeled using a discrete number of elements, each element having a simple geometry. The similarity of the various elements is one reason why the finite element method is easily amenable to computer implementation. For easy implementation, an orderly numbering scheme for the model has to be adopted.

In a one-dimensional problem, every node is permitted to displace only in the $\pm x$ direction. Thus, each node has only one *degree of freedom (dof)*. The five-node finite element model in Fig. 3.2b has five dofs. The displacements along each dof are denoted by Q_1, Q_2, \dots, Q_5 . In fact, the column vector $\mathbf{Q} = [Q_1, Q_2, \dots, Q_5]^T$ is called the *global displacement vector*. The *global load vector* is denoted by $\mathbf{F} = [F_1, F_2, \dots, F_5]^T$. The vectors \mathbf{Q} and \mathbf{F} are shown in Fig. 3.3. The sign convention used is that a displacement or load has a positive value if acting along the $+x$ direction. At this stage, conditions at the boundary are not imposed. For example, node 1 in Fig. 3.3 is fixed, which implies $Q_1 = 0$. These conditions are discussed later.

Each element has two nodes; therefore, the **element connectivity** information can be conveniently represented as shown in Fig. 3.4. Further, the element connectivity table is also given. In the connectivity table, the headings 1 and 2 refer to *local node numbers* of an element, and the corresponding node numbers on the body are called *global numbers*. Connectivity thus establishes the local-global correspondence. In this simple example, the connectivity can be easily generated since local node 1 is the same as the element number e , and local node 2 is $e + 1$. Other ways of numbering nodes or more complex geometries suggest the need for a connectivity table. The connectivity is introduced in the program using the array NOC.

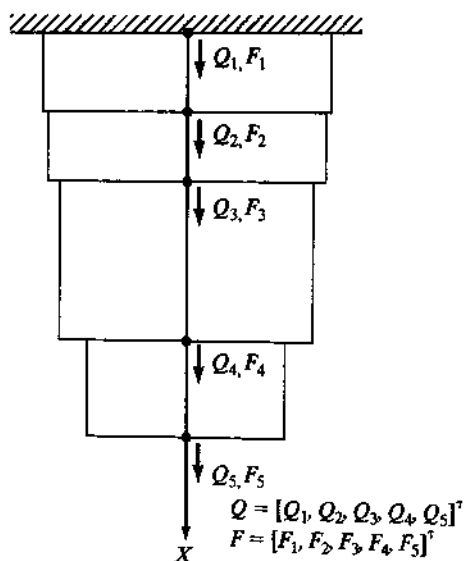


FIGURE 3.3 Q and F vectors.

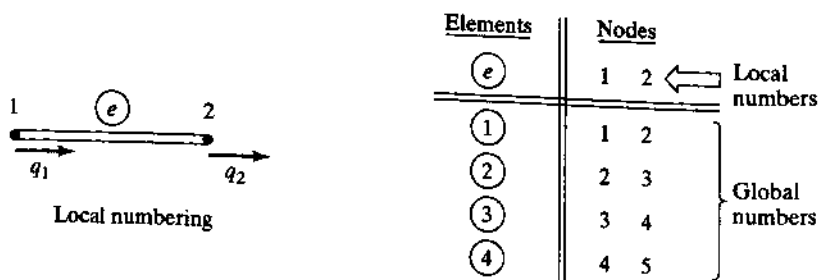
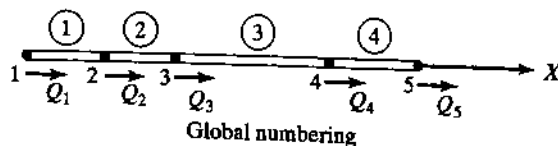
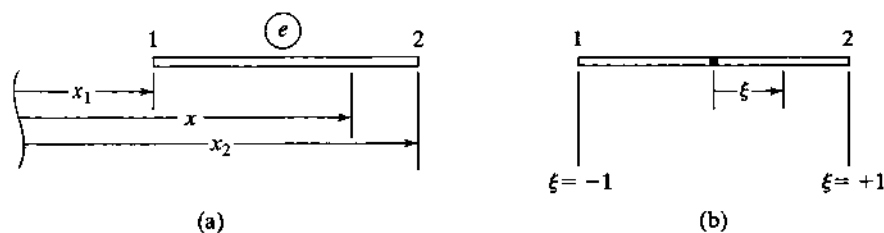


FIGURE 3.4 Element connectivity.

The concepts of dof, nodal displacements, nodal loads, and element connectivity are central to the finite element method and should be clearly understood.

3.3 COORDINATES AND SHAPE FUNCTIONS

Consider a typical finite element e in Fig. 3.5a. In the local number scheme, the first node will be numbered 1 and the second node 2. The notation $x_1 = x$ -coordinate of node 1, $x_2 = x$ -coordinate of node 2 is used. We define a **natural** or **intrinsic** coordinate system, denoted by ξ , as

FIGURE 3.5 Typical element in x - and ξ -coordinates.

$$\xi = \frac{2}{x_2 - x_1}(x - x_1) - 1 \quad (3.4)$$

From Fig. 3.5b, we see that $\xi = -1$ at node 1 and $\xi = 1$ at node 2. The length of an element is covered when ξ changes from -1 to 1 . We use this system of coordinates in defining shape functions, which are used in interpolating the displacement field.

Now the *unknown displacement field within an element will be interpolated by a linear distribution* (Fig. 3.6). This approximation becomes increasingly accurate as more elements are considered in the model. To implement this linear interpolation, linear **shape functions** will be introduced as

$$N_1(\xi) = \frac{1 - \xi}{2} \quad (3.5)$$

$$N_2(\xi) = \frac{1 + \xi}{2} \quad (3.6)$$

The shape functions N_1 and N_2 are shown in Figs. 3.7a and b, respectively. The graph of the shape function N_1 in Fig. 3.7a is obtained from Eq. 3.5 by noting that $N_1 = 1$ at $\xi = -1$, $N_1 = 0$ at $\xi = 1$, and N_1 is a straight line between the two points. Similarly, the graph of N_2 in Fig. 3.7b is obtained from Eq. 3.6. Once the shape functions are defined, the linear displacement field within the element can be written in terms of the nodal displacements q_1 and q_2 as

$$u = N_1 q_1 + N_2 q_2 \quad (3.7a)$$

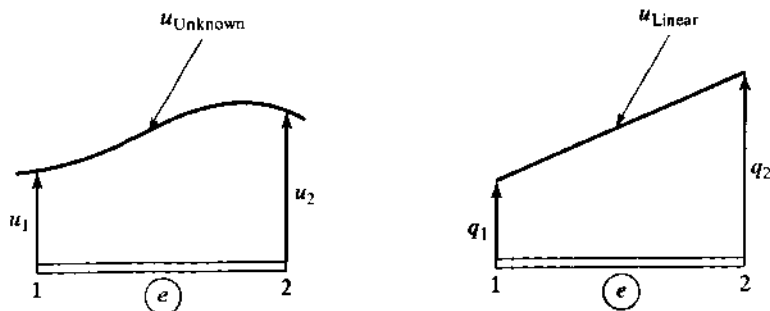


FIGURE 3.6 Linear interpolation of the displacement field within an element.

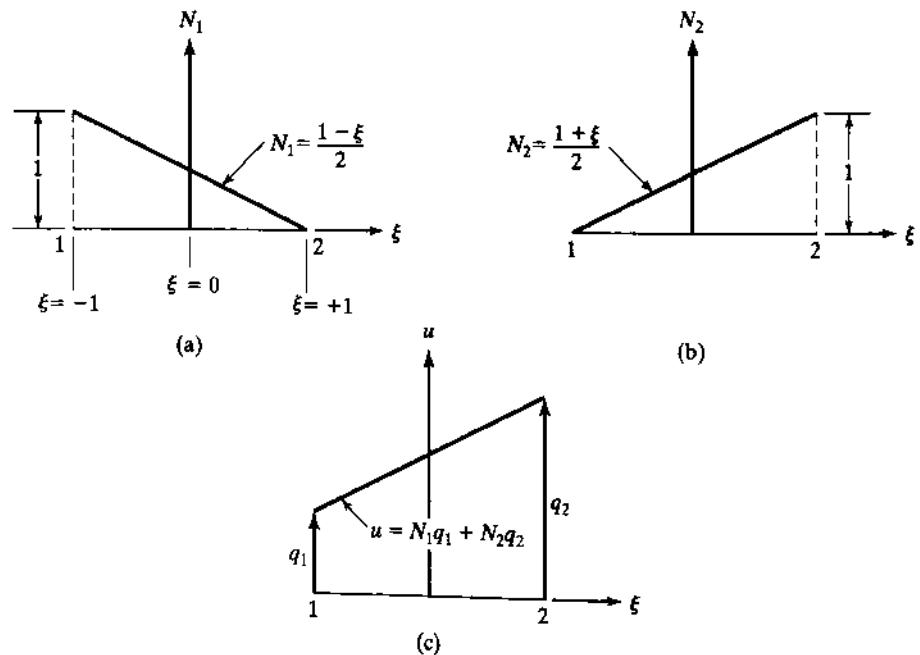


FIGURE 3.7 (a) Shape function N_1 , (b) shape function N_2 , and (c) linear interpolation using N_1 and N_2 .

or, in matrix notation, as

$$u = \mathbf{N}\mathbf{q} \quad (3.7b)$$

where

$$\mathbf{N} = [N_1, N_2] \quad \text{and} \quad \mathbf{q} = [q_1, q_2]^T \quad (3.8)$$

In these equations, \mathbf{q} is referred to as the *element displacement vector*. It is readily verified from Eq. 3.7a that $u = q_1$ at node 1, $u = q_2$ at node 2, and that u varies linearly (Fig. 3.7c).

It may be noted that the transformation from x to ξ in Eq. 3.4 can be written in terms of N_1 and N_2 as

$$x = N_1 x_1 + N_2 x_2 \quad (3.9)$$

Comparing Eqs. 3.7a and 3.9, we see that both the displacement u and the coordinate x are interpolated within the element using the *same* shape functions N_1 and N_2 . This is referred to as the *isoparametric* formulation in the literature.

Though linear shape functions have been used previously, other choices are possible. Quadratic shape functions are discussed in Section 3.9. In general, shape functions need to satisfy the following:

1. First derivatives must be finite within an element.
2. Displacements must be continuous across the element boundary.

Rigid body motion should not introduce any stresses in the element.

Example 3.1

Referring to Fig. E3.1, do the following:

- (a) Evaluate ξ , N_1 , and N_2 at point P .
 (b) If $q_1 = 0.003$ in. and $q_2 = -0.005$ in., determine the value of the displacement q at point P .

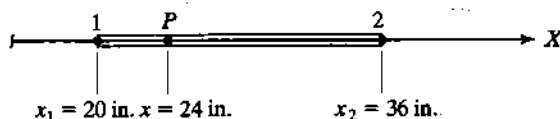


FIGURE E3.1

Solution

- (a) Using Eq. 3.4, the ξ coordinate of point P is given by

$$\begin{aligned}\xi_p &= \frac{2}{18}(24 - 20) - 1 \\ &= -0.5\end{aligned}$$

Now Eqs. 3.5 and 3.6 yield

$$N_1 = 0.75 \quad \text{and} \quad N_2 = 0.25$$

- (b) Using Eq. 3.7a, we get

$$\begin{aligned}u_p &= 0.75(0.003) + 0.25(-0.005) \\ &= 0.001 \text{ in.}\end{aligned}$$

The strain–displacement relation in Eq. 3.2 is

$$\epsilon = \frac{du}{dx}$$

Upon using the chain rule of differentiation, we obtain

$$\epsilon = \frac{du}{d\xi} \frac{d\xi}{dx} \quad (3.10)$$

From the relation between x and ξ in Eq. 3.4, we have

$$\frac{d\xi}{dx} = \frac{2}{x_2 - x_1} \quad (3.11)$$

Also, since

$$u = N_1 q_1 + N_2 q_2 = \frac{1 - \xi}{2} q_1 + \frac{1 + \xi}{2} q_2$$

we have

$$\frac{du}{d\xi} = \frac{-q_1 + q_2}{2} \quad (3.12)$$

Thus, Eq. 3.10 yields

$$\epsilon = \frac{1}{x_2 - x_1}(-q_1 + q_2) \quad (3.13)$$

The Eq. 3.13 can be written as

$$\epsilon = \mathbf{B}\mathbf{q} \quad (3.14)$$

where the (1×2) matrix \mathbf{B} , called the *element strain-displacement matrix*, is given by

$$\mathbf{B} = \frac{1}{x_2 - x_1}[-1 \quad 1] \quad (3.15)$$

Note: Use of linear shape functions results in a constant \mathbf{B} matrix and, hence, in a constant strain within the element. The stress, from Hooke's law, is

$$\sigma = E\mathbf{B}\mathbf{q} \quad (3.16)$$

The stress given by this equation is also constant within the element. For interpolation purposes, however, the stress obtained from Eq. 3.16 can be considered to be the value at the centroid of the element.

The expressions $u = \mathbf{N}\mathbf{q}$, $\epsilon = \mathbf{B}\mathbf{q}$, and $\sigma = E\mathbf{B}\mathbf{q}$ relate the displacement, strain and stress, respectively, in terms of nodal values. These expressions will now be substituted into the potential-energy expression for the bar to obtain the element stiffness and load matrices.

3.4 THE POTENTIAL-ENERGY APPROACH

The general expression for the potential energy given in Chapter 1 is

$$\Pi = \frac{1}{2} \int_L \sigma^T \epsilon A dx - \int_L u^T f A dx - \int_L u^T T dx - \sum_i u_i P_i \quad (3.17)$$

The quantities σ , ϵ , u , f , and T in Eq. 3.17 are discussed at the beginning of this chapter. In the last term, P_i represents a force acting at point i , and u_i is the x displacement at that point. The summation on i gives the potential energy due to all point loads.

Since the continuum has been discretized into finite elements, the expression for Π becomes

$$\Pi = \sum_e \frac{1}{2} \int_e \sigma^T \epsilon A dx - \sum_e \int_e u^T f A dx - \sum_e \int_e u^T T dx - \sum_i Q_i P_i \quad (3.18a)$$

The last term in Eq. 3.18a assumes that point loads P_i are applied at the nodes. This assumption makes the present derivation simpler with respect to notation and is also a common modeling practice. Equation 3.18a can be written as

$$\Pi = \sum_e U_e - \sum_e \int_e u^T f A dx - \sum_e \int_e u^T T dx - \sum_i Q_i P_i \quad (3.18b)$$

where

$$U_e = \frac{1}{2} \int \sigma^T \epsilon A dx$$

is the element strain energy.

Element Stiffness Matrix

Consider the strain energy term

$$U_e = \frac{1}{2} \int_e \sigma^T \epsilon A dx \quad (3.19)$$

Substituting for $\sigma = E\mathbf{B}\mathbf{q}$ and $\epsilon = \mathbf{B}\mathbf{q}$ into Eq. 3.19 yields

$$U_e = \frac{1}{2} \int_e \mathbf{q}^T \mathbf{B}^T E \mathbf{B} \mathbf{q} A dx \quad (3.20a)$$

or

$$U_e = \frac{1}{2} \mathbf{q}^T \int_e [\mathbf{B}^T E \mathbf{B} A dx] \mathbf{q} \quad (3.20b)$$

In the finite element model (Section 3.2), the cross-sectional area of element e , denoted by A_e , is constant. Also, \mathbf{B} is a constant matrix. Further, the transformation from x to ξ in Eq. 3.4 yields

$$dx = \frac{x_2 - x_1}{2} d\xi \quad (3.21a)$$

or

$$dx = \frac{\ell_e}{2} d\xi \quad (3.21b)$$

where $-1 \leq \xi \leq 1$, and $\ell_e = |x_2 - x_1|$ is the length of the element.

The element strain energy U_e is now written as

$$U_e = \frac{1}{2} \mathbf{q}^T \left[A_e \frac{\ell_e}{2} E_e \mathbf{B}^T \mathbf{B} \int_{-1}^1 d\xi \right] \mathbf{q} \quad (3.22)$$

where E_e is Young's modulus of element e . Noting that $\int_{-1}^1 d\xi = 2$ and substituting for \mathbf{B} from Eq. 3.15, we get

$$U_e = \frac{1}{2} \mathbf{q}^T A_e \ell_e E_e \frac{1}{\ell_e^2} \begin{Bmatrix} -1 \\ 1 \end{Bmatrix} \begin{bmatrix} -1 & 1 \end{bmatrix} \mathbf{q} \quad (3.23)$$

which results in

$$U_e = \frac{1}{2} \mathbf{q}^T \frac{A_e E_e}{\ell_e} \begin{bmatrix} 1 & -1 \\ -1 & 1 \end{bmatrix} \mathbf{q} \quad (3.24)$$

This equation is of the form

$$U_e = \frac{1}{2} \mathbf{q}^T \mathbf{k}^e \mathbf{q} \quad (3.25)$$

where the **element stiffness matrix** \mathbf{k}^e is given by

$$\mathbf{k}^e = \frac{E_e A_e}{\ell_e} \begin{bmatrix} 1 & -1 \\ -1 & 1 \end{bmatrix} \quad (3.26)$$

We note here the similarity of the strain energy expression in Eq. 3.26 with the strain energy in a simple spring, which is given as $U = \frac{1}{2} k Q^2$. Also, observe that \mathbf{k}^e is linearly proportional to the product $A_e E_e$ and inversely proportional to the length ℓ_e .

Force Terms

The element body force term $\int_e u^T f A dx$ appearing in the total potential energy is considered first. Substituting $u = N_1 q_1 + N_2 q_2$, we have

$$\int_e u^T f A dx = A_e f \int_e (N_1 q_1 + N_2 q_2) dx \quad (3.27)$$

Recall that the body force f has units of force per unit volume. In the Eq. 3.27, A_e and f are constant within the element and were consequently brought outside the integral. This equation can be written as

$$\int_e u^T f A dx = \mathbf{q}^T \begin{Bmatrix} A_e f \int_e N_1 dx \\ A_e f \int_e N_2 dx \end{Bmatrix} \quad (3.28)$$

The integrals of the shape functions described earlier can be readily evaluated by making the substitution $dx = (\ell_e/2) d\xi$. Thus,

$$\begin{aligned} \int_e N_1 dx &= \frac{\ell_e}{2} \int_{-1}^1 \frac{1 - \xi}{2} d\xi = \frac{\ell_e}{2} \\ \int_e N_2 dx &= \frac{\ell_e}{2} \int_{-1}^1 \frac{1 + \xi}{2} d\xi = \frac{\ell_e}{2} \end{aligned} \quad (3.29)$$

Alternatively, $\int_e N_1 dx$ is simply the area under the N_1 curve as shown in Fig. 3.8, which equals $\frac{1}{2} \cdot \ell_e \cdot 1 = \ell_e/2$. Similarly, $\int N_2 dx = \frac{1}{2} \cdot \ell_e \cdot 1 = \ell_e/2$. The body force term in Eq. 3.28 reduces to

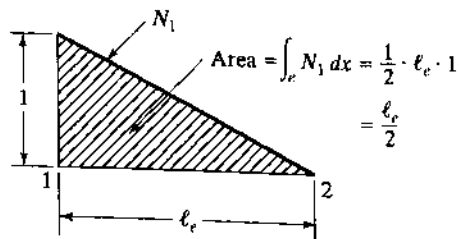


FIGURE 3.8 Integral of a shape function.

$$\int_e u^T f A dx = \mathbf{q}^T \frac{A_e}{2} \ell_e f \begin{Bmatrix} 1 \\ 1 \end{Bmatrix} \quad (3.30a)$$

which is of the form

$$\int_e u^T f A dx = \mathbf{q}^T \mathbf{f}^e \quad (3.30b)$$

The right side of this equation is of the form Displacement \times Force. Thus, the **element body force vector**, \mathbf{f}^e , is identified as

$$\mathbf{f}^e = \frac{A_e \ell_e f}{2} \begin{Bmatrix} 1 \\ 1 \end{Bmatrix} \quad (3.31)$$

The element body force vector above has a simple physical explanation. Since $A_e \ell_e$ is the volume of the element and f is the body force per unit volume, we see that $A_e \ell_e f$ gives the total body force acting on the element. The factor $\frac{1}{2}$ in Eq. 3.31 tells us that this total body force is equally distributed to the two nodes of the element.

The element *traction force term* $\int_e u^T T dx$ appearing in the total potential energy is now considered. We have

$$\int_e u^T T dx = \int_e (N_1 q_1 + N_2 q_2) T dx \quad (3.32)$$

Since the traction force T is constant within the element, we have

$$\int_e u^T T dx = \mathbf{q}^T \begin{Bmatrix} T \int_e N_1 dx \\ T \int_e N_2 dx \end{Bmatrix} \quad (3.33)$$

We have already shown that $\int_e N_1 dx = \int_e N_2 dx = \ell_e/2$. Thus, Eq. 3.33 is of the form

$$\int_e u^T T dx = \mathbf{q}^T \mathbf{T}^e \quad (3.34)$$

where the element traction-force vector is given by

$$\mathbf{T}^e = \frac{T \ell_e}{2} \begin{Bmatrix} 1 \\ 1 \end{Bmatrix} \quad (3.35)$$

We can provide a physical explanation for this equation as was given for the element body force vector.

At this stage, element matrices \mathbf{k}^e , \mathbf{f}^e , and \mathbf{T}^e have been obtained. After we account for the element connectivity (in Fig. 3.3, for example, $\mathbf{q} = [Q_1, Q_2]^T$ for element 1, $\mathbf{q} = [Q_2, Q_3]^T$ for element 2, etc.), the total potential energy in Eq. 3.18b can be written as

$$\Pi = \frac{1}{2} \mathbf{Q}^T \mathbf{K} \mathbf{Q} - \mathbf{Q}^T \mathbf{F} \quad (3.36)$$

where \mathbf{K} is the *global stiffness matrix*, \mathbf{F} is the global load vector, and \mathbf{Q} is the global displacement vector. For example, in the finite element model in Fig. 3.2b, \mathbf{K} is a (5×5)

matrix, and \mathbf{Q} and \mathbf{F} are each (5×1) vectors. \mathbf{K} is obtained as follows: Using the element connectivity information, the elements of each \mathbf{k}^e are placed in the appropriate locations in the larger \mathbf{K} matrix, and overlapping elements are then summed. The \mathbf{F} vector is similarly assembled. This process of assembling \mathbf{K} and \mathbf{F} from element stiffness and force matrices is discussed in detail in Section 3.6.

3.5 THE GALERKIN APPROACH

Following the concepts introduced in Chapter 1, we introduce a virtual displacement field

$$\phi = \phi(x) \quad (3.37)$$

and associated virtual strain

$$\epsilon(\phi) = \frac{d\phi}{dx} \quad (3.38)$$

where ϕ is an arbitrary or virtual displacement consistent with the boundary conditions. Galerkin's variational form, given in Eq. 1.43, for the one-dimensional problem considered here, is

$$\int_L \sigma^T \epsilon(\phi) A dx - \int_L \phi^T f A dx - \int_L \phi^T T dx - \sum_i \phi_i P_i = 0 \quad (3.39a)$$

This equation should hold for every ϕ consistent with the boundary conditions. The first term represents the internal virtual work, while the load terms represent the external virtual work.

On the discretized region, Eq. 3.39a becomes

$$\sum_e \int_e \epsilon^T E \epsilon(\phi) A dx - \sum_e \int_e \phi^T f A dx - \sum_e \int_e \phi^T T dx - \sum_i \phi_i P_i = 0 \quad (3.39b)$$

Note that ϵ is the strain due to the actual loads in the problem, while $\epsilon(\phi)$ is a virtual strain. Similar to the interpolation steps in Eqs. 3.7b, 3.14, and 3.16, we express

$$\begin{aligned} \phi &= \mathbf{N}\psi \\ \epsilon(\phi) &= \mathbf{B}\psi \end{aligned} \quad (3.40)$$

where $\psi = [\psi_1, \psi_2]^T$ represents the arbitrary nodal displacements of element e . Also, the global virtual displacements at the nodes are represented by

$$\Psi = [\psi_1, \psi_2, \dots, \psi_N]^T \quad (3.41)$$

Element Stiffness

Consider the first term, representing internal virtual work, in Eq. 3.39b. Substituting Eq. 3.40 into Eq. 3.39b, and noting that $\epsilon = \mathbf{B}\mathbf{q}$, we get

$$\int_e \epsilon^T E \epsilon(\phi) A dx = \int_e \mathbf{q}^T \mathbf{B}^T E \mathbf{B} \psi A dx \quad (3.42)$$

In the finite element model (Section 3.2), the cross-sectional area of element e , denoted by A_e , is constant. Also, \mathbf{B} is a constant matrix. Further, $dx = (\ell_e/2) d\xi$. Thus,

$$\int_e \epsilon^T E \epsilon(\phi) A dx = \mathbf{q}^T \left[E_e A_e \frac{\ell_e}{2} \mathbf{B}^T \mathbf{B} \int_{-1}^1 d\xi \right] \psi \quad (3.43a)$$

$$= \mathbf{q}^T \mathbf{k}^e \psi \quad (3.43b)$$

$$= \psi^T \mathbf{k}^e \mathbf{q}$$

where \mathbf{k}^e is the (symmetric) element stiffness matrix given by

$$\mathbf{k}^e = E_e A_e \ell_e \mathbf{B}^T \mathbf{B} \quad (3.44)$$

Substituting \mathbf{B} from Eq. 3.15, we have

$$\mathbf{k}^e = \frac{E_e A_e}{\ell_e} \begin{bmatrix} 1 & -1 \\ -1 & 1 \end{bmatrix} \quad (3.45)$$

Force Terms

Consider the second term in Eq. 3.39a, representing the virtual work done by the body force in an element. Using $\phi = \mathbf{N}\psi$ and $dx = \ell_e/2 d\xi$, and noting that the body force in the element is assumed constant, we have

$$\int_e \phi^T f A dx = \int_{-1}^1 \psi^T \mathbf{N}^T f A_e \frac{\ell_e}{2} d\xi \quad (3.46a)$$

$$= \psi^T \mathbf{f}^e \quad (3.46b)$$

where

$$\mathbf{f}^e = \frac{A_e \ell_e f}{2} \left\{ \begin{array}{c} \int_{-1}^1 N_1 d\xi \\ \int_{-1}^1 N_2 d\xi \end{array} \right\} \quad (3.47a)$$

is called the element body force vector. Substituting for $N_1 = (1 - \xi)/2$ and $N_2 = (1 + \xi)/2$, we obtain $\int_{-1}^1 N_1 d\xi = 1$. Alternatively, $\int_{-1}^1 N_1 d\xi$ is the area under the N_1 curve $= \frac{1}{2} \times 2 \times 1 = 1$ and $\int_{-1}^1 N_2 d\xi = 1$. Thus,

$$\mathbf{f}^e = \frac{A_e \ell_e f}{2} \begin{Bmatrix} 1 \\ 1 \end{Bmatrix} \quad (3.47b)$$

The element traction term then reduces to

$$\int_e \phi^T T dx = \psi^T \mathbf{T}^e \quad (3.48)$$

where the element traction-force vector is given by

$$\mathbf{T}^e = \frac{T \ell_e}{2} \begin{Bmatrix} 1 \\ 1 \end{Bmatrix} \quad (3.49)$$

At this stage, the element matrices \mathbf{k}^e , \mathbf{f}^e , and \mathbf{T}^e have been obtained. After accounting for the element connectivity (in Fig. 3.3, for example, $\boldsymbol{\psi} = [\psi_1, \psi_2]^T$ for element 1, $\boldsymbol{\psi} = [\Psi_2, \Psi_3]^T$ for element 2, etc.), the variational form

$$\sum_e \boldsymbol{\psi}^T \mathbf{k}^e \mathbf{q} - \sum_e \boldsymbol{\psi}^T \mathbf{f}^e - \sum_e \boldsymbol{\psi}^T \mathbf{T}^e - \sum_i \Psi_i P_i = 0 \quad (3.50)$$

can be written as

$$\boldsymbol{\Psi}^T (\mathbf{KQ} - \mathbf{F}) = 0 \quad (3.51)$$

which should hold for every $\boldsymbol{\Psi}$ consistent with the boundary conditions. Methods for handling boundary conditions are discussed shortly. The global stiffness matrix \mathbf{K} is assembled from element matrices \mathbf{k}^e using element connectivity information. Likewise, \mathbf{F} is assembled from element matrices \mathbf{f}^e and \mathbf{T}^e . This assembly is discussed in detail in the next section.

3.6 ASSEMBLY OF THE GLOBAL STIFFNESS MATRIX AND LOAD VECTOR

We noted earlier that the total potential energy written in the form

$$\Pi = \sum_e \frac{1}{2} \mathbf{q}^T \mathbf{k}^e \mathbf{q} - \sum_e \mathbf{q}^T \mathbf{f}^e - \sum_e \mathbf{q}^T \mathbf{T}^e - \sum_i P_i Q_i$$

can be written in the form

$$\Pi = \frac{1}{2} \mathbf{Q}^T \mathbf{KQ} - \mathbf{Q}^T \mathbf{F}$$

by taking element connectivity into account. This step involves assembling \mathbf{K} and \mathbf{F} from element stiffness and force matrices. The assembly of the structural stiffness matrix \mathbf{K} from element stiffness matrices \mathbf{k}^e will first be shown here.

Referring to the finite element model in Fig. 3.2b, let us consider the strain energy in, say, element 3. We have

$$U_3 = \frac{1}{2} \mathbf{q}^T \mathbf{k}^3 \mathbf{q} \quad (3.52a)$$

or, substituting for \mathbf{k}^3 ,

$$U_3 = \frac{1}{2} \mathbf{q}^T \frac{E_3 A_3}{\ell_3} \begin{bmatrix} 1 & -1 \\ -1 & 1 \end{bmatrix} \mathbf{q} \quad (3.52b)$$

For element 3, we have $\mathbf{q} = [Q_3, Q_4]^T$. Thus, we can write U_3 as

$$U_3 = \frac{1}{2} [Q_1, Q_2, Q_3, Q_4, Q_5] \begin{bmatrix} 0 & 0 & 0 & 0 & 0 \\ 0 & 0 & 0 & 0 & 0 \\ 0 & 0 & \frac{E_3 A_3}{\ell_3} & -\frac{E_3 A_3}{\ell_3} & 0 \\ 0 & 0 & -\frac{E_3 A_3}{\ell_3} & \frac{E_3 A_3}{\ell_3} & 0 \\ 0 & 0 & 0 & 0 & 0 \end{bmatrix} \begin{Bmatrix} Q_1 \\ Q_2 \\ Q_3 \\ Q_4 \\ Q_5 \end{Bmatrix} \quad (3.53)$$

From the previous equations, we see that elements of the matrix \mathbf{k}^e occupy the third and fourth rows and columns of the \mathbf{K} matrix. Consequently, when adding element-strain energies, the elements of \mathbf{k}^e are placed in the appropriate locations of the global \mathbf{K} matrix, based on the element connectivity; overlapping elements are simply added. We can denote this assembly symbolically as

$$\mathbf{K} \leftarrow \sum_e \mathbf{k}^e \quad (3.54a)$$

Similarly, the global load vector \mathbf{F} is assembled from element-force vectors and point loads as

$$\mathbf{F} \leftarrow \sum_e (\mathbf{f}^e + \mathbf{T}^e) + \mathbf{P} \quad (3.54b)$$

The Galerkin approach also gives us the same assembly procedure. An example is now given to illustrate this assembly procedure in detail. In actual computation, \mathbf{K} is stored in banded or skyline form to take advantage of symmetry and sparsity. This aspect is discussed in Section 3.7 and in greater detail in Chapter 4.

Example 3.2

Consider the bar as shown in Fig. E3.2. For each element i , A_i and ℓ_i are the cross-sectional area and length, respectively. Each element i is subjected to a traction force T_i per unit length and a body force f per unit volume. The units of T_i , f , A_i , and so on are assumed to be consistent. The Young's modulus of the material is E . A concentrated load P_2 is applied at node 2. The structural stiffness matrix and nodal load vector will now be assembled.

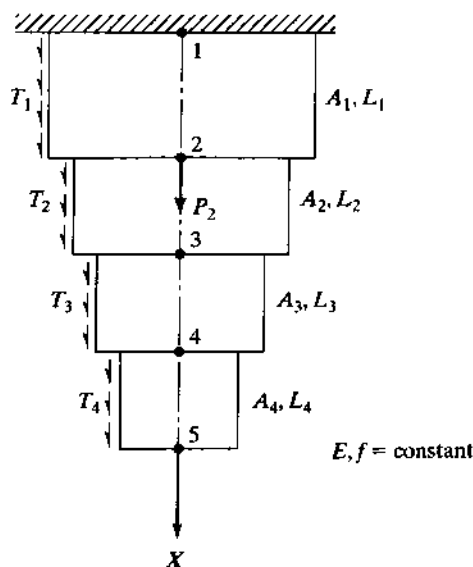


FIGURE E3.2

The element stiffness matrix for each element i is obtained from Eq. 3.26 as

$$[k^{(i)}] = \frac{EA_i}{\ell_i} \begin{bmatrix} 1 & -1 \\ -1 & 1 \end{bmatrix}$$

The element connectivity table is the following:

| Element | 1 | 2 |
|---------|---|---|
| 1 | 1 | 2 |
| 2 | 2 | 3 |
| 3 | 3 | 4 |
| 4 | 4 | 5 |

The element stiffness matrices can be "expanded" using the connectivity table and then summed (or assembled) to obtain the structural stiffness matrix as follows:*

$$\mathbf{K} = \frac{EA_1}{\ell_1} \begin{bmatrix} 1 & -1 & 0 & 0 & 0 \\ -1 & 1 & 0 & 0 & 0 \\ 0 & 0 & 0 & 0 & 0 \\ 0 & 0 & 0 & 0 & 0 \\ 0 & 0 & 0 & 0 & 0 \end{bmatrix} + \frac{EA_2}{\ell_2} \begin{bmatrix} 0 & 0 & 0 & 0 & 0 \\ 0 & 1 & -1 & 0 & 0 \\ 0 & -1 & 1 & 0 & 0 \\ 0 & 0 & 0 & 0 & 0 \\ 0 & 0 & 0 & 0 & 0 \end{bmatrix}$$

$$+ \frac{EA_3}{\ell_3} \begin{bmatrix} 0 & 0 & 0 & 0 & 0 \\ 0 & 0 & 0 & 0 & 0 \\ 0 & 0 & 1 & -1 & 0 \\ 0 & 0 & -1 & 1 & 0 \\ 0 & 0 & 0 & 0 & 0 \end{bmatrix} + \frac{EA_4}{\ell_4} \begin{bmatrix} 0 & 0 & 0 & 0 & 0 \\ 0 & 0 & 0 & 0 & 0 \\ 0 & 0 & 0 & 0 & 0 \\ 0 & 0 & 0 & 1 & -1 \\ 0 & 0 & 0 & -1 & 1 \end{bmatrix}$$

which gives

$$\mathbf{K} = E \begin{bmatrix} \frac{A_1}{\ell_1} & -\frac{A_1}{\ell_1} & 0 & 0 & 0 \\ -\frac{A_1}{\ell_1} & \left(\frac{A_1}{\ell_1} + \frac{A_2}{\ell_2}\right) & -\frac{A_2}{\ell_2} & 0 & 0 \\ 0 & -\frac{A_2}{\ell_2} & \left(\frac{A_2}{\ell_2} + \frac{A_3}{\ell_3}\right) & -\frac{A_3}{\ell_3} & 0 \\ 0 & 0 & -\frac{A_3}{\ell_3} & \left(\frac{A_3}{\ell_3} + \frac{A_4}{\ell_4}\right) & -\frac{A_4}{\ell_4} \\ 0 & 0 & 0 & -\frac{A_4}{\ell_4} & \frac{A_4}{\ell_4} \end{bmatrix}$$

*This "expansion" of element stiffness matrices as shown in Example 3.2 is merely for illustration purposes and is never explicitly carried out in the computer, since storing zeroes is inefficient. Instead, \mathbf{K} is assembled directly from \mathbf{k}^e using the connectivity table.

The global load vector is assembled as

$$\mathbf{F} = \begin{Bmatrix} \frac{A_1 \ell_1 f}{2} + \frac{\ell_1 T_1}{2} \\ \left(\frac{A_1 \ell_1 f}{2} + \frac{\ell_1 T_1}{2} \right) + \left(\frac{A_2 \ell_2 f}{2} + \frac{\ell_2 T_2}{2} \right) \\ \left(\frac{A_2 \ell_2 f}{2} + \frac{\ell_2 T_2}{2} \right) + \left(\frac{A_3 \ell_3 f}{2} + \frac{\ell_3 T_3}{2} \right) \\ \left(\frac{A_3 \ell_3 f}{2} + \frac{\ell_3 T_3}{2} \right) + \left(\frac{A_4 \ell_4 f}{2} + \frac{\ell_4 T_4}{2} \right) \\ \frac{A_4 \ell_4 f}{2} + \frac{\ell_4 T_4}{2} \end{Bmatrix} + \begin{Bmatrix} 0 \\ P_2 \\ 0 \\ 0 \\ 0 \end{Bmatrix}$$

■

3.7 PROPERTIES OF \mathbf{K}

Several important comments will now be made regarding the global stiffness matrix for the linear one-dimensional problem discussed earlier:

1. The dimension of the global stiffness \mathbf{K} is $(N \times N)$, where N is the number of nodes. This follows from the fact that each node has only one degree of freedom.
2. \mathbf{K} is symmetric.
3. \mathbf{K} is a banded matrix. That is, all elements outside of the band are zero. This can be seen in Example 3.2, just considered. In this example, \mathbf{K} can be compactly represented in banded form as

$$\mathbf{K}_{\text{banded}} = E \begin{bmatrix} \frac{A_1}{\ell_1} & -\frac{A_1}{\ell_1} \\ \frac{A_1}{\ell_1} + \frac{A_2}{\ell_2} & -\frac{A_2}{\ell_2} \\ \frac{A_2}{\ell_2} + \frac{A_3}{\ell_3} & -\frac{A_3}{\ell_3} \\ \frac{A_3}{\ell_3} + \frac{A_4}{\ell_4} & -\frac{A_4}{\ell_4} \\ \frac{A_4}{\ell_4} & 0 \end{bmatrix}$$

Note that $\mathbf{K}_{\text{banded}}$ is of dimension $[N \times \text{NBW}]$, where NBW is the half-bandwidth. In many one-dimensional problems such as the example just considered, the connectivity of element i is $i, i + 1$. In such cases, the banded matrix has only two columns (NBW = 2). In two and three dimensions, the direct formation of \mathbf{K} in banded or skyline

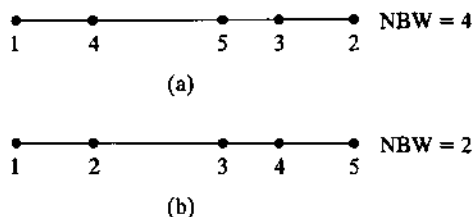


FIGURE 3.9 Node numbering and its effect on the half-bandwidth.

form from the element matrices involves some bookkeeping. This is discussed in detail at the end of Chapter 4. The reader should verify the following general formula for the half-bandwidth:

$$\text{NBW} = \max \left(\begin{array}{l} \text{Difference between dof numbers} \\ \text{connecting an element} \end{array} \right) + 1 \quad (3.55)$$

For example, consider a four-element model of a bar that is numbered as shown in Fig. 3.9a. Using Eq. 3.55, we have

$$\text{NBW} = \max(4 - 1, 5 - 4, 5 - 3, 3 - 2) + 1 = 4$$

The numbering scheme in Fig. 3.9a is bad since \mathbf{K} is almost "filled up" and consequently requires more computer storage and computation. Figure 3.9b shows the optimum numbering for minimum NBW.

Now the potential energy or Galerkin's approach has to be applied, noting the boundary conditions of the problem, to yield the finite element (equilibrium) equations. Solution of these equations yields the global displacement vector \mathbf{Q} . The stresses and reaction forces can then be recovered. These steps will now be discussed in the next section.

3.8 THE FINITE ELEMENT EQUATIONS; TREATMENT OF BOUNDARY CONDITIONS

Finite element equations are now developed after a consistent treatment of the boundary conditions.

Types of Boundary Conditions

After using a discretization scheme to model the continuum, we have obtained an expression for the total potential energy in the body as

$$\Pi = \frac{1}{2} \mathbf{Q}^T \mathbf{K} \mathbf{Q} - \mathbf{Q}^T \mathbf{F}$$

where \mathbf{K} is the structural stiffness matrix, \mathbf{F} is the global load vector, and \mathbf{Q} is the global displacement vector. As discussed previously, \mathbf{K} and \mathbf{F} are assembled from element stiffness and force matrices, respectively. We now must arrive at the equations of equilibrium, from which we can determine nodal displacements, element stresses, and support reactions.

The minimum potential-energy theorem (Chapter 1) is now invoked. This theorem is stated as follows: *Of all possible displacements that satisfy the boundary conditions of a structural system, those corresponding to equilibrium configurations make the total potential energy assume a minimum value.* Consequently, the equations of equilibrium can be obtained by minimizing, with respect to \mathbf{Q} , the potential energy $\Pi = \frac{1}{2} \mathbf{Q}^T \mathbf{K} \mathbf{Q} - \mathbf{Q}^T \mathbf{F}$ subject to boundary conditions. Boundary conditions are usually of the type

$$Q_{p_1} = a_1, Q_{p_2} = a_2, \dots, Q_{p_r} = a_r \quad (3.56)$$

That is, the displacements along dofs p_1, p_2, \dots, p_r are specified to be equal to a_1, a_2, \dots, a_r , respectively. In other words, there are r number of supports in the structure, with each support node given a specified displacement. For example, consider the bar in Fig. 3.2b. There is only one boundary condition in this problem, $Q_1 = 0$.

It is noted here that *the treatment of boundary conditions in this section is applicable to two- and three-dimensional problems as well.* For this reason, the term dof is used here instead of node, since a two-dimensional stress problem will have two degrees of freedom per node. The steps described in this section will be used in all subsequent chapters. Furthermore, a Galerkin-based argument leads to the same steps for handling boundary conditions as the energy approach used subsequently.

There are *multipoint constraints* of the type

$$\beta_1 Q_{p_1} + \beta_2 Q_{p_2} = \beta_0 \quad (3.57)$$

where β_0, β_1 , and β_2 are known constants. These types of boundary conditions are used in modeling inclined roller supports, rigid connections, or shrink fits.

It should be emphasized that improper specification of boundary conditions can lead to erroneous results. Boundary conditions eliminate the possibility of the structure moving as a rigid body. Further, boundary conditions should accurately model the physical system. Two approaches will now be discussed for handling specified displacement boundary conditions of the type given in Eq. 3.56: the **elimination approach** and the **penalty approach**. For multipoint constraints in Eq. 3.57, only the penalty approach will be given, because it is simpler to implement.

Elimination Approach

To illustrate the basic idea, consider the single boundary condition $Q_1 = a_1$. The equilibrium equations are obtained by minimizing Π with respect to \mathbf{Q} , subject to the boundary condition $Q_1 = a_1$. For an N - dof structure, we have

$$\begin{aligned} \mathbf{Q} &= [Q_1, Q_2, \dots, Q_N]^T \\ \mathbf{F} &= [F_1, F_2, \dots, F_N]^T \end{aligned}$$

The global stiffness matrix is of the form

$$\mathbf{K} = \begin{bmatrix} K_{11} & K_{12} & \cdots & K_{1N} \\ K_{21} & K_{22} & \cdots & K_{2N} \\ \vdots & & & \\ K_{N1} & K_{N2} & \cdots & K_{NN} \end{bmatrix} \quad (3.58)$$

Note that K is a symmetric matrix. The potential energy $\Pi = \frac{1}{2} \mathbf{Q}^T \mathbf{K} \mathbf{Q} - \mathbf{Q}^T \mathbf{F}$ can be written in expanded form as

$$\begin{aligned} \Pi = & \frac{1}{2} (Q_1 K_{11} Q_1 + Q_1 K_{12} Q_2 + \cdots + Q_1 K_{1N} Q_N \\ & + Q_2 K_{21} Q_1 + Q_2 K_{22} Q_2 + \cdots + Q_2 K_{2N} Q_N \\ & \cdots \\ & + Q_N K_{N1} Q_1 + Q_N K_{N2} Q_2 + \cdots + Q_N K_{NN} Q_N) \\ & - (Q_1 F_1 + Q_2 F_2 + \cdots + Q_N F_N) \end{aligned} \quad (3.59)$$

If we now substitute the boundary condition $Q_1 = a_1$ into this expression for Π , we obtain

$$\begin{aligned} \Pi = & \frac{1}{2} (a_1 K_{11} a_1 + a_1 K_{12} Q_2 + \cdots + a_1 K_{1N} Q_N \\ & + Q_2 K_{21} a_1 + Q_2 K_{22} Q_2 + \cdots + Q_2 K_{2N} Q_N \\ & \cdots \\ & + Q_N K_{N1} a_1 + Q_N K_{N2} Q_2 + \cdots + Q_N K_{NN} Q_N) \\ & - (a_1 F_1 + Q_2 F_2 + \cdots + Q_N F_N) \end{aligned} \quad (3.60)$$

Note that the displacement Q_1 has been eliminated in the potential-energy expression. Consequently, the requirement that Π take on a minimum value implies that

$$\frac{d\Pi}{dQ_i} = 0 \quad i = 2, 3, \dots, N \quad (3.61)$$

We thus obtain, from Eqs. 3.60 and 3.61,

$$\begin{aligned} K_{22} Q_2 + K_{23} Q_3 + \cdots + K_{2N} Q_N &= F_2 - K_{21} a_1 \\ K_{32} Q_2 + K_{33} Q_3 + \cdots + K_{3N} Q_N &= F_3 - K_{31} a_1 \\ \cdots \\ K_{N2} Q_2 + K_{N3} Q_3 + \cdots + K_{NN} Q_N &= F_N - K_{N1} a_1 \end{aligned} \quad (3.62)$$

These finite element equations can be expressed in matrix form as

$$\begin{bmatrix} K_{22} & K_{23} & \cdots & K_{2N} \\ K_{32} & K_{33} & \cdots & K_{3N} \\ \vdots & \vdots & \ddots & \vdots \\ K_{N2} & K_{N3} & \cdots & K_{NN} \end{bmatrix} \begin{Bmatrix} Q_2 \\ Q_3 \\ \vdots \\ Q_N \end{Bmatrix} = \begin{Bmatrix} F_2 - K_{21} a_1 \\ F_3 - K_{31} a_1 \\ \vdots \\ F_N - K_{N1} a_1 \end{Bmatrix} \quad (3.63)$$

We now observe that the $(N - 1 \times N - 1)$ stiffness matrix is obtained simply by deleting or eliminating the first row and column (in view of $Q_1 = a_1$) from the original $(N \times N)$ stiffness matrix. Equation 3.63 may be denoted as

$$\mathbf{K} \mathbf{Q} = \mathbf{F} \quad (3.64)$$

where \mathbf{K} is a reduced stiffness matrix obtained by eliminating the row and column corresponding to the specified or "support" dof. Equation 3.64 can be solved for the displacement vector \mathbf{Q} using Gaussian elimination. Note that the reduced \mathbf{K} matrix is nonsingular, provided the boundary conditions have been specified properly; the original \mathbf{K} matrix, on the other hand, is a singular matrix. Once \mathbf{Q} has been determined, the element stress can be evaluated using Eq. 3.16: $\sigma = E\mathbf{B}\mathbf{q}$, where \mathbf{q} for each element is extracted from \mathbf{Q} using element connectivity information.

Assume that displacements and stresses have been determined. It is now necessary to calculate the reaction force R_1 at the support. This reaction force can be obtained from the finite element equation (or equilibrium equation) for node 1:

$$K_{11}Q_1 + K_{12}Q_2 + \cdots + K_{1N}Q_N = F_1 + R_1 \quad (3.65)$$

Here, Q_1, Q_2, \dots, Q_N are known. F_1 , which equals the load applied at the support (if any), is also known. Consequently, the reaction force at the node that maintains equilibrium, is

$$R_1 = K_{11}Q_1 + K_{12}Q_2 + \cdots + K_{1N}Q_N - F_1 \quad (3.66)$$

Note that the elements $K_{11}, K_{12}, \dots, K_{1N}$, which form the first row of \mathbf{K} , need to be stored separately. This is because \mathbf{K} in Eq. 3.64 is obtained by deleting this row and column from the original \mathbf{K} .

The modifications to \mathbf{K} and \mathbf{F} discussed earlier are also derivable using Galerkin's variational formulation. We have Eq. 3.51 in which

$$\Psi^T(\mathbf{K}\mathbf{Q} - \mathbf{F}) = 0 \quad (3.67)$$

for every Ψ consistent with the boundary conditions of the problem. Specifically, consider the constraint

$$Q_1 = a_1 \quad (3.68)$$

Then, we require

$$\Psi_1 = 0 \quad (3.69)$$

Choosing virtual displacements $\Psi = [0, 1, 0, \dots, 0]$, $\Psi = [0, 0, 1, 0, \dots, 0]^T, \dots$, $\Psi = [0, 0, \dots, 0, 1]^T$, and substituting each of these into Eq. 3.67, we obtain precisely the equilibrium equations given in Eqs. 3.63.

The preceding discussion addressed the boundary condition $Q_1 = a_1$. This procedure can readily be generalized to handle multiple boundary conditions. The general procedure is summarized subsequently. Again, this procedure is also applicable to two- and three-dimensional problems.

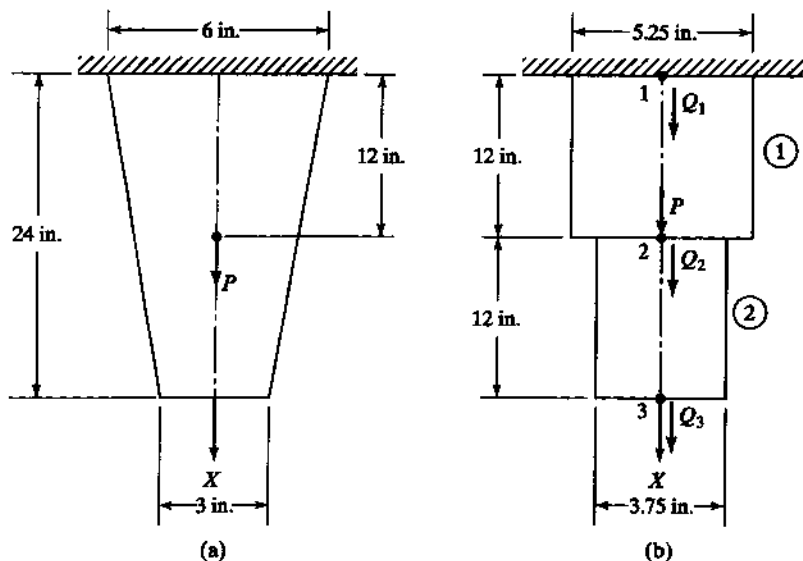


FIGURE E3.3

Solution

- (a) Using two elements, each of 12 in. in length, we obtain the finite element model in Fig. E3.3b. Nodes and elements are numbered as shown. Note that the area at the midpoint of the plate in Fig. E3.3a is 4.5 in.^2 . Consequently, the average area of element 1 is $A_1 = (6 + 4.5)/2 = 5.25 \text{ in.}^2$, and the average area of element 2 is $A_2 = (4.5 + 3)/2 = 3.75 \text{ in.}^2$. The boundary condition for this model is $Q_1 = 0$.
- (b) From Eq. 3.26, we can write down expressions for the element stiffness matrices of the two elements as

$$\mathbf{k}^1 = \frac{30 \times 10^6 \times 5.25}{12} \begin{matrix} & \begin{matrix} 1 & 2 \end{matrix} \\ \begin{matrix} \left[\begin{array}{cc} 1 & -1 \\ -1 & 1 \end{array} \right] \end{matrix} & \begin{matrix} \downarrow \\ \text{Global dof} \\ 1 \\ 2 \end{matrix} \end{matrix}$$

and

$$\mathbf{k}^2 = \frac{30 \times 10^6 \times 3.75}{12} \begin{matrix} & \begin{matrix} 2 & 3 \end{matrix} \\ \begin{matrix} \left[\begin{array}{cc} 1 & -1 \\ -1 & 1 \end{array} \right] \end{matrix} & \begin{matrix} 2 \\ 3 \end{matrix} \end{matrix}$$

Using Eq. 3.31, the element body force vectors are

$$\mathbf{f}^1 = \frac{5.25 \times 12 \times 0.2836}{2} \begin{matrix} \left\{ \begin{matrix} 1 \\ 1 \end{matrix} \right\} \\ \begin{matrix} \downarrow \\ \text{Global dof} \\ 1 \\ 2 \end{matrix} \end{matrix}$$

and

$$\mathbf{f}^2 = \frac{3.75 \times 12 \times 0.2836}{2} \begin{matrix} \left\{ \begin{matrix} 1 \\ 1 \end{matrix} \right\} \\ \begin{matrix} 2 \\ 3 \end{matrix} \end{matrix}$$

- (c) The global stiffness matrix
- \mathbf{K}
- is assembled from
- \mathbf{k}^1
- and
- \mathbf{k}^2
- as

$$\mathbf{K} = \frac{30 \times 10^6}{12} \begin{bmatrix} 1 & 2 & 3 \\ 5.25 & -5.25 & 0 \\ -5.25 & 9.00 & -3.75 \\ 0 & -3.75 & 3.75 \end{bmatrix} \begin{matrix} 1 \\ 2 \\ 3 \end{matrix}$$

The externally applied global load vector \mathbf{F} is assembled from \mathbf{f}^1 , \mathbf{f}^2 , and the point load $P = 100$ lb; as

$$\mathbf{F} = \begin{Bmatrix} 8.9334 \\ 15.3144 + 100 \\ 6.3810 \end{Bmatrix}$$

- (d) In the elimination approach, the stiffness matrix
- \mathbf{K}
- is obtained by deleting rows and columns corresponding to fixed dofs. In this problem, dof 1 is fixed. Thus,
- \mathbf{K}
- is obtained by deleting the first row and column of the original
- \mathbf{K}
- . Also,
- \mathbf{F}
- is obtained by deleting the first component of the original
- \mathbf{F}
- . The resulting equations are

$$\frac{30 \times 10^6}{12} \begin{bmatrix} 2 & 3 \\ 9.00 & -3.75 \\ -3.75 & 3.75 \end{bmatrix} \begin{Bmatrix} Q_2 \\ Q_3 \end{Bmatrix} = \begin{Bmatrix} 115.3144 \\ 6.3810 \end{Bmatrix}$$

Solution of these equations yields

$$Q_2 = 0.9272 \times 10^{-5} \text{ in.}$$

$$Q_3 = 0.9953 \times 10^{-5} \text{ in.}$$

Thus, $\mathbf{Q} = [0, 0.9272 \times 10^{-5}, 0.9953 \times 10^{-5}]^T$ in.

- (e) Using Eqs. 3.15 and 3.16, we obtain the stress in each element:

$$\begin{aligned} \sigma_1 &= 30 \times 10^6 \times \frac{1}{12} [-1 \quad 1] \begin{Bmatrix} 0 \\ 0.9272 \times 10^{-5} \end{Bmatrix} \\ &= 23.18 \text{ psi} \end{aligned}$$

and

$$\begin{aligned} \sigma_2 &= 30 \times 10^6 \times \frac{1}{12} [-1 \quad 1] \begin{Bmatrix} 0.9272 \times 10^{-5} \\ 0.9953 \times 10^{-5} \end{Bmatrix} \\ &= 1.70 \text{ psi} \end{aligned}$$

- (f) The reaction force
- R_1
- at node 1 is obtained from Eq. 3.71. This calculation requires the first row of
- \mathbf{K}
- from part (c). Also, from part (c), note that the externally applied load (due to the self-weight) at node 1 is
- $F_1 = 8.9334$
- lb. Thus,

$$\begin{aligned} R_1 &= \frac{30 \times 10^6}{12} [5.25 \quad -5.25 \quad 0] \begin{Bmatrix} 0 \\ 0.9272 \times 10^{-5} \\ 0.9953 \times 10^{-5} \end{Bmatrix} - 8.9334 \\ &= -130.6 \text{ lb} \end{aligned}$$

Evidently, the reaction is equal and opposite to the total downward load on the plate. ■

Penalty Approach

A second approach for handling boundary conditions will now be discussed. This approach is easy to implement in a computer program and retains its simplicity even when considering general boundary conditions as given in Eq. 3.57. Specified displacement boundary conditions will first be discussed. The method will then be shown to apply to problems with multipoint constraints.

Specified displacement boundary conditions. Consider the boundary condition

$$Q_1 = a_1$$

where a_1 is a known specified displacement along dof 1 of the support. The penalty approach for handling this boundary condition is now presented.

A spring with a large stiffness C is used to model the support. The magnitude of C is discussed subsequently. In this case, one end of the spring is displaced by an amount a_1 , as shown in Fig. 3.10. The displacement Q_1 along dof 1 will be approximately equal to a_1 , owing to the relatively small resistance offered by the structure. Consequently, the net extension of the spring is equal to $(Q_1 - a_1)$. The strain energy in the spring equals

$$U_s = \frac{1}{2}C(Q_1 - a_1)^2 \quad (3.72)$$

This strain energy contributes to the total potential energy. As a result,

$$\Pi_M = \frac{1}{2}\mathbf{Q}^T\mathbf{K}\mathbf{Q} + \frac{1}{2}C(Q_1 - a_1)^2 - \mathbf{Q}^T\mathbf{F} \quad (3.73)$$

The minimization of Π_M can be carried out by setting $\partial\Pi_M/\partial Q_i = 0, i = 1, 2, \dots, N$. The resulting finite element equations are

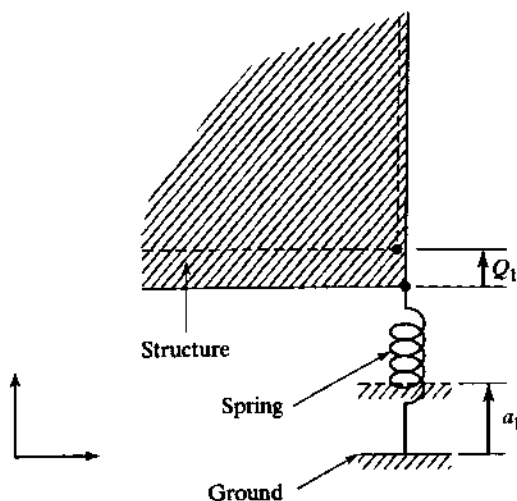


FIGURE 3.10 The penalty approach, where a spring with a large stiffness is used to model the boundary condition $Q_1 = a_1$.

$$\begin{bmatrix} (K_{11} + C) & K_{12} & \cdots & K_{1N} \\ K_{21} & K_{22} & \cdots & K_{2N} \\ \vdots & \vdots & \ddots & \vdots \\ K_{N1} & K_{N2} & \cdots & K_{NN} \end{bmatrix} \begin{Bmatrix} Q_1 \\ Q_2 \\ \vdots \\ Q_N \end{Bmatrix} = \begin{Bmatrix} F_1 + Ca_1 \\ F_2 \\ \vdots \\ F_N \end{Bmatrix} \quad (3.74)$$

Here, we see that the only modifications to handle $Q_1 = a_1$ are that a large number C gets added on to the first diagonal element of \mathbf{K} and that Ca_1 gets added on to F_1 . Solution of Eqs. 3.74 yields the displacement vector \mathbf{Q} .

The reaction force at node 1 equals the force exerted by the spring on the structure. Since the net extension of the spring is $(Q_1 - a_1)$, and the spring stiffness is C , the reaction force is given by

$$R_1 = -C(Q_1 - a_1) \quad (3.75)$$

The modifications to \mathbf{K} and \mathbf{F} given in Eqs. 3.74 are also derivable using Galerkin's approach. Consider the boundary condition $Q_1 = a_1$. To handle this, we introduce a spring with a large stiffness C with the support given a displacement equal to a_1 (Fig. 3.10). The virtual work done by the spring as a result of an arbitrary displacement Ψ is

$$\delta W_s = \text{virtual displacement} \times \text{force in spring}$$

or

$$\delta W_s = \Psi_1 C(Q_1 - a_1) \quad (3.76)$$

Thus, the variational form is

$$\Psi^T(\mathbf{KQ} - \mathbf{F}) + \Psi_1 C(Q_1 - a_1) = 0 \quad (3.77)$$

which should be valid for any Ψ . Choosing $\Psi = [1, 0, \dots, 0]^T$, $\Psi = [0, 1, 0, \dots, 0]^T, \dots, \Psi = [0, \dots, 0, 1]^T$ and substituting each in turn into Eq. 3.77, we obtain precisely the modifications shown in Eqs. 3.74. The general procedure is now summarized as follows:

Summary: Penalty Approach

Consider the boundary conditions

$$Q_{p_1} = a_1, Q_{p_2} = a_2, \dots, Q_{p_r} = a_r$$

Step 1. Modify the structural stiffness matrix \mathbf{K} by adding a large number C to each of the p_1 th, p_2 th, ..., and p_r th diagonal elements of \mathbf{K} . Also, modify the global load vector \mathbf{F} by adding Ca_1 to F_{p_1} , Ca_2 to F_{p_2} , ..., and Ca_r to F_{p_r} . Solve $\mathbf{KQ} = \mathbf{F}$ for the displacement \mathbf{Q} , where \mathbf{K} and \mathbf{F} are the modified stiffness and load matrices.

Step 2. For each element, extract the element displacement vector \mathbf{q} from the \mathbf{Q} vector, using element connectivity, and determine the element stresses.

Step 3. Evaluate the reaction force at each support from

$$R_{p_i} = -C(Q_{p_i} - a_i) \quad i = 1, 2, \dots, r \quad (3.78)$$

It should be noted that the penalty approach presented herein is an approximate approach. The accuracy of the solution, particularly the reaction forces, depends on the choice of C .

Choice of C . Let us expand the first equation in Eq. 3.74. We have

$$(K_{11} + C)Q_1 + K_{12}Q_2 + \cdots + K_{1N}Q_N = F_1 + Ca_1 \quad (3.79a)$$

Upon dividing by C , we get

$$\left(\frac{K_{11}}{C} + 1\right)Q_1 + \frac{K_{12}}{C}Q_2 + \cdots + \frac{K_{1N}}{C}Q_N = \frac{F_1}{C} + a_1 \quad (3.79b)$$

From this equation, we see that if C is chosen large enough, then $Q_1 \approx a_1$. Specifically, we see that if C is large compared to the stiffness coefficients $K_{11}, K_{12}, \dots, K_{1N}$, then $Q_1 \approx a_1$. Note that F_1 is a load applied at the support (if any), and that F_1/C is generally of small magnitude.

A simple scheme suggests itself for choosing the magnitude of C :

$$C = \max|K_{ij}| \times 10^4$$

for

$$\begin{aligned} 1 \leq i \leq N \\ 1 \leq j \leq N \end{aligned} \quad (3.80)$$

The choice of 10^4 has been found to be satisfactory on most computers. The reader may wish to choose a sample problem and experiment with this (using, say, 10^5 or 10^6) to check whether the reaction forces differ by much.

Example 3.4

Consider the bar shown in Fig. E3.4. An axial load $P = 200 \times 10^3 \text{ N}$ is applied as shown. Using the penalty approach for handling boundary conditions, do the following:

- Determine the nodal displacements.
- Determine the stress in each material.
- Determine the reaction forces.

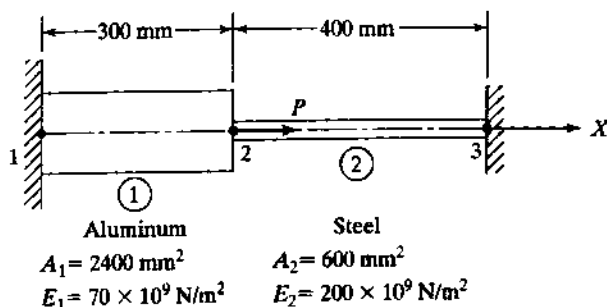


FIGURE E3.4

Solution

(a) The element stiffness matrices are

$$\mathbf{k}^1 = \frac{70 \times 10^3 \times 2400}{300} \begin{matrix} & \begin{matrix} 1 & 2 \end{matrix} \\ \begin{matrix} 1 \\ -1 \end{matrix} & \begin{bmatrix} 1 & -1 \\ -1 & 1 \end{bmatrix} \end{matrix} \leftarrow \text{Global dof}$$

and

$$\mathbf{k}^2 = \frac{200 \times 10^3 \times 600}{400} \begin{matrix} & \begin{matrix} 2 & 3 \end{matrix} \\ \begin{matrix} 1 \\ -1 \end{matrix} & \begin{bmatrix} 1 & -1 \\ -1 & 1 \end{bmatrix} \end{matrix}$$

The structural stiffness matrix that is assembled from \mathbf{k}^1 and \mathbf{k}^2 is

$$\mathbf{K} = 10^6 \begin{matrix} & \begin{matrix} 1 & 2 & 3 \end{matrix} \\ \begin{matrix} 0.56 \\ -0.56 \\ 0 \end{matrix} & \begin{bmatrix} 0.56 & -0.56 & 0 \\ -0.56 & 0.86 & -0.30 \\ 0 & -0.30 & 0.30 \end{bmatrix} \end{matrix}$$

The global load vector is

$$\mathbf{F} = [0, 200 \times 10^3, 0]^T$$

Now dofs 1 and 3 are fixed. When using the penalty approach, therefore, a large number C is added to the first and third diagonal elements of \mathbf{K} . Choosing C based on Eq. 3.80, we get

$$C = [0.86 \times 10^6] \times 10^4$$

Thus, the modified stiffness matrix is

$$\mathbf{K} = 10^6 \begin{bmatrix} 8600.56 & -0.56 & 0 \\ -0.56 & 0.86 & -0.30 \\ 0 & -0.30 & 8600.30 \end{bmatrix}$$

The finite element equations are given by

$$10^6 \begin{bmatrix} 8600.56 & -0.56 & 0 \\ -0.56 & 0.86 & -0.30 \\ 0 & -0.30 & 8600.30 \end{bmatrix} \begin{Bmatrix} Q_1 \\ Q_2 \\ Q_3 \end{Bmatrix} = \begin{Bmatrix} 0 \\ 200 \times 10^3 \\ 0 \end{Bmatrix}$$

which yields the solution

$$\mathbf{Q} = [15.1432 \times 10^{-6}, 0.23257, 8.1127 \times 10^{-6}]^T \text{ mm}$$

(b) The element stresses (Eq. 3.16) are

$$\begin{aligned} \sigma_1 &= 70 \times 10^3 \times \frac{1}{300} [-1 \quad 1] \begin{Bmatrix} 15.1432 \times 10^{-6} \\ 0.23257 \end{Bmatrix} \\ &= 54.27 \text{ MPa} \end{aligned}$$

where $1 \text{ MPa} = 10^6 \text{ N/m}^2 = 1 \text{ N/mm}^2$. Also,

$$\begin{aligned} \sigma_2 &= 200 \times 10^3 \times \frac{1}{400} \begin{bmatrix} -1 & 1 \end{bmatrix} \begin{Bmatrix} 0.23257 \\ 8.1127 \times 10^{-6} \end{Bmatrix} \\ &= -116.29 \text{ MPa} \end{aligned}$$

(c) The reaction forces are obtained from Eq. 3.78 as

$$\begin{aligned} R_1 &= -CQ_1 \\ &= -[0.86 \times 10^{10}] \times 15.1432 \times 10^{-6} \\ &= -130.23 \times 10^3 \end{aligned}$$

Also,

$$\begin{aligned} R_3 &= -CQ_3 \\ &= -[0.86 \times 10^{10}] \times 8.1127 \times 10^{-6} \\ &= -69.77 \times 10^3 \text{ N} \end{aligned}$$

Example 3.5

In Fig. E3.5a, a load $P = 60 \times 10^3 \text{ N}$ is applied as shown. Determine the displacement field, stress, and support reactions in the body. Take $E = 20 \times 10^3 \text{ N/mm}^2$.

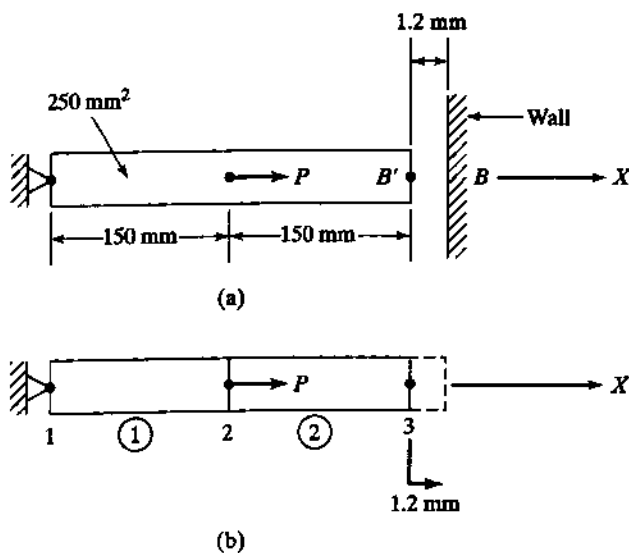


FIGURE E3.5

Solution In this problem, we should first determine whether contact occurs between the bar and the wall, B . To do this, assume that the wall does not exist. Then, the solution to the problem can be verified to be

$$Q_B = 1.8 \text{ mm}$$

where Q_B is the displacement of point B' . From this result, we see that contact does occur. The problem has to be re-solved, since the boundary conditions are now different: The displacement

at B' is specified to be 1.2 mm. Consider the two-element finite element model in Fig. 3.5b. The boundary conditions are $Q_1 = 0$ and $Q_3 = 1.2$ mm. The structural stiffness matrix \mathbf{K} is

$$\mathbf{K} = \frac{20 \times 10^3 \times 250}{150} \begin{bmatrix} 1 & -1 & 0 \\ -1 & 2 & -1 \\ 0 & -1 & 1 \end{bmatrix}$$

and the global load vector \mathbf{F} is

$$\mathbf{F} = [0, 60 \times 10^3, 0]^T$$

In the penalty approach, the boundary conditions $Q_1 = 0$ and $Q_3 = 1.2$ imply the following modifications: A large number C chosen here as $C = (2/3) \times 10^{10}$, is added on to the 1st and 3rd diagonal elements of \mathbf{K} . Also, the number $(C \times 1.2)$ gets added on to the 3rd component of \mathbf{F} . Thus, the modified equations are

$$\frac{10^5}{3} \begin{bmatrix} 20001 & -1 & 0 \\ -1 & 2 & -1 \\ 0 & -1 & 20001 \end{bmatrix} \begin{Bmatrix} Q_1 \\ Q_2 \\ Q_3 \end{Bmatrix} = \begin{Bmatrix} 0 \\ 60.0 \times 10^3 \\ 80.0 \times 10^7 \end{Bmatrix}$$

The solution is

$$\mathbf{Q} = [7.49985 \times 10^{-5}, 1.500045, 1.200015]^T \text{ mm}$$

The element stresses are

$$\begin{aligned} \sigma_1 &= 200 \times 10^3 \times \frac{1}{150} \begin{bmatrix} -1 & 1 \end{bmatrix} \begin{Bmatrix} 7.49985 \times 10^{-5} \\ 1.500045 \end{Bmatrix} \\ &= 199.996 \text{ MPa} \\ \sigma_2 &= 200 \times 10^3 \times \frac{1}{150} \begin{bmatrix} -1 & 1 \end{bmatrix} \begin{Bmatrix} 1.500045 \\ 1.200015 \end{Bmatrix} \\ &= -40.004 \text{ MPa} \end{aligned}$$

The reaction forces are

$$\begin{aligned} R_1 &= -C \times 7.49985 \times 10^{-5} \\ &= -49.999 \times 10^3 \text{ N} \end{aligned}$$

and

$$\begin{aligned} R_3 &= -C \times (1.200015 - 1.2) \\ &= -10.001 \times 10^3 \text{ N} \end{aligned}$$

The results obtained from the penalty approach have a small approximation error due to the flexibility of the support introduced. In fact, the reader may verify that the elimination approach for handling boundary conditions yields the exact reactions, $R_1 = -50.0 \times 10^3$ N and $R_3 = -10.0 \times 10^3$ N. ■

Multipoint Constraints

In problems where, for example, inclined rollers or rigid connections are to be modeled, the boundary conditions take the form

$$\beta_1 Q_{p_1} + \beta_2 Q_{p_2} = \beta_0$$

where β_0 , β_1 , and β_2 are known constants. Such boundary conditions are referred to as multipoint constraints in the literature. The penalty approach will now be shown to apply to this type of boundary condition.

Consider the modified total potential-energy expression

$$\Pi_M = \frac{1}{2} \mathbf{Q}^T \mathbf{K} \mathbf{Q} + \frac{1}{2} C (\beta_1 Q_{p_1} + \beta_2 Q_{p_2} - \beta_0)^2 - \mathbf{Q}^T \mathbf{F} \quad (3.81)$$

where C is a large number. Since C is large, Π_M takes on a minimum value only when $(\beta_1 Q_{p_1} + \beta_2 Q_{p_2} - \beta_0)$ is very small—that is, when $\beta_1 Q_{p_1} + \beta_2 Q_{p_2} \approx \beta_0$, as desired. Setting $\partial \Pi_M / \partial Q_i = 0$, $i = 1, \dots, N$ yields the modified stiffness and force matrices. These modifications are given as

$$\begin{bmatrix} K_{p_1 p_1} & K_{p_1 p_2} \\ K_{p_2 p_1} & K_{p_2 p_2} \end{bmatrix} \longrightarrow \begin{bmatrix} K_{p_1 p_1} + C\beta_1^2 & K_{p_1 p_2} + C\beta_1\beta_2 \\ K_{p_2 p_1} + C\beta_1\beta_2 & K_{p_2 p_2} + C\beta_2^2 \end{bmatrix} \quad (3.82)$$

and

$$\begin{Bmatrix} F_{p_1} \\ F_{p_2} \end{Bmatrix} \longrightarrow \begin{Bmatrix} F_{p_1} + C\beta_0\beta_1 \\ F_{p_2} + C\beta_0\beta_2 \end{Bmatrix} \quad (3.83)$$

If we consider the equilibrium equations $\partial \Pi_M / \partial Q_{p_1} = 0$ and $\partial \Pi_M / \partial Q_{p_2} = 0$ and rearrange these in the form

$$\sum_j K_{p_1 j} Q_j - F_{p_1} = R_{p_1} \quad \text{and} \quad \sum_j K_{p_2 j} Q_j - F_{p_2} = R_{p_2}$$

we obtain the reaction forces R_{p_1} and R_{p_2} , which are the reaction components along dofs p_1 and p_2 , respectively, as

$$R_{p_1} = -\frac{\partial}{\partial Q_{p_1}} \left[\frac{1}{2} C (\beta_1 Q_{p_1} + \beta_2 Q_{p_2} - \beta_0)^2 \right] \quad (3.84a)$$

and

$$R_{p_2} = -\frac{\partial}{\partial Q_{p_2}} \left[\frac{1}{2} C (\beta_1 Q_{p_1} + \beta_2 Q_{p_2} - \beta_0)^2 \right] \quad (3.84b)$$

Upon simplification, Eqs. 3.84 yield

$$R_{p_1} = -C\beta_1(\beta_1 Q_{p_1} + \beta_2 Q_{p_2} - \beta_0) \quad (3.85a)$$

and

$$R_{p_2} = -C\beta_2(\beta_1 Q_{p_1} + \beta_2 Q_{p_2} - \beta_0) \quad (3.85b)$$

We see that the penalty approach allows us to handle multipoint constraints and is again easy to implement in a computer program. A nonphysical argument is used here to arrive at the modified potential energy in Eq. 3.81. Multipoint constraints are the most general types of boundary conditions, from which other types can be treated as special cases.

Example 3.6

Consider the structure shown in Fig. E3.6a. A rigid bar of negligible mass, pinned at one end, is supported by a steel rod and an aluminum rod. A load $P = 30 \times 10^3$ N is applied as shown.

- (a) Model the structure using two finite elements. What are the boundary conditions for your model?
- (b) Develop the modified stiffness matrix and modified load vector. Solve the equations for Q . Then determine element stresses.

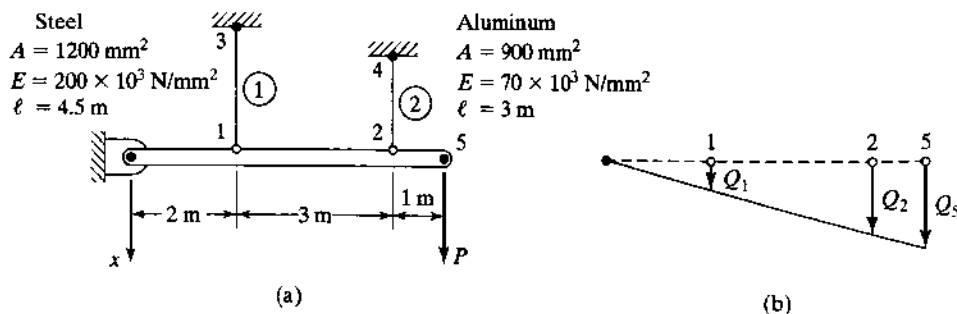


FIGURE E3.6

Solution

- (a) The problem is modeled using two elements as shown in the following connectivity table:

| CONNECTIVITY TABLE | | |
|--------------------|--------|--------|
| Element no. | Node 1 | Node 2 |
| 1 | 3 | 1 |
| 2 | 4 | 2 |

The boundary conditions at nodes 3 and 4 are obvious: $Q_3 = 0$ and $Q_4 = 0$. Now, since the rigid bar has to remain straight, Q_1 , Q_2 , and Q_5 are related as shown in Fig. E3.6b. The multipoint constraints due to the rigid bar configuration are given by

$$Q_1 - 0.333Q_5 = 0$$

$$Q_2 - 0.833Q_5 = 0$$

- (b) First, the element stiffness matrices are given by

$$\mathbf{k}^1 = \frac{200 \times 10^3 \times 1200}{4500} \begin{bmatrix} 1 & -1 \\ -1 & 1 \end{bmatrix} = 10^3 \begin{bmatrix} 53.33 & -53.33 \\ -53.33 & 53.33 \end{bmatrix} \begin{matrix} 3 \\ 1 \end{matrix}$$

and

$$\mathbf{k}^2 = \frac{70 \times 10^3 \times 900}{3000} \begin{bmatrix} 1 & -1 \\ -1 & 1 \end{bmatrix} = 10^3 \begin{bmatrix} 21 & -21 \\ -21 & 21 \end{bmatrix} \begin{matrix} 4 \\ 2 \end{matrix}$$

The global stiffness matrix \mathbf{K} is

$$\mathbf{K} = 10^3 \begin{bmatrix} 1 & 2 & 3 & 4 & 5 \\ 53.33 & 0 & -53.33 & 0 & 0 \\ 0 & 21 & 0 & -21 & 0 \\ -53.33 & 0 & 53.33 & 0 & 0 \\ 0 & -21 & 0 & 21 & 0 \\ 0 & 0 & 0 & 0 & 0 \end{bmatrix} \begin{matrix} 1 \\ 2 \\ 3 \\ 4 \\ 5 \end{matrix}$$

The \mathbf{K} matrix is modified as follows: a number $C = [53.33 \times 10^3] \times 10^4$, large in comparison to the stiffness values, is chosen. Since $Q_3 = Q_4 = 0$, C is added on to the (3, 3) and (4, 4) locations of \mathbf{K} . Next, multipoint constraints given in part (a) are considered. For the first constraint, $Q_1 - 0.333Q_5 = 0$, we note that $\beta_0 = 0$, $\beta_1 = 1$, and $\beta_2 = -0.333$. The addition to the stiffness matrix is obtained from Eqs. 3.82 as

$$\begin{bmatrix} C\beta_1^2 & C\beta_1\beta_2 \\ C\beta_1\beta_2 & C\beta_2^2 \end{bmatrix} = 10^7 \begin{bmatrix} 1 & 5 \\ 53.33 & -17.77 \\ -17.77 & 5.925926 \end{bmatrix} \begin{matrix} 1 \\ 5 \end{matrix}$$

The force addition is zero since $\beta_0 = 0$. Similarly, the consideration of the second multipoint constraint $Q_2 - 0.833Q_5 = 0$ yields the stiffness addition

$$10^7 \begin{bmatrix} 2 & 5 \\ 53.33 & -44.44 \\ -44.44 & 37.037037 \end{bmatrix} \begin{matrix} 2 \\ 5 \end{matrix}$$

On addition of all the preceding stiffnesses, we obtain the final modified equations as

$$10^3 \begin{bmatrix} 533386.7 & 0 & -53.33 & 0 & -177777.7 \\ 0 & 533354.3 & 0 & -21.0 & -444444.4 \\ -53.33 & 0 & 533386.7 & 0 & 0 \\ 0 & -21.0 & 0 & 533354.3 & 0 \\ -177777.7 & -444444.4 & 0 & 0 & 429629.6 \end{bmatrix} \begin{Bmatrix} Q_1 \\ Q_2 \\ Q_3 \\ Q_4 \\ Q_5 \end{Bmatrix} = \begin{Bmatrix} 0 \\ 0 \\ 0 \\ 0 \\ 30 \times 10^3 \end{Bmatrix}$$

The solution, obtained from a computer program that solves matrix equations, such as the one given in Chapter 2, is

$$\mathbf{Q} = [0.486 \quad 1.215 \quad 4.85 \times 10^{-5} \quad 4.78 \times 10^{-5} \quad 1.457] \text{ mm}$$

The element stresses are now recovered from Eqs. 3.15 and 3.16 as

$$\begin{aligned} \sigma_1 &= \frac{200 \times 10^3}{4500} [-1 \quad 1] \begin{Bmatrix} 4.85 \times 10^{-5} \\ 0.486 \end{Bmatrix} \\ &= 21.60 \text{ MPa} \end{aligned}$$

and

$$\sigma_2 = 28.35 \text{ MPa} \quad \blacksquare$$

In this problem, we note that the introduction of the multipoint constraints by the penalty approach makes all the diagonal stiffness values large. Thus, the results become

sensitive to errors in the calculations. Double-precision arithmetic on the computer is recommended when there are several multipoint constraints.

3.9 QUADRATIC SHAPE FUNCTIONS

So far, the unknown displacement field was interpolated by linear shape functions within each element. In some problems, however, use of quadratic interpolation leads to far more accurate results. In this section, quadratic shape functions will be introduced, and the corresponding element stiffness matrix and load vectors will be derived. The reader should note that the basic procedure is the same as that used in the linear one-dimensional element earlier.

Consider a typical three-node quadratic element, as shown in Fig. 3.11a. In the local numbering scheme, the left node will be numbered 1, the right node 2, and the midpoint 3. Node 3 has been introduced for the purposes of passing a quadratic fit and is called an *internal node*. The notation $x_i = x$ -coordinate of node i , $i = 1, 2, 3$, is used. Further, $\mathbf{q} = [q_1, q_2, q_3]^T$, where q_1, q_2 , and q_3 are the displacements of nodes 1, 2, and 3, respectively. The x -coordinate system is mapped onto a ξ -coordinate system, which is given by the transformation

$$\xi = \frac{2(x - x_3)}{x_2 - x_1} \quad (3.86)$$

From Eq. 3.86, we see that $\xi = -1, 0$, and $+1$ at nodes 1, 3, and 2 (Fig. 3.11b).

Now, in ξ -coordinates, *quadratic shape functions* N_1, N_2 , and N_3 will be introduced as

$$N_1(\xi) = -\frac{1}{2}\xi(1 - \xi) \quad (3.87a)$$

$$N_2(\xi) = \frac{1}{2}\xi(1 + \xi) \quad (3.87b)$$

$$N_3(\xi) = (1 + \xi)(1 - \xi) \quad (3.87c)$$

The shape function N_1 is equal to unity at node 1 and zero at nodes 2 and 3. Similarly, N_2 equals unity at node 2 and equals zero at the other two nodes; N_3 equals unity at node 3 and equals zero at nodes 1 and 2. The shape functions N_1, N_2 , and N_3 are graphed in Fig. 3.12. The expressions for these shape functions can be written down by inspection. For example, since $N_1 = 0$ at $\xi = 0$ and $N_1 = 0$ at $\xi = 1$, we know that N_1 must contain the product $\xi(1 - \xi)$. That is, N_1 is of the form

$$N_1 = c\xi(1 - \xi) \quad (3.88)$$

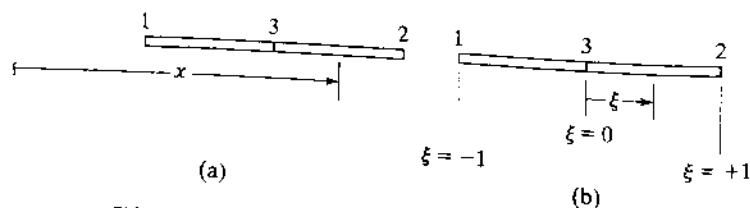
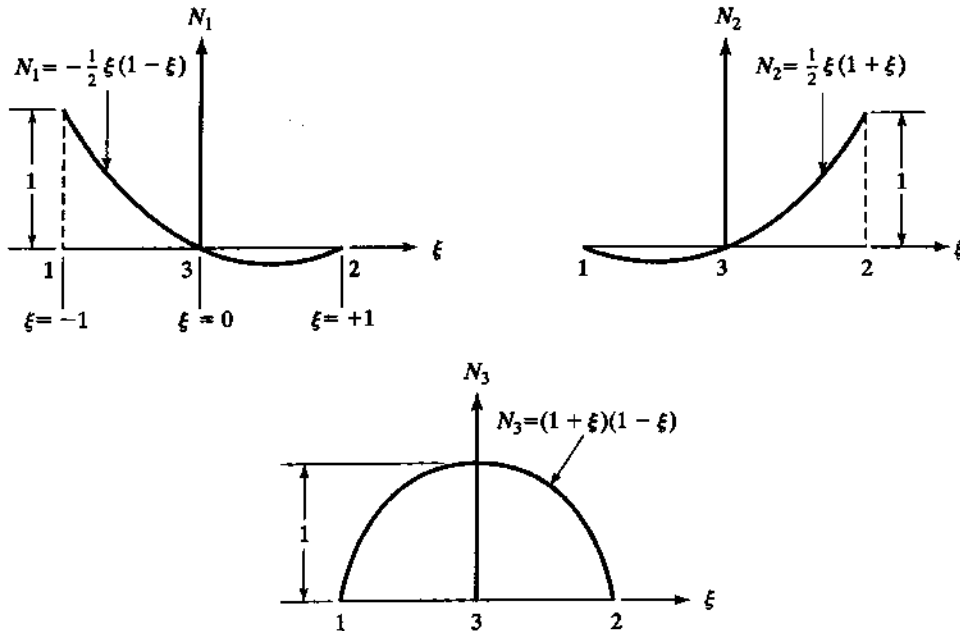


FIGURE 3.11 Quadratic element in x - and ξ -coordinates.

FIGURE 3.12 Shape functions N_1 , N_2 , and N_3 .

The constant c is now obtained from the condition $N_1 = 1$ at $\xi = -1$, which yields $c = -\frac{1}{2}$, resulting in the formula given in Eq. 3.87a. These shape functions are called *Lagrange* shape functions.

Now the displacement field within the element is written in terms of the nodal displacements as

$$u = N_1 q_1 + N_2 q_2 + N_3 q_3 \quad (3.89a)$$

or

$$u = \mathbf{N} \mathbf{q} \quad (3.89b)$$

where $\mathbf{N} = [N_1, N_2, N_3]$ is a (1×3) vector of shape functions and $\mathbf{q} = [q_1, q_2, q_3]^T$ is the (3×1) element displacement vector. At node 1, we see that $N_1 = 1$, $N_2 = N_3 = 0$, and hence $u = q_1$. Similarly, $u = q_2$ at node 2 and $u = q_3$ at node 3. Thus, u in Eq. 3.89a is a quadratic interpolation passing through q_1 , q_2 , and q_3 (Fig. 3.13).

The strain ϵ is now given by

$$\begin{aligned} \epsilon &= \frac{du}{dx} && \text{(strain-displacement relation)} \\ &= \frac{du}{d\xi} \frac{d\xi}{dx} && \text{(chain rule)} \\ &= \frac{2}{x_2 - x_1} \frac{du}{d\xi} && \text{(using Eq. 3.86)} \\ &= \frac{2}{x_2 - x_1} \left[\frac{dN_1}{d\xi}, \frac{dN_2}{d\xi}, \frac{dN_3}{d\xi} \right] \cdot \mathbf{q} && \text{(using Eq. 3.89)} \end{aligned} \quad (3.90)$$

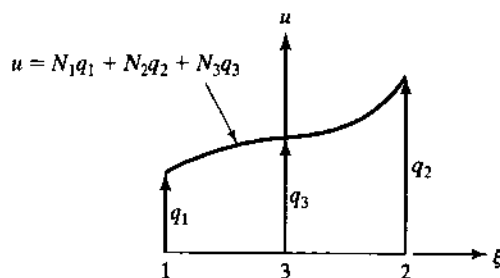


FIGURE 3.13 Interpolation using quadratic shape functions.

Using Eqs. 3.87, we have

$$\epsilon = \frac{2}{x_2 - x_1} \left[-\frac{1 - 2\xi}{2}, \frac{1 + 2\xi}{2}, -2\xi \right] \mathbf{q} \quad (3.91)$$

which is of the form

$$\epsilon = \mathbf{B} \mathbf{q} \quad (3.92)$$

where \mathbf{B} is given by

$$\mathbf{B} = \frac{2}{x_2 - x_1} \left[-\frac{1 - 2\xi}{2}, \frac{1 + 2\xi}{2}, -2\xi \right] \quad (3.93)$$

Using Hooke's law, we can write the stress as

$$\sigma = E \mathbf{B} \mathbf{q} \quad (3.94)$$

Note that since N_i are quadratic shape functions, \mathbf{B} in Eq. 3.93 is linear in ξ . This means that the strain and stress can vary linearly within the element. Recall that when using linear shape functions, the strain and stress came out to be constant within the element.

We now have expressions for u , ϵ , and σ in Eqs. 3.89b, 3.92, and 3.94, respectively. Also, we have $dx = (\ell_e/2) d\xi$ from Eq. 3.86.

Again, in the finite element model considered here, it will be assumed that cross-sectional area A_e , body force F , and traction force T are constant within the element. Substituting for u , ϵ , σ , and dx into the potential-energy expression yields

$$\begin{aligned} \Pi &= \sum_e \frac{1}{2} \int_e \sigma^T \epsilon A dx - \sum_e \int_e u^T f A dx - \sum_e \int_e u^T T dx - \sum_i Q_i P_i \\ &= \sum_e \frac{1}{2} \mathbf{q}^T \left(E_e A_e \frac{\ell_e}{2} \int_{-1}^1 [\mathbf{B}^T \mathbf{B}] d\xi \right) \mathbf{q} - \sum_e \mathbf{q}^T \left(A_e \frac{\ell_e}{2} f \int_{-1}^1 N^T d\xi \right) \\ &\quad - \sum_e \mathbf{q}^T \left(\frac{\ell_e}{2} T \int_{-1}^1 N^T d\xi \right) - \sum_i Q_i P_i \end{aligned} \quad (3.95)$$

Comparing the above equation with the general form

$$\Pi = \sum_e \frac{1}{2} \mathbf{q}^T \mathbf{k}^e \mathbf{q} - \sum_e \mathbf{q}^T \mathbf{f}^e - \sum_e \mathbf{q}^T \mathbf{T}^e - \sum_i Q_i P_i$$

yields

$$\mathbf{k}^e = \frac{E_e A_e \ell_e}{2} \int_{-1}^1 [\mathbf{B}^T \quad \mathbf{B}] d\xi \quad (3.96a)$$

which, upon substituting for \mathbf{B} in Eq. 3.93, yields

$$\mathbf{k}^e = \frac{E_e A_e}{3\ell_e} \begin{matrix} & \begin{matrix} 1 & 2 & 3 \end{matrix} & \leftarrow \text{Local dof} \\ \begin{bmatrix} 7 & 1 & -8 \\ 1 & 7 & -8 \\ -8 & -8 & 16 \end{bmatrix} & \begin{matrix} 1 \\ 2 \\ 3 \end{matrix} & \end{matrix} \quad (3.96b)$$

The element body force vector \mathbf{f}^e is given by

$$\mathbf{f}^e = \frac{A_e \ell_e f}{2} \int_{-1}^1 \mathbf{N}^T d\xi \quad (3.97a)$$

which, upon substituting for \mathbf{N} in Eqs. 3.87, yields

$$\mathbf{f}^e = A_e \ell_e f \begin{matrix} & \begin{matrix} \downarrow \text{Local dof} \\ 1 \\ 2 \\ 3 \end{matrix} & \\ \left\{ \begin{matrix} 1/6 \\ 1/6 \\ 2/3 \end{matrix} \right\} & \begin{matrix} 1 \\ 2 \\ 3 \end{matrix} & \end{matrix} \quad (3.97b)$$

Similarly, the element traction-force vector \mathbf{T}^e is given by

$$\mathbf{T}^e = \frac{\ell_e T}{2} \int_{-1}^1 \mathbf{N}^T d\xi \quad (3.98a)$$

which results in

$$\mathbf{T}^e = \ell_e T \begin{matrix} & \begin{matrix} \downarrow \text{Local dof} \\ 1 \\ 2 \\ 3 \end{matrix} & \\ \left\{ \begin{matrix} 1/6 \\ 1/6 \\ 2/3 \end{matrix} \right\} & \begin{matrix} 1 \\ 2 \\ 3 \end{matrix} & \end{matrix} \quad (3.98b)$$

The total potential energy is again of the form $\Pi = \frac{1}{2} \mathbf{Q}^T \mathbf{K} \mathbf{Q} - \mathbf{Q}^T \mathbf{F}$, where the structural stiffness matrix \mathbf{K} and nodal load vector \mathbf{F} are assembled from element stiffness matrices and load vectors, respectively.

Example 3.7

Consider the rod (a robot arm) in Fig. E3.7a, which is rotating at constant angular velocity $\omega = 30$ rad/s. Determine the axial stress distribution in the rod, using two quadratic elements. Consider only the centrifugal force. Ignore bending of the rod.

Solution A finite element model of the rod, with two quadratic elements, is shown in Fig. E3.7b. The model has a total of five degrees of freedom. The element stiffness matrices are (from Eq. 3.96b)

$$\mathbf{k}^j = \frac{10^7 \times 0.6}{3 \times 21} \begin{matrix} & \begin{matrix} 1 & 3 & 2 \end{matrix} & \leftarrow \text{Global dof} \\ \begin{bmatrix} 7 & 1 & -8 \\ 1 & 7 & -8 \\ -8 & -8 & 16 \end{bmatrix} & \begin{matrix} 1 \\ 3 \\ 2 \end{matrix} & \end{matrix}$$

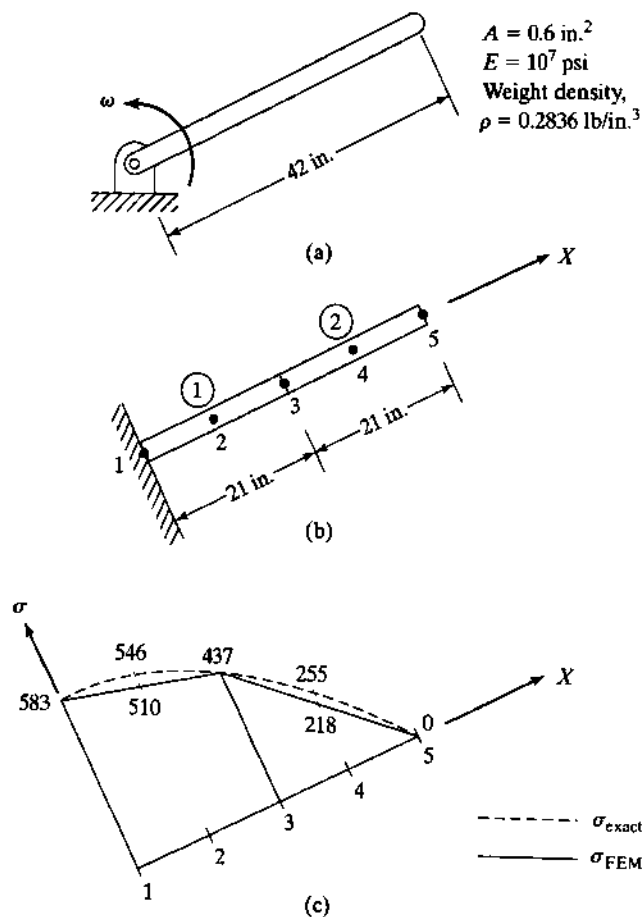


FIGURE E3.7

and

$$k^2 = \frac{10^7 \times 0.6}{3 \times 21} \begin{bmatrix} 7 & 1 & -8 \\ 1 & 7 & -8 \\ -8 & -8 & 16 \end{bmatrix} \begin{matrix} 3 \\ 5 \\ 4 \end{matrix}$$

Thus,

$$K = \frac{10^7 \times 0.6}{3 \times 21} \begin{bmatrix} 1 & 2 & 3 & 4 & 5 \\ 7 & -8 & 1 & 0 & 0 \\ -8 & 16 & -8 & 0 & 0 \\ 1 & -8 & 14 & -8 & 1 \\ 0 & 0 & -8 & 16 & -8 \\ 0 & 0 & 1 & -8 & 7 \end{bmatrix} \begin{matrix} 1 \\ 2 \\ 3 \\ 4 \\ 5 \end{matrix}$$

The body force f (lb/in.³) is given by

$$f = \frac{\rho \omega^2}{g} \text{ lb/in}^3$$

where ρ = weight density and $g = 32.2 \text{ ft/s}^2$. Note that f is a function of the distance r from the pin. Taking average values of f over each element, we have

$$\begin{aligned} f_1 &= \frac{0.2836 \times 10.5 \times 30^2}{32.2 \times 12} \\ &= 6.94 \end{aligned}$$

and

$$\begin{aligned} f_2 &= \frac{0.2836 \times 31.5 \times 30^2}{32.2 \times 12} \\ &= 20.81 \end{aligned}$$

Thus, the element body force vectors are (from Eq. 3.97b)

$$\mathbf{f}^1 = 0.6 \times 21 \times f_1 \begin{matrix} \downarrow \text{Global dof} \\ \left(\begin{array}{c} \frac{1}{6} \\ \frac{1}{6} \\ \frac{2}{3} \end{array} \right) \\ \begin{matrix} 1 \\ 3 \\ 2 \end{matrix} \end{matrix}$$

and

$$\mathbf{f}^2 = 0.6 \times 21 \times f_2 \begin{matrix} \downarrow \text{Global dof} \\ \left(\begin{array}{c} \frac{1}{6} \\ \frac{1}{6} \\ \frac{2}{3} \end{array} \right) \\ \begin{matrix} 3 \\ 5 \\ 4 \end{matrix} \end{matrix}$$

Assembling \mathbf{f}^1 and \mathbf{f}^2 , we obtain

$$\mathbf{F} = [14.57, 58.26, 58.26, 174.79, 43.70]^T$$

Using the elimination method, the finite element equations are

$$\frac{10^7 \times 0.6}{63} \begin{bmatrix} 16 & -8 & 0 & 0 \\ -8 & 14 & -8 & 1 \\ 0 & -8 & 16 & -8 \\ 0 & 1 & -8 & 7 \end{bmatrix} \begin{Bmatrix} Q_2 \\ Q_3 \\ Q_4 \\ Q_5 \end{Bmatrix} = \begin{Bmatrix} 58.26 \\ 58.26 \\ 174.79 \\ 43.7 \end{Bmatrix}$$

which yields

$$\mathbf{Q} = 10^{-3}[0, .5735, 1.0706, 1.4147, 1.5294]^T \text{ mm}$$

The stresses can now be evaluated from Eqs. 3.93 and 3.94. The element connectivity table is as follows:

| Element Number | 1 | 2 | 3 | ← Local Node Nos. |
|----------------|---|---|---|--------------------|
| 1 | 1 | 3 | 2 | ↑ Global Node Nos. |
| 2 | 3 | 5 | 4 | |

Thus,

$$\mathbf{q} = [Q_1, Q_3, Q_2]^T$$

for element 1, while

$$\mathbf{q} = [Q_3, Q_5, Q_4]^T$$

for element 2. Using Eqs. 3.93 and 3.94, we get

$$\sigma_1 = 10^7 \times \frac{2}{21} \left[-\frac{1-2\xi}{2}, \frac{1+2\xi}{2}, -2\xi \right] \begin{Bmatrix} Q_1 \\ Q_3 \\ Q_2 \end{Bmatrix}$$

where $-1 \leq \xi \leq 1$, and σ_1 denotes the stress in element 1. The stress at node 1 in element 1 is obtained by substituting $\xi = -1$ into the previous equation, which results in

$$\begin{aligned} \sigma_{1|1} &= 10^7 \times \frac{2}{21} \times 10^{-3} [-1.5, -0.5, +2.0] \begin{Bmatrix} 0 \\ 1.0706 \\ .5735 \end{Bmatrix} \\ &= 583 \text{ psi} \end{aligned}$$

The stress at node 2 (which corresponds to the midpoint of element 1) is obtained by substituting for $\xi = 0$:

$$\begin{aligned} \sigma_{1|3} &= 10^7 \times \frac{2}{21} \times 10^{-3} [-0.5, 0.5, 0] \begin{Bmatrix} 0 \\ 1.0706 \\ .5735 \end{Bmatrix} \\ &= 510 \text{ psi} \end{aligned}$$

Similarly, we obtain

$$\sigma_{1|2} = \sigma_{2|1} = 437 \text{ psi} \quad \sigma_{2|3} = 218 \text{ psi} \quad \sigma_{2|2} = 0$$

The axial distribution is shown in Fig. E3.7c. The stresses obtained from the finite element model can be compared with the exact solution, given by

$$\sigma_{\text{exact}}(x) = \frac{\rho\omega^2}{2g}(L^2 - x^2)$$

The exact stress distribution based on this equation is also shown in Fig. E3.7c. ■

3.10 TEMPERATURE EFFECTS

In this section, the stresses induced by temperature changes in an isotropic linearly elastic material will be considered. That is, the **thermal stress** problem will be considered. If the distribution of the change in temperature, $\Delta T(x)$, is known, then the strain due to this temperature change can be treated as an **initial strain**, ϵ_0 , given as

$$\epsilon_0 = \alpha \Delta T \quad (3.99)$$

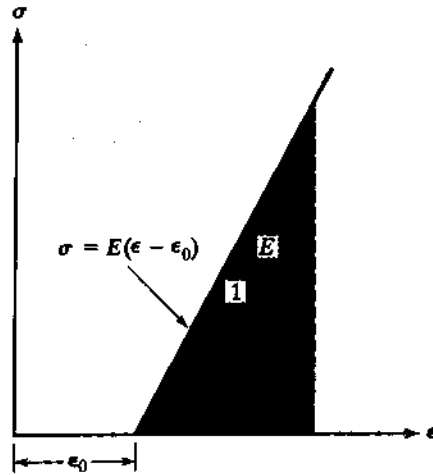


FIGURE 3.14 Stress-strain law in the presence of an initial strain.

where α is the coefficient of thermal expansion. Note that a positive ΔT implies a rise in temperature. The stress-strain law in the presence of ϵ_0 is shown in Fig. 3.14. From this figure, we see that the stress-strain relation is given by

$$\sigma = E(\epsilon - \epsilon_0) \quad (3.100)$$

The strain energy per unit volume, u_0 , is equal to the shaded area in Fig. 3.14 and is given by

$$u_0 = \frac{1}{2}\sigma(\epsilon - \epsilon_0) \quad (3.101)$$

By using Eq. 3.100, we find that Eq. 3.101 yields

$$u_0 = \frac{1}{2}(\epsilon - \epsilon_0)^T E (\epsilon - \epsilon_0) \quad (3.102a)$$

The total strain energy U in the structure is obtained by integrating u_0 over the volume of the structure:

$$U = \int_L \frac{1}{2}(\epsilon - \epsilon_0)^T E (\epsilon - \epsilon_0) A dx \quad (3.102b)$$

For a structure modeled using one-dimensional linear elements, this equation becomes

$$U = \sum_e \frac{1}{2} A_e \frac{\ell_e}{2} \int_{-1}^1 (\epsilon - \epsilon_0)^T E_e (\epsilon - \epsilon_0) d\xi \quad (3.102c)$$

Noting that $\epsilon = \mathbf{B}\mathbf{q}$, we get

$$\begin{aligned} U &= \sum_e \frac{1}{2} \mathbf{q}^T \left(E_e A_e \frac{\ell_e}{2} \int_{-1}^1 \mathbf{B}^T \mathbf{B} d\xi \right) \mathbf{q} - \sum_e \mathbf{q}^T E_e A_e \frac{\ell_e}{2} \epsilon_0 \int_{-1}^1 \mathbf{B}^T d\xi \\ &\quad + \sum_e \frac{1}{2} E_e A_e \frac{\ell_e}{2} \epsilon_0^2 \end{aligned} \quad (3.102d)$$

Examining the strain energy expression, we see that the first term on the right side yields the element stiffness matrix derived earlier in Section 3.4; the last term is a constant

term and is of no consequence since it drops out of the equilibrium equations, which are obtained by setting $d\Pi/d\mathbf{Q} = 0$. The second term yields the desired element load vector Θ^e , as a result of the temperature change:

$$\Theta^e = E_e A_e \frac{\ell_e}{2} \epsilon_0 \int_{-1}^1 \mathbf{B}^T d\xi \quad (3.103a)$$

This equation can be simplified by substituting for $\mathbf{B} = [-1 \ 1]/(x_2 - x_1)$ and noting that $\epsilon_0 = \alpha \Delta T$. Thus,

$$\Theta^e = \frac{E_e A_e \ell_e \alpha \Delta T}{x_2 - x_1} \begin{Bmatrix} -1 \\ 1 \end{Bmatrix} \quad (3.103b)$$

In Eq. 3.103b, ΔT is the average change in temperature within the element. The temperature load vector in Eq. 3.103b can be assembled along with the body force, traction-force, and point load vectors to yield the global load vector \mathbf{F} , for the structure. This assembly can be denoted as

$$\mathbf{F} = \sum_e (\mathbf{f}^e + \mathbf{T}^e + \Theta^e) + \mathbf{P} \quad (3.104)$$

After solving the finite element equations $\mathbf{K}\mathbf{Q} = \mathbf{F}$ for the displacements \mathbf{Q} , the stress in each element can be obtained from Eq. (3.100) as

$$\sigma = E(\mathbf{B}\mathbf{q} - \alpha \Delta T) \quad (3.105a)$$

or

$$\sigma = \frac{E}{x_2 - x_1} [-1 \ 1] \mathbf{q} - E\alpha \Delta T \quad (3.105b)$$

Example 3.8

An axial load $P = 300 \times 10^3 \text{ N}$ is applied at 20°C to the rod as shown in Fig. E3.8. The temperature is then raised to 60°C .

- Assemble the \mathbf{K} and \mathbf{F} matrices.
- Determine the nodal displacements and element stresses.

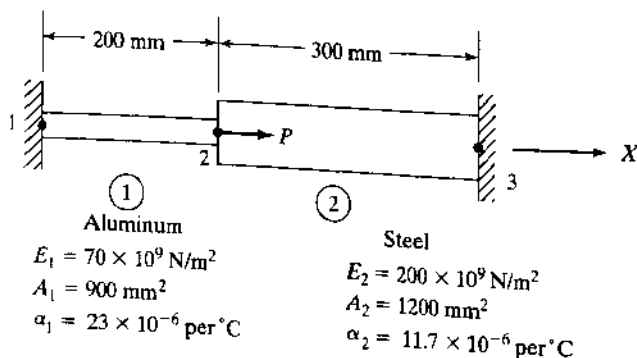


FIGURE E3.8

Solution

(a) The element stiffness matrices are

$$\mathbf{k}^1 = \frac{70 \times 10^3 \times 900}{200} \begin{bmatrix} 1 & -1 \\ -1 & 1 \end{bmatrix} \text{N/mm}$$

$$\mathbf{k}^2 = \frac{200 \times 10^3 \times 1200}{300} \begin{bmatrix} 1 & -1 \\ -1 & 1 \end{bmatrix} \text{N/mm}$$

Thus,

$$\mathbf{K} = 10^3 \begin{bmatrix} 315 & -315 & 0 \\ -315 & 1115 & -800 \\ 0 & -800 & 800 \end{bmatrix} \text{N/mm}$$

Now, in assembling \mathbf{F} , both temperature and point load effects have to be considered. The element temperature forces due to $\Delta T = 40^\circ\text{C}$ are obtained from Eq. 3.103b as

$$\Theta^1 = 70 \times 10^3 \times 900 \times 23 \times 10^{-6} \times 40 \begin{Bmatrix} -1 \\ 1 \end{Bmatrix} \begin{matrix} \downarrow \text{Global dof} \\ 1 \\ 2 \end{matrix} \text{ N}$$

and

$$\Theta^2 = 200 \times 10^3 \times 1200 \times 11.7 \times 10^{-6} \times 40 \begin{Bmatrix} -1 \\ 1 \end{Bmatrix} \begin{matrix} 2 \\ 3 \end{matrix} \text{ N}$$

Upon assembling Θ^1 , Θ^2 , and the point load, we get

$$\mathbf{F} = 10^3 \begin{Bmatrix} -57.96 \\ 57.96 - 112.32 + 300 \\ 112.32 \end{Bmatrix}$$

or

$$\mathbf{F} = 10^3 [-57.96, 245.64, 112.32]^T \text{ N}$$

(b) The elimination approach will now be used to solve for the displacements. Since dofs 1 and 3 are fixed, the first and third rows and columns of \mathbf{K} , together with the first and third components of \mathbf{F} , are deleted. This results in the scalar equation

$$10^3 [1115] Q_2 = 10^3 \times 245.64$$

yielding

$$Q_2 = 0.220 \text{ mm}$$

Thus,

$$\mathbf{Q} = [0, 0.220, 0]^T \text{ mm}$$

In evaluating element stresses, we have to use Eq. 3.105b:

$$\sigma_1 = \frac{70 \times 10^3}{200} [-1 \quad 1] \begin{Bmatrix} 0 \\ 0.220 \end{Bmatrix} - 70 \times 10^3 \times 23 \times 10^{-6} \times 40$$

$$= 12.60 \text{ MPa}$$

and

$$\begin{aligned}\sigma_2 &= \frac{200 \times 10^3}{300} [-1 \quad 1] \begin{Bmatrix} 0.220 \\ 0 \end{Bmatrix} - 200 \times 10^3 \times 11.7 \times 10^{-6} \times 40 \\ &= -240.27 \text{ MPa}\end{aligned}$$

Input Data File

```
<< 1D STRESS ANALYSIS USING BAR ELEMENT >>
EXAMPLE 3.3
NN NE NM NDIM NEN NDN
3 2 1 1 2 1
ND NL NMPC
1 3 0
Node# X-Coordinate
1 0
2 12
3 24
Elem# N1 N2 Mat# Area TempRise
1 1 2 1 5.25 0
2 2 3 1 3.75 0
DOF# Displacement
1 0
DOF# Load
1 8.9334
2 115.3144
3 6.3810
MAT# E Alpha
1 30E6 0
B1 i B2 j B3 (Multi-point constr. B1*Qi+B2*Qj=B3)
```

```
EXAMPLE 3.3
NODE NO. DISPLACEMENT
1 5.8057E-10
2 9.2726E-06
3 9.9532E-06
ELEM NO. STRESS
1 2.3180E+01
2 1.7016E+00
NODE NO. REACTION
1 -1.3063E+02
```

PROBLEMS

- 3.1. Consider the bar in Fig. P3.1. Cross-sectional area $A_e = 1.2 \text{ in.}^2$, and Young's modulus $E = 30 \times 10^6 \text{ psi}$. If $q_1 = 0.02 \text{ in.}$ and $q_2 = 0.025 \text{ in.}$, determine the following (by hand calculation):
- the displacement at point P ,
 - the strain ϵ and stress σ ,
 - the element stiffness matrix, and
 - the strain energy in the element.

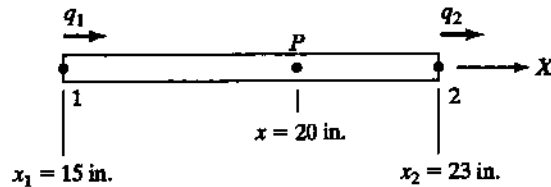


FIGURE P3.1

3.2. Find the bandwidth NBW for the one-dimensional model whose nodes are numbered as shown in Fig. P3.2.

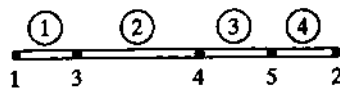


FIGURE P3.2

3.3. A finite element solution using one-dimensional, two-noded elements has been obtained for a rod as shown in Fig. P3.3:

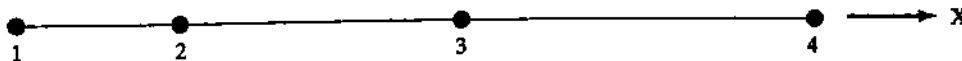


FIGURE P3.3

Displacements are as follows: $\mathbf{Q} = [-0.2, 0, 0.6, -0.1]^T$ mm, $E = 1$ N/mm², Area of each element = 1 mm², $L_{1-2} = 50$ mm, $L_{2-3} = 80$ mm, $L_{3-4} = 100$ mm.

- (i) According to the finite element theory, plot displacement $u(x)$ vs x .
- (ii) According to the finite element theory, plot strain $\epsilon(x)$ vs x .
- (iii) Determine the \mathbf{B} matrix for element 2-3.
- (iv) Determine the strain energy in element 1-2 using $U = \frac{1}{2} \mathbf{q}^T \mathbf{k} \mathbf{q}$.

3.4. Consider a finite element with shape functions $N_1(\xi)$ and $N_2(\xi)$ used to interpolate the displacement field within the element (Fig. P3.4).

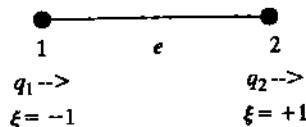


FIGURE P3.4

Derive an expression for the strain-displacement matrix \mathbf{B} , where strain $\epsilon = \mathbf{B} \mathbf{q}$, in terms of N_1 and N_2 . (Do not assume any specific form for N_1 or N_2 .) (Note: $\mathbf{q} = [q_1, q_2]^T$.)

- 3.5. It is desired to attach a spring to node 22 of a structure modeled using 1-D elements, as shown in Fig. P3.5. The banded stiffness matrix \mathbf{S} in program FEM1D can be modified to attach the spring as follows:

$$S(\underline{\quad}, \underline{\quad}) = S(\underline{\quad}, \underline{\quad}) + \underline{\quad}$$

(Fill in the blanks.)

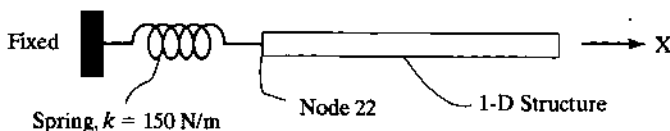


FIGURE P3.5

- 3.6. Consider the 1-D model of the structure shown in Fig. P3.6.
- Show that the assembled stiffness matrix \mathbf{K} is singular.
 - Give a sample displacement vector $\mathbf{Q}_0 \neq \mathbf{0}$ that satisfies $\mathbf{K} \mathbf{Q}_0 = \mathbf{F} = \mathbf{0}$. With the help of a sketch, discuss the significance of this displacement. What is the strain energy in the structure?
 - Prove, in general, that any nonzero solution \mathbf{Q} to a system of equations $\mathbf{K} \mathbf{Q} = \mathbf{0}$ implies that \mathbf{K} is singular.

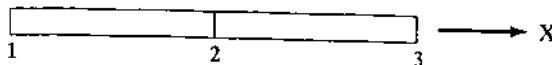
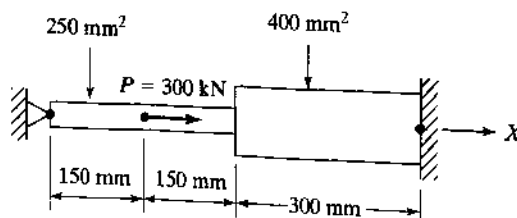


FIGURE P3.6

- 3.7. Consider the bar in Fig. 3.7 loaded as shown. Determine the nodal displacements, element stresses, and support reactions. Solve this problem by hand calculation, adopting the elimination method for handling boundary conditions. Verify your results using program FEM1D.



$$E = 200 \times 10^9 \text{ N/m}^2$$

$$(1 \text{ kN} = 1000 \text{ N})$$

FIGURE P3.7

- 3.8. Repeat Example 3.5 in the text, but use the elimination approach for handling boundary conditions. Solve by hand calculation.

- 3.9. An axial load $P = 385 \text{ kN}$ is applied to the composite block shown in Fig. P3.9. Determine the stress in each material. (*Hint:* You may name the nodes 1-2 for both the elements.)

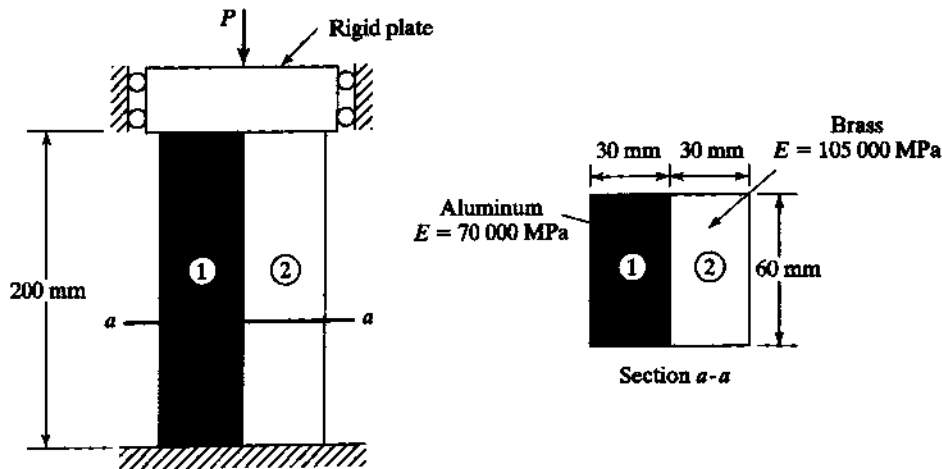


FIGURE P3.9

- 3.10. Consider the bar in Fig. P3.10. Determine the nodal displacements, element stresses, and support reactions.

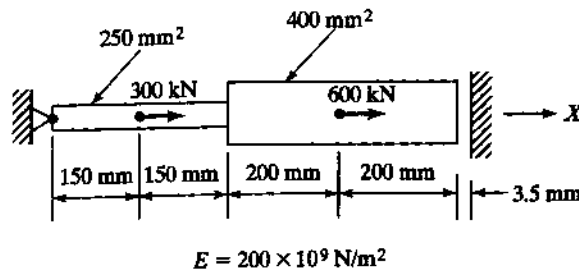


FIGURE P3.10

- 3.11. Complete Example 3.7 in the text using:
 (a) two linear finite elements and
 (b) four linear finite elements.
 Plot the stress distributions on Fig. E3.7c.
- 3.12. A tapered rod is subjected to a body force $f = x^2$ acting in the x -direction and also a point load $P = 2$ as shown in Fig. 3.12.
 (a) Use the Rayleigh-Ritz method with an assumed displacement field $u = a_0 + a_1x + a_2x^2$ to determine expressions for displacement $u(x)$ and stress $\sigma(x)$.

- (b) Solve this problem using a finite element solution with two (2) two-noded elements. Show all work such as element matrices, assembly, boundary conditions, and solution. Compare finite element and Rayleigh–Ritz solutions by providing plots of $u(x)$ vs. x and $\sigma(x)$ vs. x by the two methods.

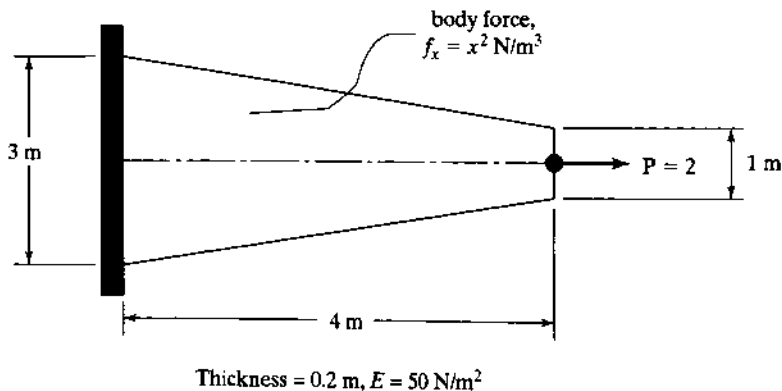


FIGURE P3.12

- 3.13. Consider the multipoint constraint $3Q_p - Q_q = 0$, where p and q are the degree of freedom numbers. Indicate what modifications need to be made to the banded stiffness matrix \mathbf{S} to implement this constraint. Also, if the bandwidth of the structure is n_1 , what will be the new bandwidth when the constraint is introduced?
- 3.14. The rigid beam in Fig. P3.14 was level before the load was applied. Find the stress in each vertical member. (*Hint:* The boundary condition is of the multipoint constraint type.)

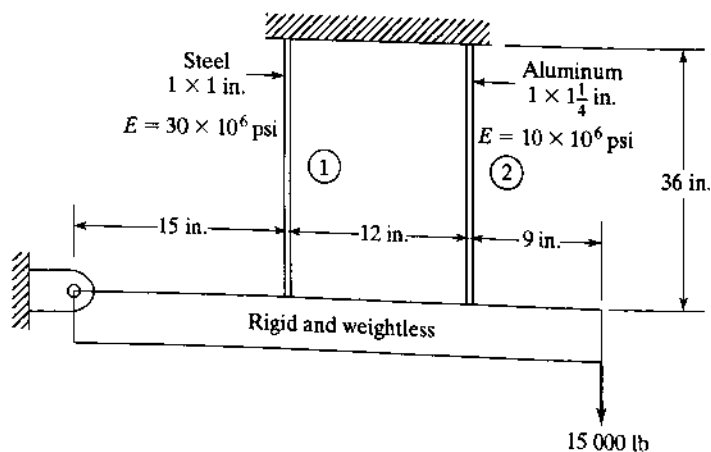


FIGURE P3.14

- 3.15. A brass bolt is fitted inside an aluminum tube, as shown in Fig. P3.15. After the nut has been fitted snugly, it is tightened one-quarter of a full turn. Given that the bolt is single threaded with a 2-mm pitch, determine the stress in bolt and tube. (*Hint:* The boundary condition is of the multipoint constraint type.)

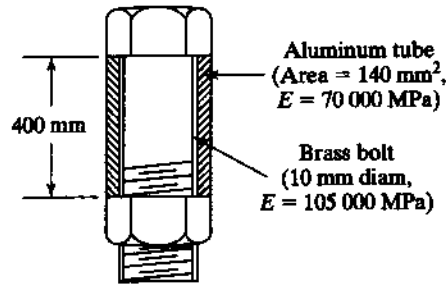


FIGURE P3.15

- 3.16. This problem reinforces the fact that once the shape functions are assumed, then all other element matrices can be derived. Certain arbitrary shape functions are given, and the reader is asked to derive the **B** and **k** matrices.

Consider the one-dimensional element shown in Fig. P3.16. The transformation

$$\xi = \frac{2}{x_2 - x_1}(x - x_1) - 1$$

is used to relate x and ξ coordinates. Let the displacement field be interpolated as

$$u(\xi) = N_1 q_1 + N_2 q_2$$

where shape functions N_1 and N_2 are assumed to be

$$N_1 = \cos \frac{\pi(1 + \xi)}{4} \quad N_2 = \cos \frac{\pi(1 - \xi)}{4}$$

- (a) Develop the relation $\epsilon = \mathbf{B}\mathbf{q}$. That is, develop the **B** matrix.
 (b) Develop the stiffness matrix, **k**. (You need not evaluate the integrals.)

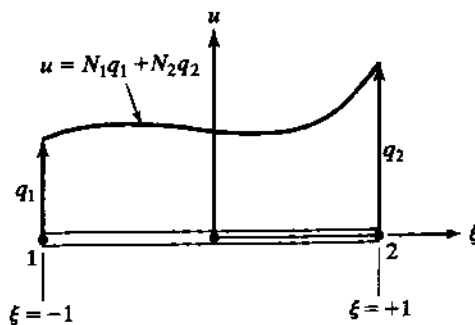


FIGURE P3.16

- 3.17. Derive the element stiffness matrix **k** for the one-dimensional tapered elements shown in Fig. P3.17a and P3.17b. (Hint: Introduce the linearity of width for part a and diameter for part b using the shape functions used for the displacement interpolation.)

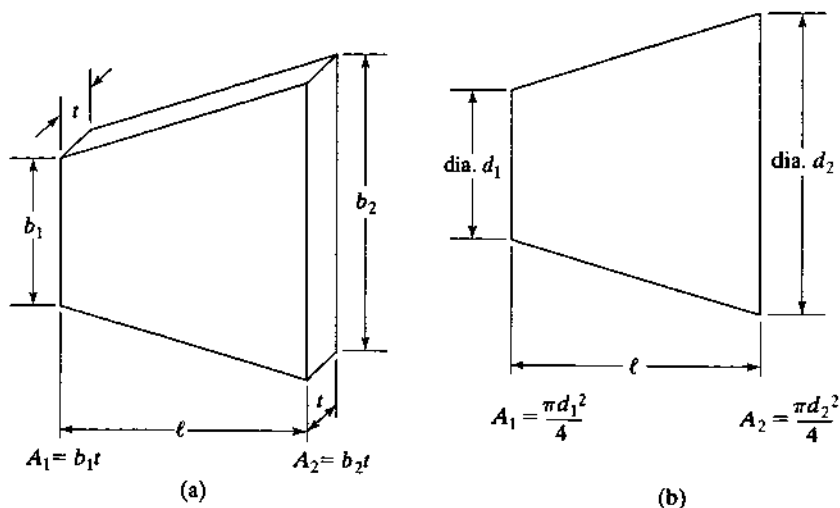


FIGURE P3.17

- 3.18. For plotting and extrapolation purposes (see Chapter 12), it is sometimes necessary to obtain nodal stress values from element stress values that are obtained from a computer run. Specifically, consider the element stresses, σ_1 , σ_2 , and σ_3 , which are constant within each element, as shown in Fig. P3.18. It is desired to obtain nodal stresses S_i , $i = 1, 2, 3, 4$, which best fit the elemental values. Obtain S_i from the least-squares criterion.

$$\text{Minimize } I = \sum_e \int_e \frac{1}{2} (\sigma - \sigma_e)^2 dx$$

where σ is expressed in terms of the nodal values s_i , using linear shape functions as

$$\sigma = N_1 s_1 + N_2 s_2$$

where 1 and 2 are the local numbers.

Plot the distribution of stress from the nodal values.

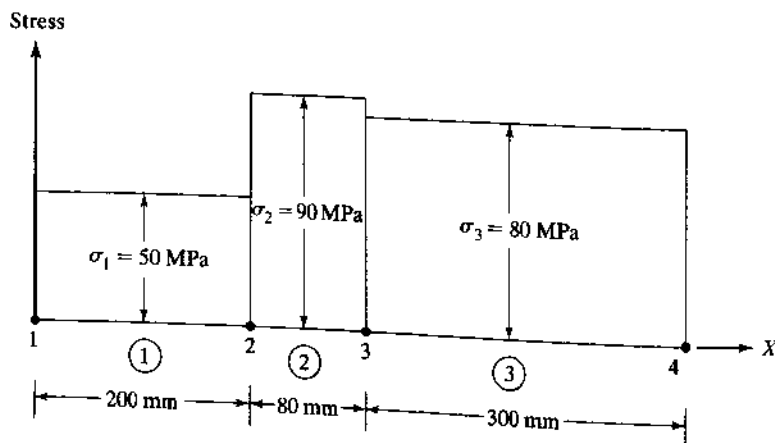


FIGURE P3.18

- 3.19. Determine the stresses in the 4 in. long bar in Fig. P3.19, using the following models:
- One linear element.
 - Two linear elements. (Note: x in, T kips/in.)

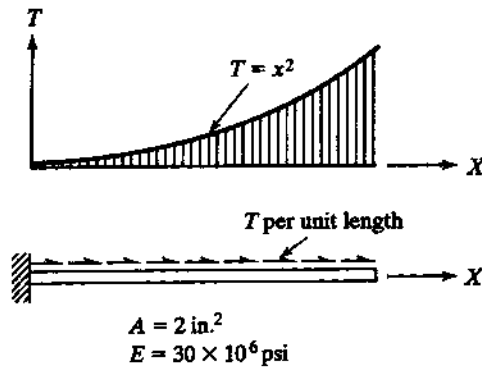


FIGURE P3.19

- 3.20. For the vertical rod shown in Fig. P3.20, find the deflection at A and the stress distribution. Use $E = 100 \text{ MPa}$ and weight per unit volume $= 0.06 \text{ N/cm}^3$. (Hint: Introduce weight contribution to the nodal loads into the program and solve using two elements and four elements.) Comment on the stress distribution.

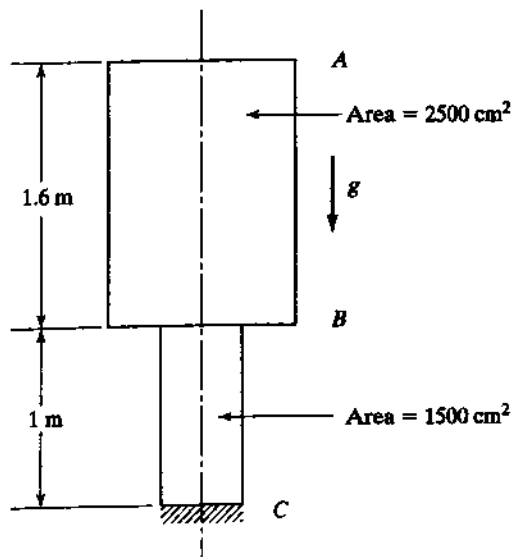


FIGURE P3.20

- 3.21. For Fig. P3.21, find the deflection at the free end under its own weight, using divisions of
- 1 element,
 - 2 elements,

- (c) 4 elements,
 - (d) 8 elements, and
 - (e) 16 elements.
- Then plot number of elements vs. deflection.

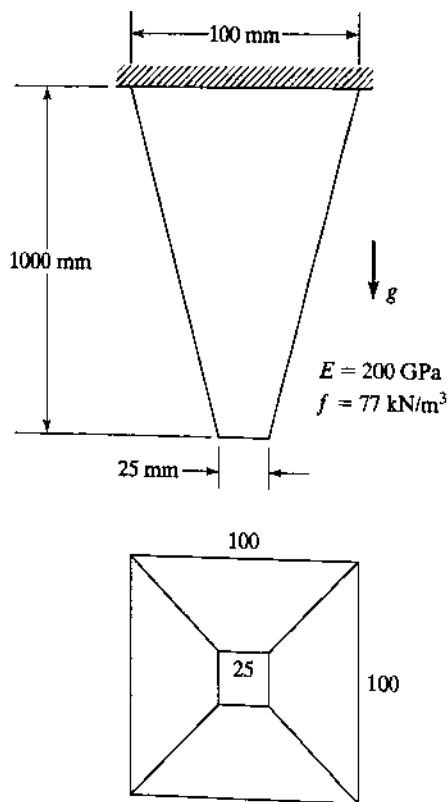


FIGURE P3.21

- 3.22. Consider the quadratic element shown in Fig. P3.22, subjected to a quadratically varying traction force (which is defined as force per unit length).
- (a) Express the traction force as a function of ξ , T_1 , T_2 , and T_3 , using the shape functions N_1 , N_2 , and N_3 .
 - (b) Derive, from the potential term $\int_e u^T T dx$, an expression for the element traction force, T^e . Leave your answer in terms of T_1 , T_2 , T_3 , and ℓ_e .

- (c) Re-solve Problem 3.19 using the exact traction load derived previously, with one quadratic element, by hand calculations.

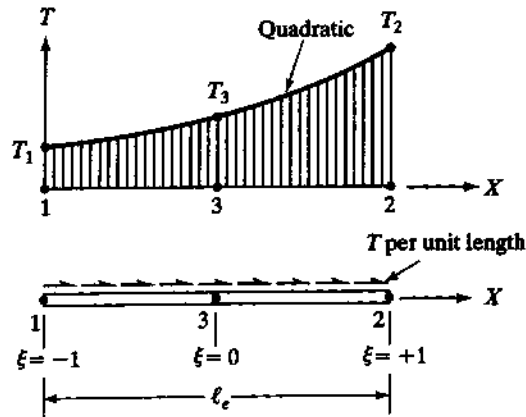


FIGURE P3.22

- 3.23. The structure in Fig. P3.23 is subjected to an increase in temperature, $\Delta T = 80^\circ\text{C}$. Determine the displacements, stresses, and support reactions. Solve this problem by hand calculation, using the elimination method for handling boundary conditions.

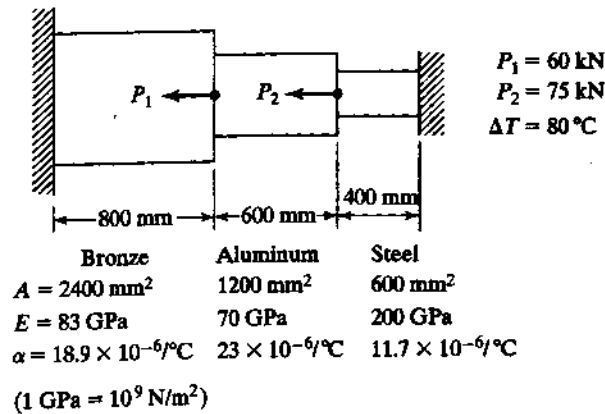


FIGURE P3.23

Program Listing

```

*****
!*          PROGRAM FEM1D          *
!*          1-D BAR ELEMENT        *
!*          WITH MULTI-POINT CONSTRAINTS *
!*          T.R.Chandrupatla and A.D.Belegundu *
*****

DefInt I-N
DefDbl A-H, O-Z
Dim NN, NE, NM, NDIM, NEN, NDN
Dim ND, NL, NMPC, NBW
Dim X(), NOC(), F(), AREA(), MAT(), DT(), S()
Dim PM(), NU(), U(), MPC(), BT(), Stress(), React()
Dim CNST
Dim Title As String, File1 As String, File2 As String
Dim Dummy As String
Private Sub cmdEnd_Click()
    End
End Sub

'===== MAIN PROGRAM =====
Private Sub cmdStart_Click()
    Call InputData
    Call Bandwidth
    Call Stiffness
    Call ModifyForBC
    Call BandSolver
    Call StressCalc
    Call ReactionCalc
    Call Output
    cmdView.Enabled = True
    cmdStart.Enabled = False
End Sub

'=====

```

```

'===== DATA INPUT FROM A FILE =====
Private Sub InputData()
    File1 = InputBox("Input File d:\dir\fileName.ext", "Name of File")
    Open File1 For Input As #1
    Line Input #1, Dummy: Input #1, Title
    Line Input #1, Dummy: Input #1, NN, NE, NM, NDIM, NEN, NDN
    Line Input #1, Dummy: Input #1, ND, NL, NMPC
    ReDim X(NN), NOC(NE, NEN), F(NN), AREA(NE), MAT(NE), DT(NE)
    ReDim PM(NM, 2), NU(ND), U(ND), MPC(NMPC, 2), BT(NMPC, 3)
    '----- READ DATA -----
    '----- Coordinates -----
    Line Input #1, Dummy
    For I = 1 To NN
        Input #1, N
        Input #1, X(N)
    Next I

```

continued

```

'----- Connectivity -----
Line Input #1, Dummy
For I = 1 To NE
  Input #1, N
  Input #1, NOC(N, 1), NOC(N, 2)
  Input #1, MAT(N), AREA(N), DT(N)
Next I
'----- Specified Displacements -----
Line Input #1, Dummy
For I = 1 To ND
  Input #1, NU(I), U(I)
Next I
'----- Component Loads -----
Line Input #1, Dummy
For I = 1 To NL
  Input #1, N
  Input #1, F(N)
Next I
'----- Material Properties -----
Line Input #1, Dummy
For I = 1 To NM
  Input #1, N
  For J = 1 To 2
    Input #1, PM(N, J)
  Next J
Next I
'----- Multi-point Constraints B1*Q1+B2*Qj=B0 -----
If NMPC > 0 Then
  Line Input #1, Dummy
  For I = 1 To NMPC
    Input #1, BT(I, 1), MPC(I, 1), BT(I, 2), MPC(I, 2), BT(I, 3)
  Next I
End If
Close #1
End Sub

```

```

'----- BANDWIDTH EVALUATION -----
Private Sub Bandwidth()
'----- Bandwidth Evaluation -----
NBW = 0
For N = 1 To NE
  NABS = NDN * Abs(NOC(N, 1) - NOC(N, 2)) + 1
  If NBW < NABS Then NBW = NABS
Next N
For I = 1 To NMPC
  NABS = Abs(MPC(I, 1) - MPC(I, 2)) + 1
  If NBW < NABS Then NBW = NABS
Next I
End Sub

```

```

===== ELEMENT STIFFNESS AND ASSEMBLY =====
Private Sub Stiffness()
  ReDim S(NN, NBW)
  '----- Stiffness Matrix -----
  For N = 1 To NE
    N1 = NOC(N, 1): N2 = NOC(N, 2): N3 = MAT(N)
    X21 = X(N2) - X(N1): EL = Abs(X21)
    EAL = PM(N3, 1) * AREA(N) / EL
    TL = PM(N3, 1) * PM(N3, 2) * DT(N) * AREA(N) * EL / X21
    '----- Temperature Loads -----
    F(N1) = F(N1) - TL
    F(N2) = F(N2) + TL
    '----- Element Stiffness in Global Locations -----
    S(N1, 1) = S(N1, 1) + EAL
    S(N2, 1) = S(N2, 1) + EAL
    IR = N1: If IR > N2 Then IR = N2
    IC = Abs(N2 - N1) + 1
    S(IR, IC) = S(IR, IC) - EAL
  Next N
End Sub
=====

```

```

===== MODIFICATION FOR BOUNDARY CONDITIONS =====
Private Sub ModifyForBC()
  '----- Decide Penalty Parameter CNST -----
  CNST = 0
  For I = 1 To NN
    If CNST < S(I, 1) Then CNST = S(I, 1)
  Next I
  CNST = CNST * 10000
  '----- Modify for Boundary Conditions -----
  '---- Displacement BC ----
  For I = 1 To ND
    N = NU(I)
    S(N, 1) = S(N, 1) + CNST
    F(N) = F(N) + CNST * U(I)
  Next I
  '---- Multi-point Constraints ----
  For I = 1 To NMPC
    I1 = MPC(I, 1): I2 = MPC(I, 2)
    S(I1, 1) = S(I1, 1) + CNST * BT(I, 1) * BT(I, 1)
    S(I2, 1) = S(I2, 1) + CNST * BT(I, 2) * BT(I, 2)
    IR = I1: If IR > I2 Then IR = I2
    IC = Abs(I2 - I1) + 1
    S(IR, IC) = S(IR, IC) + CNST * BT(I, 1) * BT(I, 2)
    F(I1) = F(I1) + CNST * BT(I, 1) * BT(I, 3)
    F(I2) = F(I2) + CNST * BT(I, 2) * BT(I, 3)
  Next I
End Sub
=====

```

```

===== SOLUTION OF EQUATIONS BANDSOLVER =====
Private Sub BandSolver()
'----- Equation Solving using Band Solver -----
  N = NN
'----- Forward Elimination -----
  For K = 1 To N - 1
    NBK = N - K + 1
    If N - K + 1 > NBW Then NBK = NBW
    For I = K + 1 To NBK + K - 1
      I1 = I - K + 1
      C = S(K, I1) / S(K, 1)
      For J = I To NBK + K - 1
        J1 = J - I + 1
        J2 = J - K + 1
        S(I, J1) = S(I, J1) - C * S(K, J2)
      Next J
      F(I) = F(I) - C * F(K)
    Next I
  Next K
'----- Back Substitution -----
  F(N) = F(N) / S(N, 1)
  For II = 1 To N - 1
    I = N - II
    NBI = N - I + 1
    If N - I + 1 > NBW Then NBI = NBW
    Sum = 0!
    For J = 2 To NBI
      Sum = Sum + S(I, J) * F(I + J - 1)
    Next J
    F(I) = (F(I) - Sum) / S(I, 1)
  Next II
End Sub
=====

```

```

===== STRESS CALCULATIONS =====
Private Sub StressCalc()
  ReDim Stress(NE)
'----- Stress Calculation -----
  For N = 1 To NE
    N1 = NOC(N, 1): N2 = NOC(N, 2): N3 = MAT(N)
    EPS = (F(N2) - F(N1)) / (X(N2) - X(N1))
    Stress(N) = PM(N3, 1) * (EPS - PM(N3, 2) * DT(N))
  Next N
End Sub
=====

```



```

===== REACTION CALCULATIONS =====
Private Sub ReactionCalc()
  ReDim React(ND)
  '----- Reaction Calculation -----
  For I = 1 To ND
    N = NU(I)
    React(I) = CNST * (U(I) - F(N))
  Next I
End Sub
=====

```

```

===== OUTPUT =====
Private Sub Output()
  '----- Print Displacements, Stresses, and Reactions
  File2 = InputBox("Output File d:\dir\fileName.ext", "Name of File")
  Open File2 For Output As #2
  Print #2, "Program FEM1D - CHANDRUPATLA & BELEGUNDU"
  Print #2, Title
  '----- Displacements -----
  Print #2, "NODE NO.", "DISPLACEMENT"
  For I = 1 To NN
    Print #2, I, Format(F(I), "0.0000E+00")
  Next I
  '----- Stresses -----
  Print #2, "ELEM NO.", "STRESS"
  For N = 1 To NE
    Print #2, N, Format(Stress(N), "0.0000E+00")
  Next N
  '----- Reactions -----
  Print #2, "NODE NO.", "REACTION"
  For I = 1 To ND
    N = NU(I)
    Print #2, N, Format(React(I), "0.0000E+00")
  Next I
  Close #2
  picBox.Print "RESULTS ARE IN FILE "; File2
End Sub

Private Sub cmdView_Click()
  Dim ALine As String, CRLF As String, File1 As String
  CRLF = Chr$(13) + Chr$(10)
  picBox.Visible = False
  txtView.Visible = True
  txtView.Text = ""
  Open File2 For Input As #1
  Do While Not EOF(1)
    Line Input #1, ALine
    txtView.Text = txtView.Text + ALine + CRLF
  Loop
  Close #1
End Sub

```

Trusses

4.1 INTRODUCTION

The finite element analysis of truss structures is presented in this chapter. Two-dimensional trusses (or plane trusses) are treated in Section 4.2. In Section 4.3, this treatment is readily generalized to handle three-dimensional trusses. A typical plane truss is shown in Fig. 4.1. A truss structure consists only of two-force members. That is, every truss element is in direct tension or compression (Fig. 4.2). In a truss, it is required that all loads and reactions are applied only at the joints and that all members are connected together at their ends by frictionless pin joints. Every engineering student has, in a course on statics, analyzed trusses using the method of joints and the method of sections. These methods, while illustrating the fundamentals of statics, become tedious when applied to large-scale statically indeterminate truss structures. Further, joint displacements are not readily obtainable. The finite element method on the other hand is applicable to statically determinate or indeterminate structures alike. The finite element method also provides joint deflections. Effects of temperature changes and support settlements can also be routinely handled.

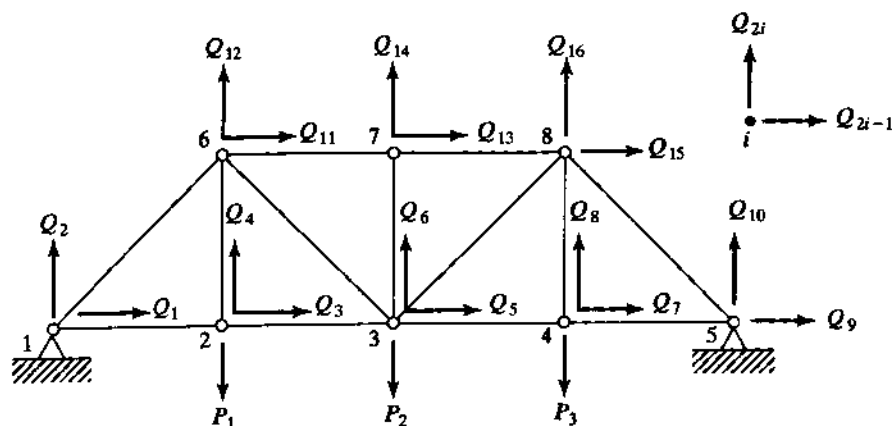


FIGURE 4.1 A two-dimensional truss.

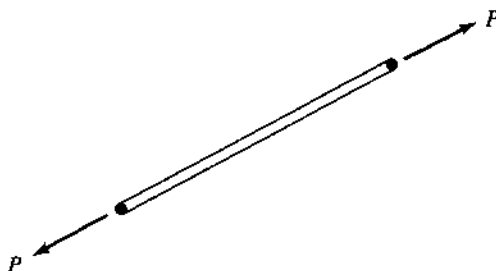


FIGURE 4.2 A two-force member.

4.2 PLANE TRUSSES

Modeling aspects discussed in Chapter 3 are now extended to the two-dimensional truss. The steps involved are discussed here.

Local and Global Coordinate Systems

The main difference between the one-dimensional structures considered in Chapter 3 and trusses is that the elements of a truss have various orientations. To account for these different orientations, **local** and **global** coordinate systems are introduced as follows:

A typical plane-truss element is shown in local and global coordinate systems in Fig. 4.3. In the local numbering scheme, the two nodes of the element are numbered 1 and 2. The local coordinate system consists of the x' -axis, which runs along the element from node 1 toward node 2. All quantities in the local coordinate system will be denoted by a prime ('). The global x -, y -coordinate system is fixed and does not depend on the orientation of the element. Note that x , y , and z form a right-handed coordinate system with the z -axis coming straight out of the paper. In the global coordinate system,

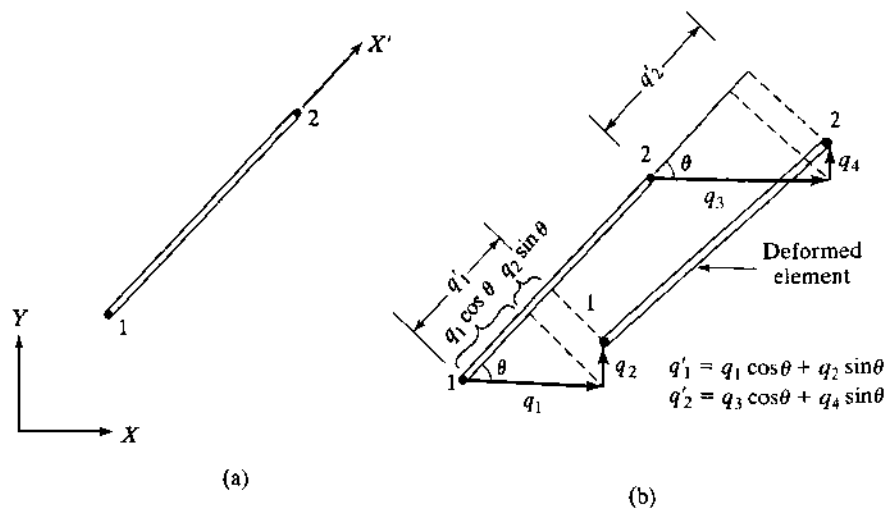


FIGURE 4.3 A two-dimensional truss element in (a) a local coordinate system and (b) a global coordinate system.

every node has two degrees of freedom (dofs). A systematic numbering scheme is adopted here: A node whose global node number is j has associated with it dofs $2j - 1$ and $2j$. Further, the global displacements associated with node j are Q_{2j-1} and Q_{2j} , as shown in Fig. 4.1.

Let q'_1 and q'_2 be the displacements of nodes 1 and 2, respectively, in the local coordinate system. Thus, the element displacement vector in the local coordinate system is denoted by

$$\mathbf{q}' = [q'_1, q'_2]^T \quad (4.1)$$

The element displacement vector in the global coordinate system is a (4×1) vector denoted by

$$\mathbf{q} = [q_1, q_2, q_3, q_4]^T \quad (4.2)$$

The relationship between \mathbf{q}' and \mathbf{q} is developed as follows: In Fig. 4.3b, we see that q'_1 equals the sum of the projections of q_1 and q_2 onto the x' -axis. Thus,

$$q'_1 = q_1 \cos \theta + q_2 \sin \theta \quad (4.3a)$$

Similarly,

$$q'_2 = q_3 \cos \theta + q_4 \sin \theta \quad (4.3b)$$

At this stage, the **direction cosines** ℓ and m are introduced as $\ell = \cos \theta$ and $m = \sin \theta$ ($= \cos \phi$). These direction cosines are the cosines of the angles that the local x' -axis makes with the global x -, y -axes, respectively. Equations 4.3a and 4.3b can now be written in matrix form as

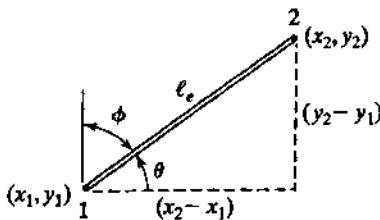
$$\mathbf{q}' = \mathbf{Lq} \quad (4.4)$$

where the **transformation matrix L** is given by

$$\mathbf{L} = \begin{bmatrix} \ell & m & 0 & 0 \\ 0 & 0 & \ell & m \end{bmatrix} \quad (4.5)$$

Formulas for Calculating ℓ and m

Simple formulas are now given for calculating the direction cosines ℓ and m from nodal coordinate data. Referring to Fig. 4.4, let (x_1, y_1) and (x_2, y_2) be the coordinates of nodes 1 and 2, respectively. We then have



$$\begin{aligned} \ell &= \cos \theta = \frac{x_2 - x_1}{\ell_e} \\ m &= \cos \phi = \frac{y_2 - y_1}{\ell_e} (= \sin \theta) \\ \ell_e &= \sqrt{(x_2 - x_1)^2 + (y_2 - y_1)^2} \end{aligned}$$

FIGURE 4.4 Direction cosines.

$$\ell = \frac{x_2 - x_1}{\ell_e} \quad m = \frac{y_2 - y_1}{\ell_e} \quad (4.6)$$

where the length ℓ_e is obtained from

$$\ell_e = \sqrt{(x_2 - x_1)^2 + (y_2 - y_1)^2} \quad (4.7)$$

The expressions in Eqs. 4.6 and 4.7 are obtained from nodal coordinate data and can readily be implemented in a computer program.

Element Stiffness Matrix

An important observation will now be made: *The truss element is a one-dimensional element when viewed in the local coordinate system.* This observation allows us to use previously developed results in Chapter 3 for one-dimensional elements. Consequently, from Eq. 3.26, the element stiffness matrix for a truss element in the local coordinate system is given by

$$\mathbf{k} = \frac{E_e A_e}{\ell_e} \begin{bmatrix} 1 & -1 \\ -1 & 1 \end{bmatrix} \quad (4.8)$$

where A_e is the element cross-sectional area and E_e is Young's modulus. The problem at hand is to develop an expression for the element stiffness matrix in the global coordinate system. This is obtainable by considering the strain energy in the element. Specifically, the element strain energy in local coordinates is given by

$$U_e = \frac{1}{2} \mathbf{q}'^T \mathbf{k}' \mathbf{q}' \quad (4.9)$$

Substituting for $\mathbf{q}' = \mathbf{L}\mathbf{q}$ into Eq. 4.9, we get

$$U_e = \frac{1}{2} \mathbf{q}^T [\mathbf{L}^T \mathbf{k}' \mathbf{L}] \mathbf{q} \quad (4.10)$$

The strain energy in global coordinates can be written as

$$U_e = \frac{1}{2} \mathbf{q}^T \mathbf{k} \mathbf{q} \quad (4.11)$$

where \mathbf{k} is the element stiffness matrix in global coordinates. From the previous equation, we obtain the element stiffness matrix in global coordinates as

$$\mathbf{k} = \mathbf{L}^T \mathbf{k}' \mathbf{L} \quad (4.12)$$

Substituting for \mathbf{L} from Eq. 4.5 and for \mathbf{k}' from Eq. 4.8, we get

$$\mathbf{k} = \frac{E_e A_e}{\ell_e} \begin{bmatrix} \ell^2 & \ell m & -\ell^2 & -\ell m \\ \ell m & m^2 & -\ell m & -m^2 \\ -\ell^2 & -\ell m & \ell^2 & \ell m \\ -\ell m & -m^2 & \ell m & m^2 \end{bmatrix} \quad (4.13)$$

The element stiffness matrices are assembled in the usual manner to obtain the structural stiffness matrix. This assembly is illustrated in Example 4.1. The computer logic for directly placing element stiffness matrices into global matrices for banded and skyline solutions is explained in Section 4.4.

The derivation of the result $\mathbf{k} = \mathbf{L}^T \mathbf{k}' \mathbf{L}$ also follows from Galerkin's variational principle. The virtual work δW as a result of virtual displacement ψ' is

$$\delta W = \psi'^T (\mathbf{k}' \mathbf{q}') \quad (4.14a)$$

Since $\psi' = \mathbf{L}\psi$ and $\mathbf{q}' = \mathbf{L}\mathbf{q}$, we have

$$\begin{aligned} \delta W &= \psi^T [\mathbf{L}^T \mathbf{k}' \mathbf{L}] \mathbf{q} \\ &= \psi^T \mathbf{k} \mathbf{q} \end{aligned} \quad (4.14b)$$

Stress Calculations

Expressions for the element stresses can be obtained by noting that a truss element in local coordinates is a simple two-force member (Fig. 4.2). Thus, the stress σ in a truss element is given by

$$\sigma = E_e \epsilon \quad (4.15a)$$

Since the strain ϵ is the change in length per unit original length,

$$\begin{aligned} \sigma &= E_e \frac{q'_2 - q'_1}{\ell_e} \\ &= \frac{E_e}{\ell_e} [-1 \quad 1] \begin{Bmatrix} q'_1 \\ q'_2 \end{Bmatrix} \end{aligned} \quad (4.15b)$$

This equation can be written in terms of the global displacements \mathbf{q} using the transformation $\mathbf{q}' = \mathbf{L}\mathbf{q}$ as

$$\sigma = \frac{E_e}{\ell_e} [-1 \quad 1] \mathbf{L} \mathbf{q} \quad (4.15c)$$

Substituting for \mathbf{L} from Eq. 4.5 yields

$$\sigma = \frac{E_e}{\ell_e} [-\ell \quad -m \quad \ell \quad m] \mathbf{q} \quad (4.16)$$

Once the displacements are determined by solving the finite element equations, the stresses can be recovered from Eq. 4.16 for each element. Note that a positive stress implies that the element is in tension and a negative stress implies compression.

Example 4.1

Consider the four-bar truss shown in Fig. E4.1a. It is given that $E = 29.5 \times 10^6$ psi and $A_e = 1 \text{ in.}^2$ for all elements. Complete the following:

- Determine the element stiffness matrix for each element.
- Assemble the structural stiffness matrix \mathbf{K} for the entire truss.
- Using the elimination approach, solve for the nodal displacement.
- Recover the stresses in each element.
- Calculate the reaction forces.

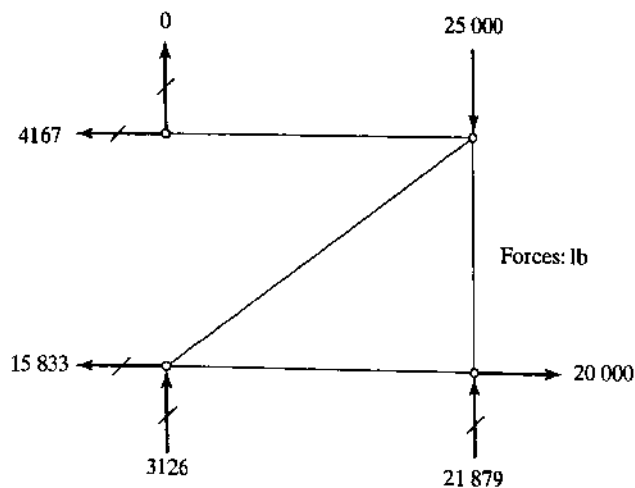
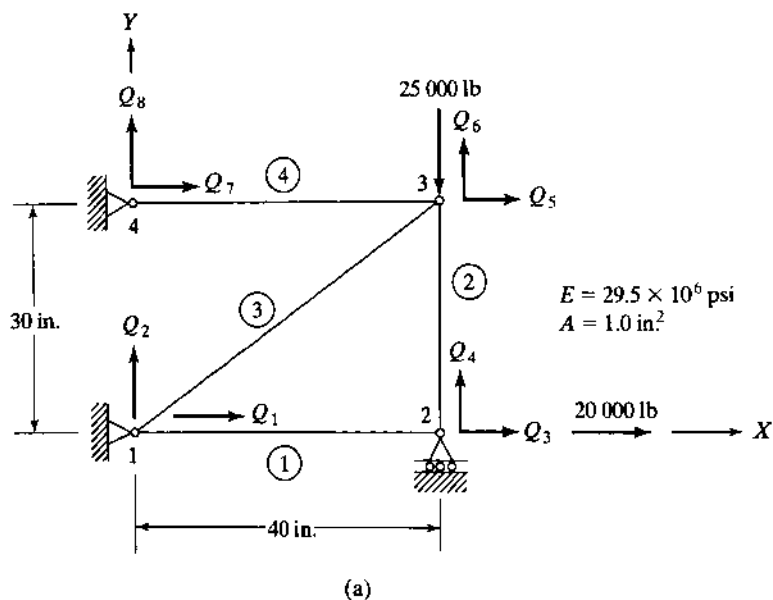


FIGURE E4.1

Solution

- (a) It is recommended that a *tabular* form be used for representing nodal coordinate data and element information. The nodal coordinate data are as follows:

| Node | x | y |
|------|----|----|
| 1 | 0 | 0 |
| 2 | 40 | 0 |
| 3 | 40 | 30 |
| 4 | 0 | 30 |

The element connectivity table is

| Element | 1 | 2 |
|---------|---|---|
| 1 | 1 | 2 |
| 2 | 3 | 2 |
| 3 | 1 | 3 |
| 4 | 4 | 3 |

Note that the user has a choice in defining element connectivity. For example, the connectivity of element 2 can be defined as 2-3 instead of 3-2 as in the previous table. However, calculations of the direction cosines will be consistent with the adopted connectivity scheme. Using formulas in Eqs. 4.6 and 4.7, together with the nodal coordinate data and the given element connectivity information, we obtain the direction cosines table:

| Element | ℓ_e | ℓ | m |
|---------|----------|--------|-----|
| 1 | 40 | 1 | 0 |
| 2 | 30 | 0 | -1 |
| 3 | 50 | 0.8 | 0.6 |
| 4 | 40 | 1 | 0 |

For example, the direction cosines of elements 3 are obtained as $\ell = (x_3 - x_1)/\ell_e = (40 - 0)/50 = 0.8$ and $m = (y_3 - y_1)/\ell_e = (30 - 0)/50 = 0.6$. Now, using Eq. 4.13, the element stiffness matrices for element 1 can be written as

$$\mathbf{k}^1 = \frac{29.5 \times 10^6}{40} \begin{bmatrix} 1 & 2 & 3 & 4 \\ 1 & 0 & -1 & 0 \\ 0 & 0 & 0 & 0 \\ -1 & 0 & 1 & 0 \\ 0 & 0 & 0 & 0 \end{bmatrix} \begin{matrix} \leftarrow \downarrow \text{Global dof} \\ 1 \\ 2 \\ 3 \\ 4 \end{matrix}$$

The global dofs associated with element 1, which is connected between nodes 1 and 2, are indicated in \mathbf{k}^1 earlier. These global dofs are shown in Fig. E4.1a and assist in assembling the various element stiffness matrices.

The element stiffness matrices of elements 2, 3, and 4 are as follows:

$$\mathbf{k}^2 = \frac{29.5 \times 10^6}{30} \begin{bmatrix} 5 & 6 & 3 & 4 \\ 0 & 0 & 0 & 0 \\ 0 & 1 & 0 & -1 \\ 0 & 0 & 0 & 0 \\ 0 & -1 & 0 & 1 \end{bmatrix} \begin{matrix} 5 \\ 6 \\ 3 \\ 4 \end{matrix}$$

$$\mathbf{k}^3 = \frac{29.5 \times 10^6}{50} \begin{bmatrix} 1 & 2 & 5 & 6 \\ .64 & .48 & -.64 & -.48 \\ .48 & .36 & -.48 & -.36 \\ -.64 & -.48 & .64 & .48 \\ -.48 & -.36 & .48 & .36 \end{bmatrix} \begin{matrix} 1 \\ 2 \\ 5 \\ 6 \end{matrix}$$

$$\mathbf{k}^4 = \frac{29.5 \times 10^6}{40} \begin{bmatrix} 7 & 8 & 5 & 6 \\ 1 & 0 & -1 & 0 \\ 0 & 0 & 0 & 0 \\ -1 & 0 & 1 & 0 \\ 0 & 0 & 0 & 0 \end{bmatrix} \begin{matrix} 7 \\ 8 \\ 5 \\ 6 \end{matrix}$$

- (b) The structural stiffness matrix \mathbf{K} is now assembled from the element stiffness matrices. By adding the element stiffness contributions, noting the element connectivity, we get

$$\mathbf{K} = \frac{29.5 \times 10^6}{600} \begin{bmatrix} 1 & 2 & 3 & 4 & 5 & 6 & 7 & 8 \\ 22.68 & 5.76 & -15.0 & 0 & -7.68 & -5.76 & 0 & 0 \\ 5.76 & 4.32 & 0 & 0 & -5.76 & -4.32 & 0 & 0 \\ -15.0 & 0 & 15.0 & 0 & 0 & 0 & 0 & 0 \\ 0 & 0 & 0 & 20.0 & 0 & -20.0 & 0 & 0 \\ -7.68 & -5.76 & 0 & 0 & 22.68 & 5.76 & -15.0 & 0 \\ -5.76 & -4.32 & 0 & -20.0 & 5.76 & 24.32 & 0 & 0 \\ 0 & 0 & 0 & 0 & -15.0 & 0 & 15.0 & 0 \\ 0 & 0 & 0 & 0 & 0 & 0 & 0 & 0 \end{bmatrix} \begin{matrix} 1 \\ 2 \\ 3 \\ 4 \\ 5 \\ 6 \\ 7 \\ 8 \end{matrix}$$

- (c) The structural stiffness matrix \mathbf{K} given above needs to be modified to account for the boundary conditions. The elimination approach discussed in Chapter 3 will be used here. The rows and columns corresponding to dofs 1, 2, 4, 7, and 8, which correspond to fixed supports, are deleted from the \mathbf{K} matrix. The reduced finite element equations are given as

$$\frac{29.5 \times 10^6}{600} \begin{bmatrix} 15 & 0 & 0 \\ 0 & 22.68 & 5.76 \\ 0 & 5.76 & 24.32 \end{bmatrix} \begin{Bmatrix} Q_3 \\ Q_5 \\ Q_6 \end{Bmatrix} = \begin{Bmatrix} 20\,000 \\ 0 \\ -25\,000 \end{Bmatrix}$$

Solution of these equations yields the displacements

$$\begin{Bmatrix} Q_3 \\ Q_5 \\ Q_6 \end{Bmatrix} = \begin{Bmatrix} 27.12 \times 10^{-3} \\ 5.65 \times 10^{-3} \\ -22.25 \times 10^{-3} \end{Bmatrix} \text{ in.}$$

The nodal displacement vector for the entire structure can therefore be written as

$$\mathbf{Q} = [0, 0, 27.12 \times 10^{-3}, 0, 5.65 \times 10^{-3}, -22.25 \times 10^{-3}, 0, 0]^T \text{ in.}$$

- (d) The stress in each element can now be determined from Eq. 4.16, as shown below. The connectivity of element 1 is 1 - 2. Consequently, the nodal displacement vector for element 1 is given by $\mathbf{q} = [0, 0, 27.12 \times 10^{-3}, 0]^T$, and Eq. 4.16 yields

$$\begin{aligned} \sigma_1 &= \frac{29.5 \times 10^6}{40} [-1 \ 0 \ 1 \ 0] \begin{Bmatrix} 0 \\ 0 \\ 27.12 \times 10^{-3} \\ 0 \end{Bmatrix} \\ &= 20\,000.0 \text{ psi} \end{aligned}$$

The stress in member 2 is given by

$$\begin{aligned} \sigma_2 &= \frac{29.5 \times 10^6}{30} [0 \ 1 \ 0 \ -1] \begin{Bmatrix} 5.65 \times 10^{-3} \\ -22.25 \times 10^{-3} \\ +27.12 \times 10^{-3} \\ 0 \end{Bmatrix} \\ &= -21\,880.0 \text{ psi} \end{aligned}$$

Following similar steps, we get

$$\sigma_3 = -5208.0 \text{ psi}$$

$$\sigma_4 = 4167.0 \text{ psi}$$

- (e) The final step is to determine the support reactions. We need to determine the reaction forces along dofs 1, 2, 4, 7, and 8, which correspond to fixed supports. These are obtained by substituting for \mathbf{Q} into the original finite element equation $\mathbf{R} = \mathbf{KQ} - \mathbf{F}$. In this substitution, only those rows of \mathbf{K} corresponding to the support dofs are needed, and $\mathbf{F} = \mathbf{0}$ for these dofs. Thus, we have

$$\begin{Bmatrix} R_1 \\ R_2 \\ R_4 \\ R_7 \\ R_8 \end{Bmatrix} = \frac{29.5 \times 10^6}{600} \begin{bmatrix} 22.68 & 5.76 & -15.0 & 0 & -7.68 & -5.76 & 0 & 0 \\ 5.76 & 4.32 & 0 & 0 & -5.76 & -4.32 & 0 & 0 \\ 0 & 0 & 0 & 20.0 & 0 & -20.0 & 0 & 0 \\ 0 & 0 & 0 & 0 & -15.0 & 0 & 15.0 & 0 \\ 0 & 0 & 0 & 0 & 0 & 0 & 0 & 0 \end{bmatrix} \begin{Bmatrix} 0 \\ 0 \\ 27.12 \times 10^{-3} \\ 0 \\ 5.65 \times 10^{-3} \\ -22.25 \times 10^{-3} \\ 0 \\ 0 \end{Bmatrix}$$

which results in

$$\begin{Bmatrix} R_1 \\ R_2 \\ R_4 \\ R_7 \\ R_8 \end{Bmatrix} = \begin{Bmatrix} -15833.0 \\ 3126.0 \\ 21879.0 \\ -4167.0 \\ 0 \end{Bmatrix} \text{ lb}$$

A free body diagram of the truss with reaction forces and applied loads is shown in Fig. E4.1b. ■

Temperature Effects

The thermal stress problem is considered here. Since a truss element is simply a one-dimensional element when viewed in the local coordinate system, the element temperature load in the local coordinate system is given by (see Eq. 3.103b)

$$\Theta' = E_c A_c \epsilon_0 \begin{Bmatrix} -1 \\ 1 \end{Bmatrix} \quad (4.17)$$

where the initial strain ϵ_0 associated with a temperature change is given by

$$\epsilon_0 = \alpha \Delta T \quad (4.18)$$

in which α is the coefficient of thermal expansion, and ΔT is the average change in temperature in the element. It may be noted that the initial strain ϵ_0 can also be induced by forcing members into places that are either too long or too short, due to fabrication errors.

We will now express the load vector in Eq. 4.17 in the global coordinate system. Since the potential energy associated with this load is the same in magnitude whether measured in the local or global coordinate systems, we have

$$\mathbf{q}'^T \Theta' = \mathbf{q}^T \Theta \quad (4.19)$$

where Θ is the load vector in the global coordinate system. Substituting for $\mathbf{q}' = \mathbf{L}\mathbf{q}$ into Eq. 4.19, we get

$$\mathbf{q}^T \mathbf{L}^T \Theta' = \mathbf{q}^T \Theta \quad (4.20)$$

Comparing the left and right sides of this equation, we obtain

$$\Theta = \mathbf{L}^T \Theta' \quad (4.21)$$

Substituting for \mathbf{L} from Eq. 4.5, we can write down the expression for the element temperature load as

$$\Theta^e = E_e A_e \epsilon_0 \begin{Bmatrix} -\ell \\ -m \\ \ell \\ m \end{Bmatrix} \quad (4.22)$$

The temperature loads, along with other externally applied loads, are assembled in the usual manner to obtain the nodal load vector \mathbf{F} . Once the displacements are obtained by solving the finite element equations, the stress in each truss element is obtained from (see Eq. 3.100)

$$\sigma = E(\epsilon - \epsilon_0) \quad (4.23)$$

This equation for the element stress can be simplified by using Eq. 4.16 and noting that $\epsilon_0 = \alpha \Delta T$, to obtain

$$\sigma = \frac{E_e}{\ell_e} [-\ell \quad -m \quad \ell \quad m] \mathbf{q} - E_e \alpha \Delta T \quad (4.24)$$

Example 4.2

The four-bar truss of Example 4.1 is considered here, but the loading is different. Take $E = 29.5 \times 10^6$ psi and $\alpha = 1/150\,000$ per $^\circ\text{F}$.

- There is an increase in temperature of 50°F in bars 2 and 3 only (Fig. E4.2a). There are no other loads on the structure. Determine the nodal displacements and element stresses as a result of this temperature increase. Use the elimination approach.
- A support settlement effect is considered here. Node 2 settles by 0.12 in. vertically down, and in addition, two point loads are applied on the structure (Fig. E4.2b). Write down (without solving) the equilibrium equations $\mathbf{K}\mathbf{Q} = \mathbf{F}$, where \mathbf{K} and \mathbf{F} are the modified structural stiffness matrix and load vector, respectively. Use the penalty approach.
- Use the program TRUSS2 to obtain the solution to part (b).

Solution

- The stiffness matrix for the truss structure has already been developed in Example 4.1. Only the load vector needs to be assembled due to the temperature increase. Using Eq. 4.22, the temperature load as a result of temperature increases in elements 2 and 3 are, respectively,

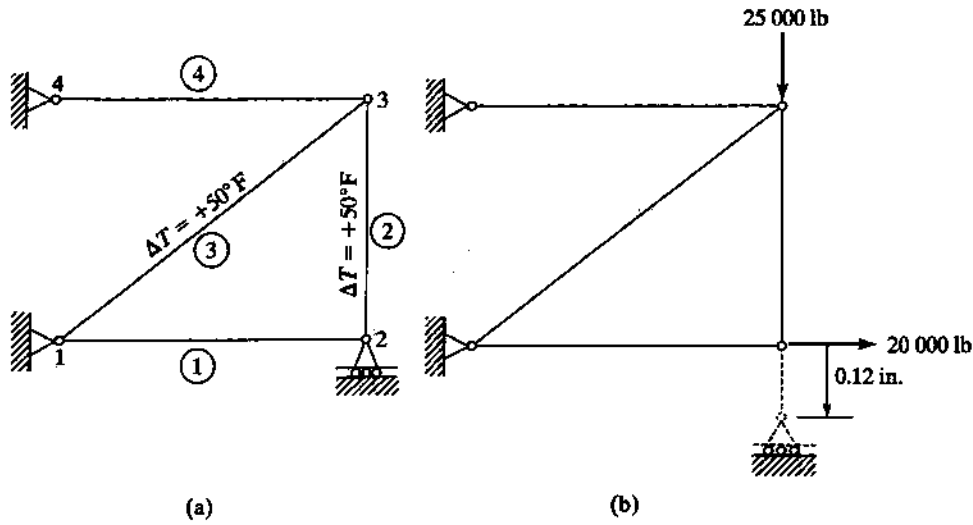


FIGURE E4.2

$$\theta^2 = \frac{29.5 \times 10^6 \times 50}{150,000} \begin{Bmatrix} 0 \\ 1 \\ 0 \\ -1 \end{Bmatrix} \begin{matrix} \downarrow \text{Global dof} \\ 5 \\ 6 \\ 3 \\ 4 \end{matrix}$$

and

$$\theta^3 = \frac{29.5 \times 10^6 \times 50}{150,000} \begin{Bmatrix} -0.8 \\ -0.6 \\ 0.8 \\ 0.6 \end{Bmatrix} \begin{matrix} 1 \\ 2 \\ 5 \\ 6 \end{matrix}$$

The θ^2 and θ^3 vectors contribute to the global load vector F . Using the elimination approach, we can delete all rows and columns corresponding to support dofs in K and F . The resulting finite element equations are

$$\frac{29.5 \times 10^6}{600} \begin{bmatrix} 15.0 & 0 & 0 \\ 0 & 22.68 & 5.76 \\ 0 & 5.76 & 24.32 \end{bmatrix} \begin{Bmatrix} Q_3 \\ Q_5 \\ Q_6 \end{Bmatrix} = \begin{Bmatrix} 0 \\ 7866.7 \\ 15733.3 \end{Bmatrix}$$

which yield

$$\begin{Bmatrix} Q_3 \\ Q_5 \\ Q_6 \end{Bmatrix} = \begin{Bmatrix} 0 \\ 0.003951 \\ 0.01222 \end{Bmatrix} \text{ in.}$$

The element stresses can now be obtained from Eq. 4.24. For example, the stress in element 2 is given as

$$\begin{aligned} \sigma_2 &= \frac{29.5 \times 10^6}{30} [0 \quad 1 \quad 0 \quad -1] \begin{Bmatrix} 0.003951 \\ 0.01222 \\ 0 \\ 0 \end{Bmatrix} - \frac{29.5 \times 10^6 \times 50}{150,000} \\ &= -8631.7 \text{ psi} \end{aligned}$$

The complete stress solution is

$$\begin{Bmatrix} \sigma_1 \\ \sigma_2 \\ \sigma_3 \\ \sigma_4 \end{Bmatrix} = \begin{Bmatrix} 0 \\ 2183 \\ -3643 \\ 2914 \end{Bmatrix} \text{ psi}$$

- (b) Support 2 settles by 0.12 in. vertically down, and two concentrated forces are applied (Fig. E4.2b). In the penalty approach for handling boundary conditions (Chapter 3), recall that a large spring constant C is added to the diagonal elements in the structural stiffness matrix at those dofs where the displacements are specified. Typically, C may be chosen 10^4 times the largest diagonal element of the unmodified stiffness matrix (see Eq. 3.80). Further, a force Ca is added to the force vector, where a is the specified displacement. In this example, for dof 4, $a = -0.12$ in., and consequently, a force equal to $-0.12C$ gets added to the fourth location in the force vector. Consequently, the modified finite element equations are given by

$$\frac{29.5 \times 10^6}{600} \begin{bmatrix} 22.68 + C & 5.76 & -15.0 & 0 & -7.68 & -5.76 & 0 & 0 \\ & 4.32 + C & 0 & 0 & -5.76 & -4.32 & 0 & 0 \\ & & 15.0 & 0 & 0 & 0 & 0 & 0 \\ & & & 20.0 + C & 0 & -20.0 & 0 & 0 \\ & & & & 22.68 & 5.76 & -15.0 & 0 \\ & & & & & 24.32 & 0 & 0 \\ & & & & & & 15.0 + C & 0 \\ & & & & & & & C \end{bmatrix} \begin{Bmatrix} Q_1 \\ Q_2 \\ Q_3 \\ Q_4 \\ Q_5 \\ Q_6 \\ Q_7 \\ Q_8 \end{Bmatrix} = \begin{Bmatrix} 0 \\ 0 \\ 20\,000 \\ -0.12C \\ 0 \\ -25\,000.0 \\ 0 \\ 0 \end{Bmatrix}$$

Symmetric

- (c) Obviously, the equations in (b) are too large for hand calculations. In the program TRUSS, that is provided, these equations are automatically generated and solved from the user's input data. The output from the program is

$$\begin{Bmatrix} Q_3 \\ Q_4 \\ Q_5 \\ Q_6 \end{Bmatrix} = \begin{Bmatrix} 0.0271200 \\ -0.1200145 \\ 0.0323242 \\ -0.1272606 \end{Bmatrix} \text{ in.}$$

and

$$\begin{Bmatrix} \sigma_1 \\ \sigma_2 \\ \sigma_3 \\ \sigma_4 \end{Bmatrix} = \begin{Bmatrix} 20\,000.0 \\ -7\,125.3 \\ -29\,791.7 \\ 23\,833.3 \end{Bmatrix} \text{ psi}$$

4.3 THREE-DIMENSIONAL TRUSSES

The 3-D truss element can be treated as a straightforward generalization of the 2-D truss element discussed earlier. The local and global coordinate systems for a 3-D truss element are shown in Fig. 4.5. Note that the local coordinate system is again the x' -axis running along the element, since a truss element is simply a two-force member. Consequently, the nodal displacement vector in local coordinates is

$$\mathbf{q}' = [q'_1, q'_2]^T \quad (4.25)$$

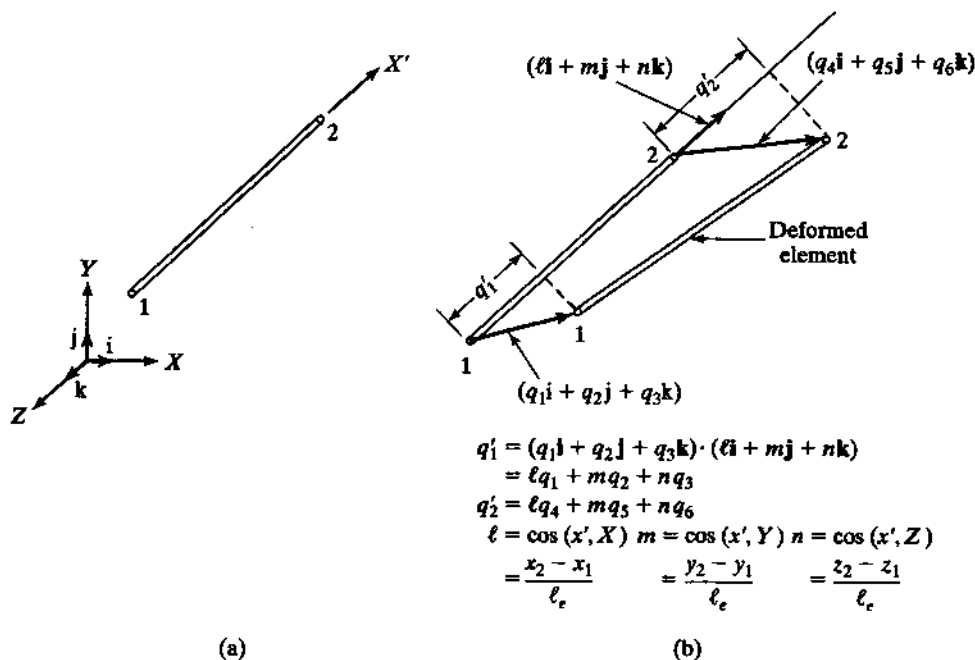


FIGURE 4.5 A three-dimensional truss element in local and global coordinate systems.

The nodal displacement vector in global coordinates is now (Fig. 4.5b)

$$\mathbf{q} = [q_1, q_2, q_3, q_4, q_5, q_6]^T \quad (4.26)$$

Referring to Fig. 4.5, we find that the transformation between local and global coordinates is

$$\mathbf{q}' = \mathbf{L}\mathbf{q} \quad (4.27)$$

where the transformation matrix \mathbf{L} is given by

$$\mathbf{L} = \begin{bmatrix} \ell & m & n & 0 & 0 & 0 \\ 0 & 0 & 0 & \ell & m & n \end{bmatrix} \quad (4.28)$$

in which ℓ , m , and n are the direction cosines of the local x' -axis with respect to the global x -, y -, and z -axes, respectively. The element stiffness matrix in global coordinates is given by Eq. 4.12, which yields

$$\mathbf{k} = \frac{E_c A_c}{\ell_e} \begin{bmatrix} \ell^2 & \ell m & \ell n & -\ell^2 & -\ell m & -\ell n \\ \ell m & m^2 & mn & -\ell m & -m^2 & -mn \\ \ell n & mn & n^2 & -\ell n & -mn & -n^2 \\ -\ell^2 & -\ell m & -\ell n & \ell^2 & \ell m & \ell n \\ -\ell m & -m^2 & -mn & \ell m & m^2 & mn \\ -\ell n & -mn & -n^2 & \ell n & mn & n^2 \end{bmatrix} \quad (4.29)$$

The formulas for calculating ℓ , m , and n are

$$\ell = \frac{x_2 - x_1}{\ell_e} \quad m = \frac{y_2 - y_1}{\ell_e} \quad n = \frac{z_2 - z_1}{\ell_e} \quad (4.30)$$

where the length ℓ_e of the element is given by

$$\ell_e = \sqrt{(x_2 - x_1)^2 + (y_2 - y_1)^2 + (z_2 - z_1)^2} \quad (4.31)$$

Generalizations of the element stress and element temperature load expressions are left as an exercise.

4.4 ASSEMBLY OF GLOBAL STIFFNESS MATRIX FOR THE BANDED AND SKYLINE SOLUTIONS

The solution of the finite element equations should take advantage of symmetry and sparsity of the global stiffness matrix. Two methods, the banded approach and the skyline approach, are discussed in Chapter 2. In the banded approach, the elements of each element stiffness matrix \mathbf{k}^e are directly placed in a banded matrix \mathbf{S} . In the skyline approach, the elements of \mathbf{k}^e are placed in a vector form with certain identification pointers. The bookkeeping aspects of this assembly procedure for banded and skyline solution are discussed in the sections that follow.

Assembly for Banded Solution

The assembly of elements of \mathbf{k}^e into a banded global stiffness matrix \mathbf{S} is now discussed for a two-dimensional truss element. Consider an element e whose connectivity is indicated as follows:

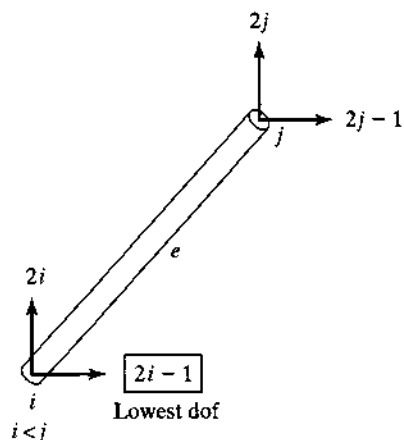
| | | | |
|---------|-----|-----|--------------------|
| Element | 1 | 2 | ← Local Node Nos. |
| e | i | j | ← Global Node Nos. |

The element stiffness with its associated degrees of freedom are

$$\mathbf{k}^e = \begin{bmatrix} 2i-1 & 2i & 2j-1 & 2j & \leftarrow \text{Global dofs} \\ k_{11} & k_{12} & k_{13} & k_{14} & 2i-1 \\ & & k_{22} & k_{23} & 2i \\ & & & k_{33} & 2j-1 \\ \text{Symmetric} & & & & k_{44} & 2j \end{bmatrix} \quad (4.32)$$

The principal diagonal of \mathbf{k}^e is placed in the first column of \mathbf{S} , the next-to-principal diagonal is placed in the second column, and so on. Thus, the correspondence between elements in \mathbf{k}^e and \mathbf{S} is given by (see Eq. 2.39)

$$k_{\alpha,\beta}^e \rightarrow S_{p,q-p+1} \quad (4.33)$$



| Element e | |
|---------------------|---------------------------------|
| Location No. I | Skyline Height $ID(I)$ |
| $2i - 1$ | $\max(1, \text{OLD})$ |
| $2i$ | $\max(2, \text{OLD})$ |
| $2j - 1$ | $\max(2j - 2i + 1, \text{OLD})$ |
| $2j$ | $\max(2j - 2i + 2, \text{OLD})$ |

$\max(X, \text{OLD}) = \text{REPLACE by } X \text{ if } X > \text{OLD}$
(start value of OLD = 0)

FIGURE 4.6 Skyline heights.

the vector ID . Then, starting from location $I = 2$, replacing the location at I by the sum $ID(I) + ID(I - 1)$ gives the pointer numbers as discussed in Chapter 2.

The next step involves assembling the element stiffness values into the column vector A . The correspondence of the global locations of the square stiffness matrix coming from an element shown in Fig. 4.6 are clearly presented in Fig. 4.7, using the diagonal pointers discussed previously. The details presented earlier have been implemented in program TRUSSKY. Other programs provided may be similarly modified for skyline solution instead of banded solution.

| | | Column | | | | |
|---------------------|--|-----------------|-----------------|---------------------------------|-----------------------------|----------|
| | | $2i - 1$ | $2i$ | $2j - 1$ | $2j$ | Row |
| Column vector A → | | $A[ID(2i - 1)]$ | $A[ID(2i) - 1]$ | $A[ID(2j - 1) - (2j - 2i)]$ | $A[ID(2j) - (2j - 2i + 1)]$ | $2i - 1$ |
| | | | $A[ID(2i)]$ | $A[ID(2j - 1) - (2j - 1 - 2i)]$ | $A[ID(2j) - (2j - 2i)]$ | $2i$ |
| | | | | $A[ID(2j - 1)]$ | $A[ID(2j) - 1]$ | $2j - 1$ |
| | | | | | $A[ID(2j)]$ | $2j$ |

FIGURE 4.7 Stiffness locations in column vector form for skyline solution.

Input Data File

```

<< 2D TRUSS ANALYSIS >>
EXAMPLE 4.1
NN NE NM NDIM NEN NDN
4 4 1 2 2 2
ND NL NMPC
5 2 0
Node# X Y
1 0 0
2 40 0
3 40 30
4 0 30
Elem# N1 N2 Mat# Area TempRise
1 1 2 1 1 0
2 3 2 1 1 0
3 3 1 1 1 0
4 4 3 1 1 0
DOF# Displacement
1 0
2 0
4 0
7 0
8 0
DOF# Load
3 20000
6 -25000
MAT# E Alpha
1 29.5E6 12E-6
B1 i B2 j B3 (Multi-point constr. B1*Qi+B2*Qj=B3)
    
```

```

Program Truss2D - CHANDRUPATLA & BELEGUNDU
Output
EXAMPLE 4.1
NODE# X-Displ Y-Displ
1 1.3241E-06 -2.6138E-07
2 2.7120E-02 -1.8294E-06
3 5.6507E-03 -2.2247E-02
4 3.4850E-07 0.0000E+00
Elem# Stress
1 2.0000E+04
2 -2.1875E+04
3 -5.2089E+03
4 4.1671E+03
DOF# Reaction
1 -1.5833E+04
2 3.1254E+03
4 2.1875E+04
7 -4.1671E+03
8 0.0000E+00
    
```

PROBLEMS

- 4.1. Consider the truss element shown in Fig. P4.1. The x -, y -coordinates of the two nodes are indicated in the figure. If $\mathbf{q} = [1.5, 1.0, 2.1, 4.3]^T \times 10^{-2}$ in., determine the following:
- the vector \mathbf{q}' ,
 - the stress in the element,
 - the \mathbf{k} matrix, and
 - the strain energy in the element.

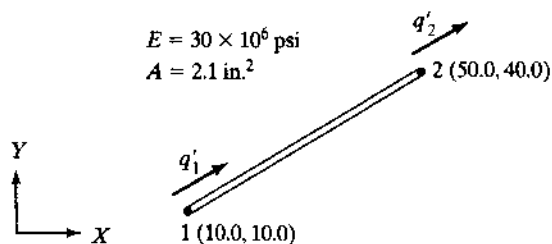


FIGURE P4.1

- 4.2. A truss element, with local node numbers 1 and 2, is shown in Fig. P4.2.
- What are the direction cosines ℓ and m .
 - Show the x' -axis, $q_1, q_2, q_3, q_4, q'_1, q'_2$ on the figure.
 - If $\mathbf{q} = [0., 0.01, -0.025, -0.05]^T$, determine q'_1, q'_2 .

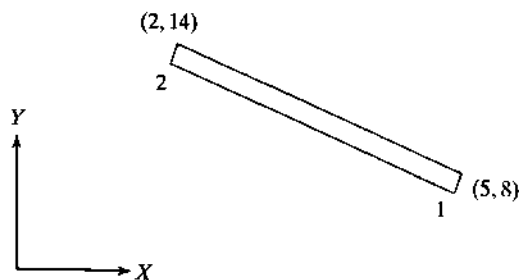


FIGURE P4.2

- 4.3. For the pin-jointed configuration shown in Fig. P4.3, determine the stiffness values K_{11}, K_{12} , and K_{22} of the global stiffness matrix.

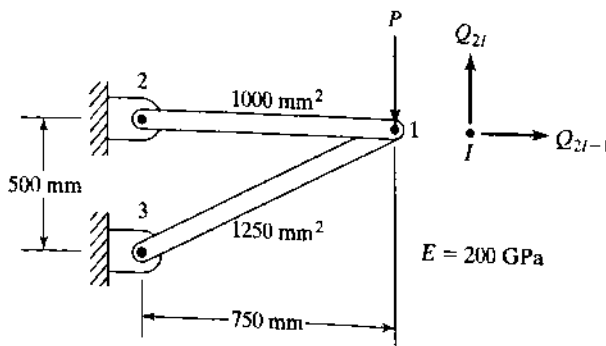


FIGURE P4.3

- 4.4. For the truss in Fig. P4.4, a horizontal load of $P = 4000$ lb is applied in the x direction at node 2.
- Write down the element stiffness matrix k for each element.
 - Assemble the K matrix.
 - Using the elimination approach, solve for Q .
 - Evaluate the stress in elements 2 and 3.
 - Determine the reaction force at node 2 in the y direction.

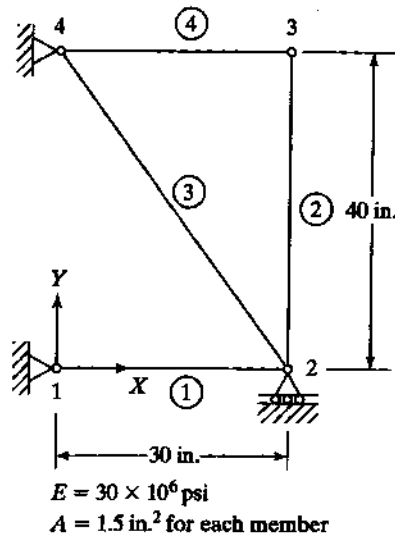


FIGURE P4.4

- 4.5. For Fig. P4.4, determine the stresses in each element due to the following support movement: support at node 2, 0.24 in. down.
- 4.6. For the two-bar truss shown in Fig. P4.6, determine the displacements of node 1 and the stress in element 1-3.

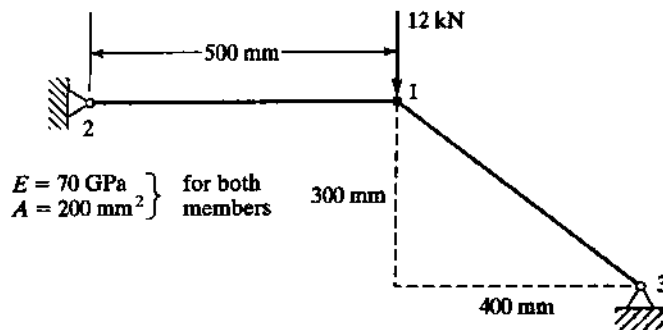


FIGURE P4.6

- 4.7. For the three-bar truss shown in Fig. P4.7, determine the displacements of node 1 and the stress in element 3.

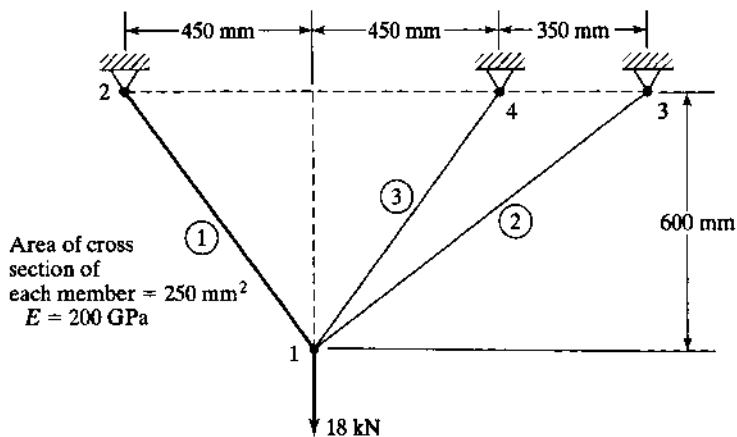


FIGURE P4.7

- 4.8. For the two-dimensional truss configuration shown in Fig. P4.8, determine the bandwidth for stiffness storage in a banded form. Choose an alternative numbering scheme and determine the corresponding bandwidth. Comment on the strategy that you use for decreasing the bandwidth.

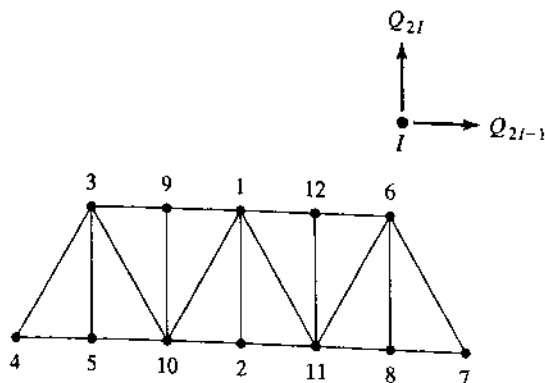


FIGURE P4.8

- 4.9. A small railroad bridge is constructed of steel members, all of which have a cross-sectional area of 3250 mm^2 . A train stops on the bridge, and the loads applied to the truss on one side of the bridge are as shown in Fig. P4.9. Estimate how much the point R moves horizontally because of this loading. Also determine the nodal displacements and element stresses.

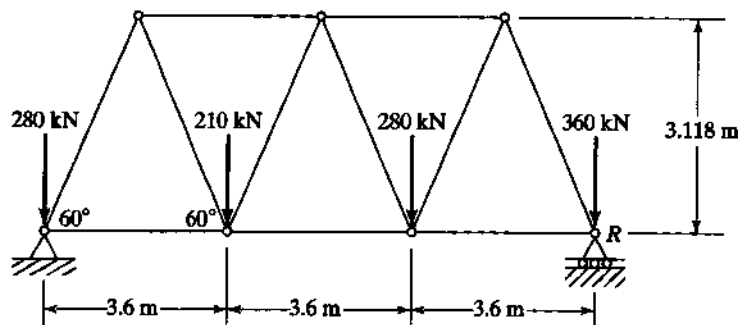


FIGURE P4.9

- 4.10. Consider the truss in Fig. P4.10 loaded as shown. Cross-sectional areas in square inches are shown in parentheses. Consider symmetry and model only one-half of the truss shown. Determine displacements and element stresses. Let $E = 30 \times 10^6 \text{ psi}$.

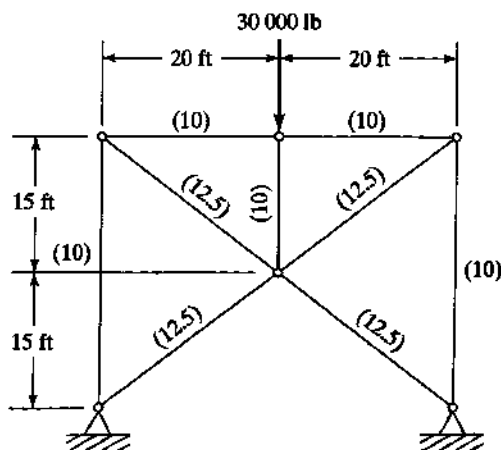


FIGURE P4.10

- 4.11. Determine the nodal displacements and element stresses in the truss in Fig. P4.11, due to each of the following conditions:
- Increase of temperature of 50°F in elements 1, 3, 7, and 8.
 - Elements 9 and 10 are $\frac{1}{4}$ in. too short and element 6 is $\frac{1}{8}$ in. too long, owing to errors in fabrication, and it was necessary to force them into place.

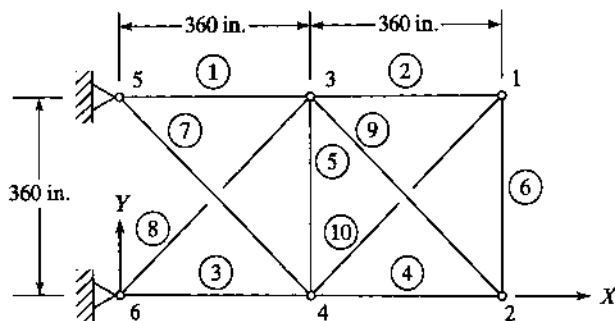


FIGURE P4.11

- (c) Support at node 6 moves 0.12 in. down. Data: Take $E = 30 \times 10^6$ psi, $\alpha = 1/150\,000$ per $^{\circ}\text{F}$. Cross-sectional areas for each element are as follows:

| Element | Area (in. ²) |
|---------|--------------------------|
| 1,3 | 25 |
| 2,4 | 12 |
| 5 | 1 |
| 6 | 4 |
| 7,8,9 | 17 |
| 10 | 5 |

- 4.12. A two-member truss is subjected to a load $P = 8000$ N. Member 1-2 is 400 mm long. Member 1-3 was manufactured to be 505 mm long instead of 500 mm. However, it was forced into place. Determine
- the stresses in the members assuming that member 1-3 was manufactured to its correct length of 500 mm and
 - the stresses in the members as a result of member 1-3 being forced into place (and the load P , of course).
- (Hint: Treat this as an initial strain problem and use the temperature load vector expression in the text.) Take cross-sectional areas = 750 mm², $E = 200$ GPa.

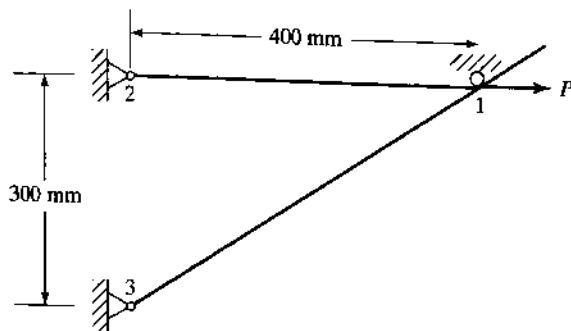


FIGURE P4.12

- 4.13. Expressions for the element stress (Eq. 4.16), and element temperature load (Eq. 4.22) were derived for a two-dimensional truss element. Generalize these expressions for a three-dimensional truss element.
- 4.14. Find deflections at nodes, stresses in members, and reactions at supports for the truss shown in Fig. P4.14 when the 150-kip load is applied.

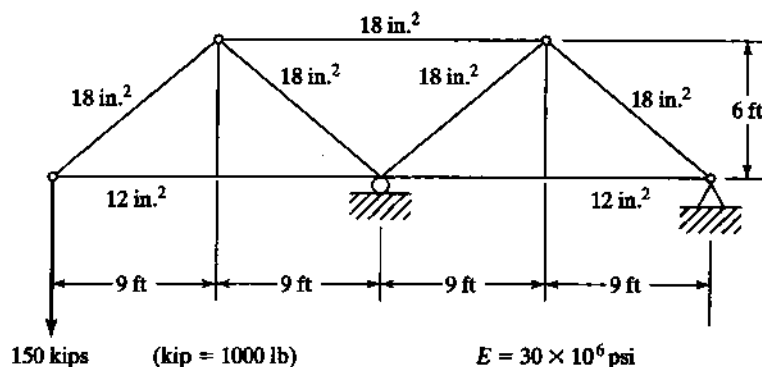


FIGURE P4.14

- 4.15. Find the deflections at the nodes for the truss configuration shown in Fig. P4.15. Area = 8 in.^2 for each member.

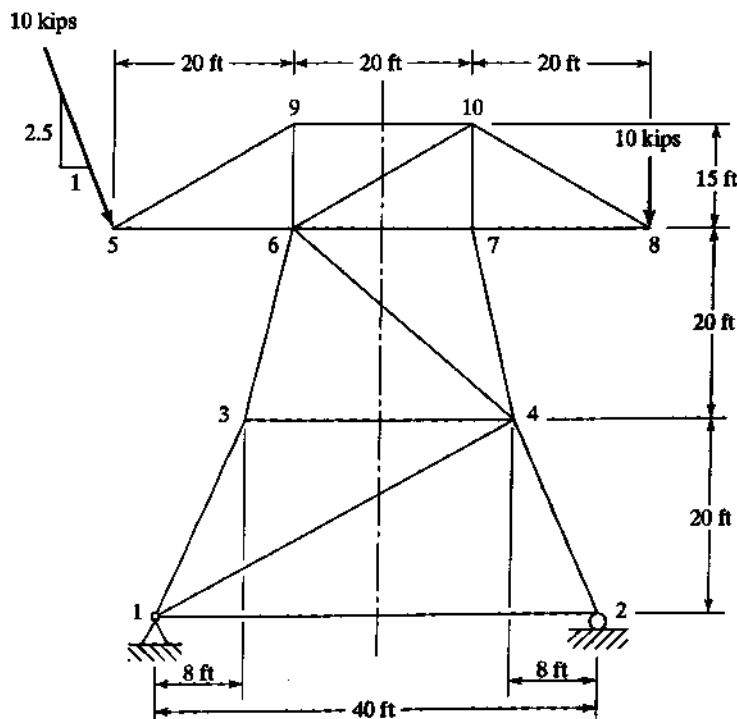


FIGURE P4.15

4.16. Modify program TRUSS2D to handle 3-D trusses and solve the problem in Fig. P4.16.

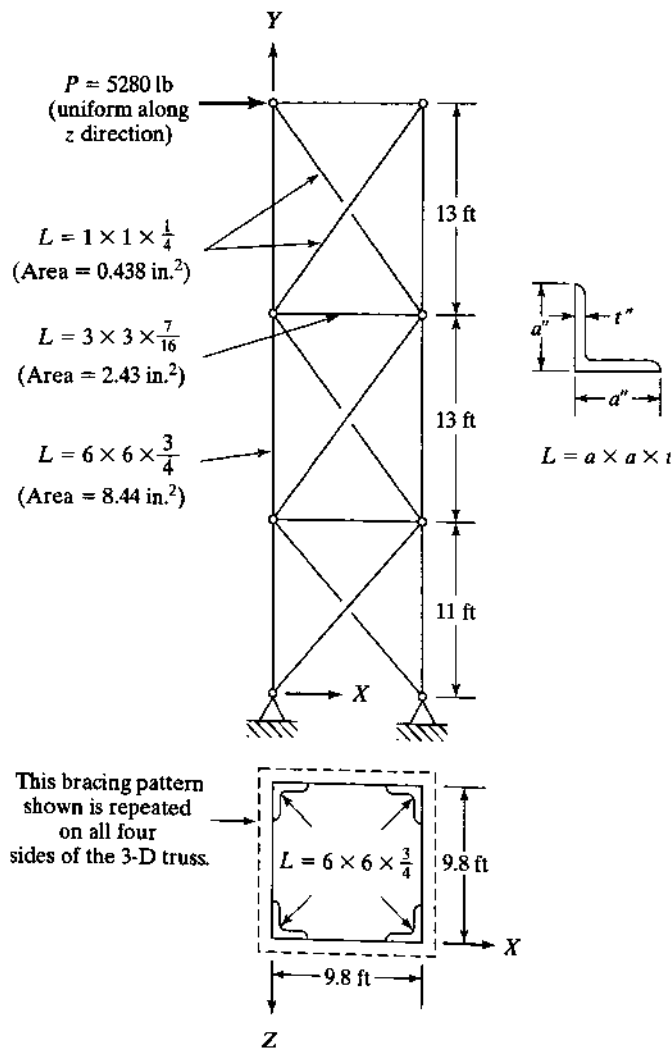


FIGURE P4.16 3-D truss model of a steel tower, supporting a water tank, and subjected to wind loads.

- 4.17. If the members in the truss in Problem 4.9 have a moment of inertia I of $8.4 \times 10^5 \text{ mm}^4$ about the axis perpendicular to the plane of the truss, check the compression members for Euler buckling. The Euler buckling load P_{cr} is given by $(\pi^2 EI)/\ell^2$. If σ_c is the compressive stress in a member, then the factor of safety for buckling may be taken as $P_{cr}/A\sigma_c$. Introduce this into the computer program TRUSS2D to calculate the factors of safety in compression members and print them in the output file.

- 4.18. (a) Analyze the three-dimensional truss shown in Fig. P4.18. Identify the tetrahedral patterns in the truss.
 (b) Generate the coordinates and connectivity if the two-stage truss shown is extended to 10 stages.

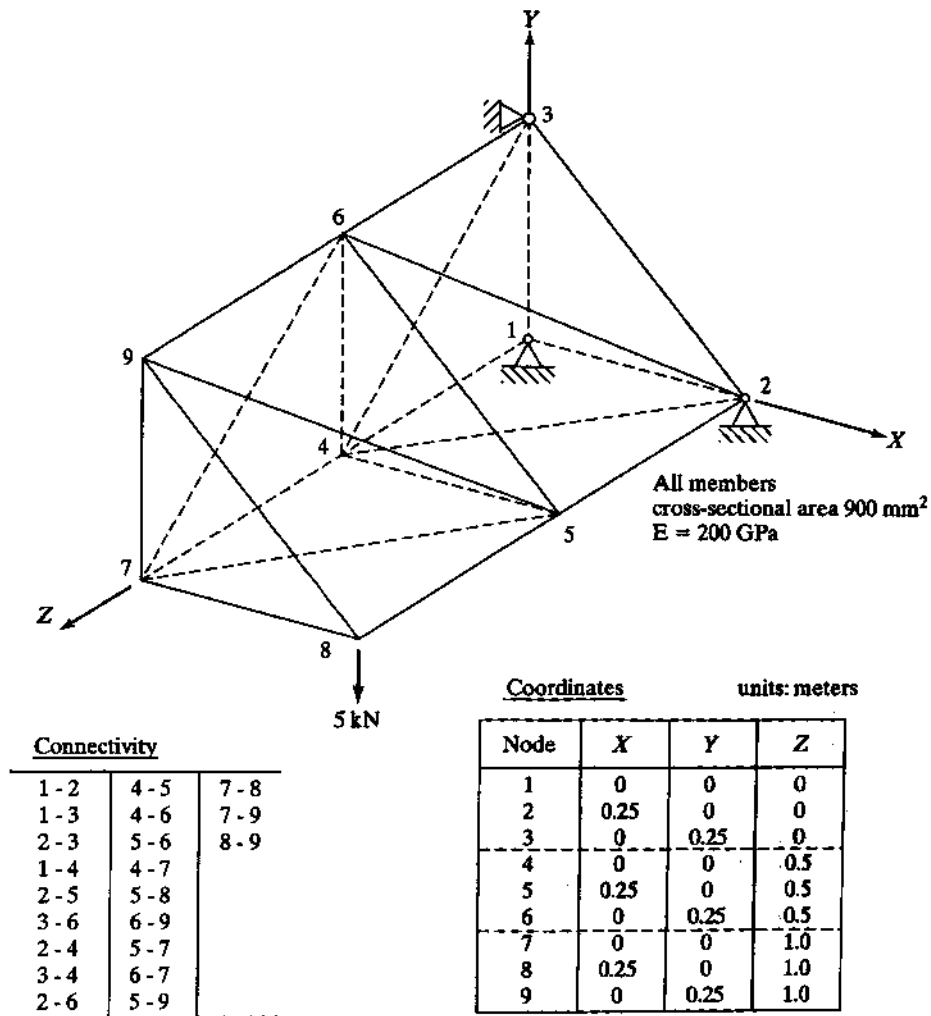


FIGURE P4.18

Program Listing

```

*****
*          PROGRAM TRUSS2D          *
*    TWO-DIMENSIONAL TRUSSES      *
*  T.R.Chandrupatla and A.D.Belegundu *
*****

===== MAIN PROGRAM =====
Private Sub cmdStart_Click()
    Call InputData
    Call Bandwidth
    Call Stiffness
    Call ModifyForBC
    Call BandSolver
    Call StressCalc
    Call ReactionCalc
    Call Output
    cmdView.Enabled = True
    cmdStart.Enabled = False
End Sub
=====

```

```

===== ELEMENT STIFFNESS AND ASSEMBLY =====
Private Sub Stiffness()
    ReDim S(NQ, NBW)
    '----- Global Stiffness Matrix -----
    For N = 1 To NE
        picBox.Print "Forming Stiffness Matrix of Element "; N
        I1 = NOC(N, 1): I2 = NOC(N, 2)
        I3 = MAT(N)
        X21 = X(I2, 1) - X(I1, 1)
        Y21 = X(I2, 2) - X(I1, 2)
        EL = Sqr(X21 * X21 + Y21 * Y21)
        EAL = PM(I3, 1) * AREA(N) / EL
        CS = X21 / EL: SN = Y21 / EL
        '----- Element Stiffness Matrix SE() -----
        SE(1, 1) = CS * CS * EAL
        SE(1, 2) = CS * SN * EAL: SE(2, 1) = SE(1, 2)
        SE(1, 3) = -CS * CS * EAL: SE(3, 1) = SE(1, 3)
        SE(1, 4) = -CS * SN * EAL: SE(4, 1) = SE(1, 4)
        SE(2, 2) = SN * SN * EAL
        SE(2, 3) = -CS * SN * EAL: SE(3, 2) = SE(2, 3)
        SE(2, 4) = -SN * SN * EAL: SE(4, 2) = SE(2, 4)
        SE(3, 3) = CS * CS * EAL
        SE(3, 4) = CS * SN * EAL: SE(4, 3) = SE(3, 4)
        SE(4, 4) = SN * SN * EAL
        '----- Temperature Load TL() -----
        EEO = PM(I3, 2) * DT(N) * PM(I3, 1) * AREA(N)
        TL(1) = -EEO * CS: TL(2) = -EEO * SN
        TL(3) = EEO * CS: TL(4) = EEO * SN
    Next N
End Sub

```

continued

```

picBox.Print ".... Placing in Global Locations"
For II = 1 To NEN
  NRT = NDN * (NOC(N, II) - 1)
  For IT = 1 To NDN
    NR = NRT + IT
    I = NDN * (II - 1) + IT
    For JJ = 1 To NEN
      NCT = NDN * (NOC(N, JJ) - 1)
      For JT = 1 To NDN
        J = NDN * (JJ - 1) + JT
        NC = NCT + JT - NR + 1
        If NC > 0 Then
          S(NR, NC) = S(NR, NC) + SE(I, J)
        End If
      Next JT
    Next JJ
    F(NR) = F(NR) + TL(I)
  Next IT
Next II
Next N
End Sub
=====

```

```

===== STRESS CALCULATIONS =====
Private Sub StressCalc()
  ReDim Stress(NE)
  '----- Stress Calculations
  For I = 1 To NE
    I1 = NOC(I, 1)
    I2 = NOC(I, 2)
    I3 = MAT(I)
    X21 = X(I2, 1) - X(I1, 1): Y21 = X(I2, 2) - X(I1, 2)
    EL = Sqr(X21 * X21 + Y21 * Y21)
    CS = X21 / EL
    SN = Y21 / EL
    J2 = 2 * I1
    J1 = J2 - 1
    K2 = 2 * I2
    K1 = K2 - 1
    DLT = (F(K1) - F(J1)) * CS + (F(K2) - F(J2)) * SN
    Stress(I) = PM(I3, 1) * (DLT / EL - PM(I3, 2) * DT(I))
  Next I
End Sub
=====

```

Two-Dimensional Problems Using Constant Strain Triangles

5.1 INTRODUCTION

The two-dimensional finite element formulation in this chapter follows the steps used in the one-dimensional problem. The displacements, traction components, and distributed body force values are functions of the position indicated by (x, y) . The displacement vector \mathbf{u} is given as

$$\mathbf{u} = [u, v]^T \quad (5.1)$$

where u and v are the x and y components of \mathbf{u} , respectively. The stresses and strains are given by

$$\boldsymbol{\sigma} = [\sigma_x, \sigma_y, \tau_{xy}]^T \quad (5.2)$$

$$\boldsymbol{\epsilon} = [\epsilon_x, \epsilon_y, \gamma_{xy}]^T \quad (5.3)$$

From Fig. 5.1, representing the two-dimensional problem in a general setting, the body force, traction vector, and elemental volume are given by

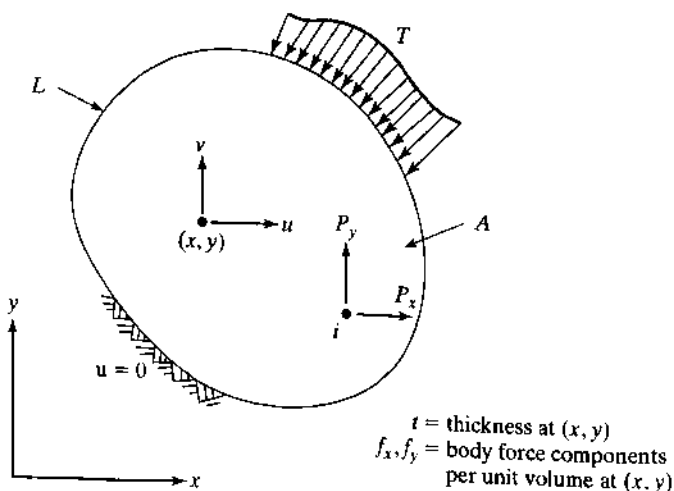


FIGURE 5.1 Two-dimensional problem.

$$\mathbf{f} = [f_x, f_y]^T \quad \mathbf{T} = [T_x, T_y]^T \quad \text{and} \quad dV = t dA \quad (5.4)$$

where t is the thickness along the z direction. The body force \mathbf{f} has the units force/unit volume, while the traction force \mathbf{T} has the units force/unit area. The strain–displacement relations are given by

$$\boldsymbol{\epsilon} = \left[\frac{\partial u}{\partial x}, \frac{\partial v}{\partial y}, \left(\frac{\partial u}{\partial y} + \frac{\partial v}{\partial x} \right) \right]^T \quad (5.5)$$

Stresses and strains are related by (see Eqs. 1.18 and 1.19)

$$\boldsymbol{\sigma} = \mathbf{D}\boldsymbol{\epsilon} \quad (5.6)$$

The region is discretized with the idea of expressing the displacements in terms of values at discrete points. Triangular elements are introduced first. Stiffness and load concepts are then developed using energy and Galerkin approaches.

5.2 FINITE ELEMENT MODELING

The two-dimensional region is divided into straight-sided triangles. Figure 5.2 shows a typical triangulation. The points where the corners of the triangles meet are called *nodes*, and each triangle formed by three nodes and three sides is called an *element*. The elements fill the entire region except a small region at the boundary. This unfilled region exists for curved boundaries, and it can be reduced by choosing smaller elements or elements with curved boundaries. The idea of the finite element method is to solve the continuous problem approximately, and this unfilled region contributes to some part of this

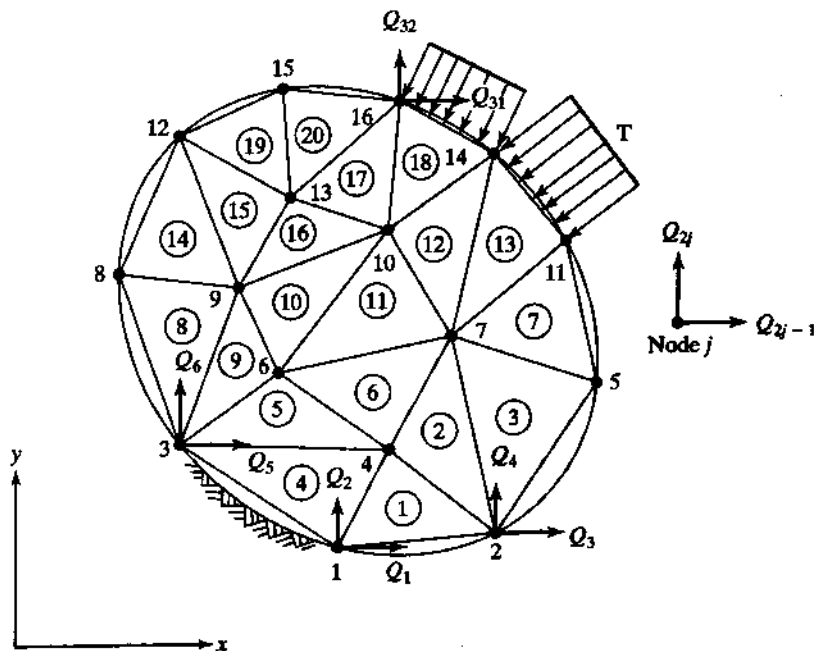


FIGURE 5.2 Finite element discretization.

approximation. For the triangulation shown in Fig. 5.2, the node numbers are indicated at the corners and element numbers are circled.

In the two-dimensional problem discussed here, each node is permitted to displace in the two directions x and y . Thus, each node has two degrees of freedom (dofs). As seen from the numbering scheme used in trusses, the displacement components of node j are taken as Q_{2j-1} in the x direction and Q_{2j} in the y direction. We denote the global displacement vector as

$$\mathbf{Q} = [Q_1, Q_2, \dots, Q_N]^T \quad (5.7)$$

where N is the number of degrees of freedom.

Computationally, the information on the triangulation is to be represented in the form of *nodal coordinates* and *connectivity*. The nodal coordinates are stored in a two-dimensional array represented by the total number of nodes and the two coordinates per node. The connectivity may be clearly seen by isolating a typical element, as shown in Fig. 5.3. For the three nodes designated locally as 1, 2, and 3, the corresponding global node numbers are defined in Fig. 5.2. This element connectivity information becomes an array of the size and number of elements and three nodes per element. A typical connectivity representation is shown in Table 5.1. Most standard finite element codes use the convention of going around the element in a counterclockwise direction to avoid calculating a negative area. However, in the program that accompanies this chapter, ordering is not necessary.

Table 5.1 establishes the correspondence of local and global node numbers and the corresponding degrees of freedom. The displacement components of a local node j in Fig. 5.3 are represented as q_{2j-1} and q_{2j} in the x and y directions, respectively. We denote the element displacement vector as

$$\mathbf{q} = [q_1, q_2, \dots, q_6]^T \quad (5.8)$$

Note that from the connectivity matrix in Table 5.1, we can extract the \mathbf{q} vector from the global \mathbf{Q} vector, an operation performed frequently in a finite element program. Also,

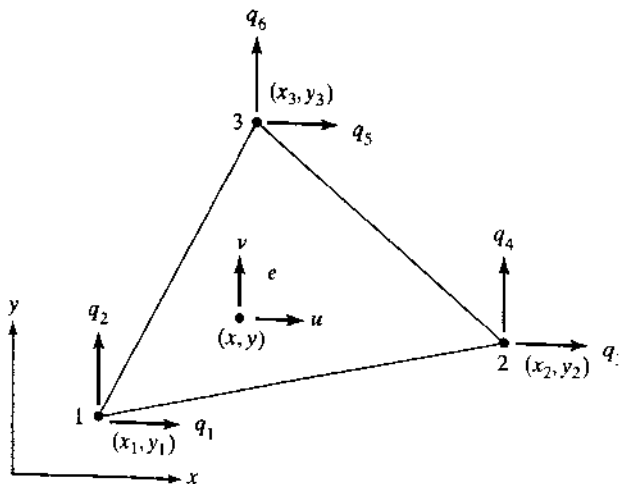


FIGURE 5.3 Triangular element.

TABLE 5.1 Element Connectivity

| Element number e | Three nodes | | |
|-----------------------|-------------|----|----|
| | 1 | 2 | 3 |
| 1 | 1 | 2 | 4 |
| 2 | 4 | 2 | 7 |
| ⋮ | | | |
| 11 | 6 | 7 | 10 |
| ⋮ | | | |
| 20 | 13 | 16 | 15 |

the nodal coordinates designated by (x_1, y_1) , (x_2, y_2) and (x_3, y_3) have the global correspondence established through Table 5.1. The local representation of nodal coordinates and degrees of freedom provides a setting for a simple and clear representation of element characteristics.

5.3 CONSTANT-STRAIN TRIANGLE (CST)

The displacements at points inside an element need to be represented in terms of the nodal displacements of the element. As discussed earlier, the finite element method uses the concept of shape functions in systematically developing these interpolations. For the constant strain triangle, the shape functions are linear over the element. The three shape functions N_1 , N_2 , and N_3 corresponding to nodes 1, 2, and 3, respectively, are shown in Fig. 5.4. Shape function N_1 is 1 at node 1 and linearly reduces to 0 at nodes 2 and 3. The values of shape function N_1 thus define a plane surface shown shaded in Fig. 5.4a. N_2 and N_3 are represented by similar surfaces having values of 1 at nodes 2 and 3, respectively, and dropping to 0 at the opposite edges. Any linear combination of these shape functions also represents a plane surface. In particular, $N_1 + N_2 + N_3$ represents a plane at a height of 1 at nodes 1, 2, and 3, and, thus, it is parallel to the triangle 123. Consequently, for every N_1 , N_2 , and N_3 ,

$$N_1 + N_2 + N_3 = 1 \quad (5.9)$$

N_1 , N_2 , and N_3 are therefore not linearly independent; only two of these are independent. The independent shape functions are conveniently represented by the pair ξ , η as

$$N_1 = \xi \quad N_2 = \eta \quad N_3 = 1 - \xi - \eta \quad (5.10)$$

where ξ , η are natural coordinates (Fig. 5.4). At this stage, the similarity with the one-dimensional element (Chapter 3) should be noted: in the one-dimensional problem the x -coordinates were mapped onto the ξ coordinates, and shape functions were defined as functions of ξ . Here, in the two-dimensional problem, the x -, y -coordinates are mapped onto the ξ -, η -coordinates, and shape functions are defined as functions of ξ and η .

The shape functions can be physically represented by area coordinates. A point (x, y) in a triangle divides it into three areas, A_1 , A_2 , and A_3 , as shown in Fig. 5.5. The shape functions N_1 , N_2 , and N_3 are precisely represented by

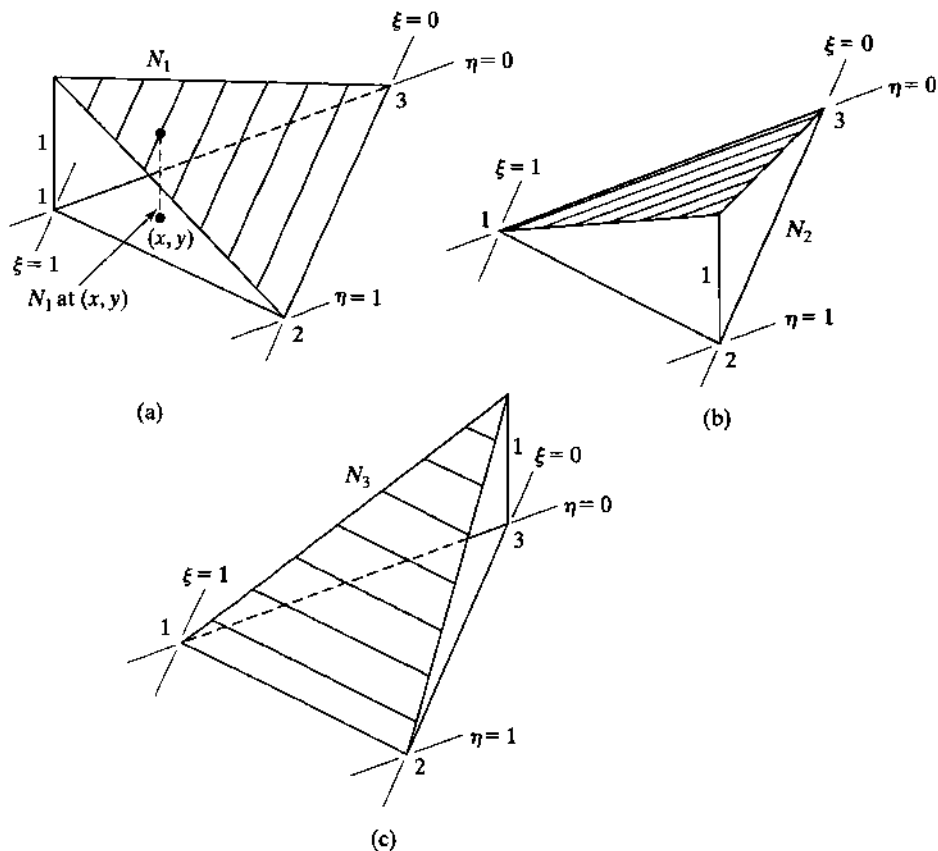


FIGURE 5.4 Shape functions.

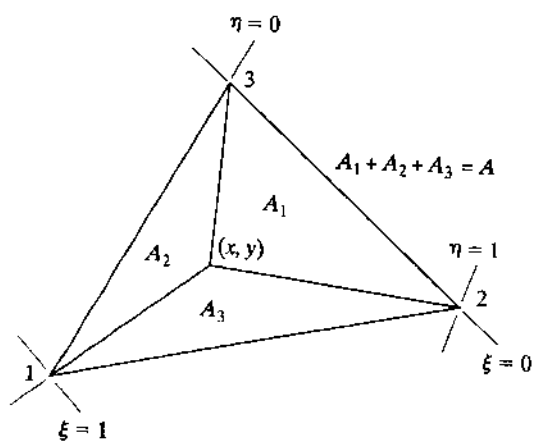


FIGURE 5.5 Area coordinates.

$$N_1 = \frac{A_1}{A} \quad N_2 = \frac{A_2}{A} \quad N_3 = \frac{A_3}{A} \quad (5.11)$$

where A is the area of the element. Clearly, $N_1 + N_2 + N_3 = 1$ at every point inside the triangle.

Isoparametric Representation

The displacements inside the element are now written using the shape functions and the nodal values of the unknown displacement field. We have

$$\begin{aligned} u &= N_1 q_1 + N_2 q_3 + N_3 q_5 \\ v &= N_1 q_2 + N_2 q_4 + N_3 q_6 \end{aligned} \quad (5.12a)$$

or, using Eq. 5.10,

$$\begin{aligned} u &= (q_1 - q_5)\xi + (q_3 - q_5)\eta + q_5 \\ v &= (q_2 - q_6)\xi + (q_4 - q_6)\eta + q_6 \end{aligned} \quad (5.12b)$$

The relations 5.12a can be expressed in a matrix form by defining a shape function matrix

$$\mathbf{N} = \begin{bmatrix} N_1 & 0 & N_2 & 0 & N_3 & 0 \\ 0 & N_1 & 0 & N_2 & 0 & N_3 \end{bmatrix} \quad (5.13)$$

and

$$\mathbf{u} = \mathbf{N}\mathbf{q} \quad (5.14)$$

For the triangular element, the coordinates x, y can also be represented in terms of nodal coordinates using the same shape functions. This is **isoparametric representation**. This approach lends to simplicity of development and retains the uniformity with other complex elements. We have

$$\begin{aligned} x &= N_1 x_1 + N_2 x_2 + N_3 x_3 \\ y &= N_1 y_1 + N_2 y_2 + N_3 y_3 \end{aligned} \quad (5.15a)$$

or

$$\begin{aligned} x &= (x_1 - x_3)\xi + (x_2 - x_3)\eta + x_3 \\ y &= (y_1 - y_3)\xi + (y_2 - y_3)\eta + y_3 \end{aligned} \quad (5.15b)$$

Using the notation, $x_{ij} = x_i - x_j$ and $y_{ij} = y_i - y_j$, we can write Eq. 5.15b as

$$\begin{aligned} x &= x_{13}\xi + x_{23}\eta + x_3 \\ y &= y_{13}\xi + y_{23}\eta + y_3 \end{aligned} \quad (5.15c)$$

This equation relates x - and y -coordinates to the ξ - and η -coordinates. Equation 5.12 expresses u and v as functions of ξ and η .

Example 5.1

Evaluate the shape functions N_1, N_2 , and N_3 at the interior point P for the triangular element shown in Fig. E5.1.

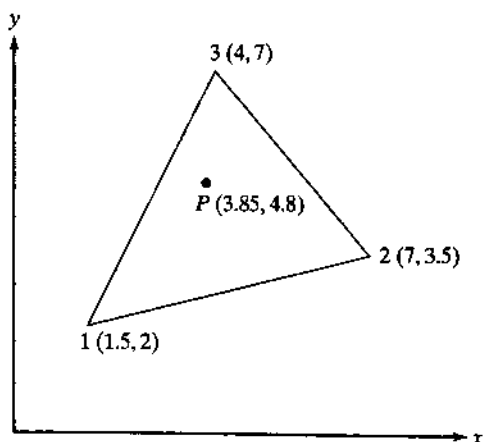


FIGURE E5.1 Examples 5.1 and 5.2.

Solution Using the isoparametric representation (Eqs. 5.15), we have

$$3.85 = 1.5N_1 + 7N_2 + 4N_3 = -2.5\xi + 3\eta + 4$$

$$4.8 = 2N_1 + 3.5N_2 + 7N_3 = -5\xi - 3.5\eta + 7$$

These two equations are rearranged in the form

$$2.5\xi - 3\eta = 0.15$$

$$5\xi + 3.5\eta = 2.2$$

Solving the equations, we obtain $\xi = 0.3$ and $\eta = 0.2$, which implies that

$$N_1 = 0.3 \quad N_2 = 0.2 \quad N_3 = 0.5$$

In evaluating the strains, partial derivatives of u and v are to be taken with respect to x and y . From Eqs. 5.12 and 5.15, we see that u , v and x , y are functions of ξ and η . That is, $u = u(x(\xi, \eta), y(\xi, \eta))$ and similarly $v = v(x(\xi, \eta), y(\xi, \eta))$. Using the chain rule for partial derivatives of u , we have

$$\frac{\partial u}{\partial \xi} = \frac{\partial u}{\partial x} \frac{\partial x}{\partial \xi} + \frac{\partial u}{\partial y} \frac{\partial y}{\partial \xi}$$

$$\frac{\partial u}{\partial \eta} = \frac{\partial u}{\partial x} \frac{\partial x}{\partial \eta} + \frac{\partial u}{\partial y} \frac{\partial y}{\partial \eta}$$

which can be written in matrix notation as

$$\begin{Bmatrix} \frac{\partial u}{\partial \xi} \\ \frac{\partial u}{\partial \eta} \end{Bmatrix} = \begin{bmatrix} \frac{\partial x}{\partial \xi} & \frac{\partial y}{\partial \xi} \\ \frac{\partial x}{\partial \eta} & \frac{\partial y}{\partial \eta} \end{bmatrix} \begin{Bmatrix} \frac{\partial u}{\partial x} \\ \frac{\partial u}{\partial y} \end{Bmatrix} \quad (5.16)$$

where the (2×2) square matrix is denoted as the *Jacobian* of the transformation, \mathbf{J} :

$$\mathbf{J} = \begin{bmatrix} \frac{\partial x}{\partial \xi} & \frac{\partial y}{\partial \xi} \\ \frac{\partial x}{\partial \eta} & \frac{\partial y}{\partial \eta} \end{bmatrix} \quad (5.17)$$

Some additional properties of the Jacobian are given in the appendix. On taking the derivative of x and y ,

$$\mathbf{J} = \begin{bmatrix} x_{13} & y_{13} \\ x_{23} & y_{23} \end{bmatrix} \quad (5.18)$$

Also, from Eq. 5.16,

$$\begin{Bmatrix} \frac{\partial u}{\partial x} \\ \frac{\partial u}{\partial y} \end{Bmatrix} = \mathbf{J}^{-1} \begin{Bmatrix} \frac{\partial u}{\partial \xi} \\ \frac{\partial u}{\partial \eta} \end{Bmatrix} \quad (5.19)$$

where \mathbf{J}^{-1} is the inverse of the Jacobian \mathbf{J} , given by

$$\mathbf{J}^{-1} = \frac{1}{\det \mathbf{J}} \begin{bmatrix} y_{23} & -y_{13} \\ -x_{23} & x_{13} \end{bmatrix} \quad (5.20)$$

$$\det \mathbf{J} = x_{13}y_{23} - x_{23}y_{13} \quad (5.21)$$

From the knowledge of the area of the triangle, it can be seen that the magnitude of $\det \mathbf{J}$ is twice the area of the triangle. If the points 1, 2, and 3 are ordered in a counterclockwise manner, $\det \mathbf{J}$ is positive in sign. We have

$$A = \frac{1}{2} |\det \mathbf{J}| \quad (5.22)$$

where $||$ represents the magnitude. Most computer codes use a counterclockwise order for the nodes and use $\det \mathbf{J}$ for evaluating the area.

Example 5.2

Determine the Jacobian of the transformation \mathbf{J} for the triangular element shown in Fig. E5.1.

Solution We have

$$\mathbf{J} = \begin{bmatrix} x_{13} & y_{13} \\ x_{23} & y_{23} \end{bmatrix} = \begin{bmatrix} -2.5 & -5.0 \\ 3.0 & -3.5 \end{bmatrix}$$

Thus, $\det \mathbf{J} = 23.75$ units. This is twice the area of the triangle. If 1, 2, 3 are in a clockwise order, then $\det \mathbf{J}$ will be negative. ■

From Eqs. 5.19 and 5.20, it follows that

$$\begin{Bmatrix} \frac{\partial u}{\partial x} \\ \frac{\partial u}{\partial y} \end{Bmatrix} = \frac{1}{\det \mathbf{J}} \begin{Bmatrix} y_{23} \frac{\partial u}{\partial \xi} - y_{13} \frac{\partial u}{\partial \eta} \\ -x_{23} \frac{\partial u}{\partial \xi} + x_{13} \frac{\partial u}{\partial \eta} \end{Bmatrix} \quad (5.23a)$$

Replacing u by the displacement v , we get a similar expression

$$\begin{Bmatrix} \frac{\partial v}{\partial x} \\ \frac{\partial v}{\partial y} \end{Bmatrix} = \frac{1}{\det \mathbf{J}} \begin{Bmatrix} y_{23} \frac{\partial v}{\partial \xi} - y_{13} \frac{\partial v}{\partial \eta} \\ -x_{23} \frac{\partial v}{\partial \xi} + x_{13} \frac{\partial v}{\partial \eta} \end{Bmatrix} \quad (5.23b)$$

Using the strain-displacement relations (5.5) and Eqs. 5.12b and 5.23, we get

$$\begin{aligned} \boldsymbol{\epsilon} &= \begin{Bmatrix} \frac{\partial u}{\partial x} \\ \frac{\partial v}{\partial y} \\ \frac{\partial u}{\partial y} + \frac{\partial v}{\partial x} \end{Bmatrix} \\ &= \frac{1}{\det \mathbf{J}} \begin{Bmatrix} y_{23}(q_1 - q_5) - y_{13}(q_3 - q_5) \\ -x_{23}(q_2 - q_6) + x_{13}(q_4 - q_6) \\ -x_{23}(q_1 - q_5) + x_{13}(q_3 - q_5) + y_{23}(q_2 - q_6) - y_{13}(q_4 - q_6) \end{Bmatrix} \end{aligned} \quad (5.24a)$$

From the definition of x_{ij} and y_{ij} , we can write $y_{31} = -y_{13}$ and $y_{12} = y_{13} - y_{23}$, and so on. The foregoing equation can be written in the form

$$\boldsymbol{\epsilon} = \frac{1}{\det \mathbf{J}} \begin{Bmatrix} y_{23}q_1 + y_{31}q_3 + y_{12}q_5 \\ x_{32}q_2 + x_{13}q_4 + x_{21}q_6 \\ x_{32}q_1 + y_{23}q_2 + x_{13}q_3 + y_{31}q_4 + x_{21}q_5 + y_{12}q_6 \end{Bmatrix} \quad (5.24b)$$

This equation can be written in matrix form as

$$\boldsymbol{\epsilon} = \mathbf{B}\mathbf{q} \quad (5.25)$$

where \mathbf{B} is a (3×6) element strain-displacement matrix relating the three strains to the six nodal displacements and is given by

$$\mathbf{B} = \frac{1}{\det \mathbf{J}} \begin{bmatrix} y_{23} & 0 & y_{31} & 0 & y_{12} & 0 \\ 0 & x_{32} & 0 & x_{13} & 0 & x_{21} \\ x_{32} & y_{23} & x_{13} & y_{31} & x_{21} & y_{12} \end{bmatrix} \quad (5.26)$$

It may be noted that all the elements of the \mathbf{B} matrix are constants expressed in terms of the nodal coordinates.

Example 5.3

Find the strain-nodal displacement matrices \mathbf{B}^e for the elements shown in Fig. E5.3. Use local numbers given at the corners.

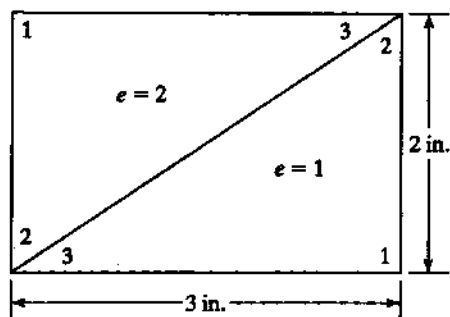


FIGURE ES.3

Solution We have

$$\mathbf{B}^1 = \frac{1}{\det \mathbf{J}} \begin{bmatrix} y_{23} & 0 & y_{31} & 0 & y_{12} & 0 \\ 0 & x_{32} & 0 & x_{13} & 0 & x_{21} \\ x_{32} & y_{23} & x_{13} & y_{31} & x_{21} & y_{12} \end{bmatrix}$$

$$= \frac{1}{6} \begin{bmatrix} 2 & 0 & 0 & 0 & -2 & 0 \\ 0 & -3 & 0 & 3 & 0 & 0 \\ -3 & 2 & 3 & 0 & 0 & -2 \end{bmatrix}$$

where $\det \mathbf{J}$ is obtained from $x_{13}y_{23} - x_{23}y_{13} = (3)(2) - (3)(0) = 6$. Using the local numbers at the corners, \mathbf{B}^2 can be written using the relationship as

$$\mathbf{B}^2 = \frac{1}{6} \begin{bmatrix} -2 & 0 & 0 & 0 & 2 & 0 \\ 0 & 3 & 0 & -3 & 0 & 0 \\ 3 & -2 & -3 & 0 & 0 & 2 \end{bmatrix} \quad \blacksquare$$

Potential-Energy Approach

The potential energy of the system, Π , is given by

$$\Pi = \frac{1}{2} \int_A \boldsymbol{\epsilon}^T \mathbf{D} \boldsymbol{\epsilon} \, dA - \int_A \mathbf{u}^T \mathbf{f} \, dA - \int_L \mathbf{u}^T \mathbf{T} \, dt - \sum_i \mathbf{u}_i^T \mathbf{P}_i \quad (5.27)$$

In the last term in Eq. 5.27, i indicates the point of application of a point load \mathbf{P}_i and $\mathbf{P}_i = [P_x, P_y]^T$. The summation in i gives the potential energy due to all point loads.

Using the triangulation shown in Fig. 5.2, the total potential energy can be written in the form

$$\Pi = \sum_e \frac{1}{2} \int_e \boldsymbol{\epsilon}^T \mathbf{D} \boldsymbol{\epsilon} \, dA - \sum_e \int_e \mathbf{u}^T \mathbf{f} \, dA - \int_L \mathbf{u}^T \mathbf{T} \, dt - \sum_i \mathbf{u}_i^T \mathbf{P}_i \quad (5.28a)$$

or

$$\Pi = \sum_e U_e - \sum_e \int_e \mathbf{u}^T \mathbf{f} \, dA - \sum_L \int_L \mathbf{u}^T \mathbf{T} \, dt - \sum_i \mathbf{u}_i^T \mathbf{P}_i \quad (5.28b)$$

where $U_e = \frac{1}{2} \int_e \boldsymbol{\epsilon}^T \mathbf{D} \boldsymbol{\epsilon} \, dA$ is the element strain energy.

Element Stiffness

We now substitute for the strain from the element strain–displacement relationship in Eq. 5.25 into the element strain energy U_e in Eq. 5.28b, to obtain

$$\begin{aligned} U_e &= \frac{1}{2} \int_e \boldsymbol{\epsilon}^T \mathbf{D} \boldsymbol{\epsilon} t_e dA \\ &= \frac{1}{2} \int_e \mathbf{q}^T \mathbf{B}^T \mathbf{D} \mathbf{B} \mathbf{q} t_e dA \end{aligned} \quad (5.29a)$$

Taking the element thickness t_e as constant over the element and remembering that all terms in the \mathbf{D} and \mathbf{B} matrices are constants, we have

$$U_e = \frac{1}{2} \mathbf{q}^T \mathbf{B}^T \mathbf{D} \mathbf{B} t_e \left(\int_e dA \right) \mathbf{q} \quad (5.29b)$$

Now, $\int_e dA = A_e$, where A_e is the area of the element. Thus,

$$U_e = \frac{1}{2} \mathbf{q}^T t_e A_e \mathbf{B}^T \mathbf{D} \mathbf{B} \mathbf{q} \quad (5.29c)$$

or

$$U_e = \frac{1}{2} \mathbf{q}^T \mathbf{k}^e \mathbf{q} \quad (5.29d)$$

where \mathbf{k}^e is the element stiffness matrix given by

$$\mathbf{k}^e = t_e A_e \mathbf{B}^T \mathbf{D} \mathbf{B} \quad (5.30)$$

For plane stress or plane strain, the element stiffness matrix can be obtained by taking the appropriate material property matrix \mathbf{D} defined in Chapter 1 and carrying out the previous multiplication on the computer. We note that \mathbf{k}^e is symmetric since \mathbf{D} is symmetric. The element connectivity as established in Table 5.1 is now used to add the element stiffness values in \mathbf{k}^e into the corresponding global locations in the global stiffness matrix \mathbf{K} , so that

$$\begin{aligned} U &= \sum_e \frac{1}{2} \mathbf{q}^T \mathbf{k}^e \mathbf{q} \\ &= \frac{1}{2} \mathbf{Q}^T \mathbf{K} \mathbf{Q} \end{aligned} \quad (5.31)$$

The global stiffness matrix \mathbf{K} is symmetric and banded or sparse. The stiffness value K_{ij} is zero when the degrees of freedom i and j are not connected through an element. If i and j are connected through one or more elements, stiffness values accumulate from these elements. For the global dof numbering shown in Fig. 5.2, the bandwidth is related to the maximum difference in node numbers of an element, over all the elements. If $i_1, i_2,$ and i_3 are node numbers of an element e , the maximum element node number difference is given by

$$m_e = \max(|i_1 - i_2|, |i_2 - i_3|, |i_3 - i_1|) \quad (5.32a)$$

The half-bandwidth is then given by

$$\text{NBW} = 2 \left(\max_{1 \leq e \leq \text{NE}} (m_e) + 1 \right) \quad (5.32b)$$

where NE is the number of elements and 2 is the number of degrees of freedom per node.

The global stiffness \mathbf{K} is in a form where all the degrees of freedom \mathbf{Q} are free. It needs to be modified to account for the boundary conditions.

Force Terms

The body force term $\int_e \mathbf{u}^T \mathbf{f}^e dA$ appearing in the total potential energy in Eq. 5.28b is considered first. We have

$$\int_e \mathbf{u}^T \mathbf{f}^e dA = t_e \int_e (u f_x + v f_y) dA$$

Using the interpolation relations given in Eq. 5.12a, we find that

$$\begin{aligned} \int_e \mathbf{u}^T \mathbf{f}^e dA &= q_1 \left(t_e f_x \int_e N_1 dA \right) + q_2 \left(t_e f_y \int_e N_1 dA \right) \\ &+ q_3 \left(t_e f_x \int_e N_2 dA \right) + q_4 \left(t_e f_y \int_e N_2 dA \right) \\ &+ q_5 \left(t_e f_x \int_e N_3 dA \right) + q_6 \left(t_e f_y \int_e N_3 dA \right) \end{aligned} \quad (5.33)$$

From the definition of shape functions on a triangle, shown in Fig. 5.4, $\int_e N_1 dA$ represents the volume of a tetrahedron with base area A_e and height of corner equal to 1 (nondimensional). The volume of this tetrahedron is given by $\frac{1}{3} \times \text{Base area} \times \text{Height}$ (Fig. 5.6) as in

$$\int_e N_1 dA = \frac{1}{3} A_e \quad (5.34)$$

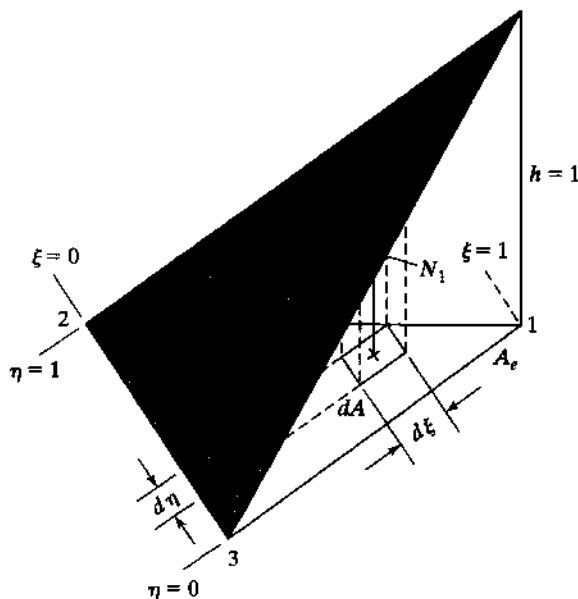
Similarly, $\int_e N_2 dA = \int_e N_3 dA = \frac{1}{3} A_e$, Equation 5.33 can now be written in the form

$$\int_e \mathbf{u}^T \mathbf{f}^e dA = \mathbf{q}^T \mathbf{f}^e \quad (5.35)$$

where \mathbf{f}^e is the element body force vector, given as

$$\mathbf{f}^e = \frac{t_e A_e}{3} [f_x, f_y, f_x, f_y, f_x, f_y]^T \quad (5.36)$$

These element nodal forces contribute to the global load vector \mathbf{F} . The connectivity in Table 5.1 needs to be used again to add \mathbf{f}^e to the global force vector \mathbf{F} . The vector \mathbf{f}^e is



$$\int_e N_1 dA = \frac{1}{3} \cdot A_e h = \frac{1}{3} \cdot A_e$$

$$\text{or } \int_e N_1 dA = \int_0^1 \int_0^{1-\xi} N_1 \det J d\eta d\xi = 2A_e \int_0^1 \int_0^{1-\xi} \xi d\eta d\xi = \frac{1}{3} \cdot A_e$$

FIGURE 5.6 Integral of a shape function.

of dimension (6×1) , whereas \mathbf{F} is $(N \times 1)$. This assembly procedure is discussed in Chapters 3 and 4. Stating this symbolically,

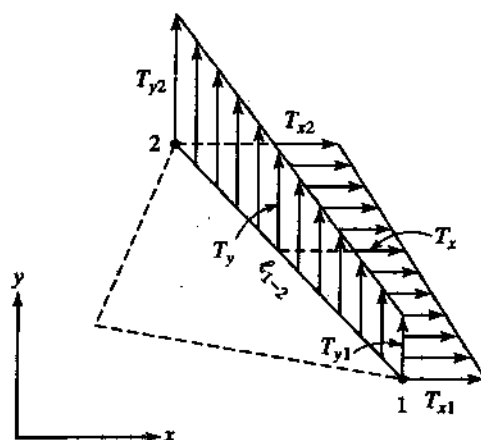
$$\mathbf{F} \longleftarrow \sum_e \mathbf{f}^e \quad (5.37)$$

A **traction force** is a distributed load acting on the surface of the body. Such a force acts on edges connecting boundary nodes. A traction force acting on the edge of an element contributes to the global load vector \mathbf{F} . This contribution can be determined by considering the traction force term $\int \mathbf{u}^T \mathbf{T} t d\ell$. Consider an edge ℓ_{1-2} , acted on by a traction T_x, T_y in units of force per unit surface area, shown in Fig. 5.7a. We have

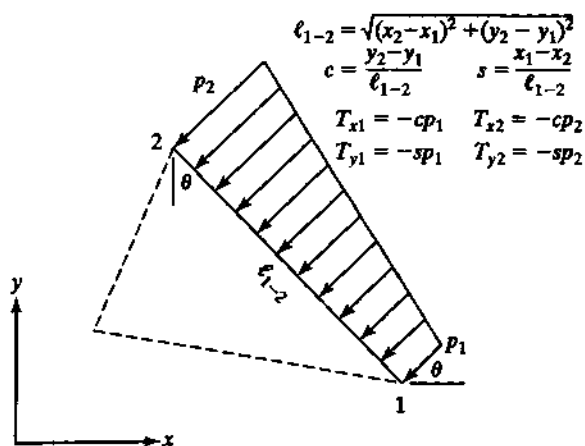
$$\int_L \mathbf{u}^T \mathbf{T} t d\ell = \int_{\ell_{1-2}} (uT_x + vT_y) t d\ell \quad (5.38)$$

Using the interpolation relations involving the shape functions

$$\begin{aligned} u &= N_1 q_1 + N_2 q_3 \\ v &= N_1 q_2 + N_2 q_4 \\ T_x &= N_1 T_{x1} + N_2 T_{x2} \\ T_y &= N_1 T_{y1} + N_2 T_{y2} \end{aligned} \quad (5.39)$$



(a) Component distribution



(b) Normal pressure

FIGURE 5.7 Traction load.

and noting that

$$\int_{\ell_{1-2}} N_1^2 d\ell = \frac{1}{3}\ell_{1-2}, \quad \int_{\ell_{1-2}} N_2^2 d\ell = \frac{1}{3}\ell_{1-2}, \quad \int_{\ell_{1-2}} N_1 N_2 d\ell = \frac{1}{6}\ell_{1-2}$$

$$\ell_{1-2} = \sqrt{(x_2 - x_1)^2 + (y_2 - y_1)^2} \quad (5.40)$$

we get

$$\int_{\ell_{1-2}} \mathbf{n}^T \mathbf{T} t d\ell = [q_1, q_2, q_3, q_4] \mathbf{T}^e \quad (5.41)$$

where \mathbf{T}^e is given by

$$\mathbf{T}^e = \frac{t \ell_{1-2}}{6} [2T_{x1} + T_{x2}, 2T_{y1} + T_{y2}, T_{x1} + 2T_{x2}, T_{y1} + 2T_{y2}]^T \quad (5.42)$$

If p_1 and p_2 are pressures acting normal to the line directed to the right as we move from 1 to 2, as shown in Fig. 5.7b, then

$$T_{x1} = -cp_1, \quad T_{x2} = -cp_2, \quad T_{y1} = -sp_1, \quad T_{y2} = -sp_2$$

where

$$s = \frac{(x_1 - x_2)}{\ell_{1-2}} \quad \text{and} \quad c = \frac{(y_2 - y_1)}{\ell_{1-2}}.$$

In Eq. 5.42, both normal and tangential distributed loads can be considered. The traction load contributions need to be added to the global force vector \mathbf{F} .

The programs given in this book expect the loads in component point load form. For distributed loads, we need to determine the equivalent point load components as illustrated in the following example.

Example 5.4

A two-dimensional plate is shown in the Fig. E5.4. Determine the equivalent point loads at nodes 7, 8, and 9 for the linearly distributed pressure load acting on the edge 7–8–9.

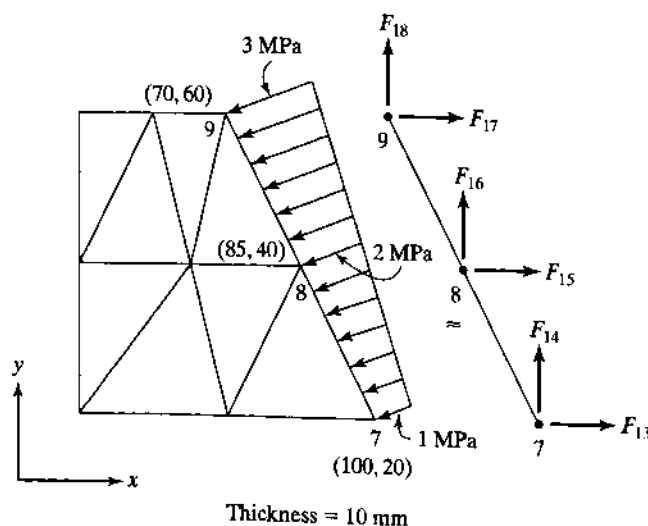


FIGURE E5.4

Solution We consider the two edges 7–8 and 8–9 separately and then merge them.

For edge 7–8

$$p_1 = 1 \text{ MPa}, \quad p_2 = 2 \text{ MPa}, \quad x_1 = 100 \text{ mm}, \quad y_1 = 20 \text{ mm}, \quad x_2 = 85 \text{ mm}, \quad y_2 = 40 \text{ mm}.$$

$$\ell_{1-2} = \sqrt{(x_1 - x_2)^2 + (y_1 - y_2)^2} = 25 \text{ mm}$$

$$c = \frac{y_2 - y_1}{\ell_{1-2}} = 0.8, \quad s = \frac{x_1 - x_2}{\ell_{1-2}} = 0.6$$

$$T_{x1} = -p_1c = -0.8, \quad T_{y1} = -p_1s = -0.6, \quad T_{x2} = -p_2c = -1.6,$$

$$T_{y2} = -p_2 s = -1.2$$

$$\begin{aligned} \mathbf{T}^1 &= \frac{10 \times 25}{6} [2T_{x1} + T_{x2}, 2T_{y1} + T_{y2}, T_{x1} + 2T_{x2}, T_{y1} + 2T_{y2}]^T \\ &= [-133.3, -100, -166.7, -125]^T \text{ N} \end{aligned}$$

These loads add to F_{13} , F_{14} , F_{15} , and F_{16} , respectively.

For edge 8-9

$$p_1 = 2 \text{ MPa}, \quad p_2 = 3 \text{ MPa}, \quad x_1 = 85 \text{ mm}, \quad y_1 = 40 \text{ mm}, \quad x_2 = 70 \text{ mm}, \quad y_2 = 60 \text{ mm},$$

$$\ell_{1-2} = \sqrt{(x_1 - x_2)^2 + (y_1 - y_2)^2} = 25 \text{ mm}$$

$$c = \frac{y_2 - y_1}{\ell_{1-2}} = 0.8, \quad s = \frac{x_1 - x_2}{\ell_{1-2}} = 0.6$$

$$T_{x1} = -p_1 c = -1.6, \quad T_{y1} = -p_1 s = -1.2, \quad T_{x2} = -p_2 c = -2.4,$$

$$T_{y2} = -p_2 s = -1.8$$

$$\begin{aligned} \mathbf{T}^2 &= \frac{10 \times 25}{6} [2T_{x1} + T_{x2}, 2T_{y1} + T_{y2}, T_{x1} + 2T_{x2}, T_{y1} + 2T_{y2}]^T \\ &= [-233.3, -175, -266.7, -200]^T \text{ N} \end{aligned}$$

These loads add to F_{15} , F_{16} , F_{17} , and F_{18} , respectively. Thus,

$$[F_{13} \quad F_{14} \quad F_{15} \quad F_{16} \quad F_{17} \quad F_{18}] = [-133.3 \quad -100 \quad -400 \quad -300 \quad -266.7 \quad -200] \text{ N}$$

The point load term is easily considered by having a node at the point of application of the point load. If i is the node at which $\mathbf{P}_i = [P_x, P_y]^T$ is applied, then

$$\mathbf{u}_i^T \mathbf{P}_i = Q_{2i-1} P_x + Q_{2i} P_y \quad (5.43)$$

Thus, P_x and P_y , the x and y components of \mathbf{P}_i , get added to the $(2i - 1)$ th and $(2i)$ th components of the global force \mathbf{F} .

The contribution of body forces, traction forces, and point loads to the global force \mathbf{F} can be represented as $\mathbf{F} \leftarrow \sum_e (\mathbf{f}^e + \mathbf{T}^e) + \mathbf{P}$.

Consideration of the strain energy and the force terms gives us the total potential energy in the form

$$\Pi = \frac{1}{2} \mathbf{Q}^T \mathbf{K} \mathbf{Q} - \mathbf{Q}^T \mathbf{F} \quad (5.44)$$

The stiffness and force modifications are made to account for the boundary conditions. Using the methods presented in Chapters 3 and 4, we have

$$\mathbf{K} \mathbf{Q} = \mathbf{F} \quad (5.45)$$

where \mathbf{K} and \mathbf{F} are modified stiffness matrix and force vector, respectively. These equations are solved by Gaussian elimination or other techniques, to yield the displacement vector \mathbf{Q} .

Example 5.5

A CST element is shown in Fig. E5.5. The element is subjected to a body force $f_x = x^2 \text{ N/m}^3$. Determine the nodal force vector \mathbf{f}^e . Take element thickness = 1 m.

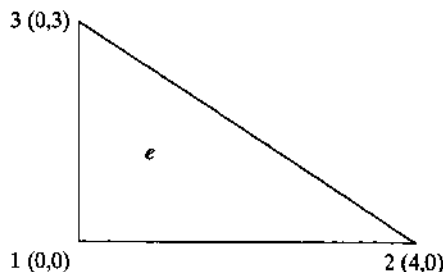


FIGURE E5.5

The work potential is $-\int_e \mathbf{f}^T \mathbf{u} dV$, where $\mathbf{f}^T = [f_x, 0]$. Substituting for $\mathbf{u} = \mathbf{N}\mathbf{q}$, we obtain the work potential in the form $-\mathbf{q}^T \mathbf{f}^e$, where $\mathbf{f}^e = \int_e \mathbf{N}^T \mathbf{f} dV$, where \mathbf{N} is given in Eq. 5.13. All y components of \mathbf{f}^e are zero. The x components at nodes 1, 2, 3 are given, respectively, by

$$\int_e \xi f_x dV, \quad \int_e \eta f_x dV, \quad \int_e (1 - \xi - \eta) f_x dV$$

We now make the following substitutions: $f_x = x^2$, $x = \xi x_1 + \eta x_2 + (1 - \xi - \eta)x_3 = 4\eta$, $dV = \det \mathbf{J} d\eta d\xi$, $\det \mathbf{J} = 2A_e$, and $A_e = 6$. Now, integration over a triangle is illustrated in Fig. 5.6. Thus,

$$\int_e \xi f_x dV = \int_0^1 \int_0^{1-\xi} \xi (16\eta^2) (12) d\eta d\xi = 3.2 \text{ N}$$

Similarly, the other integrations result in 9.6 N and 3.2 N. Thus,

$$\mathbf{f}^e = [3.2, 0, 9.6, 0, 3.2, 0]^T \text{ N} \quad \blacksquare$$

Galerkin Approach

Following the steps presented in Chapter 1, we introduce

$$\boldsymbol{\phi} = [\phi_x, \phi_y]^T \quad (5.46)$$

and

$$\boldsymbol{\epsilon}(\boldsymbol{\phi}) = \left[\frac{\partial \phi_x}{\partial x}, \frac{\partial \phi_y}{\partial y}, \frac{\partial \phi_x}{\partial y} + \frac{\partial \phi_y}{\partial x} \right]^T \quad (5.47)$$

where $\boldsymbol{\phi}$ is an arbitrary (virtual) displacement vector, consistent with the boundary conditions. The variational form is given by

$$\int_A \boldsymbol{\sigma}^T \boldsymbol{\epsilon}(\boldsymbol{\phi}) t dA - \left(\int_A \boldsymbol{\phi}^T \mathbf{f} t dA + \int_L \boldsymbol{\phi}^T \mathbf{T} t d\ell + \sum_i \phi_i^T \mathbf{P}_i \right) = 0 \quad (5.48)$$

where the first term represents the internal virtual work. The expression in parentheses represents the external virtual work. On the discretized region, the previous equation becomes

$$\sum_e \int_e \boldsymbol{\epsilon}^T \mathbf{D} \boldsymbol{\epsilon}(\boldsymbol{\phi}) t dA - \left(\sum_e \int_e \boldsymbol{\phi}^T \mathbf{f} t dA + \int_L \boldsymbol{\phi}^T \mathbf{T} t d\ell + \sum_i \phi_i^T \mathbf{P}_i \right) = 0 \quad (5.49)$$

Using the interpolation steps of Eqs. 5.12–5.14, we express

$$\phi = \mathbf{N}\psi \quad (5.50)$$

$$\epsilon(\phi) = \mathbf{B}\psi \quad (5.51)$$

where

$$\psi = [\psi_1, \psi_2, \psi_3, \psi_4, \psi_5, \psi_6]^T \quad (5.52)$$

represents the arbitrary nodal displacements of element e . The global nodal displacement variations Ψ are represented by

$$\Psi = [\Psi_1, \Psi_2, \dots, \Psi_N]^T \quad (5.53)$$

The element internal work term in Eq. 5.49 can be expressed as

$$\int_e \epsilon^T \mathbf{D} \epsilon(\phi) t \, dA = \int_e \mathbf{q}^T \mathbf{B}^T \mathbf{D} \mathbf{B} \psi t \, dA$$

Noting that all terms of \mathbf{B} and \mathbf{D} are constant and denoting t_e and A_e as thickness and area of element, respectively, we find that

$$\begin{aligned} \int_e \epsilon^T \mathbf{D} \epsilon(\phi) t \, dA &= \mathbf{q}^T \mathbf{B}^T \mathbf{D} \mathbf{B} t_e \int_e dA \psi \\ &= \mathbf{q}^T t_e A_e \mathbf{B}^T \mathbf{D} \mathbf{B} \psi \\ &= \mathbf{q}^T \mathbf{k}^e \psi \end{aligned} \quad (5.54)$$

where \mathbf{k}^e is the element stiffness matrix given by

$$\mathbf{k}^e = t_e A_e \mathbf{B}^T \mathbf{D} \mathbf{B} \quad (5.55)$$

The material property matrix \mathbf{D} is symmetric, and, hence, the element stiffness matrix is also symmetric. The element connectivity as presented in Table 5.1 is used in adding the stiffness values of \mathbf{k}^e to the global locations. Thus,

$$\begin{aligned} \sum_e \int_e \epsilon^T \mathbf{D} \epsilon(\phi) t \, dA &= \sum_e \mathbf{q}^T \mathbf{k}^e \psi = \sum_e \psi^T \mathbf{k}^e \mathbf{q} \\ &= \Psi^T \mathbf{K} \mathbf{Q} \end{aligned} \quad (5.56)$$

The global stiffness matrix \mathbf{K} is symmetric and banded. The treatment of external virtual work terms follows the steps involved in the treatment of force terms in the potential energy formulation, where \mathbf{u} is replaced by ϕ . Thus,

$$\int_e \phi^T \mathbf{f} t \, dA = \psi^T \mathbf{f}^e \quad (5.57)$$

which follows from Eq. 5.33, with \mathbf{f}^e given by Eq. 5.36. Similarly, the traction and point load treatment follows from Eqs. 5.38 and 5.43. The terms in the variational form are given by

$$\text{Internal virtual work} = \Psi^T \mathbf{K} \mathbf{Q} \quad (5.58a)$$

$$\text{External virtual work} = \Psi^T \mathbf{F} \quad (5.58b)$$

The stiffness and force matrices are modified to use the full size (all degrees of freedom), using methods suggested in Chapter 3. From the Galerkin form (Eq. 5.49), the arbitrariness of Ψ gives

$$\mathbf{KQ} = \mathbf{F} \quad (5.59)$$

where \mathbf{K} and \mathbf{F} are modified to account for boundary conditions. Equation 5.59 turns out to be the same as Eq. 5.45, obtained in the potential-energy formulation.

Stress Calculations

Since strains are constant in a constant-strain triangle (CST) element, the corresponding stresses are constant. The stress values need to be calculated for each element. Using the stress-strain relations in Eq. 5.6 and element strain-displacement relations in Eq. 5.25, we have

$$\boldsymbol{\sigma} = \mathbf{DBq} \quad (5.60)$$

The connectivity in Table 5.1 is once again needed to extract the element nodal displacements \mathbf{q} from the global displacements vector \mathbf{Q} . Equation 5.60 is used to calculate the element stresses. For interpolation purposes, the calculated stress may be used as the value at the centroid of the element.

Principal stresses and their directions are calculated using Mohr's circle relationships. The program at the end of the chapter includes the principal stress calculations.

Detailed calculations in Example 5.6 illustrate the steps involved. However, it is expected that the exercise problems at the end of the chapter will be solved using a computer.

Example 5.6

For the two-dimensional loaded plate shown in Fig. E5.6, determine the displacements of nodes 1 and 2 and the element stresses using plane stress conditions. Body force may be neglected in comparison with the external forces.

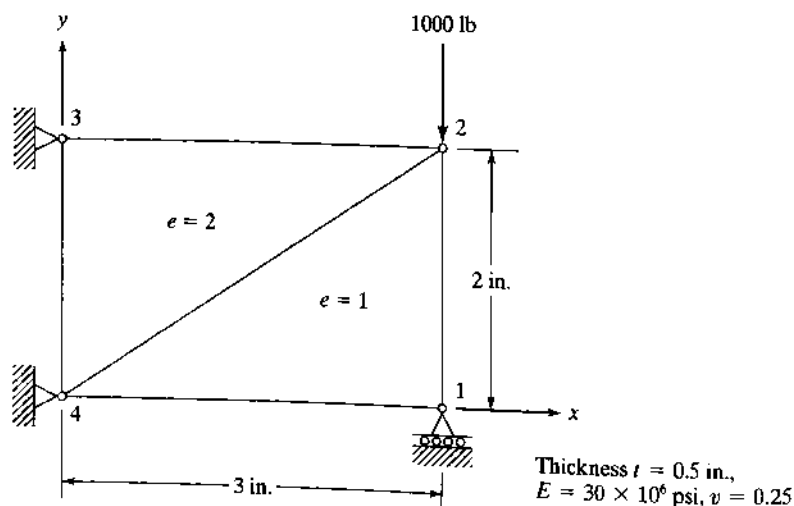


FIGURE E5.6

Solution For plane stress conditions, the material property matrix is given by

$$\mathbf{D} = \frac{E}{1-\nu^2} \begin{bmatrix} 1 & \nu & 0 \\ \nu & 1 & 0 \\ 0 & 0 & \frac{1-\nu}{2} \end{bmatrix} = \begin{bmatrix} 3.2 \times 10^7 & 0.8 \times 10^7 & 0 \\ 0.8 \times 10^7 & 3.2 \times 10^7 & 0 \\ 0 & 0 & 1.2 \times 10^7 \end{bmatrix}$$

Using the local numbering pattern used in Fig. E5.3, we establish the connectivity as follows:

| Element No. | Nodes | | |
|-------------|-------|---|---|
| | 1 | 2 | 3 |
| 1 | 1 | 2 | 4 |
| 2 | 3 | 4 | 2 |

On performing the matrix multiplication \mathbf{DB}^e , we get

$$\mathbf{DB}^1 = 10^7 \begin{bmatrix} 1.067 & -0.4 & 0 & 0.4 & -1.067 & 0 \\ 0.267 & -1.6 & 0 & 1.6 & -0.267 & 0 \\ -0.6 & 0.4 & 0.6 & 0 & 0 & -0.4 \end{bmatrix}$$

and

$$\mathbf{DB}^2 = 10^7 \begin{bmatrix} -1.067 & 0.4 & 0 & -0.4 & 1.067 & 0 \\ -0.267 & 1.6 & 0 & -1.6 & 0.267 & 0 \\ 0.6 & -0.4 & -0.6 & 0 & 0 & 0.4 \end{bmatrix}$$

These two relationships will be used later in calculating stresses using $\sigma^e = \mathbf{DB}^e \mathbf{q}$. The multiplication $t_e \mathbf{A}_e \mathbf{B}^{eT} \mathbf{DB}^e$ gives the element stiffness matrices,

$$\mathbf{k}^1 = 10^7 \begin{bmatrix} 1 & 2 & 3 & 4 & 7 & 8 \leftarrow \text{Global dof} \\ 0.983 & -0.5 & -0.45 & 0.2 & -0.533 & 0.3 \\ & 1.4 & 0.3 & -1.2 & 0.2 & -0.2 \\ & & 0.45 & 0 & 0 & -0.3 \\ & & & 1.2 & -0.2 & 0 \\ \text{Symmetric} & & & & 0.533 & 0 \\ & & & & & 0.2 \end{bmatrix}$$

$$\mathbf{k}^2 = 10^7 \begin{bmatrix} 5 & 6 & 7 & 8 & 3 & 4 \leftarrow \text{Global dof} \\ 0.983 & -0.5 & -0.45 & 0.2 & -0.533 & 0.3 \\ & 1.4 & 0.3 & -1.2 & 0.2 & -0.2 \\ & & 0.45 & 0 & 0 & -0.3 \\ & & & 1.2 & -0.2 & 0 \\ \text{Symmetric} & & & & 0.533 & 0 \\ & & & & & 0.2 \end{bmatrix}$$

In the previous element matrices, the global dof association is shown on top. In the problem under consideration, $Q_2, Q_5, Q_6, Q_7,$ and $Q_8,$ are all zero. Using the elimination approach discussed in Chapter 3, it is now sufficient to consider the stiffnesses associated with

the degrees of freedom Q_1 , Q_3 , and Q_4 . Since the body forces are neglected, the first vector has the component $F_4 = -1000$ lb. The set of equations is given by the matrix representation

$$10^7 \begin{bmatrix} 0.983 & -0.45 & 0.2 \\ -0.45 & 0.983 & 0 \\ 0.2 & 0 & 1.4 \end{bmatrix} \begin{Bmatrix} Q_1 \\ Q_3 \\ Q_4 \end{Bmatrix} = \begin{Bmatrix} 0 \\ 0 \\ -1000 \end{Bmatrix}$$

Solving for Q_1 , Q_3 , and Q_4 , we get

$$Q_1 = 1.913 \times 10^{-5} \text{ in.} \quad Q_3 = 0.875 \times 10^{-5} \text{ in.} \quad Q_4 = -7.436 \times 10^{-5} \text{ in.}$$

For element 1, the element nodal displacement vector is given by

$$\mathbf{q}^1 = 10^{-5} [1.913, 0, 0.875, -7.436, 0, 0]^T$$

The element stresses $\boldsymbol{\sigma}^1$ are calculated from $\mathbf{DB}^1 \mathbf{q}$ as

$$\boldsymbol{\sigma}^1 = [-93.3, -1138.7, -62.3]^T \text{ psi}$$

Similarly,

$$\mathbf{q}^2 = 10^{-5} [0, 0, 0, 0, 0.875, -7.436]^T$$

$$\boldsymbol{\sigma}^2 = [93.4, 23.4, -297.4]^T \text{ psi}$$

The computer results may differ slightly since the penalty approach for handling boundary conditions is used in the computer program. ■

Temperature Effects

If the distribution of the change in temperature $\Delta T(x, y)$ is known, the strain due to this change in temperature can be treated as an initial strain $\boldsymbol{\epsilon}_0$. From the theory of mechanics of solids, $\boldsymbol{\epsilon}_0$ can be represented by

$$\boldsymbol{\epsilon}_0 = [\alpha \Delta T, \alpha \Delta T, 0]^T \quad (5.61)$$

for plane stress and

$$\boldsymbol{\epsilon}_0 = (1 + \nu)[\alpha \Delta T, \alpha \Delta T, 0]^T \quad (5.62)$$

for plane strain. The stresses and strains are related by

$$\boldsymbol{\sigma} = \mathbf{D}(\boldsymbol{\epsilon} - \boldsymbol{\epsilon}_0) \quad (5.63)$$

The effect of temperature can be accounted for by considering the strain energy term. We have

$$\begin{aligned} U &= \frac{1}{2} \int (\boldsymbol{\epsilon} - \boldsymbol{\epsilon}_0)^T \mathbf{D}(\boldsymbol{\epsilon} - \boldsymbol{\epsilon}_0) t \, dA \\ &= \frac{1}{2} \int (\boldsymbol{\epsilon}^T \mathbf{D} \boldsymbol{\epsilon} - 2\boldsymbol{\epsilon}^T \mathbf{D} \boldsymbol{\epsilon}_0 + \boldsymbol{\epsilon}_0^T \mathbf{D} \boldsymbol{\epsilon}_0) t \, dA \end{aligned} \quad (5.64)$$

The first term in the previous expansion gives the stiffness matrix derived earlier. The last term is a constant, which has no effect on the minimization process. The middle term, which yields the temperature load, is now considered in detail. Using the strain-displacement relationship $\boldsymbol{\epsilon} = \mathbf{B}\mathbf{q}$,

$$\int_A \boldsymbol{\epsilon}^T \mathbf{D} \boldsymbol{\epsilon}_0 t dA = \sum_e \mathbf{q}^T (\mathbf{B}^T \mathbf{D} \boldsymbol{\epsilon}_0) t_e A_e \quad (5.65)$$

This step is directly obtained in the Galerkin approach where $\boldsymbol{\epsilon}^T$ will be $\boldsymbol{\epsilon}^T(\boldsymbol{\phi})$ and \mathbf{q}^T will be $\boldsymbol{\psi}^T$.

It is convenient to designate the element temperature load as

$$\boldsymbol{\Theta}^e = t_e A_e \mathbf{B}^T \mathbf{D} \boldsymbol{\epsilon}_0 \quad (5.66)$$

where

$$\boldsymbol{\Theta}^e = [\Theta_1, \Theta_2, \Theta_3, \Theta_4, \Theta_5, \Theta_6]^T \quad (5.67)$$

The vector $\boldsymbol{\epsilon}_0$ is the strain in Eq. 5.61 or 5.62 due to the average temperature change in the element. $\boldsymbol{\Theta}^e$ represents the element nodal load contributions that must be added to the global force vector using the connectivity.

The stresses in an element are then obtained by using Eq. 5.63 in the form

$$\boldsymbol{\sigma} = \mathbf{D}(\mathbf{B}\mathbf{q} - \boldsymbol{\epsilon}_0) \quad (5.68)$$

Example 5.7

Consider the two-dimensional loaded plate shown in Fig. E5.6. In addition to the conditions defined in Example 5.6, there is an increase in temperature of the plate of 80°F. The coefficient of linear expansion of the material α is $7 \times 10^{-6}/^\circ\text{F}$. Determine the additional displacements due to temperature. Also, calculate the stresses in element 1.

Solution We have $\alpha = 7 \times 10^{-6}/^\circ\text{F}$ and $\Delta T = 80^\circ\text{F}$. So

$$\boldsymbol{\epsilon}_0 = \begin{bmatrix} \alpha \Delta T \\ \alpha \Delta T \\ 0 \end{bmatrix} = 10^{-4} \begin{bmatrix} 5.6 \\ 5.6 \\ 0 \end{bmatrix}$$

Thickness t equals 0.5, and the area of the element A is 3 in². The element temperature loads are

$$\boldsymbol{\Theta}^1 = tA(\mathbf{DB}^1)^T \boldsymbol{\epsilon}_0$$

where \mathbf{DB}^1 is calculated in the solution of Example 5.5. On evaluation, we get

$$(\boldsymbol{\Theta}^1)^T = [11206 \quad -16800 \quad 0 \quad 16800 \quad -11206 \quad 0]^T$$

with associated dofs 1, 2, 3, 4, 7, 8, and

$$(\boldsymbol{\Theta}^2)^T = [-11206 \quad 16800 \quad 0 \quad -16800 \quad 11206 \quad 0]^T$$

with associated dofs 5, 6, 7, 8, 3, and 4.

Picking the forces for dofs 1, 3, and 4 from the previous equations, we have

$$\mathbf{F}^T = [F_1 \quad F_3 \quad F_4] = [11206 \quad 11206 \quad 16800]$$

On solving $\mathbf{KQ} = \mathbf{F}$, we get

$$[Q_1 \quad Q_3 \quad Q_4] = [1.862 \times 10^{-3} \quad 1.992 \times 10^{-3} \quad 0.934 \times 10^{-3}] \text{ in}$$

The displacements of element 1 due to temperature are

$$\mathbf{q}^1 = [1.862 \times 10^{-3} \quad 0 \quad 1.992 \times 10^{-4} \quad 0.934 \times 10^{-3} \quad 0 \quad 0]^T$$

The stresses are calculated using Eq. 5.68 as

$$\sigma^1 = (DB^1)^T q^1 - D\epsilon_0$$

On substituting for the terms on the right-hand side, we get

$$\sigma^1 = 10^4 [1.204 \quad -2.484 \quad 0.78]^T \text{ psi}$$

We note that the displacements and stresses just calculated are due to temperature change. ■

5.4 PROBLEM MODELING AND BOUNDARY CONDITIONS

The finite element method is used for computing displacements and stresses for a wide variety of problems. The physical dimensions, loading, and boundary conditions are clearly defined in some problems, similar to what we discussed in Example 5.4. In other problems, these are not clear at the outset.

An example is the problem illustrated in Fig. 5.8a. A plate with such a loading can exist anywhere in space. Since we are interested in the deformation of the body, the symmetry of the geometry and the symmetry of the loading can be used effectively. Let x and y represent the axes of symmetry as shown in Fig. 5.8b. The points along the x -axis move along x and are constrained in the y direction and points along the y -axis are constrained along the x direction. This suggests that the part, which is one-quarter of the full area, with the loading and boundary conditions as shown is all that is needed to solve the deformation and stresses.

As another example, consider an octagonal pipe under internal pressure, shown in Fig. 5.9a. By symmetry, we observe that it is sufficient to consider the 22.5° segment shown in Fig. 5.9b. The boundary conditions require that points along x and n are constrained normal to the two lines, respectively. Note that for a *circular* pipe under internal or external pressure, by symmetry, all points move radially. In this case, any radial segment may be considered. The boundary conditions for points along the x -axis in Fig. 5.9b are easily considered by using the penalty approach discussed in Chapter 3. The boundary conditions for points along the inclined direction n , which are considered perpendicular to n , are now treated in detail. If node i with degrees of freedom Q_{2i-1} and

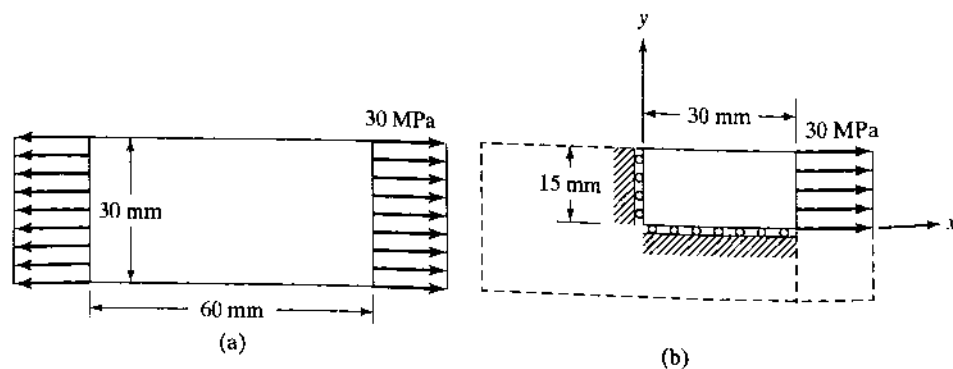


FIGURE 5.8 Rectangular plate.

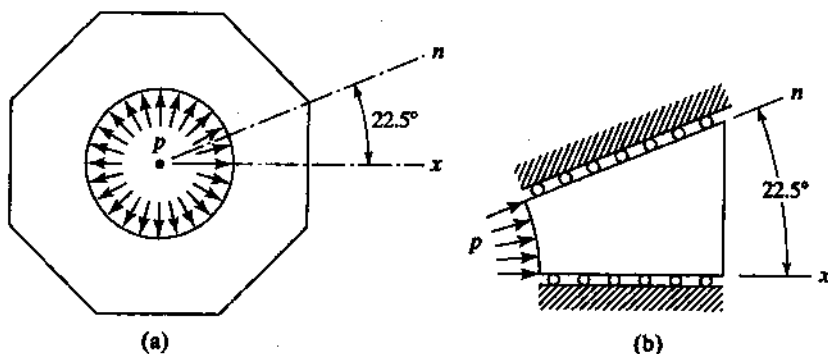


FIGURE 5.9 Octagonal pipe.

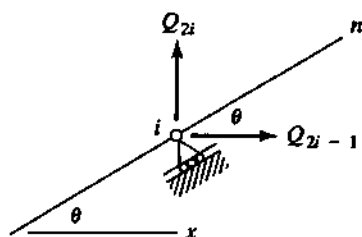


FIGURE 5.10 Inclined roller support.

Q_{2i} moves along n as seen in Fig. 5.10 and θ is the angle of inclination of n with respect to x -axis, we have

$$Q_{2i-1} \sin \theta - Q_{2i} \cos \theta = 0 \quad (5.69)$$

This boundary condition is seen to be a multipoint constraint, which is discussed in Chapter 3. Using the penalty approach presented in Chapter 3, this amounts to adding a term to the potential energy as in

$$\Pi = \frac{1}{2} \mathbf{Q}^T \mathbf{K} \mathbf{Q} - \mathbf{Q}^T \mathbf{F} + \frac{1}{2} C (Q_{2i-1} \sin \theta - Q_{2i} \cos \theta)^2 \quad (5.70)$$

where C is a large number.

The squared term in Eq. 5.70 can be written in the form

$$\frac{1}{2} C (Q_{2i-1} \sin \theta - Q_{2i} \cos \theta)^2 = \frac{1}{2} [Q_{2i-1}, Q_{2i}] \begin{bmatrix} C \sin^2 \theta & -C \sin \theta \cos \theta \\ -C \sin \theta \cos \theta & C \cos^2 \theta \end{bmatrix} \begin{Bmatrix} Q_{2i-1} \\ Q_{2i} \end{Bmatrix} \quad (5.71)$$

The terms $C \sin^2 \theta$, $-C \sin \theta \cos \theta$, and $C \cos^2 \theta$ get added to the global stiffness matrix, for every node on the incline, and the new stiffness matrix is used to solve for the displacements. Note that these modifications can also be directly obtained from Eq. 3.82 by substituting $\beta_0 = 0$, $\beta_1 = \sin \theta$, and $\beta_2 = -\cos \theta$. The contributions to the banded stiffness matrix \mathbf{S} are made in the locations $(2i - 1, 1)$, $(2i - 1, 2)$, and $(2i, 1)$ by adding $C \sin^2 \theta$, $-C \sin \theta \cos \theta$, and $C \cos^2 \theta$, respectively.

Some General Comments on Dividing into Elements

When dividing an area into triangles, avoid large aspect ratios. Aspect ratio is defined as the ratio of maximum to minimum characteristic dimensions. Observe that the best elements are those that approach an equilateral triangular configuration. Such configurations are not usually possible. A good practice may be to choose corner angles in the range of 30° to 120°.

In problems where the stresses change widely over an area, such as in notches and fillets, it is good practice to decrease the size of elements in that area to capture the stress variations. The constant-strain triangle (CST), in particular, gives constant stresses on the element. This suggests that smaller elements will better represent the distribution. Better estimates of maximum stress may be obtained even with coarser meshes by plotting and extrapolating. For this purpose, the constant element stresses may be interpreted as the values at centroids of the triangle. A method for evaluating nodal values from constant element values is presented in the postprocessing section of Chapter 12.

Coarse meshes are recommended for initial trials to check data and reasonableness of results. Errors may be fixed at this stage, before running larger numbers of elements. Increasing the number of elements in those regions where stress variations are high should give better results. This is called *convergence*. One should get a feel for convergence by successively increasing the number of elements in finite element meshes.

5.5 ORTHOTROPIC MATERIALS

Certain naturally occurring materials such as crystals of topaz and barite are orthotropic. Wood may also be considered to be orthotropic as a first approximation. Unidirectional fiber-reinforced composites also exhibit orthotropic behavior. Orthotropic materials have three mutually perpendicular planes of elastic symmetry. We will denote 1, 2, and 3 as the *principal material axes* that are normal to the planes of symmetry. For example, Fig. 5.11 shows a cross section of a tree, with 1 being the axis along the wood fibers (grain), 2 being the axis tangential to the annual rings, and 3 the axis along the radial direction. The generalized Hooke's law as referred to coordinate system 1, 2, 3 can be written as*

$$\begin{aligned}\epsilon_1 &= \frac{1}{E_1}\sigma_1 - \frac{\nu_{21}}{E_2}\sigma_2 - \frac{\nu_{31}}{E_3}\sigma_3, & \gamma_{23} &= \frac{1}{G_{23}}\tau_{23} \\ \epsilon_2 &= -\frac{\nu_{12}}{E_1}\sigma_1 + \frac{1}{E_2}\sigma_2 - \frac{\nu_{32}}{E_3}\sigma_3, & \gamma_{13} &= \frac{1}{G_{13}}\tau_{13} \\ \epsilon_3 &= -\frac{\nu_{13}}{E_1}\sigma_1 - \frac{\nu_{23}}{E_2}\sigma_2 + \frac{1}{E_3}\sigma_3, & \gamma_{12} &= \frac{1}{G_{12}}\tau_{12}\end{aligned}\quad (5.72)$$

where E_1 , E_2 , and E_3 are the Young's moduli along the principal material axes; ν_{12} is the Poisson's ratio that characterizes the decrease in the 2-direction during tension applied in the 1-direction; ν_{21} is the Poisson's ratio that characterizes the decrease in the 1-direction

*S. G. Lekhnitskij, *Anisotropic Plates*, Gordon and Breach Science Publishers, New York, 1968 (translated by S. W. Tsai and T. Cheron).

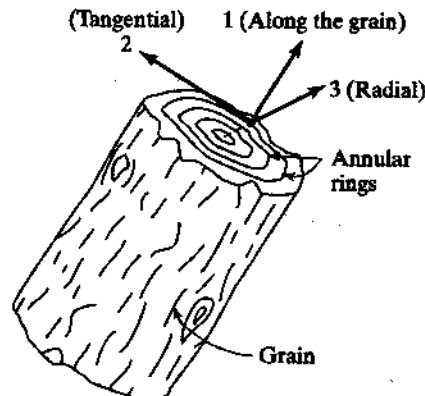


FIGURE 5.11 Wood as an orthotropic material.

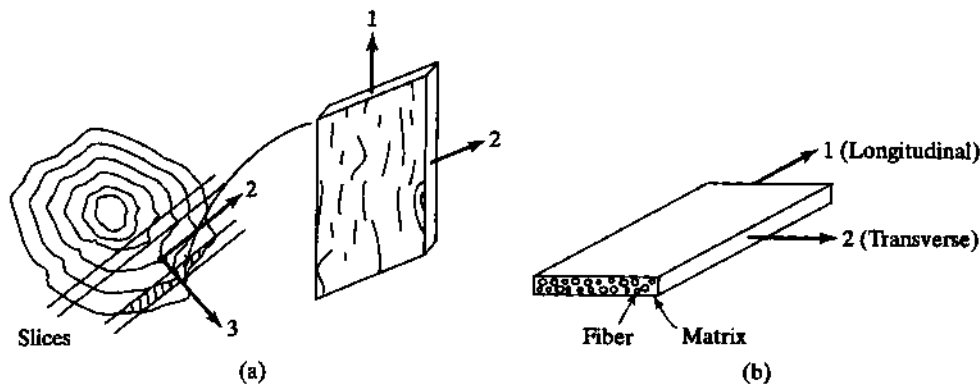


FIGURE 5.12 Plane stress orthotropic bodies. (a) wood planks, (b) unidirectional composites.

due to tension in the 2-direction, and so on; and G_{23} , G_{13} , and G_{12} are the shear moduli that characterize changes of angles between principal directions 2 and 3, 1 and 3, and 1 and 2, respectively. Due to symmetry of Eqs. 5.72, the following relations obtain:

$$E_1\nu_{21} = E_2\nu_{12}, \quad E_2\nu_{32} = E_3\nu_{23}, \quad E_3\nu_{13} = E_1\nu_{31}, \quad (5.73)$$

Thus, there are nine independent material constants. In this chapter, we will consider only the problem of plane stress. Thus, we consider a thin body that lies in the 1, 2 plane. Examples of such thin bodies are shown in Figs. 5.12a and b. Figure 5.12a shows how thin planks are obtained from a tree. Figure 5.12b shows a unidirectional composite that can be modeled as a plane stress orthotropic problem. In actual design, many layers of these unidirectional composites are stacked at different fiber orientations to form a *laminate*. A single-layer composite may be viewed as a building block for laminate constructions. In a unidirectional composite, the Young's modulus along the fibers is greater than that across. That is, $E_1 > E_2$. The axis 1 is often referred to as the *longitudinal axis*, and 2 is referred to as the *transverse axis*. In plane stress, all stresses and

displacements are assumed to be averaged across the thickness and are consequently only functions of 1, 2. The loading is confined to be in the 1, 2 plane.

Neglecting the z -component stresses, we have, from (5.72),

$$\epsilon_1 = \frac{1}{E_1}\sigma_1 - \frac{\nu_{21}}{E_2}\sigma_2, \quad \epsilon_2 = -\frac{\nu_{12}}{E_1}\sigma_1 + \frac{1}{E_2}\sigma_2, \quad \gamma_{12} = \frac{1}{G_{12}}\tau_{12} \quad (5.74)$$

These equations can be inverted to express stress in terms of strain as

$$\begin{Bmatrix} \sigma_1 \\ \sigma_2 \\ \tau_{12} \end{Bmatrix} = \begin{bmatrix} \frac{E_1}{1 - \nu_{12}\nu_{21}} & \frac{E_1\nu_{21}}{1 - \nu_{12}\nu_{21}} & 0 \\ \frac{E_2\nu_{12}}{1 - \nu_{12}\nu_{21}} & \frac{E_2}{1 - \nu_{12}\nu_{21}} & 0 \\ 0 & 0 & G_{12} \end{bmatrix} \begin{Bmatrix} \epsilon_1 \\ \epsilon_2 \\ \gamma_{12} \end{Bmatrix} \quad (5.75)$$

The 3×3 coefficient matrix in expression 5.75 will be denoted by \mathbf{D}^m , the superscript m denoting the material axes. Thus, $D_{11}^m = E_1/(1 - \nu_{12}\nu_{21})$, $D_{33}^m = G_{12}$, and so on. \mathbf{D}^m is symmetric since $E_1\nu_{21} = E_2\nu_{12}$. Four independent constants are involved here.

When an orthotropic plate is loaded parallel to its material axes, it results only in normal strains and not in shear strains. When the load is not parallel to any of its material axes, it results in both normal and shear strains. To be able to analyze general problems of this sort, we will consider an orthotropic material with its material axes oriented at an angle θ with the global x -, y -axes as shown in Fig. 5.13. Note that θ is measured counterclockwise from the x -axis to the 1-axis. A transformation matrix \mathbf{T} is introduced as

$$\mathbf{T} = \begin{bmatrix} \cos^2 \theta & \sin^2 \theta & 2 \sin \theta \cos \theta \\ \sin^2 \theta & \cos^2 \theta & -2 \sin \theta \cos \theta \\ -\sin \theta \cos \theta & \sin \theta \cos \theta & \cos^2 \theta - \sin^2 \theta \end{bmatrix} \quad (5.76)$$

The relations between the stresses (strains) in the material coordinate system and the global coordinate system are

$$\begin{Bmatrix} \sigma_1 \\ \sigma_2 \\ \tau_{12} \end{Bmatrix} = \mathbf{T} \begin{Bmatrix} \sigma_x \\ \sigma_y \\ \tau_{xy} \end{Bmatrix}, \quad \begin{Bmatrix} \epsilon_1 \\ \epsilon_2 \\ \frac{1}{2}\gamma_{12} \end{Bmatrix} = \mathbf{T} \begin{Bmatrix} \epsilon_x \\ \epsilon_y \\ \frac{1}{2}\gamma_{xy} \end{Bmatrix} \quad (5.77)$$

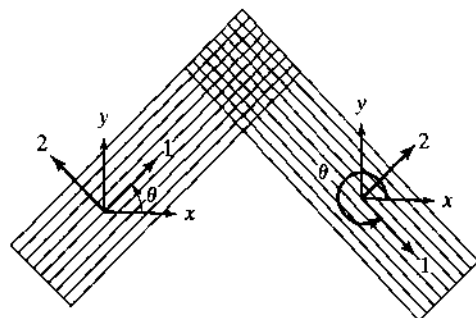


FIGURE 5.13 Orientation of material axes with respect to global axes; θ is the counterclockwise angle from x -axis to 1-axis. Note: $\theta = 330^\circ$ is equivalent to $\theta = -30^\circ$.

The important relation we need is the \mathbf{D} matrix, which relates stress and strain in the global system as

$$\begin{Bmatrix} \sigma_x \\ \sigma_y \\ \tau_{xy} \end{Bmatrix} = \begin{bmatrix} D_{11} & D_{12} & D_{13} \\ D_{12} & D_{22} & D_{23} \\ D_{13} & D_{23} & D_{33} \end{bmatrix} \begin{Bmatrix} \epsilon_x \\ \epsilon_y \\ \gamma_{xy} \end{Bmatrix} \quad (5.78)$$

It can be shown* that the \mathbf{D} matrix is related to the \mathbf{D}^m matrix as

$$\begin{aligned} D_{11} &= D_{11}^m \cos^4 \theta + 2(D_{12}^m + 2D_{33}^m) \sin^2 \theta \cos^2 \theta + D_{22}^m \sin^4 \theta \\ D_{12} &= (D_{11}^m + D_{22}^m - 4D_{33}^m) \sin^2 \theta \cos^2 \theta + D_{12}^m (\sin^4 \theta + \cos^4 \theta) \\ D_{13} &= (D_{11}^m - D_{12}^m - 2D_{33}^m) \sin \theta \cos^3 \theta + (D_{12}^m - D_{22}^m + 2D_{33}^m) \sin^3 \theta \cos \theta \\ D_{22} &= D_{11}^m \sin^4 \theta + 2(D_{12}^m + 2D_{33}^m) \sin^2 \theta \cos^2 \theta + D_{22}^m \cos^4 \theta \\ D_{23} &= (D_{11}^m - D_{12}^m - 2D_{33}^m) \sin^3 \theta \cos \theta + (D_{12}^m - D_{22}^m + 2D_{33}^m) \sin \theta \cos^3 \theta \\ D_{33} &= (D_{11}^m + D_{22}^m - 2D_{12}^m - 2D_{33}^m) \sin^2 \theta \cos^2 \theta + D_{33}^m (\sin^4 \theta + \cos^4 \theta) \end{aligned} \quad (5.79)$$

Implementation of (5.79) into the finite element program CST2 is straightforward. The existing isotropic \mathbf{D} matrix is replaced by that given in Eq. (5.79). The angle θ will be assumed to be constant within each finite element, although the angle can vary from one element to another. This variation in θ makes it possible to tailor the material so as to be most effective in resisting the loads. After equation solving and obtaining the stresses in the global coordinate system, the stresses in the material coordinate system can be obtained using Eqs. 5.77 and then inserted into an appropriate failure theory to determine the factor of safety.

Temperature Effects

We have studied how temperature strains are handled for isotropic materials. The stress-strain law is of the form $\sigma = \mathbf{D}(\epsilon - \epsilon^0)$. This same relation also holds for orthotropic materials. In material coordinates, an increase in temperature ΔT will cause normal strains, but no shearing strain. Thus, $\epsilon_1^0 = \alpha_1 \Delta T$ and $\epsilon_2^0 = \alpha_2 \Delta T$. The \mathbf{T} -matrix in Eq. 5.76 can be used to transform the coefficients of thermal expansion as

$$\begin{Bmatrix} \alpha_x \\ \alpha_y \\ \frac{1}{2} \alpha_{xy} \end{Bmatrix} = \mathbf{T} \begin{Bmatrix} \alpha_1 \\ \alpha_2 \\ 0 \end{Bmatrix} \quad (5.80)$$

The initial strain vector ϵ^0 is now given by

$$\begin{Bmatrix} \epsilon_x^0 \\ \epsilon_y^0 \\ \gamma_{xy}^0 \end{Bmatrix} = \begin{Bmatrix} \alpha_x & \Delta T \\ \alpha_y & \Delta T \\ \alpha_{xy} & \Delta T \end{Bmatrix} \quad (5.81)$$

*B. D. Agarwal and L. J. Broutman, *Analysis and Performance of Fiber Composites*, John Wiley & Sons, Inc., New York, 1980.

TABLE 5.1 Typical Properties for Some Orthotropic Materials

| Material | $E_1, 10^9$ psi | E_1/E_2 | ν_{12} | E_1/G_{12} | $\alpha_1, 10^{-6}/^\circ\text{F}$ | $\alpha_2, 10^{-6}/^\circ\text{F}$ |
|---------------------------|-----------------|-----------|------------|--------------|------------------------------------|------------------------------------|
| Balsa wood | 0.125 | 20.0 | 0.30 | 29.0 | — | — |
| Pine wood | 1.423 | 23.8 | 0.24 | 13.3 | — | — |
| Plywood | 1.707 | 2.0 | 0.07 | 17.1 | — | — |
| Boron Epoxy | 33.00 | 1.571 | 0.23 | 4.714 | 3.20 | 11.0 |
| S-glass epoxy | 7.50 | 4.412 | 0.25 | 9.375 | 3.50 | 11.0 |
| Graphite (Thornel 300) | 23.06 | 14.587 | 0.38 | 24.844 | 0.025 | 11.2 |
| Kevlar-49 | 12.04 | 14.820 | 0.34 | 39.500 | -1.22 to -1.28 | 19.4 |

Typical values of the elastic constants for some orthotropic materials, that is, wood materials and unidirectional composites, are given in Table 5.1. The unidirectional composites are made from embedding fibers in a matrix. In the table, the matrix is an epoxy resin with $E \approx 0.5 \times 10^6$ psi, $\nu = 0.3$.

Example 5.8

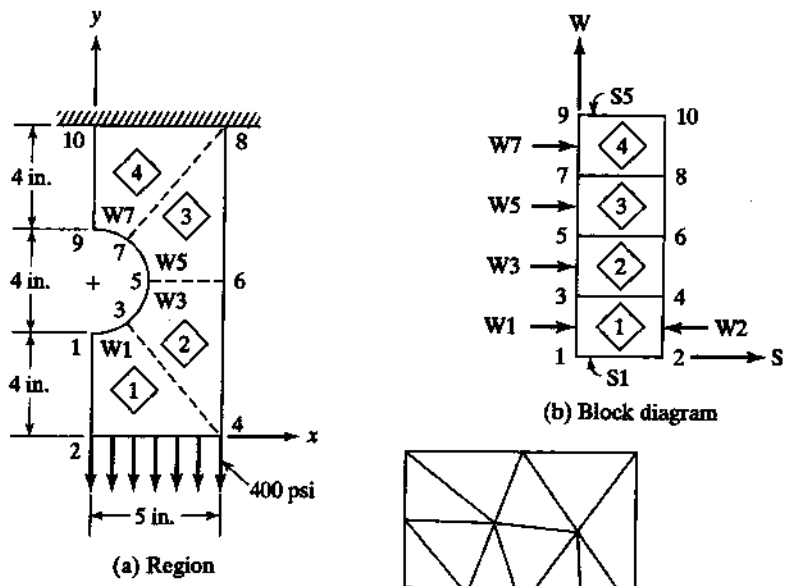
This example shows how more detailed models can be analyzed using program CST with pre- and postprocessing programs of Chapter 12.

Consider the problem shown in Fig. E5.8a. It is necessary to determine the location and magnitude of the maximum y stress in the plate.

Use of the mesh generation program MESHGEN requires mapping the region into a checkerboard and specifying the number of subdivisions for discretization. The detailed explanation of using MESHGEN is given in Chapter 12. Here, the emphasis is only on using the program to generate input data for CST. Thus, using the checkerboard in Fig. E5.8b, a 36-node, 48-element mesh is created as shown in Fig. E5.8c. Program PLOT2D has been used to generate the plot after executing MESHGEN. A text editor is then used to define the boundary conditions, loads, and material properties. The MESHGEN input file is listed subsequently. MESHGEN is run using this input file. The output of MESHGEN is then edited using any text editor. The changes and additions are shown in bold face in the CST input file, which follows the MESHGEN input file listing. Note that the structure of input files is shown in the inside front cover of the book. The resulting data file is input into CST. In summary, the order in which programs are executed is MESHGEN, PLOT2D, text editor, and CST.

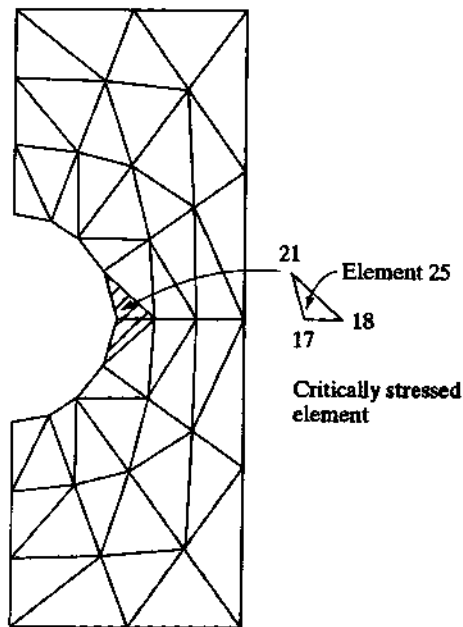
From the output, we note the maximum y stress to be 1768.0 psi occurring in the hatched region in Fig. E5.8c.

The reader is urged to follow these steps, which will help in the solution of complex problems with less effort. Programs BESTFIT and CONTOURA or CONTOURB can be used at this stage for obtaining nodal stresses and contour plots, as discussed in Chapter 12. Contour plotting with programs BESTFIT and CONTOUR is shown schematically in Fig. E5.8d. Also, the stresses in the elements may be considered to be accurate at the centroids of the elements and can be extrapolated to obtain the maximum stresses. See Figs. E6.3c or E7.2b for examples of such extrapolation. ■



STEPS

1. Divide the region into four-sided subregions
2. Create a block diagram
3. Number the blocks, corner nodes and sides on the block diagram
4. Transfer these numbers onto the region
5. Create input file and run MESHGEN.BAS
6. Run PLOT2D.BAS
7. Use text editor to prepare cst.inp see front pages of book for the structure of input file
8. Run CST
9. Run BESTFIT followed by CONTOURA.BAS and CONTOUR.BAS

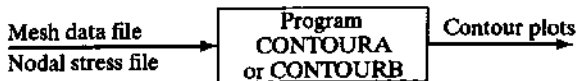


(c) Finite element mesh viewed using PLOT2D.BAS

STEP 1



STEP 2



(d) Contour plotting using programs BESTFIT and CONTOUR

FIGURE E5.8

Input Data File

```

MESHGEN Input File
Example E5.8
Number of Nodes per Element <3 or 4>
3
BLOCK DATA
#S-Spans (NS)   #W-Spans (NW)   #PairsOfEdgesMerged(NSJ)
1               4               0
SPAN DATA
S-Span#  Num-Divisions   (for each S-Span/ Single division = 1)
1        3
W-Span#  Num-Divisions   (for each W-Span/ Single division = 1)
1        2
2        2
3        2
4        2
BLOCK MATERIAL DATA (for Material Number other than 1)
Block#  Material (Void => 0   Block# = 0 completes this data)
0
BLOCK CORNER DATA
Corner#  X-Coord  Y-Coord (Corner# = 0 completes this data)
1        0        4
2        0        0
3        1.4142   4.5858
4        5        0
5        2        6
6        5        6
7        1.4142   7.4142
8        5        12
9        0        8
10       0        12
0
MID POINT DATA FOR CURVED OR GRADED SIDES
S-Side#  X-Coord  Y-Coord (Side# = 0 completes this data)
0
W-Side#  X-Coord  Y-Coord (Side# = 0 completes this data)
1        .7654    4.1522
3        1.8478   5.2346
5        1.8478   6.7654
7        .7654    7.8478
0
MERGING SIDES (Node1 is the lower number)
Pair#  Side1Node1  Side1Node2  Side2Node1  Side2Node2

```

```

CST INPUT FILE (MESHGEN OUTPUT FILE AFTER TEXT EDITING)
Example E5.8
NN NE NM NDIM NEN NDN
 36 48 1 2 3 2
ND NL NMPC
 6 3 0
Node# X Y
 1 0 4
 2 0 2.666667
-----
 35 0 10.66667
 36 0 12
Elem# Node1 Node2 Node3 Material# Thickness TempChange
 1 1 2 5 1 .4 0
 2 6 5 2 1 .4 0
 3 2 3 6 1 .4 0
46 35 34 30 1 .4 0
47 31 32 36 1 .4 0
48 36 35 31 1 .4 0
DOF# Specified Displacement
55 0
56 0
63 0
64 0
71 0
72 0
DOF# Load
8 -200
16 -400
24 -200
MAT# E PWU CTE
1 30e6 .3 0
    
```

Enter data

THICKNESS,
AND TEMP.
CHANGE

Data Added

```

<< STRESS ANALYSIS USING CONSTANT STRAIN TRIANGLE >>
EXAMPLE 5.5
NN NE NM NDIM NEN NDN
 4 2 1 2 3 2
ND NL NMPC
 5 1 0
Node# X Y
 1 3 0
 2 3 2
 3 0 2
 4 0 0
Elem# N1 N2 N3 Mat# Thickness TempRise
 1 4 1 2 1 .5 0
 2 3 4 2 1 .5 0
DOF# Displacement
 2 0
 5 0
 6 0
 7 0
 8 0
DOF# Load
 4 -1000
MAT# E Nu Alpha
 1 30E6 .25 12E-6
B1 1 B2 j B3 (Multi-point constr. B1*Q1+B2*Qj=B3)
    
```

Program Cst2D - CHANDRUPATLA & BELEGUNDU

Output

EXAMPLE 5.5

Plane Stress Analysis

| NODE# | X-Displ | Y-Displ | | | | |
|------------|-------------|-------------|-------------|-------------|-------------|--------------|
| 1 | 1.9076E-05 | -5.8618E-09 | | | | |
| 2 | 8.7326E-06 | -7.4160E-05 | | | | |
| 3 | 1.9216E-09 | -1.1840E-09 | | | | |
| 4 | -1.9216E-09 | -9.7090E-11 | | | | |
| ELEM# | SX | SY | TXY | S1 | S2 | ANGLE SX->S1 |
| 1 | -9.3122E+01 | -1.1356E+03 | -6.2082E+01 | -8.9438E+01 | -1.1393E+03 | - |
| 3.3961E+00 | | | | | | |
| 2 | 9.3122E+01 | 2.3264E+01 | -2.9661E+02 | 3.5685E+02 | -2.4047E+02 | -4.1642E+01 |
| DOF# | REACTION | | | | | |
| 2 | 8.2065E+02 | | | | | |
| 5 | -2.6902E+02 | | | | | |
| 6 | 1.6575E+02 | | | | | |
| 7 | 2.6902E+02 | | | | | |
| 8 | 1.3593E+01 | | | | | |

PROBLEMS

- 5.1. The nodal coordinates of the triangular element are shown in Fig. P5.1. At the interior point P , the x -coordinate is 3.3 and $N_1 = 0.3$. Determine N_2 , N_3 , and the y -coordinate at point P .

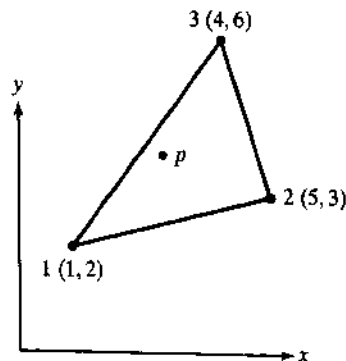


FIGURE P5.1

- 5.2. Determine the Jacobian for the $(x, y) - (\xi, \eta)$ transformation for the element shown in Fig. P5.2. Also, find the area of the triangle.

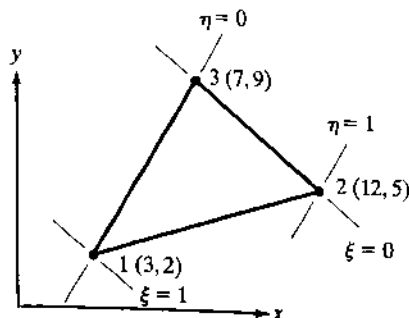


FIGURE P5.2

- 5.3. For point P located inside the triangle shown in Fig. P5.3, the shape functions N_1 and N_2 are 0.15 and 0.25, respectively. Determine the x - and y -coordinates of point P .

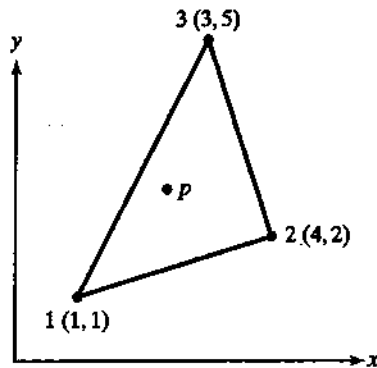


FIGURE P5.3

- 5.4. In Example 5.1, determine the shape functions using the area coordinate approach. (*Hint:* Use $\text{Area} = 0.5(x_{13}y_{23} - x_{23}y_{13})$ for triangle 1-2-3.)
- 5.5. For the triangular element shown in Figure P5.5, obtain the strain-displacement relation matrix \mathbf{B} and determine the strains ϵ_x , ϵ_y , and γ_{xy} .

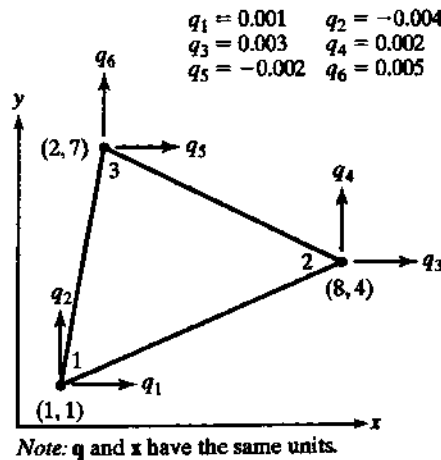


FIGURE P5.5

5.6. Figure P5.6 shows a 2-D region modeled with 12 CST elements.

- (a) Determine the bandwidth NBW (also referred to as the "half-bandwidth").
- (b) If the multipoint constraint $Q_1 = Q_{18}$ is imposed (1 and 18 are degree of freedom numbers corresponding to x displacement of node 1 and y displacement of node 9, respectively), what is the new value of NBW?

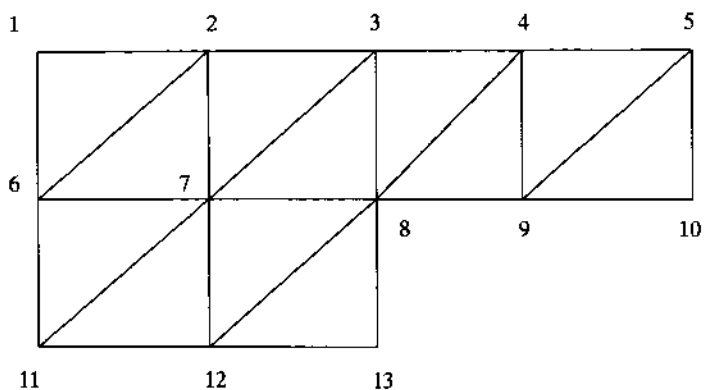


FIGURE P5.6

5.7. Indicate all the mistakes in the following finite element models with CST elements:

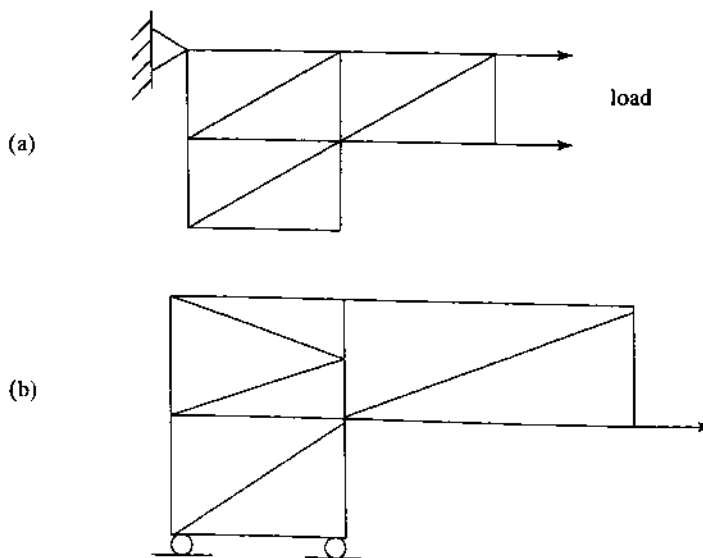


FIGURE P5.7

- 5.8. For a two-dimensional triangular element, the stress–displacement matrix DB appearing in $\sigma = DBq$ is given by

$$DB = \begin{bmatrix} 2500 & 2200 & -1500 & 1200 & -4400 & 1000 \\ 5500 & 4000 & 4100 & 2600 & -1500 & 1200 \\ 2000 & 2500 & -4000 & 1800 & 2200 & 4400 \end{bmatrix} \text{ N/mm}^3$$

If the coefficient of linear expansion is $10 \times 10^{-6}/^\circ\text{C}$, the temperature rise of the element is 100°C , and the volume of the element is 25 mm^3 , determine the equivalent temperature load θ for the element.

- 5.9. For the configuration shown in Fig. P5.9, determine the deflection at the point of load application using a one-element model. If a mesh of several triangular elements is used, comment on the stress values in the elements close to the tip.

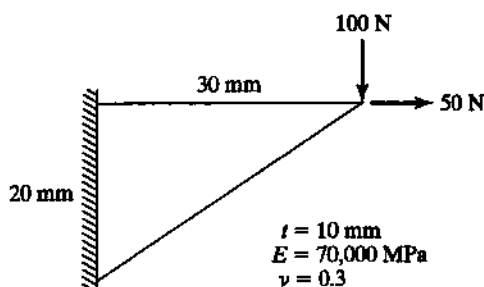


FIGURE P5.9

- 5.10. Determine the bandwidth for the two-dimensional region for the triangular element division with the node numbering shown in Fig. P5.10. How do you proceed to decrease the bandwidth?

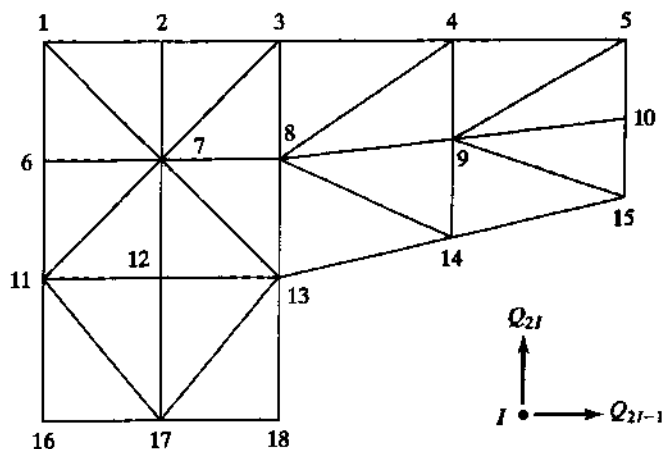


FIGURE P5.10

- 5.11. Consider the four-element CST model in Fig. P5.11 subjected to a body force $f = y^2 \text{ N/m}^3$ in the y direction. Assemble the global load vector $\mathbf{F}_{12 \times 1}$ for the model.

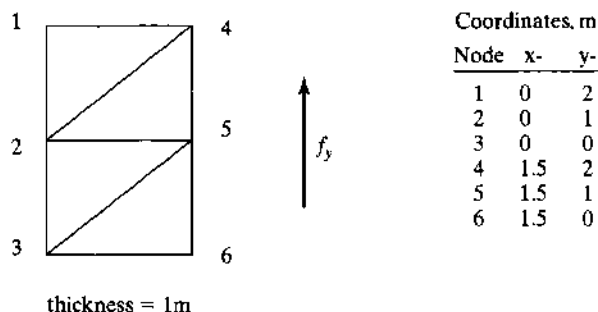


FIGURE P5.11

- 5.12. Assemble the load vector $\mathbf{F}_{6 \times 1}$ at the three nodes on the inner boundary, which is subjected to a pressure $p = 0.9 \text{ MPa}$. (See Fig. P5.12.)

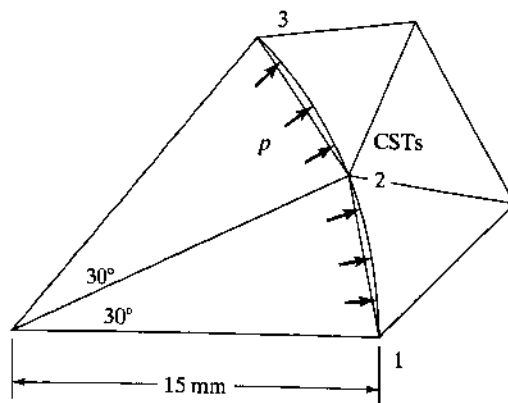


FIGURE P5.12

- 5.13. Consider the three-noded triangular element in Fig. P5.13. Express the integral for area moment of inertia $I = \int_e y^2 dA$ as

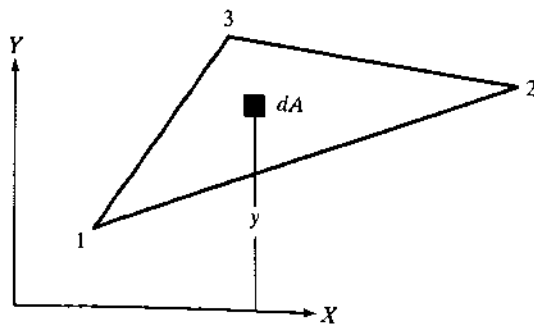


FIGURE P5.13

$$I = \mathbf{y}_e^T [\mathbf{R}] \mathbf{y}_e$$

where $\mathbf{y}_e = [y_1, y_2, y_3]^T$ = a vector of y -coordinates of the three nodes, and \mathbf{R} is a 3×3 matrix. (Hint: Interpolate y using shape functions N_i .)

- 5.14. Compute the integral $I = \int_e N_1 N_2 N_3 dA$, where N_i are the linear shape functions for a three-noded CST element.
- 5.15. Solve the plane stress problem in Fig. P5.15 using three different mesh divisions. Compare your deformation and stress results with values obtained from elementary beam theory.

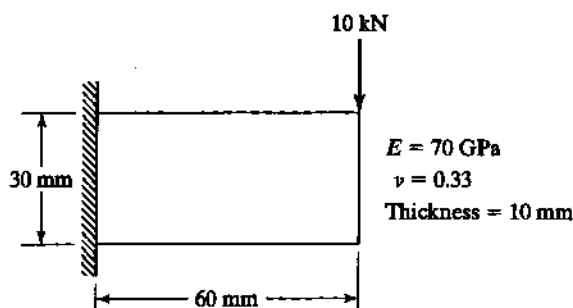


FIGURE P5.15

- 5.16. For the plate with a hole under plane stress (Fig. P5.16), find the deformed shape of the hole and determine the maximum stress distribution along AB by using stresses in elements adjacent to the line. (Note: The result in this problem is the same for any thickness. You may use $t = 1 \text{ in.}$)

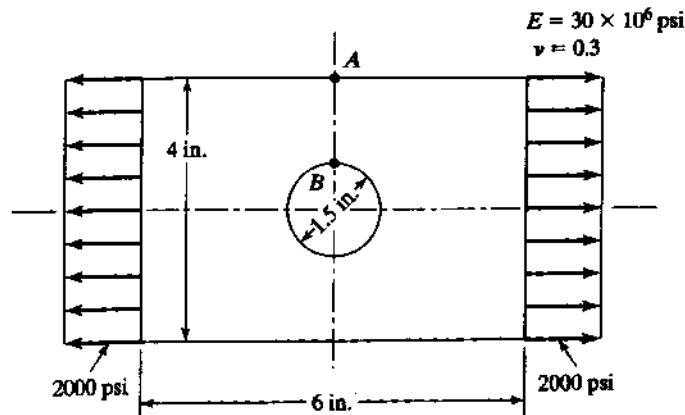


FIGURE P5.16

- 5.17. Model a half of the disk with a hole (Fig. P5.17) and find the major and minor dimensions after compression. Also, plot the distribution of maximum stress along AB .

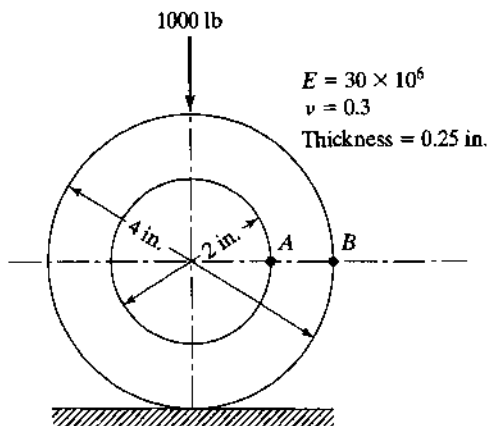


FIGURE P5.17

- 5.18. Consider the multipoint constraint

$$3Q_5 - 2Q_9 = 0.1$$

where Q_5 is the displacement along degree of freedom 5, and Q_9 is the displacement along dof 9. Write the penalty term

$$\frac{1}{2}C(3Q_5 - 2Q_9 - 0.1)^2 \text{ as } \frac{1}{2}(Q_5, Q_9)\mathbf{k}\begin{pmatrix} Q_5 \\ Q_9 \end{pmatrix} - (Q_5, Q_9)\mathbf{f}$$

and, hence, determine the stiffness additions \mathbf{k} and force additions \mathbf{f} . Then, fill in the following blanks to show how these additions are made in the computer program that uses a banded stiffness matrix \mathbf{S} :

$$S(5, 1) = S(5, 1) + \underline{\hspace{2cm}}$$

$$S(9, 1) = S(9, 1) + \underline{\hspace{2cm}}$$

$$S(5, \underline{\hspace{1cm}}) = S(5, \underline{\hspace{1cm}}) + \underline{\hspace{2cm}}$$

$$F(5) = F(5) + \underline{\hspace{2cm}}$$

$$F(9) = F(9) + \underline{\hspace{2cm}}$$

- 5.19. Model the 22.5° segment of the octagonal pipe shown in Fig. P5.19. Show the deformed configuration of the segment and the distribution of maximum in-plane shear stress. (*Hint:* For all points along CD , use stiffness modification suggested in Eq. 5.71. Also, maximum in-plane shear stress = $(\sigma_1 - \sigma_2)/2$, where σ_1 and σ_2 are the principal stresses. Assume plane strain.)

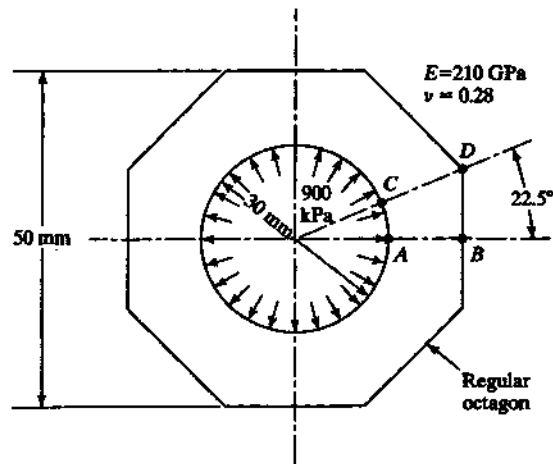


FIGURE P5.19

5.20. Determine the location and magnitude of maximum principal stress and maximum shearing stress in the fillet shown in Fig. P5.20.

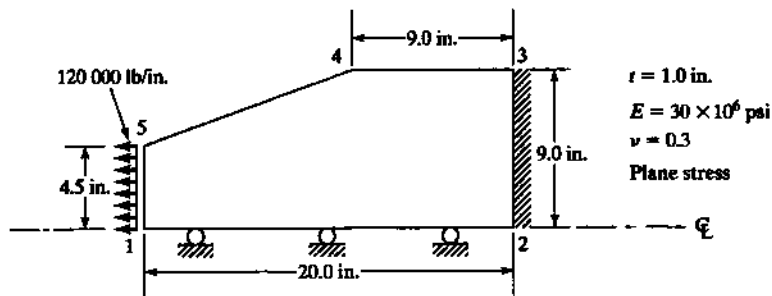


FIGURE P5.20

5.21. The torque arm in Fig. P5.21 is an automotive component, fixed at left bolt hole. Determine the location and magnitude of maximum von Mises stress, σ_{VM} , given by

$$\sigma_{VM} = \sqrt{\sigma_x^2 - \sigma_x\sigma_y + \sigma_y^2 + 3\tau_{xy}^2}$$

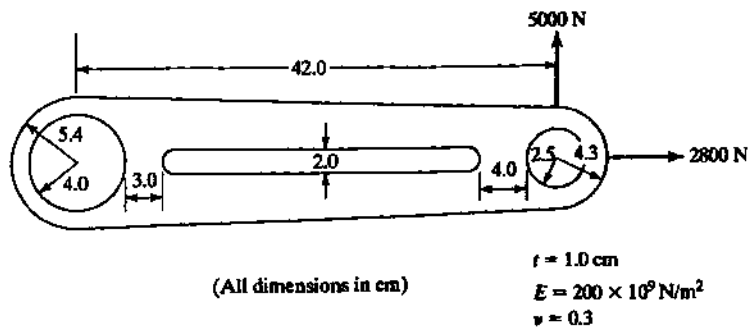


FIGURE P5.21

- 5.22. A large, flat surface of a steel body is subjected to a line load of 100 lb/in. Assuming plane strain, consider an enclosure as shown in Fig. P5.22 and determine the deformation of the surface and stress distribution in the body. (Note: Choose small elements close to the load and assume that deflection at 10 in. away is negligible.)

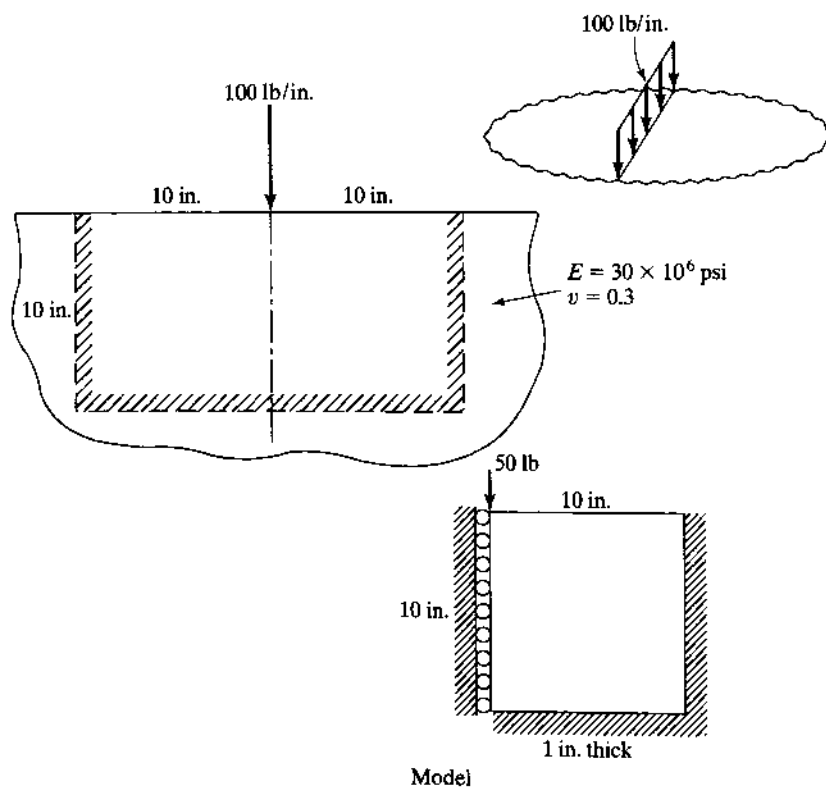


FIGURE P5.22

- 5.23. In Problem 5.22, the load is changed to a distributed load 400 lb/in.² on a 1/4-in.-wide long region, as in Fig. P5.23. Model the problem as above with this loading and find deformation of the surface and stress distribution in the body. (Note: Assume that deflection at 10 in. away is negligible.)

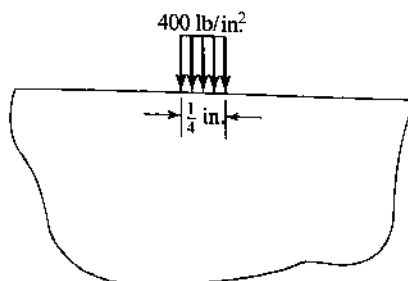


FIGURE P5.23

- 5.24. A $\frac{1}{2} \times 5$ -in. copper piece fits snugly into a short channel-shaped steel piece at room temperature, as shown in Fig. P5.24. The assembly is subjected to a uniform temperature increase of 80°F . Assuming that the properties are constant within this change and that the surfaces are bonded together, find the deformed shape and the stress distribution.

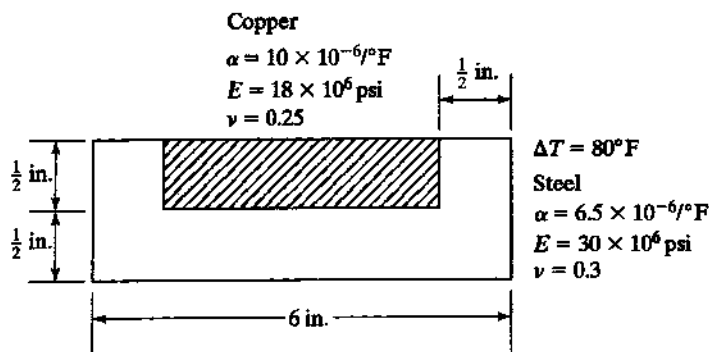


FIGURE P5.24

- 5.25. In the slotted ring shown in Fig. P5.25, two loads of magnitude P and load R are applied such that the 3-mm gap closes. Determine the magnitude of P and show the deformed shape of the part. (*Hint:* Find the deflection of gap for, say, $P = 100$ and multiply the deflections proportionately.)

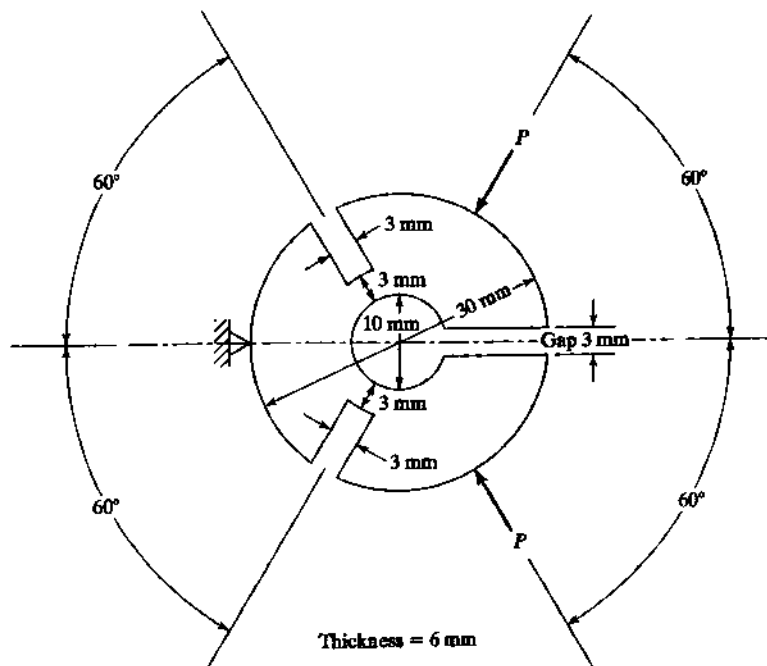


FIGURE P5.25

- 5.26. A titanium piece (A) is press-fitted into a titanium workpiece (B) as shown in Fig. P5.26. Determine the location (show on a sketch) and magnitude of maximum von Mises stress in both the parts (from your CST output file). Then, provide contour plots of the von Mises stress in each part. Data are as follows: $E = 101 \text{ GPa}$, $\nu = 0.34$.

The guidelines are (a) use less than 100 elements in all, (b) mesh each part independently, but without duplicating node or element numbers, (c) choose a value for $L_{\text{interface}}$ and then enforce multipoint constraints (MPCs) between the coincident nodes on this interface—the choice of $L_{\text{interface}}$ will involve trial-and-check as nodes that want to separate should not be forced together through the MPC, and (d) use symmetry. Assume a no-slip interface, a fixed base, and plane strain.

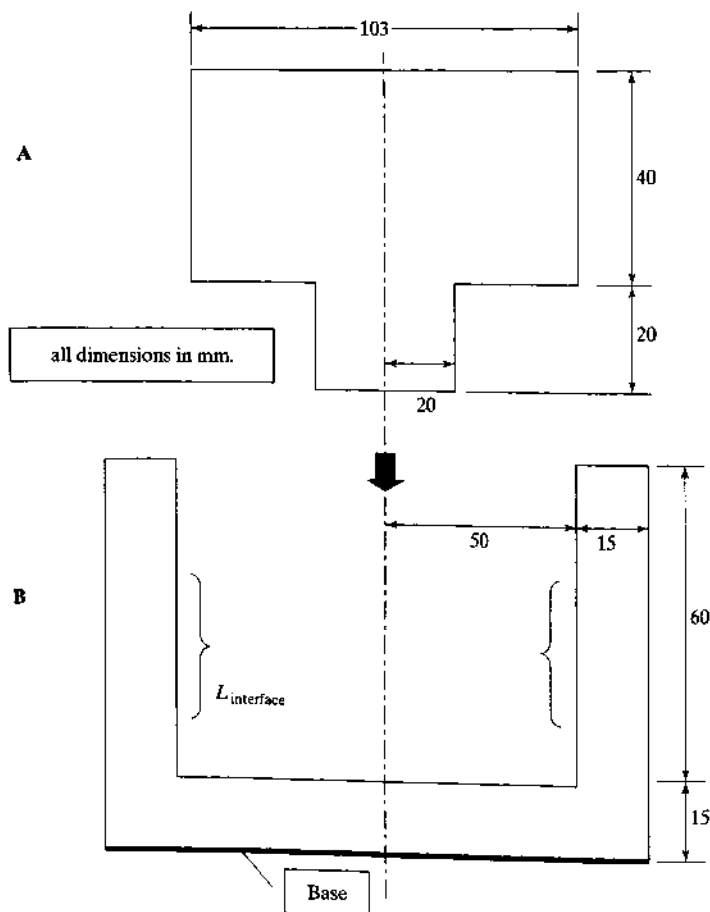


FIGURE P5.26

- 5.27. An edge crack of length a in a rectangular plate is subjected to a tensile stress σ_0 as shown in Fig. P5.27. Using a half-symmetry model, complete the following:
- (a) Determine the crack opening angle, θ ($\theta = 0$ before the load is applied).

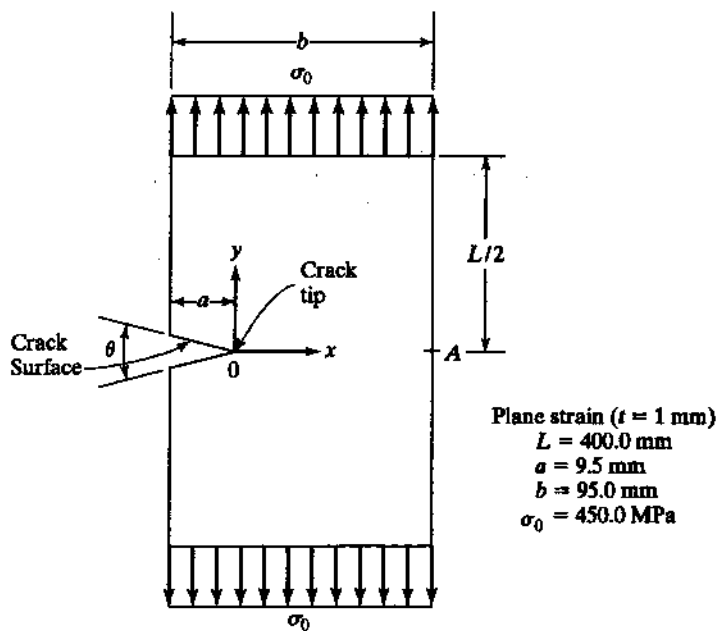


FIGURE P5.27

- (b) Plot the y stress σ_y versus x , along the line $A-O$. Assuming that $\sigma_y = \frac{K_I}{\sqrt{2\pi x}}$, use regression to estimate K_I . Compare your result for infinitely long plates, for which K_I of $= 1.2\sigma_0\sqrt{\pi a}$ is used.
- (c) Repeat part (b) for increasingly fine meshes near the crack tip.
- 5.28. Use the geometry of the plate for the plane-stress problem in P5.15. If the material of the plate is graphite-epoxy resin with fiber orientation at an angle θ to the horizontal, determine the deformation and stress values σ_x , σ_y , and σ_1 , σ_2 for $\theta = 0^\circ, 30^\circ, 45^\circ, 60^\circ$, and 90° . Properties of graphite in epoxy resin are given in Table 5.1. (*Hint:* The problem solution requires modification of program CST to incorporate the D matrix defined in Eq. 5.79.)
- 5.29. The plate with a hole in Problem 5.16 is made of pine wood. For $\theta = 0^\circ, 30^\circ, 45^\circ, 60^\circ$, and 90° , complete the following:
- Determine the deformed shape of the hole.
 - Find the stress distribution along AB and, hence, the stress concentration factor K_t . Plot K_t versus θ .

Program Listing

```

*****
**          PROGRAM CST          *
**    CONSTANT STRAIN TRIANGLE  *
** T.R.Chandrupatla and A.D.Belegundu *
*****
\===== MAIN PROGRAM =====
Private Sub cmdStart_Click()
    Call InputData
    Call Bandwidth
    Call Stiffness
    Call ModifyForBC
    Call BandSolver
    Call StressCalc
    Call ReactionCalc
    Call Output
    cmdView.Enabled = True
    cmdStart.Enabled = False
End Sub
\=====

```

```

\===== BANDWIDTH EVALUATION =====
Private Sub Bandwidth()
    '---- Bandwidth Evaluation ----
    For I = 1 To NE
        NMIN = NOC(I, 1): NMAX = NOC(I, 1)
        For J = 2 To NEN
            If NMIN > NOC(I, J) Then NMIN = NOC(I, J)
            If NMAX < NOC(I, J) Then NMAX = NOC(I, J)
        Next J
        NTMP = NDN * (NMAX - NMIN + 1)
        If NBW < NTMP Then NBW = NTMP
    Next I
    For I = 1 To NMPC
        NABS = Abs(MPC(I, 1) - MPC(I, 2)) + 1
        If NBW < NABS Then NBW = NABS
    Next I
    picBox.Print "The Bandwidth is"; NBW
End Sub
\=====

```

```

\===== ELEMENT STIFFNESS AND ASSEMBLY =====
Private Sub Stiffness()
    ReDim S(NQ, NBW)
    '---- Global Stiffness Matrix ----
    For N = 1 To NE
        picBox.Print "Forming Stiffness Matrix of Element "; N
        '---- Element Stiffness
        Call DbMat(N, 1)
        For I = 1 To 6
            For J = 1 To 6
                C = 0
            Next J
        Next I
    Next N

```

continued

```

      For K = 1 To 3
        C = C + 0.5 * Abs(DJ) * B(K, I) * DB(K, J) * TH(N)
      Next K
      SE(I, J) = C
    Next J
  Next I
  '--- Temperature Load Vector
  AL = PM(MAT(N), 3)
  C = AL * DT(N): If LC = 2 Then C = C * (1 + PNU)
  For I = 1 To 6
    TL(I) = 0.5 * C * TH(N) * Abs(DJ) * (DB(1, I) + DB(2, I))
  Next I
  picBox.Print ".... Placing in Global Locations"
  Call PlaceGlobal(N)
Next N
End Sub
=====

```

```

'===== PLACING ELEMENT STIFFNESS IN GLOBAL LOCATIONS =====
Private Sub PlaceGlobal(N)
  For II = 1 To NEN
    NRT = NDN * (NOC(N, II) - 1)
    For IT = 1 To NDN
      NR = NRT + IT
      I = NDN * (II - 1) + IT
      For JJ = 1 To NEN
        NCT = NDN * (NOC(N, JJ) - 1)
        For JT = 1 To NDN
          J = NDN * (JJ - 1) + JT
          NC = NCT + JT - NR + 1
          If NC > 0 Then
            S(NR, NC) = S(NR, NC) + SE(I, J)
          End If
        Next JT
      Next JJ
      F(NR) = F(NR) + TL(I)
    Next IT
  Next II
End Sub

```

```

===== STRESS CALCULATIONS =====
Private Sub StressCalc()
  ReDim Stress(NE, 3), PrinStress(NE, 3), PltStress(NE)
  '----- Stress Calculations
  For N = 1 To NE
    Call DbMat(N, 2)
    '--- Principal Stress Calculations
    If STR(3) = 0 Then
      S1 = STR(1): S2 = STR(2): ANG = 0
      If S2 > S1 Then
        S1 = STR(2): S2 = STR(1): ANG = 90
      End If
    Else
      C = 0.5 * (STR(1) + STR(2))
      R = Sqr(0.25 * (STR(1) - STR(2)) ^ 2 + (STR(3)) ^ 2)
      S1 = C + R: S2 = C - R
      If C > STR(1) Then
        ANG = 57.2957795 * Atn(STR(3) / (S1 - STR(1)))
        If STR(3) > 0 Then ANG = 90 - ANG
        If STR(3) < 0 Then ANG = -90 - ANG
      Else
        ANG = 57.29577951 * Atn(STR(3) / (STR(1) - S2))
      End If
    End If
    Stress(N, 1) = STR(1)
    Stress(N, 2) = STR(2)
    Stress(N, 3) = STR(3)
    PrinStress(N, 1) = S1
    PrinStress(N, 2) = S2
    PrinStress(N, 3) = ANG
    If IPL = 2 Then PltStress(N) = 0.5 * (S1 - S2)
    If IPL = 3 Then
      S3 = 0: If LC = 2 Then S3 = PNU * (S1 + S2)
      C = (S1 - S2) ^ 2 + (S2 - S3) ^ 2 + (S3 - S1) ^ 2
      PltStress(N) = Sqr(0.5 * C)
    End If
  Next N
End Sub
=====

```

```

===== B AND DB MATRICES FOR BTDB =====
Private Sub DbMat(N, ISTR)
  '----- D(), B() and DB() matrices
  '--- First the D-Matrix
  M = MAT(N): E = PM(M, 1): PNU = PM(M, 2): AL = PM(M, 3)
  '--- D() Matrix
  If LC = 1 Then
    '--- Plane Stress
    C1 = E / (1 - PNU ^ 2): C2 = C1 * PNU
  Else

```

continued

```

'--- Plane Strain
C = E / ((1 + PNU) * (1 - 2 * PNU))
C1 = C * (1 - PNU): C2 = C * PNU
End If
C3 = 0.5 * E / (1 + PNU)
D(1, 1) = C1: D(1, 2) = C2: D(1, 3) = 0
D(2, 1) = C2: D(2, 2) = C1: D(2, 3) = 0
D(3, 1) = 0: D(3, 2) = 0: D(3, 3) = C3
'--- Strain-Displacement Matrix B()
I1 = NOC(N, 1): I2 = NOC(N, 2): I3 = NOC(N, 3)
X1 = X(I1, 1): Y1 = X(I1, 2)
X2 = X(I2, 1): Y2 = X(I2, 2)
X3 = X(I3, 1): Y3 = X(I3, 2)
X21 = X2 - X1: X32 = X3 - X2: X13 = X1 - X3
Y12 = Y1 - Y2: Y23 = Y2 - Y3: Y31 = Y3 - Y1
DJ = X13 * Y23 - X32 * Y31 'DJ is determinant of Jacobian
'--- Definition of B() Matrix
B(1, 1) = Y23 / DJ: B(2, 1) = 0: B(3, 1) = X32 / DJ
B(1, 2) = 0: B(2, 2) = X32 / DJ: B(3, 2) = Y23 / DJ
B(1, 3) = Y31 / DJ: B(2, 3) = 0: B(3, 3) = X13 / DJ
B(1, 4) = 0: B(2, 4) = X13 / DJ: B(3, 4) = Y31 / DJ
B(1, 5) = Y12 / DJ: B(2, 5) = 0: B(3, 5) = X21 / DJ
B(1, 6) = 0: B(2, 6) = X21 / DJ: B(3, 6) = Y12 / DJ
'--- DB Matrix DB = D*B
For I = 1 To 3
  For J = 1 To 6
    C = 0
    For K = 1 To 3
      C = C + D(I, K) * B(K, J)
    Next K
    DB(I, J) = C
  Next J
Next I
If ISTR = 2 Then
'----- Stress Evaluation
Q(1) = F(2 * I1 - 1): Q(2) = F(2 * I1)
Q(3) = F(2 * I2 - 1): Q(4) = F(2 * I2)
Q(5) = F(2 * I3 - 1): Q(6) = F(2 * I3)
C1 = AL * DT(N): If LC = 2 Then C1 = C1 * (1 + PNU)
For I = 1 To 3
  C = 0
  For K = 1 To 6
    C = C + DB(I, K) * Q(K)
  Next K
  STR(I) = C - C1 * (D(I, 1) + D(I, 2))
Next I
End If
End Sub
'=====

```

Axisymmetric Solids Subjected to Axisymmetric Loading

6.1 INTRODUCTION

Problems involving three-dimensional axisymmetric solids or solids of revolution, subjected to axisymmetric loading, reduce to simple two-dimensional problems. Because of total symmetry about the z -axis, as seen in Fig. 6.1, all deformations and stresses are independent of the rotational angle θ . Thus, the problem needs to be looked at as a two-dimensional problem in rz , defined on the revolving area (Fig. 6.1b). Gravity forces can be considered if acting in the z direction. Revolving bodies like flywheels can be analyzed by introducing centrifugal forces in the body force term. We now discuss the axisymmetric problem formulation.

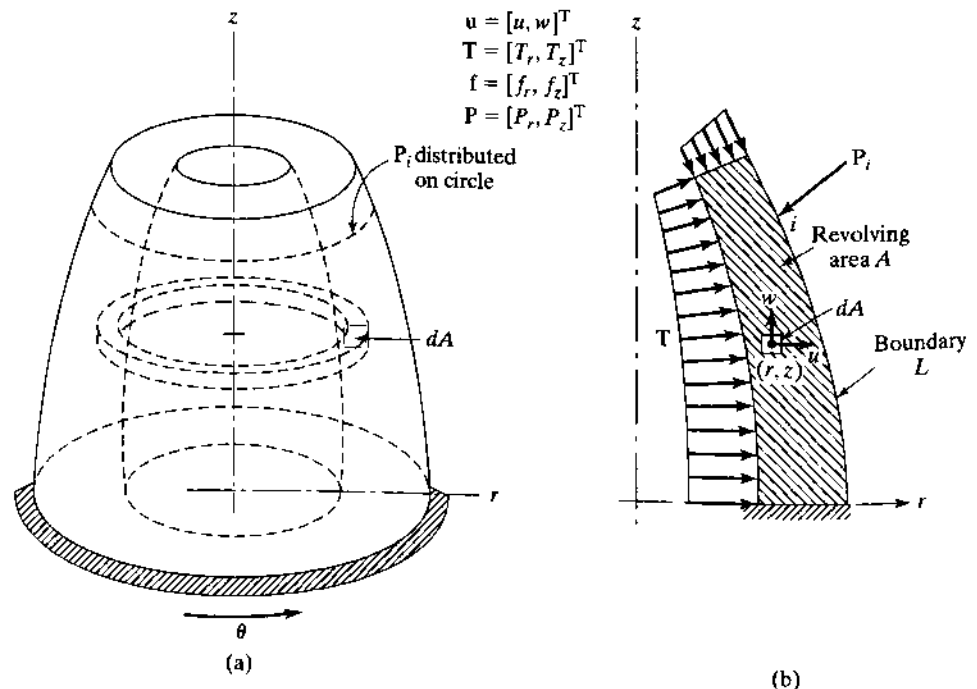


FIGURE 6.1 Axisymmetric problem.

6.2 AXISYMMETRIC FORMULATION

Considering the elemental volume shown in Fig. 6.2, the potential energy can be written in the form

$$\Pi = \frac{1}{2} \int_0^{2\pi} \int_A \boldsymbol{\sigma}^T \boldsymbol{\epsilon} r dA d\theta - \int_0^{2\pi} \int_A \mathbf{u}^T \mathbf{f} r dA d\theta - \int_0^{2\pi} \int_L \mathbf{u}^T \mathbf{T} r d\ell d\theta - \sum_i \mathbf{u}_i^T \mathbf{P}_i \quad (6.1)$$

where $r d\ell d\theta$ is the elemental surface area and the point load \mathbf{P}_i represents a line load distributed around a circle, as shown in Fig. 6.1.

All variables in the integrals are independent of θ . Thus, Eq. 6.1 can be written as

$$\Pi = 2\pi \left(\frac{1}{2} \int_A \boldsymbol{\sigma}^T \boldsymbol{\epsilon} r dA - \int_A \mathbf{u}^T \mathbf{f} r dA - \int_L \mathbf{u}^T \mathbf{T} r d\ell \right) - \sum_i \mathbf{u}_i^T \mathbf{P}_i \quad (6.2)$$

where

$$\mathbf{u} = [u, w]^T \quad (6.3)$$

$$\mathbf{f} = [f_r, f_z]^T \quad (6.4)$$

$$\mathbf{T} = [T_r, T_z]^T \quad (6.5)$$

From Fig. 6.3, we can write the relationship between strains $\boldsymbol{\epsilon}$ and displacements \mathbf{u} as

$$\begin{aligned} \boldsymbol{\epsilon} &= [\epsilon_r, \epsilon_z, \gamma_{rz}, \epsilon_\theta]^T \\ &= \left[\frac{\partial u}{\partial r}, \frac{\partial w}{\partial z}, \frac{\partial u}{\partial z} + \frac{\partial w}{\partial r}, \frac{u}{r} \right]^T \end{aligned} \quad (6.6)$$

The stress vector is correspondingly defined as

$$\boldsymbol{\sigma} = [\sigma_r, \sigma_z, \tau_{rz}, \sigma_\theta]^T \quad (6.7)$$

The stress-strain relations are given in the usual form, viz.,

$$\boldsymbol{\sigma} = \mathbf{D}\boldsymbol{\epsilon} \quad (6.8)$$

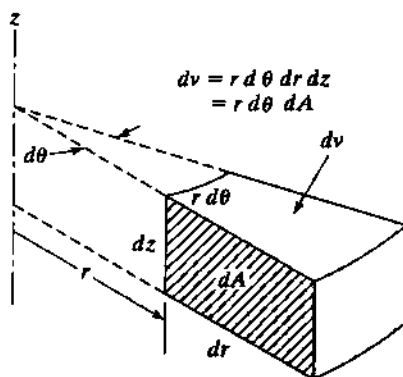


FIGURE 6.2 Elemental volume.

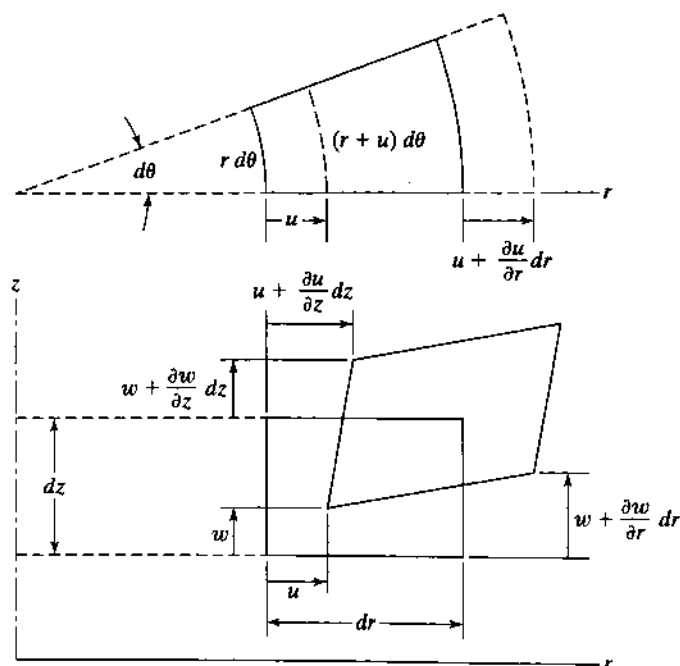


FIGURE 6.3 Deformation of elemental volume.

where the (4×4) matrix \mathbf{D} can be written by dropping the appropriate terms from the three-dimensional matrix in Chapter 1, as

$$\mathbf{D} = \frac{E(1-\nu)}{(1+\nu)(1-2\nu)} \begin{bmatrix} 1 & \frac{\nu}{1-\nu} & 0 & \frac{\nu}{1-\nu} \\ \frac{\nu}{1-\nu} & 1 & 0 & \frac{\nu}{1-\nu} \\ 0 & 0 & \frac{1-2\nu}{2(1-\nu)} & 0 \\ \frac{\nu}{1-\nu} & \frac{\nu}{1-\nu} & 0 & 1 \end{bmatrix} \quad (6.9)$$

In the Galerkin formulation, we require

$$2\pi \int_A \boldsymbol{\sigma}^T \boldsymbol{\epsilon}(\boldsymbol{\Phi}) r \, dA - \left(2\pi \int_A \boldsymbol{\Phi}^T \mathbf{f} r \, dA + 2\pi \int_L \boldsymbol{\Phi}^T \mathbf{T} r \, d\ell + \sum \boldsymbol{\Phi}_i^T \mathbf{P}_i \right) = 0 \quad (6.10)$$

where

$$\boldsymbol{\Phi} = [\phi_r, \phi_z]^T \quad (6.11)$$

$$\boldsymbol{\epsilon}(\boldsymbol{\Phi}) = \left[\frac{\partial \phi_r}{\partial r}, \frac{\partial \phi_z}{\partial z}, \frac{\partial \phi_r}{\partial z} + \frac{\partial \phi_z}{\partial r}, \frac{\phi_r}{r} \right]^T \quad (6.12)$$

6.3 FINITE ELEMENT MODELING: TRIANGULAR ELEMENT

The two-dimensional region defined by the revolving area is divided into triangular elements, as shown in Fig. 6.4. Though each element is completely represented by the area in the rz plane, in reality, it is a ring-shaped solid of revolution obtained by revolving the triangle about the z -axis. A typical element is shown in Fig. 6.5.

The definition of connectivity of elements and the nodal coordinates follow the steps involved in the CST element discussed in Section 5.3. We note here that the r - and z -coordinates, respectively, replace x and y .

Using the three shape functions N_1 , N_2 , and N_3 , we define

$$\mathbf{u} = \mathbf{N}\mathbf{q} \quad (6.13)$$

where \mathbf{u} is defined in (6.3) and

$$\mathbf{N} = \begin{bmatrix} N_1 & 0 & N_2 & 0 & N_3 & 0 \\ 0 & N_1 & 0 & N_2 & 0 & N_3 \end{bmatrix} \quad (6.14)$$

$$\mathbf{q} = [q_1, q_2, q_3, q_4, q_5, q_6]^T \quad (6.15)$$

If we denote $N_1 = \xi$ and $N_2 = \eta$, and note that $N_3 = 1 - \xi - \eta$, then Eq. 6.13 gives

$$\begin{aligned} u &= \xi q_1 + \eta q_3 + (1 - \xi - \eta) q_5 \\ w &= \xi q_2 + \eta q_4 + (1 - \xi - \eta) q_6 \end{aligned} \quad (6.16)$$

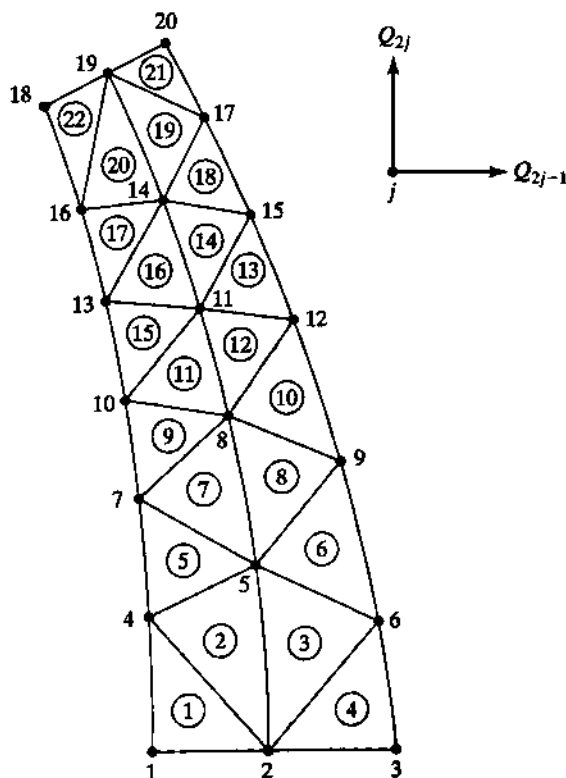


FIGURE 6.4 Triangulation.

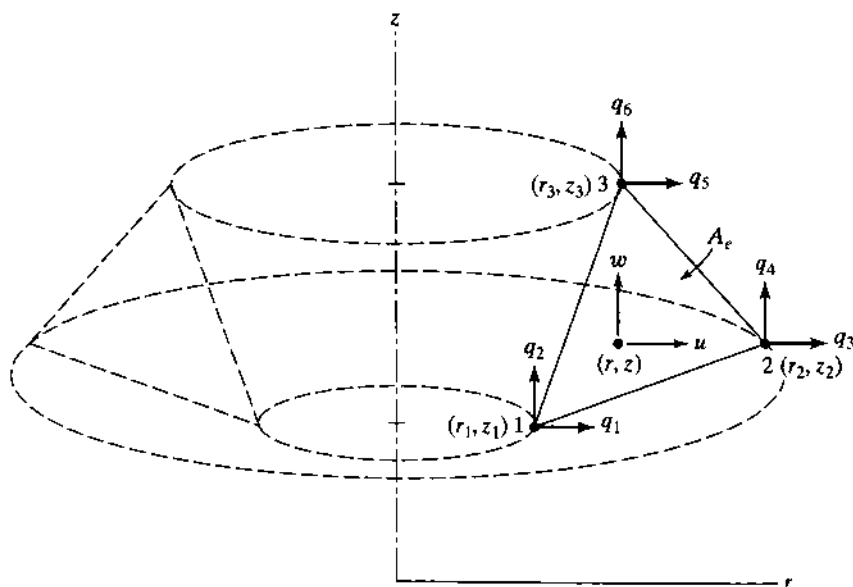


FIGURE 6.5 Axisymmetric triangular element.

By using the isoparametric representation, we find

$$\begin{aligned} r &= \xi r_1 + \eta r_2 + (1 - \xi - \eta) r_3 \\ z &= \xi z_1 + \eta z_2 + (1 - \xi - \eta) z_3 \end{aligned} \quad (6.17)$$

The chain rule of differentiation gives

$$\begin{Bmatrix} \frac{\partial u}{\partial \xi} \\ \frac{\partial u}{\partial \eta} \end{Bmatrix} = \mathbf{J} \begin{Bmatrix} \frac{\partial u}{\partial r} \\ \frac{\partial u}{\partial z} \end{Bmatrix} \quad (6.18)$$

and

$$\begin{Bmatrix} \frac{\partial w}{\partial \xi} \\ \frac{\partial w}{\partial \eta} \end{Bmatrix} = \mathbf{J} \begin{Bmatrix} \frac{\partial w}{\partial r} \\ \frac{\partial w}{\partial z} \end{Bmatrix} \quad (6.19)$$

where the Jacobian is given by

$$\mathbf{J} = \begin{bmatrix} r_{13} & z_{13} \\ r_{23} & z_{23} \end{bmatrix} \quad (6.20)$$

In the definition of \mathbf{J} earlier, we have used the notation $r_{ij} = r_i - r_j$ and $z_{ij} = z_i - z_j$. The determinant of \mathbf{J} is

$$\det \mathbf{J} = r_{13} z_{23} - r_{23} z_{13} \quad (6.21)$$

Recall that $|\det \mathbf{J}| = 2A_e$. That is, the absolute value of the determinant of \mathbf{J} equals twice the area of the element. The inverse relations for Eqs. 6.18 and 6.19 are given by

$$\begin{Bmatrix} \frac{\partial u}{\partial r} \\ \frac{\partial u}{\partial z} \end{Bmatrix} = \mathbf{J}^{-1} \begin{Bmatrix} \frac{\partial u}{\partial \xi} \\ \frac{\partial u}{\partial \eta} \end{Bmatrix} \quad \text{and} \quad \begin{Bmatrix} \frac{\partial w}{\partial r} \\ \frac{\partial w}{\partial z} \end{Bmatrix} = \mathbf{J}^{-1} \begin{Bmatrix} \frac{\partial w}{\partial \xi} \\ \frac{\partial w}{\partial \eta} \end{Bmatrix} \quad (6.22)$$

where

$$\mathbf{J}^{-1} = \frac{1}{\det \mathbf{J}} \begin{bmatrix} z_{23} & -z_{13} \\ -r_{23} & z_{13} \end{bmatrix} \quad (6.23)$$

Introducing these transformation relationships into the strain-displacement relations in Eq. 6.6 and using Eqs. 6.16, we get

$$\boldsymbol{\epsilon} = \begin{Bmatrix} \frac{z_{23}(q_1 - q_5) - z_{13}(q_3 - q_5)}{\det \mathbf{J}} \\ \frac{-r_{23}(q_2 - q_6) + r_{13}(q_4 - q_6)}{\det \mathbf{J}} \\ \frac{-r_{23}(q_1 - q_5) + r_{13}(q_3 - q_5) + z_{23}(q_2 - q_6) - z_{13}(q_4 - q_6)}{\det \mathbf{J}} \\ \frac{N_1 q_1 + N_2 q_3 + N_3 q_5}{r} \end{Bmatrix}$$

This can be written in the matrix form as

$$\boldsymbol{\epsilon} = \mathbf{B} \mathbf{q} \quad (6.24)$$

where the element strain-displacement matrix, of dimension (4×6) , is given by

$$\mathbf{B} = \begin{bmatrix} \frac{z_{23}}{\det \mathbf{J}} & 0 & \frac{z_{31}}{\det \mathbf{J}} & 0 & \frac{z_{12}}{\det \mathbf{J}} & 0 \\ 0 & \frac{r_{32}}{\det \mathbf{J}} & 0 & \frac{r_{13}}{\det \mathbf{J}} & 0 & \frac{r_{21}}{\det \mathbf{J}} \\ \frac{r_{32}}{\det \mathbf{J}} & \frac{z_{23}}{\det \mathbf{J}} & \frac{r_{13}}{\det \mathbf{J}} & \frac{z_{31}}{\det \mathbf{J}} & \frac{r_{21}}{\det \mathbf{J}} & \frac{z_{12}}{\det \mathbf{J}} \\ \frac{N_1}{r} & 0 & \frac{N_2}{r} & 0 & \frac{N_3}{r} & 0 \end{bmatrix} \quad (6.25)$$

Potential-Energy Approach

The potential energy Π on the discretized region is given by

$$\begin{aligned} \Pi = & \sum_e \left[\frac{1}{2} \left(2\pi \int_e \boldsymbol{\epsilon}^T \mathbf{D} \boldsymbol{\epsilon} dA \right) - 2\pi \int_e \mathbf{u}^T \mathbf{f} r dA - 2\pi \int_e \mathbf{u}^T \mathbf{T} r d\ell \right] \\ & - \sum \mathbf{u}_i^T \mathbf{P}_i \end{aligned} \quad (6.26)$$

The element strain energy U_e given by the first term can be written as

$$U_e = \frac{1}{2} \mathbf{q}^T \left(2\pi \int_e \mathbf{B}^T \mathbf{D} \mathbf{B} r dA \right) \mathbf{q} \quad (6.27)$$

The quantity inside the parentheses is the element stiffness matrix,

$$\mathbf{k}^e = 2\pi \int_e \mathbf{B}^T \mathbf{D} \mathbf{B} r dA \quad (6.28)$$

The fourth row in \mathbf{B} has terms of the type N_i/r . Further, this integral also has an additional r in it. As a simple approximation, \mathbf{B} and r can be evaluated at the centroid of the triangle and used as representative values for the triangle. At the centroid of the triangle,

$$N_1 = N_2 = N_3 = \frac{1}{3} \quad (6.29)$$

and

$$\bar{r} = \frac{r_1 + r_2 + r_3}{3}$$

where \bar{r} is the radius of the centroid. Denoting $\bar{\mathbf{B}}$ as the element strain-displacement matrix \mathbf{B} evaluated at the centroid, we get

$$\mathbf{k}^e = 2\pi \bar{r} \bar{\mathbf{B}}^T \mathbf{D} \bar{\mathbf{B}} \int_e dA$$

or

$$\mathbf{k}^e = 2\pi \bar{r} A_e \bar{\mathbf{B}}^T \mathbf{D} \bar{\mathbf{B}} \quad (6.30)$$

We note here that $2\pi \bar{r} A_e$ is the volume of the ring-shaped element shown in Fig. 6.5. Also, A_e is given by

$$A_e = \frac{1}{2} |\det \mathbf{J}| \quad (6.31)$$

We also use this centroid or midpoint rule* for body forces and surface tractions as discussed in the following section. Caution must be exerted for elements close to the axis of symmetry. For better results, smaller elements need to be chosen close to the axis of symmetry. Another approach is to introduce $r = N_1 r_1 + N_2 r_2 + N_3 r_3$ in the following equations and perform elaborate integration. More elaborate methods of numerical integration are discussed in Chapter 7.

Body Force Term

We first consider the body force term $2\pi \int_e \mathbf{u}^T \mathbf{f} r dA$. We have

$$\begin{aligned} 2\pi \int_e \mathbf{u}^T \mathbf{f} r dA &= 2\pi \int_e (u f_r + w f_z) r dA \\ &= 2\pi \int_e [(N_1 q_1 + N_2 q_3 + N_3 q_5) f_r + (N_1 q_2 + N_2 q_4 + N_3 q_6) f_z] r dA \end{aligned}$$

*Suggested by O. C. Zienkiewicz, *The Finite Element Method*, 3d ed. New York: McGraw-Hill, 1983.

Once again, approximating the variable quantities by their values at the centroid of the triangle, we get

$$2\pi \int_e \mathbf{u}^T \mathbf{f} r dA = \mathbf{q}^T \mathbf{f}^c \quad (6.32)$$

where the element body force vector \mathbf{f}^c is given by

$$\mathbf{f}^c = \frac{2\pi \bar{r} A_e}{3} [\bar{f}_r, \bar{f}_z, \bar{f}_r, \bar{f}_z, \bar{f}_r, \bar{f}_z]^T \quad (6.33)$$

The bar on the \mathbf{f} terms indicates that they are evaluated at the centroid. Where body force is the primary load, greater accuracy may be obtained by substituting $r = N_1 r_1 + N_2 r_2 + N_3 r_3$ into Eq. 6.32 and integrating to get nodal loads.

Rotating Flywheel

As an example, let us consider a rotating flywheel with its axis in the z direction. We consider the flywheel to be stationary and apply the equivalent radial centrifugal (inertial) force per unit volume of $\rho r \omega^2$, where ρ is the density (mass per unit volume), and ω the angular velocity in rad/s. In addition, if gravity acts along the negative z -axis, then

$$\mathbf{f} = [f_r, f_z]^T = [\rho r \omega^2, -\rho g]^T \quad (6.34)$$

and

$$\bar{f}_r = \rho \bar{r} \omega^2, \bar{f}_z = -\rho g \quad (6.35)$$

For more precise results with coarse meshes, we need to use $r = N_1 r_1 + N_2 r_2 + N_3 r_3$ and integrate.

Surface Traction

For a uniformly distributed load with components T_r and T_z , shown in Fig. 6.6, on the edge connecting nodes 1 and 2, we get

$$2\pi \int_e \mathbf{u}^T \mathbf{T} r d\ell = \mathbf{q}^T \mathbf{T}^c \quad (6.36)$$

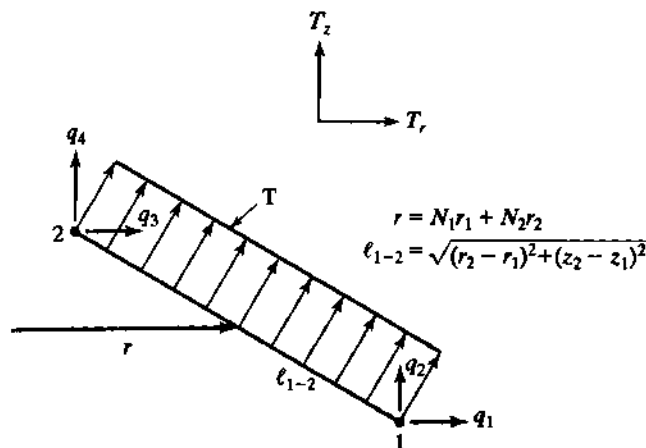


FIGURE 6.6 Surface traction.

where

$$\mathbf{q} = [q_1, q_2, q_3, q_4]^T \quad (6.37)$$

$$\mathbf{T}^e = 2\pi\ell_{1-2}[aT_r, aT_z, bT_r, bT_z]^T \quad (6.38)$$

$$a = \frac{2r_1 + r_2}{6} \quad b = \frac{r_1 + 2r_2}{6} \quad (6.39)$$

$$\ell_{1-2} = \sqrt{(r_2 - r_1)^2 + (z_2 - z_1)^2} \quad (6.40)$$

In this derivation, r is expressed as $N_1r_1 + N_2r_2$ and then integrated. When the line 1-2 is parallel to the z -axis, we have $r_1 = r_2$, which gives $a = b = 0.5r_1$.

Example 6.1

An axisymmetric body with a linearly distributed load on the conical surface is shown in Fig. E6.1. Determine the equivalent point loads at nodes 2, 4, and 6.

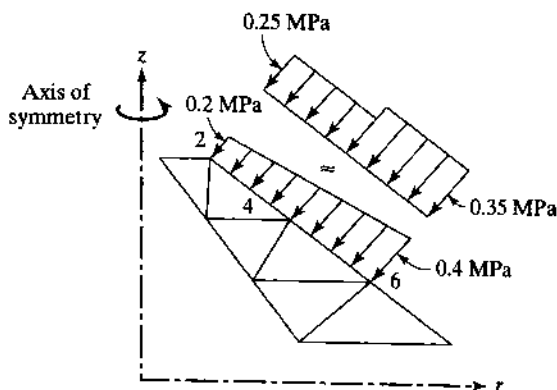


FIGURE E6.1

Solution We approximate the linearly distributed load by the average uniformly distributed loads on the edges 6-4 and 4-2 as shown in Fig. E6.1. Relationships for more precise modeling of a linearly distributed load are provided in Problem 6.12. We now consider the two edges 6-4 and 4-2 separately and then merge them.

For edge 6-4

$$p = 0.35 \text{ MPa}, \quad r_1 = 60 \text{ mm}, \quad z_1 = 40 \text{ mm}, \quad r_2 = 40 \text{ mm}, \quad z_2 = 55 \text{ mm}$$

$$\ell_{1-2} = \sqrt{(r_1 - r_2)^2 + (z_1 - z_2)^2} = 25 \text{ mm}$$

$$c = \frac{z_2 - z_1}{\ell_{1-2}} = 0.6, \quad s = \frac{r_1 - r_2}{\ell_{1-2}} = 0.8$$

$$T_r = -pc = -0.21, \quad T_z = -ps = -0.28$$

$$a = \frac{2r_1 + r_2}{6} = 26.67, \quad b = \frac{r_1 + 2r_2}{6} = 23.33$$

$$\mathbf{T}^1 = 2\pi\ell_{1-2}[aT_r, aT_z, bT_r, bT_z]^T \\ = [-879.65 \quad -1172.9 \quad -769.69 \quad -1026.25]^T \text{ N}$$

These loads add to F_{11} , F_{12} , F_7 , and F_8 , respectively.

For edge 4-2

$$p = 0.25 \text{ MPa}, \quad r_1 = 40 \text{ mm}, \quad z_1 = 55 \text{ mm}, \quad r_2 = 20 \text{ mm}, \quad z_2 = 70 \text{ mm}$$

$$\ell_{1-2} = \sqrt{(r_1 - r_2)^2 + (z_1 - z_2)^2} = 25 \text{ mm}$$

$$c = \frac{z_2 - z_1}{\ell_{1-2}} = 0.6, \quad s = \frac{r_1 - r_2}{\ell_{1-2}} = 0.8$$

$$T_r = -pc = -0.15, \quad T_z = -ps = -0.2$$

$$a = \frac{2r_1 + r_2}{6} = 16.67, \quad b = \frac{r_1 + 2r_2}{6} = 13.33$$

$$\mathbf{T}^T = 2\pi\ell_{1-2}[aT_r \quad aT_z \quad bT_r \quad bT_z]^T \\ = [-392.7 \quad -523.6 \quad -314.16 \quad -418.88]^T \text{ N}$$

These loads add to F_7 , F_8 , F_3 , and F_4 , respectively. Thus,

$$[F_3 \quad F_4 \quad F_7 \quad F_8 \quad F_{11} \quad F_{12}] = [-314.2 \quad -418.9 \quad -1162.4 \quad -1696.5 \quad -879.7 \quad -1172.9] \text{ N}$$

The load distributed along a circumference of a circle on the surface has to be applied at a point on the revolving area. We may conveniently locate a node here and add the load components.

On summing up the strain energy and force terms over all the elements and modifying for the boundary conditions while minimizing the total potential energy, we get

$$\mathbf{KQ} = \mathbf{F} \quad (6.41)$$

We note here that axisymmetric boundary conditions need be applied only on the revolving area shown in Fig. 6.1.

Galerkin Approach

In the Galerkin formulation, the consistent variation ϕ in an element is expressed as

$$\phi = \mathbf{N}\psi \quad (6.42)$$

where

$$\psi = [\psi_1, \psi_2, \dots, \psi_6]^T \quad (6.43)$$

The corresponding strain $\epsilon(\phi)$ is given by

$$\epsilon(\phi) = \mathbf{B}\psi \quad (6.44)$$

The global vector of variations Ψ is represented by

$$\Psi = [\Psi_1, \Psi_2, \Psi_3, \dots, \Psi_N]^T \quad (6.45)$$

We now introduce the interpolated displacements into the Galerkin variational form (Eq. 6.10). The first term representing the internal virtual work gives

$$\begin{aligned} \text{Internal virtual work} &= 2\pi \int_A \sigma^T \epsilon(\phi) r \, dA \\ &= \sum_e 2\pi \int_e \mathbf{q}^T \mathbf{B}^T \mathbf{D} \mathbf{B} \psi r \, dA \\ &= \sum_e \mathbf{q}^T \mathbf{k}^e \psi \end{aligned} \quad (6.46)$$

where the element stiffness \mathbf{k}^e is given by

$$\mathbf{k}^e = 2\pi r A_e \bar{\mathbf{B}}^T \bar{\mathbf{D}} \bar{\mathbf{B}} \quad (6.47)$$

We note that \mathbf{k}^e is symmetric. Using the connectivity of the elements, the internal virtual work can be expressed in the form

$$\begin{aligned} \text{Internal virtual work} &= \sum_e \mathbf{q}^T \mathbf{k}^e \boldsymbol{\psi} = \sum \boldsymbol{\psi}^T \mathbf{k}^e \mathbf{q} \\ &= \boldsymbol{\Psi}^T \mathbf{K} \mathbf{Q} \end{aligned} \quad (6.48)$$

where \mathbf{K} is the global stiffness matrix. The external virtual work terms in Eq. 6.10 involving body forces, surface tractions, and point loads can be treated in the same way as in the potential-energy approach, by replacing \mathbf{q} with $\boldsymbol{\psi}$. The summation of all the force terms over the elements then yields

$$\text{External virtual work} = \boldsymbol{\Psi}^T \mathbf{F} \quad (6.49)$$

The boundary conditions are considered using the ideas discussed in Chapter 3. The stiffness matrix \mathbf{K} and the force \mathbf{F} are modified, resulting in the same set of equations as (6.41).

Detailed calculations in the example that follows are provided for illustrating the steps involved. However, it is expected that the exercise problems at the end of the chapter will be solved using program AXISYM, which is provided.

Example 6.2

In Fig. E6.2, a long cylinder of inside diameter 80 mm and outside diameter 120 mm snugly fits in a hole over its full length. The cylinder is then subjected to an internal pressure of 2 MPa. Using two elements on the 10-mm length shown, find the displacements at the inner radius.

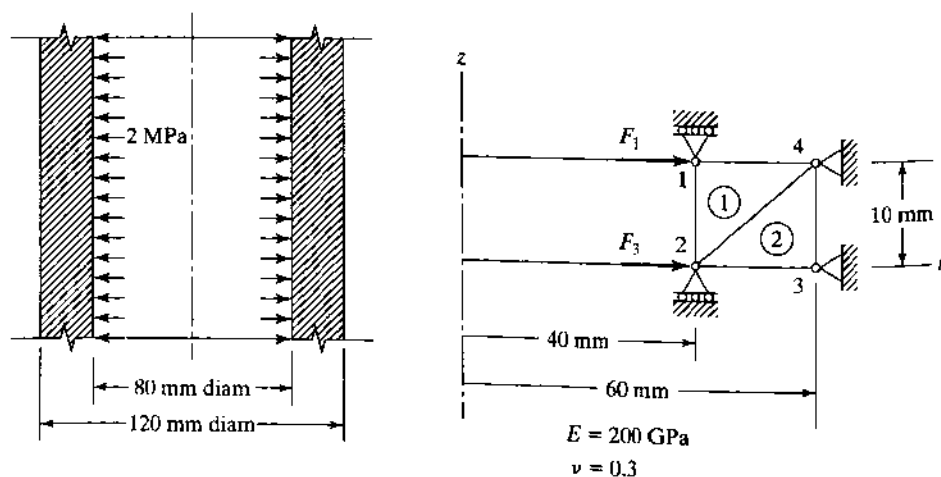


FIGURE E6.2

Solution

Consider the following table:

| Element | Connectivity | | | Node | Coordinates | |
|---------|--------------|---|---|------|-------------|----|
| | 1 | 2 | 3 | | r | z |
| 1 | 1 | 2 | 4 | 1 | 40 | 10 |
| 2 | 2 | 3 | 4 | 2 | 40 | 0 |
| | | | | 3 | 60 | 0 |
| | | | | 4 | 60 | 10 |

We will use the units of millimeters for length, newtons for force, and megapascals for stress and E . These units are consistent. On substituting $E = 200\,000$ MPa and $\nu = 0.3$, we have

$$\mathbf{D} = \begin{bmatrix} 2.69 \times 10^5 & 1.15 \times 10^5 & 0 & 1.15 \times 10^5 \\ 1.15 \times 10^5 & 2.69 \times 10^5 & 0 & 1.15 \times 10^5 \\ 0 & 0 & 0.77 \times 10^5 & 0 \\ 1.15 \times 10^5 & 1.15 \times 10^5 & 0 & 2.69 \times 10^5 \end{bmatrix}$$

for both elements, $\det \mathbf{J} = 200 \text{ mm}^2$ and $A_e = 100 \text{ mm}^2$. From Eq. 6.31, forces F_1 and F_3 are given by

$$F_1 = F_3 = \frac{2\pi r_1 \ell_e p_i}{2} = \frac{2\pi(40)(10)(2)}{2} = 2514 \text{ N}$$

The \mathbf{B} matrices relating element strains to nodal displacements are obtained first. For element 1, $\bar{r} = \frac{1}{3}(40 + 40 + 60) = 46.67 \text{ mm}$ and

$$\bar{\mathbf{B}}^1 = \begin{bmatrix} -0.05 & 0 & 0 & 0 & 0.05 & 0 \\ 0 & 0.1 & 0 & -0.1 & 0 & 0 \\ 0.1 & -0.05 & -0.1 & 0 & 0 & 0.05 \\ 0.0071 & 0 & 0.0071 & 0 & 0.0071 & 0 \end{bmatrix}$$

For element 2, $\bar{r} = \frac{1}{3}(40 + 60 + 60) = 53.33 \text{ mm}$ and

$$\bar{\mathbf{B}}^2 = \begin{bmatrix} -0.05 & 0 & 0.05 & 0 & 0 & 0 \\ 0 & 0 & 0 & -0.1 & 0 & 0.1 \\ 0 & -0.05 & -0.1 & 0.05 & 0.1 & 0 \\ 0.00625 & 0 & 0.00625 & 0 & 0.00625 & 0 \end{bmatrix}$$

The element stress-displacement matrices are obtained by multiplying \mathbf{DB} :

$$\mathbf{DB}^1 = 10^4 \begin{bmatrix} -1.26 & 1.15 & 0.082 & -1.15 & 1.43 & 0 \\ -0.49 & 2.69 & 0.082 & -2.69 & 0.657 & 0.1 \\ 0.77 & -0.385 & -0.77 & 0 & 0 & 0.385 \\ -0.384 & 1.15 & 0.191 & -1.15 & 0.766 & 0 \end{bmatrix}$$

$$\mathbf{DB}^2 = 10^4 \begin{bmatrix} -1.27 & 0 & 1.42 & -1.15 & 0.072 & 1.15 \\ -0.503 & 0 & 0.647 & -2.69 & 0.072 & 2.69 \\ 0 & -0.385 & -0.77 & 0.385 & 0.77 & 0 \\ -0.407 & 0 & 0.743 & -1.15 & 0.168 & 1.15 \end{bmatrix}$$

The stiffness matrices are obtained by finding $2\pi r A_e \bar{\mathbf{B}}^T \mathbf{D} \bar{\mathbf{B}}$ for each element:

$$\mathbf{k}^1 = 10^7 \begin{bmatrix} \text{Global dof} \rightarrow & 1 & 2 & 3 & 4 & 7 & 8 \\ 4.03 & -2.58 & -2.34 & 1.45 & -1.932 & 1.13 \\ & 8.45 & 1.37 & -7.89 & 1.93 & -0.565 \\ & & 2.30 & -0.24 & 0.16 & -1.13 \\ & & & 7.89 & -1.93 & 0 \\ \text{Symmetric} & & & & 2.25 & 0 \\ & & & & & 0.565 \end{bmatrix}$$

$$\mathbf{k}^2 = 10^7 \begin{bmatrix} \text{Global dof} \rightarrow & 3 & 4 & 5 & 6 & 7 & 8 \\ 2.05 & 0 & -2.22 & 1.69 & -0.085 & -1.69 \\ & 0.645 & 1.29 & -0.645 & -1.29 & 0 \\ & & 5.11 & -3.46 & -2.42 & 2.17 \\ & & & 9.66 & 1.05 & -9.01 \\ \text{Symmetric} & & & & 2.62 & 0.241 \\ & & & & & 9.01 \end{bmatrix}$$

Using the elimination approach, on assembling the matrices with reference to the degrees of freedom 1 and 3, we get

$$10^7 = \begin{bmatrix} 4.03 & -2.34 \\ -2.34 & 4.35 \end{bmatrix} \begin{Bmatrix} Q_1 \\ Q_3 \end{Bmatrix} = \begin{Bmatrix} 2514 \\ 2514 \end{Bmatrix}$$

so that

$$Q_1 = 0.014 \times 10^{-2} \text{ mm}$$

$$Q_3 = 0.0133 \times 10^{-2} \text{ mm}$$

Stress Calculations

From the set of nodal displacements obtained above, the element nodal displacements \mathbf{q} can be found using the connectivity. Then, using stress-strain relation in Eq. 6.8 and strain-displacement relation in Eq. 6.24, we have

$$\boldsymbol{\sigma} = \mathbf{D} \bar{\mathbf{B}} \mathbf{q} \quad (6.50)$$

where $\bar{\mathbf{B}}$ is \mathbf{B} , given in Eq. 6.25, evaluated at the centroid of the element. We also note that σ_θ is a principal stress. The two principal stresses σ_1 and σ_2 corresponding to σ_r , σ_z , and τ_{rz} can be calculated using Mohr's circle.

Example 6.3

Calculate the element stresses in the problem discussed in Example 6.2.

Solution We need to find $\boldsymbol{\sigma}^{e^T} = [\sigma_r, \sigma_z, \tau_{rz}, \sigma_\theta]^e$ for each element. From the connectivity established in Example 6.2,

$$\mathbf{q}^1 = [0.0140, 0, 0.0133, 0, 0, 0]^T \times 10^{-2}$$

$$\mathbf{q}^2 = [0.0133, 0, 0, 0, 0, 0]^T \times 10^{-2}$$

Using the product matrices \mathbf{DB}^e and \mathbf{q} in the formula

$$\boldsymbol{\sigma}^e = \mathbf{DB}^e \mathbf{q}$$

we get

$$\boldsymbol{\sigma}^1 = [-166, -58.2, 5.4, -28.4]^T \times 10^{-2} \text{ MPa}$$

$$\boldsymbol{\sigma}^2 = [-169.3, -66.9, 0, -54.1]^T \times 10^{-2} \text{ MPa} \quad \blacksquare$$

Temperature Effects

Uniform increase in temperature of ΔT introduces initial normal strains $\boldsymbol{\epsilon}_0$ given as

$$\boldsymbol{\epsilon}_0 = [\alpha \Delta T, \alpha \Delta T, 0, \alpha \Delta T]^T \quad (6.51)$$

The stresses are given by

$$\boldsymbol{\sigma} = \mathbf{D}(\boldsymbol{\epsilon} - \boldsymbol{\epsilon}_0) \quad (6.52)$$

where $\boldsymbol{\epsilon}$ is the total strain.

On substitution into the strain energy, this yields an additional term of $-\boldsymbol{\epsilon}^T \mathbf{D} \boldsymbol{\epsilon}_0$ in the potential energy Π . Using the element strain-displacement relations in Eq. 6.24, we find that

$$2\pi \int_A \boldsymbol{\epsilon}^T \mathbf{D} \boldsymbol{\epsilon}_0 r \, dA = \sum_e \mathbf{q}^T (2\pi \bar{r} A_e \bar{\mathbf{B}}^T \mathbf{D} \bar{\boldsymbol{\epsilon}}_0) \quad (6.53)$$

The consideration of the temperature effect in the Galerkin approach is rather simple. The term $\boldsymbol{\epsilon}^T$ in Eq. (6.53) is replaced by $\boldsymbol{\epsilon}^T(\boldsymbol{\phi})$.

The expression in parentheses gives element nodal load contributions. The vector $\bar{\boldsymbol{\epsilon}}_0$ is the initial strain evaluated at the centroid, representing the average temperature rise of the element. We have

$$\boldsymbol{\theta}^e = 2\pi \bar{r} A_e \bar{\mathbf{B}}^T \mathbf{D} \bar{\boldsymbol{\epsilon}}_0 \quad (6.54)$$

where

$$\boldsymbol{\theta}^e = [\theta_1, \theta_2, \theta_3, \theta_4, \theta_5, \theta_6]^T \quad (6.55)$$

6.4 PROBLEM MODELING AND BOUNDARY CONDITIONS

We have seen that the axisymmetric problem simply reduces to consideration of the revolving area. The boundary conditions need to be enforced on this area. θ independence arrests the rotation. Axisymmetry also implies that points lying on the z -axis remain radially fixed. Let us now consider some typical problems with a view to modeling them.

Cylinder Subjected to Internal Pressure

Figure 6.7 shows a hollow cylinder of length L subjected to an internal pressure. One end of the cylindrical pipe is attached to a rigid wall. In this, we need to model only the rectangular region of the length L bound between r_i and r_o . Nodes on the fixed end are constrained in the z and r directions. Stiffness and force modifications will be made for these nodes.

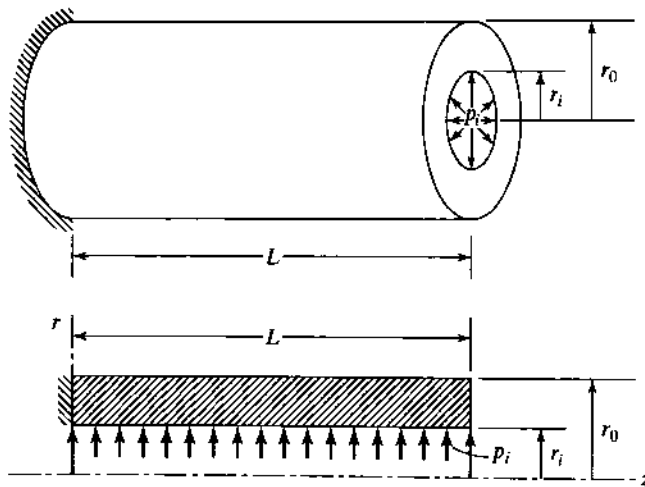


FIGURE 6.7 Hollow cylinder under internal pressure.

Infinite Cylinder

In Fig. 6.8, modeling of a cylinder of infinite length subjected to external pressure is shown. The length dimensions are assumed to remain constant. This plane strain condition is modeled by considering a unit length and restraining the end surfaces in the z direction.

Press Fit on a Rigid Shaft

Press fit of a ring of length L and internal radius r_i onto a rigid shaft of radius $r_i + \delta$ is considered in Fig. 6.9. When symmetry is assumed about the midplane, this plane is restrained in the z direction. When we impose the condition that nodes at the internal radius have to displace radially by δ , a large stiffness C is added to the diagonal locations for the radially constrained dofs and a force $C\delta$ is added to the corresponding force components. Solution of the equations gives displacements at nodes; stresses can then be evaluated.

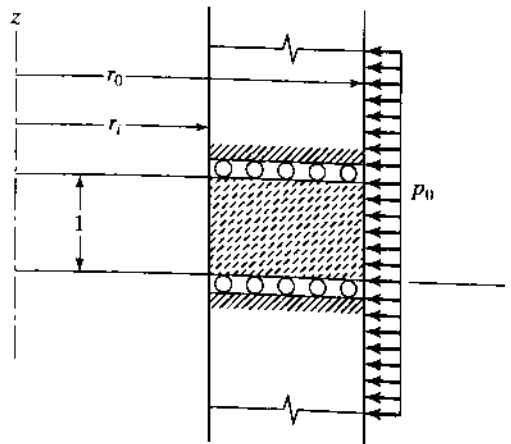


FIGURE 6.8 Cylinder of infinite length under external pressure.

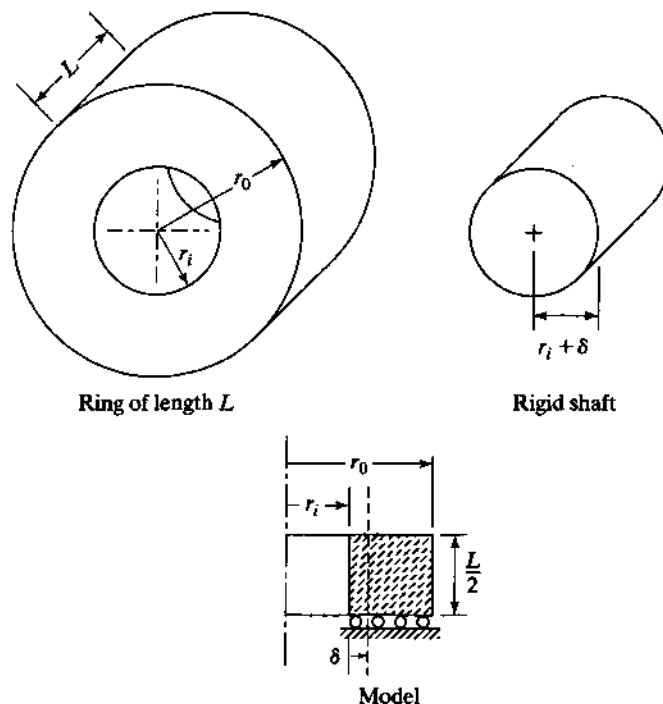


FIGURE 6.9 Press fit on a rigid shaft.

Press Fit on an Elastic Shaft

The condition at the contacting boundary leads to an interesting problem when an elastic sleeve is press fitted onto an elastic shaft. Take the problem of Fig. 6.9 stated above with the shaft also treated as elastic. A method to handle this is considered by referring to Fig. 6.10. We may define pairs of nodes on the contacting boundary, each pair consisting of one node on the sleeve and one on the shaft. If Q_i and Q_j are displacements of a typical pair along the radial degrees of freedom, we need to satisfy the multipoint constraint

$$Q_j - Q_i = \delta \quad (6.56)$$

When the term $\frac{1}{2}C(Q_j - Q_i - \delta)^2$ is added to the potential energy, the constraint is approximately enforced. The penalty approach for handling multipoint constraints is discussed in Chapter 3. Note that C is a large number. We have

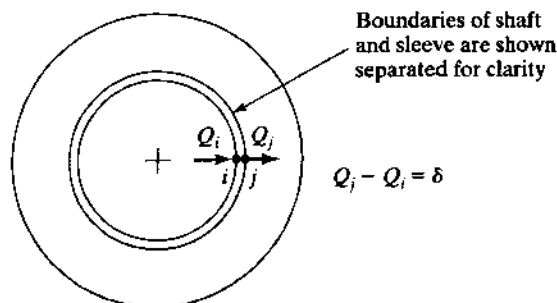


FIGURE 6.10 Elastic sleeve on an elastic shaft.

$$\frac{1}{2}C(Q_j - Q_i - \delta)^2 = \frac{1}{2}CQ_i^2 + \frac{1}{2}CQ_j^2 - \frac{1}{2}C(Q_iQ_j + Q_jQ_i) + CQ_i\delta - CQ_j\delta + \frac{1}{2}C\delta^2 \quad (6.57)$$

This implies the following modifications:

$$\begin{bmatrix} K_{ii} & K_{ij} \\ K_{ji} & K_{jj} \end{bmatrix} \rightarrow \begin{bmatrix} K_{ii} + C & K_{ij} - C \\ K_{ji} - C & K_{jj} + C \end{bmatrix} \quad (6.58)$$

and

$$\begin{bmatrix} F_i \\ F_j \end{bmatrix} \rightarrow \begin{bmatrix} F_i - C\delta \\ F_j + C\delta \end{bmatrix} \quad (6.59)$$

Belleville Spring

The Belleville spring, also called the Belleville washer, is a conical disk spring. The load is applied on the periphery of the circle and supported at the bottom as shown in Fig. 6.11a. As load is applied in the axial direction, the supporting edge moves out. Only the rectangular area shown shaded in Fig. 6.11c needs to be modeled. An axisymmetric load P is placed at the top corner, and the bottom supporting corner is constrained in the z direction. Load-deflection characteristics and stress distribution can be obtained by dividing the area into elements and using a computer program. In the Belleville spring, the load-deflection curve is *nonlinear* (Fig. 6.11b). The stiffness depends on the geometry. We can find a good approximate solution by an incremental approach. We

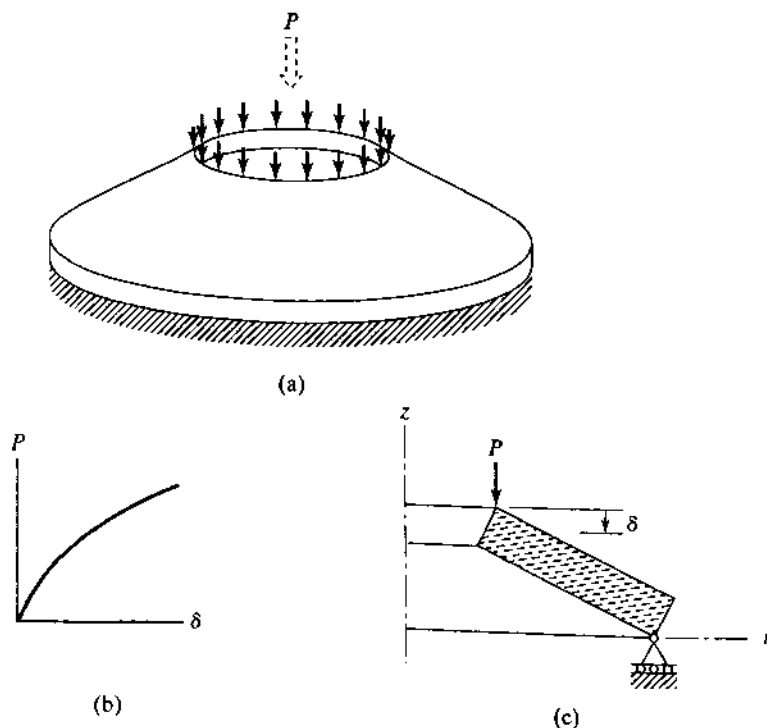


FIGURE 6.11 Belleville spring.

find the stiffness matrix $\mathbf{K}(\mathbf{x})$ for the given coordinate geometry. We obtain the displacements $\Delta \mathbf{Q}$ for an incremental loading of $\Delta \mathbf{F}$ from

$$\mathbf{K}(\mathbf{x}) \Delta \mathbf{Q} = \Delta \mathbf{F} \quad (6.60)$$

The displacements $\Delta \mathbf{Q}$ are converted to the components Δu and Δw and are added to \mathbf{x} to update the new geometry:

$$\mathbf{x} \leftarrow \mathbf{x} + \Delta \mathbf{u} \quad (6.61)$$

\mathbf{K} is recalculated for the new geometry, and the new set of equations 6.60 is solved. The process is continued until the full applied load is reached.

This example illustrates the incremental approach for geometric nonlinearity.

Thermal Stress Problem

Shown in Fig. 6.12a is a steel sleeve inserted into a rigid insulated wall. The sleeve fits snugly, and then the temperature is raised by ΔT . The stresses in the sleeve increase because of the constraint. The rectangular area of length $L/2$, bounded by r_i and r_o is considered (Fig. 6.12b), with points on the outer radius constrained radially and points on r constrained axially. The load vector is modified using the load vector from Eq. 6.55, and the finite element equations are solved.

Modeling of simple to complex problems of engineering importance have been discussed. In real life, each problem poses its own challenge. With a clear understanding of the loading, boundary conditions, and the material behavior, the modeling of a problem can be broken down into simple and easy steps.

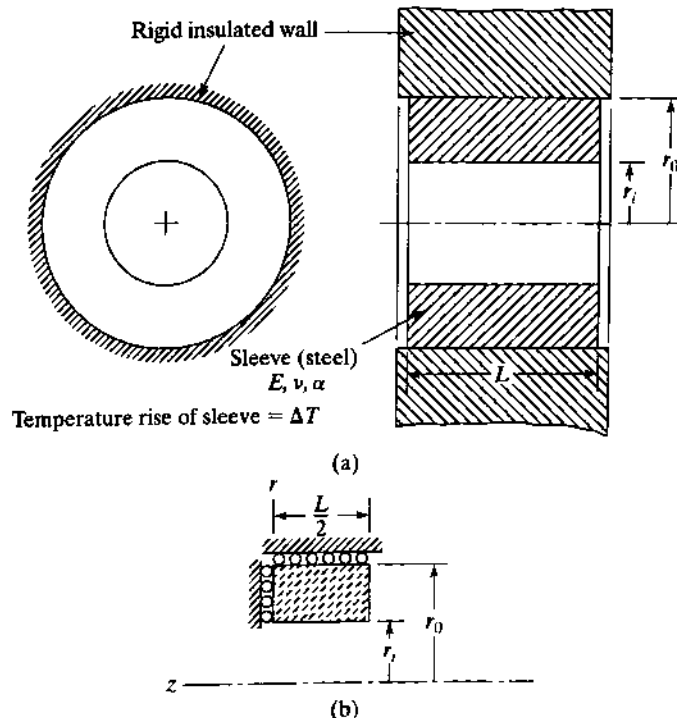


FIGURE 6.12 Thermal stress problem.

Example 6.4

A steel disk flywheel rotates at 3000 rpm. The outer diameter is 24 in., and the hole diameter is 6 in. (Fig. E6.4a). Find the value of the maximum tangential stress under the following conditions: thickness = 1 in., $E = 30 \times 10^6$ psi, Poisson's ratio = 0.3, and weight density = 0.283 lb/in.^3 .

A four-element finite element model is shown in Fig. E6.4b. The load vector is calculated from Eq. 6.34, neglecting gravity load. The result is

$$\mathbf{F} = [3449, 0, 9580, 0, 23\,380, 0, 38\,711, 0, 32\,580, 0, 18\,780, 0]^T \text{ lb}$$

The input data for program AXISYM and output are given subsequently.

The computer output gives us the tangential stresses in each of the four elements. Treating these values as centroidal values and *extrapolating* as shown in Fig. E6.4c, the maximum tangential stress occurring at the inner boundary is obtained as $\sigma_{t \max} = 8700$ psi. ■

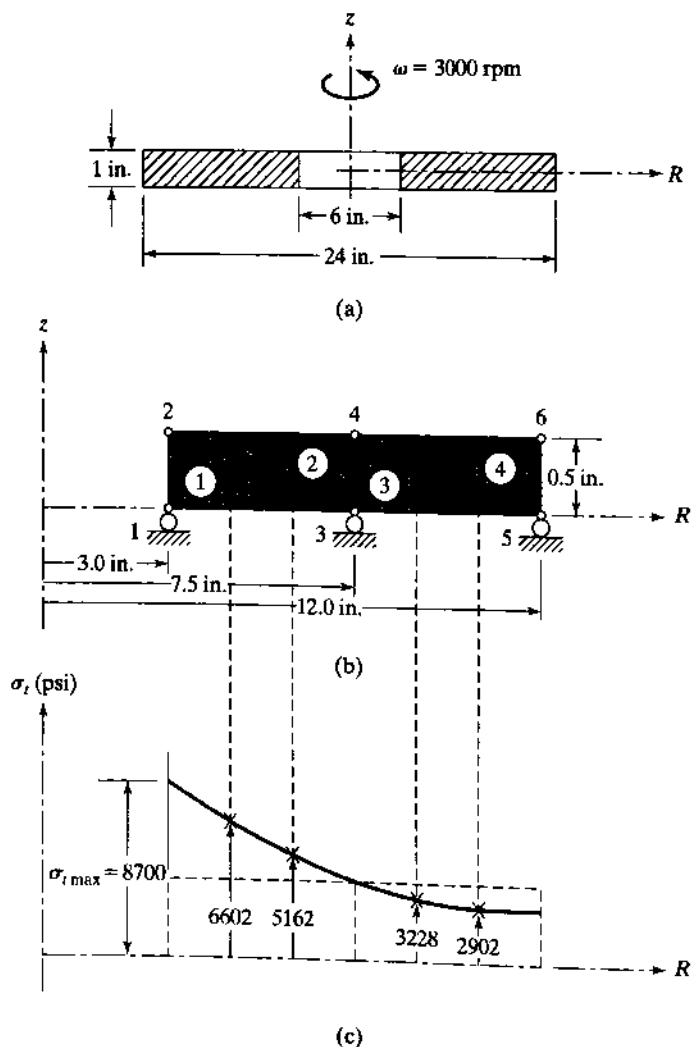


FIGURE E6.4

Input Data File

```

<< AXISYMMETRIC STRESS ANALYSIS >>
EXAMPLE 6.4
NN NE NM NDM NEN NDN
6 4 1 2 3 2
ND NL NMPC
3 6 0
Node# X Y (r z coordinates)
1 3 0
2 3 .5
3 7.5 0
4 7.5 .5
5 12 0
6 12 .5
Elem# N1 N2 N3 Mat# TempRise
1 1 3 2 1 0
2 2 3 4 1 0
3 4 3 5 1 0
4 4 5 6 1 0
DOF# Displacement
2 0
6 0
10 0
DOF# Load
1 3449
3 9580
5 23380
7 38711
9 32580
11 18780
MAT# E Nu Alpha
1 30E6 .3 12E-6
B1 i B2 j B3 (Multi-point constr. B1*Qi+B2*Qj-B3)
    
```

```

Program Axisym - CHANDRUPATLA & BELEGUNDU
Output
EXAMPLE 6.2
NODE# R-Displ Z-Displ
1 9.0031E-04 3.1892E-12
2 8.9898E-04 -4.2757E-05
3 9.0119E-04 -2.5588E-12
4 9.0291E-04 -2.6520E-05
5 9.1979E-04 -6.3050E-13
6 9.1780E-04 -1.9314E-05
ELEM# SR SZ TRZ ST S1 S2 ANGLE
SR->S1
1 1.9900E+03 1.2044E+01 -3.0815E+01 6.6017E+03 1.9904E+03 1.1564E+01
-8.9234E-01
2 1.7164E+03 4.7222E+02 8.1294E+01 5.1617E+03 1.7217E+03 4.6693E+02
3.7227E+00
3 9.9499E+02 -3.2439E+02 3.9660E+01 3.2277E+03 9.9618E+02 -3.2558E+02
1.7202E+00
4 9.7084E+02 3.0468E+00 -2.7421E+01 2.9022E+03 9.7162E+02 2.2705E+00
-1.6217E+00
    
```


PROBLEMS

- 6.1. In an axisymmetric problem, the element coordinates and displacements are as shown in the Fig. P6.1.
- What will be the value of the tangential (hoop) stress printed out by Program AXISYM?
 - What are the three principal stresses, σ_1 , σ_2 , and σ_3 ?
 - What is the vonMises stress in the element?
- Take $E = 30E6$ psi and $\nu = 0.3$. Coordinates and displacements are in inches.

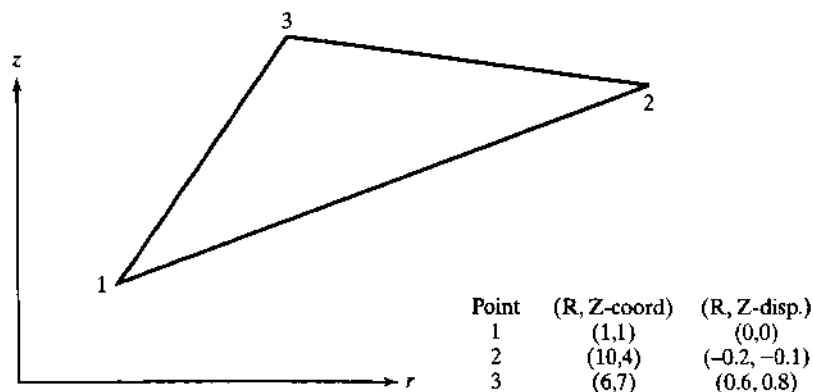


FIGURE P6.1

- 6.2. The open-ended steel cylinder shown in Fig. P6.2 is subjected to an internal pressure of 1 MPa. Find the deformed shape and the distribution of principal stresses.

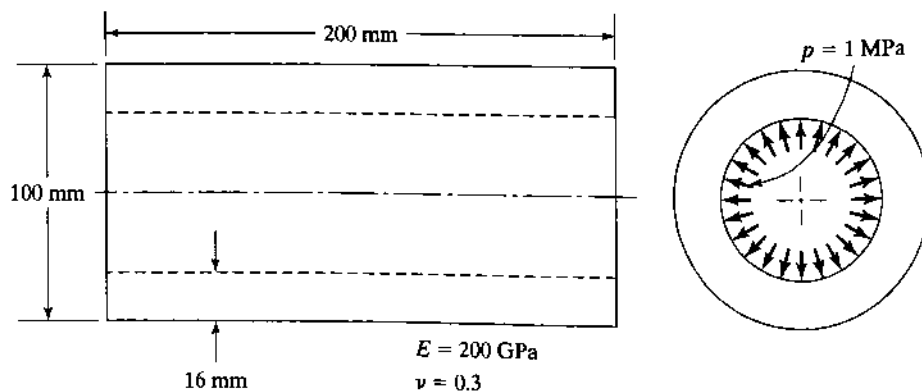


FIGURE P6.2

- 6.3. Find the deformed configuration and the stress distribution in the walls of the closed cylinder shown in Fig. P6.3.
- 6.4. Determine the diameters after deformation and the distribution of principal stresses along the radius of the infinite cylinder subjected to internal pressure as shown in Fig. P6.4.

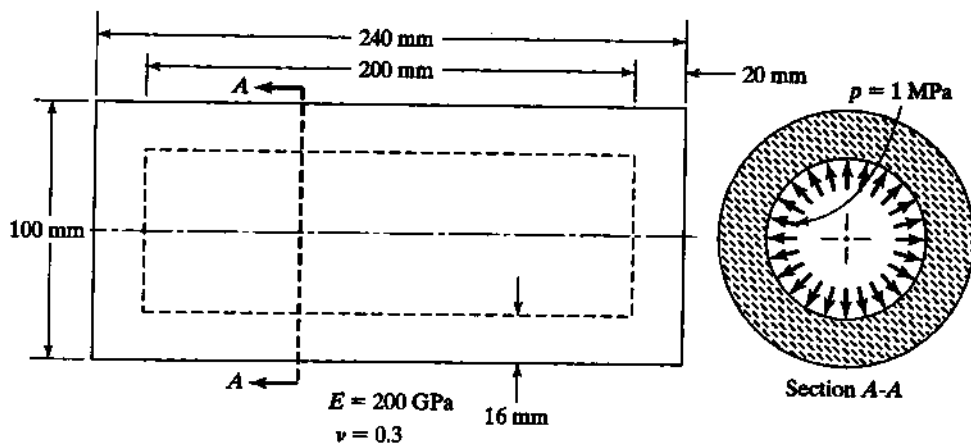


FIGURE P6.3

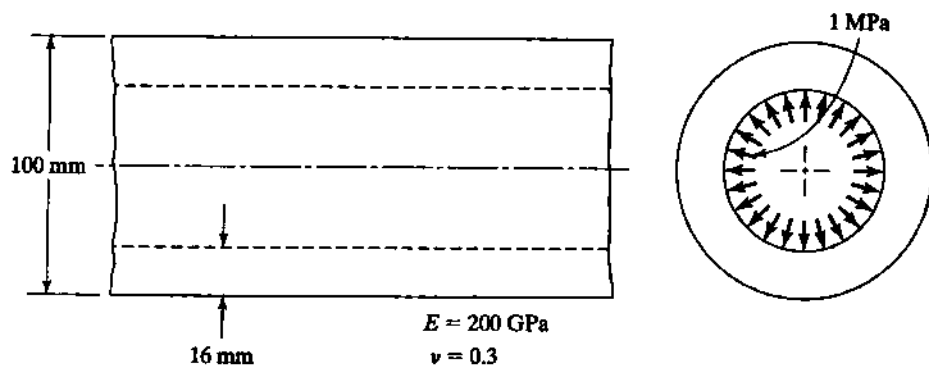


FIGURE P6.4

- 6.5. The steel sleeve of internal diameter 3 in. is press fitted onto a rigid shaft of diameter 3.01 in., as shown in Fig. P6.5. Determine (a) the outer diameter of the sleeve after fitting and (b) the stress distribution. Estimate the contact pressure by interpolating the radial stress in the neighboring elements.

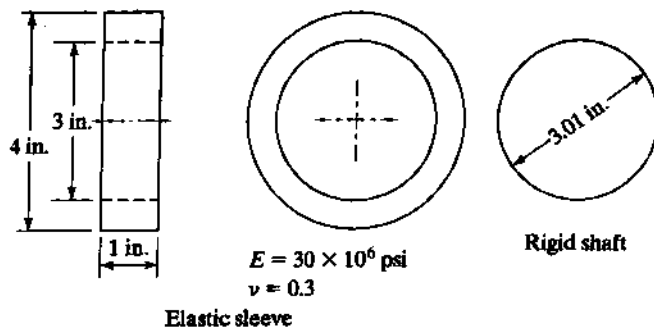


FIGURE P6.5

- 6.6. Solve Problem 6.5 if the shaft is also made out of steel.
- 6.7. The steel flywheel shown in Fig. P6.7 rotates at 3000 rpm. Find the deformed shape of the flywheel and give the stress distribution.

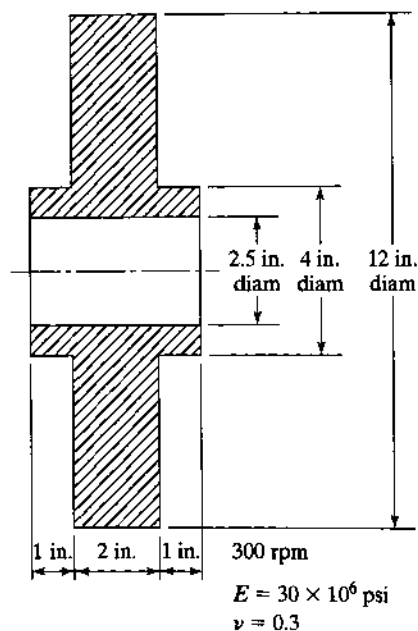


FIGURE P6.7 Flywheel.

- 6.8. The circular pad hydrostatic bearing shown in Fig. P6.8 is used for supporting slides subjected to large forces. Oil under pressure is supplied through a small hole at the center and flows out through the gap. The pressure distribution in the pocket area and the gap is shown in the figure. Find the deformed configuration of the pad and determine the stress distribution. (Note: Neglect the dimension of the oil supply hole.)

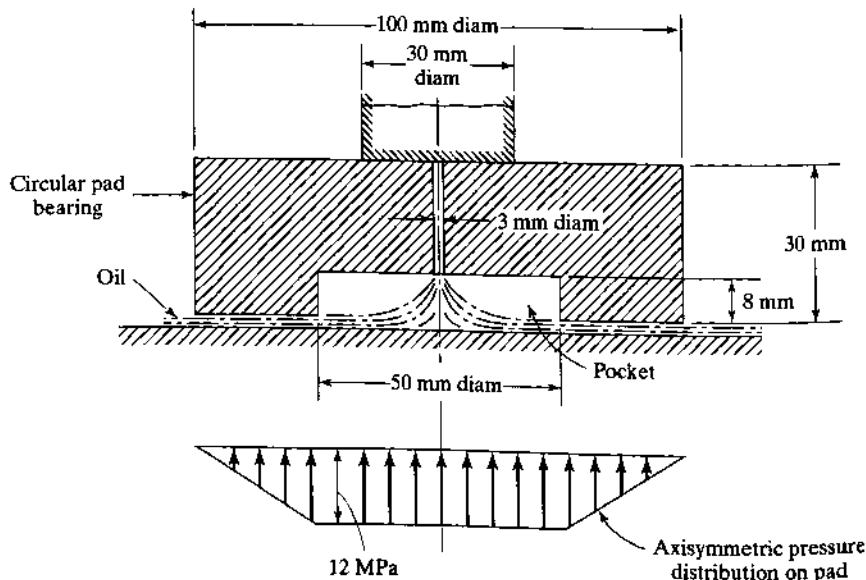


FIGURE P6.8 Hydrostatic bearing.

- 6.9. A Belleville spring is a conical disk spring. For the spring shown in Fig. P6.9, determine the axial load required to flatten the spring. Solve the problem using the incremental approach discussed in the text and plot the load-deflection curve as the spring flattens.

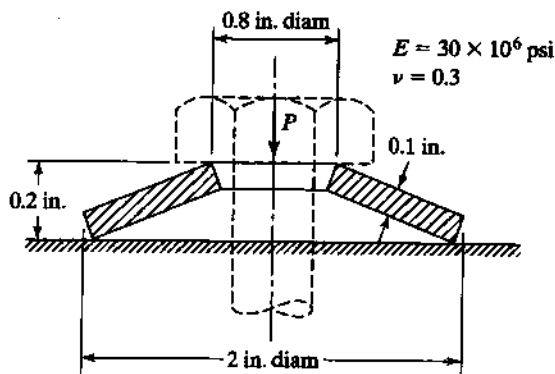


FIGURE P6.9 Belleville spring.

- 6.10. The aluminum tube shown in Fig. P6.10 fits snugly into a rigid hole at room temperature. If the temperature of the aluminum tube is increased by 40°C , find the deformed configuration and the stress distribution.

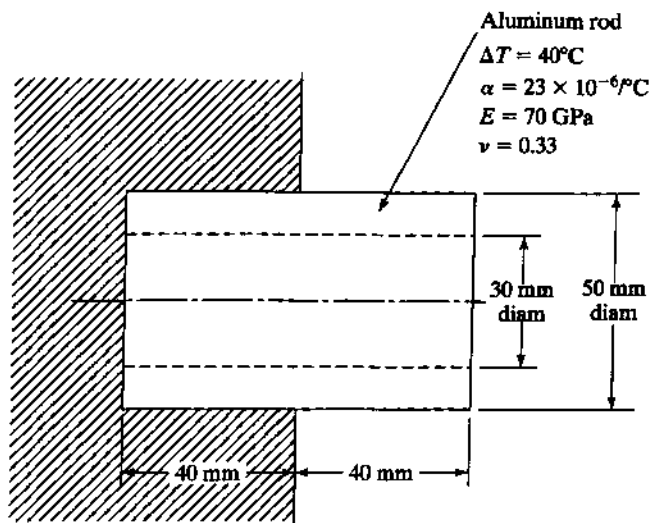


FIGURE P6.10

- 6.11. The steel water tank shown in Fig. P6.11 is bolted to a 5-m circular support. If the water is at a height of 3 m as shown, find the deformed shape and stress distribution. (Note: Pressure = ρgh , water density $\rho = 1 \text{ Mg/m}^3$, and $g = 9.8 \text{ m/s}^2$.)

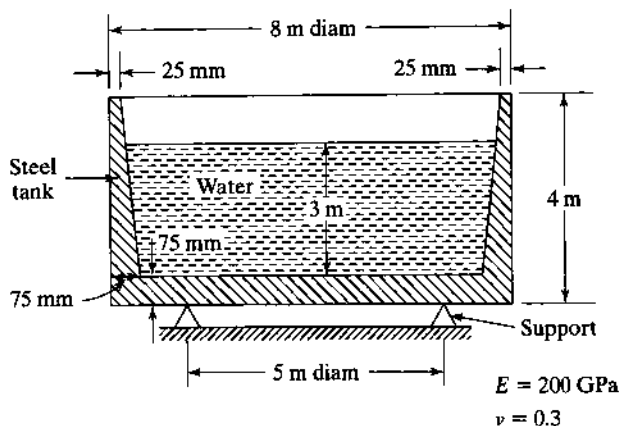


FIGURE P6.11 Water tank.

- 6.12. For the axisymmetric pressure loading shown in Fig. P6.12, determine the equivalent point loads F_1 , F_2 , F_3 , F_4 , F_7 , and F_8 .

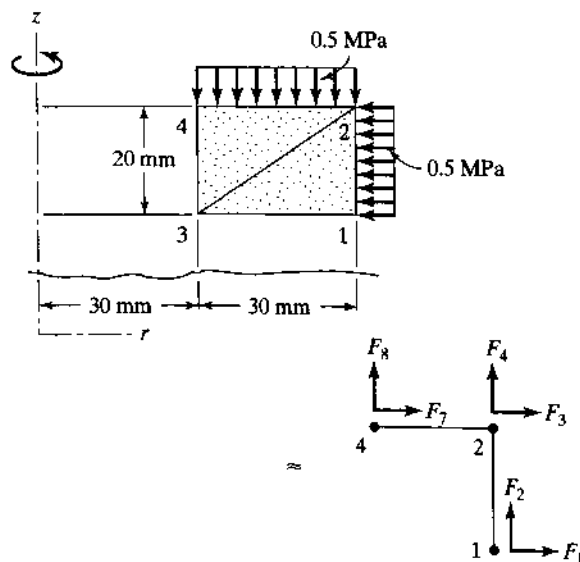


FIGURE P6.12

- 6.13. For the linearly varying distributed load on the axisymmetric conical surface shown in Fig. P6.13, complete the following:

(a) Prove that the equivalent point load vector \mathbf{T} is given by

$$\mathbf{T} = [aT_{r1} + bT_{r2}, \quad aT_{z1} + bT_{z2}, \quad bT_{r1} + cT_{r2}, \quad bT_{z1} + cT_{z2}]^T$$

where

$$a = \frac{2\pi\ell}{12}(3r_1 + r_2), \quad b = \frac{2\pi\ell}{12}(r_1 + r_2), \quad c = \frac{2\pi\ell}{12}(r_1 + 3r_2)$$

- (b) Solve the example problem 6.1 (given in Fig. E6.1) and check by how much the more precise calculations from part (a) differ from the approximation of piecewise uniform loads.

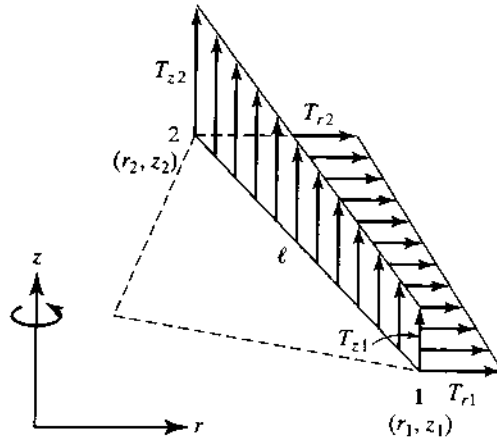


FIGURE P6.13

6.14. A cup-shaped steel die block, snugly fit in a shrink ring, is shown in Fig. P6.14a. The punch applies force on a slug placed in the die block to produce a cup-shaped part. If the process is modeled by linearly varying pressures (use the results from Problem 6.13 to compute nodal loads) on the die block as shown in Fig. P6.14b, determine the location and magnitude of maximum principal stresses in the die block for the following cases:

- (a) the die block modeled without the shrink ring,
- (b) the die block modeled with the shrink ring with no slip between the shrink ring and the die block, and
- (c) the die block modeled with the shrink ring with the assumption of frictionless axial slip. (*Hint:* You need duplicate nodes on the interface between the die block and the shrink ring. If I and J are a pair of nodes on the interface, then the multipoint constraint is $Q_{2I-1} - Q_{2J-1} = 0$. Use MESHGEN and DATAFEM programs followed by AXISYM).

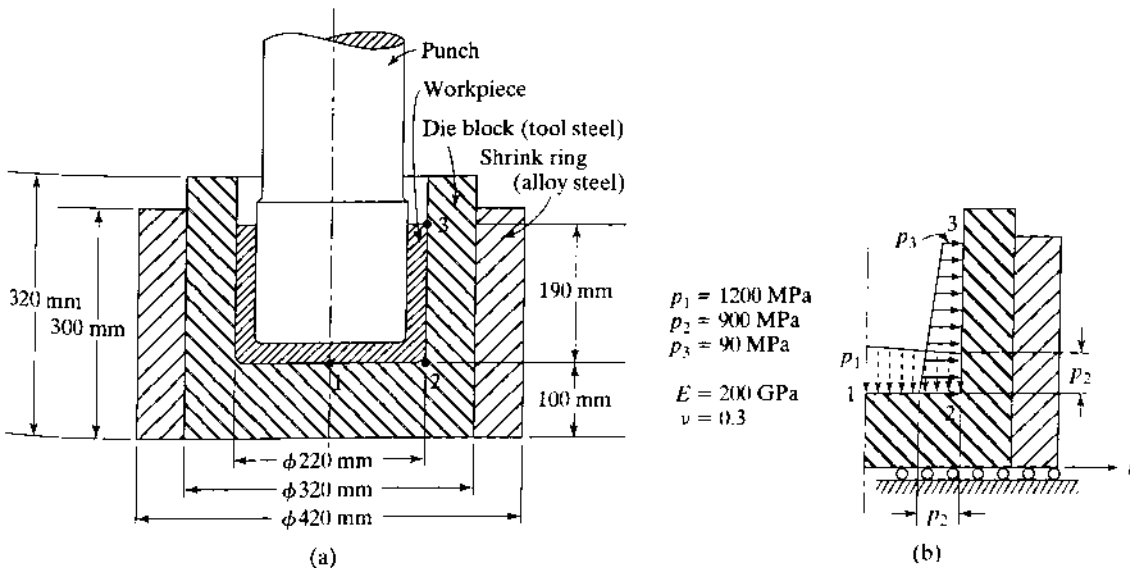


FIGURE P6.14

6.15. A 90-mm outside diameter steel disk held at 200°C above the room temperature fits snugly onto a steel shaft of 40-mm diameter at room temperature, as shown in Fig. P6.15. Determine the maximum stresses in the disk and the shaft when the assembly reaches room temperature.

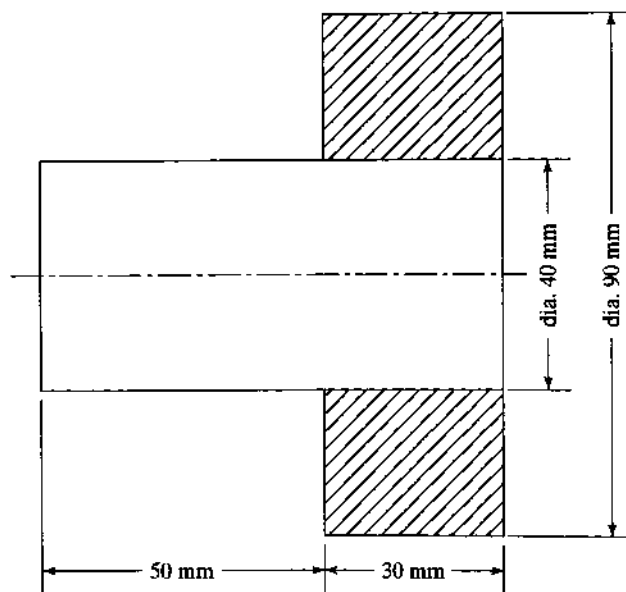


FIGURE P6.15

6.16. A syringe-plunger assembly is shown in Fig. P6.16. Model the glass syringe assuming that the 4 mm hole end is closed under test conditions. Obtain the deformation and stresses and compare the maximum principal stress with the ultimate tensile strength of glass.

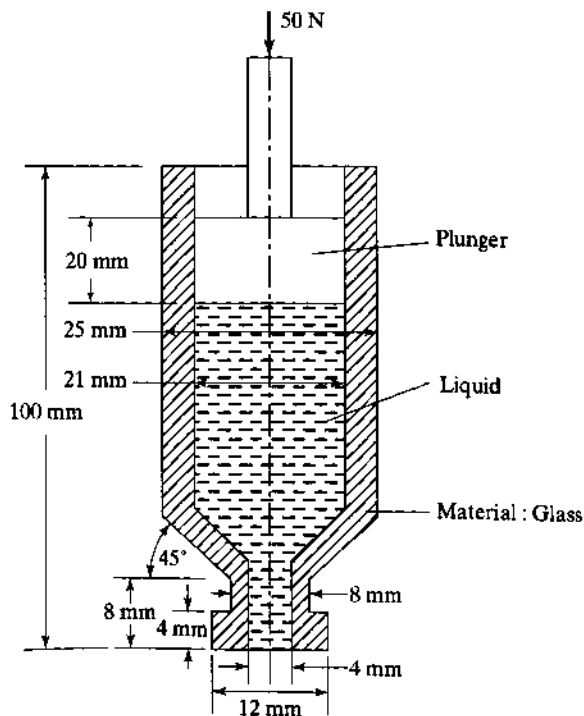


FIGURE P6.16

Program Listing

```

*****
*          PROGRAM AXISYM          *
*    AXISYMETRIC STRESS ANALYSIS  *
*      WITH TEMPERATURE           *
*  T.R.Chandrupatla and A.D.Belegundu *
*****
===== MAIN PROGRAM =====
Private Sub cmdStart_Click()
    Call InputData
    Call Bandwidth
    Call Stiffness
    Call ModifyForBC
    Call BandSolver
    Call StressCalc
    Call ReactionCalc
    Call Output
    cmdView.Enabled = True
    cmdStart.Enabled = False
End Sub
=====

```

```

===== ELEMENT STIFFNESS AND ASSEMBLY =====
Private Sub Stiffness()
    ReDim S(NQ, NBW)
    '----- Global Stiffness Matrix -----
    For N = 1 To NE
        picBox.Print "Forming Stiffness Matrix of Element "; N
    '---- Element Stiffness
        Call DbMat(N, 1, RBAR)
        For I = 1 To 6
            For J = 1 To 6
                C = 0
                For K = 1 To 4
                    C = C + Abs(DJ) * B(K, I) * DB(K, J) * PI * RBAR
                Next K
                SE(I, J) = C
            Next J
        Next I
    '---- Temperature Load Vector
        AL = PM(MAT(N), 3)
        C = AL * DT(N) * PI * RBAR * Abs(DJ)
        For I = 1 To 6
            TL(I) = C * (DB(1, I) + DB(2, I) + DB(4, I))
        Next I
        picBox.Print ".... Placing in Global Locations"
        Call PlaceGlobal(N)
    Next N
End Sub
=====

```



```

===== STRESS CALCULATIONS =====
Private Sub StressCalc()
  ReDim Stress(NE, 4), PrinStress(NE, 3), PltStress(NE)
  '----- Stress Calculations
  For N = 1 To NE
    Call DbMat(N, 2, RBAR)
    '---- Principal Stress Calculations
    If STR(3) = 0 Then
      S1 = STR(1): S2 = STR(2): ANG = 0
      If S2 > S1 Then
        S1 = STR(2): S2 = STR(1): ANG = 90
      End If
    Else
      C = 0.5 * (STR(1) + STR(2))
      R = Sqr(0.25 * (STR(1) - STR(2)) ^ 2 + (STR(3)) ^ 2)
      S1 = C + R: S2 = C - R
      If C > STR(1) Then
        ANG = 57.2957795 * Atn(STR(3) / (S1 - STR(1)))
        If STR(3) > 0 Then ANG = 90 - ANG
        If STR(3) < 0 Then ANG = -90 - ANG
      Else
        ANG = 57.29577951 * Atn(STR(3) / (STR(1) - S2))
      End If
    End If
    Stress(N, 1) = STR(1): Stress(N, 2) = STR(2)
    Stress(N, 3) = STR(3): Stress(N, 4) = STR(4)
    PrinStress(N, 1) = S1: PrinStress(N, 2) = S2
    PrinStress(N, 3) = ANG
    If IPL = 2 Then
      '---- vonMises Stress
      S3 = STR(4)
      C = (S1 - S2) ^ 2 + (S2 - S3) ^ 2 + (S3 - S1) ^ 2
      PltStress(N) = Sqr(0.5 * C)
    End If
  Next N
End Sub

```

```

===== B AND DB MATRICES FOR BTDB =====
Private Sub DbMat(N, ISTR, RBAR)
  '----- D(), B() AND DB() matrices
  '---- First the D-Matrix
  M = MAT(N): E = PM(M, 1): PNU = PM(M, 2): AL = PM(M, 3)
  C1 = E * (1 - PNU) / ((1 + PNU) * (1 - 2 * PNU)): C2 = PNU / (1 - PNU)
  For I = 1 To 4: For J = 1 To 4: D(I, J) = 0: Next J: Next I
  D(1, 1) = C1: D(1, 2) = C1 * C2: D(1, 4) = C1 * C2
  D(2, 1) = D(1, 2): D(2, 2) = C1: D(2, 4) = C1 * C2
  D(3, 3) = 0.5 * E / (1 + PNU)
  D(4, 1) = D(1, 4): D(4, 2) = D(2, 4): D(4, 4) = C1

```

continued

```

'--- Strain-Displacement Matrix B()
I1 = NOC(N, 1): I2 = NOC(N, 2): I3 = NOC(N, 3)
R1 = X(I1, 1): R2 = X(I2, 1): R3 = X(I3, 1)
Z1 = X(I1, 2): Z2 = X(I2, 2): Z3 = X(I3, 2)
R21 = R2 - R1: R32 = R3 - R2: R13 = R1 - R3
Z12 = Z1 - Z2: Z23 = Z2 - Z3: Z31 = Z3 - Z1
DJ = R13 * Z23 - R32 * Z31 'Determinant of Jacobian
RBAR = (R1 + R2 + R3) / 3
'--- Definition of B() Matrix
B(1, 1) = Z23 / DJ: B(2, 1) = 0: B(3, 1) = R32 / DJ
  B(4, 1) = 1 / (3 * RBAR)
B(1, 2) = 0: B(2, 2) = R32 / DJ: B(3, 2) = Z23 / DJ: B(4, 2) = 0
B(1, 3) = Z31 / DJ: B(2, 3) = 0: B(3, 3) = R13 / DJ
  B(4, 3) = 1 / (3 * RBAR)
B(1, 4) = 0: B(2, 4) = R13 / DJ: B(3, 4) = Z31 / DJ: B(4, 4) = 0
B(1, 5) = Z12 / DJ: B(2, 5) = 0: B(3, 5) = R21 / DJ
  B(4, 5) = 1 / (3 * RBAR)
B(1, 6) = 0: B(2, 6) = R21 / DJ: B(3, 6) = Z12 / DJ: B(4, 6) = 0
'--- DB Matrix DB = D*B
For I = 1 To 4
  For J = 1 To 6
    DB(I, J) = 0
    For K = 1 To 4
      DB(I, J) = DB(I, J) + D(I, K) * B(K, J)
    Next K
  Next J
Next I
If ISTR = 2 Then
  '----- Stress Evaluation -----
  Q(1) = F(2 * I1 - 1): Q(2) = F(2 * I1)
  Q(3) = F(2 * I2 - 1): Q(4) = F(2 * I2)
  Q(5) = F(2 * I3 - 1): Q(6) = F(2 * I3)
  C1 = AL * DT(N)
  For I = 1 To 4
    C = 0
    For K = 1 To 6: C = C + DB(I, K) * Q(K): Next K
    STR(I) = C - C1 * (D(I, 1) + D(I, 2) + D(I, 4))
  Next I
End If
End Sub

```

Two-Dimensional Isoparametric Elements and Numerical Integration

7.1 INTRODUCTION

In Chapters 5 and 6, we have developed the constant-strain triangular element for stress analysis. In this chapter, we develop four-node and higher order *isoparametric* elements and apply them to stress analysis. These elements have proved effective on a wide variety of two- and three-dimensional problems in engineering. We present the two-dimensional four-node quadrilateral in detail. Development of higher order elements follow the same basic steps used in the four-node quadrilateral. The higher order elements can capture variations in stress such as occur near fillets, holes, etc. We can view the isoparametric family of elements in a unified manner due to the simple and versatile manner in which shape functions can be derived, followed by the generation of the element stiffness matrix using numerical integration.

7.2 THE FOUR-NODE QUADRILATERAL

Consider the general quadrilateral element shown in Fig. 7.1. The local nodes are numbered as 1, 2, 3, and 4 in a *counterclockwise* fashion as shown, and (x_i, y_i) are the coordinates of node i . The vector $\mathbf{q} = [q_1, q_2, \dots, q_8]^T$ denotes the element displacement vector. The displacement of an interior point P located at (x, y) is represented as $\mathbf{u} = [u(x, y), v(x, y)]^T$.

Shape Functions

Following the steps in earlier chapters, we first develop the shape functions on a master element, shown in Fig. 7.2. The master element is defined in ξ -, η -coordinates (or *natural* coordinates) and is square shaped. The Lagrange shape functions where $i = 1, 2, 3,$ and 4 , are defined such that N_i is equal to unity at node i and is zero at other nodes. In particular, consider the definition of N_1 :

$$\begin{aligned} N_1 &= 1 && \text{at node 1} \\ &= 0 && \text{at nodes 2, 3, and 4} \end{aligned} \quad (7.1)$$

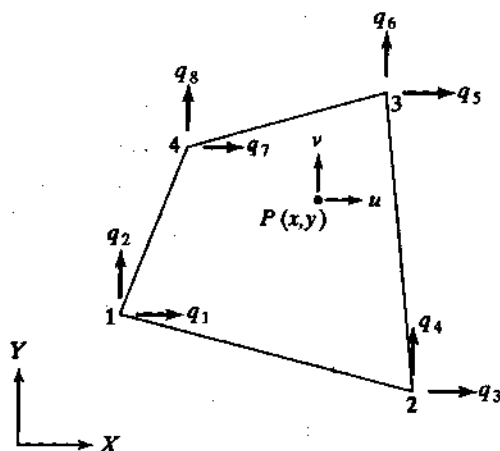
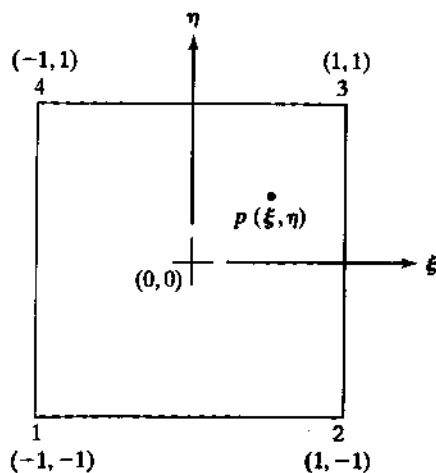


FIGURE 7.1 Four-node quadrilateral element.

FIGURE 7.2 The quadrilateral element in ξ, η space (the *master element*).

Now, the requirement that $N_1 = 0$ at nodes 2, 3, and 4 is equivalent to requiring that $N_1 = 0$ along edges $\xi = +1$ and $\eta = +1$ (Fig. 7.2). Thus, N_1 has to be of the form

$$N_1 = c(1 - \xi)(1 - \eta) \quad (7.2)$$

where c is some constant. The constant is determined from the condition $N_1 = 1$ at node 1. Since $\xi = -1$, $\eta = -1$ at node 1, we have

$$1 = c(2)(2) \quad (7.3)$$

which yields $c = \frac{1}{4}$. Thus,

$$N_1 = \frac{1}{4}(1 - \xi)(1 - \eta) \quad (7.4)$$

All the four shape functions can be written as

$$\begin{aligned} N_1 &= \frac{1}{4}(1 - \xi)(1 - \eta) \\ N_2 &= \frac{1}{4}(1 + \xi)(1 - \eta) \\ N_3 &= \frac{1}{4}(1 + \xi)(1 + \eta) \\ N_4 &= \frac{1}{4}(1 - \xi)(1 + \eta) \end{aligned} \quad (7.5)$$

While implementing in a computer program, the compact representation of Eqs. 7.5 is useful

$$N_i = \frac{1}{4}(1 + \xi\xi_i)(1 + \eta\eta_i) \quad (7.6)$$

where (ξ_i, η_i) are the coordinates of node i .

We now express the displacement field within the element in terms of the nodal values. Thus, if $\mathbf{u} = [u, v]^T$ represents the displacement components of a point located at (ξ, η) , and \mathbf{q} , dimension (8×1) , is the element displacement vector, then

$$\begin{aligned} u &= N_1q_1 + N_2q_3 + N_3q_5 + N_4q_7 \\ v &= N_1q_2 + N_2q_4 + N_3q_6 + N_4q_8 \end{aligned} \quad (7.7a)$$

which can be written in matrix form as

$$\mathbf{u} = \mathbf{N}\mathbf{q} \quad (7.7b)$$

where

$$\mathbf{N} = \begin{bmatrix} N_1 & 0 & N_2 & 0 & N_3 & 0 & N_4 & 0 \\ 0 & N_1 & 0 & N_2 & 0 & N_3 & 0 & N_4 \end{bmatrix} \quad (7.8)$$

In the isoparametric formulation, we use the *same* shape functions N_i to also express the coordinates of a point within the element in terms of nodal coordinates. Thus,

$$\begin{aligned} x &= N_1x_1 + N_2x_2 + N_3x_3 + N_4x_4 \\ y &= N_1y_1 + N_2y_2 + N_3y_3 + N_4y_4 \end{aligned} \quad (7.9)$$

Subsequently, we will need to express the derivatives of a function in x -, y -coordinates in terms of its derivatives in ξ -, η -coordinates. This is done as follows: A function $f = f(x, y)$, in view of Eqs. 7.9, can be considered to be an implicit function of ξ and η as $f = f[x(\xi, \eta), y(\xi, \eta)]$. Using the chain rule of differentiation, we have

$$\begin{aligned} \frac{\partial f}{\partial \xi} &= \frac{\partial f}{\partial x} \frac{\partial x}{\partial \xi} + \frac{\partial f}{\partial y} \frac{\partial y}{\partial \xi} \\ \frac{\partial f}{\partial \eta} &= \frac{\partial f}{\partial x} \frac{\partial x}{\partial \eta} + \frac{\partial f}{\partial y} \frac{\partial y}{\partial \eta} \end{aligned} \quad (7.10)$$

or

$$\begin{Bmatrix} \frac{\partial f}{\partial \xi} \\ \frac{\partial f}{\partial \eta} \end{Bmatrix} = \mathbf{J} \begin{Bmatrix} \frac{\partial f}{\partial x} \\ \frac{\partial f}{\partial y} \end{Bmatrix} \quad (7.11)$$

where \mathbf{J} is the Jacobian matrix

$$\mathbf{J} = \begin{bmatrix} \frac{\partial x}{\partial \xi} & \frac{\partial y}{\partial \xi} \\ \frac{\partial x}{\partial \eta} & \frac{\partial y}{\partial \eta} \end{bmatrix} \quad (7.12)$$

In view of Eqs. 7.5 and 7.9, we have

$$\mathbf{J} = \frac{1}{4} \begin{bmatrix} -(1-\eta)x_1 + (1-\eta)x_2 + (1+\eta)x_3 - (1+\eta)x_4 & -(1-\eta)y_1 + (1-\eta)y_2 + (1+\eta)y_3 - (1+\eta)y_4 \\ -(1-\xi)x_1 - (1+\xi)x_2 + (1+\xi)x_3 + (1-\xi)x_4 & -(1-\xi)y_1 - (1+\xi)y_2 + (1+\xi)y_3 + (1-\xi)y_4 \end{bmatrix} \quad (7.13a)$$

$$\equiv \begin{bmatrix} J_{11} & J_{12} \\ J_{21} & J_{22} \end{bmatrix} \quad (7.13b)$$

Equation 7.11 can be inverted as

$$\begin{Bmatrix} \frac{\partial f}{\partial x} \\ \frac{\partial f}{\partial y} \end{Bmatrix} = \mathbf{J}^{-1} \begin{Bmatrix} \frac{\partial f}{\partial \xi} \\ \frac{\partial f}{\partial \eta} \end{Bmatrix} \quad (7.14a)$$

or

$$\begin{Bmatrix} \frac{\partial f}{\partial x} \\ \frac{\partial f}{\partial y} \end{Bmatrix} = \frac{1}{\det \mathbf{J}} \begin{bmatrix} J_{22} & -J_{12} \\ -J_{21} & J_{11} \end{bmatrix} \begin{Bmatrix} \frac{\partial f}{\partial \xi} \\ \frac{\partial f}{\partial \eta} \end{Bmatrix} \quad (7.14b)$$

These expressions will be used in the derivation of the element stiffness matrix.

An additional result that will be needed is the relation

$$dx dy = \det \mathbf{J} d\xi d\eta \quad (7.15)$$

The proof of this result, found in many textbooks on calculus, is given in the appendix.

Element Stiffness Matrix

The stiffness matrix for the quadrilateral element can be derived from the strain energy in the body, given by

$$U = \int_V \frac{1}{2} \boldsymbol{\sigma}^T \boldsymbol{\epsilon} dV \quad (7.16)$$

or

$$U = \sum_e t_e \int_e \frac{1}{2} \boldsymbol{\sigma}^T \boldsymbol{\epsilon} dA \quad (7.17)$$

where t_e is the thickness of element e .

The strain-displacement relations are

$$\boldsymbol{\epsilon} = \begin{Bmatrix} \epsilon_x \\ \epsilon_y \\ \gamma_{xy} \end{Bmatrix} = \begin{Bmatrix} \frac{\partial u}{\partial x} \\ \frac{\partial v}{\partial y} \\ \frac{\partial u}{\partial y} + \frac{\partial v}{\partial x} \end{Bmatrix} \quad (7.18)$$

By considering $f = u$ in Eq. 7.14b, we have

$$\begin{Bmatrix} \frac{\partial u}{\partial x} \\ \frac{\partial u}{\partial y} \end{Bmatrix} = \frac{1}{\det \mathbf{J}} \begin{bmatrix} J_{22} & -J_{12} \\ -J_{21} & J_{11} \end{bmatrix} \begin{Bmatrix} \frac{\partial u}{\partial \xi} \\ \frac{\partial u}{\partial \eta} \end{Bmatrix} \quad (7.19a)$$

Similarly,

$$\begin{Bmatrix} \frac{\partial v}{\partial x} \\ \frac{\partial v}{\partial y} \end{Bmatrix} = \frac{1}{\det \mathbf{J}} \begin{bmatrix} J_{22} & -J_{12} \\ -J_{21} & J_{11} \end{bmatrix} \begin{Bmatrix} \frac{\partial v}{\partial \xi} \\ \frac{\partial v}{\partial \eta} \end{Bmatrix} \quad (7.19b)$$

Equations 7.18 and 7.19a,b yield

$$\boldsymbol{\epsilon} = \mathbf{A} \begin{Bmatrix} \frac{\partial u}{\partial \xi} \\ \frac{\partial u}{\partial \eta} \\ \frac{\partial v}{\partial \xi} \\ \frac{\partial v}{\partial \eta} \end{Bmatrix} \quad (7.20)$$

where \mathbf{A} is given by

$$\mathbf{A} = \frac{1}{\det \mathbf{J}} \begin{bmatrix} J_{22} & -J_{12} & 0 & 0 \\ 0 & 0 & -J_{21} & J_{11} \\ -J_{21} & J_{11} & J_{22} & -J_{12} \end{bmatrix} \quad (7.21)$$

Now, from the interpolation equations Eqs. 7.7a, we have

$$\begin{Bmatrix} \frac{\partial u}{\partial \xi} \\ \frac{\partial u}{\partial \eta} \\ \frac{\partial v}{\partial \xi} \\ \frac{\partial v}{\partial \eta} \end{Bmatrix} = \mathbf{G} \mathbf{q} \quad (7.22)$$

where

$$\mathbf{G} = \frac{1}{4} \begin{bmatrix} -(1-\eta) & 0 & (1-\eta) & 0 & (1+\eta) & 0 & -(1+\eta) & 0 \\ -(1-\xi) & 0 & -(1+\xi) & 0 & (1+\xi) & 0 & (1-\xi) & 0 \\ 0 & -(1-\eta) & 0 & (1-\eta) & 0 & (1+\eta) & 0 & -(1+\eta) \\ 0 & -(1-\xi) & 0 & -(1+\xi) & 0 & (1+\xi) & 0 & (1-\xi) \end{bmatrix} \quad (7.23)$$

Equations 7.20 and 7.22 now yield

$$\epsilon = \mathbf{B}\mathbf{q} \quad (7.24)$$

where

$$\mathbf{B} = \mathbf{A}\mathbf{G} \quad (7.25)$$

The relation $\epsilon = \mathbf{B}\mathbf{q}$ is the desired result. The strain in the element is expressed in terms of its nodal displacement. The stress is now given by

$$\sigma = \mathbf{D}\mathbf{B}\mathbf{q} \quad (7.26)$$

where \mathbf{D} is a (3×3) material matrix. The strain energy in Eq. 7.17 becomes

$$U = \sum_e \frac{1}{2} \mathbf{q}^T \left[t_e \int_{-1}^1 \int_{-1}^1 \mathbf{B}^T \mathbf{D} \mathbf{B} \det \mathbf{J} d\xi d\eta \right] \mathbf{q} \quad (7.27a)$$

$$= \sum_e \frac{1}{2} \mathbf{q}^T \mathbf{k}^e \mathbf{q} \quad (7.27b)$$

where

$$\mathbf{k}^e = t_e \int_{-1}^1 \int_{-1}^1 \mathbf{B}^T \mathbf{D} \mathbf{B} \det \mathbf{J} d\xi d\eta \quad (7.28)$$

is the element stiffness matrix of dimension (8×8) .

We note here that quantities \mathbf{B} and $\det \mathbf{J}$ in the integral in Eq. (7.28) are involved functions of ξ and η , and so the integration has to be performed numerically. Methods of numerical integration are discussed subsequently.

Element Force Vectors

Body Force A body force that is distributed force per unit volume, contributes to the global load vector \mathbf{F} . This contribution can be determined by considering the body force term in the potential-energy expression

$$\int_V \mathbf{u}^T \mathbf{f} dV \quad (7.29)$$

Using $\mathbf{u} = \mathbf{N}\mathbf{q}$, and treating the body force $\mathbf{f} = [f_x, f_y]^T$ as constant within each element, we get

$$\int_V \mathbf{u}^T \mathbf{f} dV = \sum_e \mathbf{q}^T \mathbf{f}^e \quad (7.30)$$

where the (8×1) element body force vector is given by

$$\mathbf{f}^e = t_e \left[\int_{-1}^1 \int_{-1}^1 \mathbf{N}^T \det \mathbf{J} d\xi d\eta \right] \begin{Bmatrix} f_x \\ f_y \end{Bmatrix} \quad (7.31)$$

As with the stiffness matrix derived earlier, this body force vector has to be evaluated by numerical integration.

Traction Force Assume that a constant traction force $\mathbf{T} = [T_x, T_y]^T$ —a force per unit area—is applied on edge 2-3 of the quadrilateral element. Along this edge, we have $\xi = 1$. If we use the shape functions given in Eq. 7.5, this becomes $N_1 = N_4 = 0$, $N_2 = (1 - \eta)/2$, and $N_3 = (1 + \eta)/2$. Note that the shape functions are linear functions along the edges. Consequently, from the potential, the element traction load vector is readily given by

$$\mathbf{T}^e = \frac{t_e \ell_{2-3}}{2} [0 \ 0 \ T_x \ T_y \ T_x \ T_y \ 0 \ 0]^T \quad (7.32)$$

where ℓ_{2-3} = length of edge 2-3. For varying distributed loads, we may express T_x and T_y in terms of values of nodes 2 and 3 using shape functions. Numerical integration can be used in this case.

Finally, **point** loads are considered in the usual manner by having a structural node at that point and simply adding to the global load vector \mathbf{F} .

7.3 NUMERICAL INTEGRATION

Consider the problem of numerically evaluating a one-dimensional integral of the form

$$I = \int_{-1}^1 f(\xi) d\xi \quad (7.33)$$

The *Gaussian quadrature* approach for evaluating I is given subsequently. This method has proved most useful in finite element work. Extension to integrals in two and three dimensions follows readily.

Consider the n -point approximation

$$I = \int_{-1}^1 f(\xi) d\xi \approx w_1 f(\xi_1) + w_2 f(\xi_2) + \cdots + w_n f(\xi_n) \quad (7.34)$$

where w_1, w_2, \dots , and w_n are the **weights** and ξ_1, ξ_2, \dots , and ξ_n are the sampling points or **Gauss points**. The idea behind Gaussian quadrature is to select the n Gauss points and n weights such that Eq. 7.34 provides an exact answer for polynomials $f(\xi)$ of as large a degree as possible. In other words, the idea is that if the n -point integration formula is exact for all polynomials up to as high a degree as possible, then the formula will work well even if f is not a polynomial. To get some intuition for the method, the one-point and two-point approximations are discussed in the sections that follow.

One-Point Formula. Consider the formula with $n = 1$ as

$$\int_{-1}^1 f(\xi) d\xi \approx w_1 f(\xi_1) \quad (7.35)$$

Since there are two parameters, w_1 and ξ_1 , we consider requiring the formula in Eq. 7.35 to be exact when $f(\xi)$ is a polynomial of order 1. Thus, if $f(\xi) = a_0 + a_1\xi$, then we require

$$\text{Error} = \int_{-1}^1 (a_0 + a_1\xi) d\xi - w_1 f(\xi_1) = 0 \quad (7.36a)$$

$$\text{Error} = 2a_0 - w_1(a_0 + a_1\xi_1) = 0 \quad (7.36b)$$

or

$$\text{Error} = a_0(2 - w_1) - w_1 a_1 \xi_1 = 0 \quad (7.36c)$$

From Eq. 7.36c, we see that the error is zeroed if

$$w_1 = 2 \quad \xi_1 = 0 \quad (7.37)$$

For any general f , then, we have

$$I = \int_{-1}^1 f(\xi) d\xi \approx 2f(0) \quad (7.38)$$

which is seen to be the familiar *midpoint rule* (Fig. 7.3).

Two-Point Formula. Consider the formula with $n = 2$ as

$$\int_{-1}^1 f(\xi) d\xi \approx w_1 f(\xi_1) + w_2 f(\xi_2) \quad (7.39)$$

We have four parameters to choose: w_1 , w_2 , ξ_1 , and ξ_2 . We can therefore expect the formula in Eq. 7.39 to be exact for a cubic polynomial. Thus, choosing $f(\xi) = a_0 + a_1\xi + a_2\xi^2 + a_3\xi^3$ yields

$$\text{Error} = \left[\int_{-1}^1 (a_0 + a_1\xi + a_2\xi^2 + a_3\xi^3) d\xi \right] - [w_1 f(\xi_1) + w_2 f(\xi_2)] \quad (7.40)$$

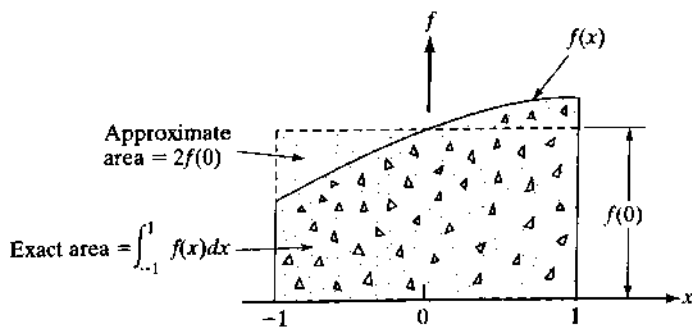


FIGURE 7.3 One-point Gauss quadrature.

Requiring zero error yields

$$\begin{aligned}w_1 + w_2 &= 2 \\w_1\xi_1 + w_2\xi_2 &= 0 \\w_1\xi_1^2 + w_2\xi_2^2 &= \frac{2}{3} \\w_1\xi_1^3 + w_2\xi_2^3 &= 0\end{aligned}\tag{7.41}$$

These nonlinear equations have the unique solution

$$w_1 = w_2 = 1 \quad -\xi_1 = \xi_2 = 1/\sqrt{3} = 0.5773502691 \dots\tag{7.42}$$

From this solution, we can conclude that n -point Gaussian quadrature will provide an exact answer if f is a polynomial of order $(2n - 1)$ or less. Table 7.1 gives the values of w_i and ξ_i for Gauss quadrature formulas of orders $n = 1$ through $n = 6$. Note that the Gauss points are located symmetrically with respect to the origin and that symmetrically placed points have the same weights. Moreover, the large number of digits given in Table 7.1 should be used in the calculations for accuracy (i.e., use double precision on the computer).

TABLE 7.1 Gauss Points and Weights for Gaussian Quadrature

$$\int_{-1}^1 f(\xi) d\xi \approx \sum_{i=1}^n w_i f(\xi_i)$$

| Number of points, n | Location, ξ_i | Weights, w_i |
|-----------------------|-------------------------------------|----------------|
| 1 | 0.0 | 2.0 |
| 2 | $\pm 1/\sqrt{3} = \pm 0.5773502692$ | 1.0 |
| 3 | ± 0.7745966692 | 0.5555555556 |
| | 0.0 | 0.8888888889 |
| 4 | ± 0.8611363116 | 0.3478548451 |
| | ± 0.3399810436 | 0.6521451549 |
| 5 | ± 0.9061798459 | 0.2369268851 |
| | ± 0.5384693101 | 0.4786286705 |
| | 0.0 | 0.5688888889 |
| 6 | ± 0.9324695142 | 0.1713244924 |
| | ± 0.6612093865 | 0.3607615730 |
| | ± 0.2386191861 | 0.4679139346 |

Example 7.1

Evaluate

$$I = \int_{-1}^1 \left[3e^x + x^2 + \frac{1}{(x+2)} \right] dx$$

using one-point and two-point Gauss quadrature.

Solution For $n = 1$, we have $w_1 = 2$, $x_1 = 0$, and

$$\begin{aligned}I &\approx 2f(0) \\ &= 7.0\end{aligned}$$

For $n = 2$, we find $w_1 = w_2 = 1$, $x_1 = -0.57735 \dots$, $x_2 = +0.57735 \dots$, and $I \approx 8.7857$. This may be compared with the exact solution

$$I_{\text{exact}} = 8.8165 \quad \blacksquare$$

Two-Dimensional Integrals

The extension of Gaussian quadrature to two-dimensional integrals of the form

$$I = \int_{-1}^1 \int_{-1}^1 f(\xi, \eta) d\xi d\eta \quad (7.43)$$

follows readily, since

$$\begin{aligned} I &\approx \int_{-1}^1 \left[\sum_{i=1}^n w_i f(\xi_i, \eta) \right] d\eta \\ &\approx \sum_{j=1}^n w_j \left[\sum_{i=1}^n w_i f(\xi_i, \eta_j) \right] \end{aligned}$$

or

$$I \approx \sum_{i=1}^n \sum_{j=1}^n w_i w_j f(\xi_i, \eta_j) \quad (7.44)$$

Stiffness Integration

To illustrate the use of Eq. 7.44, consider the element stiffness for a quadrilateral element

$$\mathbf{k}^e = t_e \int_{-1}^1 \int_{-1}^1 \mathbf{B}^T \mathbf{D} \mathbf{B} \det \mathbf{J} d\xi d\eta$$

where \mathbf{B} and $\det \mathbf{J}$ are functions of ξ and η . Note that this integral actually consists of the integral of each element in an (8×8) matrix. However, using the fact that \mathbf{k}^e is symmetric, we do not need to integrate elements below the main diagonal.

Let ϕ represent the ij th element in the integrand. That is, let

$$\phi(\xi, \eta) = t_e (\mathbf{B}^T \mathbf{D} \mathbf{B} \det \mathbf{J})_{ij} \quad (7.45)$$

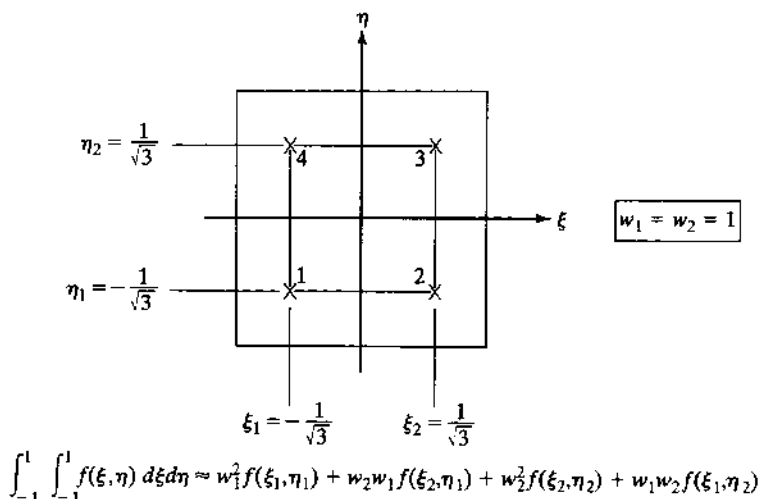
Then, if we use a 2×2 rule, we get

$$\begin{aligned} k_{ij} &\approx w_1^2 \phi(\xi_1, \eta_1) + w_1 w_2 \phi(\xi_1, \eta_2) \\ &\quad + w_2 w_1 \phi(\xi_2, \eta_1) + w_2^2 \phi(\xi_2, \eta_2) \end{aligned} \quad (7.46a)$$

where $w_1 = w_2 = 1.0$, $\xi_1 = \eta_1 = -0.57735 \dots$, and $\xi_2 = \eta_2 = +0.57735 \dots$. The Gauss points for the two-point rule used above are shown in Fig. 7.4. Alternatively, if we label the Gauss points as 1, 2, 3, and 4, then k_{ij} in Eq. 7.46a can also be written as

$$k_{ij} = \sum_{\text{IP}=1}^4 W_{\text{IP}} \phi_{\text{IP}} \quad (7.46b)$$

where ϕ_{IP} is the value of ϕ and W_{IP} is the weight factor at integration point IP. We note that $W_{\text{IP}} = (1)(1) = 1$. Computer implementation is sometimes easier using Eq. 7.46b.

FIGURE 7.4 Gaussian quadrature in two dimensions using the 2×2 rule.

We may readily follow the implementation of the previous integration procedure in program QUAD provided at the end of this chapter.

The evaluation of three-dimensional integrals is similar. For triangles, however, the weights and Gauss points are different, as discussed later in this chapter.

Stress Calculations

Unlike the constant-strain triangular element (Chapters 5 and 6), the stresses $\sigma = \mathbf{DBq}$ in the quadrilateral element are not constant within the element; they are functions of ξ and η , and consequently vary within the element. In practice, the stresses are evaluated at the Gauss points, which are also the points used for numerical evaluation of \mathbf{k}^e , where they are found to be accurate. For a quadrilateral with 2×2 integration, this gives four sets of stress values. For generating less data, one may evaluate stresses at one point per element, say, at $\xi = 0$ and $\eta = 0$. The latter approach is used in the program QUAD.

Example 7.2

Consider a rectangular element as shown in Fig. E7.1. Assume plane stress condition, $E = 30 \times 10^6$ psi, $\nu = 0.3$, and $\mathbf{q} = [0, 0, 0.002, 0.003, 0.006, 0.0032, 0, 0]^T$ in. Evaluate \mathbf{J} , \mathbf{B} , and σ at $\xi = 0$ and $\eta = 0$.

Solution Referring to Eq. 7.13a, we have

$$\mathbf{J} = \frac{1}{4} \begin{bmatrix} 2(1 - \eta) + 2(1 + \eta) & (1 + \eta) - (1 - \eta) \\ -2(1 + \xi) + 2(1 + \xi) & (1 + \xi) + (1 - \xi) \end{bmatrix}$$

$$= \begin{bmatrix} 1 & 0 \\ 0 & \frac{1}{2} \end{bmatrix}$$

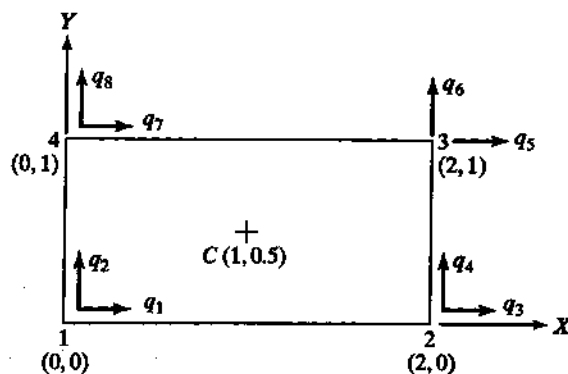


FIGURE E7.1

For this rectangular element, we find that \mathbf{J} is a constant matrix. Now, from Eqs. 7.21,

$$\mathbf{A} = \frac{1}{1/2} \begin{bmatrix} \frac{1}{2} & 0 & 0 & 0 \\ 0 & 0 & 0 & 1 \\ 0 & 1 & \frac{1}{2} & 0 \end{bmatrix}$$

Evaluating \mathbf{G} in Eq. 7.23 at $\xi = \eta = 0$ and using $\mathbf{B} = \mathbf{Q}\mathbf{G}$, we get

$$\mathbf{B}^0 = \begin{bmatrix} -\frac{1}{4} & 0 & \frac{1}{4} & 0 & \frac{1}{4} & 0 & -\frac{1}{4} & 0 \\ 0 & -\frac{1}{2} & 0 & -\frac{1}{2} & 0 & \frac{1}{2} & 0 & \frac{1}{2} \\ -\frac{1}{2} & -\frac{1}{4} & -\frac{1}{2} & \frac{1}{4} & \frac{1}{2} & \frac{1}{4} & \frac{1}{2} & -\frac{1}{4} \end{bmatrix}$$

The stresses at $\xi = \eta = 0$ are now given by the product

$$\boldsymbol{\sigma}^0 = \mathbf{D}\mathbf{B}^0\mathbf{q}$$

For the given data, we have

$$\mathbf{D} = \frac{30 \times 10^6}{(1 - 0.09)} \begin{bmatrix} 1 & 0.3 & 0 \\ 0.03 & 1 & 0 \\ 0 & 0 & 0.35 \end{bmatrix}$$

Thus,

$$\boldsymbol{\sigma}^0 = [66\ 920, 23\ 080, 40\ 960]^T \text{ psi}$$

Comment on Degenerate Quadrilaterals In some situations, we cannot avoid using degenerated quadrilaterals of the type shown in Fig. 7.5, where quadrilaterals

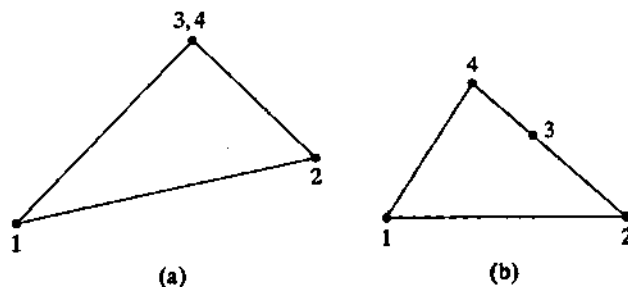


FIGURE 7.5 Degenerate four-node quadrilateral elements.

degenerate into triangles. Numerical integration will permit the use of such elements, but the errors are higher than for regular elements. Standard codes normally permit the use of such elements.

7.4 HIGHER ORDER ELEMENTS

The concepts presented earlier for the four-node quadrilateral element can be readily extended to other, higher order, isoparametric elements. In the four-node quadrilateral element, the shape functions contained terms $1, \xi, \eta,$ and $\xi\eta$. In contrast, the elements to be discussed later also contain terms such as $\xi^2\eta$ and $\xi\eta^2$, which generally provide greater accuracy. Only the shape functions \mathbf{N} are given in Eqs. 7.47. The generation of element stiffness follows the routine steps

$$\mathbf{u} = \mathbf{N}\mathbf{q} \quad (7.47a)$$

$$\boldsymbol{\epsilon} = \mathbf{B}\mathbf{q} \quad (7.47b)$$

$$\mathbf{k}^e = t_e \int_{-1}^1 \int_{-1}^1 \mathbf{B}^T \mathbf{D} \mathbf{B} \det \mathbf{J} d\xi d\eta \quad (7.47c)$$

where \mathbf{k}^e is evaluated using Gaussian quadrature.

Nine-Node Quadrilateral

The nine-node quadrilateral has been found to be very effective in finite element practice. The local node numbers for this element are shown in Fig. 7.6a. The square master element is shown in Fig. 7.6b. The shape functions are defined as follows:

Consider, first, the ξ -axis alone as shown in Fig. 7.6c. The local node numbers 1, 2, and 3 on this axis correspond to locations $\xi = -1, 0,$ and $+1$, respectively. At these nodes, we define the generic shape functions $L_1, L_2,$ and L_3 as

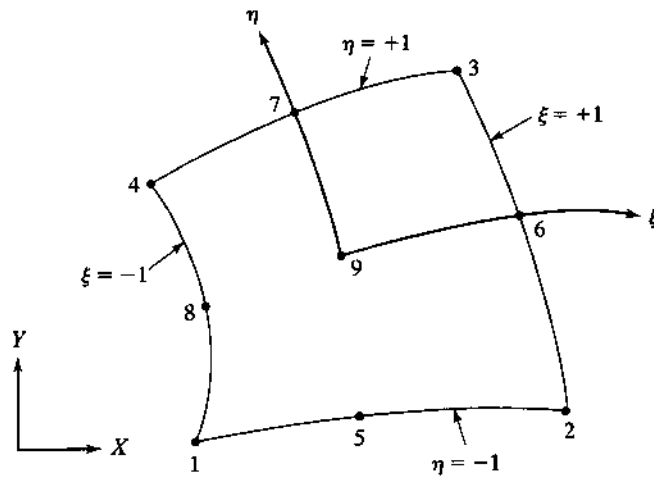
$$\begin{aligned} L_i(\xi) &= 1 && \text{at node } i \\ &= 0 && \text{at other two nodes} \end{aligned} \quad (7.48)$$

Now, consider L_1 . Since $L_1 = 0$ at $\xi = 0$ and at $\xi = +1$, we know that L_1 is of the form $L_1 = c\xi(1 - \xi)$. The constant c is obtained from $L_1 = 1$ at $\xi = -1$ as $c = -\frac{1}{2}$. Thus, $L_1(\xi) = -\xi(1 - \xi)/2$. L_2 and L_3 can be obtained by using similar arguments. We have

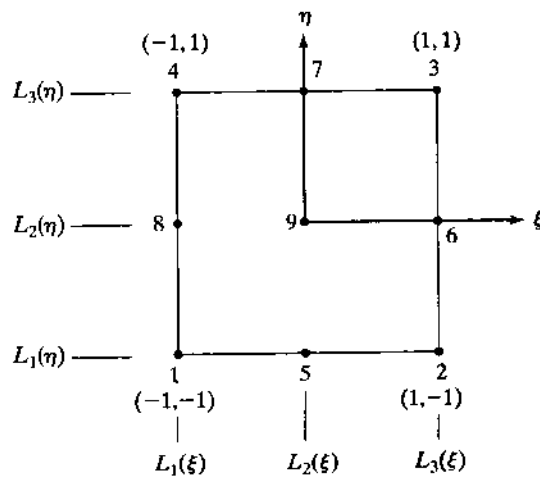
$$\begin{aligned} L_1(\xi) &= -\frac{\xi(1 - \xi)}{2} \\ L_2(\xi) &= (1 + \xi)(1 - \xi) \\ L_3(\xi) &= \frac{\xi(1 + \xi)}{2} \end{aligned} \quad (7.49a)$$

Similarly, generic shape functions can be defined along the η -axis (Fig. 7.6c) as

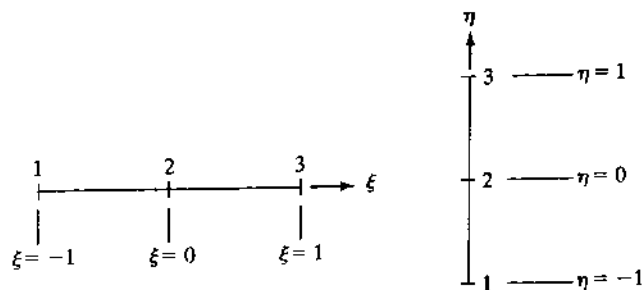
$$\begin{aligned} L_1(\eta) &= -\frac{\eta(1 - \eta)}{2} \\ L_2(\eta) &= (1 + \eta)(1 - \eta) \\ L_3(\eta) &= \frac{\eta(1 + \eta)}{2} \end{aligned} \quad (7.49b)$$



(a)



(b)



(c)

FIGURE 7.6 Nine-node quadrilateral (a) in x, y space and (b) in ξ, η space. (c) Definition of general shape functions.

Referring back to the master element in Fig. 7.6b, we observe that every node has the coordinates $\xi = -1, 0, \text{ or } +1$ and $\eta = -1, 0, \text{ or } +1$. Thus, the *product rule* that follows yields the shape functions N_1, N_2, \dots, N_9 , as

$$\begin{aligned} N_1 &= L_1(\xi)L_1(\eta) & N_5 &= L_2(\xi)L_1(\eta) & N_2 &= L_3(\xi)L_1(\eta) \\ N_8 &= L_1(\xi)L_2(\eta) & N_9 &= L_2(\xi)L_2(\eta) & N_6 &= L_3(\xi)L_2(\eta) \\ N_4 &= L_1(\xi)L_3(\eta) & N_7 &= L_2(\xi)L_3(\eta) & N_3 &= L_3(\xi)L_3(\eta) \end{aligned} \quad (7.50)$$

By the manner in which L_i are constructed, it can be readily verified that N_i equal one at node i and equal zero at other nodes, as desired.

As noted in the beginning of this section, the use of higher order terms in \mathbf{N} leads to a higher order interpolation of the displacement field as given by $\mathbf{u} = \mathbf{N}\mathbf{q}$. In addition, since $x = \sum_i N_i x_i$ and $y = \sum_i N_i y_i$, it means that higher order terms can also be used to define geometry. Thus, the elements can have curved edges if desired. However, it is possible to define a *subparametric* element by using nine-node shape functions to interpolate displacement and using only four-node quadrilateral shape functions to define geometry.

Eight-Node Quadrilateral

This element belongs to the **serendipity** family of elements. The element consists of eight nodes (Fig. 7.7a), all of which are located on the boundary. Our task is to define shape functions N_i such that $N_i = 1$ at node i and 0 at all other nodes. In defining N_i , we refer to the master element shown in Fig. 7.7b. First, we define $N_1 - N_4$. For N_1 , we note that $N_1 = 1$ at node 1 and 0 at other nodes. Thus, N_1 has to vanish along the lines $\xi = +1$, $\eta = +1$, and $\xi + \eta = -1$ (Fig. 7.7a). Consequently, N_1 is of the form

$$N_1 = c(1 - \xi)(1 - \eta)(1 + \xi + \eta) \quad (7.51)$$

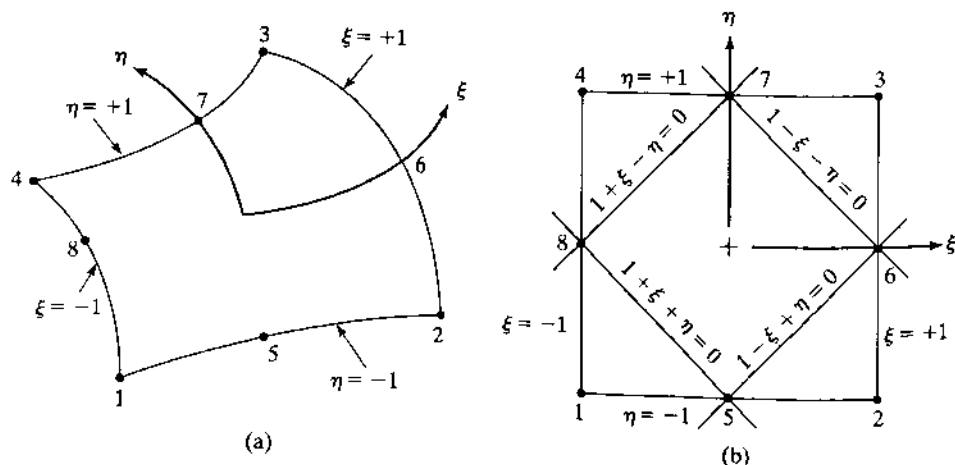


FIGURE 7.7 Eight-node quadrilateral (a) in x, y space and (b) in ξ, η space.

At node 1, $N_1 = 1$ and $\xi = \eta = -1$. Thus, $c = -\frac{1}{4}$. We thus have

$$\begin{aligned} N_1 &= -\frac{(1-\xi)(1-\eta)(1+\xi+\eta)}{4} \\ N_2 &= -\frac{(1+\xi)(1-\eta)(1-\xi+\eta)}{4} \\ N_3 &= -\frac{(1+\xi)(1+\eta)(1-\xi-\eta)}{4} \\ N_4 &= -\frac{(1-\xi)(1+\eta)(1+\xi-\eta)}{4} \end{aligned} \quad (7.52)$$

Now, we define N_5, N_6, N_7 , and N_8 at the midpoints. For N_5 , we know that it vanishes along edges $\xi = +1, \eta = +1$, and $\xi = -1$. Consequently, it has to be of the form

$$N_5 = c(1-\xi)(1-\eta)(1+\xi) \quad (7.53a)$$

$$= c(1-\xi^2)(1-\eta) \quad (7.53b)$$

The constant c in Eq. 7.53 is determined from the condition $N_5 = 1$ at node 5, or $N_5 = 1$ at $\xi = 0, \eta = -1$. Thus, $c = \frac{1}{2}$ and

$$N_5 = \frac{(1-\xi^2)(1-\eta)}{2} \quad (7.53c)$$

We have

$$\begin{aligned} N_5 &= \frac{(1-\xi^2)(1-\eta)}{2} \\ N_6 &= \frac{(1+\xi)(1-\eta^2)}{2} \\ N_7 &= \frac{(1-\xi^2)(1+\eta)}{2} \\ N_8 &= \frac{(1-\xi)(1-\eta^2)}{2} \end{aligned} \quad (7.54)$$

Six-Node Triangle

The six-node triangle is shown in Figs. 7.8a and b. By referring to the master element in Fig. 7.8b, we can write the shape functions as

$$\begin{aligned} N_1 &= \xi(2\xi - 1) & N_4 &= 4\xi\eta \\ N_2 &= \eta(2\eta - 1) & N_5 &= 4\xi\eta \\ N_3 &= \zeta(2\zeta - 1) & N_6 &= 4\xi\zeta \end{aligned} \quad (7.55)$$

where $\zeta = 1 - \xi - \eta$. Because of terms ξ^2, η^2 , etc. in the shape functions, this element is also called a *quadratic* triangle. The isoparametric representation is

$$\begin{aligned} \mathbf{u} &= \mathbf{Nq} \\ x &= \sum N_i x_i & y &= \sum N_i y_i \end{aligned} \quad (7.56)$$

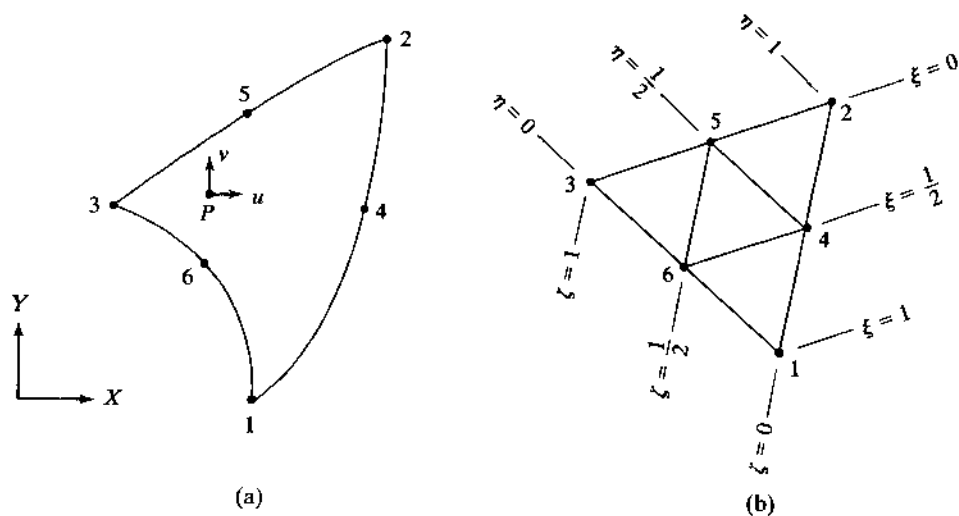


FIGURE 7.8 Six-node triangular element.

The element stiffness, which has to be integrated numerically, is given by

$$\mathbf{k}^e = t_e \int_A \int \mathbf{B}^T \mathbf{D} \mathbf{B} \det \mathbf{J} d\xi d\eta \quad (7.57)$$

The Gauss points for a triangular region differ from the square region considered earlier. The simplest is the one-point rule at the centroid with weight $w_1 = \frac{1}{2}$ and $\xi_1 = \eta_1 = \zeta_1 = \frac{1}{3}$. Equation 7.57 then yields

$$\mathbf{k}^e \approx \frac{1}{2} t_e \bar{\mathbf{B}}^T \bar{\mathbf{D}} \bar{\mathbf{B}} \det \bar{\mathbf{J}} \quad (7.58)$$

where $\bar{\mathbf{B}}$ and $\bar{\mathbf{J}}$ are evaluated at the Gauss point. Other choices of weights and Gauss points are given in Table 7.2. The Gauss points given in Table 7.2 are arranged symmetrically within the triangle. Because of triangular symmetry, the Gauss points occur in groups or *multiplicity* of one, three, or six. For multiplicity of three, if ξ -, η -, and

TABLE 7.2 Gauss Quadrature Formulas for a Triangle

$$\int_0^1 \int_0^{1-\xi} f(\xi, \eta) d\eta d\xi \approx \sum_{i=1}^n w_i f(\xi_i, \eta_i)$$

| No. of points, n | Weight, w_i | Multiplicity | ξ_i | η_i | ζ_i |
|-----------------------|------------------|--------------|---------------|---------------|---------------|
| One | $\frac{1}{2}$ | 1 | $\frac{1}{3}$ | $\frac{1}{3}$ | $\frac{1}{3}$ |
| Three | $\frac{1}{6}$ | 3 | $\frac{2}{3}$ | $\frac{1}{6}$ | $\frac{1}{6}$ |
| Three | $\frac{1}{6}$ | 3 | $\frac{1}{2}$ | $\frac{1}{2}$ | 0 |
| Four | $-\frac{9}{32}$ | 1 | $\frac{1}{3}$ | $\frac{1}{3}$ | $\frac{1}{3}$ |
| | $\frac{25}{96}$ | 3 | $\frac{3}{5}$ | $\frac{1}{5}$ | $\frac{1}{5}$ |
| Six | $\frac{1}{12}$ | 6 | 0.6590276223 | 0.2319333685 | 0.1090390090 |

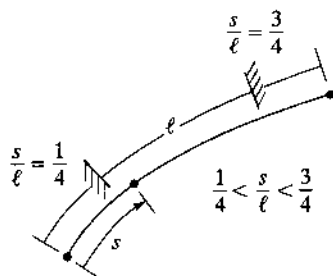


FIGURE 7.9 Restrictions on the location of a midside node.

ζ -coordinates of a Gauss point are, for instance, $(\frac{2}{3}, \frac{1}{6}, \frac{1}{6})$, then the other two Gauss points are located at $(\frac{1}{6}, \frac{2}{3}, \frac{1}{6})$ and $(\frac{1}{6}, \frac{1}{6}, \frac{2}{3})$. Note that $\zeta = 1 - \xi - \eta$, as is discussed in Chapter 5. For multiplicity of six, all six possible permutations of the ξ -, η -, and ζ -coordinates are used.

Comment on Midside Node In the higher order isoparametric elements discussed previously, we note the presence of midside nodes. The midside node should be as near as possible to the center of the side. The node should not be outside of $\frac{1}{4} < s/l < \frac{3}{4}$, as shown in Fig. 7.9. This condition ensures that $\det \mathbf{J}$ does not attain a value of zero in the element.

Comment on Temperature Effect Using the temperature strain defined in Eqs. 5.61 and 5.62 and following the derivation in Chapter 5, the nodal temperature load can be evaluated as

$$\theta^e = t_e \int_A \int \mathbf{B}^T \mathbf{D} \epsilon_0 dA = t_e \int_{-1}^1 \int_{-1}^1 \mathbf{B}^T \mathbf{D} \epsilon_0 |\det \mathbf{J}| d\xi d\eta \quad (7.59)$$

This integral is performed using numerical integration.

7.5 FOUR-NODE QUADRILATERAL FOR AXISYMMETRIC PROBLEMS

The stiffness development for the four node-quadrilateral for axisymmetric problems follows steps similar to the quadrilateral element presented earlier. The x -, y -coordinates are replaced by r , z . The main difference occurs in the development of the \mathbf{B} matrix, which relates the four strains to element nodal displacements. We partition the strain vector as

$$\boldsymbol{\epsilon} = \begin{bmatrix} \epsilon_r \\ \epsilon_z \\ \gamma_{rz} \\ \epsilon_\theta \end{bmatrix} = \begin{bmatrix} \bar{\boldsymbol{\epsilon}} \\ \epsilon_\theta \end{bmatrix} \quad (7.59)$$

where $\bar{\boldsymbol{\epsilon}} = [\epsilon_r \ \epsilon_z \ \gamma_{rz}]^T$.

Now in the relation $\boldsymbol{\epsilon} = \mathbf{B}\mathbf{q}$, we partition \mathbf{B} as $\mathbf{B} = \begin{bmatrix} \mathbf{B}_1 \\ \mathbf{B}_2 \end{bmatrix}$, such that \mathbf{B}_1 is a 3×8 matrix relating $\bar{\boldsymbol{\epsilon}}$ and \mathbf{q} by

$$\bar{\boldsymbol{\epsilon}} = \mathbf{B}_1 \mathbf{q} \quad (7.60)$$

and \mathbf{B}_2 is a row vector 1×8 relating ϵ_θ and \mathbf{q} by

$$\epsilon_\theta = \mathbf{B}_2 \mathbf{q} \quad (7.61)$$

Noting that r, z replace x, y , it is clear that \mathbf{B}_1 is same as the 3×8 matrix given in Eq. 7.24 for the four-node quadrilateral. Since $\epsilon_\theta = u/r$ and $u = N_1 q_1 + N_2 q_2 + N_3 q_3 + N_4 q_4$, \mathbf{B}_2 can be written as

$$\mathbf{B}_2 = \left[\frac{N_1}{r} \quad 0 \quad \frac{N_2}{r} \quad 0 \quad \frac{N_3}{r} \quad 0 \quad \frac{N_4}{r} \quad 0 \right] \quad (7.62)$$

On introducing these changes, the element stiffness is then obtained by performing numerical integration on

$$\mathbf{k}^e = 2\pi \int_{-1}^1 \int_{-1}^1 r \mathbf{B}^T \mathbf{D} \mathbf{B} \det \mathbf{J} d\xi d\eta \quad (7.63)$$

The force terms (in Eq. 7.31 and 7.32) are to be multiplied by the factor of 2π as in the axisymmetric triangle.

The axisymmetric quadrilateral element has been implemented in the program AXIQUAD.

7.6 CONJUGATE GRADIENT IMPLEMENTATION OF THE QUADRILATERAL ELEMENT

The ideas of the conjugate gradient method have been presented in Chapter 2. The equations are reproduced here using the notation for displacements, force and stiffness:

$$\begin{aligned} \mathbf{g}_0 &= \mathbf{K} \mathbf{Q}_0 - \mathbf{F}, & \mathbf{d}_0 &= -\mathbf{g}_0 \\ \alpha_k &= \frac{\mathbf{g}_k^T \mathbf{g}_k}{\mathbf{d}_k^T \mathbf{K} \mathbf{d}_k} \\ \mathbf{Q}_{k+1} &= \mathbf{Q}_k + \alpha_k \mathbf{d}_k \\ \mathbf{g}_{k+1} &= \mathbf{g}_k + \alpha_k \mathbf{K} \mathbf{d}_k \\ \beta_k &= \frac{\mathbf{g}_{k+1}^T \mathbf{g}_{k+1}}{\mathbf{g}_k^T \mathbf{g}_k} \\ \mathbf{d}_{k+1} &= -\mathbf{g}_{k+1} + \beta_k \mathbf{d}_k \end{aligned} \quad (7.64)$$

Here $k = 0, 1, 2, \dots$. The iterations are carried out until $\mathbf{g}_k^T \mathbf{g}_k$ reaches a small value.

We state here the steps in its implementation in finite element analysis. The main difference in this implementation is that the stiffness of each element is first generated and stored in a three-dimensional array. The stiffness of an element can be recalled from this array without recalculating for the iterations carried out. We start with the initial displacements at $\mathbf{Q}_0 = \mathbf{0}$. In the evaluation of \mathbf{g}_0 , the force modifications for the boundary conditions are implemented. The term $\mathbf{K} \mathbf{d}_k$ is evaluated by performing directly using element stiffness values by using $\sum_e \mathbf{k}^e \mathbf{d}_k^e$. The conjugate gradient approach is implemented in QUADCG.

Concluding Note

The concept of a master element defined in ξ -, η -coordinates, the definition of shape functions for interpolating displacement and geometry and use of numerical integration are all key ingredients of the isoparametric formulation. A wide variety of elements can be formulated in a unified manner. Though only stress analysis has been considered in this chapter, the elements can be applied to nonstructural problems quite readily.

Example 7.2

The problem in Example 5.8 (Fig. E5.8) is now solved using four-node quadrilateral elements using program QUAD. The loads, boundary conditions, and node locations are the same as in Fig. E5.8. The only difference is the modeling with 24 quadrilateral elements, as against 48 CST elements in Fig. E5.8. Again, MESHGEN has been used to create the mesh (Fig. E7.2a) and a text editor to define the loads, boundary conditions, and material properties.

The stresses output by program QUAD correspond to the $(0, 0)$ location in the natural coordinate system (master element). Using this fact, we *extrapolate* the y -stresses in elements 13, 14, and 15 to obtain the maximum y -stress near the semicircular edge of the plate, as shown in Fig. E7.2b. ■

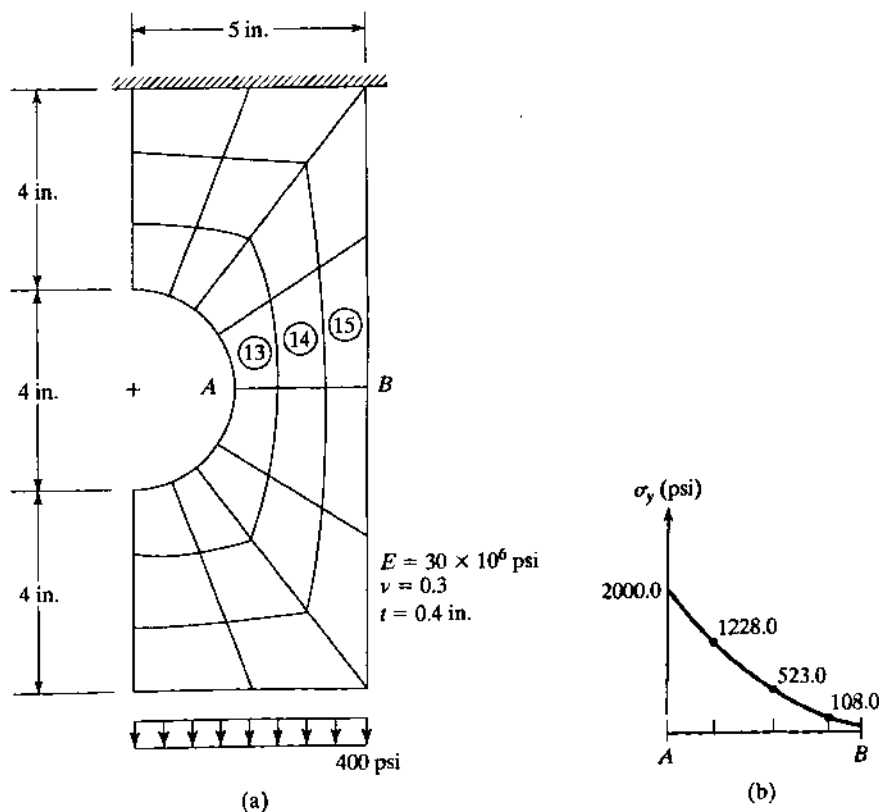


FIGURE E7.2

Input Data File

```

<< --- 2D STRESS ANALYSIS USING QUAD --- >>
PROBLEM 7.4
<< NN NE NM NDIM NEN NDN >>
9 4 1 2 4 2
<< ND NL NMPC >>
6 1 0
<< Node# Coordinates >>
1 0 0
2 0 15
3 0 30
4 30 0
5 30 15
6 30 30
7 60 0
8 60 15
9 60 30
<< Elem# Nodes Mat# Thickness TempRise >>
1 1 4 5 2 1 10 0
2 2 5 6 3 1 10 0
3 4 7 8 5 1 10 0
4 5 8 9 6 1 10 0
<< DOF# Displacement >>
1 0
2 0
3 0
4 0
5 0
6 0
<< DOF# Load >>
18 -10000
<< MAT# E Nu Alpha >>
1 70000 .33 12E-6
B1 i B2 j B3 (Multi-point constr. B1*Qi+B2*Qj=B3)

```

Program Quad - CHANDRUPATLA & BELEGUNDU**Output****PROBLEM 7.4****Plane Stress Analysis**

| NODE# | X-Displ | Y-Displ |
|-------|-------------|-------------|
| 1 | -8.8984E-07 | -2.8335E-07 |
| 2 | 1.7736E-08 | 1.5071E-07 |
| 3 | 8.7210E-07 | -3.0784E-07 |
| 4 | -8.8095E-02 | -1.3105E-01 |
| 5 | -1.2826E-03 | -1.2305E-01 |
| 6 | 8.7963E-02 | -1.2696E-01 |
| 7 | -1.1692E-01 | -3.6519E-01 |
| 8 | 3.5222E-04 | -3.7014E-01 |
| 9 | 1.2512E-01 | -3.8686E-01 |

| ELEM# | vonMises | Stresses at 4 | Integration points |
|-------|------------|---------------|-----------------------|
| 1 | 2.1336E+02 | 1.6028E+02 | 5.3779E+01 1.4114E+02 |
| 2 | 1.3696E+02 | 4.8529E+01 | 1.5995E+02 2.0832E+02 |
| 3 | 9.3736E+01 | 5.8816E+01 | 3.8024E+01 9.1475E+01 |
| 4 | 9.2307E+01 | 6.9321E+01 | 9.4183E+01 1.2010E+02 |

```

<< AXISYMMETRIC STRESS ANALYSIS >>
EXAMPLE 6.4
NN NE NM NDIM NEN NDN
 6  2  1  2    4  2
ND NL  NMPC
 3  6  0
Node#  X    Y    (r z coordinates)
 1     3    0
 2     3    .5
 3     7.5  0
 4     7.5  .5
 5     12   0
 6     12   .5
Elem#  N1  N2  N3  N4  Mat#  TempRise
 1     1  3  4  2  1  0
 2     3  5  6  4  1  0
DOF#  Displacement
 2     0
 6     0
10     0
DOF#  Load
 1    3449
 3    9580
 5   23380
 7   38711
 9   32580
11   18780
MAT#  PROP1  PROP2  PROP3
 1    30E6   .3    12E-6
B1  i  B2  j  B3 (Multi-point constr. B1*Qi+B2*Qj=B3)

```

```

Program AxiQuad - CHANDRUPATIA & BELEGUNDU
Output
EXAMPLE 6.4
NODE#  R-Displ    Z-Displ
 1  8.2970E-04  9.0276E-12
 2  8.2892E-04 -5.4296E-05
 3  8.8546E-04 -1.4325E-11
 4  8.8799E-04 -2.5290E-05
 5  9.0356E-04  5.2976E-12
 6  8.9886E-04 -1.6127E-05
ELEM#  vonMises  Stresses at 4 Integration points
 1  6.2713E+03  3.9595E+03  3.9642E+03  6.2701E+03
 2  3.0942E+03  2.3915E+03  2.3908E+03  3.1003E+03

```


PROBLEMS

- 7.1. Figure P7.1 shows a four-node quadrilateral. The (x, y) coordinates of each node are given in the figure. The element displacement vector \mathbf{q} is given as

$$\mathbf{q} = [0, 0, 0.20, 0, 0.15, 0.10, 0, 0.05]^T$$

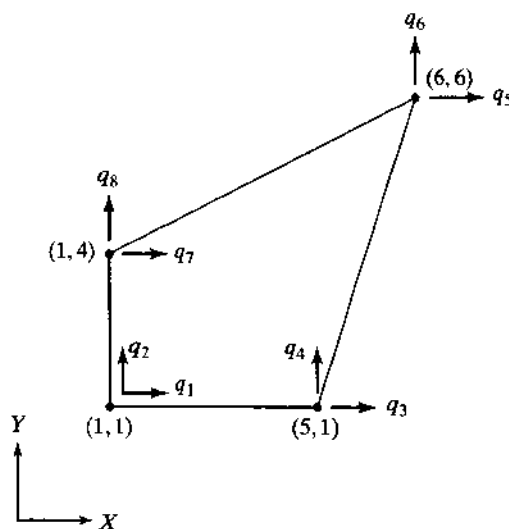


FIGURE P7.1

Find the following:

- the x, y -coordinates of a point P whose location in the master element is given by $\xi = 0.5$ and $\eta = 0.5$ and
 - the u, v displacements of the point P .
- 7.2. Using a 2×2 rule, evaluate the integral

$$\int_A \int (x^2 + xy^2) dx dy$$

by Gaussian quadrature, where A denotes the region shown in Fig. P7.1.

- 7.3. State whether the following statements are true or false:
- The shape functions are linear along an edge of a four-node quadrilateral element.
 - For isoparametric elements, such as four-, eight-, and nine-node quadrilaterals, the point $\xi = 0, \eta = 0$ in the master element corresponds to the centroid of the element in x - and y -coordinates.
 - The maximum stresses within an element occur at the Gauss points.
 - The integral of a cubic polynomial can be performed exactly using two-point Gauss quadrature.
- 7.4. Solve Problem P5.15 with four-node quadrilaterals. Use program QUAD.
- 7.5. A half-symmetry model of a culvert is shown in Fig. P7.5. The pavement load is a uniformly distributed load of 5000 N/m^2 . Using the MESHGEN program (discussed in Chapter 12), develop a finite element mesh with four-node quadrilateral elements. Using program QUAD determine the location and magnitude of maximum principal stress. First, try a mesh with about six elements and then compare results using about 18 elements.

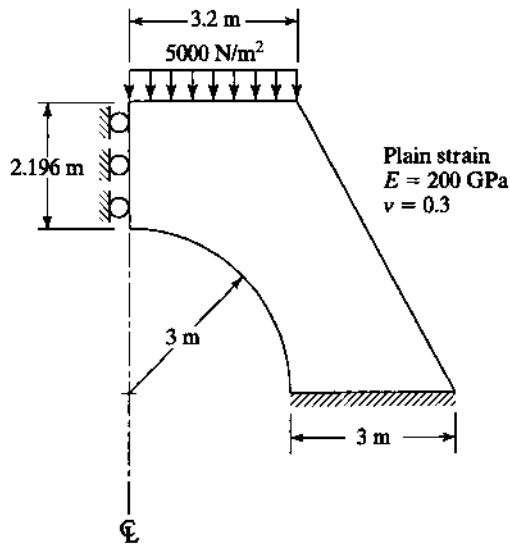


FIGURE P7.5

- 7.6. Solve Problem P5.16 using four-node quadrilateral elements (program QUAD). Compare your results with the solution obtained with CST elements. Use comparable-size meshes.
- 7.7. Solve Problem P5.17 using four-node quadrilaterals (program QUAD).
- 7.8. Solve Problem P5.20 using four-node quadrilaterals (program QUAD).
- 7.9. Develop a program for axisymmetric stress analysis with four-node quadrilateral elements. Use your program to solve Example 6.1. Compare results. [Hint: The first three rows of the **B** matrix are the same as for the plane stress problem in Eq. 7.25, and the last row can be obtained from $\epsilon_\theta = u/r$.]
- 7.10. This problem focuses on a concept used in the MESHGEN program discussed in Chapter 12. An eight-node region is shown in Fig. P7.10a. The corresponding master element or block is shown in Fig. P7.10b. The block is divided into a grid of $3 \times 3 = 9$ smaller blocks of equal size, as indicated by dotted lines. Determine the corresponding x - and y -coordinates of all the 16 nodal points, and plot the 9 subregions in Fig. P7.10a. Use the shape functions given in Eqs. 7.52 and 7.54.

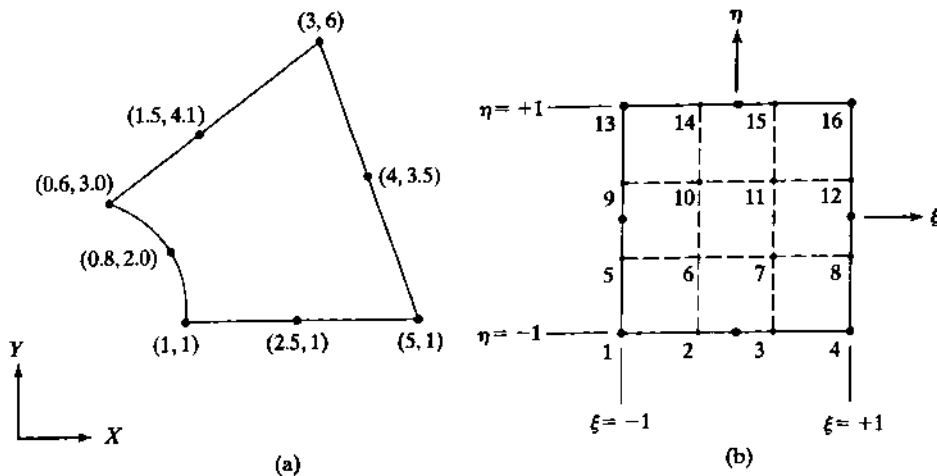


FIGURE P7.10

- 7.11. Develop a computer program for the eight-node quadrilateral. Analyze the cantilever beam shown in Fig. P7.11 with three finite elements. Compare results of x stress and center-line deflections with
- the six-element CST model and
 - elementary beam theory.

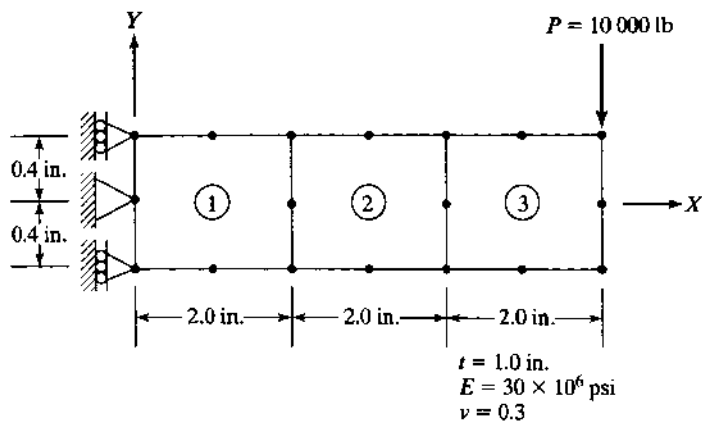


FIGURE P7.11

- 7.12. Solve Problem 6.16 using axisymmetric quadrilateral elements (Program AXIQUAD).

Program Listings

```

*****      PROGRAM QUAD      *****
*      2-D STRESS ANALYSIS USING 4-NODE      *
*      QUADRILATERAL ELEMENTS WITH TEMPERATURE      *
*      T.R.Chandrupatla and A.D.Belegundu      *
*****
'===== MAIN PROGRAM =====
Private Sub cmdStart_Click()
    Call InputData
    Call Bandwidth
    Call Stiffness
    Call ModifyForBC
    Call BandSolver
    Call StressCalc
    Call ReactionCalc
    Call Output
    cmdView.Enabled = True
    cmdStart.Enabled = False
End Sub
'=====

```

```

'===== ELEMENT STIFFNESS AND ASSEMBLY =====
Private Sub Stiffness()
    ReDim S(NQ, NBW)
    '----- Global Stiffness Matrix -----
    Call IntegPoints
    For N = 1 To NE
        picBox.Print "Forming Stiffness Matrix of Element "; N
        Call DMatrix(N)
        Call ElemStiffness(N)
        picBox.Print ".... Placing in Global Locations"
        Call PlaceGlobal(N)
    Next N
End Sub

```

```

'===== STRESS CALCULATIONS =====
Private Sub StressCalc()
    ReDim vonMisesStress(NE, 4), maxShearStress(NE, 4)
    '----- Stress Calculations
    For N = 1 To NE
        Call DMatrix(N)
        For IP = 1 To 4
            Call DbMat(N, 2, IP) '--- Get DB Matrix with Stress calculation
            '--- Von Mises Stress at Integration Point
            C = 0: If LC = 2 Then C = PNU * (STR(1) + STR(2))
            C1 = (STR(1) - STR(2)) ^ 2 + (STR(2) - C) ^ 2 + (C - STR(1)) ^ 2
            SV = Sqr(0.5 * C1 + 3 * STR(3) ^ 2)
            '--- Maximum Shear Stress R
            R = Sqr(0.25 * (STR(1) - STR(2)) ^ 2 + (STR(3)) ^ 2)
            maxShearStress(N, IP) = R
            vonMisesStress(N, IP) = SV
        Next IP
    Next N
End Sub

```

```

===== INTEGRATION POINTS =====
Private Sub IntegPoints()
'----- Integration Points XNI() -----
  C = 0.57735026919
  XNI(1, 1) = -C: XNI(1, 2) = -C
  XNI(2, 1) = C: XNI(2, 2) = -C
  XNI(3, 1) = C: XNI(3, 2) = C
  XNI(4, 1) = -C: XNI(4, 2) = C
End Sub
=====

```

```

===== D-MATRIX =====
Private Sub DMatrix(N)
'----- D() Matrix -----
  '--- Material Properties
  MATN = MAT(N)
  E = PM(MATN, 1): PNU = PM(MATN, 2)
  AL = PM(MATN, 3)
  '--- D() Matrix
  If LC = 1 Then
    '--- Plane Stress
    C1 = E / (1 - PNU ^ 2): C2 = C1 * PNU
  Else
    '--- Plane Strain
    C = E / ((1 + PNU) * (1 - 2 * PNU))
    C1 = C * (1 - PNU): C2 = C * PNU
  End If
  C3 = 0.5 * E / (1 + PNU)
  D(1, 1) = C1: D(1, 2) = C2: D(1, 3) = 0
  D(2, 1) = C2: D(2, 2) = C1: D(2, 3) = 0
  D(3, 1) = 0: D(3, 2) = 0: D(3, 3) = C3
End Sub
=====

```

```

===== ELEMENT STIFFNESS MATRIX =====
Private Sub ElemStiffness(N)
'----- Element Stiffness and Temperature Load -----
  For I = 1 To 8: For J = 1 To 8: SE(I, J) = 0: Next J: TL(I) = 0: Next I
  DTE = DT(N)
  '--- Weight Factor is ONE
  '--- Loop on Integration Points
  For IP = 1 To 4
    '--- Get DB Matrix at Integration Point IP
    Call DbMat(N, 1, IP)
    '--- Element Stiffness Matrix SE
    For I = 1 To 8
      For J = 1 To 8
        C = 0
        For K = 1 To 3

```

continued

```

      C = C + B(K, I) * DB(K, J) * DJ * TH(N)
    Next K
    SE(I, J) = SE(I, J) + C
  Next J
Next I
'--- Determine Temperature Load TL
AL = PM(MAT(N), 3)
C = AL * DTE: If LC = 2 Then C = (1 + PNU) * C
For I = 1 To 8
  TL(I) = TL(I) + TH(N) * DJ * C * (DB(1, I) + DB(2, I))
Next I
Next IP
End Sub
=====

```

```

===== B AND DB MATRICES FOR BTDB =====
Private Sub DbMat(N, ISTR, IP)
'----- DB() MATRIX -----
  XI = XNI(IP, 1): ETA = XNI(IP, 2)
  '--- Nodal Coordinates
  THICK = TH(N)
  N1 = NOC(N, 1): N2 = NOC(N, 2)
  N3 = NOC(N, 3): N4 = NOC(N, 4)
  X1 = X(N1, 1): Y1 = X(N1, 2): X2 = X(N2, 1): Y2 = X(N2, 2)
  X3 = X(N3, 1): Y3 = X(N3, 2): X4 = X(N4, 1): Y4 = X(N4, 2)
  '--- Formation of Jacobian TJ
  TJ11 = ((1 - ETA) * (X2 - X1) + (1 + ETA) * (X3 - X4)) / 4
  TJ12 = ((1 - ETA) * (Y2 - Y1) + (1 + ETA) * (Y3 - Y4)) / 4
  TJ21 = ((1 - XI) * (X4 - X1) + (1 + XI) * (X3 - X2)) / 4
  TJ22 = ((1 - XI) * (Y4 - Y1) + (1 + XI) * (Y3 - Y2)) / 4
  '--- Determinant of the JACOBIAN
  DJ = TJ11 * TJ22 - TJ12 * TJ21
  '--- A(3,4) Matrix relates Strains to Local Derivatives of u
  A(1, 1) = TJ22 / DJ: A(2, 1) = 0: A(3, 1) = -TJ21 / DJ
  A(1, 2) = -TJ12 / DJ: A(2, 2) = 0: A(3, 2) = TJ11 / DJ
  A(1, 3) = 0: A(2, 3) = -TJ21 / DJ: A(3, 3) = TJ22 / DJ
  A(1, 4) = 0: A(2, 4) = TJ11 / DJ: A(3, 4) = -TJ12 / DJ
  '--- G(4,8) Matrix relates Local Derivatives of u
  '--- to Local Nodal Displacements q(8)
  For I = 1 To 4: For J = 1 To 8
    G(I, J) = 0: Next J: Next I
  G(1, 1) = -(1 - ETA) / 4: G(2, 1) = -(1 - XI) / 4
  G(3, 2) = -(1 - ETA) / 4: G(4, 2) = -(1 - XI) / 4
  G(1, 3) = (1 - ETA) / 4: G(2, 3) = -(1 + XI) / 4
  G(3, 4) = (1 - ETA) / 4: G(4, 4) = -(1 + XI) / 4
  G(1, 5) = (1 + ETA) / 4: G(2, 5) = (1 + XI) / 4
  G(3, 6) = (1 + ETA) / 4: G(4, 6) = (1 + XI) / 4
  G(1, 7) = -(1 + ETA) / 4: G(2, 7) = (1 - XI) / 4
  G(3, 8) = -(1 + ETA) / 4: G(4, 8) = (1 - XI) / 4

```

continued

```

'--- B(3,8) Matrix Relates Strains to q
For I = 1 To 3
  For J = 1 To 8
    C = 0
    For K = 1 To 4
      C = C + A(I, K) * G(K, J)
    Next K
    B(I, J) = C
  Next J
Next I
'--- DB(3,8) Matrix relates Stresses to q(8)
For I = 1 To 3
  For J = 1 To 8
    C = 0
    For K = 1 To 3
      C = C + D(I, K) * B(K, J)
    Next K:
    DB(I, J) = C
  Next J
Next I
If ISTR = 2 Then
  '--- Stress Evaluation
  For I = 1 To NEN
    IIN = NDN * (NOC(N, I) - 1)
    II = NDN * (I - 1)
    For J = 1 To NDN
      Q(II + J) = F(IIN + J)
    Next J
  Next I
  AL = PM(MAT(N), 3)
  C1 = AL * DT(N): If LC = 2 Then C1 = C1 * (1 + PNU)
  For I = 1 To 3
    C = 0
    For K = 1 To 8
      C = C + DB(I, K) * Q(K)
    Next K
    STR(I) = C - C1 * (D(I, 1) + D(I, 2))
  Next I
End If
End Sub
=====

```

Beams and Frames

8.1 INTRODUCTION

Beams are slender members that are used for supporting transverse loading. Long horizontal members used in buildings and bridges, and shafts supported in bearings are some examples of beams. Complex structures with rigidly connected members are called frames and may be found in automobile and aeroplane structures and motion- and force-transmitting machines and mechanisms. In this chapter, we first present the finite element formulation for beams and extend these ideas to formulate and solve two-dimensional frame problems.

Beams with cross sections that are symmetric with respect to plane of loading are considered here. A general horizontal beam is shown in Fig. 8.1. Figure 8.2 shows the cross section and the bending stress distribution. For small deflections, we recall from elementary beam theory that

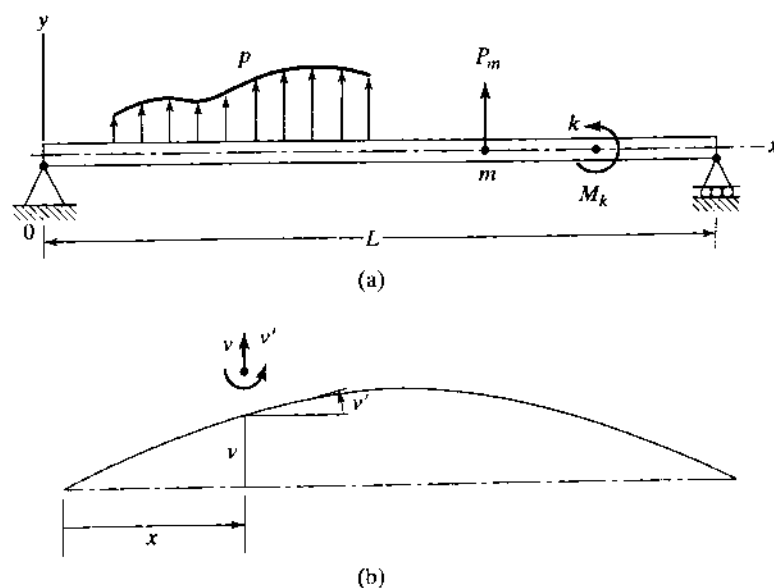


FIGURE 8.1 (a) Beam loading and (b) deformation of the neutral axis.

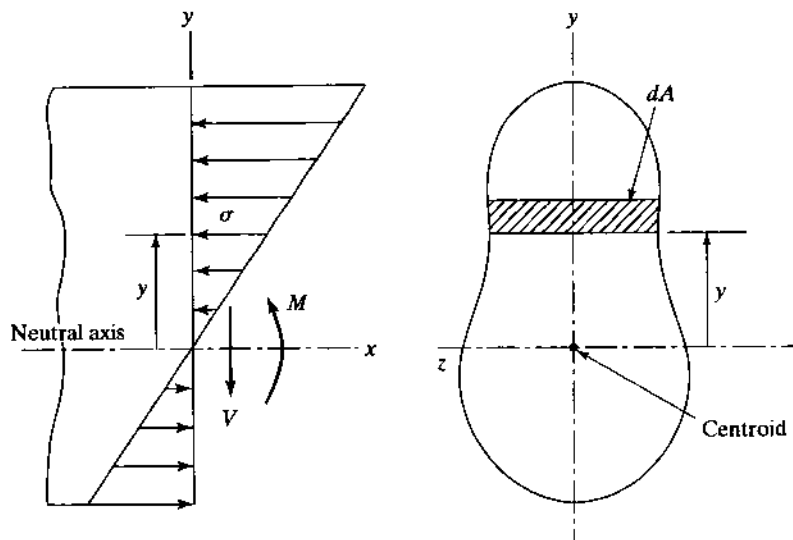


FIGURE 8.2 Beam section and stress distribution.

$$\sigma = -\frac{M}{I}y \quad (8.1)$$

$$\epsilon = \frac{\sigma}{E} \quad (8.2)$$

$$\frac{d^2v}{dx^2} = \frac{M}{EI} \quad (8.3)$$

where σ is the normal stress, ϵ is the normal strain, M is the bending moment at the section, v is the deflection of the centroidal axis at x , and I is the moment of inertia of the section about the neutral axis (z -axis passing through the centroid).

Potential-Energy Approach

The strain energy in an element of length dx is

$$\begin{aligned} dU &= \frac{1}{2} \int_A \sigma \epsilon \, dA \, dx \\ &= \frac{1}{2} \left(\frac{M^2}{EI^2} \int_A y^2 \, dA \right) dx \end{aligned}$$

Noting that $\int_A y^2 \, dA$ is the moment of inertia I , we have

$$dU = \frac{1}{2} \frac{M^2}{EI} dx \quad (8.4)$$

When Eq. 8.3 is used, the total strain energy in the beam is given by

$$U = \frac{1}{2} \int_0^L EI \left(\frac{d^2 v}{dx^2} \right)^2 dx \quad (8.5)$$

The potential energy of the beam is then given by

$$\Pi = \frac{1}{2} \int_0^L EI \left(\frac{d^2 v}{dx^2} \right)^2 dx - \int_0^L p v dx - \sum_m P_m v_m - \sum_k M_k v'_k \quad (8.6)$$

where p is the distributed load per unit length, P_m is the point load at point m , M_k is the moment of the couple applied at point k , v_m is the deflection at point m , and v'_k is the slope at point k .

Galerkin Approach

For the Galerkin formulation, we start from equilibrium of an elemental length. From Fig. 8.3, we recall that

$$\frac{dV}{dx} = p \quad (8.7)$$

$$\frac{dM}{dx} = V \quad (8.8)$$

When Eqs. 8.3, 8.7, and 8.8 are combined, the equilibrium equation is given by

$$\frac{d^2}{dx^2} \left(EI \frac{d^2 v}{dx^2} \right) - p = 0 \quad (8.9)$$

For approximate solution by the Galerkin approach, we look for the approximate solution v constructed of finite element shape functions such that

$$\int_0^L \left[\frac{d}{dx^2} \left(EI \frac{d^2 v}{dx^2} \right) - p \right] \phi dx = 0 \quad (8.10)$$

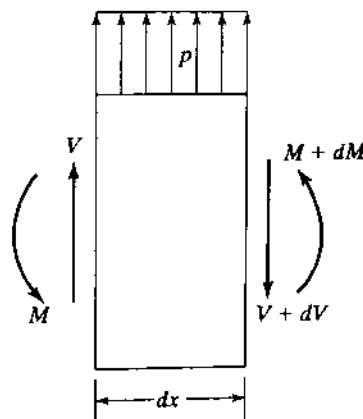


FIGURE 8.3 Free body diagram of an elemental length dx .

where ϕ is an arbitrary function using same basis functions as v . Note that ϕ is zero where v has a specified value. We integrate the first term of Eq. 8.10 by parts. The integral from 0 to L is split into intervals 0 to x_m , x_m to x_k , and x_k to L . We obtain

$$\int_0^L EI \frac{d^2 v}{dx^2} \frac{d^2 \phi}{dx^2} dx - \int_0^L p \phi dx + \frac{d}{dx} \left(EI \frac{d^2 v}{dx^2} \right) \phi \Big|_0^{x_m} + \frac{d}{dx} \left(EI \frac{d^2 v}{dx^2} \right) \phi \Big|_{x_m}^L - EI \frac{d^2 v}{dx^2} \frac{d\phi}{dx} \Big|_0^{x_k} - EI \frac{d^2 v}{dx^2} \frac{d\phi}{dx} \Big|_{x_k}^L = 0 \quad (8.11)$$

We note that $EI(d^2v/dx^2)$ equals the bending moment M from Eq. 8.3 and $(d/dx)[EI(d^2v/dx^2)]$ equals the shear force V from (8.8). Also, ϕ and M are zero at the supports. At x_m , the jump in shear force is P_m and at x_k , the jump in bending moment is $-M_k$. Thus, we get

$$\int_0^L EI \frac{d^2 v}{dx^2} \frac{d^2 \phi}{dx^2} dx - \int_0^L p \phi dx - \sum_m P_m \phi_m - \sum_k M_k \phi'_k = 0 \quad (8.12)$$

For the finite element formulation based on Galerkin's approach, v and ϕ are constructed using the same shape functions. Equation 8.12 is precisely the statement of the principle of virtual work.

8.2 FINITE ELEMENT FORMULATION

The beam is divided into elements, as shown in Fig. 8.4. Each node has two degrees of freedom. Typically, the degrees of freedom of node i are Q_{2i-1} and Q_{2i} . The degree of freedom Q_{2i-1} is transverse displacement and Q_{2i} is slope or rotation. The vector

$$\mathbf{Q} = [Q_1, Q_2, \dots, Q_{10}]^T \quad (8.13)$$

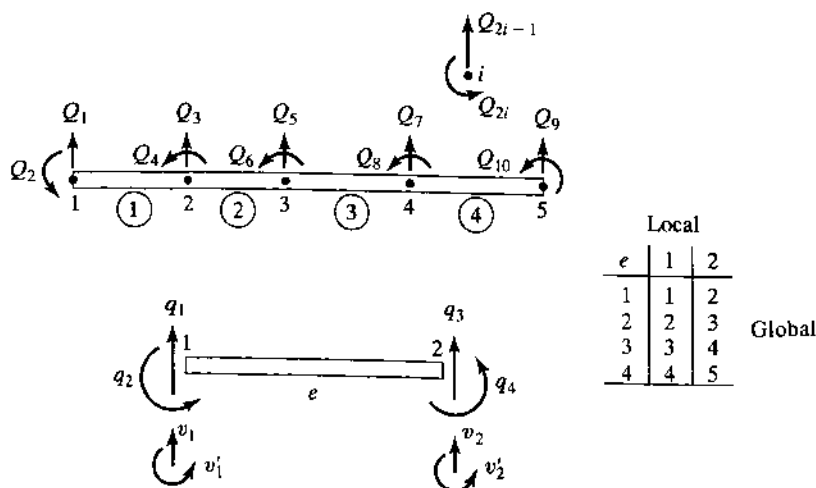


FIGURE 8.4 Finite element discretization.

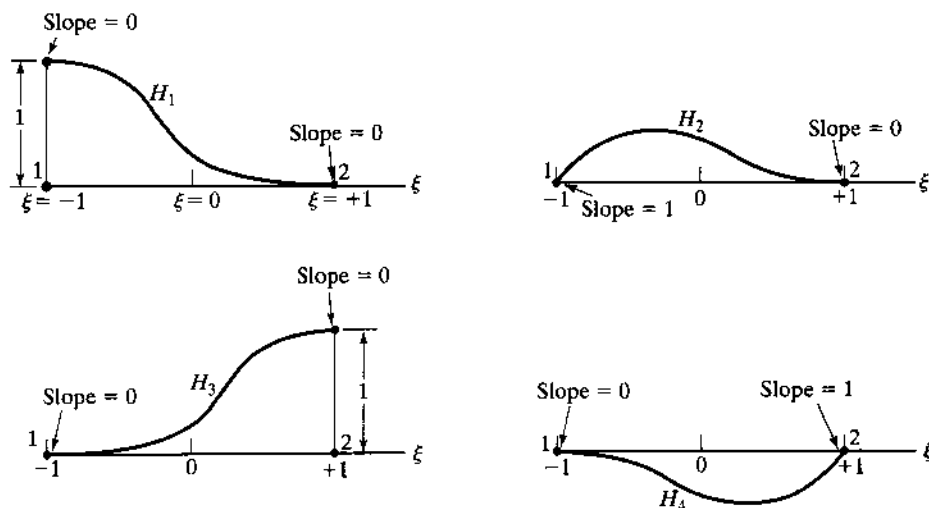


FIGURE 8.5 Hermite shape functions.

represents the global displacement vector. For a single element, the local degrees of freedom are represented by

$$\mathbf{q} = [q_1, q_2, q_3, q_4]^T \quad (8.14)$$

The local-global correspondence is easy to see from the table given in Fig. 8.4. \mathbf{q} is same as $[v_1, v'_1, v_2, v'_2]^T$. The shape functions for interpolating v on an element are defined in terms of ξ on -1 to $+1$, as shown in Fig. 8.5. *The shape functions for beam elements differ from those discussed earlier.* Since nodal values and nodal slopes are involved, we define Hermite shape functions, which satisfy nodal value and slope continuity requirements. Each of the shape functions is of cubic order represented by

$$H_i = a_i + b_i \xi + c_i \xi^2 + d_i \xi^3, \quad i = 1, 2, 3, 4 \quad (8.15)$$

The conditions given in the following table must be satisfied:

| | H_1 | H'_1 | H_2 | H'_2 | H_3 | H'_3 | H_4 | H'_4 |
|------------|-------|--------|-------|--------|-------|--------|-------|--------|
| $\xi = -1$ | 1 | 0 | 0 | 1 | 0 | 0 | 0 | 0 |
| $\xi = 1$ | 0 | 0 | 0 | 0 | 1 | 0 | 0 | 1 |

The coefficients a_i , b_i , c_i , and d_i can be easily obtained by imposing these conditions. Thus.

$$\begin{aligned} H_1 &= \frac{1}{4}(1 - \xi)^2(2 + \xi) \quad \text{or} \quad \frac{1}{4}(2 - 3\xi + \xi^3) \\ H_2 &= \frac{1}{4}(1 - \xi)^2(\xi + 1) \quad \text{or} \quad \frac{1}{4}(1 - \xi - \xi^2 + \xi^3) \\ H_3 &= \frac{1}{4}(1 + \xi)^2(2 - \xi) \quad \text{or} \quad \frac{1}{4}(2 + 3\xi - \xi^3) \\ H_4 &= \frac{1}{4}(1 + \xi)^2(\xi - 1) \quad \text{or} \quad \frac{1}{4}(-1 - \xi + \xi^2 + \xi^3) \end{aligned} \quad (8.16)$$

The Hermite shape functions can be used to write v in the form

$$v(\xi) = H_1 v_1 + H_2 \left(\frac{dv}{d\xi} \right)_1 + H_3 v_2 + H_4 \left(\frac{dv}{d\xi} \right)_2 \quad (8.17)$$

The coordinates transform by the relationship

$$\begin{aligned} x &= \frac{1 - \xi}{2} x_1 + \frac{1 + \xi}{2} x_2 \\ &= \frac{x_1 + x_2}{2} + \frac{x_2 - x_1}{2} \xi \end{aligned} \quad (8.18)$$

Since $\ell_e = x_2 - x_1$ is the length of the element, we have

$$dx = \frac{\ell_e}{2} d\xi \quad (8.19)$$

The chain rule $dv/d\xi = (dv/dx)(dx/d\xi)$ gives us

$$\frac{dv}{d\xi} = \frac{\ell_e}{2} \frac{dv}{dx} \quad (8.20)$$

Noting that dv/dx evaluated at nodes 1 and 2 is q_2 and q_4 , respectively, we have

$$v(\xi) = H_1 q_1 + \frac{\ell_e}{2} H_2 q_2 + H_3 q_3 + \frac{\ell_e}{2} H_4 q_4 \quad (8.21)$$

which may be denoted as

$$v = \mathbf{H}\mathbf{q} \quad (8.22)$$

where

$$\mathbf{H} = \left[H_1, \frac{\ell_e}{2} H_2, H_3, \frac{\ell_e}{2} H_4 \right] \quad (8.23)$$

In the total potential energy of the system, we consider the integrals as summations over the integrals over the elements. The element strain energy is given by

$$U_e = \frac{1}{2} EI \int_e \left(\frac{d^2 v}{dx^2} \right)^2 dx \quad (8.24)$$

From Eq. 8.20,

$$\frac{dv}{dx} = \frac{2}{\ell_e} \frac{dv}{d\xi} \quad \text{and} \quad \frac{d^2 v}{dx^2} = \frac{4}{\ell_e^2} \frac{d^2 v}{d\xi^2}$$

Then, substituting $v = \mathbf{H}\mathbf{q}$, we obtain

$$\left(\frac{d^2 v}{dx^2} \right)^2 = \mathbf{q}^T \frac{16}{\ell_e^4} \left(\frac{d^2 \mathbf{H}}{d\xi^2} \right)^T \left(\frac{d^2 \mathbf{H}}{d\xi^2} \right) \mathbf{q} \quad (8.25)$$

$$\left(\frac{d^2 \mathbf{H}}{d\xi^2} \right) = \left[\frac{3}{2} \xi, \frac{-1 + 3\xi}{2} \frac{\ell_e}{2}, -\frac{3}{2} \xi, \frac{1 + 3\xi}{2} \frac{\ell_e}{2} \right] \quad (8.26)$$

On substituting $dx = (\ell_e/2) d\xi$ and Eqs. 8.25 and 8.26 in Eq. 8.24, we get

$$U_e = \frac{1}{2} \mathbf{q}^T \frac{8EI}{\ell_e^3} \int_{-1}^{+1} \begin{bmatrix} \frac{9}{4} \xi^2 & \frac{3}{8} \xi(-1+3\xi)\ell_e & -\frac{9}{4} \xi^2 & \frac{3}{8} \xi(1+3\xi)\ell_e \\ \left(\frac{-1+3\xi}{4}\right)^2 \ell_e^2 & -\frac{3}{8} \xi(-1+3\xi)\ell_e & \frac{-1+9\xi^2}{16} \ell_e^2 & \\ \text{Symmetric} & \frac{9}{4} \xi^2 & -\frac{3}{8} \xi(1+3\xi)\ell_e & \\ & & \left(\frac{1+3\xi}{4}\right)^2 \ell_e^2 & \end{bmatrix} d\xi \mathbf{q} \quad (8.27)$$

Each term in the matrix needs to be integrated. Note that

$$\int_{-1}^{+1} \xi^2 d\xi = \frac{2}{3} \quad \int_{-1}^{+1} \xi d\xi = 0 \quad \int_{-1}^{+1} d\xi = 2$$

This results in the element strain energy given by

$$U_e = \frac{1}{2} \mathbf{q}^T \mathbf{k}^e \mathbf{q} \quad (8.28)$$

where the element stiffness matrix is

$$\mathbf{k}^e = \frac{EI}{\ell_e^3} \begin{bmatrix} 12 & 6\ell_e & -12 & 6\ell_e \\ 6\ell_e & 4\ell_e^2 & -6\ell_e & 2\ell_e^2 \\ -12 & -6\ell_e & 12 & -6\ell_e \\ 6\ell_e & 2\ell_e^2 & -6\ell_e & 4\ell_e^2 \end{bmatrix} \quad (8.29)$$

which is symmetric.

In the development based on Galerkin's approach (see Eq. 8.12), we note that

$$EI \frac{d^2 \phi}{dx^2} \frac{d^2 v}{dx^2} = \boldsymbol{\psi}^T EI \frac{16}{\ell_e^4} \left(\frac{d^2 \mathbf{H}}{d\xi^2} \right)^T \left(\frac{d^2 \mathbf{H}}{d\xi^2} \right) \mathbf{q} \quad (8.30)$$

where

$$\boldsymbol{\psi} = [\psi_1 \quad \psi_2 \quad \psi_3 \quad \psi_4]^T \quad (8.31)$$

is the set of generalized virtual displacements on the element, $v = \mathbf{H}\mathbf{q}$, and $\phi = \mathbf{H}\boldsymbol{\psi}$. Equation 8.30 yields the same element stiffness as Eq. 8.28 on integration, with $\boldsymbol{\psi}^T \mathbf{k}^e \mathbf{q}$ being the internal virtual work in an element.

8.3 LOAD VECTOR

The load contributions from the distributed load p in the element is first considered. We assume that the distributed load is uniform over the element:

$$\int_{\ell_e} p v dx = \left(\frac{p\ell_e}{2} \int_{-1}^{+1} \mathbf{H} d\xi \right) \mathbf{q} \quad (8.32)$$

On substituting for \mathbf{H} from Eqs. 8.16 and 8.23 and integrating, we obtain

$$\int_{\ell_e} p v dx = \mathbf{f}^e \mathbf{q} \quad (8.33)$$

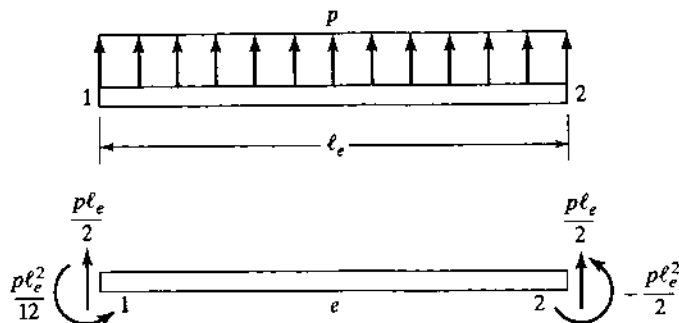


FIGURE 8.6 Distributed load on an element.

where

$$\mathbf{f}^e = \left[\frac{p\ell_e}{2}, \frac{p\ell_e^2}{12}, \frac{p\ell_e}{2}, -\frac{p\ell_e^2}{12} \right]^T \quad (8.34)$$

This equivalent load on an element is shown in Fig. 8.6. The same result is obtained by considering the term $\int_e p\phi dx$ in Eq. 8.12 for the Galerkin formulation. The point loads P_m and M_k are readily taken care of by introducing nodes at the points of application. On introducing the local-global correspondence, from the potential-energy approach, we get

$$\Pi = \frac{1}{2} \mathbf{Q}^T \mathbf{K} \mathbf{Q} - \mathbf{Q}^T \mathbf{F} \quad (8.35)$$

and from Galerkin's approach, we get

$$\Psi^T \mathbf{K} \mathbf{Q} - \Psi^T \mathbf{F} = 0 \quad (8.36)$$

where Ψ = arbitrary admissible global virtual displacement vector.

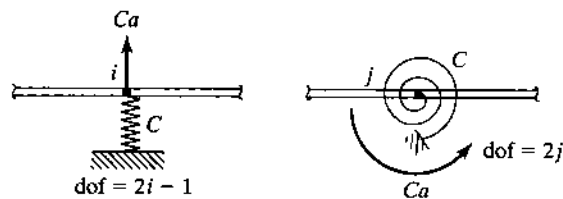
8.4 BOUNDARY CONSIDERATIONS

When the generalized displacement value is specified as a for the degree of freedom (dof) r , we follow the penalty approach and add $\frac{1}{2}C(Q_r - a)^2$ to Π and $\Psi_r C(Q_r - a)$ to the left side of the Galerkin formulation and place no restrictions on the degrees of freedom. The number C represents stiffness and is large in comparison with beam stiffness terms. This amounts to adding stiffness C to K_{rr} and load Ca to F_r (see Fig. 8.7). Both Eqs. 8.35 and 8.36 independently yield

$$\mathbf{K} \mathbf{Q} = \mathbf{F} \quad (8.37)$$

These equations are now solved to get the nodal displacements.

Reactions at constrained degrees of freedom may be calculated using Eq. 3.71 or 3.75.



a = known generalized displacement

FIGURE 8.7 Boundary conditions for a beam.

8.5 SHEAR FORCE AND BENDING MOMENT

Using the bending moment and shear force equations

$$M = EI \frac{d^2v}{dx^2} \quad V = \frac{dM}{dx} \quad \text{and} \quad v = \mathbf{Hq}$$

we get the element bending moment and shear force:

$$M = \frac{EI}{\ell_e^2} [6\xi q_1 + (3\xi - 1)\ell_e q_2 - 6\xi q_3 + (3\xi + 1)\ell_e q_4] \quad (8.38)$$

$$V = \frac{6EI}{\ell_e^3} (2q_1 + \ell_e q_2 - 2q_3 + \ell_e q_4) \quad (8.39)$$

These bending moment and shear force values are for the loading as modeled using equivalent point loads. Denoting element end equilibrium loads as R_1 , R_2 , R_3 , and R_4 , we note that

$$\begin{Bmatrix} R_1 \\ R_2 \\ R_3 \\ R_4 \end{Bmatrix} = \frac{EI}{\ell_e^3} \begin{bmatrix} 12 & 6\ell_e & -12 & 6\ell_e \\ 6\ell_e & 4\ell_e^2 & -6\ell_e & 2\ell_e^2 \\ -12 & -6\ell_e & 12 & -6\ell_e \\ 6\ell_e & 2\ell_e^2 & -6\ell_e & 4\ell_e^2 \end{bmatrix} \begin{Bmatrix} q_1 \\ q_2 \\ q_3 \\ q_4 \end{Bmatrix} + \begin{Bmatrix} \frac{-p\ell_e}{2} \\ \frac{-p\ell_e^2}{12} \\ \frac{-p\ell_e}{2} \\ \frac{p\ell_e^2}{12} \end{Bmatrix} \quad (8.40)$$

It is easily seen that the first term on the right is $\mathbf{k}^e \mathbf{q}$. Also note that the second term needs to be added only on elements with distributed load. In books on matrix structural analysis, the previous equations are written directly from element equilibrium. Also, the last vector on the right side of the equation consists of terms that are called *fixed-end reactions*. The shear forces at the two ends of the element are $V_1 = R_1$ and $V_2 = -R_3$. The end bending moments are $M_1 = -R_2$ and $M_2 = R_4$.

Example 8.1

For the beam and loading shown in Fig. E8.1, determine (1) the slopes at 2 and 3 and (2) the vertical deflection at the midpoint of the distributed load.

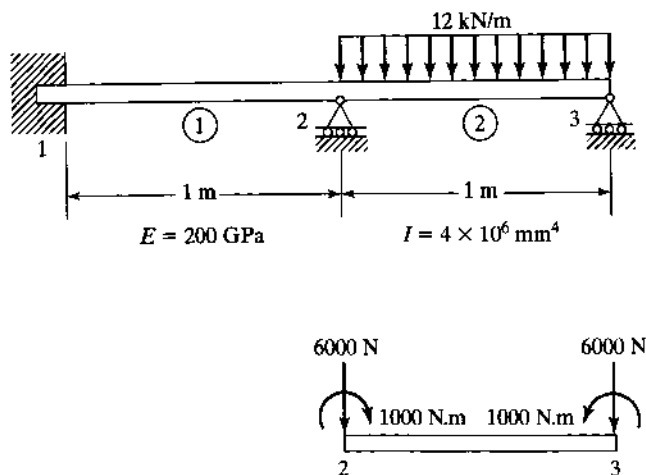


FIGURE E8.1

Solution We consider the two elements formed by the three nodes. Displacements Q_1 , Q_2 , Q_3 , and Q_5 are constrained to be zero, and Q_4 and Q_6 need to be found. Since the lengths and sections are equal, the element matrices are calculated from Eq. 8.29 as follows:

$$\frac{EI}{\ell^3} = \frac{(200 \times 10^9)(4 \times 10^{-6})}{1^3} = 8 \times 10^5 \text{ N/m}$$

$$\mathbf{k}^1 = \mathbf{k}^2 = 8 \times 10^5 \begin{bmatrix} 12 & 6 & -12 & 6 \\ 6 & 4 & -6 & 2 \\ -12 & -6 & 12 & -6 \\ 6 & 2 & -6 & 4 \end{bmatrix}$$

$$e = 1 \quad \begin{matrix} Q_1 & Q_2 & Q_3 & Q_4 \end{matrix}$$

$$e = 2 \quad \begin{matrix} Q_3 & Q_4 & Q_5 & Q_6 \end{matrix}$$

We note that global applied loads are $F_4 = -1000 \text{ N}\cdot\text{m}$ and $F_6 = +1000 \text{ N}\cdot\text{m}$ obtained from $p\ell^2/12$, as seen in Fig. 8.6. We use here the elimination approach presented in Chapter 3. Using the connectivity, we obtain the global stiffness after elimination:

$$\begin{aligned} \mathbf{K} &= \begin{bmatrix} k_{44}^{(1)} + k_{22}^{(2)} & k_{24}^{(2)} \\ k_{42}^{(2)} & k_{44}^{(2)} \end{bmatrix} \\ &= 8 \times 10^5 \begin{bmatrix} 8 & 2 \\ 2 & 4 \end{bmatrix} \end{aligned}$$

The set of equations is given by

$$8 \times 10^5 \begin{bmatrix} 8 & 2 \\ 2 & 4 \end{bmatrix} \begin{Bmatrix} Q_4 \\ Q_6 \end{Bmatrix} = \begin{Bmatrix} -1000 \\ +1000 \end{Bmatrix}$$

The solution is

$$\begin{Bmatrix} Q_4 \\ Q_6 \end{Bmatrix} = \begin{Bmatrix} -2.679 \times 10^{-4} \\ 4.464 \times 10^{-4} \end{Bmatrix}$$

For element 2, $q_1 = 0$, $q_2 = Q_4$, $q_3 = 0$, and $q_4 = Q_6$. To get vertical deflection at the midpoint of the element, use $v = \mathbf{Hq}$ at $\xi = 0$:

$$\begin{aligned} v &= 0 + \frac{\ell_e}{2} H_2 Q_4 + 0 + \frac{\ell_e}{2} H_4 Q_6 \\ &= \left(\frac{1}{2}\right)\left(\frac{1}{4}\right)(-2.679 \times 10^{-4}) + \left(\frac{1}{2}\right)\left(-\frac{1}{4}\right)(4.464 \times 10^{-4}) \\ &= -8.93 \times 10^{-5} \text{ m} \\ &= -0.0893 \text{ mm} \end{aligned}$$

8.6 BEAMS ON ELASTIC SUPPORTS

In many engineering applications, beams are supported on elastic members. Shafts are supported on ball, roller, or journal bearings. Large beams are supported on elastic walls. Beams supported on soil form a class of applications known as Winkler foundations.

Single-row ball bearings can be considered by having a node at each bearing location and adding the bearing stiffness k_B to the diagonal location of vertical degree of freedom (Fig. 8.8a). Rotational (moment) stiffness has to be considered for roller bearings and journal bearings.

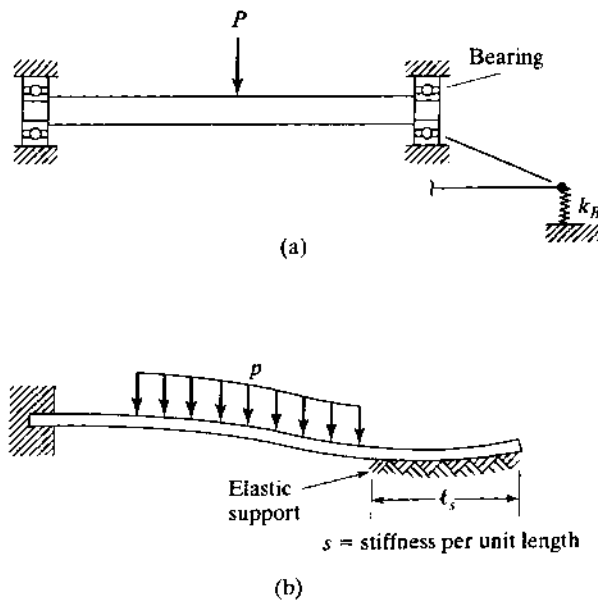


FIGURE 8.8 Elastic support.

In wide journal bearings and Winkler foundations, we use stiffness per unit length, s , of the supporting medium (Fig. 8.8b). Over the length of the support, this adds the following term to the total potential energy:

$$\frac{1}{2} \int_0^\ell sv^2 dx \quad (8.41)$$

In Galerkin's approach, this term is $\int_0^\ell sv\phi dx$. When we substitute for $v = \mathbf{H}\mathbf{q}$ for the discretized model, the previous term becomes

$$\frac{1}{2} \sum_e \mathbf{q}^T s \int_e \mathbf{H}^T \mathbf{H} dx \mathbf{q} \quad (8.42)$$

We recognize the stiffness term in this summation, namely,

$$\mathbf{k}_s^e = s \int_e \mathbf{H}^T \mathbf{H} dx = \frac{s\ell_e}{2} \int_{-1}^{+1} \mathbf{H}^T \mathbf{H} d\xi \quad (8.43)$$

On integration, we have

$$\mathbf{k}_s^e = \frac{s\ell_e}{420} \begin{bmatrix} 156 & 22\ell_e & 54 & -13\ell_e \\ 22\ell_e & 4\ell_e^2 & 13\ell_e & -3\ell_e^2 \\ 54 & 13\ell_e & 156 & -22\ell_e \\ -13\ell_e & -3\ell_e^2 & -22\ell_e & 4\ell_e^2 \end{bmatrix} \quad (8.44)$$

For elements supported on an elastic foundation, this stiffness has to be added to the element stiffness given by Eq. 8.29. Matrix \mathbf{k}_s^e is the consistent stiffness matrix for the elastic foundation.

8.7 PLANE FRAMES

Here, we consider plane structures with rigidly connected members. These members will be similar to the beams except that axial loads and axial deformations are present. The elements also have different orientations. Figure 8.9 shows a frame element. We have two displacements and a rotational deformation for each node. The nodal displacement vector is given by

$$\mathbf{q} = [q_1, q_2, q_3, q_4, q_5, q_6]^T \quad (8.45)$$

We also define the local or body coordinate system x', y' , such that x' is oriented along 1-2, with direction cosines ℓ, m (where $\ell = \cos \theta, m = \sin \theta$). These are evaluated using relationships given for the truss element, shown in Fig. 4.4. The nodal displacement vector in the local system is

$$\mathbf{q}' = [q'_1, q'_2, q'_3, q'_4, q'_5, q'_6]^T \quad (8.46)$$

Recognizing that $q'_3 = q_3$ and $q'_6 = q_6$, which are rotations with respect to the body, we obtain the local-global transformation

$$\mathbf{q}' = \mathbf{L}\mathbf{q} \quad (8.47)$$

where

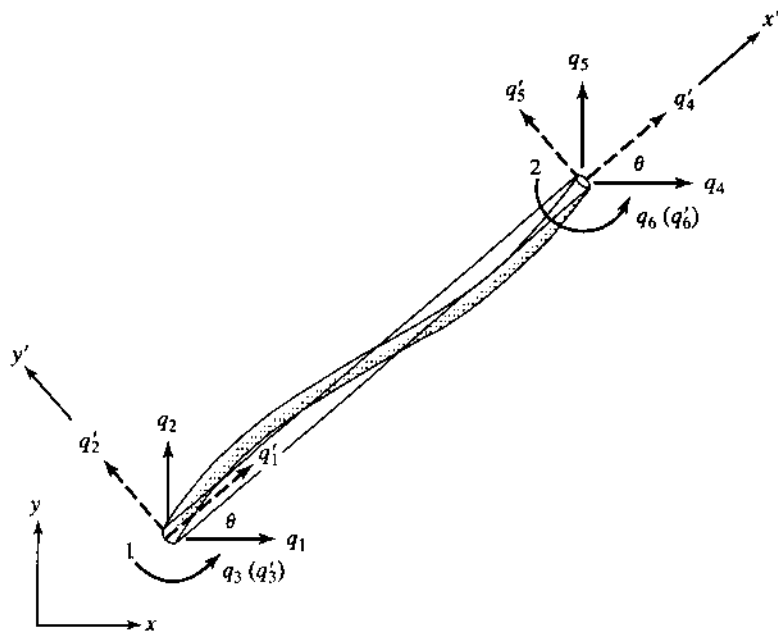


FIGURE 8.9 Frame element.

$$\mathbf{L} = \begin{bmatrix} \ell & m & 0 & 0 & 0 & 0 \\ -m & \ell & 0 & 0 & 0 & 0 \\ 0 & 0 & 1 & 0 & 0 & 0 \\ 0 & 0 & 0 & \ell & m & 0 \\ 0 & 0 & 0 & -m & \ell & 0 \\ 0 & 0 & 0 & 0 & 0 & 1 \end{bmatrix} \quad (8.48)$$

It is now observed that q'_2 , q'_3 , q'_5 , and q'_6 , are like the beam degrees of freedom, while q'_1 and q'_4 are similar to the displacements of a rod element, as discussed in Chapter 3. Combining the two stiffnesses and arranging in proper locations, we get the element stiffness for a frame element as

$$\mathbf{k}^{fe} = \begin{bmatrix} \frac{EA}{\ell_c} & 0 & 0 & \frac{-EA}{\ell_c} & 0 & 0 \\ 0 & \frac{12EI}{\ell_c^3} & \frac{6EI}{\ell_c^2} & 0 & \frac{-12EI}{\ell_c^3} & \frac{6EI}{\ell_c^2} \\ 0 & \frac{6EI}{\ell_c^2} & \frac{4EI}{\ell_c} & 0 & \frac{-6EI}{\ell_c^2} & \frac{2EI}{\ell_c} \\ -\frac{EA}{\ell_c} & 0 & 0 & \frac{EA}{\ell_c} & 0 & 0 \\ 0 & \frac{-12EI}{\ell_c^3} & \frac{-6EI}{\ell_c^2} & 0 & \frac{12EI}{\ell_c^3} & \frac{-6EI}{\ell_c^2} \\ 0 & \frac{6EI}{\ell_c^2} & \frac{2EI}{\ell_c} & 0 & \frac{-6EI}{\ell_c^2} & \frac{4EI}{\ell_c} \end{bmatrix} \quad (8.49)$$

As discussed in the development of a truss element in Chapter 4, we recognize that the element strain energy is given by

$$U_e = \frac{1}{2} \mathbf{q}'^T \mathbf{k}'^e \mathbf{q}' = \frac{1}{2} \mathbf{q}^T \mathbf{L}^T \mathbf{k}'^e \mathbf{L} \mathbf{q} \quad (8.50)$$

or in Galerkin's approach, the internal virtual work of an element is

$$W_e = \boldsymbol{\psi}'^T \mathbf{k}'^e \mathbf{q}' = \boldsymbol{\psi}^T \mathbf{L}^T \mathbf{k}'^e \mathbf{L} \mathbf{q} \quad (8.51)$$

where $\boldsymbol{\psi}'$ and $\boldsymbol{\psi}$ are virtual nodal displacements in local and global coordinate systems, respectively. From Eq. 8.50 or 8.51, we recognize the element stiffness matrix in global coordinates to be

$$\mathbf{k}^e = \mathbf{L}^T \mathbf{k}'^e \mathbf{L} \quad (8.52)$$

In the finite element program implementation, \mathbf{k}'^e can first be defined, and then this matrix multiplication can be carried out.

If there is distributed load on a member, as shown in Fig. 8.10, we have

$$\mathbf{q}'^T \mathbf{f}' = \mathbf{q}^T \mathbf{L}^T \mathbf{f} \quad (8.53)$$

where

$$\mathbf{f}' = \left[0, \frac{p\ell_e}{2}, \frac{p\ell_e^2}{12}, 0, \frac{p\ell_e}{2}, -\frac{p\ell_e^2}{12} \right]^T \quad (8.54)$$

The nodal loads due to the distributed load p are given by

$$\mathbf{f} = \mathbf{L}^T \mathbf{f}' \quad (8.55)$$

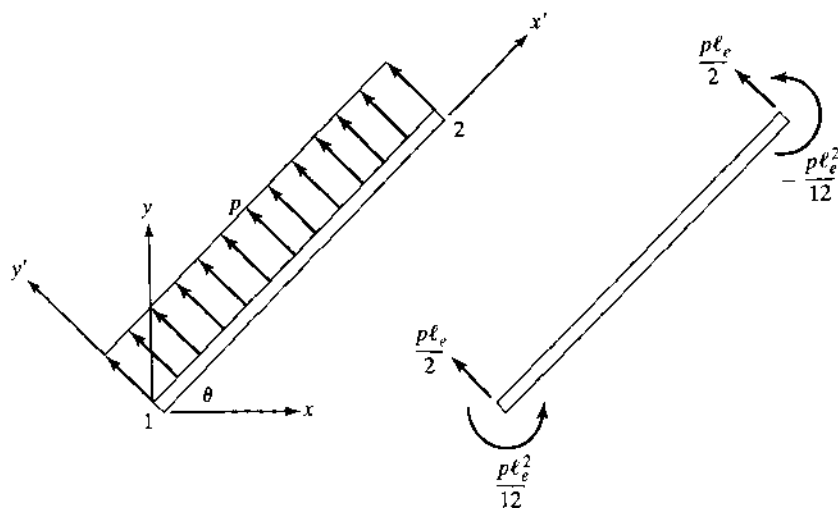


FIGURE 8.10 Distributed load on a frame element.

The values of f are added to the global load vector. Note here that positive p is in the y' direction.

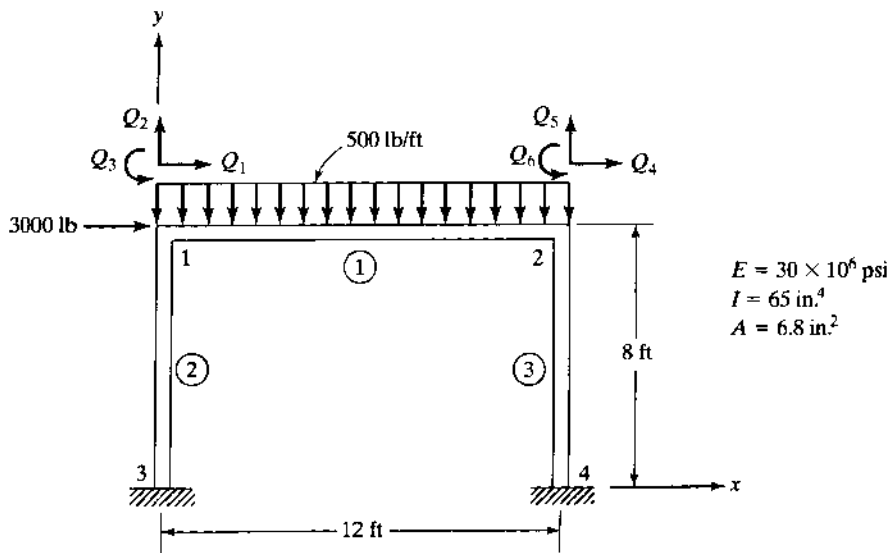
The point loads and couples are simply added to the global load vector. On gathering stiffnesses and loads, we get the system of equations

$$\mathbf{KQ} = \mathbf{F}$$

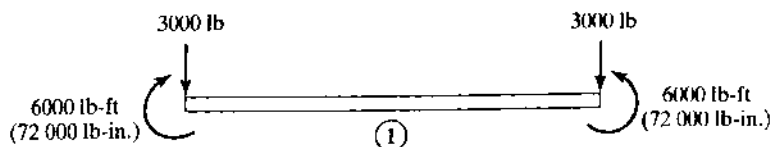
where the boundary conditions are considered by applying the penalty terms in the energy or Galerkin formulations.

Example 8.2

Determine the displacements and rotations of the joints for the portal frame shown in Fig. E8.2.



(a) Portal frame



(b) Equivalent load for element 1

FIGURE E8.2 (a) Portal frame. (b) Equivalent load for Element 1.

Solution We follow the steps given below:

Step 1. Connectivity

The connectivity is as follows:

| Element No. | Node | |
|-------------|------|---|
| | 1 | 2 |
| 1 | 1 | 2 |
| 2 | 3 | 1 |
| 3 | 4 | 2 |

Step 2. Element Stiffnesses

Element 1. Using the matrix given in Eq. 8.45 and noting that $\mathbf{k}^1 = \mathbf{k}'^1$, we find that

$$\mathbf{k}^1 = 10^4 \times \begin{bmatrix} Q_1 & Q_2 & Q_3 & Q_4 & Q_5 & Q_6 \\ 141.7 & 0 & 0 & -141.7 & 0 & 0 \\ 0 & 0.784 & 56.4 & 0 & -0.784 & 56.4 \\ 0 & 56.4 & 5417 & 0 & -56.4 & 2708 \\ -141.7 & 0 & 0 & 141.7 & 0 & 0 \\ 0 & -0.784 & -56.4 & 0 & 0.784 & -56.4 \\ 0 & 56.4 & 2708 & 0 & -56.4 & 5417 \end{bmatrix}$$

Elements 2 and 3. Local element stiffnesses for elements 2 and 3 are obtained by substituting for E, A, I and ℓ_2 in matrix \mathbf{k}' of Eq. 8.49:

$$\mathbf{k}'^2 = 10^4 \times \begin{bmatrix} 212.5 & 0 & 0 & -212.5 & 0 & 0 \\ 0 & 2.65 & 127 & 0 & -2.65 & 127 \\ 0 & 127 & 8125 & 0 & -127 & 4063 \\ -212.5 & 0 & 0 & 212.5 & 0 & 0 \\ 0 & -2.65 & -127 & 0 & 2.65 & -127 \\ 0 & 127 & 4063 & 0 & -127 & 8125 \end{bmatrix}$$

Transformation matrix L. We have noted that for element 1, $\mathbf{k} = \mathbf{k}'^1$. For elements 2 and 3, which are oriented similarly with respect to the x - and y -axes, we have $\ell = 0, m = 1$. Then,

$$\mathbf{L} = \begin{bmatrix} 0 & 1 & 0 & 0 & 0 & 0 \\ -1 & 0 & 0 & 0 & 0 & 0 \\ 0 & 0 & 1 & 0 & 0 & 0 \\ 0 & 0 & 0 & 0 & 1 & 0 \\ 0 & 0 & 0 & -1 & 0 & 0 \\ 0 & 0 & 0 & 0 & 0 & 1 \end{bmatrix}$$

Noting that $\mathbf{k}^2 = \mathbf{L}^T \mathbf{k}'^2 \mathbf{L}$, we get

$$\begin{aligned} e = 3 & \rightarrow Q_4 \quad Q_5 \quad Q_6 \\ e = 2 & \rightarrow Q_1 \quad Q_2 \quad Q_3 \end{aligned}$$

$$\mathbf{k} = 10^4 \times \begin{bmatrix} 2.65 & 0 & -127 & -2.65 & 0 & -127 \\ 0 & 212.5 & 0 & 0 & -212.5 & 0 \\ -127 & 0 & 8125 & 127 & 0 & 4063 \\ -2.65 & 0 & 127 & 2.65 & 0 & 127 \\ 0 & -212.5 & 0 & 0 & 212.5 & 0 \\ -127 & 0 & 4063 & 127 & 0 & 8125 \end{bmatrix}$$

Stiffness \mathbf{k}^1 has all its elements in the global locations. For elements 2 and 3, the shaded part of the stiffness matrix shown previously is added to the appropriate global locations of \mathbf{K} . The global stiffness matrix is given by

$$\mathbf{K} = 10^4 \times \begin{bmatrix} 144.3 & 0 & 127 & -141.7 & 0 & 0 \\ 0 & 213.3 & 56.4 & 0 & -0.784 & 56.4 \\ 127 & 56.4 & 13542 & 0 & -56.4 & 2708 \\ -141.7 & 0 & 0 & 144.3 & 0 & 127 \\ 0 & -0.784 & -56.4 & 0 & 213.3 & -56.4 \\ 0 & 56.4 & 2708 & 127 & -56.4 & 13542 \end{bmatrix}$$

From Fig. E8.2, the load vector can easily be written as

$$\mathbf{F} = \begin{pmatrix} 3\,000 \\ -3\,000 \\ -72\,000 \\ 0 \\ -3\,000 \\ +72\,000 \end{pmatrix}$$

The set of equations is given by

$$\mathbf{KQ} = \mathbf{F}$$

On solving, we get

$$\mathbf{Q} = \begin{pmatrix} 0.092 \text{ in.} \\ -0.00104 \text{ in.} \\ -0.00139 \text{ rad} \\ 0.0901 \text{ in.} \\ -0.0018 \text{ in.} \\ -3.88 \times 10^{-5} \text{ rad} \end{pmatrix}$$

8.8 THREE-DIMENSIONAL FRAMES

Three-dimensional frames, also called as *space frames*, are frequently encountered in the analysis of multistory buildings. They are also to be found in the modeling of car body and bicycle frames. A typical three-dimensional frame is shown in Fig. 8.11. Each node has six degrees of freedom (dofs) (as opposed to only three dofs in a plane frame). The dof numbering is shown in Fig. 8.11: for node J , dof $6J-5$, $6J-4$, and $6J-3$ represent

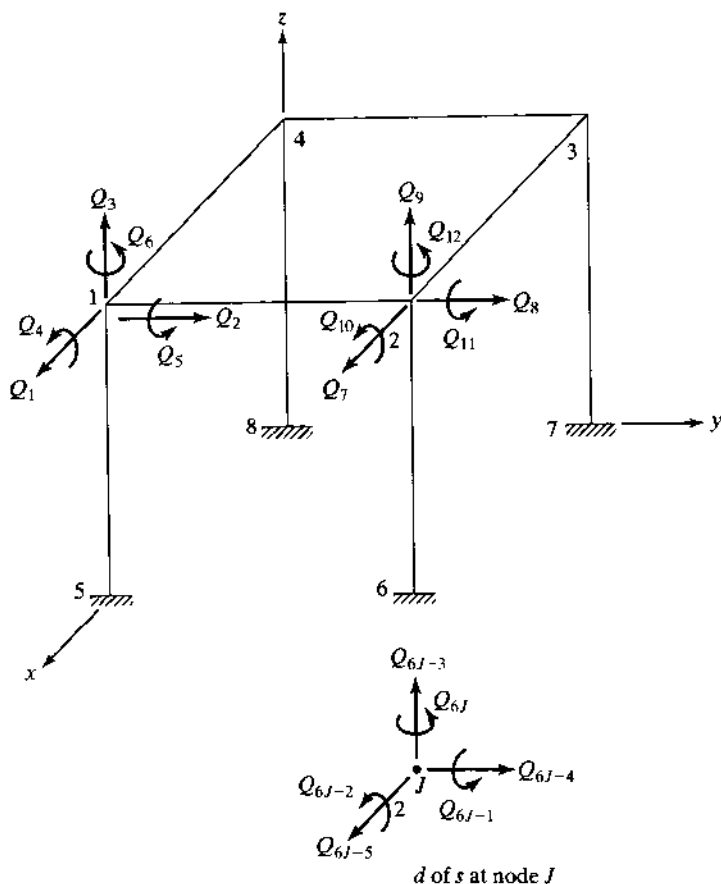


FIGURE 8.11 Degrees of freedom numbering for a three-dimensional frame.

the x -, y -, and z -translational dofs, while $6J-2$, $6J-1$, and $6J$ represent the rotational dofs along the x -, y -, and z -axes. The element displacement vectors in the local and global coordinate systems are denoted as \mathbf{q}' and \mathbf{q} , respectively. These vectors are of dimension (12×1) as shown in Fig. 8.12.

Orientation of the local x' -, y' -, and z' -coordinate system is established with the use of three points. Points 1 and 2 are the ends of the element; the x' -axis is along the line from point 1 to point 2, just as in the case of two-dimensional frames. Point 3 is any *reference point* not lying along the line joining points 1 and 2. The y' -axis is to lie in the plane defined by points 1, 2, and 3. This is shown in Fig. 8.12. The z' -axis is then automatically defined from the fact that x' , y' , and z' form a right-handed system. We note that y' and z' are the principal axes of the cross section, with $I_{y'}$ and $I_{z'}$ the principal moments of inertia. The cross-sectional properties are specified by four parameters: area A and moments of inertia $I_{y'}$, $I_{z'}$, and J . The product GJ is the torsional stiffness, where G = shear modulus. For circular or tubular cross sections, J is the polar moment of inertia. For other cross-sectional shapes, such as an I -section, the torsional stiffness is given in strength of materials texts.

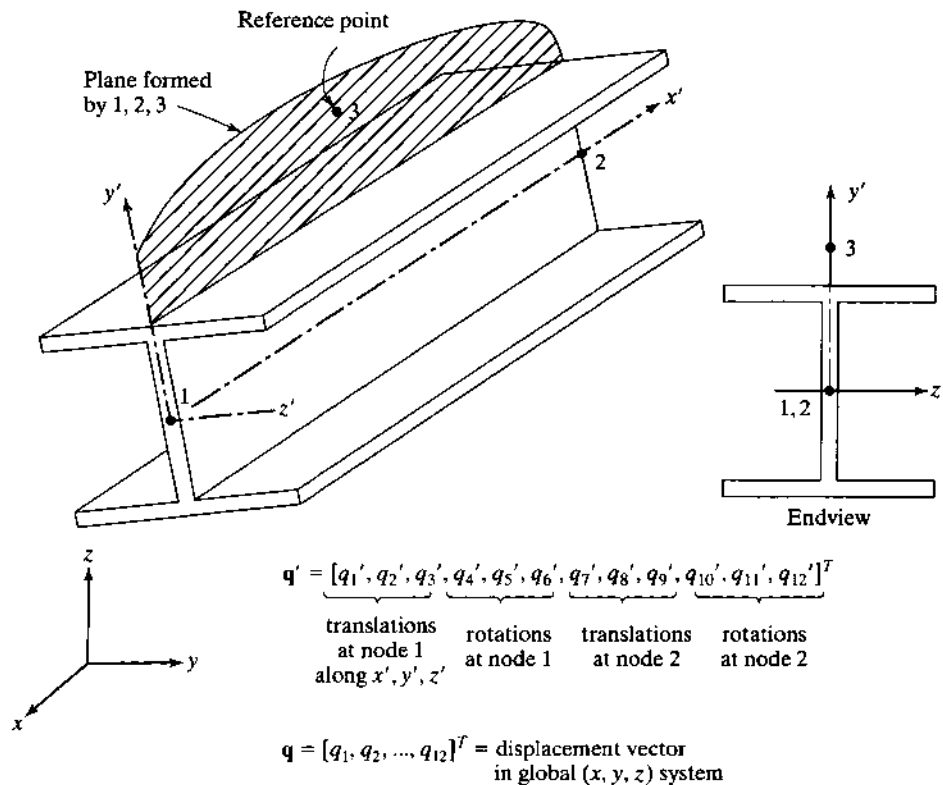


FIGURE 8.12 Three-dimensional frame element in local and global coordinate systems.

The (12×12) element stiffness matrix \mathbf{k}' in the local coordinate system is obtained by a straightforward generalization of Eq. 8.49 as

$$\mathbf{k}' = \begin{bmatrix}
 AS & 0 & 0 & 0 & 0 & 0 & -AS & 0 & 0 & 0 & 0 & 0 \\
 a_z' & 0 & 0 & 0 & b_z' & 0 & -a_z' & 0 & 0 & 0 & 0 & b_z' \\
 a_y' & 0 & -b_y' & 0 & 0 & 0 & 0 & -a_y' & 0 & -b_y' & 0 & 0 \\
 TS & 0 & 0 & 0 & 0 & 0 & 0 & 0 & -TS & 0 & 0 & 0 \\
 c_y' & 0 & 0 & 0 & 0 & 0 & b_y' & 0 & 0 & d_y' & 0 & 0 \\
 c_z' & 0 & 0 & 0 & 0 & 0 & 0 & 0 & 0 & 0 & d_z' & 0 \\
 AS & 0 & 0 & 0 & 0 & 0 & 0 & 0 & 0 & 0 & 0 & 0 \\
 a_z' & 0 & 0 & 0 & 0 & 0 & 0 & 0 & 0 & 0 & -b_z' & 0 \\
 c_y' & 0 & 0 & 0 & 0 & 0 & 0 & 0 & 0 & b_y' & 0 & 0 \\
 TS & 0 & 0 & 0 & 0 & 0 & 0 & 0 & 0 & 0 & 0 & 0 \\
 c_y' & 0 & 0 & 0 & 0 & 0 & 0 & 0 & 0 & 0 & 0 & 0 \\
 c_z' & 0 & 0 & 0 & 0 & 0 & 0 & 0 & 0 & 0 & 0 & 0
 \end{bmatrix} \quad (8.56)$$

Symmetric

where $AS = EA/l_e$, $l_e =$ length of the element, $TS = GJ/l_e$, $a_z' = 12EI_z/l_e^3$, $b_z' = 6EI_z/l_e^3$, $c_z' = 4EI_z/l_e$, $d_z' = 2EI_z/l_e$, $a_y' = 12EI_y/l_e^3$, and so on. The global-local transformation matrix is given by

$$\mathbf{q}' = \mathbf{L}\mathbf{q} \quad (8.57)$$

The (12×12) transformation matrix \mathbf{L} is defined from a (3×3) λ matrix as

$$\mathbf{L} = \begin{bmatrix} \lambda & & \mathbf{0} \\ & \lambda & \\ \mathbf{0} & & \lambda \end{bmatrix} \quad (8.58)$$

The λ is a matrix of direction cosines:

$$\lambda = \begin{bmatrix} l_1 & m_1 & n_1 \\ l_2 & m_2 & n_2 \\ l_3 & m_3 & n_3 \end{bmatrix} \quad (8.59)$$

Here, l_1 , m_1 , and n_1 are the cosines of the angles between the x' -axis and the global x -, y -, and z -axes, respectively. Similarly, l_2 , m_2 , and n_2 , are the cosines of the angles between the y' -axis and the x -, y -, and z -axes, and l_3 , m_3 , and n_3 are associated with the z' -axis. These direction cosines and hence the λ matrix are obtainable from the coordinates of the points 1, 2, and 3 as follows. We have

$$l_1 = \frac{x_2 - x_1}{l_e} \quad m_1 = \frac{y_2 - y_1}{l_e} \quad n_1 = \frac{z_2 - z_1}{l_e}$$

$$l_e = \sqrt{(x_2 - x_1)^2 + (y_2 - y_1)^2 + (z_2 - z_1)^2}$$

Now, let $\mathbf{V}_{x'} = [l_1 \quad m_1 \quad n_1]^T$ denote the unit vector along the x' -axis. Also, let

$$\mathbf{V}_{13} = \begin{bmatrix} \frac{x_3 - x_1}{l_{13}} & \frac{y_3 - y_1}{l_{13}} & \frac{z_3 - z_1}{l_{13}} \end{bmatrix}$$

where $l_{13} =$ distance between points 1 and 3. The unit vector along the z' -axis is now given by

$$\mathbf{V}_{z'} = [l_3 \quad m_3 \quad n_3]^T = \frac{\mathbf{V}_{x'} \times \mathbf{V}_{13}}{|\mathbf{V}_{x'} \times \mathbf{V}_{13}|}$$

The cross product of any two vectors is given by the determinant

$$\mathbf{u} \times \mathbf{v} = \begin{vmatrix} \mathbf{i} & \mathbf{j} & \mathbf{k} \\ u_x & u_y & u_z \\ v_x & v_y & v_z \end{vmatrix} = \begin{bmatrix} u_y v_z - v_y u_z \\ v_x u_z - u_x v_z \\ u_x v_y - v_x u_y \end{bmatrix}$$

Finally, we have the direction cosines of the y' -axis given by

$$\mathbf{V}_{y'} = [l_2 \quad m_2 \quad n_2]^T = \mathbf{V}_{z'} \times \mathbf{V}_{x'}$$

These calculations to define the \mathbf{L} matrix are coded in program FRAME3D. The element stiffness matrix in global coordinates is

$$\mathbf{k} = \mathbf{L}^T \mathbf{k}' \mathbf{L} \quad (8.60)$$

where \mathbf{k}' has been defined in Eq. 8.56.

If a distributed load with components w_y and w_z (units of force/unit length) is applied on the element, then the equivalent point loads at the ends of the member are

$$\mathbf{f}' = \left[0, \frac{w_y l_e}{2}, \frac{w_z l_e}{2}, 0, \frac{-w_z l_e^2}{12}, \frac{w_y l_e^2}{12}, 0, \frac{w_y l_e}{2}, \frac{w_z l_e}{2}, 0, \frac{w_z l_e^2}{12}, \frac{-w_y l_e^2}{12} \right]^T \quad (8.61)$$

These loads are transferred into global components by $\mathbf{f} = \mathbf{L}^T \mathbf{f}'$. After enforcing boundary conditions and solving the system equations $\mathbf{KQ} = \mathbf{F}$, we can compute the member end forces from

$$\mathbf{R}' = \mathbf{k}' \mathbf{q}' + \text{fixed-end reactions} \quad (8.62)$$

where the fixed-end reactions are the negative of the \mathbf{f}' vector and are only associated with those elements having distributed loads acting on them. The member end forces provide the bending moments and shear forces from which the beam stresses can be determined.

Example 8.3

Figure E8.3 shows a three-dimensional frame subjected to various loads. Our task is to run program FRAME3D to obtain the maximum bending moments in the structure. The input and output files are as given in the third data set, which follows the BEAM and FRAME2D data sets. From the output, we obtain the maximum $M_y = 3.680E + 0.5 \text{ N} \cdot \text{m}$ occurring in member 1 at node 1 (the first node) and maximum $M_z = -1.413E + 0.5 \text{ N} \cdot \text{m}$ occurring in member 3 at node 4. ■

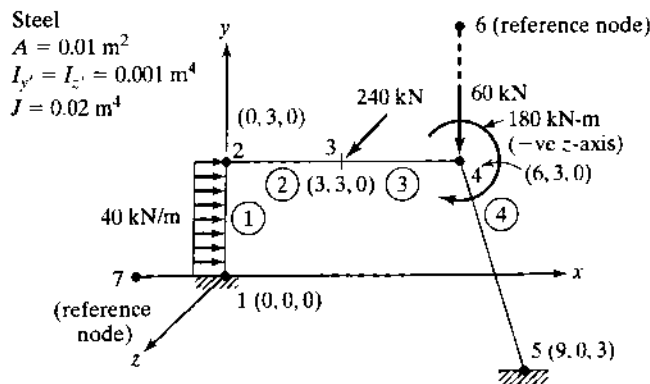


FIGURE E8.3

8.9 SOME COMMENTS

Symmetric beams and plane and space frames have been discussed in this chapter. In engineering applications, there are several challenging problems, such as frames and mechanisms with pin-jointed members, unsymmetric beams, buckling of members due to axial loads, shear considerations, and structures with large deformations. For help in formulating and analyzing such problems, the reader may refer to some advanced publications in mechanics of solids, structural analysis, elasticity and plasticity, and finite element analysis.

Input Data File

```

<< Beam Analysis >>
EXAMPLE 8.1
NN NE NM NDIM NEN NDN
3 2 1 1 2 2
ND NL NMPC
4 4 0
Node# Coordinates
1 0
2 1000
3 2000
Elem# N1 N2 Mat# Mom Inertia
1 1 2 1 4e6
2 2 3 1 4e6
DOF# Displacement
1 0
2 0
3 0
5 0
DOF# Load
3 -6000
4 -1e6
5 -6000
6 1e6
MAT# E
1 200000
Multi-point Constraints B1*Qi+B2*Qj=B3

```

```

Program Beam - CHANDRUPATLA & BELEGUNDU
Output
EXAMPLE 8.1
NODE# Displ. Rotation(radians)
1 2.0089E-11 6.6961E-09
2 -1.2723E-10 -2.6786E-04
3 -8.0357E-11 4.4643E-04
DOF# Reaction
1 -1.2857E+03
2 -4.2855E+05
3 8.1428E+03
5 5.1429E+03

```

```

<<2-D Frame Analysis >>
EXAMPLE 8.2
NN NE NM NDIM NEN NDN
4 3 1 2 2 3
ND NL NMPC
6 1 0
Node# X Y
1 0 96
2 144 96
3 0 0
4 144 0

```

continued

| ELEM# | N1 | N2 | MAT# | Area | Inertia | Distr load |
|-------|--------------|----|------|------|--------------------------------------|------------|
| 1 | 2 | 1 | 1 | 6.8 | 65 | 41.6667 |
| 2 | 3 | 1 | 1 | 6.8 | 65 | 0. |
| 3 | 4 | 2 | 1 | 6.8 | 65 | 0. |
| DOF# | Displacement | | | | | |
| 7 | 0 | | | | | |
| 8 | 0 | | | | | |
| 9 | 0 | | | | | |
| 10 | 0 | | | | | |
| 11 | 0 | | | | | |
| 12 | 0 | | | | | |
| DOF# | Load | | | | | |
| 1 | 3000 | | | | | |
| MAT# | E | | | | | |
| 1 | 30e6 | | | | | |
| B1 | i | B2 | j | B3 | (Multi-point constr. B1*Qi+B2*Qj=B3) | |

Program Frame2D - CHANDRUPATLA & BELEGUNDU

Output

EXAMPLE 8.2

| NODE# | X-Displ | Y-Displ | Z-Rotation |
|-------|------------|-------------|-------------|
| 1 | 9.1770E-02 | -1.0358E-03 | -1.3874E-03 |
| 2 | 9.0122E-02 | -1.7877E-03 | -3.8835E-05 |
| 3 | 4.9167E-10 | -1.6255E-09 | -4.4410E-08 |
| 4 | 1.7237E-09 | -2.8053E-09 | -8.3320E-08 |

Member End-Forces

Member# 1

| | | |
|-------------|-------------|-------------|
| 2.3342E+03 | -7.9884E+02 | -3.9255E+04 |
| -2.3342E+03 | 7.9884E+02 | -7.5778E+04 |

Member# 2

| | | |
|-------------|-------------|------------|
| 2.2012E+03 | 6.6580E+02 | 6.0139E+04 |
| -2.2012E+03 | -6.6580E+02 | 3.7778E+03 |

Member# 3

| | | |
|-------------|-------------|------------|
| 3.7988E+03 | 2.3342E+03 | 1.1283E+05 |
| -3.7988E+03 | -2.3342E+03 | 1.1125E+05 |

DOF# Reaction

| | |
|----|-------------|
| 7 | -6.6580E+02 |
| 8 | 2.2012E+03 |
| 9 | 6.0139E+04 |
| 10 | -2.3342E+03 |
| 11 | 3.7988E+03 |
| 12 | 1.1283E+05 |

<<3-D Frame Analysis >>

EXAMPLE 8.3

| NN | NE | NM | NDIM | NEN | NDN | NNREF |
|----|----|----|------|-----|-----|-------|
| 5 | 4 | 1 | 3 | 2 | 6 | 2 |

ND NL NMPC

12 3 0

| Node# | X | Y | Z |
|-------|---|---|---|
| 1 | 0 | 0 | 0 |
| 2 | 0 | 3 | 0 |
| 3 | 3 | 3 | 0 |

continued

| | | | | | | | | | | | |
|-------|-------------------|----|--------|------|--------------------------------------|------|------|------|---------|-------|--|
| 4 | 6 | 3 | 0 | | | | | | | | |
| 5 | 9 | 0 | 3 | | | | | | | | |
| 6 | 6 | 6 | 0 | | | | | | | | |
| 7 | -3 | 0 | 0 | | | | | | | | |
| Elem# | N1 | N2 | Ref_Pt | Mat# | Area | Iy | Iz | J | UDLy' | UDLz' | |
| 1 | 1 | 2 | 7 | 1 | .01 | 1E-3 | 1E-3 | 2E-3 | -40000. | 0. | |
| 2 | 2 | 3 | 6 | 1 | .01 | 1E-3 | 1E-3 | 2E-3 | 0. | 0. | |
| 3 | 3 | 4 | 6 | 1 | .01 | 1E-3 | 1E-3 | 2E-3 | 0. | 0. | |
| 4 | 4 | 5 | 6 | 1 | .01 | 1E-3 | 1E-3 | 2E-3 | 0. | 0. | |
| DOF# | Displacement | | | | | | | | | | |
| 1 | 0 | | | | | | | | | | |
| 2 | 0 | | | | | | | | | | |
| 3 | 0 | | | | | | | | | | |
| 4 | 0 | | | | | | | | | | |
| 5 | 0 | | | | | | | | | | |
| 6 | 0 | | | | | | | | | | |
| 25 | 0 | | | | | | | | | | |
| 26 | 0 | | | | | | | | | | |
| 27 | 0 | | | | | | | | | | |
| 28 | 0 | | | | | | | | | | |
| 29 | 0 | | | | | | | | | | |
| 30 | 0 | | | | | | | | | | |
| DOF# | Load | | | | | | | | | | |
| 15 | 240000 | | | | | | | | | | |
| 20 | -60000 | | | | | | | | | | |
| 24 | -180000 | | | | | | | | | | |
| MAT# | Prop1(E) Prop2(G) | | | | | | | | | | |
| 1 | 200E9 80E9 | | | | | | | | | | |
| B1 | i | B2 | j | B3 | (Multi-point constr. B1*Qi+B2*Qj=B3) | | | | | | |

Program Frame3D - CHANDRUPATLA & BELEGONDU

Output

EXAMPLE 8.3

| Node#) | X-Displ | Y-Displ | Z-Displ | X-Rot | Y-Rot | Z-Rot |
|--------|------------|------------|-----------|-----------|------------|------------|
| 1) | 3.127E-09 | 1.972E-09 | 9.900E-09 | 2.760E-08 | -7.145E-09 | 5.348E-09 |
| 2) | -1.868E-03 | 3.944E-05 | 5.310E-03 | 2.550E-03 | -1.786E-03 | 1.108E-03 |
| 3) | -1.985E-03 | 3.141E-03 | 9.842E-03 | 2.025E-03 | -2.452E-04 | 7.624E-04 |
| 4) | -2.103E-03 | 3.431E-03 | 6.241E-03 | 1.500E-03 | 1.836E-03 | -7.662E-04 |
| 5) | 5.873E-09 | -6.472E-09 | 8.100E-09 | 6.985E-09 | 8.429E-09 | -1.101E-09 |

Member End-Forces

| | | | | | | |
|---------|------------|------------|------------|------------|------------|------------|
| Member# | 1 | | | | | |
| | -2.629E+04 | -1.830E+04 | -1.320E+05 | 9.526E+04 | 3.680E+05 | -1.013E+05 |
| | 2.629E+04 | 1.830E+04 | 1.320E+05 | -9.526E+04 | 2.800E+04 | 4.641E+04 |
| Member# | 2 | | | | | |
| | 7.830E+04 | -2.629E+04 | -1.320E+05 | 2.800E+04 | 9.526E+04 | -1.641E+04 |
| | -7.830E+04 | 2.629E+04 | 1.320E+05 | -2.800E+04 | 3.007E+05 | -6.247E+04 |
| Member# | 3 | | | | | |
| | 7.830E+04 | -2.629E+04 | 1.080E+05 | 2.800E+04 | -3.007E+05 | 6.247E+04 |
| | -7.830E+04 | 2.629E+04 | -1.080E+05 | -2.800E+04 | -2.328E+04 | -1.413E+05 |
| Member# | 4 | | | | | |
| | 1.574E+05 | 5.600E+03 | 2.100E+04 | -1.959E+04 | 1.465E+04 | -4.713E+04 |
| | -1.574E+05 | -5.600E+03 | -2.100E+04 | 1.959E+04 | -1.238E+05 | 7.623E+04 |

PROBLEMS

- 8.1. Find the deflection at the load and the slopes at the ends for the steel shaft shown in Fig. P8.1. Consider the shaft to be simply supported at bearings *A* and *B*.

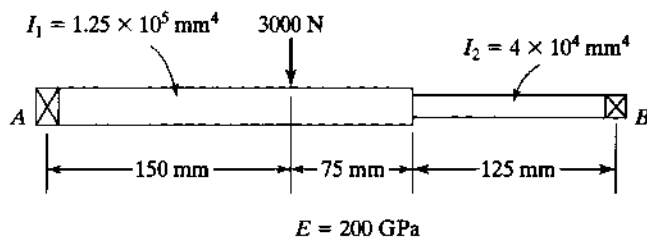


FIGURE P8.1 Problems 8.1 and 8.4.

- 8.2. A three-span beam is shown in Fig. P8.2. Determine the deflection curve of the beam and evaluate the reactions at the supports.

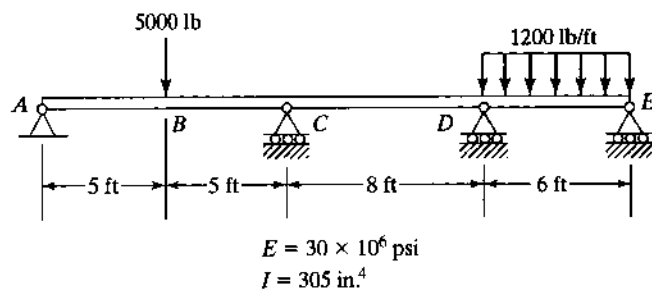


FIGURE P8.2

- 8.3. A reinforced concrete slab floor is shown in Fig. P8.3. Using a unit width of the slab in the *z* direction, determine the deflection curve of the neutral surface under its own weight.

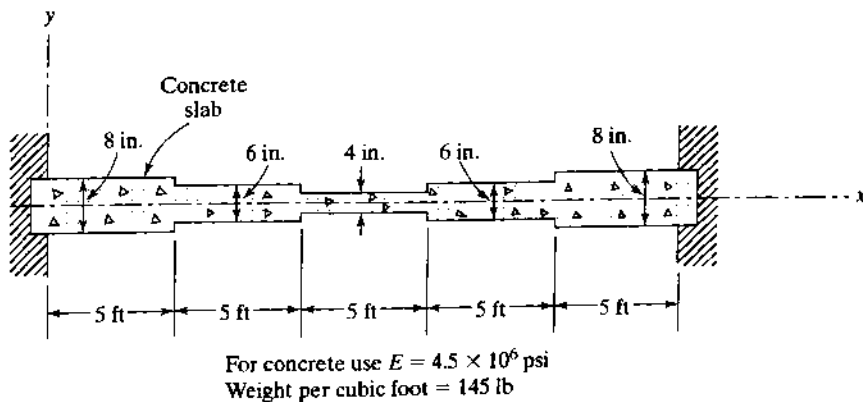


FIGURE P8.3

- 8.4. In the shaft shown in Fig. P8.1, determine the deflection at the loads and the slopes at the ends if the bearings at A and B have radial stiffnesses of 20 and 12 kN/mm, respectively.
- 8.5. Figure P8.5 shows a beam AD pinned at A and welded at B and C to long and slender rods BE and CF . A load of 3000 lb is applied at D as shown. Model the beam AD using beam elements and determine deflections at B , C , and D and stresses in rods BE and CF .

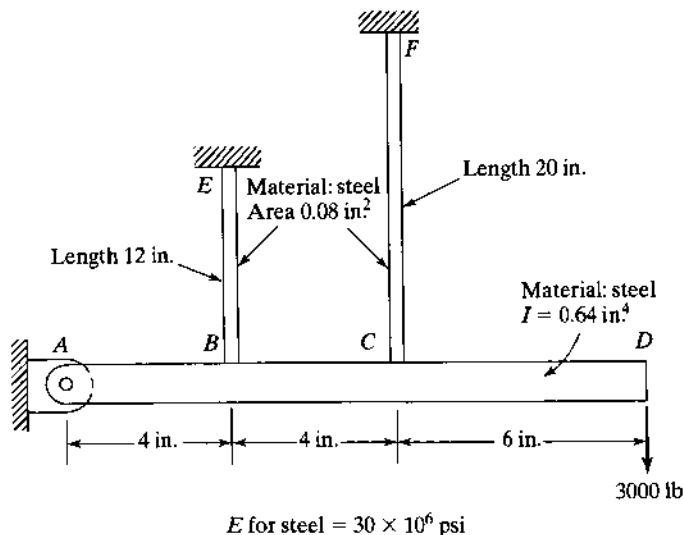


FIGURE P8.5

- 8.6. Figure P8.6 shows a cantilever beam with three rectangular openings. Find the deflections for the beam shown and compare the deflections with a beam without openings.

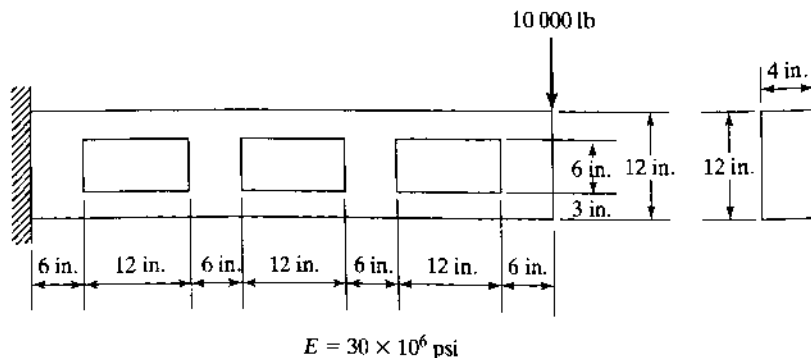


FIGURE P8.6

- 8.7. A simplified section of a machine tool spindle is shown in Fig. P8.7. Bearing B has a radial stiffness of $60 \text{ N}/\mu\text{m}$ and a rotational stiffness (against moment) of $8 \times 10^5 \text{ N}\cdot\text{m}/\text{rad}$. Bearing C has a radial stiffness of $20 \text{ N}/\mu\text{m}$ and its rotational stiffness can be neglected. For a load of 1000 N, as shown, determine the deflection and slope at A . Also, give the deflected shape of the spindle center line ($1 \mu\text{m} = 10^{-6} \text{ m}$).

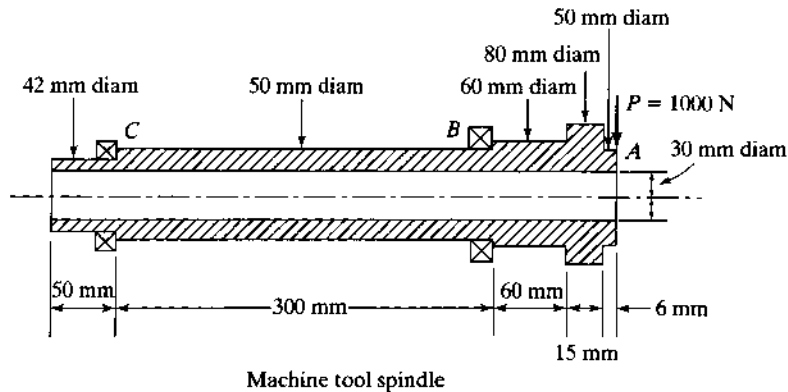


FIGURE P8.7

- 8.8. Determine the deflection at the center of BC for the frame shown in Fig. P8.8, using program FRAME2D. Also determine the reactions at A and D .

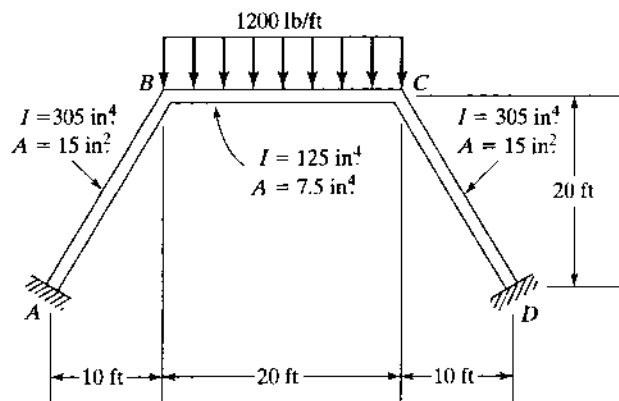


FIGURE P8.8

- 8.9. Figure P8.9 shows a hollow square section with two loading conditions. Using a 1-in. width perpendicular to the section, determine the deflection at the load for each of the two cases.

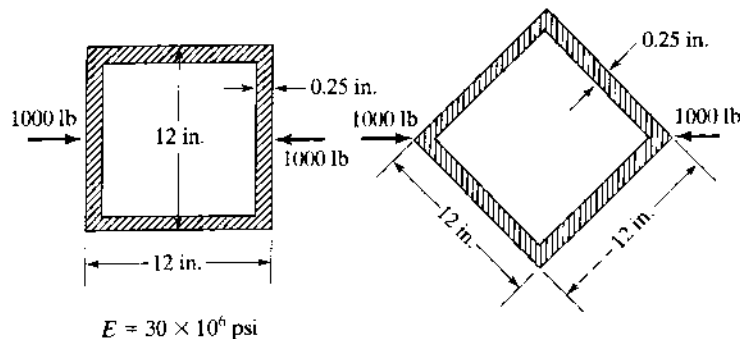


FIGURE P8.9

- 8.10. Figure P8.10 shows a five-member steel frame subjected to loads at the free end. The cross section of each member is a tube of wall thickness $t = 1$ cm and mean radius $R = 6$ cm. Determine the following:
- the displacement of node 3 and
 - the maximum axial compressive stress in a member.

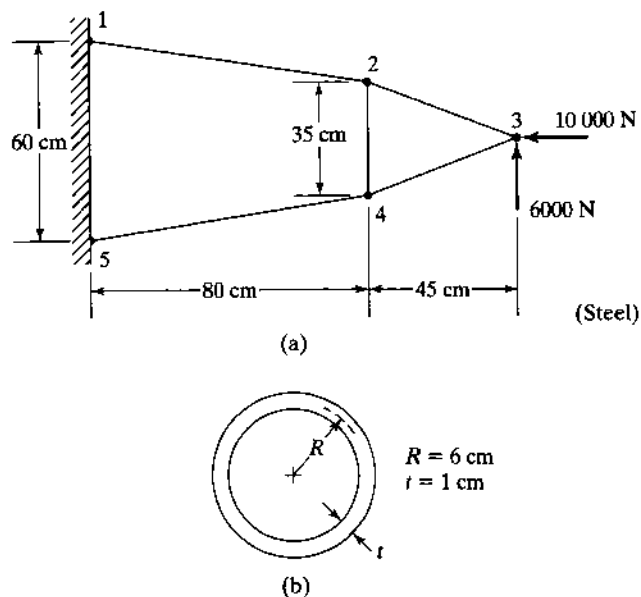


FIGURE P8.10

- 8.11. Dimensions of a common paper staple are shown in Fig. P8.11. While the staple is penetrating into the paper, a force of about 120 N is applied. Find the deformed shape for the following cases:
- load uniformly distributed on the horizontal member and pinned condition at A at entry;
 - load as in (a) with fixed condition at A after some penetration;
 - load divided into two point loads, with A pinned; and
 - load as in (c) with A fixed.

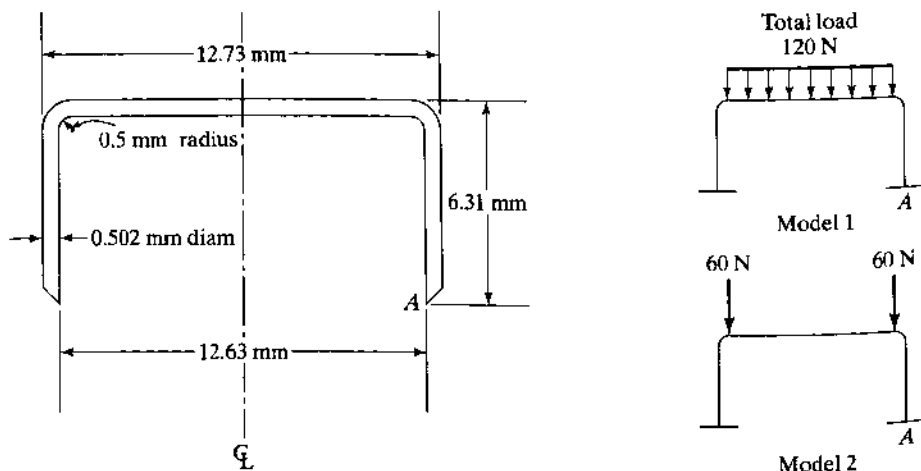


FIGURE P8.11

- 8.12. A commonly used street light arrangement is shown in Fig. P8.12. Assuming fixed condition at A , compare the deformed shapes for the following two cases:
 (a) without the rod BC (that is, only member ACD supports the light) and
 (b) with tie rod BC .

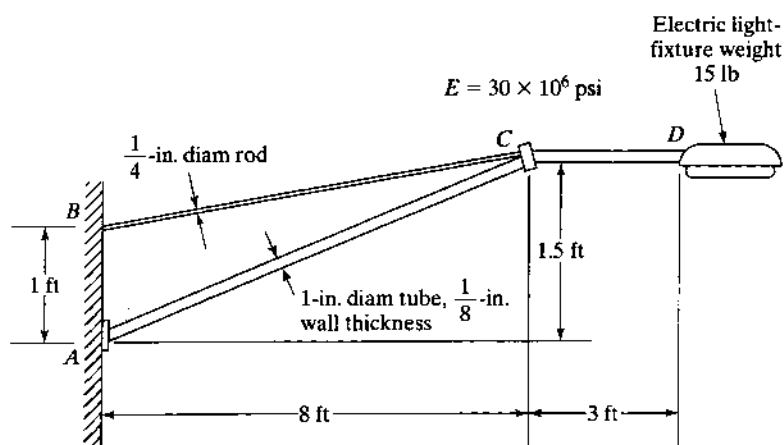


FIGURE P8.12

- 8.13. Figure P8.13a shows a cab of a van. A simplified finite element frame model is shown in Fig. P8.13b. The model consists of 28 nodes. $x-z$ is a plane of symmetry; thus, nodes $1' - 13'$ have the same x - and z -coordinates as nodes $1 - 13$, with y -coordinates reversed in sign. Each beam element is made of steel with $A = 0.2 \text{ in.}^2$, $I_y = I_z = 0.003 \text{ in.}^4$, and $J = 0.006 \text{ in.}^4$. The loading corresponds to a frontal impact test based on Swedish standards and consists of a load at node 1 (only) with components $F_x = -3194.0 \text{ lb}$ and $F_y = -856.0 \text{ lb}$. Treat nodes 11, $11'$, 12, and $12'$ as fixed (boundary conditions). Nodal coordinates in inches are as follows:

| Node | x | y | z | Node | x | y | z |
|------|------|------|------|------|------|------|------|
| 1 | 58.0 | 38.0 | 0 | 9 | 0 | 38.0 | 75.0 |
| 2 | 48.0 | 38.0 | 0 | 10 | 58.0 | 17.0 | 42.0 |
| 3 | 31.0 | 38.0 | 0 | 11 | 58.0 | 17.0 | 0 |
| 4 | 17.0 | 38.0 | 22.0 | 12 | 0 | 17.0 | 0 |
| 5 | 0 | 38.0 | 24.0 | 13 | 0 | 17.0 | 24.0 |
| 6 | 58.0 | 38.0 | 42.0 | 14 | 18.0 | 0 | 72.0 |
| 7 | 48.0 | 38.0 | 42.0 | 15 | 0 | 0 | 37.5 |
| 8 | 36.0 | 38.0 | 70.0 | | | | |

(Note: Number the nodes to keep bandwidth to a minimum.)

Determine the deflections at nodes 1, 2, 6, 7, 10, and 11 and the location and magnitude of the maximum bending moments using program FRAME3D.

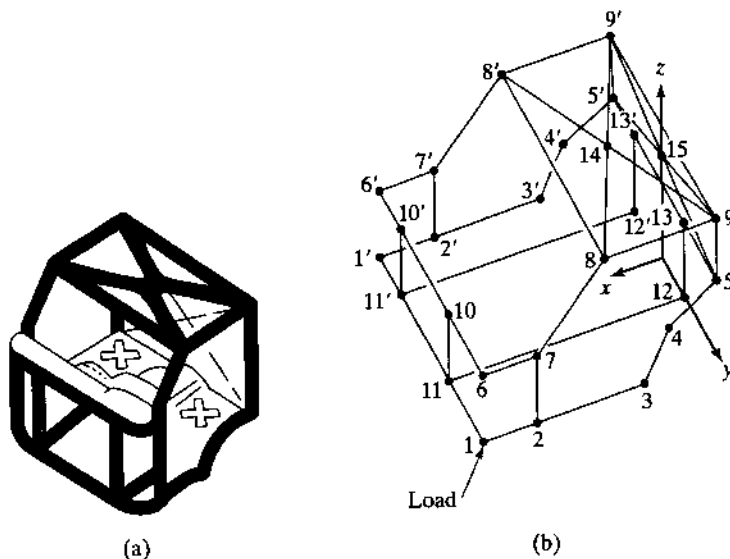
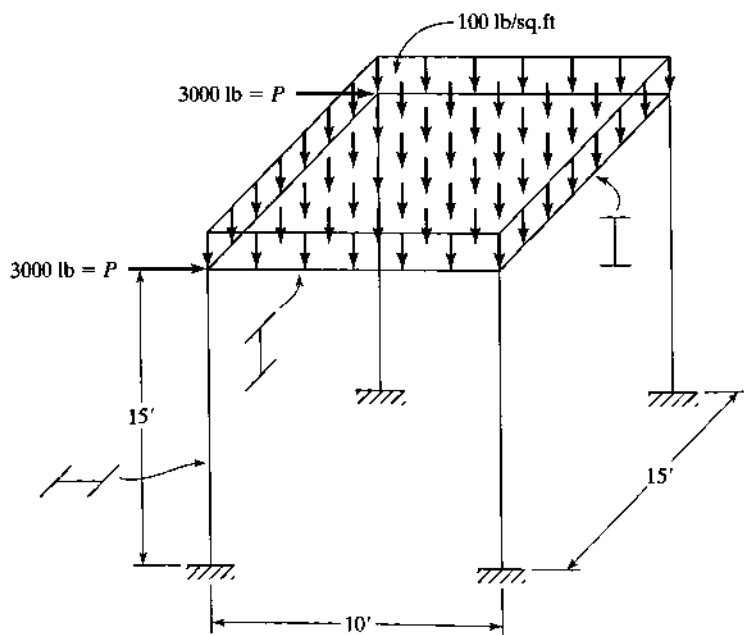


FIGURE P8.13 (a) Van Frame. (b) Frame finite element model.

8.14. Consider the steel frame in Figure P8.14, which is subjected to a wind load and roof load as shown. Determine the bending moments in the structure (maximum M_y and M_z).



| | Area (in. ²) | I_y (in. ⁴) | I_z (in. ⁴) | J (in. ⁴) |
|---------|-----------------------------|------------------------------|------------------------------|----------------------------|
| Columns | 6.0 | 3.75 | 51.0 | 0.24 |
| Beams | 3.0 | 1.26 | 17.0 | 0.08 |

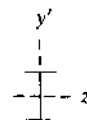


FIGURE P8.14

Program Listings

```

*****
!*          PROGRAM BEAM          *
!*          Beam Bending Analysis *
!* T.R.Chandrupatia and A.D.Belegundu *
*****
\===== MAIN PROGRAM =====
Private Sub cmdStart_Click()
    Call InputData
    Call Bandwidth
    Call Stiffness
    Call ModifyForBC
    Call BandSolver
    Call ReactionCalc
    Call Output
    cmdView.Enabled = True
    cmdStart.Enabled = False
End Sub

```

```

\===== ELEMENT STIFFNESS AND ASSEMBLY =====
Private Sub Stiffness()
    ReDim S(NQ, NBW)
    '----- Global Stiffness Matrix -----
    For N = 1 To NE
        picBox.Print "Forming Stiffness Matrix of Element "; N
        N1 = NOC(N, 1)
        N2 = NOC(N, 2)
        M = MAT(N)
        EL = Abs(X(N1) - X(N2))
        EIL = PM(M, 1) * SMI(N) / EL ^ 3
        '----- Element Stiffness Matrix -----
        SE(1, 1) = 12 * EIL
        SE(1, 2) = EIL * 6 * EL
        SE(1, 3) = -12 * EIL
        SE(1, 4) = EIL * 6 * EL
        SE(2, 1) = SE(1, 2)
        SE(2, 2) = EIL * 4 * EL * EL
        SE(2, 3) = -EIL * 6 * EL
        SE(2, 4) = EIL * 2 * EL * EL
        SE(3, 1) = SE(1, 3)
        SE(3, 2) = SE(2, 3)
        SE(3, 3) = EIL * 12
        SE(3, 4) = -EIL * 6 * EL
        SE(4, 1) = SE(1, 4)
        SE(4, 2) = SE(2, 4)
        SE(4, 3) = SE(3, 4)
        SE(4, 4) = EIL * 4 * EL * EL
        picBox.Print ".... Placing in Global Locations"
        Call PlaceGlobal(N)
    Next N
End Sub
\=====

```

```

***** PROGRAM FRAME2D *****
*      2-D FRAME ANALYSIS BY FEM      *
* T.R.Chandrupatla and A.D.Belegundu *
*****
\===== MAIN PROGRAM =====
Private Sub cmdStart_Click()
    Call InputData
    Call Bandwidth
    Call Stiffness
    Call AddLoads
    Call ModifyForBC
    Call BandSolver
    Call EndActions
    Call ReactionCalc
    Call Output
    cmdView.Enabled = True
    cmdStart.Enabled = False
End Sub
\=====

```

```

\===== ELEMENT STIFFNESS AND ASSEMBLY =====
Private Sub Stiffness()
    ReDim S(NQ, NBW)
    '----- Global Stiffness Matrix -----
    For N = 1 To NE
        picBox.Print "Forming Stiffness Matrix of Element "; N
        ISTF = 2
        Call Elstif(N)
        picBox.Print "... Placing in Global Locations"
        Call PlaceGlobal(N)
    Next N
End Sub

```

```

\===== ELEMENT STIFFNESS =====
Private Sub Elstif(N)
    '----- Element Stiffness Matrix -----
    I1 = NOC(N, 1): I2 = NOC(N, 2): M = MAT(N)
    X21 = X(I2, 1) - X(I1, 1)
    Y21 = X(I2, 2) - X(I1, 2)
    EL = Sqr(X21 * X21 + Y21 * Y21)
    EAL = PM(M, 1) * ARIN(N, 1) / EL
    EIZL = PM(M, 1) * ARIN(N, 2) / EL
    For I = 1 To 6
        For J = 1 To 6
            SEP(I, J) = 0!
        Next J
    Next I
Next I

```

continued

```

SEP(1, 1) = EAL: SEP(1, 4) = -EAL: SEP(4, 4) = EAL
SEP(2, 2) = 12 * EIZL / EL ^ 2: SEP(2, 3) = 6 * EIZL / EL
SEP(2, 5) = -SEP(2, 2): SEP(2, 6) = SEP(2, 3)
SEP(3, 3) = 4 * EIZL: SEP(3, 5) = -6 * EIZL / EL: SEP(3, 6) = 2 * EIZL
SEP(5, 5) = 12 * EIZL / EL ^ 2: SEP(5, 6) = -6 * EIZL / EL
SEP(6, 6) = 4 * EIZL
For I = 1 To 6
For J = 1 To 6
    SEP(J, I) = SEP(I, J)
Next J: Next I
'----- CONVERT ELEMENT STIFFNESS MATRIX TO GLOBAL SYSTEM
DCOS(1, 1) = X21 / EL: DCOS(1, 2) = Y21 / EL: DCOS(1, 3) = 0
DCOS(2, 1) = -DCOS(1, 2): DCOS(2, 2) = DCOS(1, 1): DCOS(2, 3) = 0
DCOS(3, 1) = 0: DCOS(3, 2) = 0: DCOS(3, 3) = 1
For I = 1 To 6
For J = 1 To 6
    ALAMBDA(I, J) = 0!
Next J: Next I
For K = 1 To 2
    IK = 3 * (K - 1)
    For I = 1 To 3
    For J = 1 To 3
        ALAMBDA(I + IK, J + IK) = DCOS(I, J)
    Next J: Next I
Next K
If ISTF = 1 Then Exit Sub
For I = 1 To 6
For J = 1 To 6
    SE(I, J) = 0
    For K = 1 To 6
        SE(I, J) = SE(I, J) + SEP(I, K) * ALAMBDA(K, J)
    Next K
Next J: Next I
For I = 1 To 6: For J = 1 To 6: SEP(I, J) = SE(I, J): Next J: Next I
For I = 1 To 6: For J = 1 To 6: SE(I, J) = 0
For K = 1 To 6
    SE(I, J) = SE(I, J) + ALAMBDA(K, I) * SEP(K, J)
Next K
Next J: Next I
End Sub

```

```

'===== LOADS DUE TO UNIFORMLY DISTRIBUTED LOAD =====
Private Sub AddLoads()
'----- Loads due to uniformly distributed load on element
For N = 1 To NE
If Abs(UDL(N)) > 0 Then
    ISTF = 1
    Call Elstif(N)
    I1 = NOC(N, 1): I2 = NOC(N, 2)
    X21 = X(I2, 1) - X(I1, 1): Y21 = X(I2, 2) - X(I1, 2)
    EL = Sqr(X21 * X21 + Y21 * Y21)

```


continued

```

ED(1) = 0: ED(4) = 0
ED(2) = UDL(N) * EL / 2: ED(5) = ED(2)
ED(3) = UDL(N) * EL ^ 2 / 12: ED(6) = -ED(3)
For I = 1 To 6
  EDP(I) = 0
  For K = 1 To 6
    EDP(I) = EDP(I) + ALAMBDA(K, I) * ED(K)
  Next K
Next I
For I = 1 To 3
  F(3 * I1 - 3 + I) = F(3 * I1 - 3 + I) + EDP(I)
  F(3 * I2 - 3 + I) = F(3 * I2 - 3 + I) + EDP(I + 3)
Next I
End If
Next N
End Sub

```

```

===== MEMBER END FORCES =====
Private Sub EndActions()
  ReDim EF(NE, 6)
  '----- Calculating Member End-Forces
  For N = 1 To NE
    ISTF = 1
    Call Elstif(N)
    I1 = NOC(N, 1): I2 = NOC(N, 2)
    For I = 1 To 3
      ED(I) = F(3 * I1 - 3 + I): ED(I + 3) = F(3 * I2 - 3 + I)
    Next I
    For I = 1 To 6: EDP(I) = 0
      For K = 1 To 6
        EDP(I) = EDP(I) + ALAMBDA(I, K) * ED(K)
      Next K: Next I
    '----- END FORCES DUE TO DISTRIBUTED LOADS
    If Abs(UDL(N)) > 0 Then
      ED(1) = 0: ED(4) = 0: ED(2) = -UDL(N) * EL / 2: ED(5) = ED(2)
      ED(3) = -UDL(N) * EL ^ 2 / 12: ED(6) = -ED(3)
    Else
      For K = 1 To 6: ED(K) = 0: Next K
    End If
    For I = 1 To 6 : EF(N, I) = ED(I)
      For K = 1 To 6
        EF(N, I) = EF(N, I) + SEP(I, K) * EDP(K)
      Next K: Next I
    Next N
  End Sub

```

```

***** PROGRAM FRAME3D *****
* 3-D FRAME ANALYSIS BY FEM *
* T.R.Chandrupatla and A.D.Belegundu *
*****
===== MAIN PROGRAM =====
Private Sub cmdStart_Click()

```

```

Call InputData
Call Bandwidth
Call Stiffness
Call AddLoads
Call ModifyForBC
Call BandSolver
Call EndActions
Call ReactionCalc
Call Output
cmdView.Enabled = True
cmdStart.Enabled = False
End Sub
=====

```

```

===== ELEMENT STIFFNESS AND ASSEMBLY =====
Private Sub Stiffness()
  ReDim S(NQ, NBW)
  '----- Global Stiffness Matrix -----
  For N = 1 To NE
    picBox.Print "Forming Stiffness Matrix of Element "; N
    ISTF = 2
    Call Elstif(N)
    picBox.Print ".... Placing in Global Locations"
    Call PlaceGlobal(N)
  Next N
End Sub
=====

```

```

===== ELEMENT STIFFNESS =====
Private Sub Elstif(N)
  '----- Element Stiffness Matrix -----
  I1 = NOC(N, 1): I2 = NOC(N, 2): I3 = NOC(N, 3): M = MAT(N)
  X21 = X(I2, 1) - X(I1, 1)
  Y21 = X(I2, 2) - X(I1, 2)
  Z21 = X(I2, 3) - X(I1, 3)
  EL = Sqr(X21 * X21 + Y21 * Y21 + Z21 * Z21)
  EAL = PM(M, 1) * ARIN(N, 1) / EL
  EIYL = PM(M, 1) * ARIN(N, 2) / EL: EIZL = PM(M, 1) * ARIN(N, 3) / EL
  GJL = PM(M, 2) * ARIN(N, 4) / EL
  For I = 1 To 12
    For J = 1 To 12
      SEP(I, J) = 0!
    Next J: Next I
  SEP(1, 1) = EAL: SEP(1, 7) = -EAL: SEP(7, 7) = EAL
  SEP(4, 4) = GJL: SEP(4, 10) = -GJL: SEP(10, 10) = GJL
  SEP(2, 2) = 12 * EIZL / EL ^ 2: SEP(2, 6) = 6 * EIZL / EL
  SEP(2, 8) = -SEP(2, 2): SEP(2, 12) = SEP(2, 6)
  SEP(3, 3) = 12 * EIYL / EL ^ 2: SEP(3, 5) = -6 * EIYL / EL
  SEP(3, 9) = -SEP(3, 3): SEP(3, 11) = SEP(3, 5)
  SEP(5, 5) = 4 * EIYL: SEP(5, 9) = 6 * EIYL / EL: SEP(5, 11) = 2 * EIYL

```

continued

```

SEP(6, 6) = 4 * EIZL: SEP(6, 8) = -6 * EIZL / EL: SEP(6, 12) = 2 * EIZL
SEP(8, 8) = 12 * EIZL / EL ^ 2: SEP(8, 12) = -6 * EIZL / EL
SEP(9, 9) = 12 * EIYL / EL ^ 2: SEP(9, 11) = 6 * EIYL / EL
SEP(11, 11) = 4 * EIYL: SEP(12, 12) = 4 * EIZL
For I = 1 To 12
  For J = I To 12
    SEP(J, I) = SEP(I, J)
  Next J: Next I
'--- CONVERT ELEMENT STIFFNESS MATRIX TO GLOBAL SYSTEM
DCOS(1, 1) = X21 / EL: DCOS(1, 2) = Y21 / EL: DCOS(1, 3) = Z21 / EL
EIP1 = X(I3, 1) - X(I1, 1): EIP2 = X(I3, 2) - X(I1, 2)
EIP3 = X(I3, 3) - X(I1, 3)
C1 = DCOS(1, 2) * EIP3 - DCOS(1, 3) * EIP2
C2 = DCOS(1, 3) * EIP1 - DCOS(1, 1) * EIP3
C3 = DCOS(1, 1) * EIP2 - DCOS(1, 2) * EIP1
CC = Sqr(C1 * C1 + C2 * C2 + C3 * C3)
DCOS(3, 1) = C1 / CC: DCOS(3, 2) = C2 / CC: DCOS(3, 3) = C3 / CC
DCOS(2, 1) = DCOS(3, 2) * DCOS(1, 3) - DCOS(1, 2) * DCOS(3, 3)
DCOS(2, 2) = DCOS(1, 1) * DCOS(3, 3) - DCOS(3, 1) * DCOS(1, 3)
DCOS(2, 3) = DCOS(3, 1) * DCOS(1, 2) - DCOS(1, 1) * DCOS(3, 2)
For I = 1 To 12: For J = 1 To 12
  ALAMBDA(I, J) = 0!
Next J: Next I
For K = 1 To 4
  IK = 3 * (K - 1)
  For I = 1 To 3
    For J = 1 To 3
      ALAMBDA(I + IK, J + IK) = DCOS(I, J)
    Next J: Next I
Next K
If ISTF = 1 Then Exit Sub
For I = 1 To 12
  For J = 1 To 12
    SE(I, J) = 0
    For K = 1 To 12
      SE(I, J) = SE(I, J) + SEP(I, K) * ALAMBDA(K, J)
    Next K
  Next J: Next I
For I = 1 To 12: For J = 1 To 12: SEP(I, J) = SE(I, J): Next J: Next I
For I = 1 To 12
  For J = 1 To 12
    SE(I, J) = 0
    For K = 1 To 12
      SE(I, J) = SE(I, J) + ALAMBDA(K, I) * SEP(K, J)
    Next K
  Next J: Next I
End Sub

```

```

===== LOADS DUE TO UNIFORMLY DISTRIBUTED LOAD =====
Private Sub AddLoads()
'----- Loads due to uniformly distributed load on element
For N = 1 To NE
If Abs(UDL(N, 1)) > 0 Or Abs(UDL(N, 2)) > 0 Then
ISTF = 1
Call Elstif(N)
I1 = NOC(N, 1): I2 = NOC(N, 2)
X21 = X(I2, 1) - X(I1, 1)
Y21 = X(I2, 2) - X(I1, 2)
Z21 = X(I2, 3) - X(I1, 3)
EL = Sqr(X21 * X21 + Y21 * Y21 + Z21 * Z21)
ED(1) = 0: ED(4) = 0: ED(7) = 0: ED(10) = 0
ED(2) = UDL(N, 1) * EL / 2: ED(8) = ED(2)
ED(6) = UDL(N, 1) * EL ^ 2 / 12: ED(12) = -ED(6)
ED(3) = UDL(N, 2) * EL / 2: ED(9) = ED(3)
ED(5) = -UDL(N, 2) * EL ^ 2 / 12: ED(11) = -ED(5)
For I = 1 To 12
EDP(I) = 0
For K = 1 To 12
EDP(I) = EDP(I) + ALAMBDA(K, I) * ED(K)
Next K
Next I
For I = 1 To 6
F(6 * I1 - 6 + I) = F(6 * I1 - 6 + I) + EDP(I)
F(6 * I2 - 6 + I) = F(6 * I2 - 6 + I) + EDP(I + 6)
Next I
End If
Next N
End Sub

```

```

===== MEMBER END FORCES =====
Private Sub EndActions()
ReDim EF(NE, 12)
'----- Calculating Member End-Forces
For N = 1 To NE
ISTF = 1
Call Elstif(N)
I1 = NOC(N, 1): I2 = NOC(N, 2)
For I = 1 To 6
ED(I) = F(6 * I1 - 6 + I): ED(I + 6) = F(6 * I2 - 6 + I)
Next I
For I = 1 To 12
EDP(I) = 0
For K = 1 To 12
EDP(I) = EDP(I) + ALAMBDA(I, K) * ED(K)
Next K
Next I

```

continued

```

'--- END FORCES DUE TO DISTRIBUTED LOADS
  If Abs(UDL(N, 1)) > 0 Or Abs(UDL(N, 2)) > 0 Then
    ED(1) = 0: ED(4) = 0: ED(7) = 0: ED(10) = 0
    ED(2) = -UDL(N, 1) * EL / 2: ED(8) = ED(2)
    ED(6) = -UDL(N, 1) * EL ^ 2 / 12: ED(12) = -ED(6)
    ED(3) = -UDL(N, 2) * EL / 2: ED(9) = ED(3)
    ED(5) = UDL(N, 2) * EL ^ 2 / 12: ED(11) = -ED(5)
  Else
    For K = 1 To 12: ED(K) = 0: Next K
  End If
  For I = 1 To 12
    EF(N, I) = ED(I)
    For K = 1 To 12
      EF(N, I) = EF(N, I) + SEP(I, K) * EDP(K)
    Next K
  Next I
Next N
End Sub

```

Three-Dimensional Problems in Stress Analysis

9.1 INTRODUCTION

Most engineering problems are three dimensional. So far, we have studied the possibilities of finite element analysis of simplified models, where rod elements, constant-strain triangles, axisymmetric elements, beams, and so on give reasonable results. In this chapter, we deal with the formulation of three-dimensional stress-analysis problems. The four-node tetrahedral element is presented in detail. Problem modeling and brick elements are also discussed. In addition, frontal solution method is introduced.

We recall from the formulation given in Chapter 1 that

$$\mathbf{u} = [u, v, w]^T \quad (9.1)$$

where u , v , and w are displacements in the x , y , and z directions, respectively. The stresses and strains are given by

$$\boldsymbol{\sigma} = [\sigma_x, \sigma_y, \sigma_z, \tau_{yz}, \tau_{xz}, \tau_{xy}]^T \quad (9.2)$$

$$\boldsymbol{\epsilon} = [\epsilon_x, \epsilon_y, \epsilon_z, \gamma_{yz}, \gamma_{xz}, \gamma_{xy}]^T \quad (9.3)$$

The stress-strain relations are given by

$$\boldsymbol{\sigma} = \mathbf{D}\boldsymbol{\epsilon} \quad (9.4)$$

where \mathbf{D} is a (6×6) symmetric matrix. For isotropic materials, \mathbf{D} is given by Eq. 1.15.

The strain-displacement relations are given by

$$\boldsymbol{\epsilon} = \left[\frac{\partial u}{\partial x}, \frac{\partial v}{\partial y}, \frac{\partial w}{\partial z}, \frac{\partial v}{\partial z} + \frac{\partial w}{\partial y}, \frac{\partial u}{\partial z} + \frac{\partial w}{\partial x}, \frac{\partial u}{\partial y} + \frac{\partial v}{\partial x} \right]^T \quad (9.5)$$

The body force and traction vectors are given by

$$\mathbf{f} = [f_x, f_y, f_z]^T \quad (9.6)$$

$$\mathbf{T} = [T_x, T_y, T_z]^T \quad (9.7)$$

The total potential and the Galerkin/virtual work form for three dimensions are given in Chapter 1.

9.2 FINITE ELEMENT FORMULATION

We divide the volume into four-node tetrahedra. Each node is assigned a number and the x -, y -, and z -coordinates are read in. A typical element e is shown in Fig. 9.1. The connectivity may be defined as shown in Table 9.1.

For each local node i we assign the three degrees of freedom q_{3i-2} , q_{3i-1} , and q_{3i} , and for the corresponding global node I , we assign Q_{3I-2} , Q_{3I-1} , Q_{3I} . Thus, the element and global displacement vectors are

$$\mathbf{q} = [q_1, q_2, q_3, \dots, q_{12}]^T \quad (9.8)$$

$$\mathbf{Q} = [Q_1, Q_2, Q_3, \dots, Q_N]^T \quad (9.9)$$

where N is the total number of degrees of freedom for the structure, three per node. We define four Lagrange-type shape functions N_1 , N_2 , N_3 , and N_4 , where shape function N_i has a value of 1 at node i and is zero at the other three nodes. Specifically, N_1 is 0 at

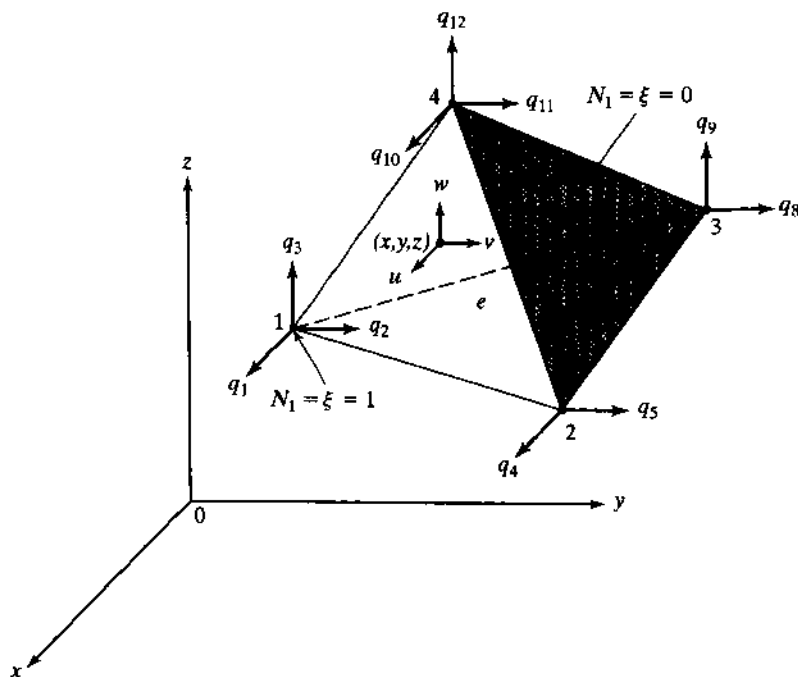


FIGURE 9.1 Tetrahedral element.

TABLE 9.1 Connectivity

| Element No. | Nodes | | | |
|-------------|-------|-----|-----|-----|
| | 1 | 2 | 3 | 4 |
| e | I | J | K | L |

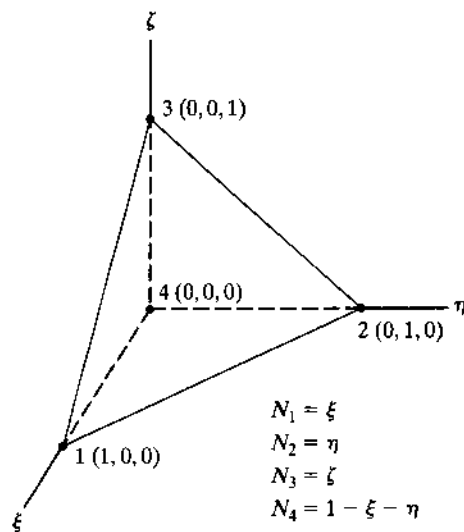


FIGURE 9.2 Master element for shape functions.

nodes 2, 3, and 4 and linearly increases to 1 at node 1. Using the master element shown in Fig. 9.2, we can define the shape functions as

$$N_1 = \xi \quad N_2 = \eta \quad N_3 = \zeta \quad N_4 = 1 - \xi - \eta - \zeta \quad (9.10)$$

The displacements u , v , and w at \mathbf{x} can be written in terms of the unknown nodal values as

$$\mathbf{u} = \mathbf{N}\mathbf{q} \quad (9.11)$$

where

$$\mathbf{N} = \begin{bmatrix} N_1 & 0 & 0 & N_2 & 0 & 0 & N_3 & 0 & 0 & N_4 & 0 & 0 \\ 0 & N_1 & 0 & 0 & N_2 & 0 & 0 & N_3 & 0 & 0 & N_4 & 0 \\ 0 & 0 & N_1 & 0 & 0 & N_2 & 0 & 0 & N_3 & 0 & 0 & N_4 \end{bmatrix} \quad (9.12)$$

It is easy to see that the shape functions given by Eq. 9.10 can be used to define the coordinates x , y , and z of the point at which the displacements u , v , and w are interpolated. The isoparametric transformation is given by

$$\begin{aligned} x &= N_1 x_1 + N_2 x_2 + N_3 x_3 + N_4 x_4 \\ y &= N_1 y_1 + N_2 y_2 + N_3 y_3 + N_4 y_4 \\ z &= N_1 z_1 + N_2 z_2 + N_3 z_3 + N_4 z_4 \end{aligned} \quad (9.13)$$

which, on substituting for N_i from Eq. 9.10 and using the notation $x_{ij} = x_i - x_j$, $y_{ij} = y_i - y_j$, $z_{ij} = z_i - z_j$, yields

$$\begin{aligned} x &= x_4 + x_{14}\xi + x_{24}\eta + x_{34}\zeta \\ y &= y_4 + y_{14}\xi + y_{24}\eta + y_{34}\zeta \\ z &= z_4 + z_{14}\xi + z_{24}\eta + z_{34}\zeta \end{aligned} \quad (9.14)$$

Using the chain rule for partial derivatives, say, of u , we have

$$\begin{pmatrix} \frac{\partial u}{\partial \xi} \\ \frac{\partial u}{\partial \eta} \\ \frac{\partial u}{\partial \zeta} \end{pmatrix} = \mathbf{J} \begin{pmatrix} \frac{\partial u}{\partial x} \\ \frac{\partial u}{\partial y} \\ \frac{\partial u}{\partial z} \end{pmatrix} \quad (9.15)$$

Thus, the partial derivatives with respect to ξ , η , and ζ are related to x , y , and z derivatives by the foregoing relationship. The Jacobian of the transformation is given by

$$\mathbf{J} = \begin{bmatrix} \frac{\partial x}{\partial \xi} & \frac{\partial y}{\partial \xi} & \frac{\partial z}{\partial \xi} \\ \frac{\partial x}{\partial \eta} & \frac{\partial y}{\partial \eta} & \frac{\partial z}{\partial \eta} \\ \frac{\partial x}{\partial \zeta} & \frac{\partial y}{\partial \zeta} & \frac{\partial z}{\partial \zeta} \end{bmatrix} = \begin{bmatrix} x_{14} & y_{14} & z_{14} \\ x_{24} & y_{24} & z_{24} \\ x_{34} & y_{34} & z_{34} \end{bmatrix} \quad (9.16)$$

We note here that

$$\det \mathbf{J} = x_{14}(y_{24}z_{34} - y_{34}z_{24}) + y_{14}(z_{24}x_{34} - z_{34}x_{24}) + z_{14}(x_{24}y_{34} - x_{34}y_{24}) \quad (9.17)$$

The volume of the element is given by

$$V_e = \left| \int_0^1 \int_0^{1-\xi} \int_0^{1-\xi-\eta} \det \mathbf{J} \, d\xi \, d\eta \, d\zeta \right| \quad (9.18)$$

Since $\det \mathbf{J}$ is constant,

$$V_e = |\det \mathbf{J}| \int_0^1 \int_0^{1-\xi} \int_0^{1-\xi-\eta} d\xi \, d\eta \, d\zeta \quad (9.19)$$

Using the polynomial integral formula

$$\int_0^1 \int_0^{1-\xi} \int_0^{1-\xi-\eta} \xi^m \eta^n \zeta^p \, d\xi \, d\eta \, d\zeta = \frac{m! \, n! \, p!}{(m+n+p+3)!} \quad (9.20)$$

we get

$$V_e = \frac{1}{6} |\det \mathbf{J}| \quad (9.21)$$

The inverse relation corresponding to Eq. 9.15 is given by

$$\begin{pmatrix} \frac{\partial u}{\partial x} \\ \frac{\partial u}{\partial y} \\ \frac{\partial u}{\partial z} \end{pmatrix} = \mathbf{A} \begin{pmatrix} \frac{\partial u}{\partial \xi} \\ \frac{\partial u}{\partial \eta} \\ \frac{\partial u}{\partial \zeta} \end{pmatrix} \quad (9.22)$$

where \mathbf{A} is the inverse of the Jacobian matrix \mathbf{J} given in Eq. 9.16:

$$\mathbf{A} = \mathbf{J}^{-1} = \frac{1}{\det \mathbf{J}} \begin{bmatrix} y_{24}z_{34} - y_{34}z_{24} & y_{34}z_{14} - y_{14}z_{34} & y_{14}z_{24} - y_{24}z_{14} \\ z_{24}x_{34} - z_{34}x_{24} & z_{34}x_{14} - z_{14}x_{34} & z_{14}x_{24} - z_{24}x_{14} \\ x_{24}y_{34} - x_{34}y_{24} & x_{34}y_{14} - x_{14}y_{34} & x_{14}y_{24} - x_{24}y_{14} \end{bmatrix} \quad (9.23)$$

Using the strain-displacement relations in Eq. 9.5, the relation between derivatives in x , y , and z and ξ , η , and ζ in Eq. 9.22 and the assumed displacement field $\mathbf{u} = \mathbf{N}\mathbf{q}$ in Eq. 9.11, we get

$$\boldsymbol{\epsilon} = \mathbf{B}\mathbf{q} \quad (9.24)$$

where \mathbf{B} is a (6×12) matrix given by

$$\mathbf{B} = \begin{bmatrix} A_{11} & 0 & 0 & A_{12} & 0 & 0 & A_{13} & 0 & 0 & -\tilde{A}_1 & 0 & 0 \\ 0 & A_{21} & 0 & 0 & A_{22} & 0 & 0 & A_{23} & 0 & 0 & -\tilde{A}_2 & 0 \\ 0 & 0 & A_{31} & 0 & 0 & A_{32} & 0 & 0 & A_{33} & 0 & 0 & -\tilde{A}_3 \\ 0 & A_{31} & A_{21} & 0 & A_{32} & A_{22} & 0 & A_{33} & A_{23} & 0 & -\tilde{A}_3 & -\tilde{A}_2 \\ A_{31} & 0 & A_{11} & A_{32} & 0 & A_{12} & A_{33} & 0 & A_{13} & -\tilde{A}_3 & 0 & -\tilde{A}_1 \\ A_{21} & A_{11} & 0 & A_{22} & A_{12} & 0 & A_{23} & A_{13} & 0 & -\tilde{A}_2 & -\tilde{A}_1 & 0 \end{bmatrix} \quad (9.25)$$

where $\tilde{A}_1 = A_{11} + A_{12} + A_{13}$, $\tilde{A}_2 = A_{21} + A_{22} + A_{23}$, and $\tilde{A}_3 = A_{31} + A_{32} + A_{33}$. All the terms of \mathbf{B} are constants. Thus, Eq. 9.24 gives constant strains after the nodal displacements are calculated.

Element Stiffness

The element strain energy in the total potential is given by

$$\begin{aligned} U_e &= \frac{1}{2} \int_e \boldsymbol{\epsilon}^T \mathbf{D} \boldsymbol{\epsilon} dV \\ &= \frac{1}{2} \mathbf{q}^T \mathbf{B}^T \mathbf{D} \mathbf{B} \mathbf{q} \int_e dV \\ &= \frac{1}{2} \mathbf{q}^T V_e \mathbf{B}^T \mathbf{D} \mathbf{B} \mathbf{q} \\ &= \frac{1}{2} \mathbf{q}^T \mathbf{k}^e \mathbf{q} \end{aligned} \quad (9.26)$$

where the element stiffness matrix \mathbf{k}^e is given by

$$\mathbf{k}^e = V_e \mathbf{B}^T \mathbf{D} \mathbf{B} \quad (9.27)$$

in which V_e is the volume of the element given by $\frac{1}{6} |\det \mathbf{J}|$. In the Galerkin approach, the internal virtual work of the element comes out to be

$$\int_e \boldsymbol{\sigma}^T \boldsymbol{\epsilon}(\phi) dV = \boldsymbol{\psi}^T V_e \mathbf{B}^T \mathbf{D} \mathbf{B} \mathbf{q} \quad (9.28)$$

which gives the element stiffness in Eq. 9.27.

Force Terms

The potential term associated with body force is

$$\int_e \mathbf{u}^T \mathbf{f} dV = \mathbf{q}^T \iiint \mathbf{N}^T \mathbf{f} \det \mathbf{J} d\xi d\eta d\zeta \quad (9.29)$$

$$= \mathbf{q}^T \mathbf{f}^e$$

Using the integration formula in Eq. 9.20, we have

$$\mathbf{f}^e = \frac{V_e}{4} [f_x, f_y, f_z, f_x, f_y, f_z, \dots, f_z]^T \quad (9.30)$$

For Eq. 9.30, the element body force vector \mathbf{f}^e is of dimension 12×1 . Note that $V_e f_x$ is the x component of the body force, which is distributed to the degrees of freedom q_1, q_4, q_7 , and q_{10} .

Let us now consider uniformly distributed traction on the boundary surface. The boundary surface of a tetrahedron is a triangle. Without loss of generality, if A_e is the boundary surface on which traction is applied, formed by local nodes 1, 2, and 3, then

$$\int_{A_e} \mathbf{u}^T \mathbf{T} dA = \mathbf{q}^T \int_{A_e} \mathbf{N}^T \mathbf{T} dA = \mathbf{q}^T \mathbf{T}^e \quad (9.31)$$

The element traction load vector is given by

$$\mathbf{T}^e = \frac{A_e}{3} [T_x, T_y, T_z, T_x, T_y, T_z, T_x, T_y, T_z, 0, 0, 0] \quad (9.32)$$

The stiffnesses and forces are gathered into global locations using element connectivity. Point loads are added into proper locations of the force vector. Boundary conditions are considered using penalty or other approaches. The energy and Galerkin approaches yield the set of equations

$$\mathbf{KQ} = \mathbf{F} \quad (9.33)$$

9.3 STRESS CALCULATIONS

After these equations are solved, the element nodal displacements \mathbf{q} can be obtained. Since $\boldsymbol{\sigma} = \mathbf{D}\boldsymbol{\epsilon}$ and $\boldsymbol{\epsilon} = \mathbf{B}\mathbf{q}$, the element stresses are given by

$$\boldsymbol{\sigma} = \mathbf{DBq} \quad (9.34)$$

The three principal stresses can be calculated by using the relationships in Eq. 9.35. The three invariants of the (3×3) stress tensor are

$$I_1 = \sigma_x + \sigma_y + \sigma_z$$

$$I_2 = \sigma_x \sigma_y + \sigma_y \sigma_z + \sigma_x \sigma_z - \tau_{yz}^2 - \tau_{xz}^2 - \tau_{xy}^2 \quad (9.35)$$

$$I_3 = \sigma_x \sigma_y \sigma_z + 2\tau_{yz} \tau_{xz} \tau_{xy} - \sigma_x \tau_{yz}^2 - \sigma_y \tau_{xz}^2 - \sigma_z \tau_{xy}^2$$

We define

$$\begin{aligned}
 a &= \frac{I_1^2}{3} - I_2 \\
 b &= -2\left(\frac{I_1}{3}\right)^3 + \frac{I_1 I_2}{3} - I_3 \\
 c &= 2\sqrt{\frac{a}{3}} \\
 \theta &= \frac{1}{3} \cos^{-1}\left(-\frac{3b}{ac}\right)
 \end{aligned} \tag{9.36}$$

The principal stresses are given by

$$\begin{aligned}
 \sigma_1 &= \frac{I_1}{3} + c \cos \theta \\
 \sigma_2 &= \frac{I_1}{3} + c \cos\left(\theta + \frac{2\pi}{3}\right) \\
 \sigma_3 &= \frac{I_1}{3} + c \cos\left(\theta + \frac{4\pi}{3}\right)
 \end{aligned} \tag{9.37}$$

9.4 MESH PREPARATION

While complex three-dimensional regions can be effectively filled by tetrahedral elements, similar to triangular elements filling a two-dimensional region, it is a tedious affair to carry out manual data preparation. To overcome this, for simple regions, it is easier to divide the regions into eight-node blocks. Consider the master cube shown in Fig. 9.3. The cube can be divided into five tetrahedra, as shown in Fig. 9.4, with the connectivity as given in Table 9.2.

In this division, the first four elements are of equal volume and element 5 has twice the volume of other elements. In this case, care must be taken to match element edges on adjacent blocks.

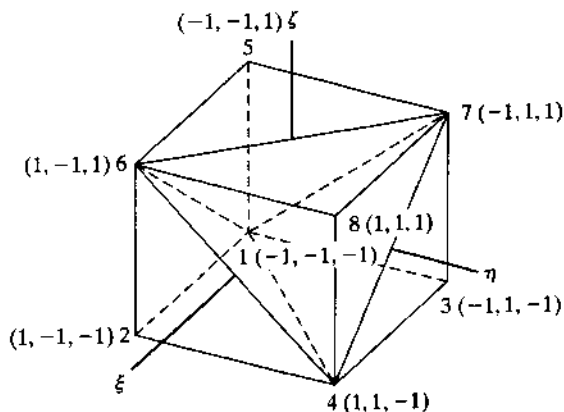


FIGURE 9.3 Cube for tetrahedral division.

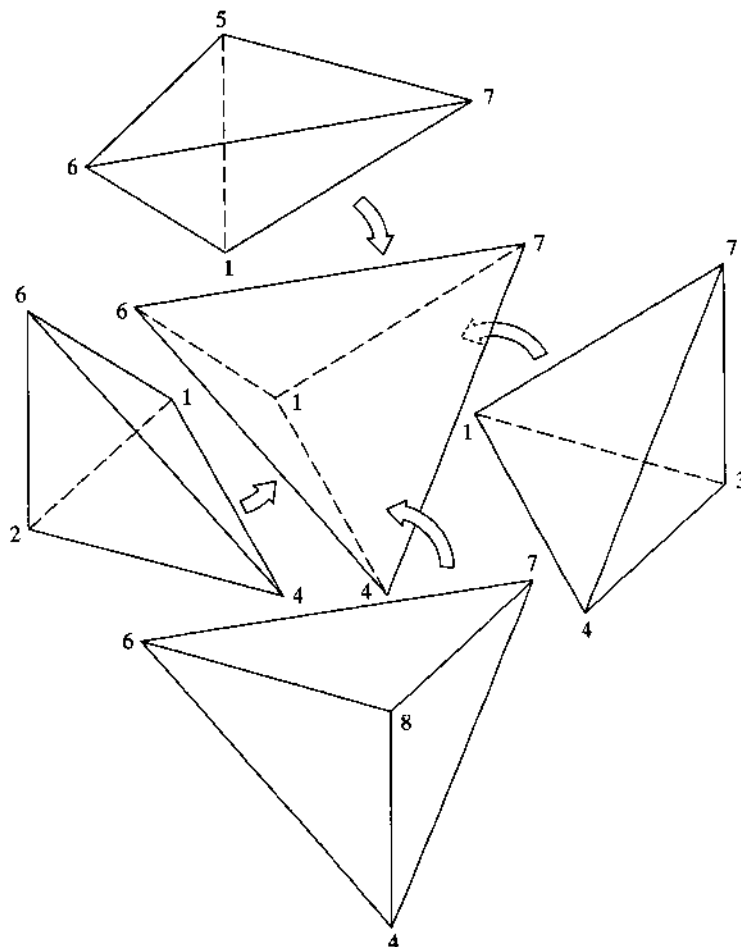


FIGURE 9.4 Division of a cube into five tetrahedra.

TABLE 9.2 Five Tetrahedra

| Element No. | Nodes | | | |
|-------------|-------|---|---|---|
| | 1 | 2 | 3 | 4 |
| 1 | 1 | 4 | 2 | 6 |
| 2 | 1 | 4 | 3 | 7 |
| 3 | 6 | 7 | 5 | 1 |
| 4 | 6 | 7 | 8 | 4 |
| 5 | 1 | 4 | 6 | 7 |

The master cube can also be divided into six elements with equal volume. A typical division is given in Table 9.3. The element division of one-half of the cube is shown in Fig. 9.5. For the division shown in Table 9.3, the same division pattern repeats for adjacent elements.

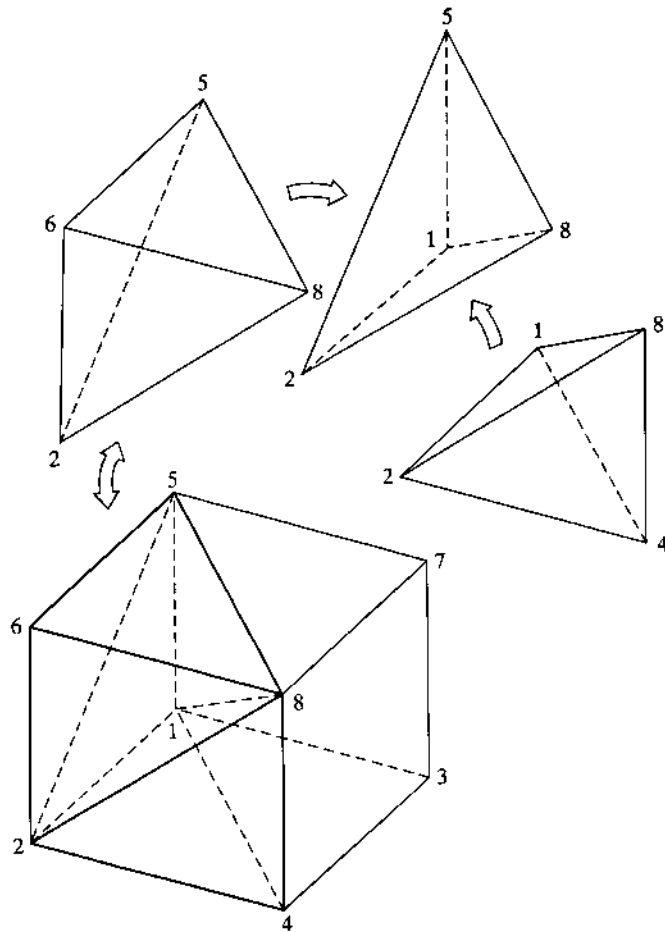


FIGURE 9.5 Division of a cube into six tetrahedra.

TABLE 9.3 Six Tetrahedra

| Element No. | Nodes | | | |
|-------------|-------|---|---|---|
| | 1 | 2 | 3 | 4 |
| 1 | 1 | 2 | 4 | 8 |
| 2 | 1 | 2 | 8 | 5 |
| 3 | 2 | 8 | 5 | 6 |
| 4 | 1 | 3 | 4 | 7 |
| 5 | 1 | 7 | 8 | 5 |
| 6 | 1 | 8 | 4 | 7 |

Use of $\det \mathbf{J}$ in the calculation of \mathbf{B} in Eq. 9.24 and use of $|\det \mathbf{J}|$ in the estimation of element volume V_e enables us to use element node numbers in any order. Among solid elements, this holds for four-node tetrahedra, since every node is connected to the other three. Some codes may still require consistent numbering schemes.

Program TETRA is included in the disk.

Example 9.1

Figure E9.1 shows a four-node tetrahedral object. The coordinate dimensions shown are in inches. The material is steel with $E = 30 \times 10^6$ psi and $\nu = 0.3$. Nodes 2, 3, and 4 are fixed, and a 1000 lb load is applied at node 1 as shown. Determine the displacement of node 1 using a single element.

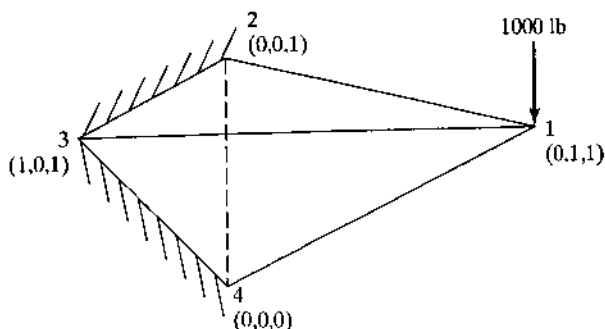


FIGURE E9.1

Solution The Jacobian \mathbf{J} given in Eq. 9.16 is easily calculated using the nodal coordinates:

$$\mathbf{J} = \begin{bmatrix} 0 & 1 & 1 \\ 0 & 0 & 1 \\ 1 & 0 & 1 \end{bmatrix}$$

and $\det \mathbf{J} = 1$. The inverse of the Jacobian, \mathbf{A} , is calculated using Eq. 9.23:

$$\mathbf{A} = \begin{bmatrix} 0 & -1 & 1 \\ 1 & -1 & 0 \\ 0 & 1 & 0 \end{bmatrix}$$

Using the elements of \mathbf{A} , the strain-displacement matrix \mathbf{B} can be evaluated using Eq. 9.25. In the product, $\mathbf{B}\mathbf{q}$, only the first three columns multiply the first three components of \mathbf{q} . The last six components of \mathbf{q} are zero. When we use the strike-off approach in assembling the stiffness matrix $\mathbf{k} = V_e \mathbf{B}^T \mathbf{D} \mathbf{B}$, we need to deal with the first three columns of \mathbf{B} . Partitioning $\mathbf{B} = [\mathbf{B}_1 \mathbf{B}_2]$ with \mathbf{B}_1 representing the first three columns, the modified 3×3 stiffness matrix \mathbf{K} is given by $\mathbf{B}_1^T \mathbf{D} \mathbf{B}_1$. The volume of the element V_e is given by $\frac{1}{6}$.

\mathbf{B}_1 is calculated using the first three columns of \mathbf{B} defined in Eq. 9.25 as

$$\mathbf{B}_1 = \begin{bmatrix} 0 & 0 & 0 \\ 0 & 1 & 0 \\ 0 & 0 & 0 \\ 0 & 0 & 1 \\ 0 & 0 & 0 \\ 1 & 0 & 0 \end{bmatrix}$$

The stress-strain relation matrix \mathbf{D} is evaluated using Eq. 1.15 from Chapter 1:

$$\mathbf{D} = 10^7 \begin{bmatrix} 4.038 & 1.731 & 1.731 & 0 & 0 & 0 \\ 1.731 & 4.038 & 1.731 & 0 & 0 & 0 \\ 1.731 & 1.731 & 4.038 & 0 & 0 & 0 \\ 0 & 0 & 0 & 1.154 & 0 & 0 \\ 0 & 0 & 0 & 0 & 1.154 & 0 \\ 0 & 0 & 0 & 0 & 0 & 1.154 \end{bmatrix}$$

The modified stiffness matrix is given by

$$\mathbf{K} = V_e \mathbf{B}_1^T \mathbf{D} \mathbf{B}_1 = 10^6 \begin{bmatrix} 1.923 & 0 & 0 \\ 0 & 6.731 & 0 \\ 0 & 0 & 1.923 \end{bmatrix}$$

The force vector is $\mathbf{F} = [0 \ 0 \ -1000]^T$. Solving for $\mathbf{KQ} = \mathbf{F}$, we get $\mathbf{Q} = [0 \ 0 \ -.00052]^T$.

We note that for this one-element case, the modified stiffness is a diagonal matrix for the geometry of the problem chosen. ■

9.5 HEXAHEDRAL ELEMENTS AND HIGHER ORDER ELEMENTS

In the hexahedral elements, a consistent node-numbering scheme must be followed for defining the connectivity. For an eight-node hexahedral or brick element, we consider the mapping onto a cube of 2-unit sides placed symmetrically with ξ -, η -, and ζ -coordinates as shown in Fig. 9.6. The corresponding element in two dimensions is the four-node quadrilateral discussed in Chapter 7.

On the master cube, the Lagrange shape functions can be written as

$$N_i = \frac{1}{8} (1 + \xi_i \xi) (1 + \eta_i \eta) (1 + \zeta_i \zeta) \quad i = 1 \text{ to } 8 \quad (9.38)$$

where (ξ_i, η_i, ζ_i) represents the coordinates of node i of the element in the (ξ, η, ζ) system. The element nodal displacements are represented by the vector

$$\mathbf{q} = [q_1, q_2, \dots, q_{24}]^T \quad (9.39)$$

We use the shape functions N_i to define displacements at any point inside the element in terms of its nodal values:

$$\begin{aligned} u &= N_1 q_1 + N_2 q_4 + \dots + N_8 q_{22} \\ v &= N_1 q_2 + N_2 q_5 + \dots + N_8 q_{23} \\ w &= N_1 q_3 + N_2 q_6 + \dots + N_8 q_{24} \end{aligned} \quad (9.40)$$

Also,

$$\begin{aligned} x &= N_1 x_1 + N_2 x_2 + \dots + N_8 x_8 \\ y &= N_1 y_1 + N_2 y_2 + \dots + N_8 y_8 \\ z &= N_1 z_1 + N_2 z_2 + \dots + N_8 z_8 \end{aligned} \quad (9.41)$$

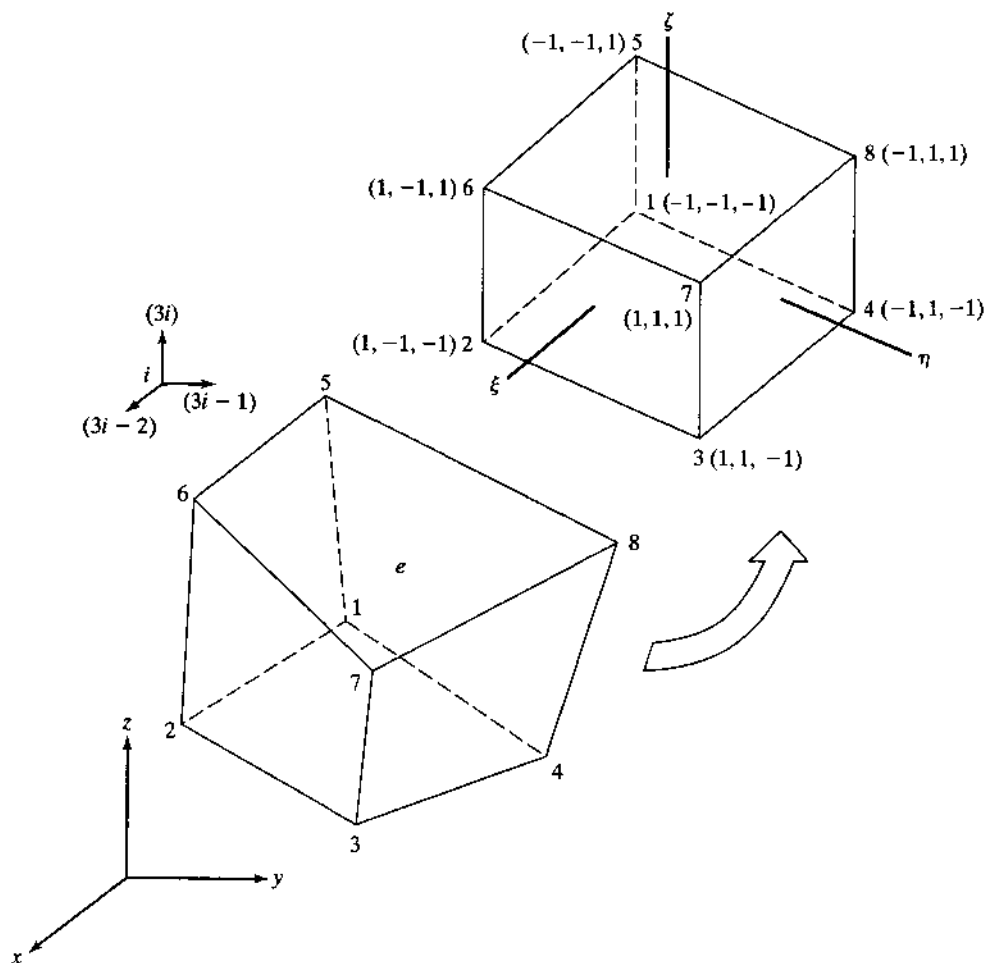


FIGURE 9.6 Hexahedral element.

Following the steps used in the development of the quadrilateral element in Chapter 7, we can get the strains in the form

$$\epsilon = \mathbf{B}q \quad (9.42)$$

The element stiffness matrix is given by

$$\mathbf{k}^e = \int_{-1}^{+1} \int_{-1}^{+1} \int_{-1}^{+1} \mathbf{B}^T \mathbf{D} \mathbf{B} |\det \mathbf{J}| d\xi d\eta d\zeta \quad (9.43)$$

where we have used $dV = |\det \mathbf{J}| d\xi d\eta d\zeta$ and \mathbf{J} is the (3×3) Jacobian matrix. The integration in Eq. 9.43 is performed numerically using Gauss quadrature.

Higher order elements, for example, 10-node tetrahedral elements or 20-node and 27-node hexahedral elements, can be developed using the ideas discussed in Chapter 7. Temperature effect is treated in a very similar manner, as in the case of the quadrilateral in Chapter 7. Program HEXAFRON is included in the disk.

9.6 PROBLEM MODELING

In solving a problem, the first step is to start with a coarse model. The data needed will be nodal coordinates, element nodal connectivity, material properties, constraint conditions, and nodal loads. In the three-dimensional cantilever shown in Fig. 9.7, the geometry and loading conditions demand a three-dimensional model. Element and connectivities can easily be established by defining the four 8-cornered blocks. We can model the first block, near the base of the cantilever, as a hexahedral element with connectivity 2-1-5-6-3-4-8-7. For each subsequent block, the connectivity can be generated by increasing each number in the current set by four. Coordinates of nodes can be generated using the shape functions of Eq. 9.38 for geometry definition. These aspects will be discussed in Chapter 12. Alternatively, each block in the 3-D cantilever can be modeled using tetrahedral elements. For the repeating block pattern shown in Fig. 9.6, the six-element division given in Table 9.3 may be used.

The consideration of boundary conditions follows those presented for one- and two-dimensional problems. However, to give a general idea of constraints and their consideration in finite element analysis, we refer to Fig. 9.8. A point fully restrained is a

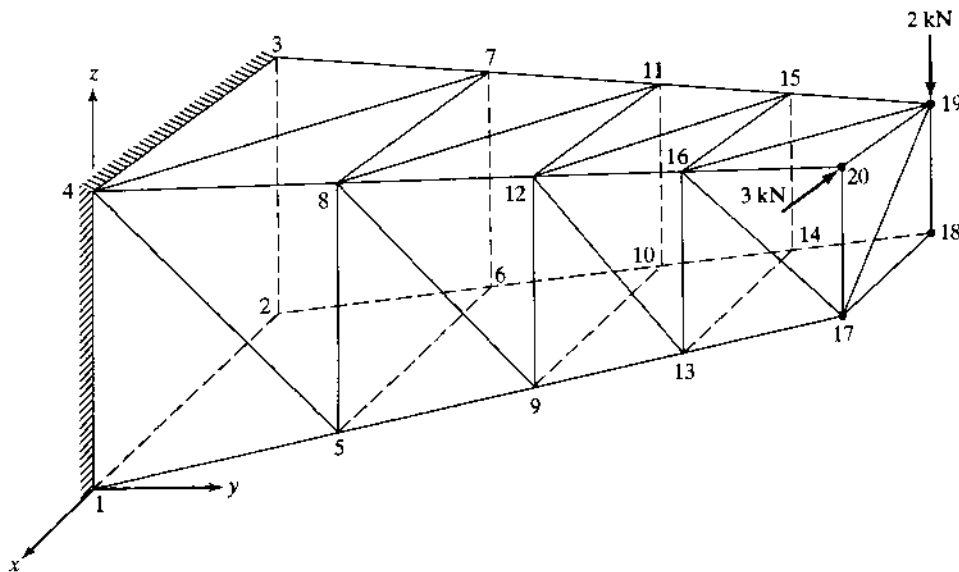


FIGURE 9.7 Three-dimensional elastic body.

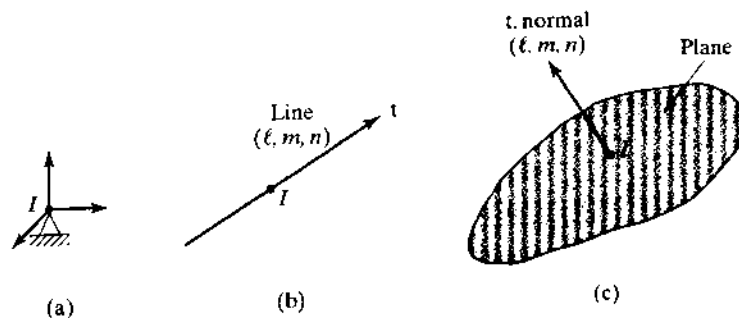


FIGURE 9.8 Nodal constraints: (a) point constraint, (b) line constraint, (c) plane constraint.

point constraint. This is considered by adding a large stiffness C to the diagonal locations corresponding to degrees of freedom of node I . When the node is constrained to move along a line, say, \mathbf{t} , with direction cosines (ℓ, m, n) , the penalty term comes from setting $\mathbf{u} \times \mathbf{t} = \mathbf{0}$. This results in the addition of following stiffness terms when the node is constrained along a line:

$$\begin{array}{l} 3I - 2 \\ 3I - 1 \\ 3I \end{array} \begin{bmatrix} 3I - 2 & 3I - 1 & 3I \\ C(1 - \ell^2) & -C\ell m & -C\ell n \\ & C(1 - m^2) & -Cmn \\ \text{Symmetric} & & C(1 - n^2) \end{bmatrix}$$

When a node is forced to lie on a plane with normal direction \mathbf{t} , shown in Fig. 9.8c, the penalty terms come from $\mathbf{u} \cdot \mathbf{t} = 0$. This requires that the following terms be added to the stiffness matrix:

$$\begin{array}{l} 3I - 2 \\ 3I - 1 \\ 3I \end{array} \begin{bmatrix} 3I - 2 & 3I - 1 & 3I \\ C\ell^2 & C\ell m & C\ell n \\ & C m^2 & C m n \\ \text{Symmetric} & & C n^2 \end{bmatrix}$$

Figure 9.9 shows a pyramid-shaped metal part and its finite element model. We observe here that nodes at A and B are line-constrained and nodes along C and D are plane-constrained. This discussion should help one to handle the modeling of three-dimensional problems with relative ease.

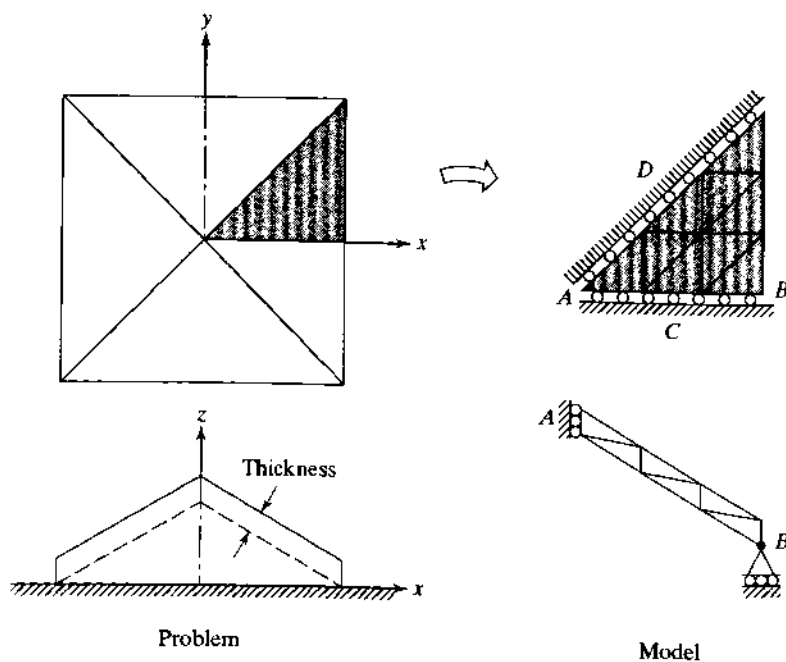
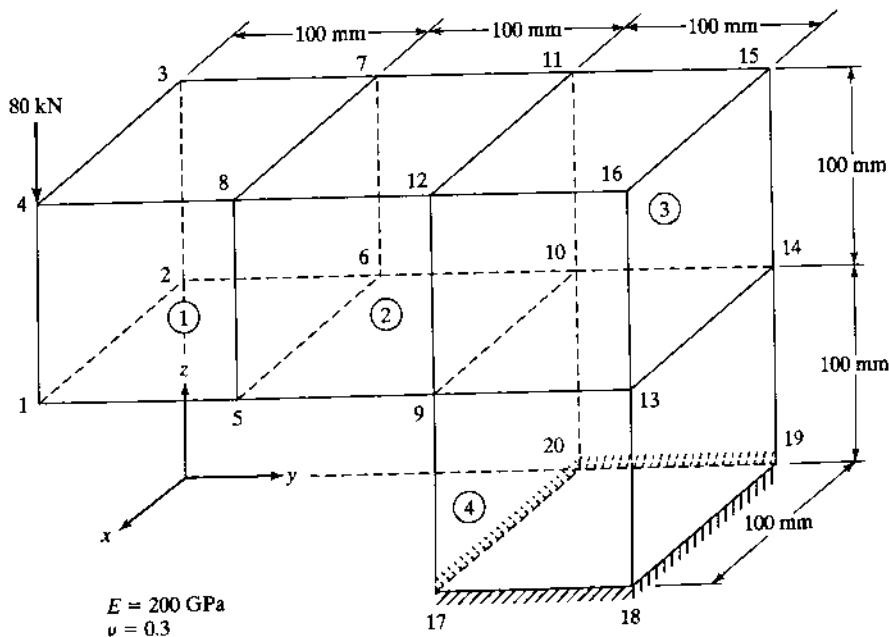


FIGURE 9.9 Metal part with a pyramid surface.

9.7 FRONTAL METHOD FOR FINITE ELEMENT MATRICES

In three-dimensional problems, the size of the stiffness matrix increases rapidly even with the banded method of handling. An alternative direct method that results in considerable saving in the use of computer memory is called the *frontal method*. In this method, the order of element numbering plays a more important role than the order of node numbering. The frontal method relies on the fact that a degree of freedom can be eliminated as soon as all stiffness values in rows and columns for that dof are complete. Irons* observed that all of the dof for a node can be eliminated when it appears for the last time as we assemble in the ascending order of elements. In the example illustrated in Fig. 9.10, nodes 1, 2, 3, and 4 appear for the last time in element 1. The dof corresponding to all these nodes can be eliminated as soon as element 1 is assembled. Once a dof is eliminated, the corresponding equation is no more necessary until backsubstitution. This equation can be written to an external device such as a tape or hard disk for backsubstitution in the



| Element No. | Nodes | | | | | | | | Front Size | |
|-------------|-------|-----|-----|-----|-----|-----|-----|-----|------------|------------|
| | 1 | 2 | 3 | 4 | 5 | 6 | 7 | 8 | Assembled | Eliminated |
| 1 | -1 | -2 | -3 | -4 | 5 | 6 | 7 | 8 | 8 | 4 |
| 2 | -5 | -6 | -7 | -8 | 9 | 10 | 11 | 12 | 8 | 4 |
| 3 | 9 | 10 | -11 | -12 | 13 | 14 | -15 | -16 | 8 | 4 |
| 4 | -9 | -10 | -14 | -13 | -17 | -20 | -19 | -18 | 8 | 0 |

Block size = $8 \times$ dof per node

FIGURE 9.10 Example for frontal method.

*Bruce M. Irons, "A frontal solution program for finite element analysis." *Int. J. for Numerical Methods in Eng.*, Vol. 2, 5-32 (1970).

reverse order. As we assemble an element, the active matrix size grows, and when some degrees of freedom are eliminated, the matrix size shrinks. The active matrix size can be compared to the action of an accordion. The largest block size needed can be determined using a prefront routine that employs a modified element connectivity matrix.

Connectivity and Prefront Routine

The first step is to determine the last appearance of a node. This is simplified by looking for the first appearance of the node as we proceed in the descending order of elements. In the element where this occurs, a negative sign is added to the node number in the connectivity array. The node-number modification is shown in the table in Fig. 9.10 for the hexahedral element example. After this operation is carried out for all the node numbers, we are ready to determine the block size. Let us first evaluate the front size in terms of the number of nodes. At the assembly of the first element, the nodal front size is 8. The dofs corresponding to four nodes are now eliminated. The nodal front size shrinks to 4. The assembly of element 2 adds four new nodes; thus, the front grows to size 8. As seen from the table in Fig. 9.10, the maximum nodal front size is 8, which corresponds to 24 dofs. The block size IBL needed is 24×24 . By the banded storage method, the maximum matrix size for the problem is 60×36 (verify this using bandwidth evaluation). The prefront routine in the program uses a simple algorithm to evaluate this block size. In the actual program, a small modification is introduced to handle multipoint constraints. This aspect is discussed later. First, the stiffness matrix $S(\text{IBL}, \text{IBL})$ is defined. An index array $\text{INDX}(\text{IBL})$, initialized as $\text{INDX}(I)=I$ for $I=1$ to IBL is defined. We also define the global dof array $\text{ISBL}(\text{IBL})$ initialized to all zeros and $\text{IEBL}()$ of size equal to the number of dofs per element. The front size NFRON and number of variables ready for elimination NTOGO are initialized to zero. The element assembly starts at this initial setting.

Element Assembly and Consideration of Specified dof

Consider now the assembly of a new element when NFRON is at some level and all the variables ready for elimination have been eliminated; that is, NTOGO is zero. We consider the dof of each node of an element using connectivity. Consider the j th dof, say, IDF, of an element and, say, the corresponding node is i . The first search is made in the NFRON locations $\text{ISBL}(\text{INDX}(L)), L=1$ to NFRON if the dof IDF is already in the set. If IDF is already in the set at $L=K$, then we set $\text{IEBL}(j)=\text{INDX}(K)$. If IDF is not in the set, then we find the next open location as follows: We set $K=\text{NFRON}+1$ and set $\text{ISBL}(\text{INDX}(K))=\text{IDF}$ and $\text{IEBL}(j)=\text{INDX}(K)$. NFRON is incremented by 1 (that is, set $\text{NFRON}=\text{NFRON}+1$). If node i is negative in the element connectivity, then this dof will be ready for elimination and must be floated into NTOGO. If IDF is a dof that has a specified value, a large penalty number CNST is added into the location $S(\text{INDX}(K), \text{INDX}(K))$, and CNST times the specified value is added into the global force location $F(\text{IDF})$. If $K > \text{NTOGO}$, the floating operation is carried out as follows: The number in $\text{INDX}(\text{NTOGO}+1)$ is exchanged with the number in $\text{INDX}(K)$, and NTOGO is incremented by 1. When all the element dofs are completed, $\text{IEBL}()$ will have the locations in $S()$ where the element stiffness is to be assembled. The element stiffness matrix $\text{SE}()$ is added into the $S()$ locations using $\text{IEBL}()$. The variables in $\text{INDX}(I)$ from $I=1$ to NTOGO are now ready for elimination. The relationships of various arrays used in the assembly process are shown in Fig. 9.11.

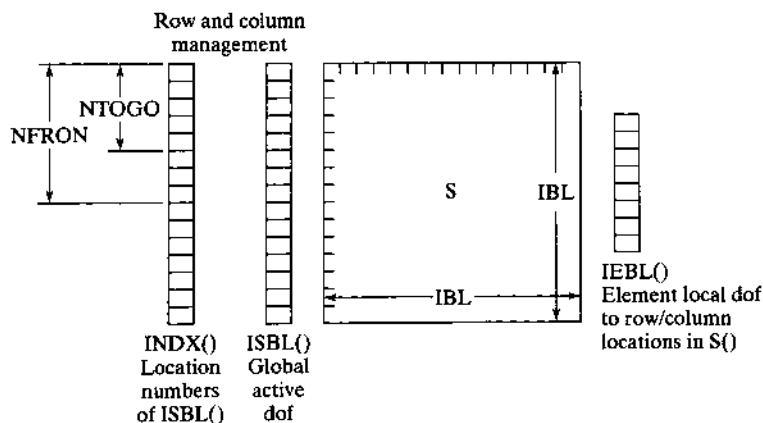


FIGURE 9.11 Stiffness assembly for frontal method.

Elimination of Completed dof

We eliminate the variable in the location $INDX(1)$ by reducing the active equations $INDX(2)$ through $INDX(NFRON)$. The equation $INDX(1)$ is written to the disk by writing the stiffness values and the corresponding dof numbers. In the BASIC program, the data are written to a random-access file. Now $INDX(1)$ is open. A few integer exchange operations are done to simplify the elimination process. First, the number at $INDX(NTOGO)$ is exchanged with the number at $INDX(1)$; then the number at $INDX(NTOGO)$ is exchanged with the number at $INDX(NFRON)$. $NTOGO$ and $NFRON$ are each decremented by 1. Once again, the reduction is carried out from $INDX(2)$ through $INDX(NFRON)$. The process continues for each element until $NTOGO$ is zero or $NFRON$ is 1.

Backsubstitution

Backsubstitution is a straightforward process. In the last equation, there is a stiffness value, a variable number, and the right-hand side. This variable is easily determined. The last but one equation will have two stiffnesses and two variable numbers and the right-hand side. Since one of the variables has already been determined, the other one is calculated and so on. The backsubstitution can even be carried out independently, if needed.

Consideration of Multipoint Constraints

Multipoint constraints of the type $\beta_1 Q_i + \beta_2 Q_j = \beta_0$ are easily considered by treating each constraint as an element of 2 dof. The penalty parameter $CNST$ is determined using the first element diagonal stiffness values. The equivalent element stiffness and right-hand side for the multipoint constraint are, respectively,

$$CNST \begin{bmatrix} \beta_1^2 & \beta_1 \beta_2 \\ \beta_1 \beta_2 & \beta_2^2 \end{bmatrix} \quad \text{and} \quad CNST \begin{bmatrix} \beta_1 \beta_0 \\ \beta_2 \beta_0 \end{bmatrix}$$

In the implementation of this boundary condition, these stiffnesses are first introduced into $S()$ and then the regular element stiffnesses are introduced. The same procedure introduced into the PREFRONT with dofs used instead of node numbers gives the needed block size. Assembly and elimination are then similar to the procedure discussed previously.

Example 9.2

The L-shaped beam shown in Fig. 9.10 is analyzed using program HEXAFRON. The input and output data and the program listing are given below. ■

Input Data File

```

<< PROGRAM HEXAFRON >>
3-D ANALYSIS USING HEXAHEDRAL ELEMENT
NN NE NM NDIM NEN NDN
20 4 1 3 8 3
ND NL NCH NPR NMPC
12 1 1 3 0
Node# X Y Z
1 100 0 100
2 0 0 100
3 0 0 200
4 100 0 200
5 100 100 100
6 0 100 100
7 0 100 200
8 100 100 200
9 100 200 100
10 0 200 100
11 0 200 200
12 100 200 200
13 100 300 100
14 0 300 100
15 0 300 200
16 100 300 200
17 100 200 0
18 100 300 0
19 0 300 0
20 0 200 0
Elem# N1 N2 N3 N4 N5 N6 N7 N8 MAT# Temprise
1 1 2 3 4 5 6 7 8 1 0
2 5 6 7 8 9 10 11 12 1 0
3 9 10 11 12 13 14 15 16 1 0
4 9 10 14 13 17 20 19 18 1 0
DOF# Displacement
49 0
50 0
51 0
52 0
53 0
54 0
55 0
56 0
57 0
58 0
59 0
60 0
DOF# Load
12 -80000
MAT# E Nu Alpha
1 200000 0.3 0
B1 i B2 j B3 (Multi-point constr. B1*Qi+B2*Qj=B3)

```

Program HexaFront - CHANDRUPATLA & BELEGUNDU
Output

3-D ANALYSIS USING HEXAHEDRAL ELEMENT

| NODE# | X-Displ | Y-Displ | Z-Displ |
|-------|-------------|-------------|-------------|
| 1 | -2.1569E-02 | -3.7894E-03 | -4.0983E-01 |
| 2 | -2.5306E-02 | -3.3079E-03 | -3.3229E-01 |
| 3 | 5.7350E-02 | -1.7896E-01 | -3.2676E-01 |
| 4 | 5.7756E-02 | -1.8449E-01 | -4.2780E-01 |
| 5 | -6.8253E-03 | -1.0487E-02 | -2.2309E-01 |
| 6 | -1.0750E-02 | -1.1683E-02 | -1.6711E-01 |
| 7 | 4.9096E-02 | -1.7250E-01 | -1.6707E-01 |
| 8 | 4.2791E-02 | -1.7376E-01 | -2.1738E-01 |
| 9 | 1.3643E-02 | -3.3666E-02 | -4.7867E-02 |
| 10 | -6.0295E-05 | -3.2558E-02 | -2.9338E-02 |
| 11 | 3.2541E-02 | -1.4954E-01 | -3.7397E-02 |
| 12 | 2.7862E-02 | -1.4804E-01 | -6.3003E-02 |
| 13 | 3.6578E-03 | -3.8342E-02 | 2.9087E-02 |
| 14 | 1.1886E-02 | -4.1411E-02 | 3.9684E-02 |
| 15 | 2.6633E-02 | -1.3842E-01 | 5.5799E-02 |
| 16 | 2.0606E-02 | -1.3494E-01 | 3.9583E-02 |
| 17 | 2.8995E-15 | -1.8921E-15 | -1.2335E-14 |
| 18 | -1.6015E-15 | 1.9503E-15 | 5.2437E-15 |
| 19 | 1.6597E-15 | 9.6746E-16 | 8.9381E-15 |
| 20 | -2.9577E-15 | -1.0256E-15 | -8.9381E-15 |

vonMises Stresses at 8 Integration points in ELEM# 1

| | | | |
|------------|------------|------------|------------|
| 2.3359E+01 | 1.5984E+01 | 1.8545E+01 | 4.0582E+01 |
| 2.9929E+01 | 1.7910E+01 | 1.4849E+01 | 4.3396E+01 |

vonMises Stresses at 8 Integration points in ELEM# 2

| | | | |
|------------|------------|------------|------------|
| 3.1416E+01 | 2.6193E+01 | 3.5722E+01 | 2.8272E+01 |
| 6.1174E+01 | 3.8615E+01 | 3.5948E+01 | 5.1608E+01 |

vonMises Stresses at 8 Integration points in ELEM# 3

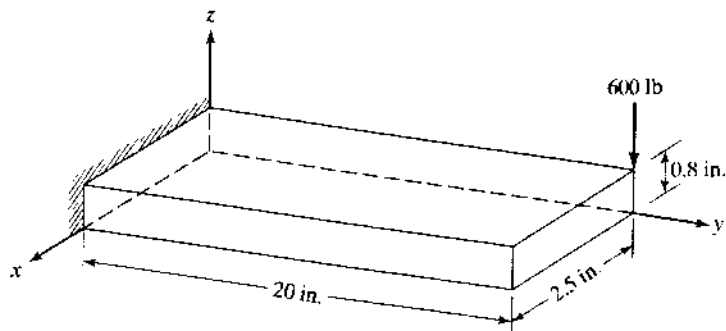
| | | | |
|------------|------------|------------|------------|
| 4.5462E+01 | 5.2393E+01 | 3.4486E+01 | 3.2530E+01 |
| 3.0872E+01 | 4.1090E+01 | 2.6155E+01 | 2.1852E+01 |

vonMises Stresses at 8 Integration points in ELEM# 4

| | | | |
|------------|------------|------------|------------|
| 5.8590E+01 | 4.6398E+01 | 4.8482E+01 | 4.1407E+01 |
| 5.1148E+01 | 3.8853E+01 | 4.9391E+01 | 3.8936E+01 |

PROBLEMS

9.1. Determine the deflections at the corner points of the steel cantilever beam shown in Fig. P9.1.



$$E = 30 \times 10^6 \text{ psi}$$

$$\nu = 0.3$$

FIGURE P9.1

- 9.2. A cast iron hollow member used in a machine tool structure is fixed at one end and loaded at the other, as shown in Fig. P9.2. Find the deflection at the load and maximum principal stresses. Compare the values with the structure without an opening.

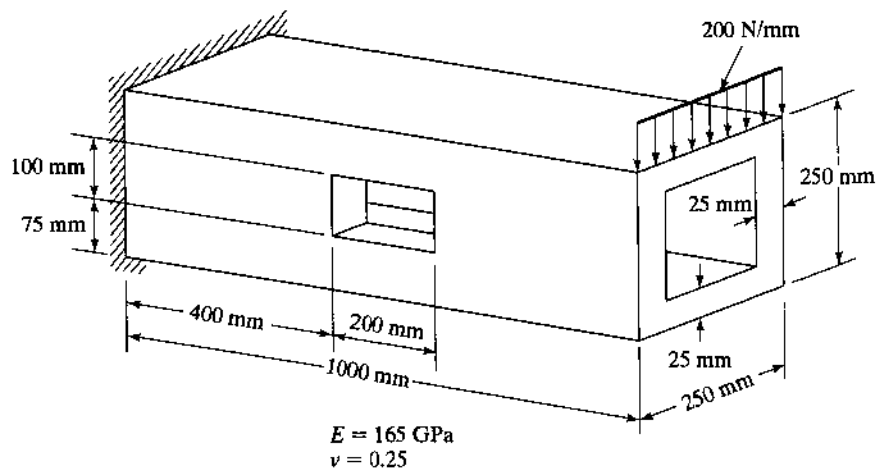


FIGURE P9.2

- 9.3. An S-shaped block used in force measurement is subjected to a load as shown in Fig. P9.3. Determine the amount by which the block is compressed. Take $E = 70\,000 \text{ N/mm}^2$ and $\nu = 0.3$.

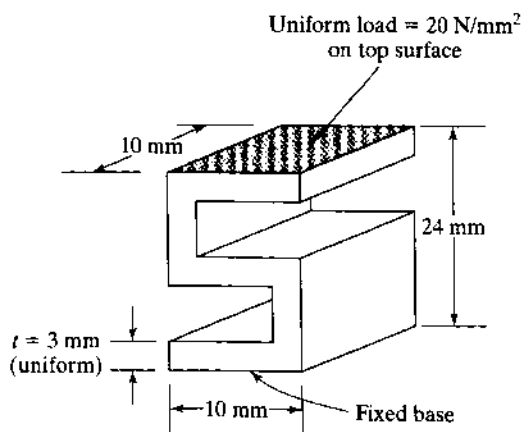


FIGURE P9.3

- 9.4. A device is hydraulically loaded as shown in Fig. P9.4. Plot the deformed configuration and determine the magnitude and location of the maximum principal stresses.

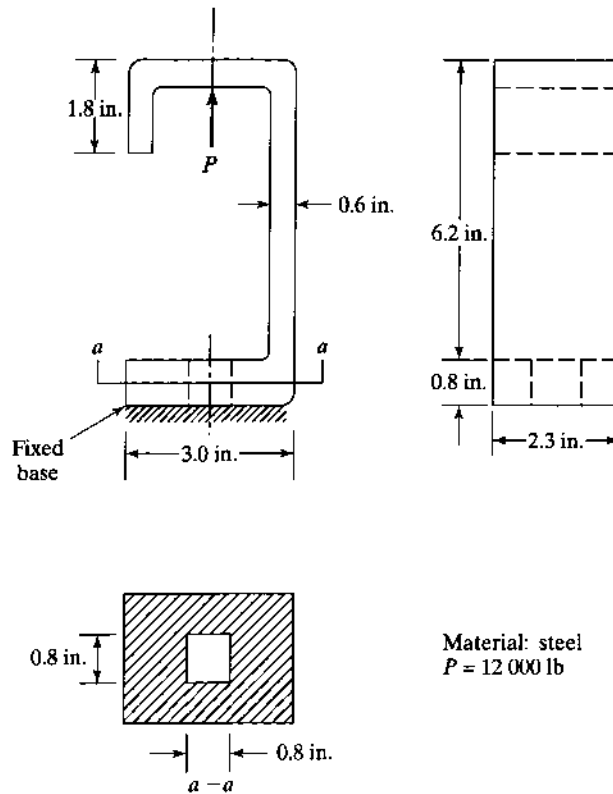


FIGURE P9.4

- 9.5. A portion of the brake pedal in an automobile is modeled as shown in Fig. P9.5. Determine the deflection at the pedal for a 500-N load.

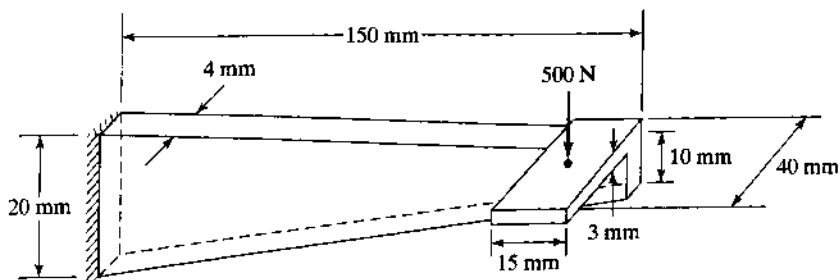
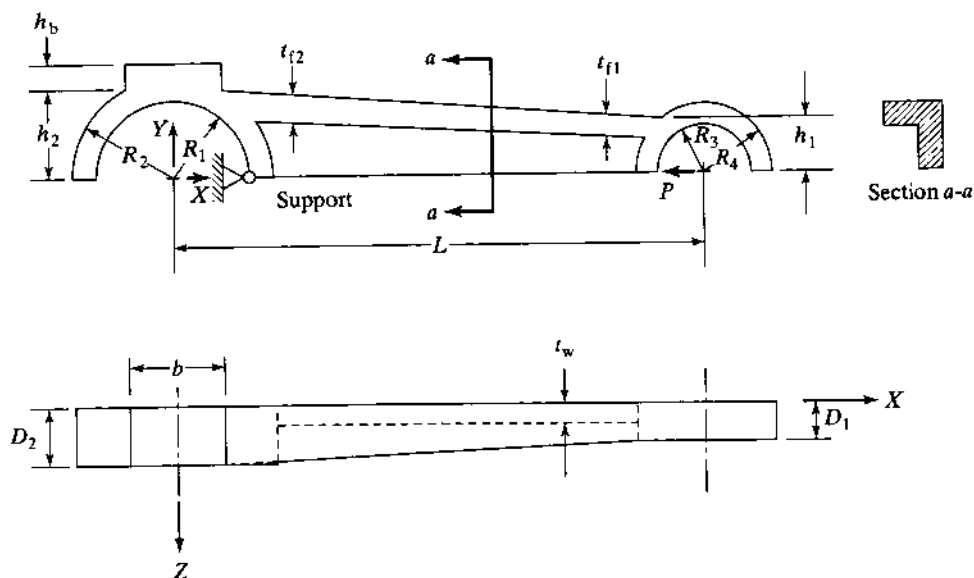


FIGURE P9.5

- 9.6. Determine the axial elongation and location and magnitude of maximum von Mises stress in the connecting rod shown in Fig. P9.6.



$\frac{1}{4}$ Symmetry model: x, z and x, y are planes of symmetry.

Dimensions (mm)

$$R_1 = 20 \quad R_2 = 26 \quad R_3 = 12 \quad R_4 = 18 \quad L = 140$$

$$t_{f1} = 4 \quad t_{f2} = 6 \quad t_w = 5 \quad h_b = 7$$

$$h_1 = 14 \quad h_2 = 23 \quad D_1 = 10 \quad D_2 = 15 \quad b = 12.1$$

$P = 30000$ -N compression

Material: steel

FIGURE P9.6

9.7 An overhanging beam made of rigidly bonded steel and aluminum plates is shown in Fig. P9.7. The aluminum plate has a constant thickness of 10 mm. Due to a manufacturing defect, the steel plate has straight edges, a thickness of 9 mm at one of the free ends, and 10 mm at other corners. From the position shown, if the temperature is raised 60°C , determine the following:

- the deformed shape,
- the maximum vertical deflection and its location, and
- the maximum von Mises stress and its location.

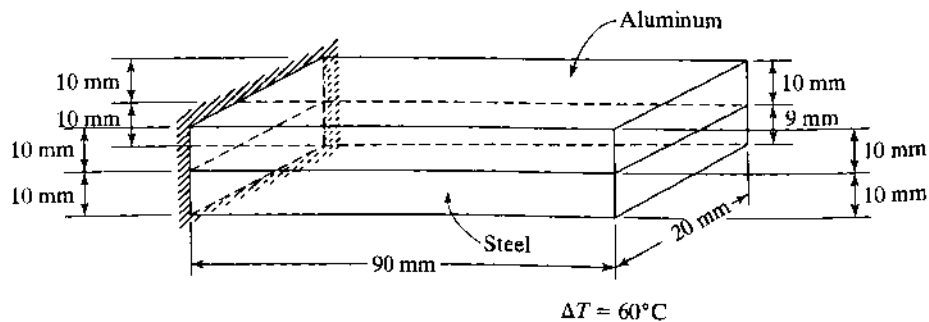


FIGURE P9.7

Program Listings

```

*****          PROGRAM HEXAFRON          *****
!*   3-D STRESS ANALYSIS USING 8-NODE   *
!*   ISOPARAMETRIC HEXAHEDRAL ELEMENT   *
!*   USING FRONTAL SOLVER               *
!*   T.R.Chandrupatla and A.D.Belegundu *
*****
\===== MAIN PROGRAM =====
Private Sub cmdStart_Click()
  Call InputData
  Call PreFront
  RecordLen = Len(Adat)
  '--- Scratch file for writing
  Open "SCRATCH.DAT" For Random As #3 Len = RecordLen
  Call Stiffness
  Call BackSub
  Close #3
  Kill "SCRATCH.DAT"
  Call StressCalc
  Call ReactionCalc
  Call Output
  cmdView.Enabled = True
  cmdStart.Enabled = False
End Sub
\=====

```

```

\===== SUBROUTINE PREFRONT =====
Private Sub PreFront()
  '----- Mark Last Appearance of Node / Make it negative in NOC()
  ' Last appearance is first appearance for reverse element order
  NEDF = NEN + NDN
  For I = 1 To NN
    II = 0
    For J = NE To 1 Step -1
      For K = 1 To NEN
        If I = NOC(J, K) Then
          II = 1
          Exit For
        End If
      Next K
      If II = 1 Then Exit For
    Next J
    NOC(J, K) = -I
  Next I
  '==== Block Size Determination
  NQ = NN * NDN
  ReDim IDE(NQ)
  For I = 1 To NQ: IDE(I) = 0: Next I
  For I = 1 To NMPC: For J = 1 To 2: IDE(MPC(I, J)) = 1: Next J: Next I
  IFRON = 0: For I = 1 To NQ: IFRON = IFRON + IDE(I): Next I
  IBL = IFRON

```

continued

```

For N = 1 To NE
  INEG = 0
  For I = 1 To NEN
    I1 = NOC(N, I): IA = NDN * (Abs(I1) - 1)
    For J = 1 To NDN
      IA = IA + 1
      If IDE(IA) = 0 Then
        IFRON = IFRON + 1: IDE(IA) = 1
      End If
    Next J
    If I1 < 0 Then INEG = INEG + 1
  Next I
  If IBL < IFRON Then IBL = IFRON
  IFRON = IFRON - NDN * INEG
Next N
Erase IDE
ReDim ISBL(IBL), S(IBL, IBL), IEBL(NEDF), INDX(IBL)
NFRON = 0: NTOGO = 0: NDCNT = 0
For I = 1 To IBL: INDX(I) = I: Next I
End Sub

```

```

===== GLOBAL STIFFNESS MATRIX =====
Private Sub Stiffness()
  '----- Global Stiffness Matrix -----
  Call IntegPoints
  MTN1 = 0
  For N = 1 To NE
    picBox.Print "Forming Stiffness Matrix of Element "; N
    MTN = MAT(N)
    If MTN <> MTN1 Then
      Call DMatrix(N)
    End If
    Call ElemStiffness(N)
    If N = 1 Then
      CNST = 0
      For I = 1 To NEDF: CNST = CNST + SE(I, I): Next I
      CNST = 100000000000# * CNST
      Call MpcFron
    End If
    '----- Account for temperature loads QT()
    For I = 1 To NEN
      IL = 3 * (I - 1): IG = 3 * (Abs(NOC(N, I)) - 1)
      For J = 1 To 3
        IL = IL + 1: IG = IG + 1
        F(IG) = F(IG) + QT(IL)
      Next J
    Next I
    Call Front(N)          'Frontal assembly and Forward Elimination
  Next N
End Sub
=====

```

```

'===== STRESS CALCULATIONS =====
Private Sub StressCalc()
  ReDim vonMisesStress(NE, 8)
  '----- Stress Calculations
  MTN1 = 0
  For N = 1 To NE
    MTN = MAT(N)
    If MTN <> MTN1 Then
      Call DMatrix(N)
    End If
    For IP = 1 To 8
      '--- Von Mises Stress at Integration Points
      Call DbMat(N, 2, IP) '--- Get DB Matrix with Stress calculation
      '--- Calculation of Von Mises Stress at IP
      SIV1 = STR(1) + STR(2) + STR(3)
      SIV2 = STR(1) * STR(2) + STR(2) * STR(3) + STR(3) * STR(1)
      SIV2 = SIV2 - STR(4) ^ 2 - STR(5) ^ 2 - STR(6) ^ 2
      vonMisesStress(N, IP) = Sqr(SIV1 * SIV1 - 3 * SIV2)
    Next IP
  Next N
End Sub

```

```

'===== INTEGRATION POINTS =====
Private Sub IntegPoints()
  '----- Integration Points XNI() -----
  C = 0.57735026919
  XI(1, 1) = -1: XI(2, 1) = -1: XI(3, 1) = -1
  XI(1, 2) = 1: XI(2, 2) = -1: XI(3, 2) = -1
  XI(1, 3) = 1: XI(2, 3) = 1: XI(3, 3) = -1
  XI(1, 4) = -1: XI(2, 4) = 1: XI(3, 4) = -1
  XI(1, 5) = -1: XI(2, 5) = -1: XI(3, 5) = 1
  XI(1, 6) = 1: XI(2, 6) = -1: XI(3, 6) = 1
  XI(1, 7) = 1: XI(2, 7) = 1: XI(3, 7) = 1
  XI(1, 8) = -1: XI(2, 8) = 1: XI(3, 8) = 1
  For I = 1 To 8
    XNI(1, I) = C * XI(1, I): XNI(2, I) = C * XI(2, I)
    XNI(3, I) = C * XI(3, I)
  Next I
End Sub

```

```

'===== D-MATRIX =====
Private Sub DMatrix(N)
  '--- D() Matrix relating Stresses to Strains
  E = PM(MTN, 1): PNU = PM(MTN, 2): AL = PM(MTN, 3)
  C1 = E / ((1 + PNU) * (1 - 2 * PNU))
  C2 = 0.5 * E / (1 + PNU)
  For I = 1 To 6: For J = 1 To 6: D(I, J) = 0: Next J: Next I
  D(1, 1) = C1 * (1 - PNU): D(1, 2) = C1 * PNU: D(1, 3) = D(1, 2)
  D(2, 1) = D(1, 2): D(2, 2) = D(1, 1): D(2, 3) = D(1, 2)
  D(3, 1) = D(1, 3): D(3, 2) = D(2, 3): D(3, 3) = D(1, 1)
  D(4, 4) = C2: D(5, 5) = C2: D(6, 6) = C2
  MTN1 = MTN
End Sub

```

```

'===== ELEMENT STIFFNESS MATRIX =====
Private Sub ElemStiffness(N)
'----- Element Stiffness -----
For I = 1 To 24: For J = 1 To 24
SE(I, J) = 0: Next J: QT(I) = 0: Next I
DTE = DT(N)
'--- Weight Factor is ONE
'--- Loop on Integration Points
For IP = 1 To 8
'--- Get DB Matrix at Integration Point IP
Call DbMat(N, 1, IP)
'--- Element Stiffness Matrix SE
For I = 1 To 24
For J = 1 To 24
For K = 1 To 6
SE(I, J) = SE(I, J) + B(K, I) * DB(K, J) * DJ
Next K
Next J
Next I
'--- Determine Temperature Load QT()
C = AL * DTE
For I = 1 To 24
DSUM = DB(1, I) + DB(2, I) + DB(3, I)
QT(I) = QT(I) + C * Abs(DJ) * DSUM / 6
Next I
Next IP
End Sub

```

```

'===== DB MATRIX =====
Private Sub DbMat(N, ISTR, IP)
'----- DB() MATRIX -----
'--- Gradient of Shape Functions - The GN() Matrix
For I = 1 To 3
For J = 1 To 8
C = 1
For K = 1 To 3
If K <> I Then
C = C * (1 + XI(K, J) * XNI(K, IP))
End If
Next K
GN(I, J) = 0.125 * XI(I, J) * C
Next J
Next I
'--- Formation of Jacobian TJ
For I = 1 To 3
For J = 1 To 3
TJ(I, J) = 0
For K = 1 To 8
KN = Abs(NOC(N, K))
TJ(I, J) = TJ(I, J) + GN(I, K) * X(KN, J)
Next K
Next J
Next I

```

continued

```

'--- Determinant of the JACOBIAN
DJ1 = TJ(1, 1) * (TJ(2, 2) * TJ(3, 3) - TJ(3, 2) * TJ(2, 3))
DJ2 = TJ(1, 2) * (TJ(2, 3) * TJ(3, 1) - TJ(3, 3) * TJ(2, 1))
DJ3 = TJ(1, 3) * (TJ(2, 1) * TJ(3, 2) - TJ(3, 1) * TJ(2, 2))
DJ = DJ1 + DJ2 + DJ3
'--- Inverse of the Jacobian AJ()
AJ(1, 1) = (TJ(2, 2) * TJ(3, 3) - TJ(2, 3) * TJ(3, 2)) / DJ
AJ(1, 2) = (TJ(3, 2) * TJ(1, 3) - TJ(3, 3) * TJ(1, 2)) / DJ
AJ(1, 3) = (TJ(1, 2) * TJ(2, 3) - TJ(1, 3) * TJ(2, 2)) / DJ
AJ(2, 1) = (TJ(2, 3) * TJ(3, 1) - TJ(2, 1) * TJ(3, 3)) / DJ
AJ(2, 2) = (TJ(1, 1) * TJ(3, 3) - TJ(1, 3) * TJ(3, 1)) / DJ
AJ(2, 3) = (TJ(1, 3) * TJ(2, 1) - TJ(1, 2) * TJ(2, 3)) / DJ
AJ(3, 1) = (TJ(2, 1) * TJ(3, 2) - TJ(2, 2) * TJ(3, 1)) / DJ
AJ(3, 2) = (TJ(1, 2) * TJ(3, 1) - TJ(1, 1) * TJ(3, 2)) / DJ
AJ(3, 3) = (TJ(1, 1) * TJ(2, 2) - TJ(1, 2) * TJ(2, 1)) / DJ
'--- H() Matrix relates local derivatives of u to local
      displacements q
For I = 1 To 9
  For J = 1 To 24
    H(I, J) = 0
  Next J
Next I
For I = 1 To 3
  For J = 1 To 3
    IR = 3 * (I - 1) + J
    For K = 1 To 8
      IC = 3 * (K - 1) + I
      H(IR, IC) = GN(J, K)
    Next K
  Next J
Next I
'--- G() Matrix relates strains to local derivatives of u
For I = 1 To 6
  For J = 1 To 9
    G(I, J) = 0
  Next J
Next I
G(1, 1) = AJ(1, 1): G(1, 2) = AJ(1, 2): G(1, 3) = AJ(1, 3)
G(2, 4) = AJ(2, 1): G(2, 5) = AJ(2, 2): G(2, 6) = AJ(2, 3)
G(3, 7) = AJ(3, 1): G(3, 8) = AJ(3, 2): G(3, 9) = AJ(3, 3)
G(4, 4) = AJ(3, 1): G(4, 5) = AJ(3, 2): G(4, 6) = AJ(3, 3)
G(4, 7) = AJ(2, 1): G(4, 8) = AJ(2, 2): G(4, 9) = AJ(2, 3)
G(5, 1) = AJ(3, 1): G(5, 2) = AJ(3, 2): G(5, 3) = AJ(3, 3)
G(5, 7) = AJ(1, 1): G(5, 8) = AJ(1, 2): G(5, 9) = AJ(1, 3)
G(6, 1) = AJ(2, 1): G(6, 2) = AJ(2, 2): G(6, 3) = AJ(2, 3)
G(6, 4) = AJ(1, 1): G(6, 5) = AJ(1, 2): G(6, 6) = AJ(1, 3)

```


continued

```

'---- B() Matrix relates strains to q
For I = 1 To 6
  For J = 1 To 24
    B(I, J) = 0
    For K = 1 To 9
      B(I, J) = B(I, J) + G(I, K) * H(K, J)
    Next K
  Next J
Next I
'---- DB() Matrix relates stresses to q
For I = 1 To 6
  For J = 1 To 24
    DB(I, J) = 0
    For K = 1 To 6
      DB(I, J) = DB(I, J) + D(I, K) * B(K, J)
    Next K
  Next J
Next I
If ISTR = 1 Then Exit Sub
'---- Element Nodal Displacements stored in QT()
For I = 1 To 8
  IIN = 3 * (Abs(NOC(N, I)) - 1)
  II = 3 * (I - 1)
  For J = 1 To 3
    QT(II + J) = F(IIN + J)
  Next J
Next I
'---- Stress Calculation STR = DB * Q
For I = 1 To 6
  STR(I) = 0
  For J = 1 To 24
    STR(I) = STR(I) + DB(I, J) * QT(J)
  Next J
  STR(I) = STR(I) - CAL * (D(I, 1) + D(I, 2) + D(I, 3))
Next I
End Sub

```

```

'===== MULTIPOINT CONSTRAINTS =====
Private Sub MpcFron()
'----- Modifications for Multipoint Constraints by Penalty Method
For I = 1 To NMPC
  I1 = MPC(I, 1)
  IFL = 0
  For J = 1 To NFRON
    J1 = INDX(J)
    If I1 = ISBL(J1) Then
      IFL = 1: Exit For
    End If
  Next J
  If IFL = 0 Then
    NFRON = NFRON + 1: J1 = INDX(NFRON): ISBL(J1) = I1
  End If

```

continued

```

I2 = MPC(I, 2)
IFL = 0
For K = 1 To NFRON
  K1 = INDX(K)
  If K1 = ISBL(K1) Then
    IFL = 1: Exit For
  End If
Next K
If IFL = 0 Then
  NFRON = NFRON + 1: K1 = INDX(NFRON): ISBL(K1) = I2
End If
'----- Stiffness Modification
S(J1, J1) = S(J1, J1) + CNST * BT(I, 1) ^ 2
S(K1, K1) = S(K1, K1) + CNST * BT(I, 2) ^ 2
S(J1, K1) = S(J1, K1) + CNST * BT(I, 1) * BT(I, 2)
S(K1, J1) = S(J1, K1)
'----- Force Modification
F(I1) = F(I1) + CNST * BT(I, 3) * BT(I, 1)
F(I2) = F(I2) + CNST * BT(I, 3) * BT(I, 2)
Next I
End Sub

```

End Sub

FRONTAL METHOD

```

Private Sub Front(N)
'----- Frontal Method Assembly and Elimination -----
'----- Assembly of Element N -----
For I = 1 To NEN
  I1 = NOC(N, I): IA = Abs(I1): IS1 = Sgn(I1)
  IDF = NDN * (IA - 1): IE1 = NDN * (I - 1)
  For J = 1 To NDN
    IDF = IDF + 1: IE1 = IE1 + 1: IFL = 0
    If NFRON > NTOGO Then
      For II = NTOGO + 1 To NFRON
        IX = INDX(II)
        If IDF = ISBL(IX) Then
          IFL = 1: Exit For
        End If
      Next II
    End If
    If IFL = 0 Then
      NFRON = NFRON + 1: II = NFRON: IX = INDX(II)
    End If
    ISBL(IX) = IDF: IE1 = IE1 + 1
    If IS1 = -1 Then
      NTOGO = NTOGO + 1
      ITEMP = INDX(NTOGO)
      INDX(NTOGO) = INDX(II)
      INDX(II) = ITEMP
    End If
  Next J
Next I

```

continued

```

For I = 1 To NEDF
  I1 = IEBL(I)
  For J = 1 To NEDF
    J1 = IEBL(J)
    S(I1, J1) = S(I1, J1) + SE(I, J)
  Next J
Next I

```

```

-----
If NDCNT < ND Then

```

```

  Modification for displacement BCs / Penalty Approach -----

```

```

  For I = 1 To NTOGO
    I1 = INDX(I)
    IG = ISBL(I1)
    For J = 1 To ND
      If IG = NU(J) Then
        S(I1, I1) = S(I1, I1) + CNST
        F(IG) = F(IG) + CNST * U(J)
        NDCNT = NDCNT + 1      'Counter for check
      Exit For
    End If
  Next J
Next I
End If

```

```

-----
Elimination of completed variables -----

```

```

  NTG1 = NTOGO
  For II = 1 To NTG1
    IPV = INDX(1): IPG = ISBL(IPV)
    Pivot = S(IPV, IPV)
    Write separator "0" and PIVOT value to disk -----
    Adat.VarNum = 0
    Adat.Coeff = Pivot
    ICOUNT = ICOUNT + 1
    Put #3, ICOUNT, Adat
    S(IPV, IPV) = 0
    For I = 2 To NFRON
      I1 = INDX(I): IG = ISBL(I1)
      If S(I1, IPV) <> 0 Then
        C = S(I1, IPV) / Pivot: S(I1, IPV) = 0
        For J = 2 To NFRON
          J1 = INDX(J)
          If S(IPV, J1) <> 0 Then
            S(I1, J1) = S(I1, J1) - C * S(IPV, J1)
          End If
        Next J
        F(IG) = F(IG) - C * F(IPG)
      End If
    Next I
    For J = 2 To NFRON

```

continued

```

'----- Write Variable# and Reduced Coeff/PIVOT to disk -----
      J1 = INDX(J)
      If S(IPV, J1) <> 0 Then
        ICOUNT = ICOUNT + 1: IBA = ISBL(J1)
        Adat.VarNum = IBA
        Adat.Coeff = S(IPV, J1) / Pivot
        Put #3, ICOUNT, Adat
        S(IPV, J1) = 0
      End If
    Next J
    ICOUNT = ICOUNT + 1
'----- Write Eliminated Variable# and RES/PIVOT to disk -----
    Adat.VarNum = IPG
    Adat.Coeff = F(IPG) / Pivot
    F(IPG) = 0
    Put #3, ICOUNT, Adat
'----- (NTOGO) into (1); (NFRON) into (NTOGO)
'----- IPV into (NFRON) and reduce front & NTOGO sizes by 1
    If NTOGO > 1 Then
      INDX(1) = INDX(NTOGO)
    End If
    INDX(NTOGO) = INDX(NFRON): INDX(NFRON) = IPV
    NFRON = NFRON - 1: NTOGO = NTOGO - 1
  Next II
End Sub

```

```

\===== BACKSUBSTITUTION =====
Private Sub BackSub()
'===== Backsubstitution
  Do While ICOUNT > 0
    Get #3, ICOUNT, Adat
    ICOUNT = ICOUNT - 1
    N1 = Adat.VarNum
    F(N1) = Adat.Coeff
    Do
      Get #3, ICOUNT, Adat
      ICOUNT = ICOUNT - 1
      N2 = Adat.VarNum
      If N2 = 0 Then Exit Do
      F(N1) = F(N1) - Adat.Coeff * F(N2)
    Loop
  Loop
End Sub

```

Scalar Field Problems

10.1 INTRODUCTION

In previous chapters, the unknowns in the problem represented components of a *vector* field. In a two-dimensional plate, for example, the unknown quantity is the vector field $\mathbf{u}(x, y)$, where \mathbf{u} is a (2×1) displacement vector. On the other hand, quantities such as temperature, pressure, and stream potentials are *scalar* in nature. In two-dimensional steady-state heat conduction, for example, the temperature field $T(x, y)$ is the unknown to be determined.

In this chapter, the finite element method for solving such problems is discussed. In Section 10.2, one-dimensional and two-dimensional steady-state heat conduction are considered, as well as temperature distribution in fins. Section 10.3 deals with torsion of solid shafts. Scalar field problems related to fluid flow, seepage, electric/magnetic fields, and flow in ducts are defined in Section 10.4.

The striking feature of scalar field problems is that they are to be found in almost all branches of engineering and physics. Most of them can be viewed as special forms of the general Helmholtz equation, given by

$$\frac{\partial}{\partial x} \left(k_x \frac{\partial \phi}{\partial x} \right) + \frac{\partial}{\partial y} \left(k_y \frac{\partial \phi}{\partial y} \right) + \frac{\partial}{\partial z} \left(k_z \frac{\partial \phi}{\partial z} \right) + \lambda \phi + Q = 0 \quad (10.1)$$

together with boundary conditions on ϕ and its derivatives. In the Eq. 10.1, $\phi = \phi(x, y, z)$ is the field variable that is to be determined. Table 10.1 lists some of the engineering problems described by Eq. 10.1. For example, if we set $\phi = T$, $k_x = k_y = k$, and $\lambda = 0$ and consider only x and y , we get $\partial^2 T / \partial x^2 + \partial^2 T / \partial y^2 + Q = 0$, which describes the heat-conduction problem for temperature T , where k is the thermal conductivity and Q is the heat source/sink. Mathematically, we can develop the finite element method for various field problems in a general manner by considering Eq. 10.1. The solution to specific problems can then be obtained by suitable definition of variables. We discuss here the heat-transfer and torsion problems in some detail. These are important in themselves, because they provide us an opportunity to understand the physical problem and how to handle different boundary conditions needed for modeling. Once the steps are understood, extension to other areas in engineering should present no difficulty. While in other chapters, both energy and Galerkin approaches were used to derive element matrices, by Galerkin's approach is used here owing to its greater generality for field problems.

TABLE 10.1 Examples of Scalar Field Problems in Engineering

| Problem | Equation | Field variable | Parameter | Boundary conditions |
|------------------------------|--|------------------------------|--------------------------------------|---|
| Heat conduction | $k \left(\frac{\partial^2 T}{\partial x^2} + \frac{\partial^2 T}{\partial y^2} \right) + Q = 0$ | Temperature, T | Thermal conductivity, k | $T = T_0, -k \frac{\partial T}{\partial n} = q_0$ $-k \frac{\partial T}{\partial n} = h(T - T_\infty)$ |
| Torsion | $\left(\frac{\partial^2 \theta}{\partial x^2} + \frac{\partial^2 \theta}{\partial y^2} \right) + 2 = 0$ | Stress function, θ | | $\theta = 0$ |
| Potential flow | $\left(\frac{\partial^2 \psi}{\partial x^2} + \frac{\partial^2 \psi}{\partial y^2} \right) = 0$ | Stream function, ψ | | $\psi = \psi_0$ |
| Seepage and groundwater flow | $k \left(\frac{\partial^2 \phi}{\partial x^2} + \frac{\partial^2 \phi}{\partial y^2} \right) + Q = 0$ | Hydraulic potential, ϕ | Hydraulic conductivity, k | $\phi = \phi_0$ $\frac{\partial \phi}{\partial n} = 0$ $\phi = y$ |
| Electric potential | $\epsilon \left(\frac{\partial^2 u}{\partial x^2} + \frac{\partial^2 u}{\partial y^2} \right) = -\rho$ | Electric potential, u | Permittivity, ϵ | $u = u_0, \frac{\partial u}{\partial n} = 0$ |
| Fluid flow in ducts | $\left(\frac{\partial^2 W}{\partial X^2} + \frac{\partial^2 W}{\partial Y^2} \right) + 1 = 0$ | Nondimensional velocity, W | | $W = 0$ |
| Acoustics | $\left(\frac{\partial^2 p}{\partial x^2} + \frac{\partial^2 p}{\partial y^2} \right) + k^2 p = 0$ | Pressure p (complex) | Wave number, $k^2 = \omega^2/c^2$ | $p = p_0,$ $\frac{1}{ik\rho c} \frac{\partial p}{\partial n} = v_0$ |

10.2 STEADY-STATE HEAT TRANSFER

We now discuss the finite element formulation for the solution of steady-state heat-transfer problems. Heat transfer occurs when there is a temperature difference within a body or between a body and its surrounding medium. Heat is transferred in the form of conduction, convection, and thermal radiation. Only conduction and convection modes are treated here.

The heat flow through the wall of a heated room on a winter day is an example of conduction. The conduction process is quantified by Fourier's law. In a thermally isotropic medium, Fourier's law for two-dimensional heat flow is given by

$$q_x = -k \frac{\partial T}{\partial x} \quad q_y = -k \frac{\partial T}{\partial y} \quad (10.2)$$

where $T = T(x, y)$ is a temperature field in the medium, q_x and q_y are the components of the heat flux (W/m^2), k is the thermal conductivity ($\text{W}/\text{m} \cdot ^\circ\text{C}$), and $\partial T/\partial x$, $\partial T/\partial y$ are the temperature gradients along x and y , respectively. The resultant heat flux $\mathbf{q} = q_x \mathbf{i} + q_y \mathbf{j}$ is at right angles to an isotherm or a line of constant temperature (Fig. 10.1). Note that $1 \text{ W} = 1 \text{ J/s} = 1 \text{ N} \cdot \text{m/s}$. The minus sign in Eq. 10.2 reflects the fact that heat is transferred in the direction of decreasing temperature. Thermal conductivity k is a material property.

In convection heat transfer, there is transfer of energy between a fluid and a solid surface as a result of a temperature difference. There can be free or natural convection, such as the circulation pattern set up while boiling water in a kettle due to hot water rising and cooler water moving down, or there can be forced convection, such as when the fluid flow is caused by a fan. The governing equation is of the form

$$q = h(T_s - T_\infty) \quad (10.3)$$

where q is the convective heat flux (W/m^2), h is the convection heat-transfer coefficient or film coefficient ($\text{W}/\text{m}^2 \cdot ^\circ\text{C}$), and T_s and T_∞ are the surface and fluid temperatures, respectively. The film coefficient h is a property of the flow and depends on various factors, such as whether convection is natural or forced, whether the flow is laminar or turbulent, the type of fluid, and the geometry of the body.

In addition to conduction and convection, heat transfer can also occur in the form of thermal radiation. The radiation heat flux is proportional to the fourth power of the

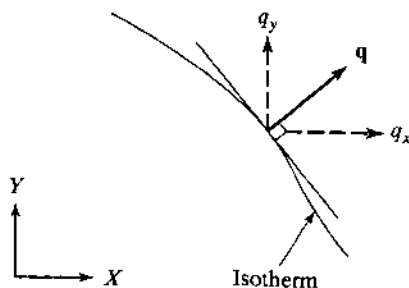


FIGURE 10.1 Heat flux in two dimensions.

absolute temperature, which causes the problem to be nonlinear. This mode of heat transfer is not considered here.

One-Dimensional Heat Conduction

We now turn our attention to the steady-state heat-conduction problem in one dimension. Our objective is to determine the temperature distribution. In one-dimensional steady-state problems, a temperature gradient exists along only one coordinate axis, and the temperature at each point is independent of time. Many engineering systems fall into this category.

Governing equation Consider heat conduction in a plane wall with uniform heat generation (Fig. 10.2). Let A be the area normal to the direction of heat flow and let Q (W/m^3) be the internal heat generated per unit volume. A common example of heat generation is the heat produced in a wire carrying a current I and having a resistance R through a volume V , which results in $Q = I^2 R/V$. A control volume is shown in Fig. 10.2. Since the heat rate (heat flux \times area) that is entering the control volume plus the heat rate generated equals the heat rate leaving the control volume, we have

$$qA + QA dx = \left(q + \frac{dq}{dx} dx \right) A \quad (10.4)$$

Canceling qA from both sides yields

$$Q = \frac{dq}{dx} \quad (10.5)$$

Substituting Fourier's law

$$q = -k \frac{dT}{dx} \quad (10.6)$$

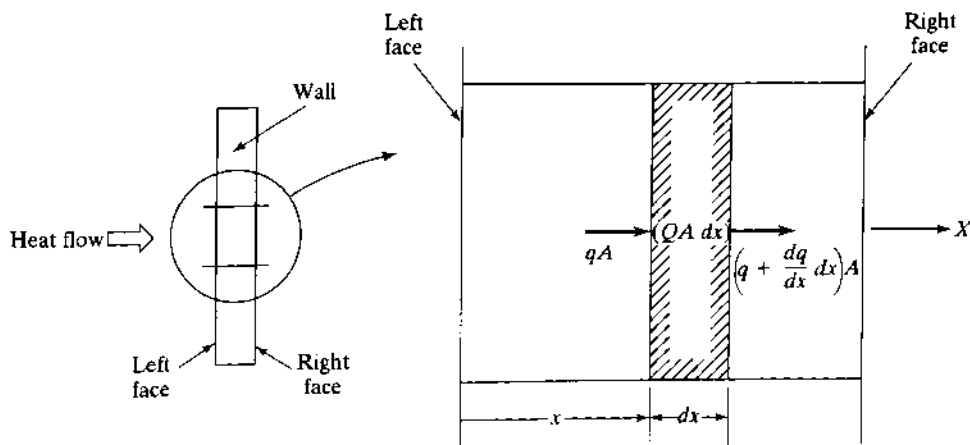


FIGURE 10.2 One-dimensional heat conduction.

Galerkin's approach for heat conduction The element matrices will now be derived using Galerkin's approach. The problem is

$$\frac{d}{dx} \left(k \frac{dT}{dx} \right) + Q = 0$$

$$T|_{x=0} = T_0 \quad q|_{x=L} = h(T_L - T_\infty) \quad (10.15)$$

If an approximate solution T is desired, Galerkin's approach is to solve

$$\int_0^L \phi \left[\frac{d}{dx} \left(k \frac{dT}{dx} \right) + Q \right] dx = 0 \quad (10.16)$$

for every ϕ constructed from the same basis functions as those of T , with $\phi(0) = 0$. ϕ can be thought of as a virtual temperature change that is consistent with boundary conditions. Thus, $\phi = 0$, where T is specified. Integrating the first term by parts, we have

$$\phi k \frac{dT}{dx} \Big|_0^L - \int_0^L k \frac{d\phi}{dx} \frac{dT}{dx} dx + \int_0^L \phi Q dx = 0 \quad (10.17)$$

Now,

$$\phi k \frac{dT}{dx} \Big|_0^L = \phi(L)k(L) \frac{dT}{dx}(L) - \phi(0)k(0) \frac{dT}{dx}(0) \quad (10.18a)$$

Since $\phi(0) = 0$ and $q = -k(L)(dT(L)/dx) = h(T_L - T_\infty)$, we get

$$\phi k \frac{dT}{dx} \Big|_0^L = -\phi(L)h(T_L - T_\infty) \quad (10.18b)$$

Thus, Eq. 10.17 becomes

$$-\phi(L)h(T_L - T_\infty) - \int_0^L k \frac{d\phi}{dx} \frac{dT}{dx} dx + \int_0^L \phi Q dx = 0 \quad (10.19)$$

We now use the isoparametric relations $T = \mathbf{N}^T \mathbf{T}^e$, etc., defined in Eqs. 10.11–10.14. Further, a global virtual-temperature vector is denoted as $\Psi = [\Psi_1, \Psi_2, \dots, \Psi_L]^T$, and the test function within each element is interpolated as

$$\phi = \mathbf{N}\Psi \quad (10.20)$$

Analogous to $dT/dx = \mathbf{B}_T \mathbf{T}^e$ in Eq. 10.13b, we have

$$\frac{d\phi}{dx} = \mathbf{B}_T \Psi \quad (10.21)$$

Thus, Eq. 10.19 becomes

$$-\Psi_L h(T_L - T_\infty) - \sum_e \Psi^T \left(\frac{k_e \ell_e}{2} \int_{-1}^1 \mathbf{B}_T^T \mathbf{B}_T d\xi \right) \mathbf{T}^e + \sum_e \Psi^T \frac{Q_e \ell_e}{2} \int_{-1}^1 \mathbf{N}^T d\xi = 0 \quad (10.22)$$

$$-\Psi_L h T_L + \Psi_L h T_\infty - \Psi^T \mathbf{K}_T \mathbf{T} + \Psi^T \mathbf{R} = 0 \quad (10.23)$$

which should be satisfied for all Ψ with $\Psi_1 = 0$. The global matrices \mathbf{K}_T and \mathbf{R} are assembled from element matrices \mathbf{k}_T and \mathbf{r}_Q , as given in

$$\mathbf{k}_T = \frac{k_e}{\ell_e} \begin{bmatrix} 1 & -1 \\ -1 & 1 \end{bmatrix} \quad (10.24)$$

$$\mathbf{r}_Q = \frac{Q_e \ell_e}{2} \begin{Bmatrix} 1 \\ 1 \end{Bmatrix} \quad (10.25)$$

When each Ψ is chosen in turn as $[0, 1, 0, \dots, 0]^T, [0, 0, 1, 0, \dots, 0]^T, \dots, [0, 0, \dots, 0, 1]^T$ and since $T_1 = T_0$, then Eq. 10.23 yields

$$\begin{bmatrix} K_{22} & K_{23} & \cdots & K_{2L} \\ K_{32} & K_{33} & \cdots & K_{3L} \\ \vdots & \vdots & \ddots & \vdots \\ K_{L2} & K_{L3} & \cdots & (K_{LL} + h) \end{bmatrix} \begin{Bmatrix} T_2 \\ T_3 \\ \vdots \\ T_L \end{Bmatrix} = \begin{Bmatrix} R_2 \\ R_3 \\ \vdots \\ (R_L + hT_\infty) \end{Bmatrix} - \begin{Bmatrix} K_{21}T_0 \\ K_{31}T_0 \\ \vdots \\ K_{L1}T_0 \end{Bmatrix} \quad (10.26)$$

We observe that Eq. 10.26 can be solved for T_2, T_3, \dots, T_L . We thus note that the Galerkin approach naturally leads to the elimination for handling nonzero specified temperature $T = T_0$ at node 1. However, it is also possible to develop Galerkin's method with a penalty approach to handle $T_1 = T_0$. In this case, the equations are as given by

$$\begin{bmatrix} (K_{11} + C) & K_{12} & \cdots & K_{1L} \\ K_{21} & K_{22} & \cdots & K_{2L} \\ \vdots & \vdots & \ddots & \vdots \\ K_{L1} & K_{L2} & \cdots & (K_{LL} + h) \end{bmatrix} \begin{Bmatrix} T_1 \\ T_2 \\ \vdots \\ T_L \end{Bmatrix} = \begin{Bmatrix} (R_1 + CT_0) \\ R_2 \\ \vdots \\ (R_L + hT_\infty) \end{Bmatrix} \quad (10.27)$$

Example 10.1

A composite wall consists of three materials, as shown in Fig. E10.1a. The outer temperature is $T_0 = 20^\circ\text{C}$. Convection heat transfer takes place on the inner surface of the wall with $T_\infty = 800^\circ\text{C}$ and $h = 25 \text{ W/m}^2 \cdot ^\circ\text{C}$. Determine the temperature distribution in the wall.

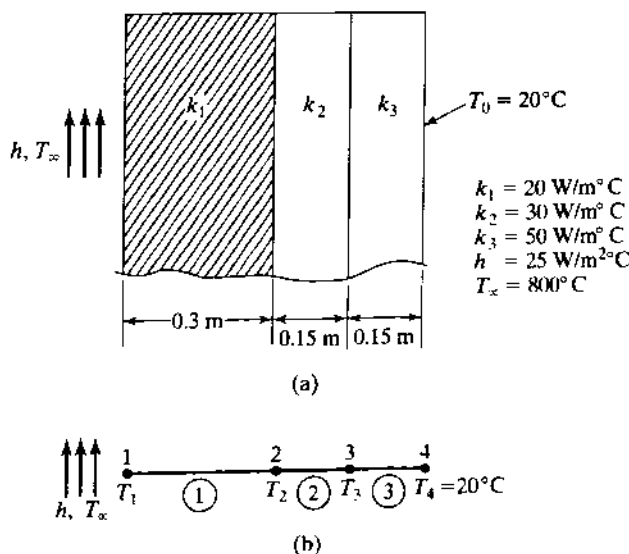


FIGURE E10.1

Solution A three-element finite element model of the wall is shown in Fig. E10.1b. The element conductivity matrices are

$$\mathbf{k}_T^{(1)} = \frac{20}{0.3} \begin{bmatrix} 1 & -1 \\ -1 & 1 \end{bmatrix} \quad \mathbf{k}_T^{(2)} = \frac{30}{0.15} \begin{bmatrix} 1 & -1 \\ -1 & 1 \end{bmatrix}$$

$$\mathbf{k}_T^{(3)} = \frac{50}{0.15} \begin{bmatrix} 1 & -1 \\ -1 & 1 \end{bmatrix}$$

The global $\mathbf{K} = \Sigma \mathbf{k}_T$ is obtained from these matrices as

$$\mathbf{K} = 66.7 \begin{bmatrix} 1 & -1 & 0 & 0 \\ -1 & 4 & -3 & 0 \\ 0 & -3 & 8 & -5 \\ 0 & 0 & -5 & 5 \end{bmatrix}$$

Now, since convection occurs at node 1, the constant $h = 25$ is added to the (1, 1) location of \mathbf{K} . This results in

$$\mathbf{K} = 66.7 \begin{bmatrix} 1.375 & -1 & 0 & 0 \\ -1 & 4 & -3 & 0 \\ 0 & -3 & 8 & -5 \\ 0 & 0 & -5 & 5 \end{bmatrix}$$

Since no heat generation Q occurs in this problem, the heat rate vector \mathbf{R} consists only of hT_∞ in the first row. That is,

$$\mathbf{R} = [25 \times 800, 0, 0, 0]^T$$

The specified temperature boundary condition $T_4 = 20^\circ\text{C}$, will now be handled by the penalty approach. We choose C based on

$$C = \max |\mathbf{K}_{ij}| \times 10^4$$

$$= 66.7 \times 8 \times 10^4$$

Now, C gets added to (4, 4) location of \mathbf{K} , while CT_4 is added to the fourth row of \mathbf{R} . The resulting equations are

$$66.7 \begin{bmatrix} 1.375 & -1 & 0 & 0 \\ -1 & 4 & -3 & 0 \\ 0 & -3 & 8 & -5 \\ 0 & 0 & -5 & 80005 \end{bmatrix} \begin{Bmatrix} T_1 \\ T_2 \\ T_3 \\ T_4 \end{Bmatrix} = \begin{Bmatrix} 25 \times 800 \\ 0 \\ 0 \\ 10672 \times 10^4 \end{Bmatrix}$$

The solution is

$$\mathbf{T} = [304.6, 119.0, 57.1, 20.0]^T \text{ } ^\circ\text{C}$$

Comment. The boundary condition $T_4 = 20^\circ\text{C}$ can also be handled by the elimination approach. The fourth row and column of \mathbf{K} is deleted, and \mathbf{R} is modified according to Eq. 3.70. The resulting equations are

$$66.7 \begin{bmatrix} 1.375 & -1 & 0 \\ -1 & 4 & -3 \\ 0 & -3 & 8 \end{bmatrix} \begin{bmatrix} T_1 \\ T_2 \\ T_3 \end{bmatrix} = \begin{bmatrix} 25 \times 800 \\ 0 \\ 0 + 6670 \end{bmatrix}$$

which yields

$$[T_1, T_2, T_3] = [304.6, 119.0, 57.1]^\circ\text{C} \quad \blacksquare$$

Heat flux boundary condition Certain physical situations are modeled using the boundary condition

$$q = q_0 \quad \text{at } x = 0 \quad (10.28)$$

where q_0 is a specified heat flux on the boundary. If $q = 0$, then the surface is perfectly insulated. A nonzero value of q_0 occurs, for example, due to an electrical heater or pad where one face is in contact with the wall and the other face is insulated. It is important to note that the input heat flux q_0 has a sign convention associated with it: q_0 is input as a positive value if heat is flowing out of the body and as a negative value if heat is flowing into the body. The boundary condition in Eq. 10.28 is handled by adding $(-q_0)$ to the heat rate vector. The resulting equations are

$$\mathbf{KT} = \mathbf{R} + \begin{Bmatrix} -q_0 \\ 0 \\ \vdots \\ 0 \end{Bmatrix} \quad (10.29)$$

The sign convention for specified heat flux given in Eq. 10.29 is clear if we consider the heat transfer occurring at a boundary. Let n be the outward normal (in 1-D problems, $n = +x$ or $-x$). The heat flow in the body towards the $+n$ direction is $q = -k \partial T / \partial n$, where $\partial T / \partial n < 0$. Thus, q is > 0 and since this heat flows out of the body, we have the boundary condition $q = q_0$ with the stated sign convention.

Comment on forced and natural boundary conditions In this problem, boundary conditions of the type $T = T_0$, which is on the field variable itself, are called *forced* boundary conditions. On the other hand, the boundary condition $q|_{x=0} = q_0$, or equivalently, $-k dT/dx_{x=0} = q_0$ is called a *natural* boundary condition involving the derivative of the field variable. Further, it is evident from Eq. 10.29 that the homogeneous natural boundary condition $q = q_0 = 0$ does not require any modifications in the element matrices. These are automatically satisfied at the boundary, in an average sense.

Example 10.2

Heat is generated in a large plate ($k = 0.8 \text{ W/m} \cdot ^\circ\text{C}$) at the rate of 4000 W/m^3 . The plate is 25 cm thick. The outside surfaces of the plate are exposed to ambient air at 30°C with a convective heat-transfer coefficient of $20 \text{ W/m}^2 \cdot ^\circ\text{C}$. Determine the temperature distribution in the wall.

Solution The problem is symmetric about the centerline of the plate. A two-element finite element model is shown in Fig. E10.2. The left end is insulated ($q = 0$) because no heat can flow across a line of symmetry. Noting that $k/\ell = 0.8/0.0625 = 12.8$, we have

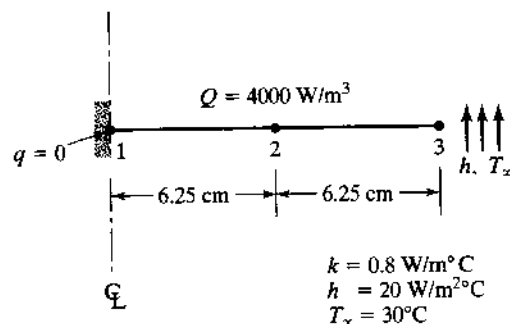


FIGURE E10.2

$$\mathbf{K} = \begin{bmatrix} 12.8 & -12.8 & 0 \\ -12.8 & 25.6 & -12.8 \\ 0 & -12.8 & (12.8 + 20) \end{bmatrix}$$

The heat rate vector is assembled from the heat source (Eq. 10.25) as well as due to convection as

$$\mathbf{R} = [125 \quad 250 \quad (125 + 20 \times 30)]^T$$

Solution of $\mathbf{KT} = \mathbf{R}$ yields

$$[T_1, T_2, T_3] = [94.0, 84.3, 55.0]^\circ\text{C}$$

In concluding 1-D heat conduction, we note that all element matrices described earlier were derived using Galerkin's approach. It is also possible to derive these matrices using an energy approach based on minimizing the functional

$$\Pi_T = \int_0^L \frac{1}{2} k \left(\frac{dT}{dx} \right)^2 dx - \int_0^L QT dx + \frac{1}{2} h (T_L - T_\infty)^2 \quad (10.30) \quad \blacksquare$$

One-Dimensional Heat Transfer in Thin Fins

A fin is an extended surface that is added onto a structure to increase the rate of heat removal. A familiar example is in the motorcycle where fins extend from the cylinder head to quickly dissipate heat through convection. We present here the finite element method for analyzing heat transfer in thin rectangular fins (Fig. 10.5). This problem differs from the conduction problem discussed previously in that both conduction and convection occur within the body.

Consider a thin rectangular fin as shown in Fig. 10.6. The problem can be treated as one dimensional, because the temperature gradients along the width and across the thickness are negligible. The governing equation may be derived from the conduction equation with heat source, given by

$$\frac{d}{dx} \left(k \frac{dT}{dx} \right) + Q = 0$$

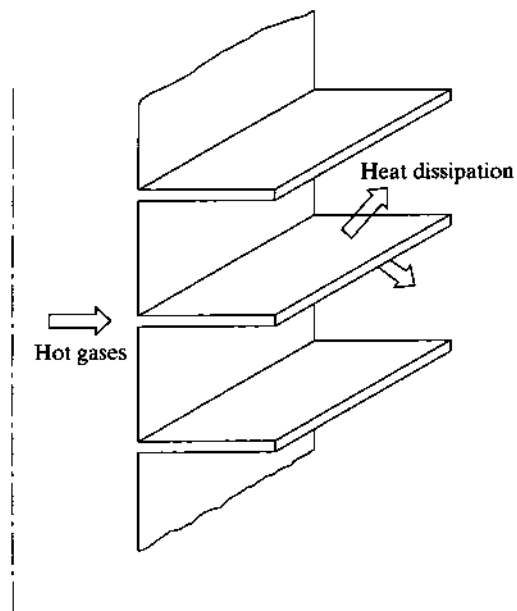


FIGURE 10.5 An array of thin rectangular fins.

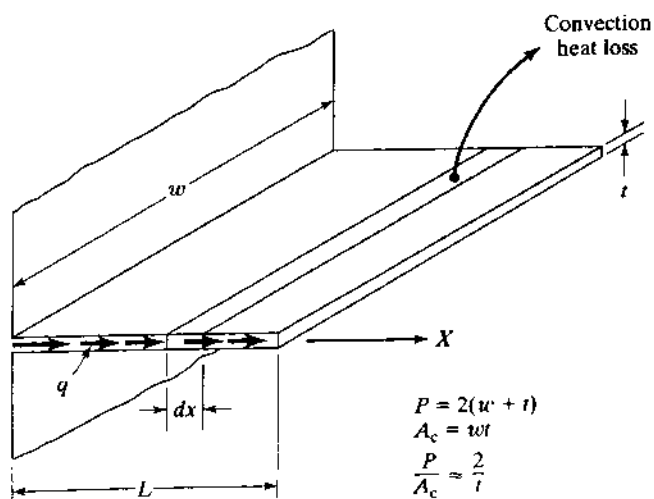


FIGURE 10.6 Heat flow in a thin rectangular fin.

The convection heat loss in the fin can be considered as a negative heat source

$$\begin{aligned} Q &= -\frac{(P dx)h(T - T_\infty)}{A_c dx} \\ &= -\frac{Ph}{A_c}(T - T_\infty) \end{aligned} \quad (10.31)$$

where P = perimeter of fin and A_c = area of cross section. Thus, the governing equation is

$$\frac{d}{dx}\left(k \frac{dT}{dx}\right) - \frac{Ph}{A_c}(T - T_\infty) = 0 \quad (10.32)$$

We present our analysis for the case when the base of the fin is held at T_0 and the tip of the fin is insulated (heat going out of the tip is negligible). The boundary conditions are then given by

$$T = T_0 \quad \text{at } x = 0 \quad (10.33a)$$

$$q = 0 \quad \text{at } x = L \quad (10.33b)$$

The finite element method: Galerkin approach The element matrices and heat-rate vectors for solving Eq. 10.32 with the boundary conditions in Eqs. 10.33 will now be developed. Galerkin's approach is attractive since we do not have to set up the functional that is to be minimized. Element matrices can be derived directly from the differential equation. Let $\phi(x)$ be any function satisfying $\phi(0) = 0$ using same basis as T . We require that

$$\int_0^L \phi \left[\frac{d}{dx}\left(k \frac{dT}{dx}\right) - \frac{Ph}{A_c}(T - T_\infty) \right] dx = 0 \quad (10.34)$$

Integrating the first term by parts, we have

$$\phi k \frac{dT}{dx} \Big|_0^L - \int_0^L k \frac{d\phi}{dx} \frac{dT}{dx} dx - \frac{Ph}{A_c} \int_0^L \phi T dx + \frac{Ph}{A_c} T_\infty \int_0^L \phi dx = 0 \quad (10.35)$$

Using $\phi(0) = 0$, $k(L)[dT(L)/dx] = 0$, and the isoparametric relations

$$dx = \frac{\ell_e}{2} d\xi \quad T = \mathbf{N}\mathbf{T}^e \quad \phi = \mathbf{N}\psi \quad \frac{dT}{dx} = \mathbf{B}_T \mathbf{T}^e \quad \frac{d\phi}{dx} = \mathbf{B}_T \psi$$

we get

$$\begin{aligned} & - \sum_e \psi^T \left[\frac{k_c \ell_e}{2} \int_{-1}^1 \mathbf{B}_T^T \mathbf{B}_T d\xi \right] \mathbf{T}^e - \frac{Ph}{A_c} \sum_e \psi^T \int_{-1}^1 \mathbf{N}^T \mathbf{N} d\xi \mathbf{T}^e \\ & + \frac{Ph T_\infty}{A_c} \sum_e \psi^T \frac{\ell_e}{2} \int_{-1}^1 \mathbf{N}^T d\xi = 0 \end{aligned} \quad (10.36)$$

We define

$$\mathbf{h}_T = \frac{Ph \ell_e}{A_c} \frac{1}{2} \int_{-1}^1 \mathbf{N}^T \mathbf{N} d\xi = \frac{Ph \ell_e}{A_c} \frac{1}{6} \begin{bmatrix} 2 & 1 \\ 1 & 2 \end{bmatrix} \quad (10.37a)$$

or, since $P/A_c \approx 2/t$ (Fig. 10.6),

$$\mathbf{h}_T \approx \frac{h\ell_e}{3t} \begin{bmatrix} 2 & 1 \\ 1 & 2 \end{bmatrix} \quad (10.37b)$$

and

$$\mathbf{r}_\infty = \frac{Ph}{A_c} T_\infty \frac{\ell_e}{2} \int_{-1}^1 \mathbf{N}^T d\xi = \frac{PhT_\infty \ell_e}{A_c} \frac{1}{2} \begin{Bmatrix} 1 \\ 1 \end{Bmatrix} \quad (10.38a)$$

or

$$\mathbf{r}_\infty \approx \frac{hT_\infty \ell_e}{t} \begin{Bmatrix} 1 \\ 1 \end{Bmatrix} \quad (10.38b)$$

Equation 10.36 reduces to

$$-\sum_e \Psi^T (\mathbf{k}_T + \mathbf{h}_T) \mathbf{T}^e + \sum_e \Psi^T \mathbf{r}_\infty = 0 \quad (10.39)$$

or

$$-\Psi^T (\mathbf{K}_T + \mathbf{H}_T) + \Psi^T \mathbf{R}_\infty = 0$$

which should hold for all Ψ satisfying $\Psi_1 = 0$.

Denoting $K_{ij} = (\mathbf{K}_T + \mathbf{H}_T)_{ij}$, we obtain

$$\begin{bmatrix} K_{22} & K_{23} & \cdots & K_{2L} \\ K_{32} & K_{33} & \cdots & K_{3L} \\ \vdots & \vdots & \ddots & \vdots \\ K_{L2} & K_{L3} & \cdots & K_{LL} \end{bmatrix} \begin{Bmatrix} T_2 \\ T_3 \\ \vdots \\ T_L \end{Bmatrix} = \begin{Bmatrix} \mathbf{R}_\infty \end{Bmatrix} - \begin{Bmatrix} K_{21}T_0 \\ K_{31}T_0 \\ \vdots \\ K_{L1}T_0 \end{Bmatrix} \quad (10.40)$$

which can be solved for \mathbf{T} . These equations incorporate the elimination approach for handling the boundary condition $T = T_0$. Other types of boundary conditions as discussed for heat conduction can also be considered for fin problems.

Example 10.3

A metallic fin, with thermal conductivity $k = 360 \text{ W/m} \cdot ^\circ\text{C}$, 0.1 cm thick, and 10 cm long, extends from a plane wall whose temperature is 235°C . Determine the temperature distribution and amount of heat transferred from the fin to the air at 20°C with $h = 9 \text{ W/m}^2 \cdot ^\circ\text{C}$. Take the width of fin to be 1 m.

Solution Assume that the tip of the fin is insulated. Using a three-element finite element model (Fig. E10.3) and assembling \mathbf{K}_T , \mathbf{H}_T , \mathbf{R}_∞ as given previously, we find that Eq. 10.40 yields

$$\begin{aligned} & \left[\frac{360}{3.33 \times 10^{-2}} \begin{bmatrix} 2 & -1 & 0 \\ -1 & 2 & -1 \\ 0 & -1 & 1 \end{bmatrix} + \frac{9 \times 3.33 \times 10^{-2}}{3 \times 10^{-3}} \begin{bmatrix} 4 & 1 & 0 \\ 1 & 4 & 1 \\ 0 & 1 & 2 \end{bmatrix} \right] \begin{Bmatrix} T_2 \\ T_3 \\ T_4 \end{Bmatrix} \\ & = \frac{9 \times 20 \times 3.33 \times 10^{-2}}{10^{-3}} \begin{Bmatrix} 2 \\ 2 \\ 1 \end{Bmatrix} - \begin{Bmatrix} -10711 \times 235 \\ 0 \\ 0 \end{Bmatrix} \end{aligned}$$

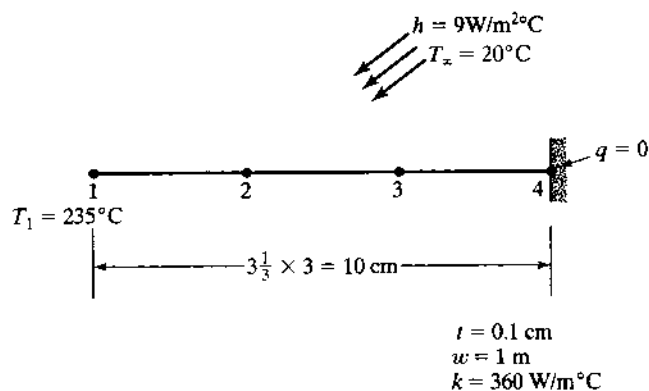


FIGURE E10.3

The solution is

$$[T_2, T_3, T_4] = [209.8, 195.2, 190.5]^\circ\text{C}$$

The total heat loss in the fin can now be computed as

$$H = \sum_e H_e$$

The loss H_e in each element is

$$H_e = h(T_{av} - T_\infty)A_s$$

where $A_s = 2 \times (1 \times 0.0333) \text{ m}^2$, and T_{av} is the average temperature within the element. We obtain

$$H_{\text{loss}} = 334.3 \text{ W/m}$$

Two-Dimensional Steady-State Heat Conduction

Our objective here is to determine the temperature distribution $T(x, y)$ in a long, prismatic solid in which two-dimensional conduction effects are important. An example is a chimney of rectangular cross section, as shown in Fig. 10.7. Once the temperature distribution is known, the heat flux can be determined from Fourier's law.

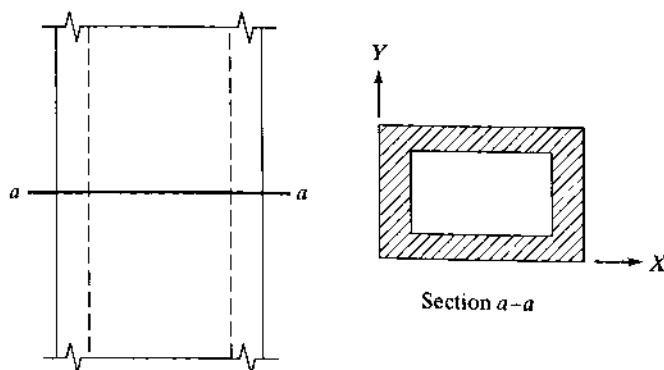


FIGURE 10.7 Two-dimensional model for heat conduction in a chimney.

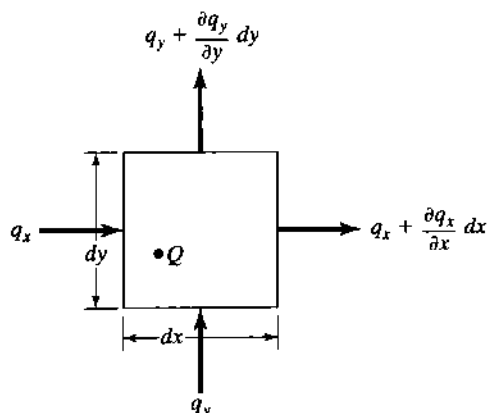


FIGURE 10.8 A differential control volume for heat transfer.

Differential equation Consider a differential control volume in the body, as shown in Fig. 10.8. The control volume has a constant thickness τ in the z direction. The heat generation Q is denoted by Q (W/m^3). Since the heat rate (= heat flux \times area) entering the control volume plus the heat rate generated equals the heat rate coming out, we have (Fig. 10.8)

$$q_x dy \tau + q_y dx \tau + Q dx dy \tau = \left(q_x + \frac{\partial q_x}{\partial x} dx \right) dy \tau + \left(q_y + \frac{\partial q_y}{\partial y} dy \right) dx \tau \quad (10.41)$$

or, upon canceling terms,

$$\frac{\partial q_x}{\partial x} + \frac{\partial q_y}{\partial y} - Q = 0 \quad (10.42)$$

Substituting for $q_x = -k \partial T / \partial x$ and $q_y = -k \partial T / \partial y$ into Eq. 10.42, we get the **heat-diffusion equation**

$$\frac{\partial}{\partial x} \left(k \frac{\partial T}{\partial x} \right) + \frac{\partial}{\partial y} \left(k \frac{\partial T}{\partial y} \right) + Q = 0 \quad (10.43)$$

We note that this partial differential equation is a special case of the Helmholtz equation given in Eq. 10.1.

Boundary conditions The governing equation, Eq. 10.43, has to be solved together with certain boundary conditions. These boundary conditions are of three types, as shown in Fig. 10.9: (1) specified temperature $T = T_0$ on S_T , (2) specified heat flux $q_n = q_0$ on S_q , and (3) convection $q_n = h(T - T_\infty)$ on S_c . The interior of the body is denoted by A , and the boundary is denoted as $S = (S_T + S_q + S_c)$. Further, q_n is the heat flux normal to the boundary. The sign convention adopted here for specifying q_0 is that $q_0 > 0$ if heat is flowing out of the body, while $q_0 < 0$ if heat is flowing into the body.

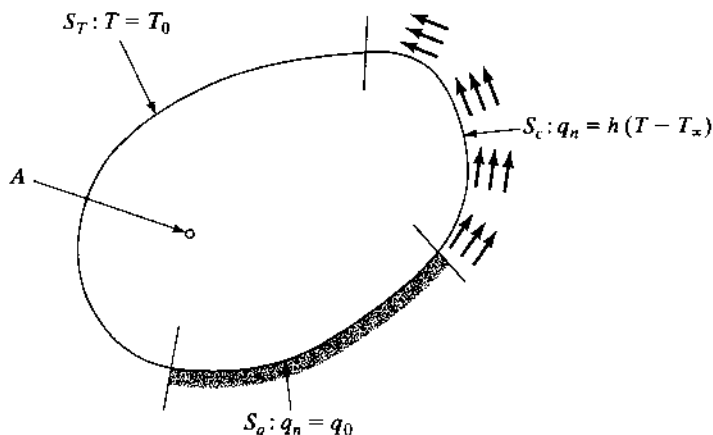


FIGURE 10.9 Boundary conditions for 2-D heat conduction.

The triangular element The triangular element (Fig. 10.10) will be used to solve the heat-conduction problem. Extension to quadrilateral or other isoparametric elements follows in a similar manner as discussed earlier for stress analysis.

Consider a constant length of the body perpendicular to the x, y plane. The temperature field within an element is given by

$$T = N_1 T_1 + N_2 T_2 + N_3 T_3 \quad (10.44)$$

or

$$T = \mathbf{N} \mathbf{T}^e$$

where $\mathbf{N} = [\xi, \eta, 1 - \xi - \eta]$ are the element-shape functions and $\mathbf{T}^e = [T_1, T_2, T_3]^T$. Referring to Chapter 5, we also have

$$\begin{aligned} x &= N_1 x_1 + N_2 x_2 + N_3 x_3 \\ y &= N_1 y_1 + N_2 y_2 + N_3 y_3 \end{aligned} \quad (10.45)$$

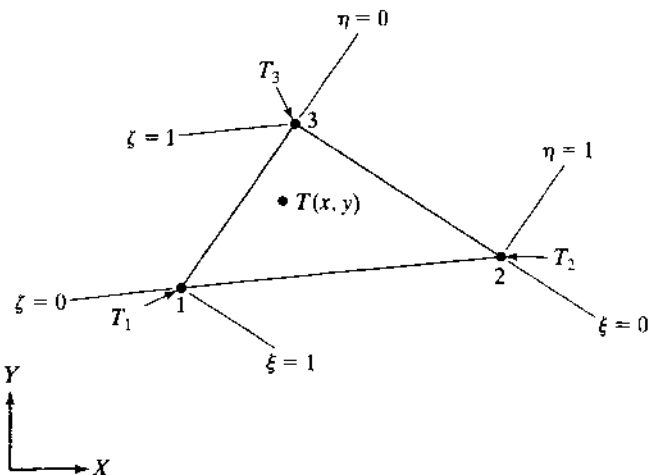


FIGURE 10.10 The linear triangular element for scalar field problems.

Further, the chain rule of differentiation yields

$$\begin{aligned}\frac{\partial T}{\partial \xi} &= \frac{\partial T}{\partial x} \frac{\partial x}{\partial \xi} + \frac{\partial T}{\partial y} \frac{\partial y}{\partial \xi} \\ \frac{\partial T}{\partial \eta} &= \frac{\partial T}{\partial x} \frac{\partial x}{\partial \eta} + \frac{\partial T}{\partial y} \frac{\partial y}{\partial \eta}\end{aligned}\quad (10.46)$$

or

$$\begin{Bmatrix} \frac{\partial T}{\partial \xi} \\ \frac{\partial T}{\partial \eta} \end{Bmatrix} = \mathbf{J} \begin{Bmatrix} \frac{\partial T}{\partial x} \\ \frac{\partial T}{\partial y} \end{Bmatrix}\quad (10.47)$$

In Eq. 10.47, \mathbf{J} is the Jacobian matrix given by

$$\mathbf{J} = \begin{bmatrix} x_{13} & y_{13} \\ x_{23} & y_{23} \end{bmatrix}\quad (10.48)$$

where $x_{ij} = x_i - x_j$, $y_{ij} = y_i - y_j$, and $|\det \mathbf{J}| = 2A_c$, where A_c is the area of the triangle. Equation 10.47 yields

$$\begin{Bmatrix} \frac{\partial T}{\partial x} \\ \frac{\partial T}{\partial y} \end{Bmatrix} = \mathbf{J}^{-1} \begin{Bmatrix} \frac{\partial T}{\partial \xi} \\ \frac{\partial T}{\partial \eta} \end{Bmatrix}\quad (10.49a)$$

$$= \frac{1}{\det \mathbf{J}} \begin{bmatrix} y_{23} & -y_{13} \\ -x_{23} & x_{13} \end{bmatrix} \begin{bmatrix} 1 & 0 & -1 \\ 0 & 1 & -1 \end{bmatrix} \mathbf{T}^e\quad (10.49b)$$

which can be written as

$$\begin{Bmatrix} \frac{\partial T}{\partial x} \\ \frac{\partial T}{\partial y} \end{Bmatrix} = \mathbf{B}_T \mathbf{T}^e\quad (10.50)$$

where

$$\mathbf{B}_T = \frac{1}{\det \mathbf{J}} \begin{bmatrix} y_{23} & -y_{13} & (y_{13} - y_{23}) \\ -x_{23} & x_{13} & (x_{23} - x_{13}) \end{bmatrix}\quad (10.51a)$$

$$= \frac{1}{\det \mathbf{J}} \begin{bmatrix} y_{23} & y_{31} & y_{12} \\ x_{32} & x_{13} & x_{21} \end{bmatrix}\quad (10.51b)$$

Galerkin approach[†] Consider the heat-conduction problem

$$\frac{\partial}{\partial x} \left(k \frac{\partial T}{\partial x} \right) + \frac{\partial}{\partial y} \left(k \frac{\partial T}{\partial y} \right) + Q = 0\quad (10.52)$$

[†]The functional approach would be based on minimizing

$$\pi_T = \frac{1}{2} \int_A \int \left[k \left(\frac{\partial T}{\partial x} \right)^2 + k \left(\frac{\partial T}{\partial y} \right)^2 - 2QT \right] dA + \int_{S_c} q_0 T dS + \int_{S_h} \frac{1}{2} h (T - T_\infty)^2 dS$$

with the boundary conditions

$$T = T_0 \quad \text{on } S_T \quad q_n = q_0 \quad \text{on } S_q \quad q_n = h(T - T_\infty) \quad \text{on } S_c \quad (10.53)$$

In Galerkin's approach, we seek an approximate solution T such that

$$\int_A \int \phi \left[\frac{\partial}{\partial x} \left(k \frac{\partial T}{\partial x} \right) + \frac{\partial}{\partial y} \left(k \frac{\partial T}{\partial y} \right) \right] dA + \int_A \int \phi Q dA = 0 \quad (10.54)$$

for every $\phi(x, y)$ constructed from the same basis functions as those used for T and satisfying $\phi = 0$ on S_T . Noting that

$$\phi \frac{\partial}{\partial x} \left(k \frac{\partial T}{\partial x} \right) = \frac{\partial}{\partial x} \left(\phi k \frac{\partial T}{\partial x} \right) - k \frac{\partial \phi}{\partial x} \frac{\partial T}{\partial x}$$

we find that Eq. 10.54 gives

$$\begin{aligned} \int_A \int \left\{ \left[\frac{\partial}{\partial x} \left(\phi k \frac{\partial T}{\partial x} \right) + \frac{\partial}{\partial y} \left(\phi k \frac{\partial T}{\partial y} \right) \right] - \left[k \frac{\partial \phi}{\partial x} \frac{\partial T}{\partial x} + k \frac{\partial \phi}{\partial y} \frac{\partial T}{\partial y} \right] \right\} dA \\ + \int_A \int \phi Q dA = 0 \end{aligned} \quad (10.55)$$

From the notation $q_x = -k(\partial T/\partial x)$ and $q_y = -k(\partial T/\partial y)$, and the divergence theorem, the first term in Eq. 10.55 above is

$$\begin{aligned} - \int_A \int \left[\frac{\partial}{\partial x} (\phi q_x) + \frac{\partial}{\partial y} (\phi q_y) \right] dA &= - \int_S \phi [q_x n_x + q_y n_y] dS \\ &= - \int_S \phi q_n dS \end{aligned} \quad (10.56)$$

where n_x and n_y are the direction cosines of the unit normal \mathbf{n} to the boundary and $q_n = q_x n_x + q_y n_y = \mathbf{q} \cdot \mathbf{n}$ is the normal heat flow along the unit outward normal, which is specified by boundary conditions. Since $S = S_T + S_q + S_c$, $\phi = 0$ on S_T , $q_n = q_0$ on S_q , and $q_n = h(T - T_\infty)$ on S_c , Eq. 10.55 reduces to

$$\begin{aligned} - \int_{S_q} \phi q_0 dS - \int_{S_c} \phi h(T - T_\infty) dS - \int_A \int \left(k \frac{\partial \phi}{\partial x} \frac{\partial T}{\partial x} + k \frac{\partial \phi}{\partial y} \frac{\partial T}{\partial y} \right) dA \\ + \int_A \int \phi Q dA = 0 \end{aligned} \quad (10.57)$$

Now, we introduce the isoparametric relations for the triangular element such as $T = \mathbf{N}\mathbf{T}^e$, given in Eqs. 10.47–10.55. Further, we denote the global virtual-temperature vector as Ψ whose dimension equals number of nodes in the finite element model. The virtual temperature distribution within each element is interpolated as

$$\phi = \mathbf{N}\Psi \quad (10.58a)$$

Moreover, just as $[\partial T/\partial x \quad \partial T/\partial y]^T = \mathbf{B}_T \mathbf{T}^e$, we have

$$\left[\frac{\partial \phi}{\partial x}, \frac{\partial \phi}{\partial y} \right]^T = \mathbf{B}_T \Psi \quad (10.58b)$$

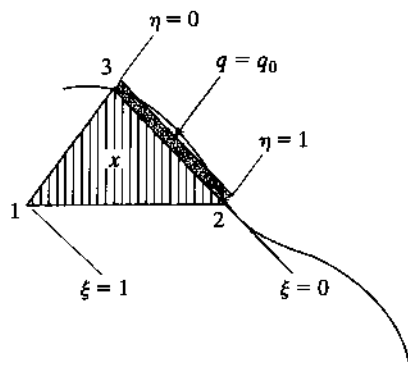


FIGURE 10.11 Specified heat flux boundary conduction on edge 2-3 of a triangular element.

Now, consider the first term in Eq. 10.57:

$$\int_{S_q} \phi q_0 dS = \sum_e \psi^T q_0 \mathbf{N}^T dS \quad (10.59)$$

If edge 2-3 is on the boundary (Fig. 10.11), we have $\mathbf{N} = [0, \eta, 1 - \eta] dS = \ell_{2-3} d\eta$, and it follows that

$$\int_{S_q} \phi q_0 dS = \sum_e \psi^T q_0 \ell_{2-3} \int_0^1 \mathbf{N}^T d\eta \quad (10.60a)$$

$$= \sum_e \psi^T \mathbf{r}_q \quad (10.60b)$$

where

$$\mathbf{r}_q = \frac{q_0 \ell_{2-3}}{2} [0 \quad 1 \quad 1]^T \quad (10.61)$$

Next, consider

$$\int_{S_c} \phi h(T - T_\infty) dS = \int_{S_c} \phi h T dS - \int_{S_c} \phi h T_\infty dS \quad (10.62a)$$

If edge 2-3 is the convection edge of the element, then

$$\begin{aligned} \int_{S_c} \phi h(T - T_\infty) dS &= \sum_e \psi^T \left[h \ell_{2-3} \int_0^1 \mathbf{N}^T \mathbf{N} d\eta \right] \mathbf{T}^e - \sum_e \psi^T h T_\infty \ell_{2-3} \int_0^1 \mathbf{N}^T d\eta \\ &= \sum_e \psi^T \mathbf{h}_T \mathbf{T}^e - \sum_e \psi^T \mathbf{r}_\infty \end{aligned} \quad (10.62b)$$

Substituting for $\mathbf{N} = [0, \eta, 1 - \eta]$, we get

$$\mathbf{h}_T = \frac{h \ell_{2-3}}{6} \begin{bmatrix} 0 & 0 & 0 \\ 0 & 2 & 1 \\ 0 & 1 & 2 \end{bmatrix} \quad (10.63)$$

$$\mathbf{r}_\infty = \frac{h T_\infty \ell_{2-3}}{2} [0 \quad 1 \quad 1]^T \quad (10.64)$$

Next,

$$\int_A \int k \left(\frac{\partial \phi}{\partial x} \frac{\partial T}{\partial x} + \frac{\partial \phi}{\partial y} \frac{\partial T}{\partial y} \right) dA = \int_A \int k \left[\frac{\partial \phi}{\partial x} \frac{\partial \phi}{\partial y} \right] \left\{ \begin{array}{l} \frac{\partial T}{\partial x} \\ \frac{\partial T}{\partial y} \end{array} \right\} dA \quad (10.65a)$$

$$= \sum_e \Psi^T \left[k_e \int_e \mathbf{B}_T^T \mathbf{B}_T dA \right] \mathbf{T}^e \quad (10.65b)$$

$$= \sum_e \Psi^T \mathbf{k}_T \mathbf{T}^e \quad (10.65c)$$

where

$$\mathbf{k}_T = k_e A_e \mathbf{B}_T^T \mathbf{B}_T \quad (10.66)$$

Finally, if $Q = Q_e$ is constant within the element,

$$\int_A \int \phi Q dA = \sum_e \Psi^T Q_e \int_e \mathbf{N} dA = \sum_e \Psi^T \mathbf{r}_Q$$

where

$$\mathbf{r}_Q = \frac{Q_e A_e}{3} [1 \quad 1 \quad 1]^T \quad (10.67)$$

Other distributions of Q within the element are considered in the exercises at the end of this chapter. Thus, Eq. 10.57 is of the form

$$- \sum_e \Psi^T \mathbf{r}_q - \sum_e \Psi^T \mathbf{h}_T \mathbf{T}^e + \sum_e \Psi^T \mathbf{r}_\infty - \sum_e \Psi^T \mathbf{k}_T \mathbf{T}^e + \sum_e \Psi^T \mathbf{r}_Q = 0 \quad (10.68)$$

or

$$\Psi^T (\mathbf{R}_\infty - \mathbf{R}_q + \mathbf{R}_Q) - \Psi^T (\mathbf{H}_T + \mathbf{K}_T) \mathbf{T} = 0 \quad (10.69)$$

which is to hold for all Ψ satisfying $\Psi = 0$ at nodes on S_T . We thus obtain

$$\mathbf{K}^E \mathbf{T}^E = \mathbf{R}^E \quad (10.70)$$

where $\mathbf{K} = \sum_e (\mathbf{k}_T + \mathbf{h}_T)$, $\mathbf{R} = \sum_e (\mathbf{r}_\infty - \mathbf{r}_q + \mathbf{r}_Q)$, and superscript E represents the familiar modifications made to \mathbf{K} and \mathbf{R} to handle $T = T_0$ on S_T by the elimination approach. Alternatively, the Penalty approach can also be used to handle $T = T_0$.

Example 10.4

A long bar of rectangular cross section, having thermal conductivity of $1.5 \text{ W/m} \cdot ^\circ\text{C}$ is subjected to the boundary conditions shown in Fig. E10.4a. Two opposite sides are maintained at a uniform temperature of 180°C ; one side is insulated, and the remaining side is subjected to a convection process with $T_\infty = 25^\circ\text{C}$ and $h = 50 \text{ W/m}^2 \cdot ^\circ\text{C}$. Determine the temperature distribution in the bar.

Solution A five-node, three-element finite element model of the problem is shown in Fig. E10.4b, where symmetry about the horizontal axis is used. Note that the line of symmetry is shown as insulated, since no heat can flow across it.

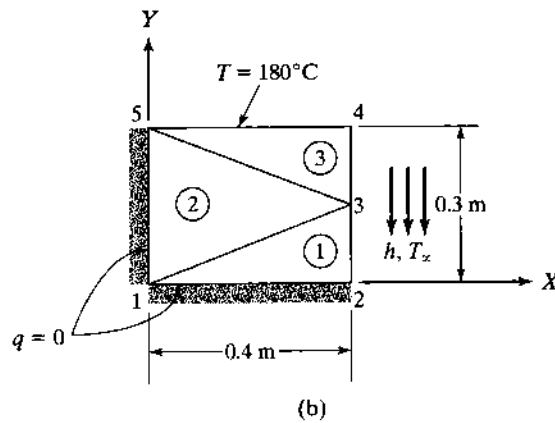
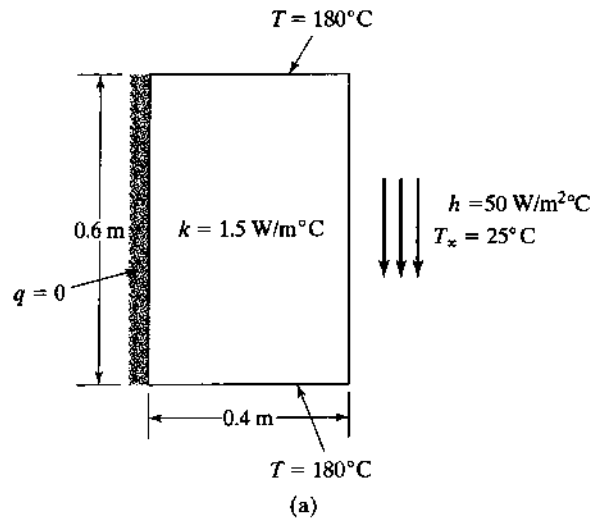


FIGURE E10.4

The element matrices are developed as follows. The element connectivity is defined as in the following table:

| Element | 1 | 2 | 3 | ← local |
|---------|---|---|---|---------|
| 1 | 1 | 2 | 3 | ↑ |
| 2 | 5 | 1 | 3 | global |
| 3 | 5 | 4 | 3 | ↓ |

We have

$$\mathbf{B}_T = \frac{1}{\det \mathbf{J}} \begin{bmatrix} y_{23} & y_{31} & y_{12} \\ x_{32} & x_{13} & x_{21} \end{bmatrix}$$

For each element,

$$\mathbf{B}_T^{(1)} = \frac{1}{0.06} \begin{bmatrix} -0.15 & 0.15 & 0 \\ 0 & -0.4 & 0.4 \end{bmatrix}$$

$$\mathbf{B}_T^{(2)} = \frac{1}{0.12} \begin{bmatrix} -0.15 & -0.15 & 0.3 \\ 0.4 & -0.4 & 0 \end{bmatrix}$$

$$\mathbf{B}_T^{(3)} = \frac{-1}{0.06} \begin{bmatrix} 0.15 & -0.15 & 0 \\ 0 & -0.4 & 0.4 \end{bmatrix}$$

Then, $\mathbf{k}_T = kA_e \mathbf{B}_T^T \mathbf{B}_T$ yields

$$\begin{aligned} \mathbf{k}_T^{(1)} &= (1.5)(0.03) \mathbf{B}_T^{(1)T} \mathbf{B}_T^{(1)} \\ &= \begin{matrix} & \begin{matrix} 1 & 2 & 3 \end{matrix} \\ \begin{matrix} 1 \\ 2 \\ 3 \end{matrix} & \begin{bmatrix} 0.28125 & -0.28125 & 0 \\ -0.28125 & 2.28125 & -2.0 \\ 0 & -2.0 & 2.0 \end{bmatrix} \end{matrix} \end{aligned}$$

$$\mathbf{k}_T^{(2)} = \begin{matrix} & \begin{matrix} 5 & 1 & 3 \end{matrix} \\ \begin{matrix} 5 \\ 1 \\ 3 \end{matrix} & \begin{bmatrix} 1.14 & -0.86 & -0.28125 \\ -0.86 & 1.14 & -0.28125 \\ -0.28125 & -0.28125 & 0.5625 \end{bmatrix} \end{matrix}$$

$$\mathbf{k}_T^{(3)} = \begin{matrix} & \begin{matrix} 5 & 4 & 3 \end{matrix} \\ \begin{matrix} 5 \\ 4 \\ 3 \end{matrix} & \begin{bmatrix} 0.28125 & -0.28125 & 0 \\ -0.28125 & 2.28125 & -2.0 \\ 0 & -2.0 & 2.0 \end{bmatrix} \end{matrix}$$

Now the matrices \mathbf{h}_T for elements with convection edges are developed. Since both elements 1 and 3 have edges 2-3 (in local node numbers) as convection edges, the formula

$$\mathbf{h}_T = \frac{h\ell_{2,3}}{6} \begin{bmatrix} 0 & 0 & 0 \\ 0 & 2 & 1 \\ 0 & 1 & 2 \end{bmatrix}$$

can be used, resulting in

$$\mathbf{h}_T^{(1)} = \begin{matrix} & \begin{matrix} 1 & 2 & 3 \end{matrix} \\ \begin{matrix} 1 \\ 2 \\ 3 \end{matrix} & \begin{bmatrix} 0 & 0 & 0 \\ 0 & 2.5 & 1.25 \\ 0 & 1.25 & 2.5 \end{bmatrix} \end{matrix} \quad \mathbf{h}_T^{(3)} = \begin{matrix} & \begin{matrix} 5 & 4 & 3 \end{matrix} \\ \begin{matrix} 5 \\ 4 \\ 3 \end{matrix} & \begin{bmatrix} 0 & 0 & 0 \\ 0 & 2.5 & 1.25 \\ 0 & 1.25 & 2.5 \end{bmatrix} \end{matrix}$$

The matrix $\mathbf{K} = \Sigma(\mathbf{k}_T + \mathbf{h}_T)$ is now assembled. The elimination approach for handling the boundary conditions $T = 180^\circ\text{C}$ at nodes 4 and 5 results in striking out these rows and columns. However, these fourth and fifth rows are used subsequently for modifying the \mathbf{R} vector. The result is

$$\mathbf{K} = \begin{matrix} & \begin{matrix} 1 & 2 & 3 \end{matrix} \\ \begin{matrix} 1 \\ 2 \\ 3 \end{matrix} & \begin{bmatrix} 1.42125 & -0.28125 & -0.28125 \\ -0.28125 & 4.78125 & -0.75 \\ -0.28125 & -0.75 & 9.5625 \end{bmatrix} \end{matrix}$$

Now the heat-rate vector \mathbf{R} is assembled from element convection contributions. The formula

$$\mathbf{r}_\infty = \frac{hT_\infty \ell_{2-3}}{2} [0 \quad 1 \quad 1]$$

results in

$$\mathbf{r}_\infty^{(1)} = \frac{(50)(25)(0.15)}{2} \begin{bmatrix} 1 & 2 & 3 \\ 0 & 1 & 1 \end{bmatrix}$$

and

$$\mathbf{r}_\infty^{(3)} = \frac{(50)(25)(0.15)}{2} \begin{bmatrix} 5 & 4 & 3 \\ 0 & 1 & 1 \end{bmatrix}$$

Thus,

$$\mathbf{R} = 93.75 \begin{bmatrix} 1 & 2 & 3 \\ 0 & 1 & 2 \end{bmatrix}^T$$

In the elimination approach, \mathbf{R} gets modified according to Eq. 3.70. Solution of $\mathbf{KT} = \mathbf{R}$ then yields

$$[T_1, T_2, T_3] = [124.5, 34.0, 45.4]^\circ\text{C}$$

Note: A large temperature gradient exists along the line connecting nodes 2 and 4. This is because node 4 is maintained at 180°C , while node 2 has a temperature close to the ambient temperature of $T_\infty = 25^\circ\text{C}$ because of the relatively large value of h . This fact implies that our finite element model should capture this large temperature gradient by having sufficient number of nodes along line 2-4. In fact, a model with only two nodes (as opposed to three as used here) will lead to an incorrect solution for the temperatures. Also, with the three-element model considered here, heat-flow values (see computer output) are not accurate. A more detailed model is necessary. ■

It is also noted that a thermal-stress analysis can now be performed once the temperature distribution is known, as discussed in Chapter 5.

Two-Dimensional Fins

In Fig. 10.12a, a thin plate is receiving heat from a pipe and then dissipating it to the surrounding media (air) by convection. We may assume that the temperature gradients are negligible in the z direction, thus, the problem is two-dimensional. Our interest is to determine the temperature distribution $T(x, y)$ in the plate. The plate is the fin here. Considering a differential area dA , the convection heat loss from both lateral surfaces of the fin is $2h(T - T_\infty) dA$. Treating this heat loss as a negative heat source per unit volume, $Q = -2h(T - T_\infty)/t$, where $t =$ thickness of the plate. Equation 10.43 yields the differential equation for two-dimensional fins, namely,

$$\frac{\partial}{\partial x} \left(k \frac{\partial T}{\partial x} \right) + \frac{\partial}{\partial y} \left(k \frac{\partial T}{\partial y} \right) - C(T - T_\infty) + Q = 0 \quad (10.71)$$

where $C = -2h/t$. Another example of a two-dimensional fin may be found in electronic packaging. The thin plate shown in Fig. 10.12b is subjected to a heat source from the surface underneath generated from electronic chips or other circuitry. Pin fins are attached to the top surface to dissipate the heat. As shown in the figure, the plate may

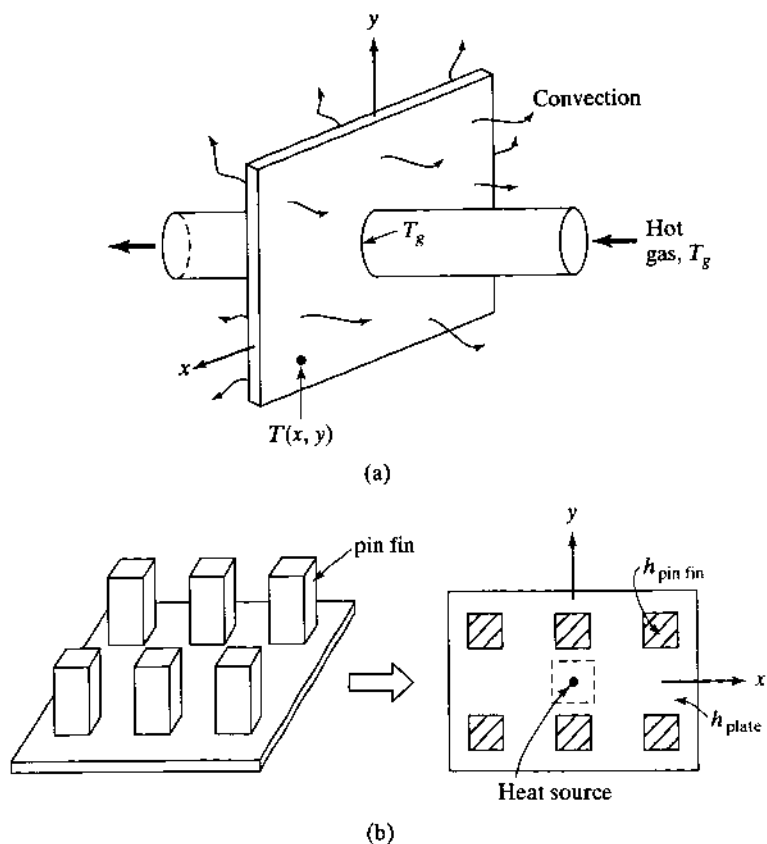


FIGURE 10.12 Two-dimensional fins.

be considered as a two-dimensional fin with higher convective heat-transfer coefficients where the pin fins are attached. In fact, these coefficients may be related to the fin size and material. Maximum temperature at the surface of the chip will be of importance in this analysis. The conductivity matrix \mathbf{k} in Eq. 10.66 and the right-hand-side heat-rate vector \mathbf{r}_Q in Eq. 10.67 get augmented by the matrices

$$+\frac{CA_c}{12} \begin{bmatrix} 2 & 1 & 1 \\ 1 & 2 & 1 \\ 1 & 1 & 2 \end{bmatrix} \quad \text{and} \quad +CT_\infty \frac{A_c}{3} \begin{bmatrix} 1 \\ 1 \\ 1 \end{bmatrix} \quad (10.72)$$

respectively.

Preprocessing for Program Heat2D

The input data file for program HEAT2D can be created, in most part, using the MESH-GEN program. Mesh generation is as usual. Treat specified temperatures as “constrained degrees of freedom,” nodal heat sources as “loads,” element heat sources as “element characteristics” (enter zero if there are none), and thermal conductivity as “material

property." The only thing that remains is the heat flux and convection boundary conditions along the edges; for this, simply edit the data file that you have created and enter this information as per the format of Example 10.4 that has been provided at the end of this chapter. Note that in heat conduction each node has only one degree of freedom.

10.3 TORSION

Consider a prismatic rod of arbitrary cross-sectional shape, which is subjected to a twisting moment M as shown in Fig. 10.13. The problem is to determine shearing stresses τ_{xz} and τ_{yz} (Fig. 10.14) and the angle of twist per unit length, α . It can be shown that the solution of such problems, with simply connected cross sections, reduces to solving the two-dimensional equation

$$\frac{\partial^2 \theta}{\partial x^2} + \frac{\partial^2 \theta}{\partial y^2} + 2 = 0 \quad \text{in } A \quad (10.73)$$

$$\theta = 0 \quad \text{on } S \quad (10.74)$$

where A is interior and S is the boundary of the cross section. Again, we note that Eq. 10.73 is a special case of Helmholtz's equations given in Eq. 10.1. In Eq. 10.74, θ is called the **stress function**, since once θ is known, then shearing stresses are obtained as

$$\tau_{xz} = G\alpha \frac{\partial \theta}{\partial y} \quad \tau_{yz} = -G\alpha \frac{\partial \theta}{\partial x} \quad (10.75)$$

with α determined from

$$M = 2G\alpha \int_A \int \theta \, dA \quad (10.76)$$

where G is the shear modulus of the material. The finite element method for solving Eqs. 10.73 and 10.74 will now be given.

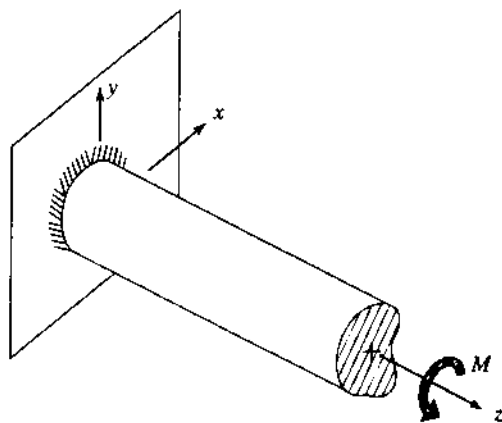


FIGURE 10.13 A rod of arbitrary cross section subjected to a torque.

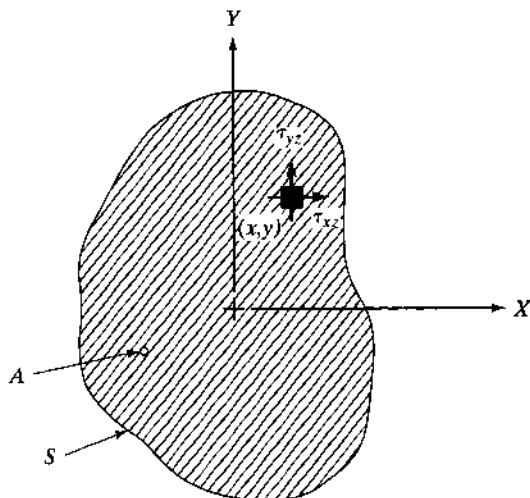


FIGURE 10.14 Shearing stresses in torsion.

Triangular Element

The stress function θ within a triangular element is interpolated as

$$\theta = \mathbf{N}\theta^e \quad (10.77)$$

where $\mathbf{N} = [\xi, \eta, 1 - \xi - \eta]$ are the usual shape functions, and $\theta^e = [\theta_1, \theta_2, \theta_3]^T$ are the nodal values of θ . Furthermore, we have the isoparametric relations (Chapter 5)

$$\begin{aligned} x &= N_1x_1 + N_2x_2 + N_3x_3 \\ y &= N_1y_1 + N_2y_2 + N_3y_3 \\ \begin{Bmatrix} \frac{\partial \theta}{\partial \xi} \\ \frac{\partial \theta}{\partial \eta} \end{Bmatrix} &= \begin{bmatrix} \frac{\partial x}{\partial \xi} & \frac{\partial y}{\partial \xi} \\ \frac{\partial x}{\partial \eta} & \frac{\partial y}{\partial \eta} \end{bmatrix} \begin{Bmatrix} \frac{\partial \theta}{\partial x} \\ \frac{\partial \theta}{\partial y} \end{Bmatrix} \end{aligned} \quad (10.78)$$

or

$$\begin{bmatrix} \frac{\partial \theta}{\partial \xi} & \frac{\partial \theta}{\partial \eta} \end{bmatrix}^T = \mathbf{J} \begin{bmatrix} \frac{\partial \theta}{\partial x} & \frac{\partial \theta}{\partial y} \end{bmatrix}^T$$

where the Jacobian matrix is given by

$$\mathbf{J} = \begin{bmatrix} x_{13} & y_{13} \\ x_{23} & y_{23} \end{bmatrix} \quad (10.79)$$

with $x_{ij} = x_i - x_j$, $y_{ij} = y_i - y_j$, and $|\det \mathbf{J}| = 2A_e$. The preceding equations yield

$$\begin{bmatrix} \frac{\partial \theta}{\partial x} & \frac{\partial \theta}{\partial y} \end{bmatrix}^T = \mathbf{B}\theta^e \quad (10.80a)$$

or

$$[-\tau_{yz} \quad \tau_{xz}]^T = G\alpha \mathbf{B}\theta^e \quad (10.80b)$$

where

$$\mathbf{B} = \frac{1}{\det \mathbf{J}} \begin{bmatrix} y_{23} & y_{31} & y_{12} \\ x_{32} & x_{13} & x_{21} \end{bmatrix} \quad (10.81)$$

The fact that identical relations also apply to the heat-conduction problem in the previous section show the similarity of treating all field problems by the finite element method.

Galerkin Approach[†]

The problem in Eqs. 10.73–10.74 will now be solved using Galerkin's approach. The problem is to find the approximate solution θ such that

$$\int_A \int \phi \left(\frac{\partial^2 \theta}{\partial x^2} + \frac{\partial^2 \theta}{\partial y^2} + 2 \right) dA = 0 \quad (10.82)$$

for every $\phi(x, y)$ constructed from the same basis as θ and satisfying $\phi = 0$ on S . Since

$$\phi \frac{\partial^2 \theta}{\partial x^2} = \frac{\partial}{\partial x} \left(\phi \frac{\partial \theta}{\partial x} \right) - \frac{\partial \phi}{\partial x} \frac{\partial \theta}{\partial x}$$

we have

$$\begin{aligned} \int_A \int \left[\frac{\partial}{\partial x} \left(\phi \frac{\partial \theta}{\partial x} \right) + \frac{\partial}{\partial y} \left(\phi \frac{\partial \theta}{\partial y} \right) \right] dA - \int_A \int \left(\frac{\partial \phi}{\partial x} \frac{\partial \theta}{\partial x} + \frac{\partial \phi}{\partial y} \frac{\partial \theta}{\partial y} \right) dA \\ + \int_A \int 2\phi dA = 0 \end{aligned} \quad (10.83)$$

Using the divergence theorem, the first term in the previous expression reduces to

$$\int_A \int \left[\frac{\partial}{\partial x} \left(\phi \frac{\partial \theta}{\partial x} \right) + \frac{\partial}{\partial y} \left(\phi \frac{\partial \theta}{\partial y} \right) \right] dA = \int_S \phi \left(\frac{\partial \theta}{\partial x} n_x + \frac{\partial \theta}{\partial y} n_y \right) dS = 0 \quad (10.84)$$

where the right side is equated to zero owing to the boundary condition $\phi = 0$ on S . Equation 10.83 becomes

$$\int_A \int \left[\frac{\partial \phi}{\partial x} \frac{\partial \theta}{\partial x} + \frac{\partial \phi}{\partial y} \frac{\partial \theta}{\partial y} \right] dA - \int_A \int 2\phi dA = 0 \quad (10.85)$$

Now, we introduce the isoparametric relations $\theta = \mathbf{N}\theta^e$, etc., as given in Eqs. 10.77–10.81. Further, we denote the global virtual-stress function vector as Ψ whose dimension equals number of nodes in the finite element model. The virtual-stress function within each element is interpolated as

$$\phi = \mathbf{N}\Psi \quad (10.86)$$

[†]The functional approach would be based on minimizing

$$\pi = G\alpha^2 \int_A \int \left\{ \frac{1}{2} \left[\left(\frac{\partial \theta}{\partial x} \right)^2 + \left(\frac{\partial \theta}{\partial y} \right)^2 \right] - 2\theta \right\} dA$$

Moreover, we have

$$\left[\frac{\partial \phi}{\partial x} \quad \frac{\partial \phi}{\partial y} \right]^T = \mathbf{B}\psi \quad (10.87)$$

Substituting these into Eq. 10.85 and noting that

$$\left(\frac{\partial \phi}{\partial x} \frac{\partial \theta}{\partial x} + \frac{\partial \phi}{\partial y} \frac{\partial \theta}{\partial y} \right) = \left(\frac{\partial \phi}{\partial x} \quad \frac{\partial \phi}{\partial y} \right) \left\{ \begin{array}{c} \frac{\partial \theta}{\partial x} \\ \frac{\partial \theta}{\partial y} \end{array} \right\}$$

we get

$$\sum_e \psi^T \mathbf{k} \theta^e - \sum_e \psi^T \mathbf{f} = 0 \quad (10.88)$$

where

$$\mathbf{k} = A_e \mathbf{B}^T \mathbf{B} \quad (10.89)$$

$$\mathbf{f} = \frac{2A_e}{3} [1, 1, 1]^T \quad (10.90)$$

Equation 10.88 can be written as

$$\Psi^T (\mathbf{K}\Theta - \mathbf{F}) = 0 \quad (10.91)$$

which should hold for all Ψ satisfying $\Psi_i = 0$ at nodes i on the boundary. We thus have

$$\mathbf{K}\Theta = \mathbf{F} \quad (10.92)$$

where rows and columns of \mathbf{K} and \mathbf{F} that correspond to boundary nodes have been deleted.

Example 10.5

Consider the shaft with a rectangular cross section shown in Fig. E10.5a. Determine, in terms of M and G , the angle of twist per unit length.

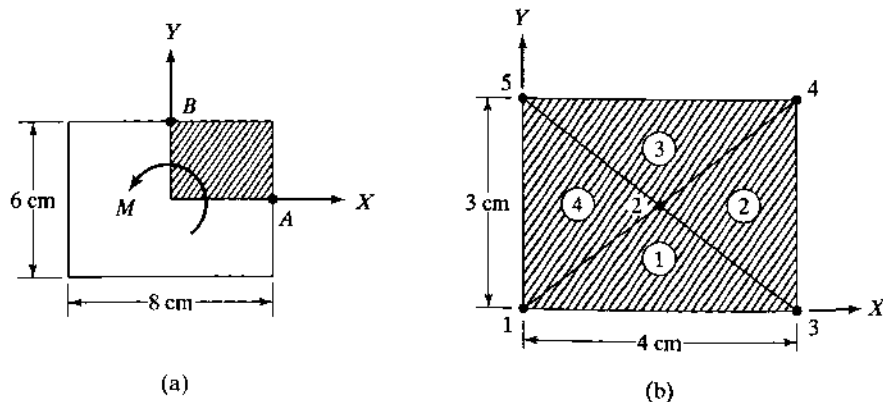


FIGURE E10.5

Solution A finite element model of a quadrant of this cross section is shown in Fig. E10.5b. We define the element connectivity as in the following table:

| Element | 1 | 2 | 3 |
|---------|---|---|---|
| 1 | 1 | 3 | 2 |
| 2 | 3 | 4 | 2 |
| 3 | 4 | 5 | 2 |
| 4 | 5 | 1 | 2 |

Using the relations

$$\mathbf{B} = \frac{1}{\det \mathbf{J}} \begin{bmatrix} y_{23} & y_{31} & y_{12} \\ x_{32} & x_{13} & x_{21} \end{bmatrix}$$

and

$$\mathbf{k} = A_e \mathbf{B}^T \mathbf{B}$$

we get

$$\mathbf{B}^{(1)} = \frac{1}{6} \begin{bmatrix} -1.5 & 1.5 & 0 \\ -2 & -2 & 4 \end{bmatrix} \quad \mathbf{k}^{(1)} = \frac{1}{2} \begin{bmatrix} 1 & 2 & 3 \\ 1.042 & 0.292 & -1.333 \\ & 1.042 & -1.333 \\ \text{Symmetric} & & 2.667 \end{bmatrix}$$

Similarly,

$$\mathbf{k}^{(2)} = \frac{1}{2} \begin{bmatrix} 3 & 4 & 2 \\ 1.042 & -0.292 & -0.75 \\ & 1.042 & -0.75 \\ \text{Symmetric} & & 1.5 \end{bmatrix}$$

$$\mathbf{k}^{(3)} = \frac{1}{2} \begin{bmatrix} 4 & 5 & 2 \\ 1.042 & 0.292 & -1.333 \\ & 1.042 & -1.333 \\ \text{Symmetric} & & 2.667 \end{bmatrix}$$

$$\mathbf{k}^{(4)} = \frac{1}{2} \begin{bmatrix} 5 & 1 & 2 \\ 1.042 & -0.292 & -0.75 \\ & 1.042 & -0.75 \\ \text{Symmetric} & & 1.5 \end{bmatrix}$$

Similarly, the element load vector $\mathbf{f} = (2A_e/3)[1, 1, 1]^T$ for each element is

$$\mathbf{f}^{(i)} = \begin{Bmatrix} 2 \\ 2 \\ 2 \end{Bmatrix} \quad i = 1, 2, 3, 4$$

We can now assemble \mathbf{K} and \mathbf{F} . Since the boundary conditions are

$$\theta_3 = \theta_4 = \theta_5 = 0$$

we are interested only in degrees of freedom 1 and 2. Thus, the finite element equations are

$$\frac{1}{2} \begin{bmatrix} 2.084 & -2.083 \\ -2.083 & 8.334 \end{bmatrix} \begin{Bmatrix} \Theta_1 \\ \Theta_2 \end{Bmatrix} = \begin{Bmatrix} 4 \\ 8 \end{Bmatrix}$$

The solution is

$$[\Theta_1, \Theta_2] = [7.676, 3.838]$$

Consider the equation

$$M = 2G\alpha \int_A \int \theta \, dA$$

Using $\theta = \mathbf{N}\theta^e$, and noting that $\int_c \mathbf{N} \, dA = (A_e/3)[1, 1, 1]$, we get

$$M = 2G\alpha \left[\sum_c \frac{A_e}{3} (\theta_1^e + \theta_2^e + \theta_3^e) \right] \times 4$$

This multiplication by 4 is because the finite element model represents only one-quarter of the rectangular cross section. Thus, we get the angle of twist per unit length to be

$$\alpha = 0.004 \frac{M}{G}$$

For given values of M and G , we can thus determine the value of α . Further, the shearing stresses in each element can be calculated from Eq. 10.80b. ■

10.4 POTENTIAL FLOW, SEEPAGE, ELECTRIC AND MAGNETIC FIELDS, AND FLUID FLOW IN DUCTS

We have discussed steady-state heat conduction and torsion problems in some detail. Other examples of field problems occurring in engineering are briefly discussed subsequently. Their solution follows the same procedure as for heat conduction and torsion problems, since the governing equations are special cases of the general Helmholtz equation, as discussed in the introduction to this chapter. In fact, the computer program HEAT2D can be used to solve the problems given in this section.

Potential Flow

Consider steady-state irrotational flow of an incompressible, nonviscous fluid around a cylinder, as shown in Fig. 10.15a. The velocity of the incoming flow is u_0 . We want to determine the flow velocities near the cylinder. The solution of this problem is given by

$$\frac{\partial^2 \psi}{\partial x^2} + \frac{\partial^2 \psi}{\partial y^2} = 0 \quad (10.93)$$

where ψ is a stream function (m^3/s) per meter in the z direction. The value of ψ is constant along a stream line. A stream line is a line that is tangent to the velocity vector. By definition, there is no flow crossing a stream line. The flow between two adjacent stream

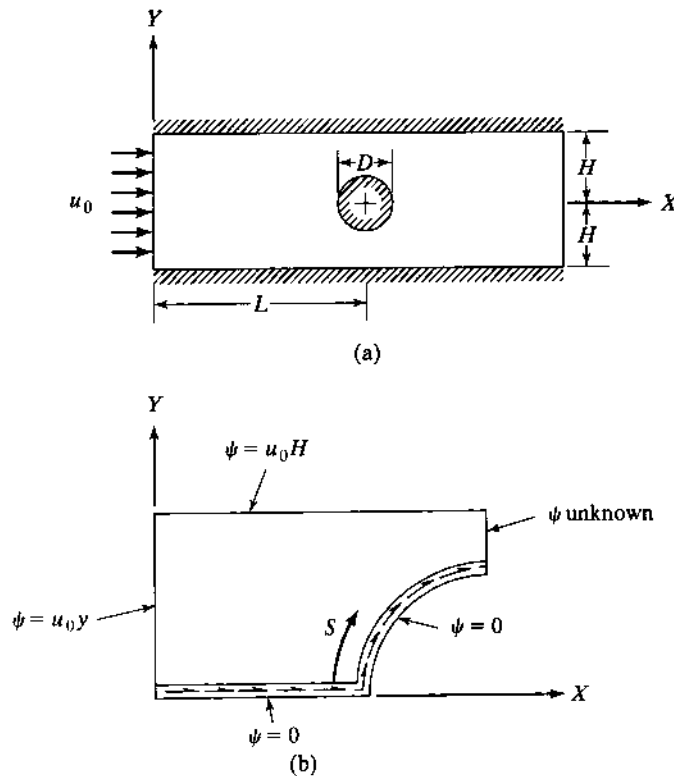


FIGURE 10.15 (a) Flow of an ideal fluid around a cylinder, and (b) boundary conditions for the finite element model.

lines can be thought of as the flow through a tube. Once the stream function $\psi = \psi(x, y)$ is known, the velocity components u and v along x and y , respectively, are obtained as

$$u = \frac{\partial \psi}{\partial y} \quad v = \frac{-\partial \psi}{\partial x} \quad (10.94)$$

Thus, the stream function ψ is analogous to the stress function in the torsion problem. Further, the rate of flow Q through a region bounded by two stream lines A and B is

$$Q = \psi_B - \psi_A \quad (10.95)$$

To illustrate the boundary conditions and use of symmetry, we consider one quadrant of Fig. 10.15a as shown in Fig. 10.15b. First, note that velocities depend only on derivatives of ψ . Thus, we may choose the reference or base value of ψ ; in Fig. 10.15b, we have chosen $\psi = 0$ at all nodes on the x -axis. Then, along the y -axis, we have $u = u_0$ or $\partial \psi / \partial y = u_0$. This is integrated to give the boundary condition $\psi = u_0 y$. That is, for each node i along the y -axis, we have $\psi = u_0 y_i$. Along all nodes on $y = H$, we therefore have $\psi = u_0 H$. On the cylinder we now know that the velocity of the flow into the cylinder is zero. That is, $\partial \psi / \partial s = 0$ (Fig. 10.15b). Integrating this with the fact that $\psi = 0$ at the bottom of the cylinder results in $\psi = 0$ at all nodes along the cylinder. Thus, the fixed boundary is a stream line, as is to be expected.

Seepage

Flow of water that occurs in land drainage or seepage under dams can, under certain conditions, be described by Laplace's equation

$$\frac{\partial}{\partial x} \left(k_x \frac{\partial \phi}{\partial x} \right) + \frac{\partial}{\partial y} \left(k_y \frac{\partial \phi}{\partial y} \right) = 0 \quad (10.96)$$

where $\phi = \phi(x, y)$ is the hydraulic potential (or hydraulic head) and k_x and k_y are the hydraulic conductivity in the x and y directions, respectively. The fluid velocity components are obtained from Darcy's law as $v_x = -k_x(\partial\phi/\partial x)$, $v_y = -k_y(\partial\phi/\partial y)$. Equation 10.96 is similar to the heat conduction equation. Lines of $\phi = \text{constant}$ are called equipotential surfaces, across which flow occurs. Equation 10.96 can include a source or sink Q (see Table 10.1), representing discharge per unit volume, to solve problems where pumps are removing water from an aquifer.

The appropriate boundary conditions associated with Eq. 10.96 are illustrated in the problem of water seepage through an earth dam (Fig. 10.16). The region to be modeled is shown shaded in the figure. Along the left and right surfaces, we have the boundary condition

$$\phi = \text{constant} \quad (10.97)$$

The impermeable bottom surface corresponds to the natural boundary condition, $\partial\phi/\partial n = 0$, where n is the normal, and does not affect the element matrices; the values of ϕ there are unknowns. The top of the region is a *line of seepage* (free surface) where $\partial\phi/\partial n = 0$ and ϕ has its value equal to the y -coordinate:

$$\phi = y \quad (10.98a)$$

This boundary condition requires iterative solution of the finite element analysis since the location of the boundary is unknown. We first assume a location for the line of seepage and impose the boundary condition $\phi = y_i$ at nodes i on the surface. Then, we solve for $\phi = \tilde{\phi}$ and check the error $(\tilde{\phi}_i - y_i)$. Based on this error, we update the locations of the nodes and obtain a new line of seepage. This process is repeated until the error is

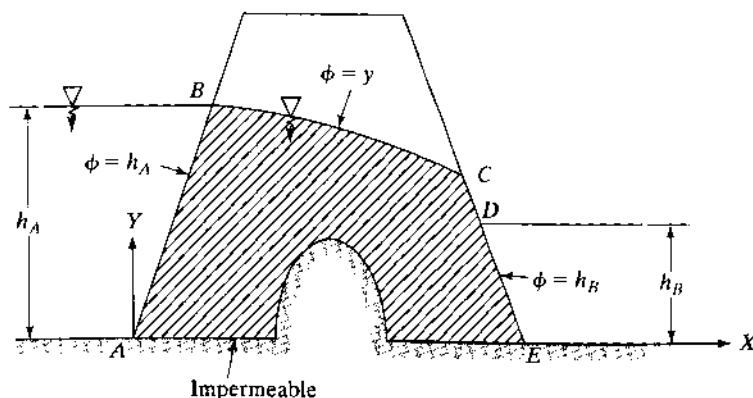


FIGURE 10.16 Seepage through an earth dam.

sufficiently small. Finally, portion CD in Fig. 10.16 is a *surface of seepage*. If no evaporation is taking place in this surface, then we have the boundary condition

$$\phi = \bar{y} \quad (10.98b)$$

where \bar{y} is the coordinate of the surface.

Electrical and Magnetic Field Problems

In the area of electrical engineering, there are several interesting problems involving scalar and vector fields in two and three dimensions. We consider here some of the typical two-dimensional scalar field problems. In an isotropic dielectric medium with a permittivity of ϵ (F/m) and a volume charge density ρ (C/m³), the electric potential u (V) must satisfy (Fig. 10.17)

$$\epsilon \left(\frac{\partial^2 u}{\partial x^2} + \frac{\partial^2 u}{\partial y^2} \right) = -\rho \quad (10.99)$$

where

$$u = a \quad \text{on } S_1 \quad u = b \quad \text{on } S_2$$

Unit thickness may be assumed without loss of generality.

Finite element formulation may proceed from the minimization of the stored field energy

$$\Pi = \frac{1}{2} \int_A \int \epsilon \left[\left(\frac{\partial u}{\partial x} \right)^2 + \left(\frac{\partial u}{\partial y} \right)^2 \right] dx dy - \int_A \rho u dA \quad (10.100)$$

In Galerkin's formulation, we seek the approximate solution u such that

$$\int_A \int \epsilon \left(\frac{\partial u}{\partial x} \frac{\partial \phi}{\partial x} + \frac{\partial u}{\partial y} \frac{\partial \phi}{\partial y} \right) dx dy - \int_A \rho \phi dA = 0 \quad (10.101)$$

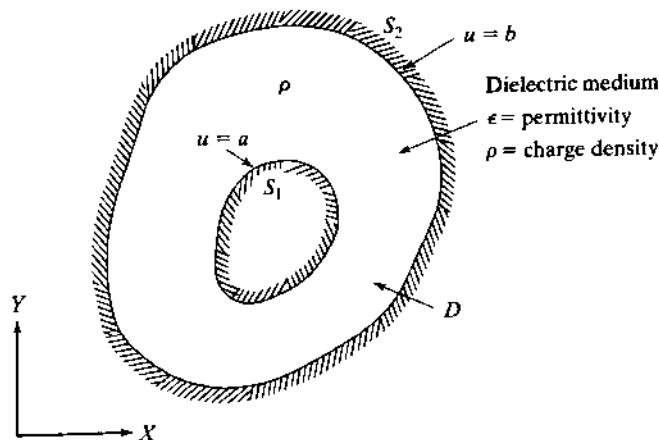


FIGURE 10.17 Electric potential problem.

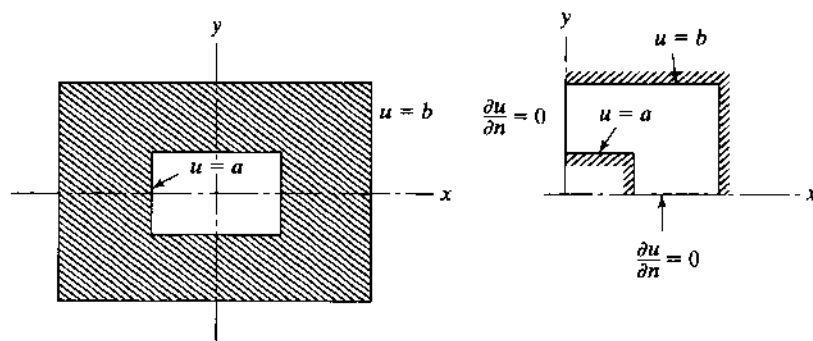


FIGURE 10.18 Rectangular coaxial cable.

for every ϕ constructed from the basis functions of u , satisfying $\phi = 0$ on S_1 and S_2 . In Eq. 10.101, integration by parts has been carried out.

Permittivity ϵ for various materials is defined in terms of relative permittivity ϵ_R and permittivity of free space $\epsilon_0 (= 8.854 \times 10^{-12} \text{F/m})$ as $\epsilon = \epsilon_R \epsilon_0$. Relative permittivity of rubber is in the range of 2.5–3. The coaxial cable problem is a typical example of Eq. 10.99 with $\rho = 0$. Figure 10.18 shows the section of a coaxial cable of rectangular cross section. By symmetry, only a quarter of the section need be considered. On the separated boundary, $\partial u / \partial n = 0$ is a natural boundary condition, which is satisfied automatically in the potential and Galerkin formulations. Another example is the determination of the electrical field distribution between two parallel plates (Fig. 10.19). Here, the field extends to infinity. Since the field drops as we move away from the plates, an arbitrary large domain D is defined, enclosing the plates symmetrically. The dimensions of this enclosure may be 5–10 times the plate dimensions. However, we may use larger elements away from the plates. On the boundary S , we may typically set $u = 0$.

If u is the magnetic field potential, and μ is the permeability (H/m), the field equation is

$$\mu \left(\frac{\partial^2 u}{\partial x^2} + \frac{\partial^2 u}{\partial y^2} \right) = 0 \quad (10.102)$$

where u is the scalar magnetic potential (A). Permeability μ is defined in terms relative permeability μ_R and permeability of free space $\mu_0 (-4\pi \times 10^{-7} \text{H/m})$ as $\mu = \mu_R \mu_0$.

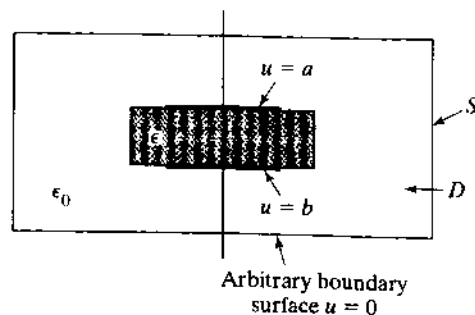


FIGURE 10.19 Parallel strips separated by dielectric medium.

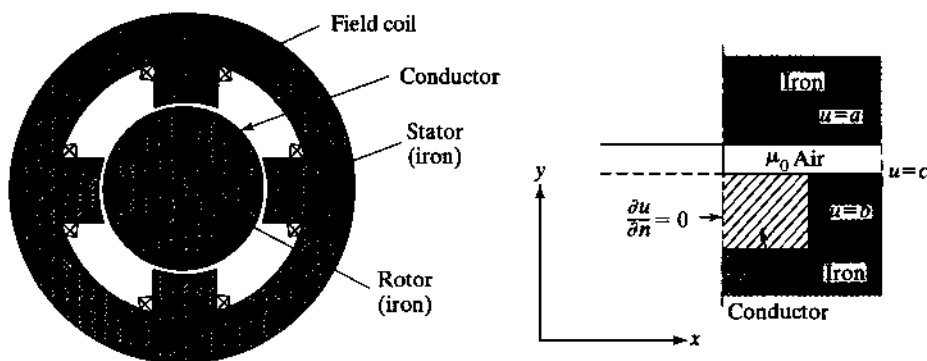


FIGURE 10.20 Model of a simple electric motor.

for pure iron is about 4000, and for aluminum or copper it is about 1. Consider a typical application in an electric motor with no current flowing through the conductor, as shown in Fig. 10.20. We have $u = a$ and $u = b$ on the iron surface; $u = c$ is used on an arbitrarily defined boundary. ($u = 0$ may be used if the boundary is set at a large distance relative to the gap.)

The ideas may be easily extended to axisymmetric coaxial cable problems. Problems in three dimensions can be considered using the steps developed in Chapter 9.

Fluid Flow in Ducts

The pressure drop occurring in the flow of a fluid in long, straight, uniform pipes and ducts is given by the equation

$$\Delta p = 2f\rho v_m^2 \frac{L}{D_h} \quad (10.103)$$

where f is the Fanning friction factor, ρ is the density, v_m is the mean velocity of fluid, L is the length of duct, and $D_h = (4 \times \text{area})/\text{perimeter}$ is the hydraulic diameter. The finite element method for determining the Fanning friction factor f for fully developed laminar flow in ducts of general cross-sectional shape will now be discussed.

Let fluid flow be in the z direction, with x, y being the plane of the cross section. A force balance (Fig. 10.21) yields

$$0 = pA - \left(p + \frac{dp}{dz} \Delta z \right) A - \tau_w P \Delta z \quad (10.104a)$$

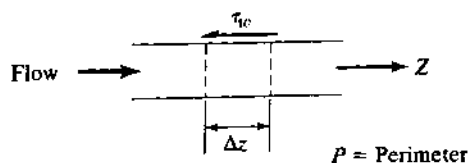


FIGURE 10.21 Force balance for fluid flow in a duct.

or

$$-\frac{dp}{dz} = \frac{4\tau_w}{D_h} \quad (10.104b)$$

where τ_w is the shear stress at the wall. The friction factor is defined as the ratio $f = \tau_w/(\rho v_m^2/2)$. The Reynolds number is defined as $Re = v_m D_h/\nu$, where $\nu = \mu/\rho$ is the kinematic viscosity, with μ representing absolute viscosity. Thus, from previous equations, we get

$$-\frac{dp}{dz} = \frac{2\mu v_m f Re}{D_h^2} \quad (10.105)$$

The momentum equation is given by

$$\mu \left(\frac{\partial^2 w}{\partial x^2} + \frac{\partial^2 w}{\partial y^2} \right) - \frac{dp}{dz} = 0 \quad (10.106)$$

where $w = w(x, y)$ is the velocity of the fluid in the z direction. We introduce the nondimensional quantities

$$X = \frac{x}{D_h} \quad Y = \frac{y}{D_h} \quad W = \frac{w}{2\nu_m f Re} \quad (10.107)$$

Equations 10.105–10.107 result in

$$\frac{\partial^2 W}{\partial X^2} + \frac{\partial^2 W}{\partial Y^2} + 1 = 0 \quad (10.108)$$

Since the velocity of the fluid in contact with the wall of the duct is zero, we have $w = 0$ on the boundary, and hence,

$$W = 0 \quad \text{on boundary} \quad (10.109)$$

The solution of Eqs. 10.108 and 10.109 by the finite element method follows the same steps as for the heat conduction or torsion problems. Once W is known, then its average value may be determined from

$$W_m = \frac{\int_A W dA}{\int_A dA} \quad (10.110)$$

The integral $\int_A W dA$ may be readily evaluated using the element-shape functions. For example, with CST elements, we get $\int_A W dA = \sum_e [A_e(w_1 + w_2 + w_3)/3]$. Once W_m is obtained, Eq. 10.107 is used to get

$$W_m = \frac{w_m}{2\nu_m f Re} = \frac{\nu_m}{2\nu_m f Re} \quad (10.111)$$

which yields

$$f = \frac{1/(2W_m)}{Re} \quad (10.112)$$

Our aim is to determine the constant $1/(2W_m)$, which depends only on the cross-sectional shape. In preparing input data to solve Eqs. 10.108–10.109, we should remember that the nodal coordinates are in nondimensional form, as given in Eq. 10.107.

Acoustics

A very interesting physical phenomenon that can be modeled using Helmholtz's equation in Eq. 10.1 occurs in acoustics. Consider the wave equation in linear acoustics, given by

$$\nabla^2 p - \frac{1}{c^2} \frac{\partial^2 p}{\partial t^2} = 0 \quad (10.113)$$

where p is a scalar quantity, a function of position and time, representing the change in pressure from some ambient value, and c = speed of the sound wave in the media. In many situations, the acoustical disturbance and hence the response is sinusoidal (harmonic) in time. That is, we may represent p as

$$p(\mathbf{x}, t) = p_{\text{amp}}(\mathbf{x}) \cos(\omega t - \phi) \quad (10.114)$$

where p_{amp} is the amplitude or peak pressure, ω is the angular frequency in radians/s, and ϕ is the phase. Substituting Eq. 10.114 into Eq. 10.113, we obtain the Helmholtz equation

$$\nabla^2 p_{\text{amp}} + k^2 p_{\text{amp}} = 0 \quad \text{in } V \quad (10.115)$$

where $k = \omega/c$ is called the wave number, and V represents the acoustic space. Upon solving Eq. 10.115 for the pressure amplitude, we may obtain the pressure function from Eq. 10.114.

Use of complex arithmetic greatly simplifies the handling of amplitude and phase in acoustics. Note the following complex arithmetic concepts: First, a complex number is represented as $a + ib$, where a is the real part and b is the imaginary part, with $i = \sqrt{-1}$ being the imaginary unit. Second, $e^{-i\phi} = \cos \phi - i \sin \phi$. We may now write p in Eq. (10.114) as

$$p = \text{Re}\{p_{\text{amp}} e^{-i(\omega t - \phi)}\} = \text{Re}\{p_{\text{amp}} e^{i\phi} e^{-i\omega t}\} = \text{Re}\{\hat{p} e^{-i\omega t}\} \quad (10.116)$$

where Re denotes the real part of the complex number. In Eq. 10.116, $\hat{p} = p_{\text{amp}}(\cos \phi + i \sin \phi)$. For example, assume that

$$\hat{p} = 3 - 4i$$

Then we have $p_{\text{amp}} = \sqrt{(3^2 + 4^2)} = 5$ and $\phi = \tan^{-1}(-4/3) = -53.1^\circ = -0.927$ rad, resulting in the pressure $p = 5 \cos(\omega t + 0.927)$.

If we substitute for $p = \text{Re}\{\hat{p} e^{-i\omega t}\}$ into the wave equation, we see that the complex pressure term \hat{p} also satisfies Helmholtz equation

$$\nabla^2 \hat{p} + k^2 \hat{p} = 0 \quad \text{in } V \quad (10.117)$$

Boundary Conditions

A vibrating or stationary surface S adjacent to the fluid imposes boundary conditions, which must be accounted for while solving Eq. 10.117. Common types of boundary conditions are as follows:

- (i) Specified pressure: $\hat{p} = \hat{p}_0$ on S_1 . For example, $p = 0$ is a pressure release condition that occurs when a sound wave encounters the atmosphere (ambient surrounding).
- (ii) Specified normal velocity: $v_n = v_{n0}$ on S_2 , where $v_n = \boldsymbol{\nu} \cdot \mathbf{n}$. This states that the normal component of the wave velocity at the solid (impenetrable) surface must be the same as that of the surface itself. Noting that velocity at a point may be specified as a complex quantity, just as in Eq. 10.116, with $\boldsymbol{\nu} = \mathcal{R}_e\{\hat{\boldsymbol{\nu}}e^{-i\omega t}\}$, the boundary condition can be written as $\hat{v}_n = \hat{v}_{n0}$ on S_2 . Equivalently, this condition can be written as

$$\frac{1}{ik\rho c} \nabla \hat{p} \cdot \mathbf{n} = \hat{v}_{n0} \quad (10.118a)$$

If the surface is stationary, then the condition takes the form

$$\frac{\partial \hat{p}}{\partial n} = \nabla \hat{p} \cdot \mathbf{n} = 0 \quad (10.118b)$$

- (iii) There is also the "mixed" boundary condition involving both p and $\frac{\partial p}{\partial n}$, which occurs when the surface is porous. The impedance Z is specified, where $\hat{p} = Z(\omega)\hat{v}_n$, where \hat{v}_n is the inward normal velocity.

Finally, acoustics in an open region (with no enclosed surface) requires the pressure field to satisfy the Sommerfeld conditions at a distance far from the sound source. However, boundary-element methods are more popular in such situations. Later, we focus on interior acoustic cavities (closed regions) with impenetrable surfaces. Thus, we consider only solution of Eq. 10.117 with the boundary conditions in (i) and (ii).

One-Dimensional Acoustics

In one dimension, Eq. 10.117 reduces to

$$\frac{d^2 \hat{p}}{dx^2} + k^2 \hat{p} = 0 \quad (10.119)$$

Assume that the problem is a duct or tube, with a piston vibrating the air at the left end (at $x = 0$) and a rigid wall at the right end at $x = L$. Thus, the boundary conditions are

$$\left. \frac{d\hat{p}}{dx} \right|_{x=L} = 0 \quad \text{and} \quad \left. \frac{d\hat{p}}{dx} \right|_{x=0} = ik\rho cv_0 \quad (10.120)$$

Galerkin's approach requires the equation

$$\int_0^L \phi \left[\frac{d^2 \hat{p}}{dx^2} + k^2 \hat{p} \right] dx = 0$$

to be satisfied for every choice of an arbitrary pressure field $\phi(x)$. If the pressure \hat{p} was specified at a point, then ϕ must equal zero at that point. Here, however, pressure

boundary conditions are absent. Now, following the Galerkin procedure, identical to 1-D heat transfer in thin fins (see Eq. 10.33 and Eq. 10.121), we obtain

$$\phi(L) \frac{d\hat{p}}{dx}(L) - \phi(0) \frac{d\hat{p}}{dx}(0) - \int_0^L \frac{d\hat{p}}{dx} \frac{d\phi}{dx} dx + k^2 \int_0^L \phi \hat{p} dx = 0 \quad (10.121)$$

Using two-node elements with the usual linear shape functions, we have

$$\phi = \mathbf{N}\psi, \hat{p} = \mathbf{N}\hat{\mathbf{p}}, \frac{d\hat{p}}{dx} = \mathbf{B}\hat{\mathbf{p}}, \frac{d\phi}{dx} = \mathbf{B}\psi$$

where $\psi = [\psi_1, \psi_2]^T$ is the arbitrary pressure field at the ends of an element and, as before, $\mathbf{N} = [N_1, N_2]$, $\mathbf{B} = \frac{1}{x_2 - x_1}[-1, 1]$, $\hat{\mathbf{p}} = [\hat{p}_1, \hat{p}_2]^T$ = nodal pressure vector.

Using these, we get

$$\int_{\ell_e} \frac{d\hat{p}}{dx} \frac{d\phi}{dx} dx = \hat{\mathbf{p}}^T \mathbf{k}\psi, \quad \int_{\ell_e} \phi \hat{p} dx = \hat{\mathbf{p}}^T \mathbf{m}\psi$$

where \mathbf{k} and \mathbf{m} are the acoustic stiffness and mass matrices, respectively, given by

$$\mathbf{k} = \frac{1}{\ell_e} \begin{bmatrix} 1 & -1 \\ -1 & 1 \end{bmatrix} \quad \mathbf{m} = \frac{\ell_e}{6} \begin{bmatrix} 2 & 1 \\ 1 & 2 \end{bmatrix} \quad (10.122)$$

The integral over the entire length of the tube leads to the usual assembly of element matrices as

$$\int_0^L \frac{d\hat{p}}{dx} \frac{d\phi}{dx} dx = \mathbf{\Psi}^T \mathbf{K}\hat{\mathbf{P}} \quad \text{and} \quad \int_0^L \phi \hat{p} dx = \mathbf{\Psi}^T \mathbf{M}\hat{\mathbf{P}} \quad (10.123)$$

where $\hat{\mathbf{P}}$ and $\mathbf{\Psi}$ are global nodal vectors of dimension $(N \times 1)$, with N = number of nodes in the model. Referring to Eq. 10.121, and using Eq. 10.120, we have

$$\phi(L) \frac{d\hat{p}}{dx}(L) - \phi(0) \frac{d\hat{p}}{dx}(0) = -\phi(0) ik\rho c v_0$$

Denoting $\mathbf{F} = -ik\rho c v_0 [1, 0, 0, 0, \dots, 0]^T$ and noting that $\phi(0) = \Psi_1$, we can write $-\phi(0) ik\rho c v_0 = \mathbf{\Psi}^T \mathbf{F}$. Substituting this and Eq. 10.120 into Eq. 10.121, and noting that $\mathbf{\Psi}$ is arbitrary, we get

$$\mathbf{K}\hat{\mathbf{P}} - k^2 \mathbf{M}\hat{\mathbf{P}} = \mathbf{F} \quad (10.124)$$

Equation 10.124 may be solved as $\hat{\mathbf{P}} = [\mathbf{K} - k^2 \mathbf{M}]^{-1} \mathbf{F}$. However, determining modes of the system (as explained subsequently) and then using these to solve for $\hat{\mathbf{P}}$ is more efficient and gives better physical understanding.

1-D Axial Vibrations

As is well known in dynamic systems, if the forcing function \mathbf{F} coincides with the natural frequency of the system, resonance occurs. In the present context of acoustics in a tube, if the piston vibrates the air in the tube at certain frequencies, the air reflected from the fixed end will arrive at the piston face just as the piston begins its next stroke. That is,

The following input data file was created for use with Program Jacobi:

Banded Stiffness and Mass for 1-D Acoustic Vibrations

Num. of DOF Bandwidth

7 2

Banded Stiffness Matrix

1 -1

2 -1

2 -1

2 -1

2 -1

2 -1

1 0

Banded Mass Matrix

.333333 .166667

.666667 .166667

.666667 .166667

.666667 .166667

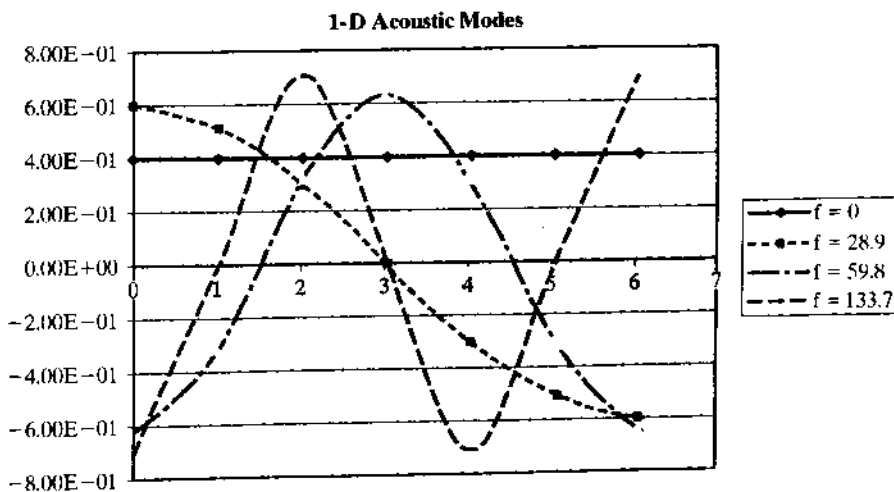
.666667 .166667

.666667 .166667

.333333 .166667

Solution The solution for the eigenvalues and eigenvectors are plotted in Fig. E10.6b.

Note that frequency in cps is obtained from the eigenvalue as $f, \text{cps} = \frac{c \cdot \sqrt{\lambda_n}}{2\pi}$.



We note that the first few frequencies match the theoretical values, $f_n = mc/2L$, $m = 1, 2, \dots$ quite well. Higher order elements that better maintain the boundary conditions are indicated for accurate prediction of higher frequencies. Comparison between finite element solution and theory for the various natural frequencies in cps is tabulated as follows:

| | | | | |
|----------------|------|------|------|-------|
| Finite Element | 28.9 | 59.8 | 94.6 | 133.7 |
| Theory | 28.6 | 57.2 | 85.8 | 114.3 |

Two-Dimensional Acoustics

The two-dimensional problem considered here is

$$\frac{\partial^2 \hat{p}}{\partial x^2} + \frac{\partial^2 \hat{p}}{\partial y^2} + k^2 \hat{p} = 0 \quad \text{in } A \quad (10.126)$$

together with the boundary conditions

$$\hat{p} = \hat{p}_0 \quad \text{on } S_1$$

and

$$\frac{1}{ik\rho c} \nabla \hat{p} \cdot \mathbf{n} = \hat{v}_{n0} \quad \text{on } S_2 \quad (10.127)$$

Galerkin's variational principle requires that the equation

$$\int_A \phi \left(\frac{\partial^2 \hat{p}}{\partial x^2} + \frac{\partial^2 \hat{p}}{\partial y^2} + k^2 \hat{p} \right) dA = 0 \quad (10.128)$$

must be satisfied for every ϕ , $\phi = 0$ on S_1 . Following the procedure used in the heat conduction problem earlier, with three-node triangles, the student should be able to arrive at the equations

$$[\mathbf{K} - k^2 \mathbf{M}] \hat{\mathbf{P}} = \mathbf{F} \quad (10.129)$$

where \mathbf{K} and \mathbf{M} are assembled from element matrices

$$\mathbf{k} = A_e \mathbf{B}^T \mathbf{B},$$

where

$$\mathbf{B} = \frac{1}{2A_e} \begin{bmatrix} y_{23} & y_{31} & y_{12} \\ x_{32} & x_{13} & x_{21} \end{bmatrix}, \quad \mathbf{m} = \frac{A_e}{12} \begin{bmatrix} 2 & 1 & 1 \\ 1 & 2 & 1 \\ 1 & 1 & 2 \end{bmatrix}$$

$$\mathbf{F} = -ik\rho c \int_{S_2} \hat{v}_{n0} \mathbf{N} dS \quad (10.130)$$

Computation of \mathbf{F} is similar to the computation of force vector from surface tractions in Chapter 5. As in the one-dimensional case, acoustic modes can be obtained by setting $\mathbf{F} = 0$ and solving the resulting eigenvalue problem.

10.5 CONCLUSION

We have seen that all the field equations stem from the Helmholtz equations. Our presentation stressed the physical problems rather than considering one general equation with different variables and constants. This approach should help us identify the proper boundary conditions for modeling a variety of problems in engineering.

Input Data File

```

HEATID DATA FILE
EXAMPLE 10.1
NE #BOUNDARY CONDITIONS (B.C.'S) #NODAL HEAT SOURCES
3 2 0
ELEM# THERMAL CONDUCTIVITY
1 20.
2 30.
3 50.
NODE COORDINATE
1 0
2 .3
3 .45
4 .6
NODE BC-TYPE followed by T0(if TEMP) or q0(if HFLUX) or H and Tinf(if CONV)
1 CONV
25 800
4 TEMP
20
NODE HEAT SOURCE

```

Program HeatID - CHANDRUPATLA & BELEGUNDU**Output**

```

EXAMPLE 10.1
NODE# TEMPERATURE
1 3.0476E+02
2 1.1905E+02
3 5.7145E+01
4 2.0002E+01

```

TWO-DIMENSIONAL HEAT ANALYSIS**EXAMPLE 10.4**

```

NN NE NM NDIM NEN NDN
5 3 1 2 3 1

```

```

ND NL NMPC
2 0 0

```

```

Node# X Y
1 0 0
2 .4 0
3 .4 .15
4 .4 .3
5 0 .3

```

```

Elem# N1 N2 N3 MAT# Elem_Heat_Source
1 1 2 3 1 0
2 1 3 5 1 0
3 4 3 5 1 0

```

```

DOF# Displacement (SPECIFIED TEMPERATURE)
4 180.
5 180.

```

```

DOF# Load (NODAL HEAT SOURCE)
MAT# ThermalConductivity
1 1.5

```

```

No. of edges with Specified Heat flux FOLLOWED BY two edges & q0 (positive if
out)
0

```

continued

```

No.of Edges with Convection FOLLOWED BY edge(2 nodes) & h & Tinf
2
2 3 50 25
3 4 50 25

```

Program Heat2D - CHANDRUPATLA & BELEGUNDU

Output

EXAMPLE 10.4

| NODE# | Temperature |
|-------|-------------|
| 1 | 1.2450E+02 |
| 2 | 3.4045E+01 |
| 3 | 4.5351E+01 |
| 4 | 1.8000E+02 |
| 5 | 1.8000E+02 |

==== Conduction Heat Flow per Unit Area in Each Element =====

| ELEM# | $Q_x = -K \cdot DT/Dx$ | $Q_y = -K \cdot DT/Dy$ |
|-------|------------------------|------------------------|
| 1 | 3.3919E+02 | -1.1306E+02 |
| 2 | 4.0086E+02 | -2.7752E+02 |
| 3 | 5.0925E-04 | -1.3465E+03 |

PROBLEMS

- 10.1. Consider a brick wall (Fig. P10.1) of thickness $L = 30$ cm, $k = 0.7$ W/m \cdot $^{\circ}$ C. The inner surface is at 28° C and the outer surface is exposed to cold air at -15° C. The heat-transfer coefficient associated with the outside surface is $h = 40$ W/m 2 \cdot $^{\circ}$ C. Determine the steady-state temperature distribution within the wall and also the heat flux through the wall. Use a two-element model, and obtain the solution by hand calculations. Assume one-dimensional flow. Then prepare input data and run program HEAT1D.

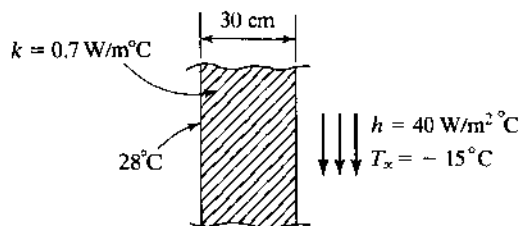


FIGURE P10.1

- 10.2. Heat is entering into a large plate at the rate of $q_0 = -300$ W/m 2 as in Fig. P10.2. The plate is 25 mm thick. The outside surface of the plate is maintained at a temperature of 10° C. Using two finite elements, solve for the vector of nodal temperatures T . Thermal conductivity $k = 1.0$ W/m \cdot $^{\circ}$ C.
- 10.3. Refer to Fig. P10.3. The outside of a heating tape is insulated, while the inside is attached to one face of a 2-cm-thick stainless steel plate ($k = 16.6$ W/m \cdot $^{\circ}$ C). The other face of the plate is exposed to the surroundings, which are at a temperature of 20° C. Heat is supplied at a rate of 500 W/m 2 . Determine the temperature of the face to which the heating tape is attached. Use program HEAT1D.

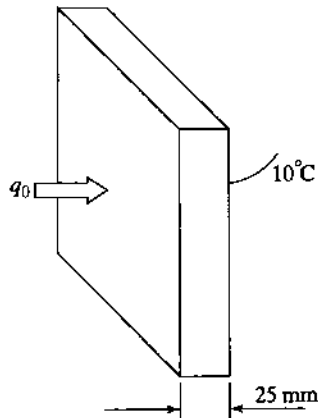


FIGURE P10.2

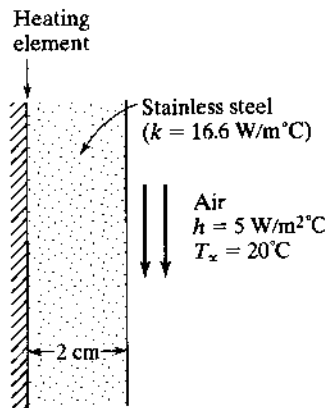


FIGURE P10.3

- 10.4. Consider a pin fin (Fig. P10.4) having a diameter of $\frac{5}{16}$ in. and length of 5 in. At the root, the temperature is 150°F . The ambient temperature is 80°F and $h = 6\text{ BTU}/(\text{h} \cdot \text{ft}^2 \cdot ^\circ\text{F})$. Take $k = 24.8\text{ BTU}/(\text{h} \cdot \text{ft} \cdot ^\circ\text{F})$. Assume that the tip of the fin is insulated. Using a two-element model, determine the temperature distribution and heat loss in the fin (by hand calculations).

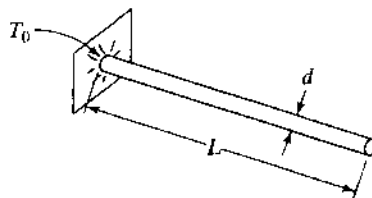


FIGURE P10.4

- 10.5. In our derivation using Galerkin's approach for straight rectangular fins, we assume that the fin tip is insulated. Modify the derivation to account for the case when convection occurs from the tip of the fin as well. Repeat Example 10.4 with this type of boundary condition.
- 10.6. A point P is located inside the triangle as shown in Fig. P10.6. Assuming a linear distribution, determine the temperature at P . Coordinates of the various points are given in the following table:

| Point | X -coordinate | Y -coordinate |
|-------|-----------------|-----------------|
| 1 | 1 | 1 |
| 2 | 10 | 4 |
| 3 | 6 | 7 |
| P | 7 | 4 |

Temperatures at nodes 1, 2, 3 are 120, 140, 80 degrees C respectively

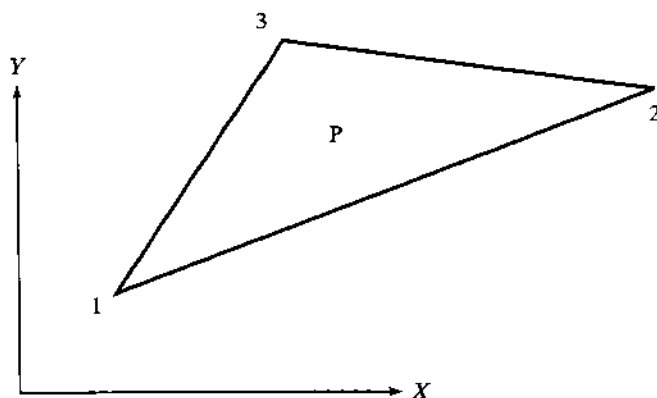


FIGURE P10.6

- 10.7. Consider a mesh for a heat-conduction problem shown in Fig. P10.7. Determine the (half) bandwidth, NBW .

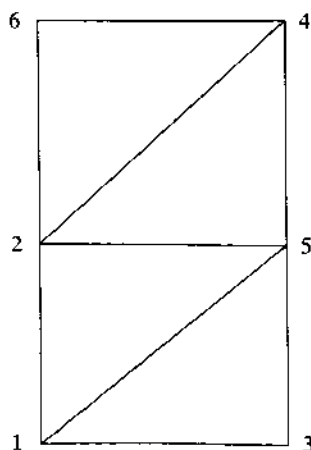


FIGURE P10.7

10.8. Using Galerkin's approach on a heat conduction problem has resulted in the equations

$$(\psi_1, \psi_2) \left\{ \begin{bmatrix} 6 & -2 \\ -2 & 4 \end{bmatrix} \begin{pmatrix} T_1 \\ T_2 \end{pmatrix} - \begin{pmatrix} 10 \\ 20 \end{pmatrix} \right\} = 0$$

- (a) Determine the temperature T_2 if $T_1 = 30^\circ$.
 (b) Determine the temperatures (T_1, T_2) if $T_1 - T_2 = 20^\circ$.
- 10.9. Assume that the heat source vector is linearly distributed within a three-noded triangular element with $\mathbf{Q}^e = [Q_1, Q_2, Q_3]^T$ being the nodal values.
 (a) Derive an expression for the heat-rate vector \mathbf{r}_Q . Show whether your expression reduces to Eq. 10.67 when Q is a constant or $Q_1 = Q_2 = Q_3$.
 (b) Derive the element heat-rate vector \mathbf{r}_Q due to a point heat source of magnitude Q_0 located at (ξ_0, η_0) within the element.
- 10.10. A long steel tube (Fig. P10.10a) with inner radius $r_1 = 3$ cm and outer radius $r_2 = 5$ cm and $k = 20$ W/m \cdot° C has its inner surface heated at a rate $q_0 = -100\,000$ W/m 2 . (The minus sign indicates that heat flows into the body.) Heat is dissipated by convection from the outer surface into a fluid at temperature $T_\infty = 120^\circ$ C and $h = 400$ W/m $^2\cdot^\circ$ C. Considering the eight-element, nine-node finite element model shown in Fig. P10.6b, determine the following:
 (a) The boundary conditions for the model.
 (b) The temperatures T_1, T_2 at the inner and outer surfaces, respectively. Use program HEAT2D.

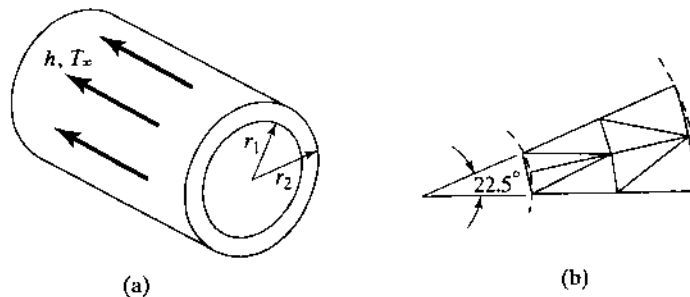


FIGURE P10.10

- 10.11. Solve Example 10.4 with a fine mesh consisting of about 100 elements. View the isotherms using CONTOUR. Plot temperature as a function of x, y . Also, calculate the total heat flow into the plate and the total heat leaving the plate. Is the difference zero? Explain.
- 10.12. In P10.10, assume that the steel tube is free of stress at a room temperature $T = 30^\circ$ C. Determine the thermal stresses in the tube using program AXISYM. Take $E = 200,000$ MPa and $\nu = 0.3$.
- 10.13. The brick chimney shown in Fig. P10.13 is 6 m high. The inside surfaces are at a uniform temperature of 100° C and the outside surfaces are held at a uniform temperature of 30° C. Using a quarter-symmetry model and preprocessing program MESHGEN (plus a little editing as discussed in the text), determine the total rate of heat transfer through the chimney wall. Thermal conductivity of the brick used is 0.72 W/m \cdot° C. (For thermal conductivities of various materials, see F. W. Schmidt et al., *Introduction to Thermal Sciences*, 2nd ed., John Wiley & Sons, Inc., New York, 1993.)

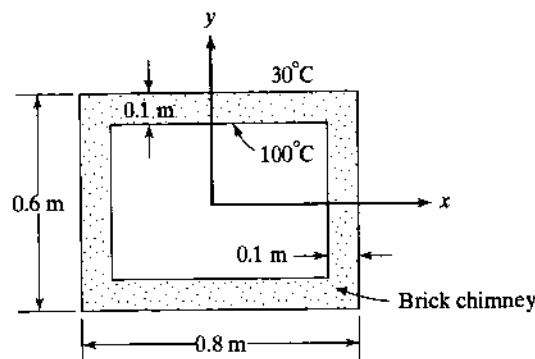


FIGURE P10.13

- 10.14.** A large industrial furnace is supported on a long column of fireclay brick, which is 1×1 m on a side (Fig. P10.11). During steady-state operation, installation is such that three surfaces of the column are maintained at 600°K while the remaining surface is exposed to an airstream for which $T_\infty = 300^\circ\text{K}$ and $h = 12 \text{ W/m}^2 \cdot ^\circ\text{K}$. Determine, using program HEAT2D, the temperature distribution in the column and the heat rate to the airstream per unit length of column. Take $k = 1 \text{ W/m} \cdot ^\circ\text{K}$.

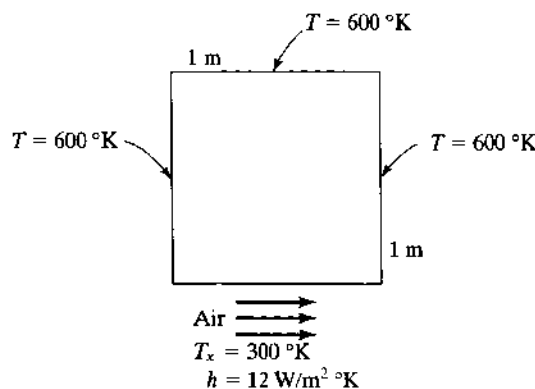


FIGURE P10.14

- 10.15.** Figure 10.15 shows a two-dimensional fin. A hot pipe running through the thin plate results in the inner surface being maintained at a specified temperature of 80°C . Thickness of plate = 0.2 cm , $k = 100 \text{ W/m} \cdot ^\circ\text{C}$, and $T_\infty = 20^\circ\text{C}$. Determine the temperature distribution in the plate. (You will need to modify program HEAT2D to account for the matrices in Eq. 10.72.)
- 10.16.** A thermal diffuser of axisymmetric shape is shown in Fig. P10.16. The thermal diffuser receives a constant thermal flux of magnitude $q_1 = 400\,000 \text{ W/m}^2 \cdot ^\circ\text{C}$ from a solid-state device on which the diffuser is mounted. At the opposite end, the diffuser is kept at a uniform value of $T = 0^\circ\text{C}$ by isothermizing heatpipes. The lateral surface of the diffuser is insulated, and thermal conductivity $k = 200 \text{ W/m} \cdot ^\circ\text{C}$. The differential equation is

$$\frac{1}{r} \frac{\partial}{\partial r} \left(r \frac{\partial T}{\partial r} \right) + \frac{\partial^2 T}{\partial z^2} = 0$$

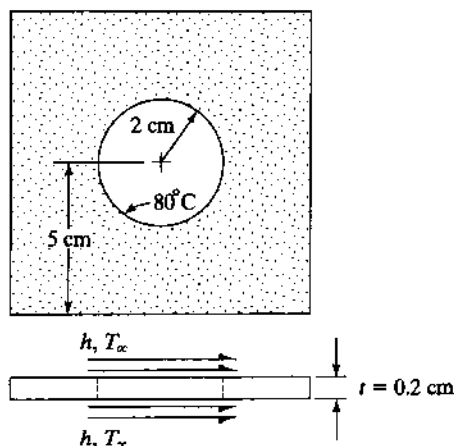


FIGURE P10.15

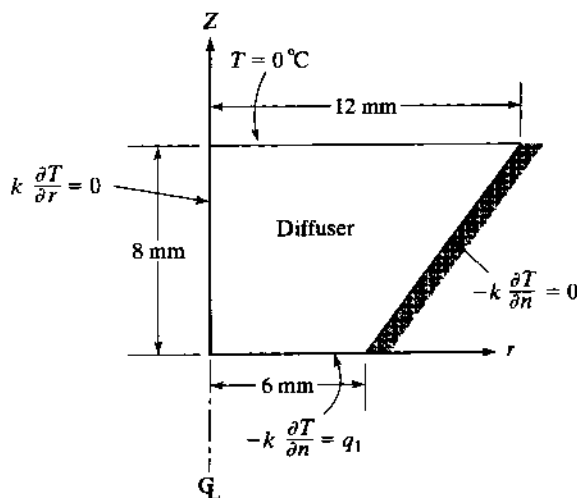


FIGURE P10.16

Develop an axisymmetric element to determine the temperature distribution and the outward heat flux at the heatpipes. Refer to Chapter 6 for details on the axisymmetric element.

- 10.17.** Develop a four-node quadrilateral for heat conduction and solve problem 10.11. Refer to Chapter 7 for details pertaining to the quadrilateral element. Compare your solution with use of three-node triangles.
- 10.18.** The L-shaped beam in Fig. P10.18, which supports a floor slab in a building, is subjected to a twisting moment T in $\cdot\text{lb}$. Determine the following, using program TORSION:
- The angle of twist per unit length, α .
 - The contribution of each finite element to the total twisting moment.
- Leave your answers in terms of torque T and shear modulus G . Verify your answers by refining the finite element grid.

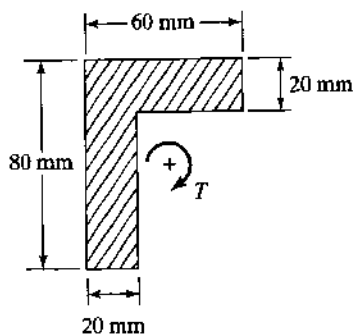


FIGURE P10.18

- 10.19.** The cross section of the steel beam in Fig. P10.19 is subjected to a torque $T = 5000$ in/lb. Determine, using program TORSION, the angle of twist and the location and magnitude of the maximum shearing stresses.

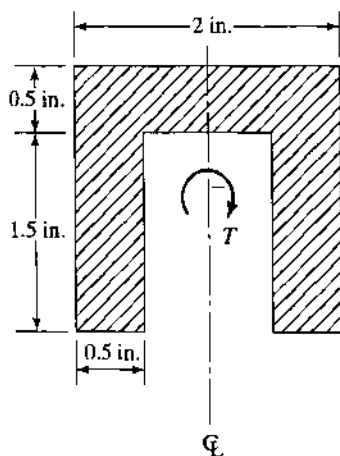


FIGURE P10.19

- 10.20.** For Fig. 10.14a in the text, let $u^0 = 1$ m/s, $L = 5$ m, $D = 1.5$ m, and $H = 2.0$ m. Determine the velocity field using a coarse grid and a fine grid (with smaller elements nearer the cylinder). In particular, determine the maximum velocity in the flow. Comment on the relation of this problem to a stress-concentration problem.
- 10.21.** Determine and plot the stream lines for the flow in the venturi meter shown in Fig. P10.21. The incoming flow has a velocity of 100 cm/s. Also plot the velocity distribution at the waist $a-a$.

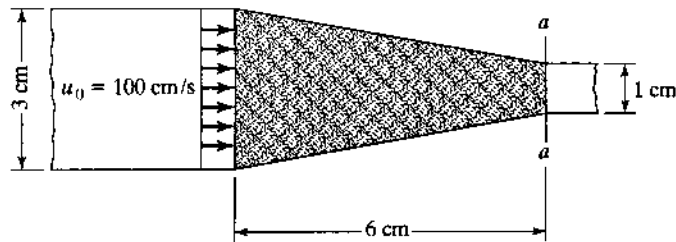


FIGURE P10.21

- 10.22. The dam shown in Fig. P10.22 rests on a homogeneous isotropic soil which has confined impermeable boundaries as shown. The walls and base of the dam are impervious. The dam retains water at a constant height of 5 m, the downstream level being zero. Determine and plot the equipotential lines, and find the quantity of water seeping underneath the dam per unit width of the dam. Take hydraulic conductivity $k = 30$ m/day.

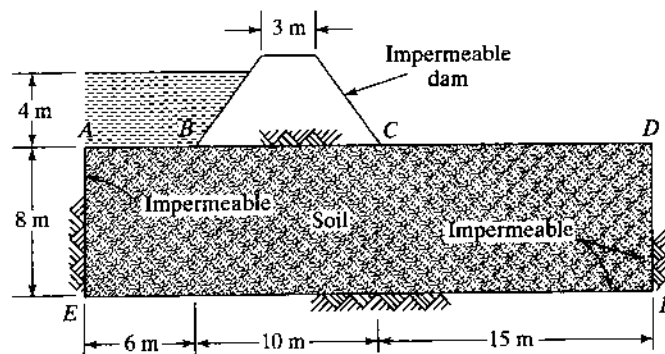


FIGURE P10.22

- 10.23. For the dam section shown in Fig. P10.23, $k = 0.003$ ft/min. Determine the following:
- The line of seepage.
 - The quantity of seepage per 100-ft length of the dam.
 - The length of the surface of seepage a .

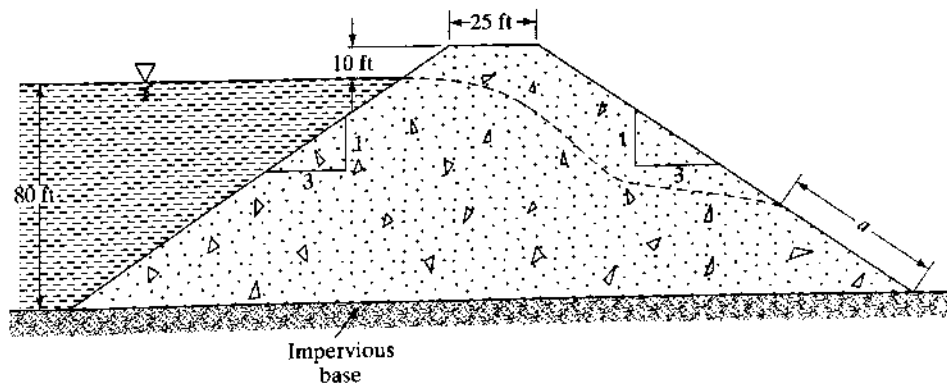


FIGURE P10.23

- 10.24. For the triangular duct shown in Fig. P10.24, obtain the constant C , which relates the Fanning friction factor f to the Reynolds number R_e as $f = C/R_e$. Use triangular finite elements. Verify your answer by refining the finite element model. Compare your result for C with that for a square duct having the same perimeter.

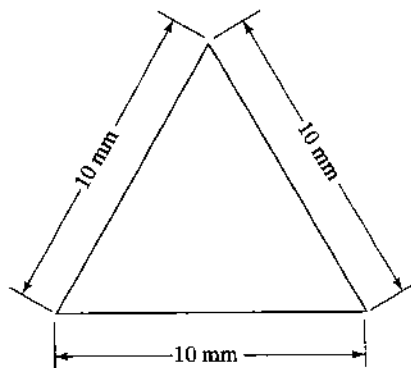


FIGURE P10.24

- 10.25. Figure P10.25 shows the cross section of a rectangular coaxial cable. At the inner surface of the dielectric insulator ($\epsilon_R = 3$), a voltage of 100 V is applied. If the voltage at the outer surface is zero, determine the voltage field distribution in the annular space.

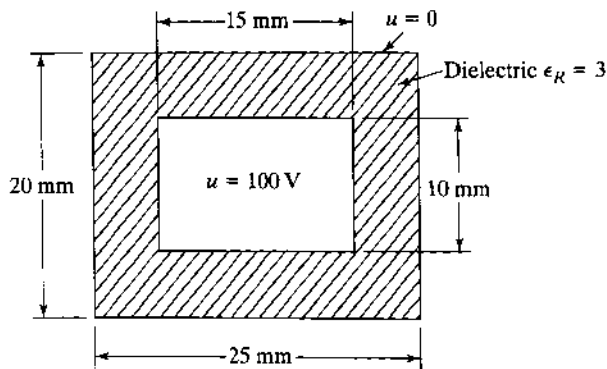


FIGURE P10.25

- 10.26. A pair of strip lines, shown in Fig. P10.26, is separated by a dielectric medium $\epsilon_R = 5.4$. The strips are enclosed by a fictitious box $2 \times 1 \text{ m}$ with enclosed space having $\epsilon_R = 1$. Assuming $u = 0$ on the boundary of this box, find the voltage field distribution. (Use large elements away from the strip plates.)

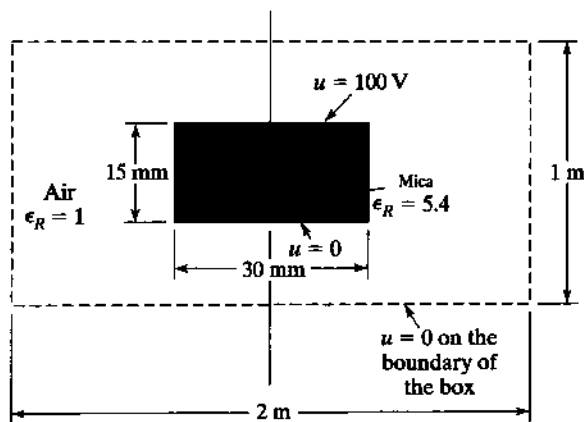


FIGURE P10.26

- 10.27. Determine the scalar magnetic potential u for the simplified model of the slot in an electric-motor armature shown in Fig. P10.27.

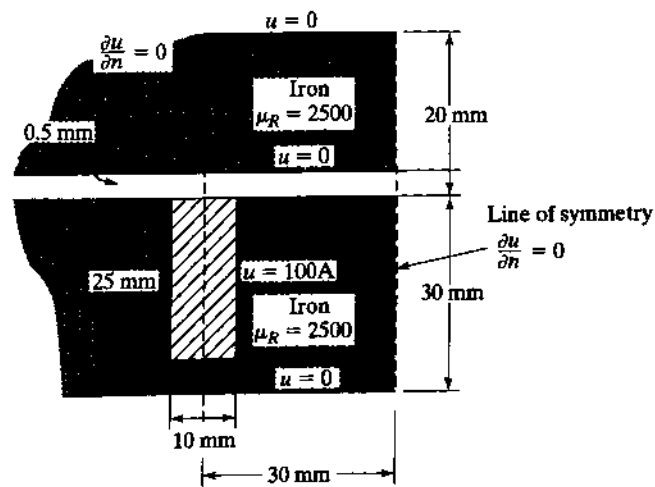


FIGURE P10.27

- 10.28. Repeat Example 10.6 with
 (a) 12 elements,
 (b) 24 elements, and
 (c) 48 elements.
 Plot convergence curves of frequency, cps Vs Number of elements.

- 10.29. Consider a tube of length 6 m as in Fig. P10.29. Fluid in the tube is air; thus, $c = 343$ m/s. One end is rigid while the other end is a pressure-release condition, as shown. Determine the mode shapes and natural frequencies, and compare then with the analytical solution

$$f_n = \left(m + \frac{1}{2}\right) \frac{c}{2L}. \text{ Adopt a six-element model.}$$

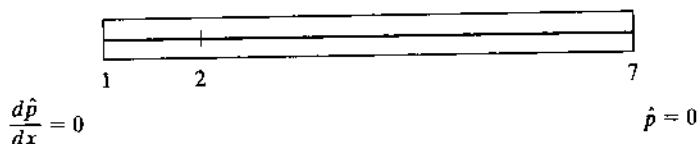


FIGURE P10.29

- 10.30. Derive the element matrices in Eq. 10.130 from Galerkin's variational statement in Eq. 10.128.
- 10.31. Solve the eigenvalue problem resulting from the two-dimensional problem in Eq. 10.129 and solve for the first four modes of the rectangular room/cavity shown in Fig. 10.31. Dimensions of the cavity are $L_x, L_y, L_z = (20 \text{ m}, 10 \text{ m}, 0.1 \text{ m})$. Provide plots of the mode shapes, and compare the natural frequencies with the analytical solution $c = 343$ m/s. Try a coarse mesh and a fine mesh. Use the equation

$$f_{\ell,m,n} = \frac{c}{2} \sqrt{\left(\frac{\ell}{L_x}\right)^2 + \left(\frac{m}{L_y}\right)^2 + \left(\frac{n}{L_z}\right)^2} \quad \text{cps, } \ell, m, n = 0, 1, 2, \dots$$

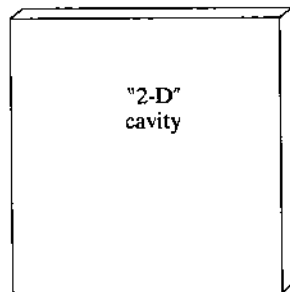


FIGURE P10.31

Program Listings

```

*****
**      PROGRAM HEAT1D      *
**  FOR 1D HEAT AND FIELD PROBLEMS *
**  T.R.Chandrupatla and A.D.Belegundu *
*****
===== MAIN PROGRAM =====
Private Sub cmdStart_Click()
  Call InputData
  Call Stiffness
  Call ModifyForBC
  Call BandSolver
  Call Output
  cmdView.Enabled = True
  cmdStart.Enabled = False
End Sub
=====

```

```

===== DATA INPUT FROM A FILE =====
Private Sub InputData()
  File1 = InputBox("Input File d:\dir\fileName.ext", "Name of File")
  Open File1 For Input As #1
  Line Input #1, Dummy: Input #1, Title
  Line Input #1, Dummy
  Input #1, NE, NBC, NQ
  NN = NE + 1
  NBW = 2 'NBW is half the bandwidth
  ReDim X(NN), S(NN, NBW), TC(NE), F(NN), V(NBC), H(NBC), NB(NBC)
  ReDim BC(NBC)
  '----- READ DATA -----
  '----- Element Thermal Conductivity -----
  Line Input #1, Dummy
  For I = 1 To NE
    Input #1, N
    Input #1, TC(N)
  Next I
  '----- Coordinates -----
  Line Input #1, Dummy
  For I = 1 To NN
    Input #1, N
    Input #1, X(N)
  Next I
  '----- Boundary Conditions -----
  Line Input #1, Dummy
  For I = 1 To NBC
    Input #1, NB(I), BC$(I)
    If BC(I) = "TEMP" Or BC(I) = "temp" Then Input #1, V(I)
    If BC(I) = "HFLUX" Or BC(I) = "hflux" Then Input #1, V(I)
    If BC(I) = "CONV" Or BC(I) = "conv" Then Input #1, H(I), V(I)
  Next I

```

continued

```

'----- Calculate and Input Nodal Heat Source Vector -----
Line Input #1, Dummy
For I = 1 To NN: F(I) = 0: Next I
For I = 1 To NQ
    Input #1, N
    Input #1, F(N)
Next I
Close #1
End Sub
=====

```

```

'===== ELEMENT STIFFNESS AND ASSEMBLY =====
Private Sub Stiffness()
    ReDim S(NN, NBW)
    '----- Stiffness Matrix -----
    For J = 1 To NBW
        For I = 1 To NN: S(I, J) = 0: Next I: Next J
    For I = 1 To NE
        I1 = I: I2 = I + 1
        ELL = Abs(X(I2) - X(I1))
        EKL = TC(I) / ELL
        S(I1, 1) = S(I1, 1) + EKL
        S(I2, 1) = S(I2, 1) + EKL
        S(I1, 2) = S(I1, 2) - EKL: Next I
    End Sub
=====

```

```

'===== MODIFICATION FOR BOUNDARY CONDITIONS =====
Private Sub ModifyForBC()
    '----- Decide Penalty Parameter CNST -----
    AMAX = 0
    For I = 1 To NN
        If S(I, 1) > AMAX Then AMAX = S(I, 1)
    Next I
    CNST = AMAX * 10000
    For I = 1 To NBC
        N = NB(I)
        If BC(I) = "CONV" Or BC(I) = "conv" Then
            S(N, 1) = S(N, 1) + H(I)
            F(N) = F(N) + H(I) * V(I)
        ElseIf BC(I) = "HFLUX" Or BC(I) = "hflux" Then
            F(N) = F(N) - V(I)
        Else
            S(N, 1) = S(N, 1) + CNST
            F(N) = F(N) + CNST * V(I)
        End If
    Next I
End Sub
=====

```

```

*****
!*      PROGRAM HEAT2D      *
!*  HEAT 2-D WITH 3-NODED TRIANGLES  *
!*  FOR 2D HEAT AND FIELD PROBLEMS  *
!*  T.R.Chandrupatla and A.D.Belegundu *
*****
\===== MAIN PROGRAM =====
Private Sub cmdStart_Click()
    Call InputData
    Call Bandwidth
    Call Stiffness
    Call ModifyForBC
    Call BandSolver
    Call HeatFlowCalc
    Call Output
    cmdView.Enabled = True
    cmdStart.Enabled = False
End Sub
\=====

```

```

\===== DATA INPUT FROM A FILE =====
Private Sub InputData()
    Dim msg As String, File As String
    File = InputBox("Input File d:\dir\fileName.txt", "Name of File")
    Open File For Input As #1
    msg = " 1) No Plot Data" & Chr(13)
    msg = msg + " 2) Create Data File Containing Nodal Temperatures" & Chr(13)
    msg = msg + "    Choose 1 or 2"
    IPL = InputBox(msg, "Plot Choice", 1) '--- default is no data
    Line Input #1, Dummy: Input #1, Title
    Line Input #1, Dummy: Input #1, NN, NE, NM, NDIM, NEN, NDN
    Line Input #1, Dummy: Input #1, ND, NL, NMPC
    NMPC = 0
    '--- ND = NO. OF SPECIFIED TEMPERATURES
    '--- NL = NO. OF NODAL HEAT SOURCES
    'NOTE!! NMPC = 0 FOR THIS PROGRAM
    '--- EHS(I) = ELEMENT HEAT SOURCE, I = 1,...,NE
    ReDim X(NN, 2), NOC(NE, 3), MAT(NE), PM(NM, 1), F(NN)
    ReDim NU(ND), U(ND), EHS(NE)
    '===== READ DATA =====
    '----- Coordinates
    Line Input #1, Dummy
    For I = 1 To NN
        Input #1, N
        For J = 1 To NDIM
            Input #1, X(N, J)
        Next J
    Next I
    '----- Connectivity, Material#, Element Heat Source
    Line Input #1, Dummy
    For I = 1 To NE
        Input #1, N

```

continued

```

      For J = 1 To NEN
        Input #1, NOC(N, J)
      Next J
      Input #1, MAT(N), EHS(N)
    Next I
    '----- Temperature BC
    Line Input #1, Dummy
    For I = 1 To ND
      Input #1, NU(I), U(I)
    Next I
    '----- Nodal Heat Sources
    Line Input #1, Dummy
    For I = 1 To NN: F(I) = 0: Next I
    For I = 1 To NL
      Input #1, N
      Input #1, F(N)
    Next I

    '----- Thermal Conductivity of Material
    Line Input #1, Dummy
    For I = 1 To NM
      Input #1, N, PM(N, 1)
    Next I

    'No. of edges with Specified Heat flux FOLLOWED BY two edges
    '& q0 (positive if out)
    Line Input #1, Dummy
    Input #1, NHF
    If NHF > 0 Then
      ReDim NFLUX(NHF, 2), FLUX(NHF)
      For I = 1 To NHF
        Input #1, NFLUX(I, 1), NFLUX(I, 2), FLUX(I)
      Next I
    End If

    'No. of Edges with Convection FOLLOWED BY edge(2 nodes) & h & Tinf
    Line Input #1, Dummy
    Input #1, NCV
    If NCV > 0 Then
      ReDim NCONV(NCV, 2), H(NCV), TINF(NCV)
      For I = 1 To NCV
        Input #1, NCONV(I, 1), NCONV(I, 2), H(I), TINF(I)
      Next I
    End If
    Close #1
  End Sub
  -----

```

```

===== ELEMENT STIFFNESS AND ASSEMBLY =====
Private Sub Stiffness()
  '----- Initialization of Conductivity Matrix and Heat Rate Vector
  ReDim S(NN, NBW)
  For I = 1 To NN
    For J = 1 To NBW
      S(I, J) = 0
    Next J
  Next I
  If NHF > 0 Then
    For I = 1 To NHF
      N1 = NFLUX(I, 1): N2 = NFLUX(I, 2)
      V = FLOX(I)
      ELEN = Sqr((X(N1, 1) - X(N2, 1)) ^ 2 + (X(N1, 2) - X(N2, 2)) ^ 2)
      F(N1) = F(N1) - ELEN * V / 2
      F(N2) = F(N2) - ELEN * V / 2
    Next I
  End If
  If NCV > 0 Then
    For I = 1 To NCV
      N1 = NCONV(I, 1): N2 = NCONV(I, 2)
      ELEN = Sqr((X(N1, 1) - X(N2, 1)) ^ 2 + (X(N1, 2) - X(N2, 2)) ^ 2)
      F(N1) = F(N1) + ELEN * H(I) * TINF(I) / 2
      F(N2) = F(N2) + ELEN * H(I) * TINF(I) / 2
      S(N1, 1) = S(N1, 1) + H(I) * ELEN / 3
      S(N2, 1) = S(N2, 1) + H(I) * ELEN / 3
      If N1 >= N2 Then
        N3 = N1: N1 = N2: N2 = N3
      End If
      S(N1, N2 - N1 + 1) = S(N1, N2 - N1 + 1) + H(I) * ELEN / 6
    Next I
  End If
  '----- Conductivity Matrix
  ReDim BT(2, 3)
  For I = 1 To NE
    I1 = NOC(I, 1): I2 = NOC(I, 2): I3 = NOC(I, 3)
    X32 = X(I3, 1) - X(I2, 1): X13 = X(I1, 1) - X(I3, 1)
    X21 = X(I2, 1) - X(I1, 1)
    Y23 = X(I2, 2) - X(I3, 2): Y31 = X(I3, 2) - X(I1, 2)
    Y12 = X(I1, 2) - X(I2, 2)
    DETJ = X13 * Y23 - X32 * Y31
    AREA = 0.5 * Abs(DETJ)
    '---- Element Heat Sources
    If EHS(I) <> 0 Then
      C = EHS(I) * AREA / 3
      F(I1) = F(I1) + C: F(I2) = F(I2) + C: F(I3) = F(I3) + C
    End If
    BT(1, 1) = Y23: BT(1, 2) = Y31: BT(1, 3) = Y12
    BT(2, 1) = X32: BT(2, 2) = X13: BT(2, 3) = X21
    For II = 1 To 3
      For JJ = 1 To 2
        BT(JJ, II) = BT(JJ, II) / DETJ
      Next JJ
    Next II
  Next II

```

continued

```

For II = 1 To 3
  For JJ = 1 To 3
    III = NOC(I, II): II2 = NOC(I, JJ)
    If III <= II2 Then
      Sum = 0
      For J = 1 To 2
        Sum = Sum + BT(J, II) * BT(J, JJ)
      Next J
      IC = II2 - III + 1
      S(III, IC) = S(III, IC) + Sum * AREA * PM(MAT(I), 1)
    End If
  Next JJ
Next II
Next I
End Sub
=====

```

```

===== HEAT FLOW CALCULATIONS =====
Private Sub HeatFlowCalc()
  ReDim Q(NE, 2)
  For I = 1 To NE
    I1 = NOC(I, 1): I2 = NOC(I, 2): I3 = NOC(I, 3)
    X32 = X(I3, 1) - X(I2, 1): X13 = X(I1, 1) - X(I3, 1)
    X21 = X(I2, 1) - X(I1, 1)
    Y23 = X(I2, 2) - X(I3, 2): Y31 = X(I3, 2) - X(I1, 2)
    Y12 = X(I1, 2) - X(I2, 2)
    DETJ = X13 * Y23 - X32 * Y31
    BT(1, 1) = Y23: BT(1, 2) = Y31: BT(1, 3) = Y12
    BT(2, 1) = X32: BT(2, 2) = X13: BT(2, 3) = X21
    For II = 1 To 3
      For JJ = 1 To 2
        BT(JJ, II) = BT(JJ, II) / DETJ
      Next JJ
    Next II
    QX = BT(1, 1) * F(II) + BT(1, 2) * F(I2) + BT(1, 3) * F(I3)
    QX = -QX * PM(MAT(I), 1)
    QY = BT(2, 1) * F(II) + BT(2, 2) * F(I2) + BT(2, 3) * F(I3)
    QY = -QY * PM(MAT(I), 1)
    Q(I, 1) = QX
    Q(I, 2) = QY
  Next I
End Sub
=====

```

Dynamic Considerations

11.1 INTRODUCTION

In Chapters 3–9, we have discussed the static analysis of structures. Static analysis holds when the loads are slowly applied. When the loads are suddenly applied, or when the loads are of a variable nature, the mass and acceleration effects come into the picture. If a solid body, such as an engineering structure, is deformed elastically and suddenly released, it tends to vibrate about its equilibrium position. This periodic motion due to the restoring strain energy is called **free vibration**. The number of cycles per unit time is called the **frequency**. The maximum displacement from the equilibrium position is the **amplitude**. In the real world, the vibrations subside with time due to damping action. In the simplest vibration model, the damping effects are neglected. The undamped free-vibration model of a structure gives significant information about its dynamic behavior. We present here the considerations needed to apply finite elements to the analysis of undamped free vibrations of structures.

11.2 FORMULATION

We define the Lagrangean by

$$L = T - \Pi \quad (11.1)$$

where T is the kinetic energy and Π is the potential energy.

Hamilton's principle For an arbitrary time interval from t_1 to t_2 , the state of motion of a body extremizes the functional

$$I = \int_{t_1}^{t_2} L dt \quad (11.2)$$

If L can be expressed in terms of the generalized variables $(q_1, q_2, \dots, q_n, \dot{q}_1, \dot{q}_2, \dots, \dot{q}_n)$ where $\dot{q}_i = dq_i/dt$, then the equations of motion are given by

$$\frac{d}{dt} \left(\frac{\partial L}{\partial \dot{q}_i} \right) - \frac{\partial L}{\partial q_i} = 0 \quad i = 1 \text{ to } n \quad (11.3)$$

To illustrate the principle, let us consider two point masses connected by springs. Consideration of distributed masses follows the example.

Example 11.1

Consider the spring-mass system in Fig. E11.1. The kinetic and potential energies are given by

$$T = \frac{1}{2}m_1\dot{x}_1^2 + \frac{1}{2}m_2\dot{x}_2^2$$

$$\Pi = \frac{1}{2}k_1x_1^2 + \frac{1}{2}k_2(x_2 - x_1)^2$$

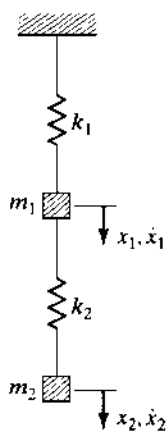


FIGURE E11.1

Using $L = T - \Pi$, we obtain the equations of motion

$$\frac{d}{dt} \left(\frac{\partial L}{\partial \dot{x}_1} \right) - \frac{\partial L}{\partial x_1} = m_1\ddot{x}_1 + k_1x_1 - k_2(x_2 - x_1) = 0$$

$$\frac{d}{dt} \left(\frac{\partial L}{\partial \dot{x}_2} \right) - \frac{\partial L}{\partial x_2} = m_2\ddot{x}_2 + k_2(x_2 - x_1) = 0$$

which can be written in the form

$$\begin{bmatrix} m_1 & 0 \\ 0 & m_2 \end{bmatrix} \begin{Bmatrix} \ddot{x}_1 \\ \ddot{x}_2 \end{Bmatrix} + \begin{bmatrix} (k_1 + k_2) & -k_2 \\ -k_2 & k_2 \end{bmatrix} \begin{Bmatrix} x_1 \\ x_2 \end{Bmatrix} = \mathbf{0}$$

which is of the form

$$\mathbf{M}\ddot{\mathbf{x}} + \mathbf{K}\mathbf{x} = \mathbf{0} \quad (11.4)$$

where \mathbf{M} is the mass matrix, \mathbf{K} is the stiffness matrix, and $\ddot{\mathbf{x}}$ and \mathbf{x} are vectors representing accelerations and displacements. ■

Solid Body with Distributed Mass

We now consider a solid body with distributed mass (Fig. 11.1). The potential-energy term has already been considered in Chapter 1. The kinetic energy is given by

$$T = \frac{1}{2} \int_V \dot{\mathbf{u}}^T \dot{\mathbf{u}} \rho dV \quad (11.5)$$

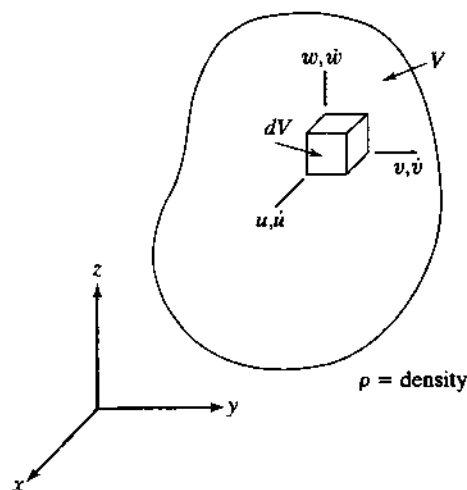


FIGURE 11.1 Body with distributed mass.

where ρ is the density (mass per unit volume) of the material and

$$\dot{\mathbf{u}} = [\dot{u}, \dot{v}, \dot{w}]^T \quad (11.6)$$

is the velocity vector of the point at \mathbf{x} , with components \dot{u} , \dot{v} , and \dot{w} . In the finite element method, we divide the body into elements, and in each element, we express \mathbf{u} in terms of the nodal displacements \mathbf{q} , using shape functions \mathbf{N} . Thus,

$$\mathbf{u} = \mathbf{N}\mathbf{q} \quad (11.7)$$

In dynamic analysis, the elements of \mathbf{q} are dependent on time, while \mathbf{N} represents (spatial) shape functions defined on a master element. The velocity vector is then given by

$$\dot{\mathbf{u}} = \mathbf{N}\dot{\mathbf{q}} \quad (11.8)$$

When Eq. 11.8 is substituted into Eq. 11.5, the kinetic energy T_e in element e is

$$T_e = \frac{1}{2} \dot{\mathbf{q}}^T \left[\int_e \rho \mathbf{N}^T \mathbf{N} dV \right] \dot{\mathbf{q}} \quad (11.9)$$

where the bracketed expression is the element mass matrix

$$\mathbf{m}^e = \int_e \rho \mathbf{N}^T \mathbf{N} dV \quad (11.10)$$

This mass matrix is consistent with the shape functions chosen and is called the *consistent mass matrix*. Mass matrices for various elements are given in the next section. On summing over all the elements, we get

$$T = \sum_e T_e = \sum_e \frac{1}{2} \dot{\mathbf{q}}^T \mathbf{m}^e \dot{\mathbf{q}} = \frac{1}{2} \dot{\mathbf{Q}}^T \mathbf{M} \dot{\mathbf{Q}} \quad (11.11)$$

The potential energy is given by

$$\Pi = \frac{1}{2} \mathbf{Q}^T \mathbf{K} \mathbf{Q} - \mathbf{Q}^T \mathbf{F} \quad (11.12)$$

Using the Lagrangean $L = T - \Pi$, we obtain the equation of motion:

$$\mathbf{M} \ddot{\mathbf{Q}} + \mathbf{K} \mathbf{Q} = \mathbf{F} \quad (11.13)$$

For free vibrations the force \mathbf{F} is zero. Thus,

$$\mathbf{M} \ddot{\mathbf{Q}} + \mathbf{K} \mathbf{Q} = 0 \quad (11.14)$$

For the steady-state condition, starting from the equilibrium state, we set

$$\mathbf{Q} = \mathbf{U} \sin \omega t \quad (11.15)$$

where \mathbf{U} is the vector of nodal amplitudes of vibration and ω (rad/s) is the circular frequency ($=2\pi f$, f = cycles/s or Hz). Introducing Eq. 11.15 into Eq. 11.14, we have

$$\mathbf{K} \mathbf{U} = \omega^2 \mathbf{M} \mathbf{U} \quad (11.16)$$

This is the generalized eigenvalue problem

$$\mathbf{K} \mathbf{U} = \lambda \mathbf{M} \mathbf{U} \quad (11.17)$$

where \mathbf{U} is the eigenvector, representing the vibrating mode, corresponding to the eigenvalue λ . The eigenvalue λ is the square of the circular frequency ω . The frequency f in hertz (cycles per second) is obtained from $f = \omega/(2\pi)$.

The previous equations can also be obtained by using D'Alembert's principle and the principle of virtual work. Galerkin's approach applied to equations of motion of an elastic body also yields this set of equations.

11.3 ELEMENT MASS MATRICES

Since the shape functions for various elements have been discussed in detail in the earlier chapters, we now give the element mass matrices. Treating the material density ρ to be constant over the element, we have, from Eq. 11.10,

$$\mathbf{m}^e = \rho \int_e \mathbf{N}^T \mathbf{N} dV \quad (11.18)$$

One-dimensional bar element For the bar element shown in Fig. 11.2,

$$\begin{aligned} \mathbf{q}^T &= [q_1 \quad q_2] \\ \mathbf{N} &= [N_1 \quad N_2] \end{aligned} \quad (11.19)$$

where

$$\begin{aligned} N_1 &= \frac{1 - \xi}{2} & N_2 &= \frac{1 + \xi}{2} \\ \mathbf{m}^e &= \rho \int_e \mathbf{N}^T \mathbf{N} A dx = \frac{\rho A_e \ell_e}{2} \int_{-1}^{+1} \mathbf{N}^T \mathbf{N} d\xi \end{aligned}$$

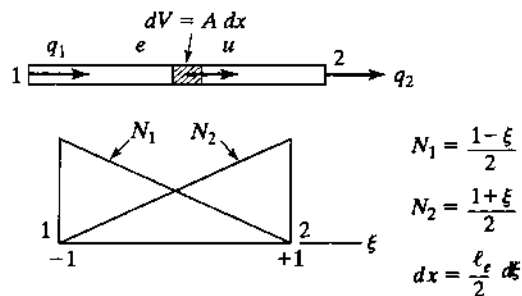


FIGURE 11.2 Bar element.

On carrying out the integration of each term in $\mathbf{N}^T \mathbf{N}$, we find that

$$\mathbf{m}^e = \frac{\rho A_e l_e}{6} \begin{bmatrix} 2 & 1 \\ 1 & 2 \end{bmatrix} \quad (11.20)$$

Truss element For the truss element shown in Fig. 11.3,

$$\begin{aligned} \mathbf{u}^T &= [u \quad v] \\ \mathbf{q}^T &= [q_1 \quad q_2 \quad q_3 \quad q_4] \\ \mathbf{N} &= \begin{bmatrix} N_1 & 0 & N_2 & 0 \\ 0 & N_1 & 0 & N_2 \end{bmatrix} \end{aligned} \quad (11.21)$$

where

$$N_1 = \frac{1-\xi}{2} \quad N_2 = \frac{1+\xi}{2}$$

in which ξ is defined from -1 to $+1$. Then,

$$\mathbf{m}^e = \frac{\rho A_e l_e}{6} \begin{bmatrix} 2 & 0 & 1 & 0 \\ 0 & 2 & 0 & 1 \\ 1 & 0 & 2 & 0 \\ 0 & 1 & 0 & 2 \end{bmatrix} \quad (11.22)$$

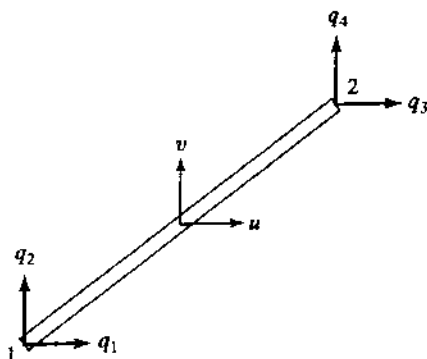


FIGURE 11.3 Truss element.

CST element For the plane stress and plane strain conditions for the CST element shown in Fig. 11.4, we have, from Chapter 5,

$$\begin{aligned} \mathbf{u}^T &= [u \quad v] \\ \mathbf{q}^T &= [q_1 \quad q_2 \quad \cdots \quad q_6] \\ \mathbf{N} &= \begin{bmatrix} N_1 & 0 & N_2 & 0 & N_3 & 0 \\ 0 & N_1 & 0 & N_2 & 0 & N_3 \end{bmatrix} \end{aligned} \quad (11.23)$$

The element mass matrix is then given by

$$\mathbf{m}^e = \rho t_e \int_e \mathbf{N}^T \mathbf{N} dA$$

Noting that $\int_e N_1^2 dA = \frac{1}{6} A_e$, $\int_e N_1 N_2 dA = \frac{1}{12} A_e$, etc., we have

$$\mathbf{m}^e = \frac{\rho t_e A_e}{12} \begin{bmatrix} 2 & 0 & 1 & 0 & 1 & 0 \\ & 2 & 0 & 1 & 0 & 1 \\ & & 2 & 0 & 1 & 0 \\ & & & 2 & 0 & 1 \\ \text{Symmetric} & & & & 2 & 0 \\ & & & & & 2 \end{bmatrix} \quad (11.24)$$

Axisymmetric triangular element For the axisymmetric triangular element, we have

$$\mathbf{u}^T = [u \quad w]$$

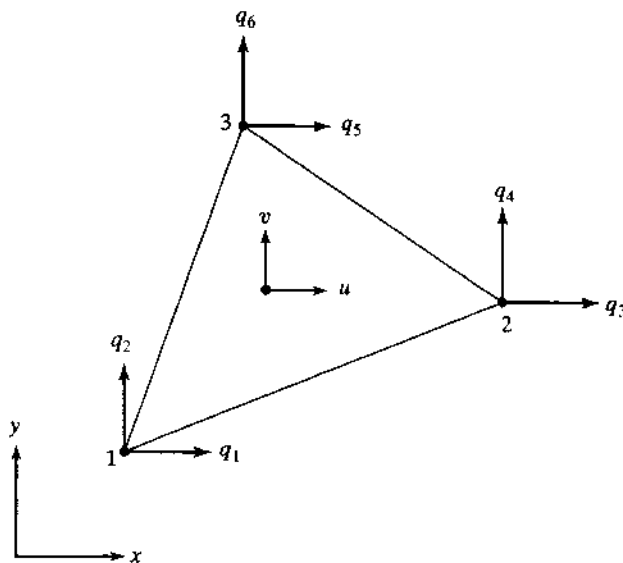


FIGURE 11.4 CST element.

where u and w are the radial and axial displacements, respectively. The vectors \mathbf{q} and \mathbf{N} are similar to those for the triangular element given in Eq. 11.23. We have

$$\mathbf{m}^e = \int_e \rho \mathbf{N}^T \mathbf{N} dV = \int_e \rho \mathbf{N}^T \mathbf{N} 2\pi r dA \quad (11.25)$$

Since $r = N_1 r_1 + N_2 r_2 + N_3 r_3$, we have

$$\mathbf{m}^e = 2\pi\rho \int_e (N_1 r_1 + N_2 r_2 + N_3 r_3) \mathbf{N}^T \mathbf{N} dA$$

Noting that

$$\int_e N_1^3 dA = \frac{2A_e}{20}, \int_e N_1^2 N_2 dA = \frac{2A_e}{60}, \int_e N_1 N_2 N_3 dA = \frac{2A_e}{120}, \text{etc.}$$

we get

$$\mathbf{m}_e = \frac{\pi\rho A_e}{10} \begin{bmatrix} \frac{4}{3}r_1 + 2\bar{r} & 0 & 2\bar{r} - \frac{r_3}{3} & 0 & 2\bar{r} - \frac{r_2}{3} & 0 \\ & \frac{4}{3}r_1 + 2\bar{r} & 0 & 2\bar{r} - \frac{r_3}{3} & 0 & 2\bar{r} - \frac{r_2}{3} \\ & & \frac{4}{3}r_2 + 2\bar{r} & 0 & 2\bar{r} - \frac{r_1}{3} & 0 \\ & & & \frac{4}{3}r_2 + 2\bar{r} & 0 & 2\bar{r} - \frac{r_1}{3} \\ \text{Symmetric} & & & & \frac{4}{3}r_3 + 2\bar{r} & 0 \\ & & & & & \frac{4}{3}r_3 + 2\bar{r} \end{bmatrix} \quad (11.26)$$

where

$$\bar{r} = \frac{r_1 + r_2 + r_3}{3} \quad (11.27)$$

Quadrilateral element For the quadrilateral element for plane stress and plane strain,

$$\begin{aligned} \mathbf{u}^T &= [u \quad v] \\ \mathbf{q}^T &= [q_1 \quad q_2 \quad \cdots \quad q_8] \\ \mathbf{N} &= \begin{bmatrix} N_1 & 0 & N_2 & 0 & N_3 & 0 & N_4 & 0 \\ 0 & N_1 & 0 & N_2 & 0 & N_3 & 0 & N_4 \end{bmatrix} \end{aligned} \quad (11.28)$$

The mass matrix is then given by

$$\mathbf{m}^e = \rho t_e \int_{-1}^1 \int_{-1}^1 \mathbf{N}^T \mathbf{N} \det \mathbf{J} d\xi d\eta \quad (11.29)$$

This integral needs to be evaluated by numerical integration.

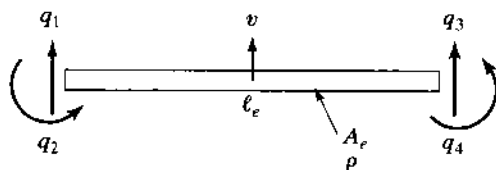


FIGURE 11.5 Beam element.

Beam element For the beam element shown in Fig. 11.5, we use the Hermite shape functions given in Chapter 8. We have

$$v = \mathbf{H}\mathbf{q}$$

$$\mathbf{m}^e = \int_{-1}^{+1} \mathbf{H}^T \mathbf{H} \rho A_e \frac{\ell_e}{2} d\xi \quad (11.30)$$

On integrating, we get

$$\mathbf{m}^e = \frac{\rho A_e \ell_e}{420} \begin{bmatrix} 156 & 22\ell_e & 54 & -13\ell_e \\ & 4\ell_e^2 & 13\ell_e & -3\ell_e^2 \\ \text{Symmetric} & & 156 & -22\ell_e \\ & & & 4\ell_e^2 \end{bmatrix} \quad (11.31)$$

Frame element We refer to Fig. 8.9, showing the frame element. In the body coordinate system x', y' , the mass matrix can be seen as a combination of bar element and beam element. Thus, the mass matrix in the prime system is given by

$$\mathbf{m}^{e'} = \begin{bmatrix} 2a & 0 & 0 & a & 0 & 0 \\ & 156b & 22\ell_e^2 b & 0 & 54b & -13\ell_e b \\ & & 4\ell_e^2 b & 0 & 13\ell_e b & -3\ell_e^2 b \\ & & & 2a & 0 & 0 \\ \text{Symmetric} & & & & 156b & -22\ell_e b \\ & & & & & 4\ell_e^2 b \end{bmatrix} \quad (11.32)$$

where

$$a = \frac{\rho A_e \ell_e}{6} \quad \text{and} \quad b = \frac{\rho A_e \ell_e}{420}$$

Using the transformation matrix \mathbf{L} given by Eq. 8.48, we now obtain the mass matrix \mathbf{m}^e in the global system:

$$\mathbf{m}^e = \mathbf{L}^T \mathbf{m}^{e'} \mathbf{L} \quad (11.33)$$

Tetrahedral element For the tetrahedral element presented in Chapter 9,

$$\mathbf{u}^T = [u \quad v \quad w]$$

$$\mathbf{N} = \begin{bmatrix} N_1 & 0 & 0 & N_2 & 0 & 0 & N_3 & 0 & 0 & N_4 & 0 & 0 \\ 0 & N_1 & 0 & 0 & N_2 & 0 & 0 & N_3 & 0 & 0 & N_4 & 0 \\ 0 & 0 & N_1 & 0 & 0 & N_2 & 0 & 0 & N_3 & 0 & 0 & N_4 \end{bmatrix} \quad (11.34)$$

The mass matrix of the element is then given by

$$\mathbf{m}^e = \frac{\rho V_e}{20} \begin{bmatrix} 2 & 0 & 0 & 1 & 0 & 0 & 1 & 0 & 0 & 1 & 0 & 0 \\ & 2 & 0 & 0 & 1 & 0 & 0 & 1 & 0 & 0 & 1 & 0 \\ & & 2 & 0 & 0 & 1 & 0 & 0 & 1 & 0 & 0 & 1 \\ & & & 2 & 0 & 0 & 1 & 0 & 0 & 1 & 0 & 0 \\ & & & & 2 & 0 & 0 & 1 & 0 & 0 & 1 & 0 \\ \text{Symmetric} & & & & & 2 & 0 & 0 & 1 & 0 & 0 & 1 \\ & & & & & & 2 & 0 & 0 & 1 & 0 & 0 \\ & & & & & & & 2 & 0 & 0 & 1 & 0 \\ & & & & & & & & 2 & 0 & 0 & 1 \\ & & & & & & & & & 2 & 0 & 0 \\ & & & & & & & & & & 2 & 0 \\ & & & & & & & & & & & 2 \end{bmatrix} \quad (11.35)$$

Lumped mass matrices Consistent mass matrices have been presented. Practicing engineers also use lumped mass techniques, where the total element mass in each direction is distributed equally to the nodes of the element, and the masses are associated with translational degrees of freedom only. For the truss element, the lumped mass approach gives a mass matrix of

$$\mathbf{m}^e = \frac{\rho A_e \ell_e}{2} \begin{bmatrix} 1 & 0 & 0 & 0 \\ & 1 & 0 & 0 \\ & & 1 & 0 \\ \text{Symmetric} & & & 1 \end{bmatrix} \quad (11.36)$$

For the beam element, the lumped element mass matrix is

$$\mathbf{m}^e = \frac{\rho A_e \ell_e}{2} \begin{bmatrix} 1 & 0 & 0 & 0 \\ & 0 & 0 & 0 \\ & & 1 & 0 \\ \text{Symmetric} & & & 0 \end{bmatrix} \quad (11.37)$$

Consistent mass matrices yield more accurate results for flexural elements such as beams. The lumped mass technique is easier to handle since only diagonal elements are involved. The natural frequencies obtained from lumped mass techniques are lower than the exact values. In our presentation, we discuss techniques for determining the eigenvalues and eigenvectors with consistent mass formulations. The programs presented can be used for lumped mass cases also.

11.4 EVALUATION OF EIGENVALUES AND EIGENVECTORS

The generalized problem in free vibration is that of evaluating an eigenvalue $\lambda (= \omega^2)$, which is a measure of the frequency of vibration together with the corresponding eigenvector \mathbf{U} indicating the mode shape, as in Eq. 11.17, restated here:

$$\mathbf{K}\mathbf{U} = \lambda\mathbf{M}\mathbf{U} \quad (11.38)$$

We observe here that \mathbf{K} and \mathbf{M} are symmetric matrices. Further, \mathbf{K} is positive definite for properly constrained problems.

Properties of Eigenvectors

For a positive definite symmetric stiffness matrix of size n , there are n real eigenvalues and corresponding eigenvectors satisfying Eq. 11.38. The eigenvalues may be arranged in ascending order:

$$0 \leq \lambda_1 \leq \lambda_2 \leq \dots \leq \lambda_n \quad (11.39)$$

If $\mathbf{U}_1, \mathbf{U}_2, \dots, \mathbf{U}_n$ are the corresponding eigenvectors, we have

$$\mathbf{K}\mathbf{U}_i = \lambda_i\mathbf{M}\mathbf{U}_i \quad (11.40)$$

The eigenvectors possess the property of being orthogonal with respect to both the stiffness and mass matrices:

$$\mathbf{U}_i^T\mathbf{M}\mathbf{U}_j = 0 \quad \text{if } i \neq j \quad (11.41a)$$

$$\mathbf{U}_i^T\mathbf{K}\mathbf{U}_j = 0 \quad \text{if } i \neq j \quad (11.41b)$$

The lengths of eigenvectors are generally normalized so that

$$\mathbf{U}_i^T\mathbf{M}\mathbf{U}_i = 1 \quad (11.42a)$$

The foregoing normalization of the eigenvectors leads to the relation

$$\mathbf{U}_i^T\mathbf{K}\mathbf{U}_i = \lambda_i \quad (11.42b)$$

In many codes, other normalization schemes are also used. The length of an eigenvector may be fixed by setting its largest component to a preset value, say, unity.

Eigenvalue–Eigenvector Evaluation

The eigenvalue–eigenvector evaluation procedures fall into the following basic categories:

1. Characteristic polynomial technique
2. Vector iteration methods
3. Transformation methods

Characteristic polynomial From Eq. 11.38, we have

$$(\mathbf{K} - \lambda\mathbf{M})\mathbf{U} = \mathbf{0} \quad (11.43)$$

If the eigenvector is to be nontrivial, the required condition is

$$\det(\mathbf{K} - \lambda\mathbf{M}) = 0 \quad (11.44)$$

This represents the characteristic polynomial in λ .

Example 11.2

Determine the eigenvalues and eigenvectors for the stepped bar shown in Fig. E11.2a.

Solution Gathering the stiffness and mass values corresponding to the degrees of freedom Q_2 and Q_3 , we get the eigenvalue problem

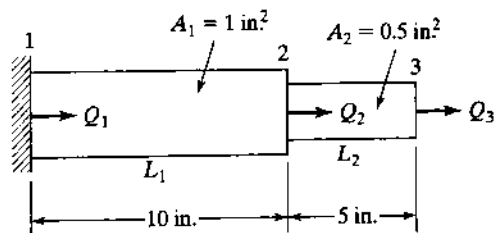
$$E \begin{bmatrix} \left(\frac{A_1}{L_1} + \frac{A_2}{L_2}\right) & -\frac{A_2}{L_2} \\ -\frac{A_2}{L_2} & \frac{A_2}{L_2} \end{bmatrix} \begin{Bmatrix} U_2 \\ U_3 \end{Bmatrix} = \lambda \frac{\rho}{6} \begin{bmatrix} 2(A_1 L_1 + A_2 L_2) & A_2 L_2 \\ A_2 L_2 & 2A_2 L_2 \end{bmatrix} \begin{Bmatrix} U_2 \\ U_3 \end{Bmatrix}$$

We note here that the density is

$$\rho = \frac{f}{g} = \frac{0.283}{32.2 \times 12} = 7.324 \times 10^{-4} \text{ lbs}^2/\text{in.}^4$$

Substituting the values, we get

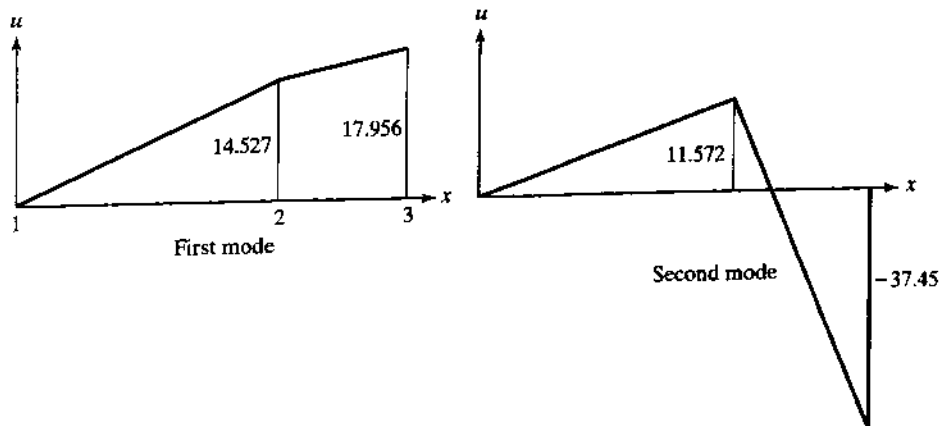
$$30 \times 10^6 \begin{bmatrix} 0.2 & -0.1 \\ -0.1 & 0.1 \end{bmatrix} \begin{Bmatrix} U_2 \\ U_3 \end{Bmatrix} = \lambda 1.22 \times 10^{-4} \begin{bmatrix} 25 & 2.5 \\ 2.5 & 5 \end{bmatrix} \begin{Bmatrix} U_2 \\ U_3 \end{Bmatrix}$$



$$E = 30 \times 10^6 \text{ psi}$$

$$\text{Specific weight } f = 0.283 \text{ lb/in.}^3$$

(a)



(b)

FIGURE E11.2

The characteristic equation is

$$\det \begin{bmatrix} (6 \times 10^6 - 30.5 \times 10^{-4}\lambda) & (-3 \times 10^6 - 3.05 \times 10^{-4}\lambda) \\ (-3 \times 10^6 - 3.05 \times 10^{-4}\lambda) & (3 \times 10^6 - 6.1 \times 10^{-4}\lambda) \end{bmatrix} = 0$$

which simplifies to

$$1.77 \times 10^{-6}\lambda^2 - 1.465 \times 10^4\lambda + 9 \times 10^{12} = 0$$

The eigenvalues are

$$\lambda_1 = 6.684 \times 10^8$$

$$\lambda_2 = 7.61 \times 10^9$$

Note that $\lambda = \omega^2$, where ω is the circular frequency given by $2\pi f$ and f = frequency in hertz (cycles/s).

These frequencies are

$$f_1 = 4115 \text{ Hz}$$

$$f_2 = 13\,884 \text{ Hz}$$

The eigenvector for λ_1 is found from

$$(\mathbf{K} - \lambda_1\mathbf{M})\mathbf{U}_1 = \mathbf{0}$$

which gives

$$10^6 \begin{bmatrix} 3.96 & -3.204 \\ -3.204 & 2.592 \end{bmatrix} \begin{Bmatrix} U_2 \\ U_3 \end{Bmatrix}_1 = \mathbf{0}$$

The two previous equations are not independent, since the determinant of the matrix is zero. This gives

$$3.96U_2 = 3.204U_3$$

Thus,

$$\mathbf{U}_1^T = [U_2, 1.236U_2]$$

For normalization, we set

$$\mathbf{U}_1^T \mathbf{M} \mathbf{U}_1 = 1$$

On substituting for \mathbf{U}_1 , we get

$$\mathbf{U}_1^T = [14.527 \quad 17.956]$$

The eigenvector corresponding to the second eigenvalue is similarly found to be

$$\mathbf{U}_2^T = [11.572 \quad -37.45]$$

The mode shapes are shown in Fig. E11.2b. ■

Implementation of characteristic polynomial approach on computers is rather tedious and requires further mathematical considerations. We now discuss the other two categories.

Vector iteration methods Various vector iteration methods use the properties of the *Rayleigh quotient*. For the generalized eigenvalue problem given by Eq. 11.38, we define the Rayleigh quotient

$$Q(\mathbf{v}) = \frac{\mathbf{v}^T \mathbf{K} \mathbf{v}}{\mathbf{v}^T \mathbf{M} \mathbf{v}} \quad (11.45)$$

where \mathbf{v} is arbitrary vector. A fundamental property of the Rayleigh quotient is that it lies between the smallest and the largest eigenvalue:

$$\lambda_1 \leq Q(\mathbf{v}) \leq \lambda_n \quad (11.46)$$

Power iteration, inverse iteration, and subspace iteration methods use this property. Power iteration leads to evaluation of the largest eigenvalue. Subspace iteration technique is suitable for large-scale problems and is used in several codes. The inverse iteration scheme can be used in evaluating the lowest eigenvalues. We present here the inverse iteration scheme and give a computer program for banded matrices.

Inverse Iteration Method In the inverse iteration scheme, we start with a trial vector \mathbf{u}^0 . The iterative solution proceeds as follows:

Step 0. Estimate an initial trial vector \mathbf{u}^0 . Set iteration index $k = 0$.

Step 1. Set $k = k + 1$.

Step 2. Determine right side $\mathbf{v}^{k-1} = \mathbf{M} \mathbf{u}^{k-1}$.

Step 3. Solve equations $\mathbf{K} \hat{\mathbf{u}}^k = \mathbf{v}^{k-1}$.

Step 4. Denote $\hat{\mathbf{v}}^k = \mathbf{M} \hat{\mathbf{u}}^k$.

Step 5. Estimate eigenvalue $\lambda^k = \frac{\hat{\mathbf{u}}^{kT} \mathbf{v}^{k-1}}{\hat{\mathbf{u}}^{kT} \hat{\mathbf{v}}^k}$. (11.47)

Step 6. Normalize eigenvector $\mathbf{u}^k = \frac{\hat{\mathbf{u}}^k}{(\hat{\mathbf{u}}^{kT} \hat{\mathbf{v}}^k)^{1/2}}$.

Step 7. Check for tolerance $\left| \frac{\lambda^k - \lambda^{k-1}}{\lambda^k} \right| \leq \text{tolerance}$.

If satisfied, denote the eigenvector \mathbf{u}^k as \mathbf{U} and exit. Otherwise, go to step 1.

The algorithm just described converges to the lowest eigenvalue, provided the trial vector does not coincide with one of the eigenvectors. Other eigenvalues can be evaluated by shifting, or by taking the trial vector from a space that is M orthogonal to the calculated eigenvectors.

Shifting We define a shifted stiffness matrix as

$$\mathbf{K}_s = \mathbf{K} + s\mathbf{M} \quad (11.48)$$

where \mathbf{K}_s is the shifted matrix. Now the shifted eigenvalue problem is

$$\mathbf{K}_s \mathbf{U} = \lambda_s \mathbf{M} \mathbf{U} \quad (11.49)$$

We state here without proof that the eigenvectors of the shifted problem are the same as those of the original problem. The eigenvalues get shifted by s :

$$\lambda_s = \lambda + s \quad (11.50)$$

Orthogonal Space Higher eigenvalues can be obtained by the inverse iteration method by choosing the trial vector from a space M -orthogonal to the calculated eigenvectors. This can be done effectively by the Gram-Schmidt process. Let U_1, U_2, \dots, U_m be the first m eigenvectors already determined. The trial vector for each iteration is then taken as

$$\mathbf{u}^{k-1} = \mathbf{u}^{k-1} - (\mathbf{u}^{k-1T} \mathbf{M} \mathbf{U}_1) \mathbf{U}_1 - (\mathbf{u}^{k-1T} \mathbf{M} \mathbf{U}_2) \mathbf{U}_2 - \dots - (\mathbf{u}^{k-1T} \mathbf{M} \mathbf{U}_m) \mathbf{U}_m \quad (11.51)$$

This is the Gram-Schmidt process, which results in the evaluation of λ_{m+1} and \mathbf{U}_{m+1} . This is used in the program given in this chapter. Equation 11.51 is implemented after step 1 in the algorithm given in Eq. 11.51.

Example 11.3

Evaluate the lowest eigenvalue and the corresponding eigenmode for the beam shown in Fig. E11.3a.

Solution Using only the degrees of freedom $Q_3, Q_4, Q_5,$ and Q_6 , we obtain the stiffness and mass matrices:

$$\mathbf{K} = 10^3 \begin{bmatrix} 355.56 & 0 & -177.78 & 26.67 \\ & 10.67 & -26.67 & 2.667 \\ \text{Symmetric} & & 177.78 & -26.67 \\ & & & 5.33 \end{bmatrix}$$

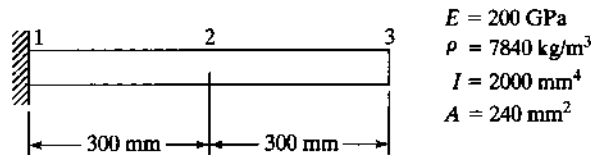
$$\mathbf{M} = \begin{bmatrix} 0.4193 & 0 & 0.0726 & -.0052 \\ & .000967 & .0052 & -.00036 \\ \text{Symmetric} & & 0.2097 & -.0089 \\ & & & .00048 \end{bmatrix}$$

The inverse iteration program requires the creation of a data file. The format of the file for the preceding problem is as follows:

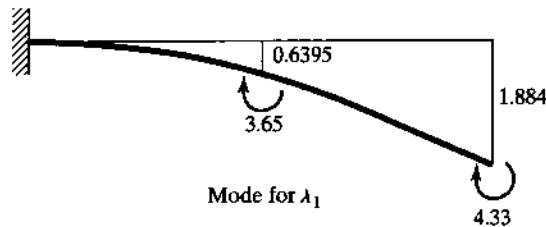
Data File:

```

TITLE
      NDOF      NBW
      4          4
Banded Stiffness Matrix
      3.556E5           0          -1.778E5          2.667E4
      1.067E4          -2.667E4          2.667E3           0
      1.778E5          -2.667E4           0           0
      5.333E3           0           0           0
  
```



(a)



(b)

FIGURE E11.3

Banded Mass Matrix

| | | | |
|----------|---------|----------|---------|
| 0.4193 | 0 | 0.0726 | -0.0052 |
| 0.000967 | 0.0052 | -0.00036 | 0 |
| 0.2097 | -0.0089 | 0 | 0 |
| 0.00048 | 0 | 0 | 0 |

The first line of data contains the values of n = dimension of the matrices and nbw = half-band width. This is followed by \mathbf{K} and \mathbf{M} matrices in banded form. (See Chapter 2.) The two titles are part of the data file. Though these data were created by hand calculations, it is possible to write a program, as discussed at the end of this chapter.

Feeding this data file into the inverse iteration program, INVITR, gives the lowest eigenvalue,

$$\lambda_1 = 2.03 \times 10^4$$

and the corresponding eigenvector or mode shape,

$$\mathbf{U}_1^T = [0.64, 3.65, 1.88, 4.32]$$

λ_1 corresponds to a circular frequency of 142.48 rad/s or 22.7 Hz ($= 142.48/2\pi$). The mode shape is shown in Fig. E11.3b. ■

Transformation methods The basic approach here is to transform the matrices to a simpler form and then determine the eigenvalues and eigenvectors. The major methods in this category are the generalized Jacobi method and the QR method. These methods are suitable for large-scale problems. In the QR method, the matrices are first reduced to tridiagonal form using Householder matrices. The generalized Jacobi method uses the transformation to simultaneously diagonalize the stiffness and mass matrices. This method needs the full matrix locations and is quite efficient for calculating all

eigenvalues and eigenvectors for small problems. We present here the generalized Jacobi method as an illustration of the transformation approach.

If all the eigenvectors are arranged as columns of a square matrix \mathbf{U} and all eigenvalues as the diagonal elements of a square matrix $\mathbf{\Lambda}$, then the generalized eigenvalue problem can be written in the form

$$\mathbf{KU} = \mathbf{MUA} \quad (11.52)$$

where

$$\mathbf{U} = [\mathbf{U}_1, \mathbf{U}_2, \dots, \mathbf{U}_n] \quad (11.53)$$

$$\mathbf{\Lambda} = \begin{bmatrix} \lambda_1 & & & 0 \\ & \lambda_2 & & \\ & & \ddots & \\ 0 & & & \lambda_n \end{bmatrix} \quad (11.54)$$

Using the M -orthonormality of the eigenvectors, we have

$$\mathbf{U}^T \mathbf{KU} = \mathbf{\Lambda} \quad (11.55a)$$

and

$$\mathbf{U}^T \mathbf{MU} = \mathbf{I} \quad (11.55b)$$

where \mathbf{I} is the identity matrix.

Generalized Jacobi Method

In the generalized Jacobi method, a series of transformations $\mathbf{P}_1, \mathbf{P}_2, \dots, \mathbf{P}_\ell$ are used such that if \mathbf{P} represents the product

$$\mathbf{P} = \mathbf{P}_1 \mathbf{P}_2 \dots \mathbf{P}_\ell \quad (11.56)$$

then the off-diagonal terms of $\mathbf{P}^T \mathbf{KP}$ and $\mathbf{P}^T \mathbf{MP}$ are zero. In practice, the off-diagonal terms are set to be less than a small tolerance. If we denote these diagonal matrices as

$$\hat{\mathbf{K}} = \mathbf{P}^T \mathbf{KP} \quad (11.57a)$$

and

$$\hat{\mathbf{M}} = \mathbf{P}^T \mathbf{MP} \quad (11.57b)$$

then the eigenvectors are given by

$$\mathbf{U} = \hat{\mathbf{M}}^{-1/2} \mathbf{P} \quad (11.58)$$

and

$$\mathbf{\Lambda} = \hat{\mathbf{M}}^{-1} \hat{\mathbf{K}} \quad (11.59)$$

where

$$\hat{\mathbf{M}}^{-1} = \begin{bmatrix} \hat{M}_{11}^{-1} & & & 0 \\ & \hat{M}_{22}^{-1} & & \\ & & \ddots & \\ 0 & & & \hat{M}_{nn}^{-1} \end{bmatrix} \quad (11.60)$$

$$\hat{\mathbf{M}}^{-1/2} = \begin{bmatrix} \hat{M}_{11}^{-1/2} & & & 0 \\ & \hat{M}_{22}^{-1/2} & & \\ & & \ddots & \\ 0 & & & \hat{M}_{nn}^{-1/2} \end{bmatrix} \quad (11.61)$$

Computationally, Eq. 11.58 indicates that each row of \mathbf{P} is divided by the square root of the diagonal element of $\hat{\mathbf{M}}$, and Eq. 11.59 indicates that each diagonal element of $\hat{\mathbf{K}}$ is divided by the diagonal element of $\hat{\mathbf{M}}$.

We mentioned that the diagonalization follows in several steps. At step k , we choose a transformation matrix \mathbf{P}_k given by

$$\mathbf{P}_k = \begin{array}{c} \text{Row} \\ \downarrow \end{array} \begin{array}{c} \text{Column} \rightarrow \\ \begin{matrix} i & & & j \end{matrix} \end{array} \begin{bmatrix} 1 & & & \\ & 1 & & \\ & & \ddots & \\ & & & 1 \end{bmatrix} \begin{array}{c} \\ \\ \\ \alpha \\ \\ \\ \beta \\ \\ \\ 1 \\ \\ \\ 1 \end{array} \quad (11.62)$$

\mathbf{P}_k has all diagonal elements equal to 1, has a value of α at row i and column j and β at row j and column i , and has all other elements equal to zero. The scalars α and β are chosen so that the ij locations of $\mathbf{P}_k^T \mathbf{K} \mathbf{P}_k$ and $\mathbf{P}_k^T \mathbf{M} \mathbf{P}_k$ are simultaneously zero. This is represented by

$$\alpha K_{ii} + (1 + \alpha\beta)K_{ij} + \beta K_{jj} = 0 \quad (11.63)$$

$$\alpha M_{ii} + (1 + \alpha\beta)M_{ij} + \beta M_{jj} = 0 \quad (11.64)$$

where $K_{ii}, K_{ij}, \dots, M_{ii}, \dots$ are elements of the stiffness and mass matrices. The solution of these equations is as follows:

Denote

$$A = K_{ij}M_{ij} - M_{ij}K_{ij}$$

$$B = K_{jj}M_{ij} - M_{jj}K_{ij}$$

$$C = K_{ij}M_{jj} - M_{ij}K_{jj}$$

Then α and β are given by

$$A \neq 0, B \neq 0: \quad \alpha = \frac{-0.5C + \text{sgn}(C)\sqrt{0.25C^2 + AB}}{A}$$

$$\beta = -\frac{A\alpha}{B}$$

$$A = 0: \quad \beta = 0$$

$$\alpha = -\frac{K_{ij}}{K_{jj}}$$

$$B = 0: \quad \alpha = 0$$

$$\beta = -\frac{K_{ij}}{K_{jj}}$$

When both A and B are zero, any one of the two values listed can be chosen. (Note: There is no summation on repeated indices these expressions.)

In the generalized Jacobi program given at the end of the chapter, the elements of \mathbf{K} and \mathbf{M} are zeroed out in the order indicated in Fig. 11.6. Once \mathbf{P}_k is defined by determining α and β , $\mathbf{P}_k^T[\]\mathbf{P}_k$ can be performed on \mathbf{K} and \mathbf{M} as shown in Fig. 11.7. Also by

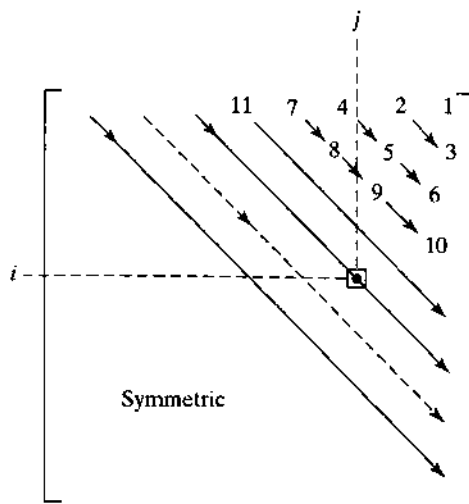
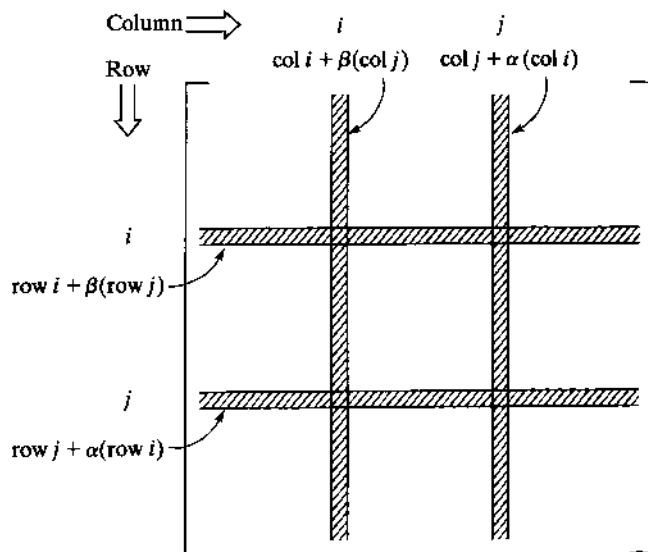


FIGURE 11.6 Diagonalization.

FIGURE 11.7 Multiplication $\mathbf{P}_k^T [] \mathbf{P}$.

starting with $\mathbf{P} = \mathbf{I}$, the product $\mathbf{P}\mathbf{P}_k$ is computed after each step. When all elements are covered as shown in Fig. 11.6, one pass is completed. After the operations at step k , some of the previously zeroed elements are altered. Another pass is conducted to check for the value of diagonal elements. The transformation is performed if the element at ij is larger than a tolerance value. A tolerance of $10^{-6} \times$ smallest K_{ii} is used for stiffness, and $10^{-6} \times$ largest M_{ii} is used for the mass. The tolerance can be redefined for higher accuracy. The process stops when all off-diagonal elements are less than the tolerance.

If the diagonal masses are less than the tolerance, the diagonal value is replaced by the tolerance value; thus, a large eigenvalue will be obtained. In this method, \mathbf{K} need not be positive definite.

Example 11.4

Determine all the eigenvalues and eigenvectors for the beam discussed in Example 11.3 using program JACOBI.

Solution The input data for JACOBI is same as that for INVITR. However, the program converts to full matrices in calculations. Convergence occurs at the fourth sweep. The solution is as follows:

$$\lambda_1 = 2.0304 \times 10^4 \text{ (22.7 Hz)}$$

$$\mathbf{U}_1^T = [0.64, 3.65, 1.88, 4.32]$$

$$\lambda_2 = 8.0987 \times 10^5 \text{ (143.2 Hz)}$$

$$\mathbf{U}_2^T = [-1.37, 1.39, 1.901, 15.27]$$

$$\lambda_3 = 9.2651 \times 10^6 \text{ (484.4 Hz)}$$

$$\mathbf{U}_3^T = [-0.20, 27.16, -2.12, -33.84]$$

$$\lambda_4 = 7.7974 \times 10^7 \text{ (1405.4 Hz)}$$

$$\mathbf{U}_4^T = [0.8986, 30.89, 3.546, 119.15]$$

Note that the eigenvalues are arranged in ascending order after they are evaluated. ■

Tridiagonalization and Implicit Shift Approach

We present here a powerful method for evaluating eigenvalues and eigenvectors using the implicit shift approach. We first bring the problem $\mathbf{Kx} = \lambda \mathbf{Mx}$ to the standard form $\mathbf{Ax} = \lambda \mathbf{x}$. Householder reflection steps are then applied to bring the matrix to a tridiagonal form. Implicit symmetric QR step is applied with Wilkinson shift* to diagonalize the matrix. These steps are now provided in detail.

Bringing Generalized Problem to Standard Form

We observe that the mass matrix \mathbf{M} is positive semidefinite. Positive semidefinite matrices have the property that if the diagonal element is zero, all the nondiagonal elements in the row and column are zero. In such a case, a small mass equal to the tolerance value say $10^{-6} \times \text{largest } M_{ii}$ is added at the diagonal location. This makes the mass matrix positive definite. Correspondingly, this yields a higher eigenvalue. The first step in bringing the problem to the standard form is to perform the *Cholesky* decomposition of \mathbf{M} using the calculations presented in Chapter 2:

$$\mathbf{M} = \mathbf{LL}^T \quad (11.65)$$

Symmetric manipulation of the generalized eigenvalue problem yields the form

$$\mathbf{L}^{-1} \mathbf{K} (\mathbf{L}^{-1})^T \mathbf{Lx} = \lambda \mathbf{Lx} \quad (11.66)$$

Denoting $\mathbf{A} = \mathbf{L}^{-1} \mathbf{K} (\mathbf{L}^{-1})^T$ and $\mathbf{y} = \mathbf{Lx}$, we get the standard form

$$\mathbf{Ay} = \lambda \mathbf{y} \quad (11.67)$$

This problem has the same eigenvalues as the generalized problem. The eigenvectors \mathbf{x} are evaluated by the forward substitution performed on

$$\mathbf{Lx} = \mathbf{y} \quad (11.68)$$

In the computer implementation, \mathbf{A} is obtained in two steps $\mathbf{LB} = \mathbf{K}$ and $\mathbf{LA} = \mathbf{B}^T$. These two forward-substitution steps are more efficient than finding the inverse and performing the multiplication steps.

*Golub, H. G., and C. F. Van Loan, *Matrix Computations*, Third Edition, (Baltimore: The Johns Hopkins University Press, 1996).

Example 11.5

Bring the generalized problem $\mathbf{Kx} = \lambda \mathbf{Mx}$ to standard form $\mathbf{Ay} = \lambda \mathbf{y}$, given that

$$\mathbf{K} = \begin{bmatrix} 4 & 1 & 2 & 1 \\ 1 & 3 & 1 & 2 \\ 2 & 1 & 4 & 2 \\ 1 & 2 & 2 & 4 \end{bmatrix} \quad \text{and} \quad \mathbf{M} = \begin{bmatrix} 1 & 1 & 1 & 2 \\ 1 & 2 & 1 & 2 \\ 1 & 1 & 2 & 2 \\ 2 & 2 & 2 & 5 \end{bmatrix}$$

Solution We make use of the Cholesky decomposition algorithm given in Chapter 2 to decompose $\mathbf{M} = \mathbf{LL}^T$. \mathbf{L} is obtained as

$$\mathbf{L} = \begin{bmatrix} 1 & 0 & 0 & 0 \\ 1 & 1 & 0 & 0 \\ 1 & 0 & 1 & 0 \\ 2 & 0 & 0 & 1 \end{bmatrix}$$

Solving for $\mathbf{LK} = \mathbf{B}$, which is a forward-substitution operation, we get

$$\mathbf{B} = \begin{bmatrix} 4 & 1 & 2 & 1 \\ -3 & 2 & -1 & 1 \\ -2 & 0 & 2 & 1 \\ -7 & 0 & -2 & 2 \end{bmatrix}$$

Another forward-substitution step of solving $\mathbf{LA} = \mathbf{B}^T$ gives

$$\mathbf{A} = \begin{bmatrix} 4 & -3 & -2 & -7 \\ -3 & 5 & 2 & 7 \\ -2 & 2 & 4 & 5 \\ -7 & 7 & 5 & 16 \end{bmatrix}$$

The standard form is now $\mathbf{Ay} = \lambda \mathbf{y}$, with $\mathbf{Lx} = \mathbf{y}$. ■

Tridiagonalization

There are several different methods available to transform a symmetric matrix to tridiagonal form. We use the *Householder reflection* ideas in the tridiagonalization process. Given a unit vector \mathbf{w} normal to a hyperplane, the reflected vector \mathbf{b} of vector \mathbf{a} , shown in Fig. 11.8, is given by

$$\mathbf{b} = \mathbf{a} - 2(\mathbf{w}^T \mathbf{a})\mathbf{w} \quad (11.69)$$

This can be put in the form

$$\mathbf{b} = \mathbf{H}\mathbf{a} \quad (11.70)$$

where

$$\mathbf{H} = \mathbf{I} - 2\mathbf{w}\mathbf{w}^T \quad \text{with} \quad \mathbf{w}^T \mathbf{w} = 1 \quad (11.71)$$

is the Householder transformation. This transformation, which reflects a vector about a plane for which \mathbf{w} is the normal direction, has some interesting properties:

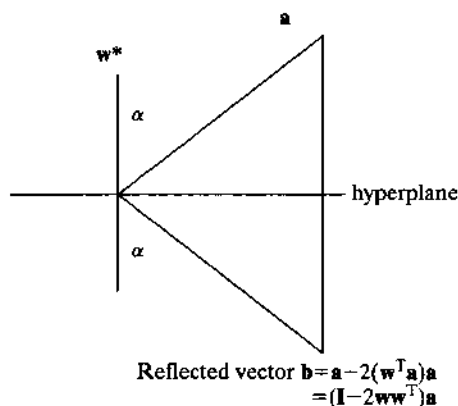


FIGURE 11.8 Householder reflection.

1. The Householder transformation is symmetric (i.e., $\mathbf{H}^T = \mathbf{H}$).
2. Its inverse is itself (i.e., $\mathbf{H}\mathbf{H} = \mathbf{I}$).

It is thus an orthogonal transformation.

If a vector \mathbf{a} has to be along the unit vector \mathbf{e}_1 after reflection, it is easy to see from Fig. 11.8 that \mathbf{w} is the unit vector in the direction given by $\mathbf{a} \pm |\mathbf{a}|\mathbf{e}_1$. The reflected vector is along $-\mathbf{e}_1$, if \mathbf{w} is along $\mathbf{a} + |\mathbf{a}|\mathbf{e}_1$. We choose vector $\mathbf{a} + |\mathbf{a}|\mathbf{e}_1$ or $\mathbf{a} - |\mathbf{a}|\mathbf{e}_1$, whichever has a larger magnitude. This reduces numerical errors in the calculation. We note that this is accomplished by taking \mathbf{w} along $\mathbf{a} + \text{sign}(a_1)|\mathbf{a}|\mathbf{e}_1$, where a_1 is the component of \mathbf{a} along the unit vector \mathbf{e}_1 . The steps involved in the tridiagonalization process are illustrated by extending the Example 11.5. The symmetric matrix in $\mathbf{A}\mathbf{y} = \lambda\mathbf{y}$ is

$$\mathbf{A} = \begin{bmatrix} 4 & -3 & -2 & -7 \\ -3 & 5 & 2 & 7 \\ -2 & 2 & 4 & 5 \\ -7 & 7 & 5 & 16 \end{bmatrix}$$

To start the tridiagonalization, we make use of the vector $[-3 \ -2 \ -7]^T$, which is made up of the elements below the diagonal in column 1. Consider this as vector \mathbf{a} , which we would like to bring to $\mathbf{e}_1 = [1 \ 0 \ 0]^T$. We have $|\mathbf{a}| = \sqrt{3^2 + 2^2 + 7^2} = 7.874$. \mathbf{w}_1 is then the unit vector along $\mathbf{a} - |\mathbf{a}|\mathbf{e}_1 = [-10.874 \ -2 \ -7]^T$. The length of this vector is $\sqrt{10.874^2 + 2^2 + 7^2} = 13.086$. The unit vector is $\mathbf{w}_1 = [-0.831 \ -0.1528 \ -0.5349]^T$. Denoting $\mathbf{H}_1 = [\mathbf{I} - 2\mathbf{w}_1\mathbf{w}_1^T]^T$, we have

$$\mathbf{H}_1 \begin{bmatrix} -3 \\ -2 \\ -7 \end{bmatrix} = \begin{bmatrix} 7.874 \\ 0 \\ 0 \end{bmatrix}$$

in the first column and $[-3 \ -2 \ -7]\mathbf{H}_1 = [7.874 \ 0 \ 0]$ in the first row. Thus the first row of the tridiagonal matrix \mathbf{T} is $[4 \ 7.874 \ 0 \ 0]^T$ and this matrix is symmetric.

Multiplication from both sides on the 3×3 partition is performed as follows:

$$\mathbf{H}_1 \begin{bmatrix} 5 & 2 & 7 \\ 2 & 4 & 5 \\ 7 & 5 & 16 \end{bmatrix} \mathbf{H}_1 = \begin{bmatrix} 21.0161 & -0.7692 & 0.9272 \\ -0.7692 & 2.4395 & 0.2041 \\ 0.9272 & 0.2041 & 1.5443 \end{bmatrix}$$

\mathbf{H}_1 is not formed at this stage. If the partitioned matrix is designated as \mathbf{B} , the multiplication is easily implemented by using the formula

$$\mathbf{H}_1 \mathbf{B} \mathbf{H}_1 = [\mathbf{I} - 2\mathbf{w}_1 \mathbf{w}_1^T] \mathbf{B} [\mathbf{I} - 2\mathbf{w}_1 \mathbf{w}_1^T] = \mathbf{B} - 2\mathbf{w}_1 \mathbf{b}^T - 2\mathbf{b} \mathbf{w}_1^T + 4\beta \mathbf{w}_1 \mathbf{w}_1^T \quad (11.72)$$

where $\mathbf{b} = \mathbf{B} \mathbf{w}_1$, $\beta = \mathbf{w}_1^T \mathbf{b}$.

At the next step, the vector $[-0.7692 \ 0.9272]^T$ is reflected to line up along $[1 \ 0]^T$. The magnitude of the vector is 1.2047. \mathbf{w}_2 is the vector along $[(-0.7692 - 1.2047)0.9272]^T$. The unit vector \mathbf{w}_2 for this is $[-0.9051 \ 0.4252]^T$. On performing the multiplication with the partitioned 2×2 matrix and placing in the 4×4 matrix \mathbf{T} , we get the tridiagonal matrix

$$\mathbf{T} = \begin{bmatrix} 4 & 7.874 & 0 & 0 \\ 7.874 & 21.0161 & 1.2047 & \\ & 1.2047 & 1.7087 & -0.4022 \\ & & -0.4022 & 2.271 \end{bmatrix} = \begin{bmatrix} d_1 & b_1 & 0 & 0 \\ b_1 & d_2 & b_2 & 0 \\ 0 & b_2 & d_3 & b_3 \\ 0 & 0 & b_3 & d_4 \end{bmatrix} \quad (11.73)$$

In this development, the tridiagonal matrix is stored in two vectors \mathbf{d} and \mathbf{b} . The original matrix \mathbf{A} is used for storing the Householder vectors \mathbf{w}_1 , \mathbf{w}_2 , etc. as follows:

$$\mathbf{A} = \begin{bmatrix} 1 & 0 & 0 & 0 \\ -0.831 & 1 & 0 & 0 \\ -0.1528 & -0.9051 & 1 & 0 \\ -0.5349 & 0.4252 & 0 & 1 \end{bmatrix}$$

The product of $\mathbf{H}_1 \mathbf{H}_2$ is easily performed in place inside \mathbf{A} . First, it is the product of \mathbf{H}_2 and the lower right 2×2 identity matrix, to obtain

$$\mathbf{A} = \begin{bmatrix} 1 & 0 & 0 & 0 \\ -0.831 & 1 & 0 & 0 \\ -0.1528 & 0 & -0.6385 & 0.7696 \\ -0.5349 & 0 & 0.7696 & 0.6385 \end{bmatrix}$$

Then the multiplication of \mathbf{H}_2 and the lower right 3×3 matrix gives

$$\mathbf{A} = \begin{bmatrix} 1 & 0 & 0 & 0 \\ 0 & -0.381 & -0.522 & -0.7631 \\ 0 & -0.254 & -0.7345 & 0.6292 \\ 0 & -0.889 & 0.4336 & 0.1473 \end{bmatrix}$$

This matrix represents the current contribution to the eigenvectors. We now discuss the steps to diagonalize the matrix and finding the eigenvectors.

Implicit Symmetric QR Step with Wilkinson Shift for Diagonalization*

The inverse iteration may be applied to the tridiagonal matrix to get desired eigenvalues. If all eigenvalues and eigenvectors are desired, the implicit shift ideas of Wilkinson provide a remarkably fast algorithm. The order of convergence with this method is cubic. The shift value μ for the *Wilkinson shift* is taken as the eigenvalue of the bottom 2×2 matrix of the tridiagonal matrix close to d_n , viz.,

$$\mu = d_n + t - \text{sign}(t)\sqrt{b_{n-1}^2 + t^2} \quad (11.74)$$

where $t = 0.5(d_{n-1} - d_n)$. The implicit shift is carried out by performing a Givens rotation \mathbf{G}_1 . $c (= \cos \theta)$ and $s (= \sin \theta)$ are chosen such that we get zero in the second position as follows:

$$\mathbf{G}_1 \begin{bmatrix} d_1 - \mu \\ b_1 \end{bmatrix} = \begin{bmatrix} c & -s \\ s & c \end{bmatrix} \begin{bmatrix} d_1 - \mu \\ b_1 \end{bmatrix} = \begin{bmatrix} \times \\ 0 \end{bmatrix} \quad (11.75)$$

We note that if $r = \sqrt{b_1^2 + (d_1 - \mu)^2}$, $c = -(d_1 - \mu)/r$ and $s = b_1/r$. We perform the rotation $\mathbf{G}_1 \mathbf{T} \mathbf{G}_1^T$ on the tridiagonal matrix on the first two rows from the left and first two columns from the right. Note that the rotation is calculated based on shift μ , but the shift itself is not performed. This is implicit shift. We refer to the tridiagonal matrix in Eq. 11.73. With $d_3 = 1.7087$, $d_4 = 2.2751$, and $b_3 = -0.4022$, we have $t = -0.2832$ and $\mu = 2.4838$. With $d_1 - \mu = 1.5162$, $b_1 = 7.874$, and $r = 8.0186$, we get $c = -0.1891$

and $s = 0.982$. We then get from Eq. 11.75, $\mathbf{G}_1 = \begin{bmatrix} c & -s \\ s & c \end{bmatrix} = \begin{bmatrix} -0.1891 & -0.982 \\ 0.982 & -0.1891 \end{bmatrix}$.

After this rotation, two additional elements, each with value $a = -1.18297$, are introduced at (3,1) and (1,3), and the matrix is no longer tridiagonal.

$$\mathbf{G}_1 \mathbf{T} \mathbf{G}_1^T = \begin{bmatrix} 23.3317 & -4.1515 & -1.18297 & 0 \\ -4.1515 & 1.6844 & -0.2278 & 0 \\ -1.18297 & -0.2278 & 1.7087 & -0.4022 \\ 0 & 0 & -0.4022 & 2.2751 \end{bmatrix}$$

Givens rotation \mathbf{G}_2 is then applied to rows 2, 3 and columns 2, 3 with reference to -4.1515 and -1.18297 such that the elements at (3,1) and (1,3) become zero. We get

$$\mathbf{G}_2 = \begin{bmatrix} c & -s \\ s & c \end{bmatrix} = \begin{bmatrix} 0.9617 & 0.274 \\ -0.274 & 0.9617 \end{bmatrix}. \text{ This leads to}$$

$$\mathbf{G}_2 \mathbf{T} \mathbf{G}_2^T = \begin{bmatrix} 23.3317 & -4.3168 & 0 & 0 \\ -4.3168 & 1.5662 & -0.1872 & -0.1102 \\ 0 & -0.1872 & 1.8269 & -0.3868 \\ 0 & -0.1102 & -0.3868 & 2.2751 \end{bmatrix}$$

Givens rotation \mathbf{G}_3 is then applied with respect to elements at (3,2) and (4,2) to make the locations (4,2) and (2,4) zero. We get $\mathbf{G}_3 = \begin{bmatrix} c & -s \\ s & c \end{bmatrix} = \begin{bmatrix} 0.8617 & 0.5074 \\ -0.5074 & 0.8617 \end{bmatrix}$.

*Wilkinson, J. H., "Global Convergence of Tridiagonal QR Algorithm with Origin Shifts," *Linear Algebra and Its Applications*, 1: 409-420 (1968).

After this application, the resulting matrix is tridiagonal. The off-diagonal elements at the bottom become smaller:

$$\mathbf{G}_3 \mathbf{T} \mathbf{G}_3^T = \begin{bmatrix} 23.3317 & -4.3168 & 0 & 0 \\ -4.3168 & 1.5662 & -0.2172 & 0 \\ 0 & -0.2172 & 1.6041 & 0.00834 \\ 0 & 0 & 0.00834 & 2.498 \end{bmatrix}$$

The eigenvector matrix is updated by multiplying \mathbf{A} with the Given's rotations $\mathbf{A} \mathbf{G}_1^T \mathbf{G}_2^T \mathbf{G}_3^T$.

The iteration process is repeated until the off diagonal element b_3 (b_{n-1} for $n \times n$ matrix) becomes small in magnitude (say, less than 10^{-8}). d_4 is an eigenvalue. The process is now repeated on the 3×3 tridiagonal matrix obtained by excluding row 4 and column 4. This is continued till each of the off-diagonal terms approaches zero. All eigenvalues are thus evaluated. Wilkinson has shown that this procedure cubically converges to diagonal form. The eigenvalues are 24.1567, 0.6914, 1.6538, and 2.4981, and the corresponding eigenvectors, after multiplying by \mathbf{L}^{-1} (a forward-substitution operation given by Eq. 11.68), are the columns of the matrix

$$\begin{bmatrix} -2.6278 & -0.1459 & 0.0934 & 0.2543 \\ 0.3798 & 0.1924 & -0.8112 & 0.4008 \\ 0.2736 & 0.1723 & -0.2780 & -0.9045 \\ 0.8055 & -0.5173 & 0.2831 & 0.0581 \end{bmatrix}$$

This algorithm for finding the eigenvalues and eigenvectors of the generalized eigenvalue problem is implemented in the program GENEIGEN.

11.5 INTERFACING WITH PREVIOUS FINITE ELEMENT PROGRAMS AND A PROGRAM FOR DETERMINING CRITICAL SPEEDS OF SHAFTS

Once the stiffness matrix \mathbf{K} and mass matrix \mathbf{M} for a structure are known, then the inverse iteration or Jacobi programs that are provided can be used to determine the natural frequencies and mode shapes. The finite element programs for rod, truss, beam, and elasticity problems that we used in previous chapters can be readily modified to output the banded \mathbf{K} and \mathbf{M} matrices onto a file. This file is then input into the inverse iteration program, which gives the natural frequencies and mode shapes.

We have provided the BEAMKM program, which outputs the banded \mathbf{K} and \mathbf{M} matrices for a beam. This output file is then provided to program INVITR, which calculates the eigenvalues and eigenvectors (mode shapes). Example 11.5 illustrates the use of these two programs. Program CSTKM, which outputs \mathbf{K} and \mathbf{M} matrices for the CST element, has also been provided.

Example 11.5

Determine the lowest critical speed (or transverse natural frequency) of the shaft shown in Fig. E11.5. The shaft has two lumped weights, W_1 and W_2 , representing flywheels, as shown. Take $E = 30 \times 10^6$ psi and mass density of shaft $\rho = 0.0007324 \text{ lb} \cdot \text{s}^2/\text{in}^4$ ($= 0.283 \text{ lb}/\text{in}^3$).

Solution The lumped weights W_1 and W_2 correspond to lumped masses W_1/g and W_2/g , respectively, where $g = 386 \text{ in./s}^2$. Program BEAMKM is executed, followed by program INVITR. The input data and solution are given at the end of the next section.

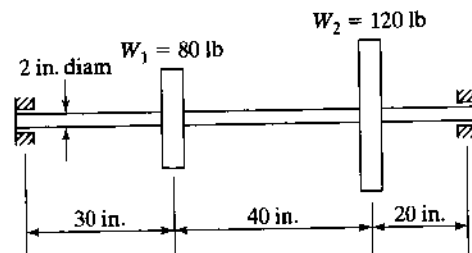


FIGURE E11.5

Now, we can obtain the critical speed in rpm from the eigenvalue 4042 as

$$\begin{aligned} n &= \sqrt{\lambda} \times \frac{60}{2\pi} \text{ rpm} \\ &= \sqrt{4042} \times \frac{60}{2\pi} \\ &= 607 \text{ rpm} \end{aligned}$$

This example illustrates how the inverse iteration and Jacobi programs given in this chapter can be interfaced with other programs for vibration analysis. ■

11.6 GUYAN REDUCTION

Often, large finite element models with thousands of degrees of freedom (dof) are used for stress and deformation analysis of ships, aircraft, automobiles, nuclear reactors, and the like. It is clearly impractical and unnecessary to perform dynamic analyses using the detailed representation that is required for static analysis. Furthermore, design and control methods work best for systems with a small number of degrees of freedom. To overcome this difficulty, dynamic reduction techniques have been developed to reduce the number of degrees of freedom prior to performing dynamic analysis. Guyan reduction is one of the popular methods for dynamic reduction.* We have to make the decision as to which dof are to be retained and which are to be omitted. For example, Fig. 11.9 shows how a reduced model is obtained by omitting certain dof. The omitted dof correspond to those at which the applied and inertial forces are negligible.

The reduced stiffness and mass matrices are obtained as follows: The equations of motion (see Eq. 11.13) are $\mathbf{M}\ddot{\mathbf{Q}} + \mathbf{K}\mathbf{Q} = \mathbf{F}$. If we group the inertial force together with the applied force, we can write the equations as $\mathbf{K}\mathbf{Q} = \mathbf{F}$. We will partition \mathbf{Q} as

$$\mathbf{Q} = \begin{Bmatrix} \mathbf{Q}_r \\ \mathbf{Q}_o \end{Bmatrix} \quad (11.76)$$

where \mathbf{Q}_r = retained set and \mathbf{Q}_o = omitted set. Typically, the retained set is about 20% of the total dof. The equations of motion can now be written in partitioned form as

$$\begin{bmatrix} \mathbf{K}_{rr} & \mathbf{K}_{ro} \\ \mathbf{K}_{ro}^T & \mathbf{K}_{oo} \end{bmatrix} \begin{Bmatrix} \mathbf{Q}_r \\ \mathbf{Q}_o \end{Bmatrix} = \begin{Bmatrix} \mathbf{F}_r \\ \mathbf{F}_o \end{Bmatrix} \quad (11.77)$$

*Guyan, R. J. "Reduction in stiffness and mass matrices," *AIAA Journal*, vol. 3, no. 2, p. 380, Feb. 1965.

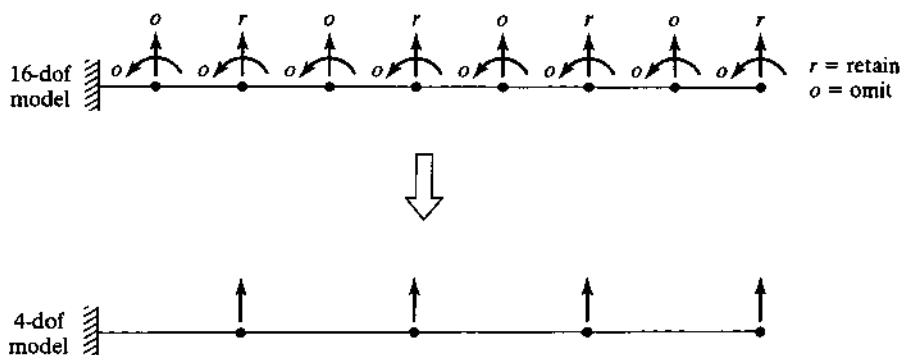


FIGURE 11.9 Guyan reduction.

The idea is to choose the omitted set such that the components of \mathbf{F}_o are small. Thus, we should retain those dof in the r -set with large concentrated masses, which are loaded (in transient-response analysis) and which are needed to adequately describe the mode shape. Setting $\mathbf{F}_o = 0$, the lower part of Eq. 11.76 yields

$$\mathbf{Q}_o = -\mathbf{K}_{oo}^{-1}\mathbf{K}_{ro}^T\mathbf{Q}_r \quad (11.78)$$

The strain energy in the structure is $U = \frac{1}{2}\mathbf{Q}^T\mathbf{K}\mathbf{Q}$. This can be written as

$$U = \frac{1}{2}\begin{bmatrix} \mathbf{Q}_r^T & \mathbf{Q}_o^T \end{bmatrix} \begin{bmatrix} \mathbf{K}_{rr} & \mathbf{K}_{ro} \\ \mathbf{K}_{ro}^T & \mathbf{K}_{oo} \end{bmatrix} \begin{bmatrix} \mathbf{Q}_r \\ \mathbf{Q}_o \end{bmatrix}$$

Upon substituting Eq. 11.77 into the equation just described, we can write $U = \frac{1}{2}\mathbf{Q}_r^T\mathbf{K}_r\mathbf{Q}_r$, where

$$\mathbf{K}_r = \mathbf{K}_{rr} - \mathbf{K}_{ro}\mathbf{K}_{oo}^{-1}\mathbf{K}_{ro}^T \quad (11.79)$$

is the reduced stiffness matrix. To obtain an expression for the reduced mass matrix, we consider the kinetic energy $V = \frac{1}{2}\mathbf{Q}^T\mathbf{M}\mathbf{Q}$. Upon partitioning the mass matrix and using Eq. 11.78, we can write the kinetic energy as $V = \frac{1}{2}\mathbf{Q}_r^T\mathbf{M}_r\mathbf{Q}_r$, where

$$\mathbf{M}_r = \mathbf{M}_{rr} - \mathbf{M}_{ro}\mathbf{K}_{oo}^{-1}\mathbf{K}_{ro}^T - \mathbf{K}_{ro}\mathbf{K}_{oo}^{-1}\mathbf{M}_{oo}^T + \mathbf{K}_{ro}\mathbf{K}_{oo}^{-1}\mathbf{M}_{oo}\mathbf{K}_{oo}^{-1}\mathbf{K}_{ro}^T \quad (11.80)$$

is the reduced mass matrix. With the reduced stiffness and mass matrices, only a smaller eigenvalue problem needs to be solved:

$$\mathbf{K}_r\mathbf{U}_r = \lambda\mathbf{M}_r\mathbf{U}_r \quad (11.81)$$

Then we recover

$$\mathbf{U}_o = -\mathbf{K}_{oo}^{-1}\mathbf{K}_{ro}^T\mathbf{U}_r \quad (11.82)$$

Example 11.6

In Example 11.3, the eigenvalues and mode shapes of a cantilever beam were determined based on a four-dof model. We will apply Guyan reduction to this problem based on omitting the rotational dofs and see how our results compare with the full model. Referring to Fig. E11.3, Q_3 and Q_5 refer to the translational dofs while Q_4 and Q_6 refer to the rotational

dofs. Thus, the retained set is Q_3 and Q_5 and the omitted set is Q_4 and Q_6 . Extracting the appropriate components from the full 4×4 \mathbf{K} and \mathbf{M} matrices, we obtain

$$\begin{aligned} \mathbf{k}_{rr} &= 1000 \begin{bmatrix} 355.6 & -177.78 \\ -177.78 & 177.78 \end{bmatrix} & \mathbf{k}_{ro} &= 1000 \begin{bmatrix} 0 & 26.67 \\ -26.67 & -26.67 \end{bmatrix} \\ \mathbf{k}_{oo} &= 1000 \begin{bmatrix} 10.67 & 2.667 \\ 2.667 & 5.33 \end{bmatrix} & \mathbf{m}_{rr} &= \begin{bmatrix} 0.4193 & 0.0726 \\ 0.0726 & 0.2097 \end{bmatrix} \\ \mathbf{m}_{ro} &= \begin{bmatrix} 0 & -0.0052 \\ 0.0052 & -0.0089 \end{bmatrix} & \mathbf{m}_{oo} &= \begin{bmatrix} 0.000967 & -0.00036 \\ -0.00036 & 0.00048 \end{bmatrix} \end{aligned}$$

From Eqs. 11.68 and 11.69, we obtain the reduced matrices

$$\mathbf{K}_r = 10000 \begin{bmatrix} 20.31 & -6.338 \\ -6.338 & 2.531 \end{bmatrix}, \quad \mathbf{M}_r = \begin{bmatrix} 0.502 & 0.1 \\ 0.1 & 0.155 \end{bmatrix}$$

An input data file is prepared and program JACOBI is used to solve the eigenvalue problem in (11.70). The solution is

$$\begin{aligned} \lambda_1 &= 2.025 \times 10^4, & U_r^1 &= [0.6401 \quad 1.888]^T \\ \lambda_2 &= 8.183 \times 10^5, & U_r^2 &= [1.370 \quad -1.959]^T \end{aligned}$$

Using Eq. 11.71, we obtain the eigenvector components corresponding to the omitted dof as

$$U_o^1 = [3.61 \quad 4.438]^T \quad \text{and} \quad U_o^2 = [-0.838 \quad -16.238]^T$$

In this example, the results correlate quite well with the solution of the unreduced system. ■

11.7 RIGID BODY MODES

In certain situations (such as in helicopter frames, flexible spacecraft structures, or flat panels that are placed on soft supports), we are faced with the task of determining mode shapes of structures that are freely suspended in space. These structures have rigid body modes as well as deformation modes. The rigid body modes correspond to translations and rotations of the entire structure along the x -, y -, and z -axes, respectively. Thus, there are six (6) rigid body modes for a three-dimensional body in space. Modes 7, 8, ... correspond to deformation modes, which are to be determined from an eigenvalue analysis. It should be recognized that the stiffness matrix \mathbf{K} is singular when rigid body modes are present. This follows from the fact that a finite translation or rotation \mathbf{U}^0 does not create any internal forces or stresses in the structure. Thus, $\mathbf{K}\mathbf{U}^0 = \mathbf{0}$. Since $\mathbf{U}^0 \neq \mathbf{0}$, \mathbf{K} has to be a singular matrix. Further, we can write $\mathbf{K}\mathbf{U}^0 = \mathbf{0}$ as $\mathbf{K}\mathbf{U}^0 = (0)\mathbf{M}\mathbf{U}^0$ from which we see that a rigid mode is associated with a zero eigenvalue. Specifically, the first six rigid body modes are associated with six zero eigenvalues.

Steps in many eigenvalue evaluation algorithms given require that \mathbf{K} be nonsingular and also positive definite (i.e., that all eigenvalues be positive). This can be effected by **shifting** as given in Eqs. 11.48–11.50. Thus, with a shift factor $s > 0$, we work with a positive definite matrix \mathbf{K}_s , even though the original stiffness matrix is singular.

Using JACOBI or GENEIGEN These methods do not require that the stiffness matrix be positive definite. Thus, they may be directly used on the unconstrained structure. Note that the first six eigenvalues (for a three-dimensional structure) will be zero representing the rigid modes. If small negative values are output as a result of round-off, these may be ignored—avoid taking their square root in computing the frequency within the programs.

Using INVTR Using the inverse iteration program to handle rigid body modes is more involved. We need to define the rigid body modes in the program and then mass-normalize them. Let $\mathbf{U}_1^0, \mathbf{U}_2^0, \dots, \mathbf{U}_6^0$ represent six rigid body modes. After defining these, each is mass normalized as

$$\mathbf{U}_i^0 = \frac{\mathbf{U}_i^0}{(\mathbf{U}_i^0)^T \mathbf{M} (\mathbf{U}_i^0)} \quad i = 1, \dots, 6 \quad (11.83)$$

Subsequently, each trial eigenvector is chosen as in Eq. 11.51 from a space M -orthogonal to all previously calculated eigenvectors *including* the six normalized rigid body modes. Rigid body modes may be readily defined as follows: Consider a general three-dimensional body as shown in Fig. 11.10. In general, a node I will have six degrees of freedom, labeled $Q_{6*I-5}, Q_{6*I-4}, \dots, Q_{6*I}$, corresponding $x, y,$ and z translations and rotations about $x, y,$ and z -axes, respectively. Defining the first mode to be a translation along x -axis, we have $Q(6*I - 5, 1) = 1$ and $Q(6*I - 4, 1) = Q(6*I - 3, 1) = Q(6*I - 2, 1) = Q(6*I - 1, 1) = Q(6*I, 1) = 0$, where the first subscript is the degree-of-freedom number and the second is the mode number. Similarly, translations along y - and z -axes define modes $\mathbf{Q}(\cdot, 2)$ and $\mathbf{Q}(\cdot, 3)$, respectively. Now, consider the sixth rigid body mode corresponding to a rotation of the body about the z -axis, by an angle θ . That is, a rotation in the x - y plane. We can choose an arbitrary value for θ . Choosing the centroid as a reference point about which the body rotates, we can write the translational displacement vector δ of any node I in the body as

$$\delta = \mathbf{V}' - \mathbf{V}, \quad \text{where} \quad \mathbf{V}' = [\mathbf{R}] \mathbf{V}$$

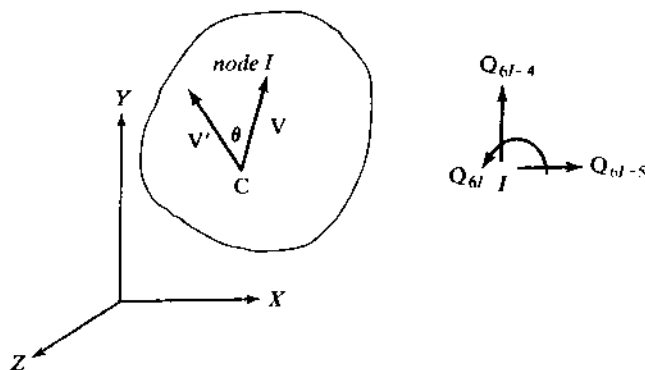


FIGURE 11.10 Rigid body rotation about z -axis.

For this equation, $\mathbf{V} = \mathbf{x}_i - \mathbf{x}_c$ and $\mathbf{R} = \begin{bmatrix} \cos \theta & -\sin \theta \\ \sin \theta & \cos \theta \end{bmatrix}$ is a rotation matrix. From δ , we obtain $Q(6^*I - 5, 6) = \delta_x$ and $Q(6^*I - 4, 6) = \delta_y$. Remaining components are $Q(6^*I - 3, 6) = 0$, $Q(6^*I - 2, 6) = 0$, $Q(6^*I - 1, 6) = 0$, and $Q(6^*I, 6) = \theta$ (in radians). Rotations about x - and y -axes can similarly be considered.

An example problem involving rigid body modes is presented in Example 11.7.

Example 11.7

Consider a two-dimensional steel beam, modeled using four elements as shown in Fig. E11.7a. In this beam model, each node has a vertical translational and a counter-clockwise rotational dof. No axial dofs are included. Taking the beam length to be 60 mm, E as 200 Gpa, and ρ as 7850 kg/m³ rectangular cross section of width 6 mm and depth 1 mm (thus, inertia $I = 0.5 \text{ mm}^4$), and the shift factor $s = -10^8$, we obtain the first three natural frequencies to be 1440 Hz, 3997 Hz, and 7850 Hz, respectively. The corresponding mode shapes are shown in Fig. E11.7b. Both programs JACOBI and INVTR give similar results. Program JACOBI is easier to implement. In program INVTR, two rigid body modes corresponding to vertical translation and rotation were introduced. Mass normalization of these involved Eq. 11.82, which needed special care as \mathbf{M} is in banded form. ■

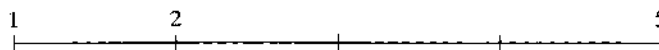


FIGURE E11.7a Unconstrained beam.

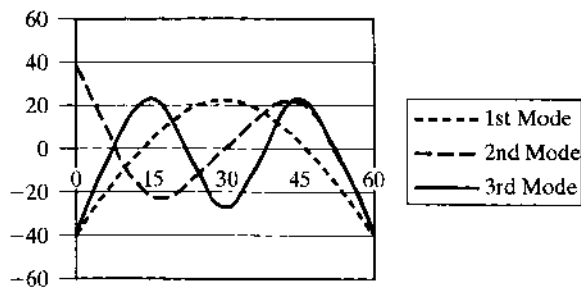


FIGURE E11.7b Mode shapes for unconstrained beam.

11.8 CONCLUSION

In this chapter, the application of finite elements for free vibrations is discussed in a general setting using consistent mass matrices. Solution techniques and computer programs are given. These programs can be integrated with static analysis programs to get dynamic behavior of structures. Natural frequencies and mode shapes of structures give us the needed data concerning what excitation frequencies should be avoided.

Input Data File

```

<< PROGRAM BEAMKM >>
EXAMPLE11.5
NN NE NM NDIM NEN NDN
4 3 1 1 2 2
ND NL NMPC
2 0 0
Node# X
1 0
2 30
3 70
4 90
Elem# N1 N2 MAT# Mom_Inertia Area
1 1 2 1 .7854 3.1416
2 2 3 1 .7854 3.1416
3 3 4 1 .7854 3.1416
DOF# Displacement
1 0
7 0
DOF# Load
MAT# E MassDensity
1 3E+07 .0007324

```

OUTPUT FROM BEAMKM FOR INPUT TO INVITR, JACOBI, OR GENEIGEN

```

Stiffness and Mass for Data in File ex115.inp
Num. of DOF Bandwidth
8 4
Banded Stiffness Matrix
7.068601E+10 157080 -10472 157080
3141600 -157080 1570800 0
14889.88 -68722.5 -4417.875 88357.5
5497800 -88357.5 1178100 0
39760.88 265072.5 -35343 353430
7068600 -353430 2356200 0
7.068603E+10 -353430 0 0
4712400 0 0 0
Banded Mass Matrix
2.563869E-02 .1084714 8.87493E-03 -6.409672E-02
.591662 6.409672E-02 -.4437465 0
.2670774 8.436662E-02 1.183324E-02 -.1139497
1.99412 .1139497 -1.051844 0
.3621584 -.1446285 5.91662E-03 -2.848743E-02
1.577765 2.848743E-02 -.1314804 0
1.709246E-02 -.0482095 0 0
.1753073 0 0 0
Starting Vector for Inverse Iteration
1 1 1 1 1 1 1

```

OUTPUT FROM INVITR

```

Name of Input File Eigen.inp
Name of Output File InvItr.out
Tolerance <default 1E-6.
Number Eigenvalues Desired 2
Program InvItr - CHANDRUPATLA & BELEGUNDU
Eigenvalues & Eigenvectors for data in file: Eigen.inp

```

continued

```

Eigenvalue Number 1      Iteration Number 3
Eigenvalue = 4.0420E+03  Omega = 6.3577E+01  Freq Hz = 1.0119E+01
Eigenvector
2.1040E-08  5.5269E-02  1.3783E+00  2.7575E-02  1.0495E+00  -4.2193E-02
2.6005E-08  -5.7648E-02

```

```

Eigenvalue Number 2      Iteration Number 4
Eigenvalue = 4.3184E+04  Omega = 2.0781E+02  Freq Hz = 3.3074E+01
Eigenvector
8.9643E-08  8.1562E-02  1.3010E+00  -2.9044E-02  -1.2374E+00  5.0888E-03  -
1.4669E-07  9.0721E-02

```

```

Program Geneigen - CHANDRUPATLA & BELEGUNDU
Eigenvalues & Eigenvectors for data in file: Eigen.inp

```

```

Eigenvalue Number 1
Eigenvalue = 4.0420E+03  Omega = 6.3577E+01  Freq Hz = 1.0119E+01
Eigenvector
-2.1038E-08  -5.5266E-02  -1.3783E+00  -2.7576E-02  -1.0496E+00  4.2193E-02  -
2.6009E-08  5.7650E-02

```

```

Eigenvalue Number 2
Eigenvalue = 4.3184E+04  Omega = 2.0781E+02  Freq Hz = 3.3074E+01
Eigenvector
-8.9646E-08  -8.1578E-02  -1.3015E+00  2.9034E-02  1.2370E+00  -5.0751E-03
1.4669E-07  -9.0704E-02

```

```

Eigenvalue Number 3
Eigenvalue = 1.2073E+06  Omega = 1.0988E+03  Freq Hz = 1.7488E+02
Eigenvector
1.3652E-06  3.9771E-01  1.1407E-01  -4.4556E-01  3.6412E-01  2.6176E-01
9.1308E-07  -1.7764E-01

```

```

Eigenvalue Number 4
Eigenvalue = 4.5038E+06  Omega = 2.1222E+03  Freq Hz = 3.3776E+02
Eigenvector
4.3420E-06  7.7777E-01  -5.3689E-01  -1.7096E-01  -1.2843E-01  -6.2376E-01  -
3.4292E-06  4.8458E-01

```

```

Eigenvalue Number 5
Eigenvalue = 1.4837E+07  Omega = 3.8518E+03  Freq Hz = 6.1304E+02
Eigenvector
-1.1403E-05  -1.1700E+00  3.6043E-01  -7.5974E-01  1.5876E-01  -4.7676E-01  -
9.6374E-06  9.1415E-01

```

```

Eigenvalue Number 6
Eigenvalue = 4.3449E+07  Omega = 6.5916E+03  Freq Hz = 1.0491E+03
Eigenvector
-9.8104E-06  -5.0560E-01  -1.1210E-02  -5.4875E-01  -3.8044E-01  -7.6675E-01
3.8771E-05  -2.3385E+00

```

continue

| | | | | | | |
|---|-------------|-------------|------------|-------------|------------|---|
| Eigenvalue Number 7 | | | | | | |
| Eigenvalue = 1.3157E+13 Omega = 3.6272E+06 Freq Hz = 5.7729E+05 | | | | | | |
| Eigenvector | | | | | | |
| -1.3618E+01 | 2.7177E+00 | -2.1183E-01 | 2.6427E-01 | -4.1855E-03 | 1.6685E-01 | - |
| 8.2693E-01 | -1.0295E-01 | | | | | |
| Eigenvalue Number 8 | | | | | | |
| Eigenvalue = 1.8936E+13 Omega = 4.3515E+06 Freq Hz = 6.9256E+05 | | | | | | |
| Eigenvector | | | | | | |
| -9.9205E-01 | 2.6900E-01 | 3.6973E-03 | 1.1670E-01 | 1.3534E-01 | 1.8317E-01 | |
| 1.6337E+01 | 4.6521E+00 | | | | | |

PROBLEMS

- 11.1. Consider *axial* vibration of the steel bar shown in Fig. P11.1.
- Develop the global stiffness and mass matrices.
 - By hand calculations, determine the lowest natural frequency and mode shape using the inverse iteration algorithm.
 - Verify your results in (b) using programs INVTR and JACOBI.
 - Verify the properties in Eqs. 11.41a and 11.41b.

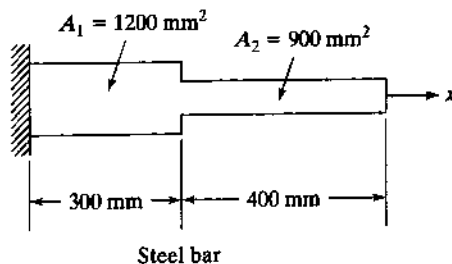


FIGURE P11.1

- 11.2. By hand calculations, determine the natural frequencies and mode shapes for the rod in P11.1 using the characteristic polynomial technique.
- 11.3. Use a lumped mass model for the rod in P11.1, and compare the results obtained with the consistent mass model. Use program INVTR or JACOBI.
- 11.4. Determine all natural frequencies of the simply supported beam shown in Fig. P11.4. Compare the results obtained using the following:
- a one-element model and
 - a two-element model.
- Use either program INVTR or JACOBI.

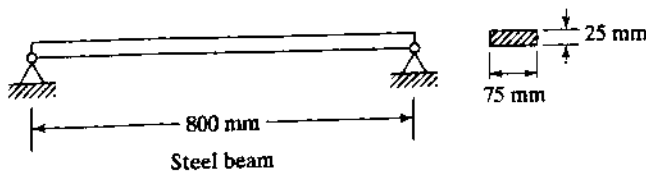


FIGURE P11.4

- 11.5. Determine, with the help of program BEAMKM, the two lowest natural frequencies (critical speeds) of the steel shaft shown in Fig. P11.5, considering the following cases:
- The three journals are like simple supports.
 - Each journal bearing is like a spring of stiffness equal to 25,000 lb/in.

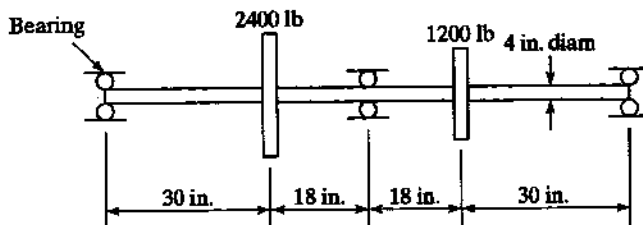


FIGURE P11.5

- 11.6. The existence of a crack renders an overall reduction in the stiffness of a structure. A crack in a bending member, such as a beam, suggests a slope discontinuity at the section containing the crack, even though the displacement is still continuous there. Thus, the effect of a fracture at a section may be represented by torsional spring connecting two elements, whose torsional stiffness k may be determined analytically or experimentally. Consider the cracked cantilever beam shown in Fig. P 11.6.
- Discuss how you will model this using beam elements. Write down the boundary conditions at the cracked section, and the resulting modifications to the stiffness matrix.
 - Determine the first three natural frequencies and mode shapes and compare these with those of an uncracked beam of same dimensions. Take $k = 8 \times 10^6$ in.-lb and $E = 30 \times 10^6$ psi.

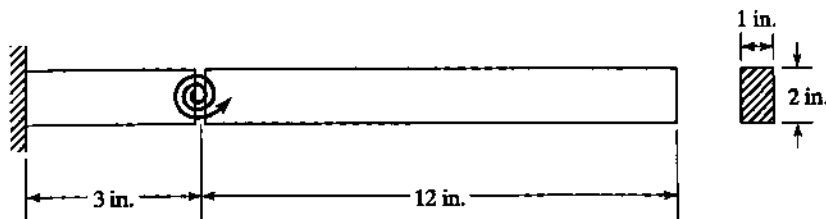


FIGURE P11.6

- 11.7. A simplified model of a steel turbine blade is shown in Fig. P11.7. We want to determine the lowest resonant frequency with motion in x direction and corresponding mode shape. It is important that we do not excite this resonant frequency to avoid contact of the blades with the casing. The outer ring connecting all the blades is represented as a lumped mass. Use programs CSTKM and INVITR.
- 11.8. Figure P11.8 shows a beam modeled using four-node quadrilateral elements. Develop a program that will generate the banded K and M matrices. Then use program INVITR to determine the two lowest natural frequencies and mode shapes. Compare your results with those obtained using beam elements.

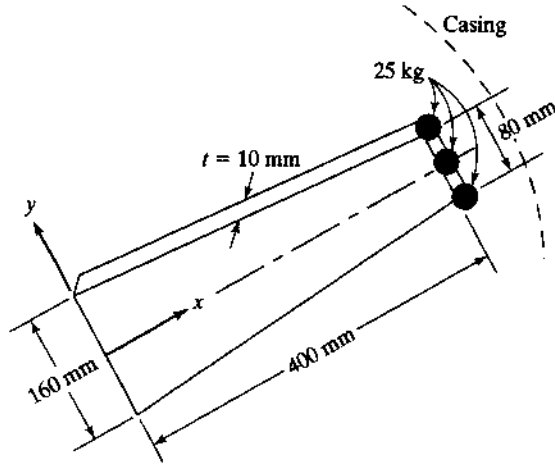


FIGURE P11.7

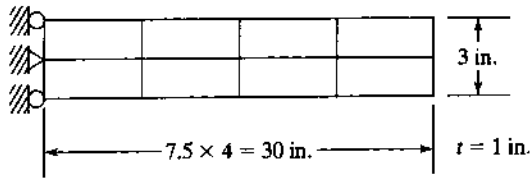


FIGURE P11.8 Steel beam.

11.9. Determine the two lowest natural frequencies and mode shapes for the one-bay, two-story planar steel frame shown in Fig. P11.9. You need to develop a program, analogous to BEAMKM, that will generate the banded \mathbf{K} and \mathbf{M} matrices and then use program INVITR.

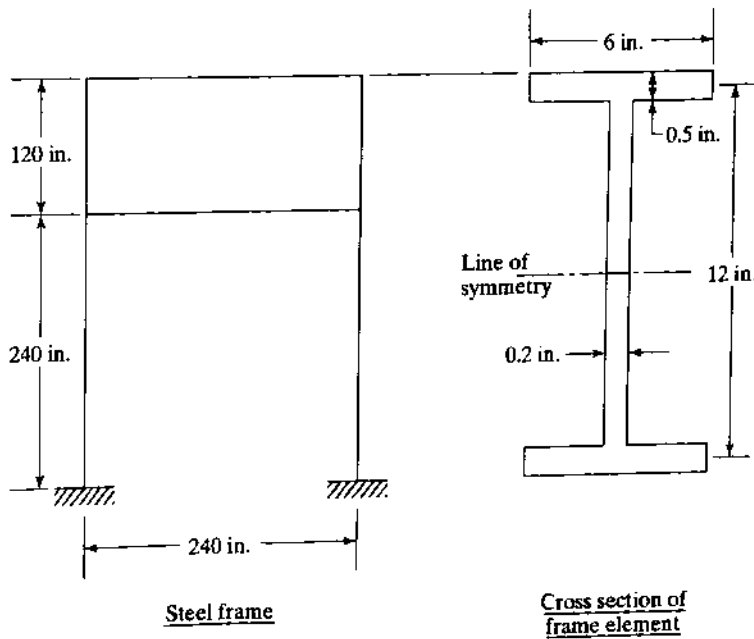


FIGURE P11.9

- 11.10.** For the signal pole arrangement shown in Fig. P11.10, a two-dimensional frame, determine the natural frequencies and mode shapes. (Note: Develop a program in line with BEAMKM to write stiffness and mass matrices to a file. Then an eigenvalue routine like INVTR can be run.)

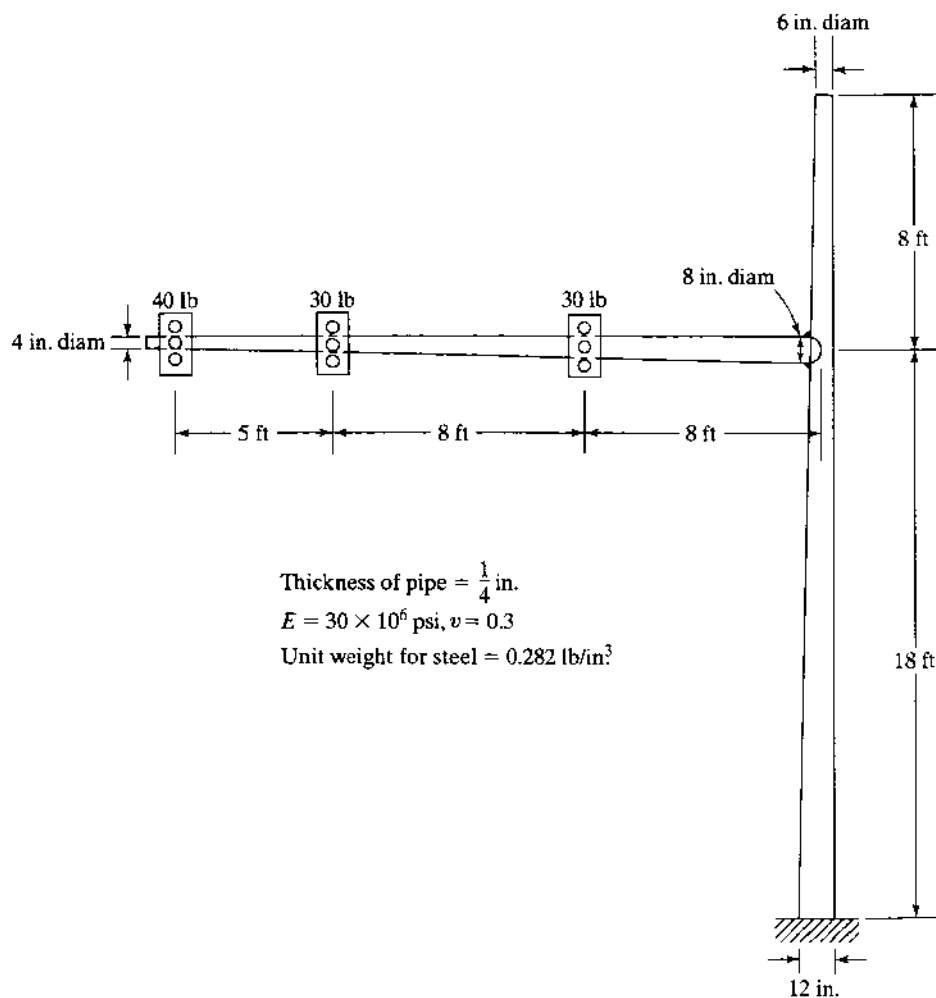


FIGURE P11.10

- 11.11.** Consider the shaft in Example 11.5. Using Guyan reduction, reduce the eight-dof beam model to a two-dof model retaining the translational dof at the flywheels. Compare these frequencies and mode shapes with those obtained from the eight-dof model. Use BEAMKM and JACOBI programs. Also state which modes are missing in the reduced model.

11.12. Reduce the following symmetric matrix to tridiagonal form:

$$\begin{bmatrix} 6 & 1 & 2 & 0 & 0 \\ 1 & 3 & 1 & 2 & 0 \\ 2 & 1 & 2 & 1 & 0 \\ 0 & 2 & 1 & 2 & 1 \\ 0 & 0 & 0 & 1 & 3 \end{bmatrix}$$

11.13. Reduce the following two matrices simultaneously to diagonal form using Jacobi's approach:

$$\mathbf{K} = \begin{bmatrix} 4 & 3 & 2 & 0 \\ 3 & 3 & 1 & 0 \\ 2 & 1 & 2 & 1 \\ 0 & 0 & 1 & 4 \end{bmatrix} \quad \mathbf{M} = \begin{bmatrix} 3 & 1 & 2 & 0 \\ 1 & 2 & 1 & 0 \\ 2 & 1 & 3 & 1 \\ 0 & 0 & 1 & 2 \end{bmatrix}$$

11.14. Consider the beam model shown in Fig. P11.14. Each beam node has a vertical translational degree of freedom (dof) and a counter-clockwise rotational dof. No axial dofs are included. Take the beam length to be 60 mm, rectangular cross section of width 6 mm and depth 1 mm (thus, $I = 0.5 \text{ mm}^4$), and obtain the first three natural frequencies for the different cases that follow. Plot the mode shapes. (After obtaining the output from eigensolver, which contains nodal displacements of the mode shapes, you can interpolate using Hermite cubic shape functions and then use MATLAB or other programs to plot the discretized curve.) Take material to be steel, with $E = 200 \text{ GPa}$ and $\rho = 7850 \text{ kg/m}^3$.

(a) Left end is fixed.

(b) Left end is fixed and a concentrated mass M is attached to the right end (node 5). Take $M = 5\%$ of the beam mass.

(c) Beam is unconstrained, and a mass M is attached to the right end as in (b).

For cases (a) and (b), you can use program INVITR, JACOBI, or GENEIGEN. For (c), use program JACOBI or GENEIGEN.

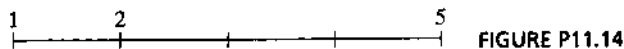


FIGURE P11.14

11.15. A rigid body with mass M and inertia I_C about its center of gravity is welded on to the end of a planar beam element as shown in Fig. P11.15. By writing the kinetic energy of the mass as $\frac{1}{2}Mv^2 + \frac{1}{2}I_C\omega^2$, and relating v and ω to \dot{Q}_1 and \dot{Q}_2 , determine the (2×2) mass matrix contribution to the beam node.

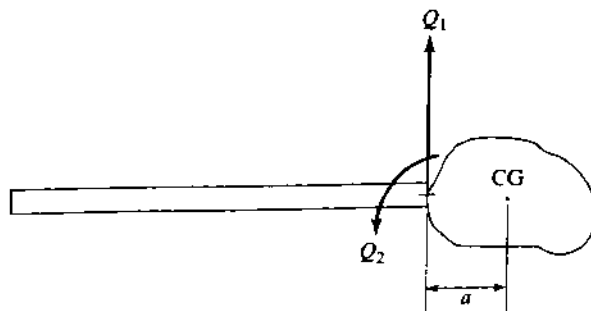


FIGURE P11.15

Program Listings

```

*****
*          PROGRAM BEAMEM          *
* STIFFNESS AND MASS GENERATION  *
* T.R.Chandrupatla and A.D.Belegundu *
*****
===== MAIN PROGRAM =====
Private Sub cmdStart_Click()
    Call InputData
    Call Bandwidth
    Call StiffnMass
    Call ModifyForBC
    Call AddSprMass
    Call Output
    cmdView.Enabled = True
    cmdStart.Enabled = False
End Sub
=====

```

```

===== STIFFNESS AND MASS =====
Private Sub StiffnMass()
    ReDim S(NQ, NEW), GM(NQ, NEW)
    '----- Global Stiffness and Mass Matrices -----
    For N = 1 To NE
        picBox.Print "Forming Stiffness and Mass Matrices of Element "; N
        Call ElemStiffMass(N)
        picBox.Print ".... Placing in Global Locations"
        For II = 1 To NEN
            NRT = NDN * (NOC(N, II) - 1)
            For IT = 1 To NDN
                NR = NRT + IT
                I = NDN * (II - 1) + IT
                For JJ = 1 To NEN
                    NCT = NDN * (NOC(N, JJ) - 1)
                    For JT = 1 To NDN
                        J = NDN * (JJ - 1) + JT
                        NC = NCT + JT - NR + 1
                        If NC > 0 Then
                            S(NR, NC) = S(NR, NC) + SE(I, J)
                            GM(NR, NC) = GM(NR, NC) + EM(I, J)
                        End If
                    Next JT
                Next JJ
            Next IT
        Next II
    Next N
End Sub

```

```

===== ELEMENT STIFFNESS AND MASS =====
Private Sub ElemStiffMass(N)
'----- Element Stiffness and Mass Matrices -----
N1 = NOC(N, 1)
N2 = NOC(N, 2)
M = MAT(NE)
EL = Abs(X(N1) - X(N2))
'--- Element Stiffness
EIL = PM(M, 1) * SMI(N) / EL ^ 3
SE(1, 1) = 12 * EIL
SE(1, 2) = EIL * 6 * EL
SE(1, 3) = -12 * EIL
SE(1, 4) = EIL * 6 * EL
SE(2, 1) = SE(1, 2)
SE(2, 2) = EIL * 4 * EL * EL
SE(2, 3) = -EIL * 6 * EL
SE(2, 4) = EIL * 2 * EL * EL
SE(3, 1) = SE(1, 3)
SE(3, 2) = SE(2, 3)
SE(3, 3) = EIL * 12
SE(3, 4) = -EIL * 6 * EL
SE(4, 1) = SE(1, 4)
SE(4, 2) = SE(2, 4)
SE(4, 3) = SE(3, 4)
SE(4, 4) = EIL * 4 * EL * EL
'--- Element Mass
RHO = PM(M, 2)
C1 = RHO * AREA(N) * EL / 420
EM(1, 1) = 156 * C1
EM(1, 2) = 22 * EL * C1
EM(1, 3) = 54 * C1
EM(1, 4) = -13 * EL * C1
EM(2, 1) = EM(1, 2)
EM(2, 2) = 4 * EL * EL * C1
EM(2, 3) = 13 * EL * C1
EM(2, 4) = -3 * EL * EL * C1
EM(3, 1) = EM(1, 3)
EM(3, 2) = EM(2, 3)
EM(3, 3) = 156 * C1
EM(3, 4) = -22 * EL * C1
EM(4, 1) = EM(1, 4)
EM(4, 2) = EM(2, 4)
EM(4, 3) = EM(3, 4)
EM(4, 4) = 4 * EL * EL * C1
End Sub

```

```

===== ADD SPRINGS/MASSES =====
Private Sub AddSprMass()
'----- Additional Springs and Lumped Masses -----
Do
N = InputBox("Dof# = 0 Exits this", "DOF# with Spring Support", 0)
If N = 0 Then Exit Do
C = InputBox(N, "Support Stiffness at Dof ", 0)
S(N, 1) = S(N, 1) + C
Loop

```

```

Do
  N = InputBox("Dof# = 0 Exits this", "DOF# with Lumped Mass", 0)
  If N = 0 Then Exit Do
  C = InputBox(N, "Lumped Mass at", 0)
  GM(N, 1) = GM(N, 1) + C
Loop
End Sub

```

```

'===== MODIFY FOR BC =====
Private Sub ModifyForBC()
  '----- Decide Penalty Parameter CNST -----
  CNST = 0
  For I = 1 To NQ
    If CNST < S(I, 1) Then CNST = S(I, 1)
  Next I
  CNST = CNST * 10000
  '----- Modify for Boundary Conditions -----
  '--- Displacement BC ---
  For I = 1 To ND
    N = NU(I)
    S(N, 1) = S(N, 1) + CNST
    F(N) = F(N) + CNST * U(I)
  Next I
  '--- Multi-point Constraints ---
  For I = 1 To NMPC
    I1 = MPC(I, 1): I2 = MPC(I, 2)
    S(I1, 1) = S(I1, 1) + CNST * BT(I, 1) * BT(I, 1)
    S(I2, 1) = S(I2, 1) + CNST * BT(I, 2) * BT(I, 2)
    IR = I1: If IR > I2 Then IR = I2
    IC = Abs(I2 - I1) + 1
    S(IR, IC) = S(IR, IC) + CNST * BT(I, 1) * BT(I, 2)
    F(I1) = F(I1) + CNST * BT(I, 1) * BT(I, 3)
    F(I2) = F(I2) + CNST * BT(I, 2) * BT(I, 3)
  Next I
End Sub

```

```

***** PROGRAM INVITE *****
** Inverse Iteration Method *
** for Eigenvalues and Eigenvectors *
** Searching in Subspace *
** for Banded Matrices *
** T.R.Chandrupatla and A.D.Belegundu *
*****
Defint I-N
DefDbl A-H, O-Z
Dim NQ, NBW
Dim S(), GM(), EV1(), EV2(), EVC(), EVL()
Dim EVT(), EVS(), ST(), NITER()
Dim TOL, SH, NEV, NEV1, ITMAX, PI
Dim Title As String, File1 As String, File2 As String
Dim Dummy As String
Private Sub cmdEnd_Click()
  End
End Sub

```

continued

```

===== MAIN PROGRAM =====
Private Sub cmdStart_Click()
  Call InputData
  Call BanSolve1      '<----Stiffness to Upper Triangle
  Call InverseIter
  Call Output
  cmdView.Enabled = True
  cmdStart.Enabled = False
End Sub
=====

```

```

===== DATA INPUT FROM A FILE =====
Private Sub InputData()
  File1 = InputBox("Input File d:\dir\fileName.ext", "Name of File")
  TOL = InputBox("Enter Value", "Tolerance", 0.000001)
  NEV = InputBox("Enter Number", "Number of Eigenvalues Desired", 1)
  SH = 0
  Open File1 For Input As #1
  Line Input #1, Title: Line Input #1, Dummy: Input #1, NQ, NBW
  ReDim S(NQ, NBW), GM(NQ, NBW), EV1(NQ), EV2(NQ), NITER(NEV)
  ReDim EVT(NQ), EVS(NQ), ST(NQ), EVC(NQ, NEV), EVL(NEV)
  '===== READ DATA =====
  '----- Read in Banded Stiffness Matrix -----
  Line Input #1, Dummy
  For I = 1 To NQ: For J = 1 To NBW
    Input #1, S(I, J)
  Next J: Next I
  '----- Read in Banded Mass Matrix -----
  Line Input #1, Dummy
  For I = 1 To NQ: For J = 1 To NBW
    Input #1, GM(I, J)
  Next J: Next I
  '----- Starting Vector for Inverse Iteration -----
  Line Input #1, Dummy
  For I = 1 To NQ: Input #1, ST(I): Next I
  Close #1
  SH = InputBox("SHIFT", "Shift Value for Eigenvalue", 0)
  If SH <> 0 Then
    For I = 1 To NQ: For J = 1 To NBW
      S(I, J) = S(I, J) - SH * GM(I, J)
    Next J: Next I
  End IfEnd Sub

```

```

===== INVERSE ITERATION =====
Private Sub InverseIter()
  ITMAX = 50: NEV1 = NEV
  PI = 3.14159
  For NV = 1 To NEV
    '--- Starting Value for Eigenvector ---
    For I = 1 To NQ: EV1(I) = ST(I): Next I
    EL2 = 0: ITER = 0
  Next NV

```


continued

```

Do
  EL1 = EL2
  ITER = ITER + 1
  If ITER > ITMAX Then
    picBox.Print "No Convergence for Eigenvalue# "; NV
    NEV1 = NV - 1
    Exit Sub
  End If
  If NV > 1 Then
    '----- Starting Vector Orthogonal to
    '----- Evaluated Vectors
    For I = 1 To NV - 1
      CV = 0
      For K = 1 To NQ
        KA = K - NBW + 1: KZ = K + NBW - 1
        If KA < 1 Then KA = 1
        If KZ > NQ Then KZ = NQ
        For L = KA To KZ
          If L < K Then
            K1 = L: L1 = K - L + 1
          Else
            K1 = K: L1 = L - K + 1
          End If
          CV = CV + EVS(K) * GM(K1, L1) * EVC(L, I)
        Next L
      Next K
      For K = 1 To NQ
        EV1(K) = EV1(K) - CV * EVC(K, I)
      Next K
    Next I
  End If
  For I = 1 To NQ
    IA = I - NBW + 1: IZ = I + NBW - 1: EVT(I) = 0
    If IA < 1 Then IA = 1
    If IZ > NQ Then IZ = NQ
    For K = IA To IZ
      If K < I Then
        I1 = K: K1 = I - K + 1
      Else
        I1 = I: K1 = K - I + 1
      End If
      EVT(I) = EVT(I) + GM(I1, K1) * EV1(K)
    Next K
    EV2(I) = EVT(I)
  Next I
  =====

  Call BanSolve2          '<--- Reduce Right Side and Solve
  C1 = 0: C2 = 0
  For I = 1 To NQ
    C1 = C1 + EV2(I) * EVT(I)
  Next I
  For I = 1 To NQ
    IA = I - NBW + 1: IZ = I + NBW - 1: EVT(I) = 0

```

continue

```

    If IA < 1 Then IA = 1
    If IZ > NQ Then IZ = NQ
    For K = IA To IZ
      If K < I Then
        I1 = K: K1 = I - K + 1
      Else
        I1 = I: K1 = K - I + 1
      End If
      EVT(I) = EVT(I) + GM(I1, K1) * EV2(K)
    Next K
  Next I
  For I = 1 To NQ
    C2 = C2 + EV2(I) * EVT(I)
  Next I
  EL2 = C1 / C2
  C2 = Sqr(C2)
  For I = 1 To NQ
    EV1(I) = EV2(I) / C2
    EVS(I) = EV1(I)
  Next I
  Loop While Abs(EL2 - EL1) / Abs(EL2) > TOL
  For I = 1 To NQ
    EVC(I, NV) = EV1(I)
  Next I
  NITER(NV) = ITER
  EL2 = EL2 + SH
  EVL(NV) = EL2
Next NV
End Sub

```

```

'===== BAND SOLVER FOR MULTIPLE RIGHT HAND SIDES =====
Private Sub BanSolve1()
  '----- Gauss Elimination LDU Approach (for Symmetric Banded Matrices)
  '----- Multiple Right hand sides
  '----- Reduction to Upper Triangular Form
  For K = 1 To NQ - 1
    NK = NQ - K + 1
    If NK > NBW Then NK = NBW
    For I = 2 To NK
      C1 = S(K, I) / S(K, 1)
      I1 = K + I - 1
      For J = I To NK
        J1 = J - I + 1
        S(I1, J1) = S(I1, J1) - C1 * S(K, J)
      Next J
    Next I
  Next K
End Sub
Private Sub BanSolve2()
  '----- Reduction of the right hand side
  For K = 1 To NQ - 1
    NK = NQ - K + 1

```

continued

```

If NK > NBW Then NK = NBW
For I = 2 To NK: I1 = K + I - 1
  C1 = 1 / S(K, 1)
  EV2(I1) = EV2(I1) - C1 * S(K, I) * EV2(K)
Next I
Next K
'----- Backsubstitution
EV2(NQ) = EV2(NQ) / S(NQ, 1)
For II = 1 To NQ - 1
  I = NQ - II: C1 = 1 / S(I, 1)
  NI = NQ - I + 1
  If NI > NBW Then NI = NBW
  EV2(I) = C1 * EV2(I)
  For K = 2 To NI
    EV2(I) = EV2(I) - C1 * S(I, K) * EV2(I + K - 1)
  Next K
Next II
End Sub

```

```

'===== OUTPUT =====
Private Sub Output()
'==== Print Displacements, Stresses, and Reactions
File2 = InputBox("Output File d:\dir\fileNames.ext", "Name of File")
Open File2 For Output As #2
Print #2, "Program Invtr - CHANDRUPATLA & BELEGUNDU"
Print #2, "Eigenvalues & Eigenvectors for data in file: "; File1
'----- Eigenvalues and Eigenvectors -----
If NEV1 < NEV Then
  Print #2, "Convergence for "; NEV1; " Eigenvalues Only."
  NEV = NEV1
End If
For NV = 1 To NEV
  Print #2,
  Print #2, "Eigenvalue Number "; NV;
  Print #2, " Iteration Number "; NITER(NV)
  Print #2, "Eigenvalue = ";
  Print #2, Format(EVL(NV), "0.0000E+00 ");
  OMEGA = Sqr(EVL(NV)): FREQ = 0.5 * OMEGA / PI
  Print #2, "Omega = ";
  Print #2, Format(OMEGA, "0.0000E+00 ");
  Print #2, "Freq Hz = ";
  Print #2, Format(FREQ, "0.0000E+00");
  Print #2, "Eigenvector "
  For I = 1 To NQ
    Print #2, Format(EVC(I, NV), "0.0000E+00 ");
  Next I
  Print #2,
Next NV
Close #2
picBox.Print "RESULTS ARE IN FILE "; File2
End Sub

```

Preprocessing and Postprocessing

12.1 INTRODUCTION

Finite element analysis involves three stages of activity: preprocessing, processing, and postprocessing. Preprocessing involves the preparation of data, such as nodal coordinates, connectivity, boundary conditions, and loading and material information. The processing stage involves stiffness generation, stiffness modification, and solution of equations, resulting in the evaluation of nodal variables. Other derived quantities, such as gradients or stresses, may be evaluated at this stage. The processing stage is presented in detail in earlier chapters, where the data were prepared in a formatted input file. The postprocessing stage deals with the presentation of results. Typically, the deformed configuration, mode shapes, temperature, and stress distribution are computed and displayed at this stage. A complete finite element analysis is a logical interaction of the three stages. The preparation of data and postprocessing require considerable effort if all data are to be handled manually. The tedium of handling the data and the possibility of errors creeping in as the number of elements increase are discouraging factors for the finite element analyst. In the following sections, we present a systematic development of preprocessing and postprocessing considerations. This should make finite element analysis a more interesting computational tool. We first present a general-purpose mesh generation scheme for two-dimensional plane problems.

12.2 MESH GENERATION

Region and Block Representation

The basic idea of a mesh-generation scheme is to generate element connectivity data and nodal-coordinate data by reading in input data for a few key points. We present here the theory and computer implementation of a mesh-generation scheme suggested by Zienkiewicz and Philips.* In this scheme, a complex region is divided into eight-noded quadrilaterals, which are then viewed in the form of a rectangular block pattern. Consider the region shown in Fig. 12.1. The full rectangular block pattern is convenient for

*Zienkiewicz, O. C., and D. V. Philips, "An automatic mesh generation scheme for plane and curved surfaces by 'isoparametric' coordinates." *International Journal for Numerical Methods in Engineering* 3: 519-528 (1971).

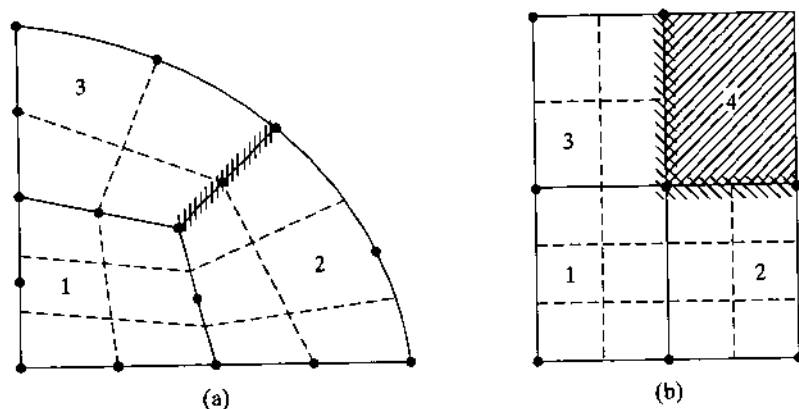


FIGURE 12.1 (a) Region and (b) block diagram.

node numbering. To match the pattern in the region, the block number 4 is to be treated as void and the two hatched edges need to be merged. In general, a complex region is viewed as a rectangle, composed of rectangular blocks, with some blocks left as void and some edges identified to be merged.

Block Corner Nodes, Sides, and Subdivisions

A general configuration of the full rectangle composed of blocks is shown in Fig. 12.2. We represent the sides of the rectangle as S and W , with respective numbers of spans of NS and NW . For consistent coordinate mapping, S , W , and the third coordinate direction Z must form a right-hand system. For mesh generation, each span is subdivided. Spans KS and KW are divided into $NSD(KS)$ and $NWD(KW)$ divisions, respectively. Since the node numbering will be carried out in the S direction first and incremented in the W direction next, the bandwidth of resulting matrices will be small if total number of divisions in the S direction is less than the total number in the W direction. S and W are chosen to represent short and wide directions in this sense. In this scheme, the bandwidth is a minimum when there are no void blocks and there is no side merging. We note here that the total number of nodes in the S and W directions are

$$\begin{aligned} NNS &= 1 + \sum_{KS=1}^{NS} NSD(KS) \\ NNW &= 1 + \sum_{KW=1}^{NW} NWD(KW) \end{aligned} \quad (12.1)$$

The maximum possible nodes for quadrilateral or triangular division is taken as $NNT (= NNS \times NNW)$. We define an array $NNAR(NNT)$ to define the nodes in the problem. We also define a block identifier array $IDBLK(NSW)$, which stores the material number in the location representing the block. A zero is stored in the location corresponding to a void block. The x - and y -coordinates of all valid block corner nodes are read into $XB(NGN, 2)$. The program is given for planar regions. By introducing the z -coordinate, three-dimensional surfaces can be modeled. Two arrays, $SR(NSR, 2)$ and $WR(NWR, 2)$, are used for storing the coordinates of the nodes on the corresponding

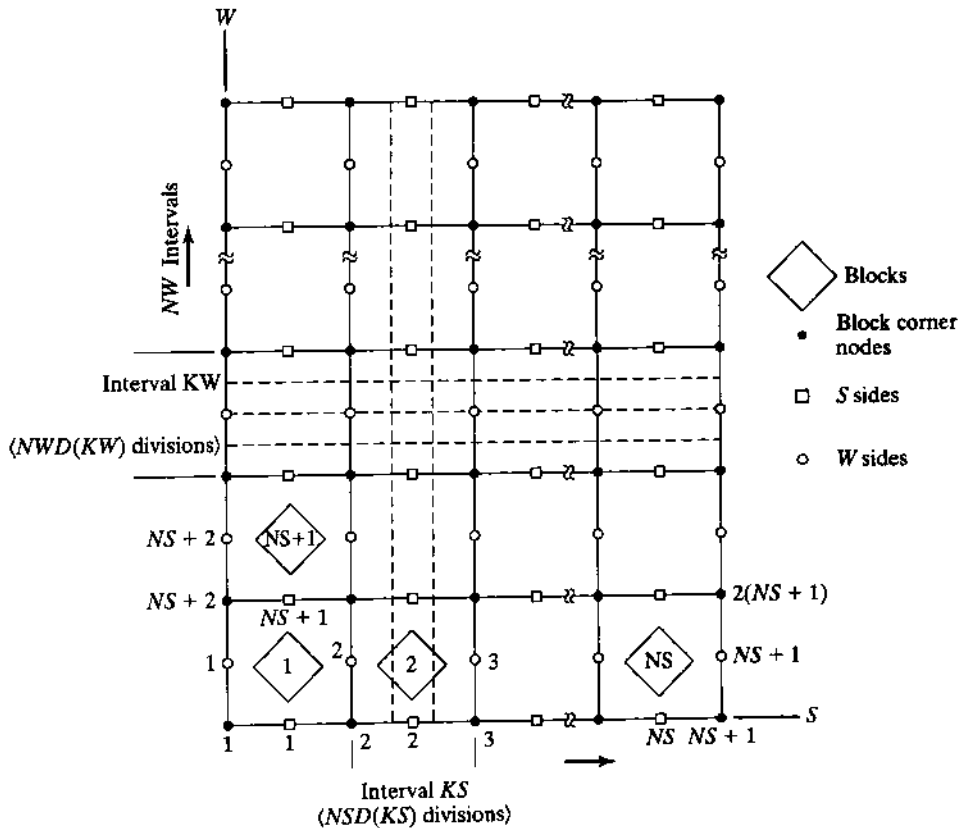


FIGURE 12.2 Numbering of corner nodes and sides.

sides. First, we generate the nodes for all sides, assuming that the side is a straight line and the node is at the midpoint between the corner nodes. This represents the default configuration. Then, for sides that are curved and for those straight sides with nodes not located at physical midpoints, the x - and y -coordinates are read into $SR(.,2)$ and $WR(.,2)$, at appropriate locations. The sides to be merged are identified by the end node numbers of the sides. We now discuss the node numbering and coordinate-generation schemes.

Generation of node numbers We present the node-numbering strategy by means of an example. Consider the region and block representation shown in Fig. 12.1. The node numbering scheme is shown in Fig. 12.3. We have two blocks in the S direction and two in the W direction. Block 4 is void. Array $NNAR(30)$ has all the locations defined. Edges 18–20 and 18–28 are to be merged. We first initialize the array $NNAR(30)$ by putting -1 at each of its locations. We then cover each of the void blocks and put zero where nodes do not exist. Existence of neighboring blocks is checked in implementing this process. For side merging, at the node locations of the side with higher node numbers, the location numbers of the corresponding nodes of the merging side are entered. The final node numbering is a simple process. We sweep along S and then increment

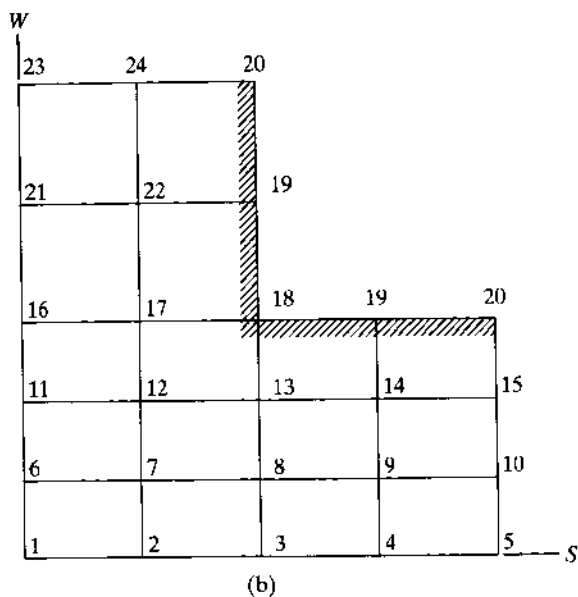
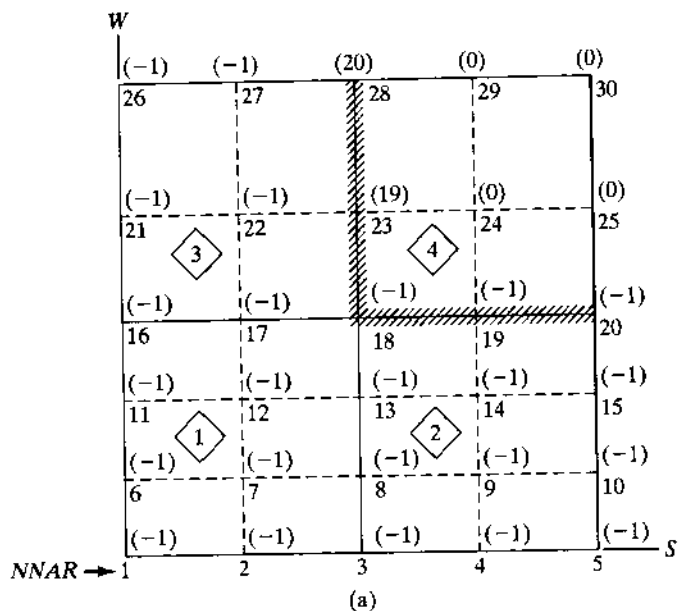


FIGURE 12.3 Node numbering.

along W . The node numbers are incremented by 1 whenever the location has a negative value. When the value is zero, it is skipped. If the location has a positive value, it indicates side merging and the corresponding node number from the location indicated by the value is inserted. The scheme is simple and nodal coordinate checking is not necessary in this process.

Generation of coordinates and connectivity Here we use the shape functions for isoparametric mapping for an eight-noded quadrilateral developed in Chapter 7. We refer to Fig. 12.4, which establishes the relationships for the master block or ξ - η block, the S - W block, and the region block or x - y block. The first step is one of extracting the global coordinates of corner and midside nodes of the block under consideration. For a general node $N1$, the ξ - and η -coordinates are obtained using the number of divisions.

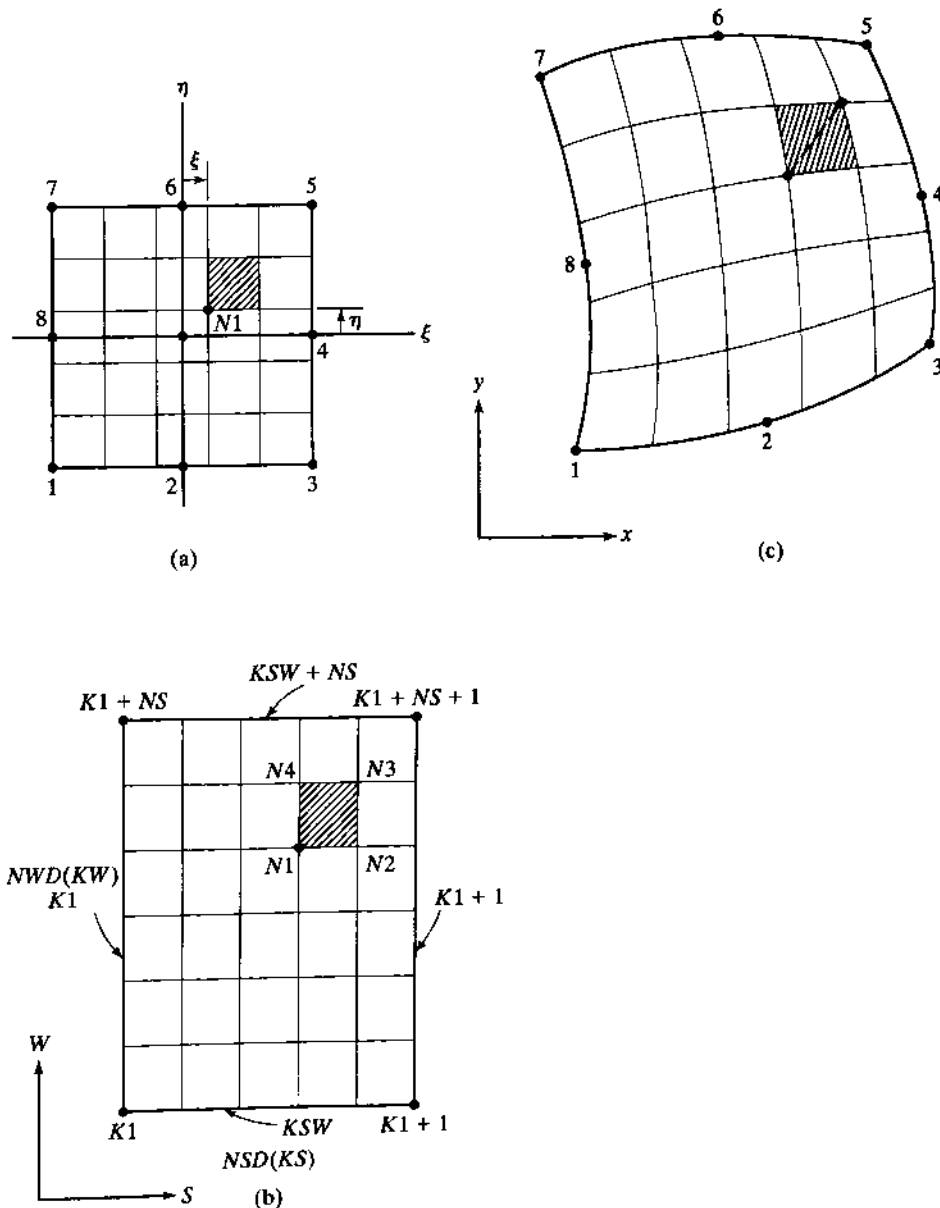


FIGURE 12.4 Coordinates and connectivity: (a) master block for shape functions, (b) block for node numbers, and (c) block in region.

The coordinates of $N1$ are given by

$$x = \sum_{I=1}^8 SH(I) \cdot X(I)$$

$$y = \sum_{I=1}^8 SH(I) \cdot Y(I) \tag{12.2}$$

where $SH()$ are shape functions and $X()$ and $Y()$ are corner node coordinates. For the small rectangular shaded division with lower left corner $N1$, shown in Fig. 12.4, the other three nodes $N2, N3,$ and $N4$ are computed. For quadrilateral elements, we use $N1-N2-N3-N4$ as the element, with the first element of the block starting at the lower left corner. The element numbers for the next block start after the last number of the previous block. For triangular element division, each rectangle is divided into two triangles, $N1-N2-N3$ and $N3-N4-N1$. The triangular division is readjusted to connect the diagonal of shorter length. The process of coordinate and connectivity generation is skipped for void blocks.

This is a general-purpose mesh-generation scheme with the capability to model complex problems. This scheme can be readily generalized to model three-dimensional surfaces by introducing the z -coordinate. To illustrate the use of the program, we consider a few examples.

Examples of mesh generation In the first example shown in Fig. 12.5, there are four blocks. The default material number for all blocks is 1. Material number for

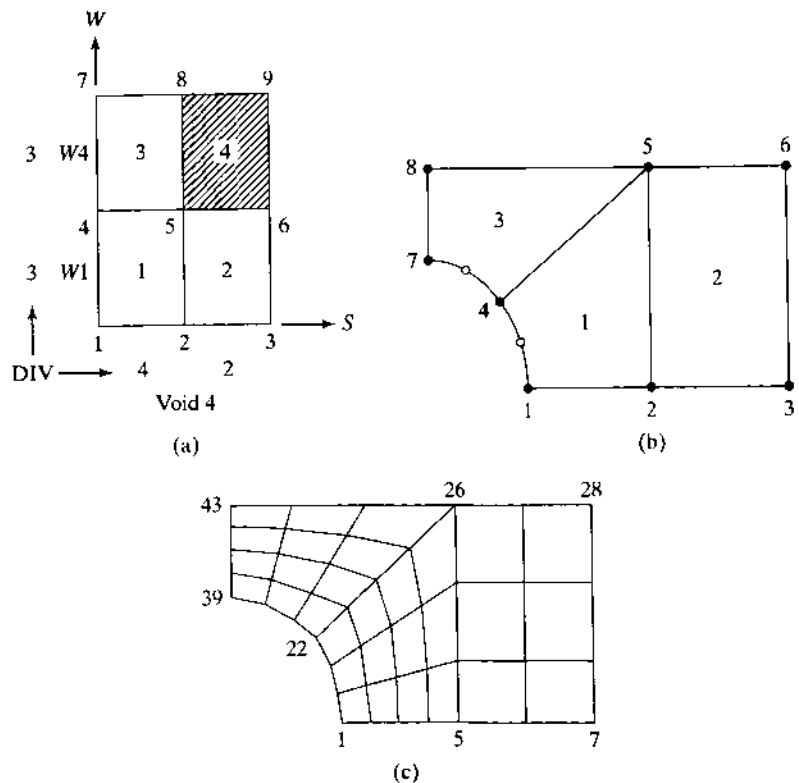


FIGURE 12.5 Example mesh 1: (a) block diagram, (b) region, and (c) mesh.

block 4 is read in as zero to represent void space. S spans 1 and 2 are divided into four and two divisions, respectively. W spans 1 and 2 are each divided into three divisions. The coordinates of corner nodes 1–8 and the coordinates of midpoints of curved sides $W1$ and $W4$ are read in. The generated mesh with node numbers is also shown in Fig. 12.5. If triangular mesh is desired, the shorter diagonal of each quadrilateral will be joined.

In the second example, shown in Fig. 12.6, we model a full annular region. To achieve a minimum bandwidth, the block diagram shown in Fig. 12.6a is suggested. Blocks 2 and 5 are void space. The side 1–2 merges with 4–3, and side 9–10 merges with 12–11. Coordinates of all corner nodes and the midpoints of $W1, W2, \dots, W8$ of the block diagram need to be given. The resulting mesh for the span divisions shown in the block diagram is given in Fig. 12.6c.

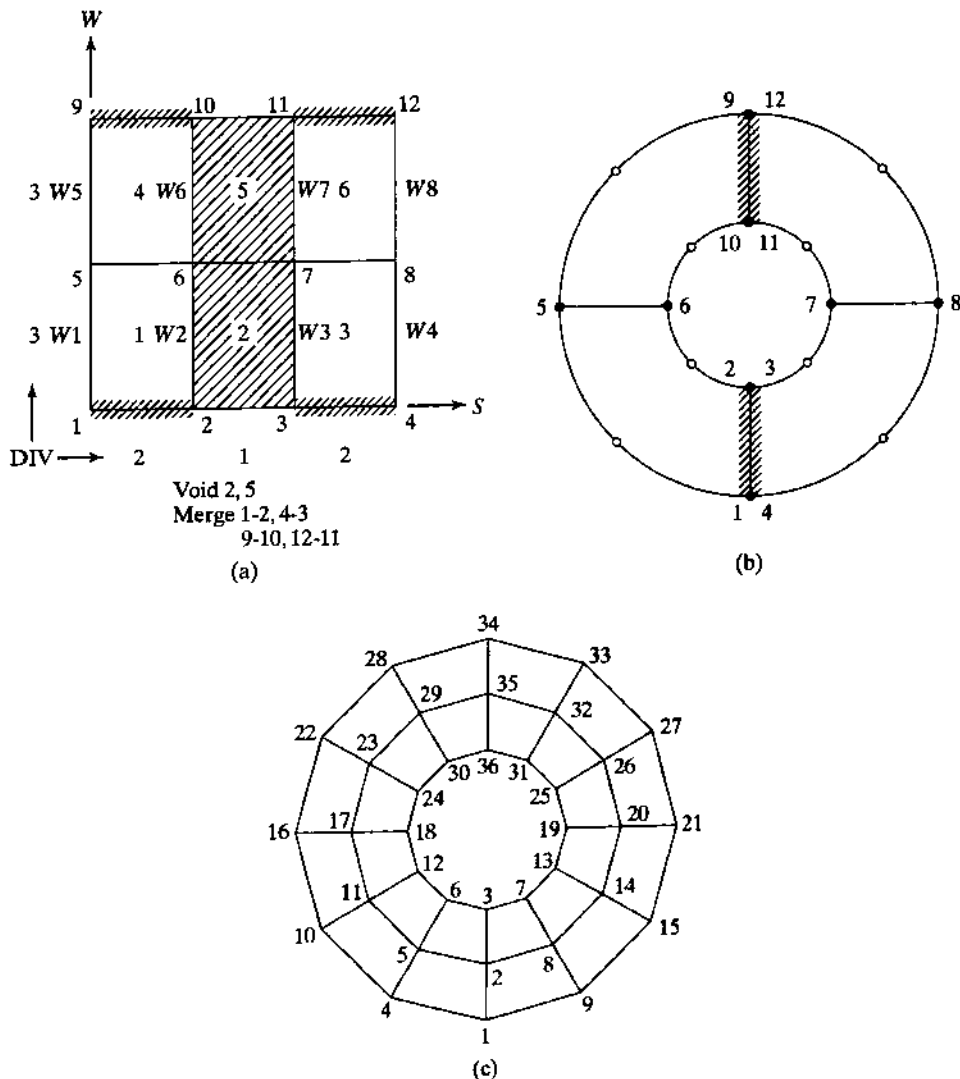


FIGURE 12.6 Example mesh 2: (a) block diagram, (b) region, and (c) mesh.

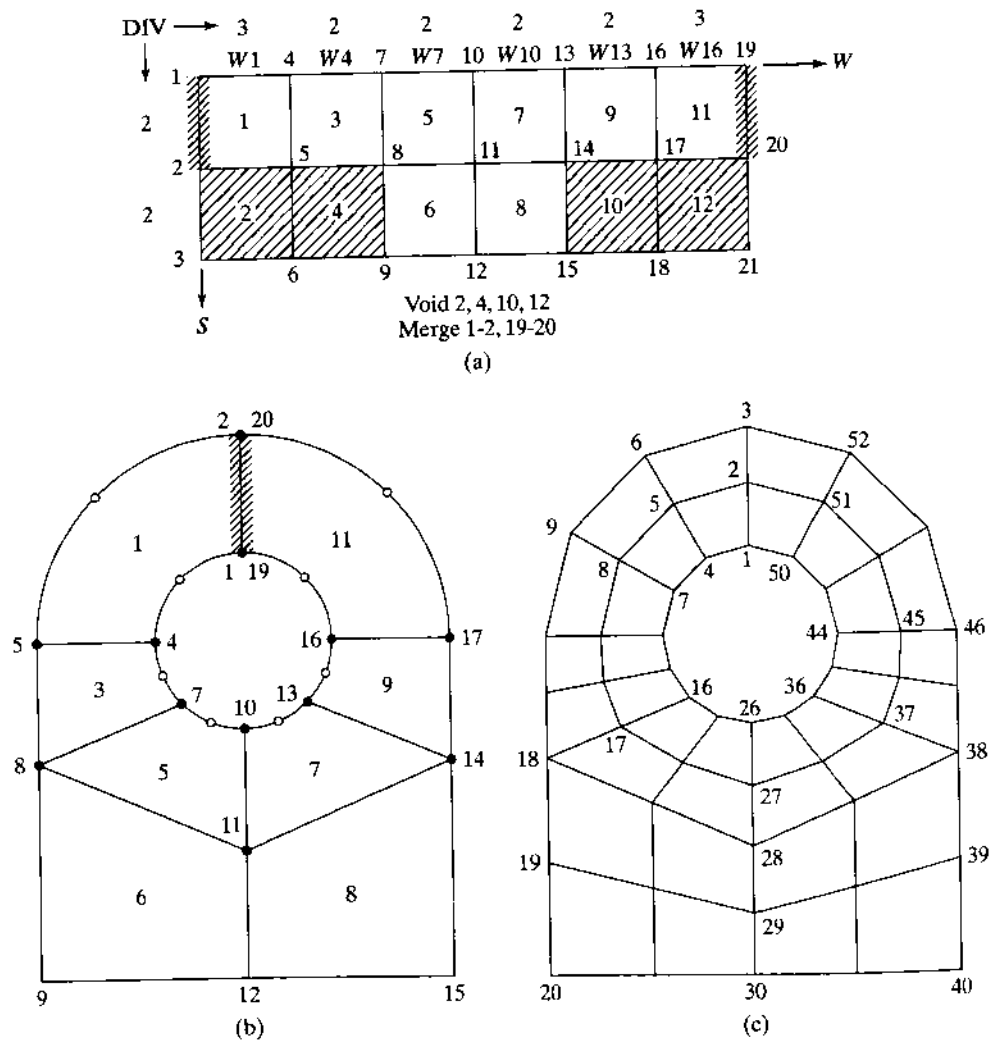


FIGURE 12.7 Example mesh 3: (a) block diagram, (b) region, and (c) mesh.

Figure 12.7 shows an eyelet. The full geometric shape is modeled. The block diagram shows void blocks and span divisions. Merging sides are indicated. Coordinates of all corner points of the block diagram are to be read in. The coordinates of midpoints of curved sides $W1, W2, W4, W7, W10, W13, W16,$ and $W17$ have to be input. The mesh is shown for quadrilateral elements.

Division of a region and making a block diagram form the first step in the preparation of data for mesh generation.

Mesh plotting The generated data are saved in a file. The convenient way of reviewing the coordinate and connectivity data is by plotting it using the computer. The plots will quickly reveal if there are any errors. Points to be readjusted can easily be

identified. The program PLOT2D can be used for plotting two-dimensional meshes on the screen. In mesh plotting, we scan each element and draw the element boundaries using the connectivity information. The coordinate bounds must first be adjusted for the screen resolution and size.

Data handling and editing In simple problems with small number of elements and nodes, it is convenient to prepare data directly using a text editor. For larger problems, the user may generate the data files by using the MESHGEN program. Output of the MESHGEN program essentially consists of nodal coordinates and element connectivity. A text editor is then used to add loading, boundary conditions, material properties, and some other information to the mesh data file. The format for the data file is common for all problems and is given on the inside front cover of this book. Importantly, an example input file is provided at the end of every chapter. For two-dimensional problems, the program PLOT2D can be used to read the data and plot meshes on the screen.

The data thus created can be processed by the finite element programs presented in earlier chapters. The finite element program processes the data and calculates nodal variable quantities, such as displacements and temperatures, and element quantities, such as stresses and gradients. The stage is now set for postprocessing.

12.3 POSTPROCESSING

We discuss here the aspects of plotting a displaced configuration, plotting nodal data in the form of contour plots, such as isotherms and isobars, and conversion of element-oriented data into best fitting nodal values. We restrict our discussion here to two-dimensional problems; however, the ideas can be extended to three-dimensional problems with some additional effort.

Deformed Configuration and Mode Shape

Plotting a deformed or displaced shape is a simple extension of PLOT2D. If the displacements or components of the eigenvector are read into the matrix $U(NN, 2)$ and the coordinates are stored in $X(NN, 2)$, we can define the displaced position matrix $XP(NN, 2)$ so that

$$XP(I, J) = X(I, J) + \alpha U(I, J) \quad \begin{array}{l} J = 1, 2 \\ I = 1, \dots, NN \end{array} \quad (12.3)$$

where α is a magnification factor so chosen that the largest component of $\alpha U(I, J)$ is of reasonable proportion in relation to the body size and NN represents the number of nodes. One may try this largest component to be about 10% of the body-size parameter. In the program PLOT2D, we need to make changes to read displacements $U(NN, 2)$, decide the value of α , and replace \mathbf{X} by $\mathbf{X} + \alpha \mathbf{U}$.

Contour Plotting

Contour plotting of a scalar nodal variable such as temperature is straightforward for three-noded triangular elements. We consider the variable f on one triangular element shown in Fig. 12.8. The nodal values are f_1, f_2 , and f_3 at the three nodes 1, 2, and 3, respectively. The function f is interpolated using the linear shape functions used for the constant strain triangle. f represents a plane surface with values f_1, f_2 , and f_3 at the three nodes. We check for each desired level. Say \hat{f} represents a typical level for contour map. If \hat{f} lies in the interval f_2-f_3 , it also lies in one of the intervals f_1-f_2 or f_1-f_3 . Say it lies in the interval f_2-f_3 , as shown in Fig. 12.8. Then f has the value of \hat{f} at points A and B and is constant along the line AB . Determination of the coordinates of points A and B will give us the contour line AB . The coordinates of point A can be obtained from

$$\xi = \frac{\hat{f} - f_2}{f_3 - f_2}$$

$$x_A = \xi x_3 + (1 - \xi)x_2$$

$$y_A = \xi y_3 + (1 - \xi)y_2 \quad (12.4)$$

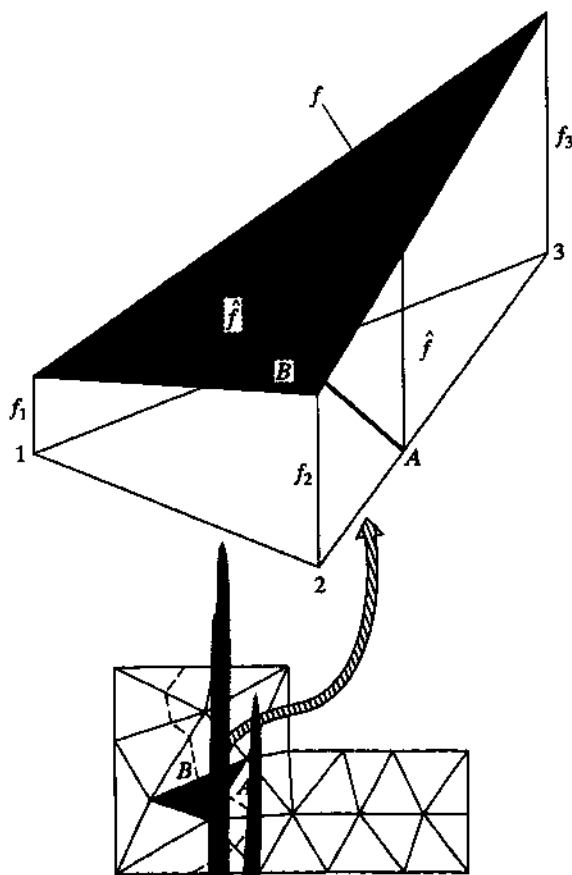


FIGURE 12.8 Constant level of variation f .

The coordinates of point B can be obtained by replacing the indices 2 and 3 by 1 and 3, respectively.

The program CONTOURA plots the variable FF represented by its nodal values. The coordinate, connectivity, and function data are read in from data files. In the first part of the program, the boundary limits are set on the screen. The function limits are found and the number of contour levels is read in. The boundary of the region is plotted on the screen. Each element is then scanned for the function levels and the constant value lines are drawn. The result is a contour map.

In addition, in CONTOURA, the number of levels is fixed at 10 and each level is associated with a distinct color. Violet is the lowest level, and red is set as the highest level, with intermediate colors roughly in the order of the rainbow spectrum. CONTOURB uses the idea of filling the color in a closed subregion of an element. Thus, for the same data used for CONTOURA, CONTOURB plots color bands. Both CONTOURA and CONTOURB also work for four-noded quadrilateral elements. The contour plot idea presented for the triangle is also used for the quadrilateral by introducing an interior point and considering the four triangles. There are other contour algorithms specifically for quadrilaterals, and interested readers are encouraged to search the literature in this area.

There are also some quantities, such as stresses, temperature, and velocity gradients, which are constant over triangular elements. For these, the contour mapping requires the evaluation of nodal values. We present here the procedure for evaluating the nodal values for least-squares fit. The procedure discussed is useful in diverse situations, such as smoothing data obtained in image processing. The least squares fit for a four-noded quadrilateral is also presented following the best fit for the triangle.

Nodal Values from Known Constant Element Values for a Triangle

We evaluate the nodal values that minimize the least-squares error. We consider here triangular elements with constant function values. A triangular element having function value f_e is shown in Fig. 12.9. Let f_1 , f_2 , and f_3 be the local nodal values. The interpolated function is given by

$$f = \mathbf{Nf} \quad (12.5)$$

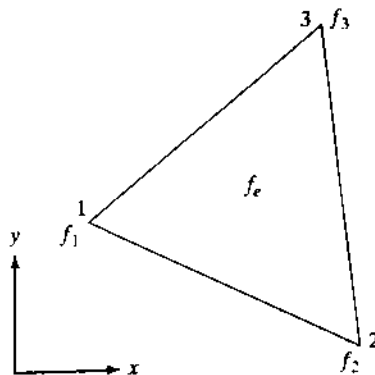


FIGURE 12.9 Triangular element for least-squares fit study.

where

$$\mathbf{N} = [N_1, N_2, N_3] \quad (12.6)$$

is the vector of shape functions and

$$\mathbf{f} = [f_1, f_2, f_3]^T \quad (12.7)$$

The squared error may be represented by

$$E = \sum_e \frac{1}{2} \int_e (f - f_e)^2 dA \quad (12.8)$$

On expanding and substituting from Eq. 12.5, we get

$$E = \sum_e \left[\frac{1}{2} \mathbf{f}^T \left(\int_e \mathbf{N}^T \mathbf{N} dA \right) \mathbf{f} - \mathbf{f}^T \left(f_e \int_e \mathbf{N}^T dA \right) + \frac{1}{2} f_e^2 A \right] \quad (12.9)$$

Noting that the last term is a constant, we write the equation in the form

$$E = \sum_e \left[\frac{1}{2} \mathbf{f}^T \mathbf{W}^e \mathbf{f} - \mathbf{f}^T \mathbf{R}^e \right] + \text{constant} \quad (12.10)$$

where

$$\mathbf{W}^e = \int_e \mathbf{N}^T \mathbf{N} dA = \frac{A_e}{12} \begin{bmatrix} 2 & 1 & 1 \\ 1 & 2 & 1 \\ 1 & 1 & 2 \end{bmatrix} \quad (12.11)$$

$$\mathbf{R}^e = f_e \int_e \mathbf{N}^T dA = \frac{f_e A_e}{3} \begin{Bmatrix} 1 \\ 1 \\ 1 \end{Bmatrix} \quad (12.12)$$

$\int_e \mathbf{N}^T \mathbf{N} dA$ is similar to the evaluation of mass matrix for a triangle in Chapter 11. On assembling the stiffness \mathbf{W}^e and load vector from \mathbf{R}^e , we get

$$E = \frac{1}{2} \mathbf{F}^T \mathbf{W} \mathbf{F} - \mathbf{F}^T \mathbf{R} + \text{constant} \quad (12.13)$$

where \mathbf{F} is the global nodal-value vector given by

$$\mathbf{F} = [F_1, F_2, \dots, F_{NN}]^T \quad (12.14)$$

For least-squares error, setting the derivatives of E with respect to each F_i to be zero, we get

$$\mathbf{W} \mathbf{F} = \mathbf{R} \quad (12.15)$$

Here \mathbf{W} is a banded symmetric matrix. The set of equations is solved using the equation solving techniques used in other finite element programs. The program BESTFIT takes the mesh data and element value data $FS(NE)$ and evaluates the nodal data $F(NN)$ for a three-noded triangle.

Least Squares Fit for a Four-Noded Quadrilateral

Let $\mathbf{q} = [q_1 \ q_2 \ q_3 \ q_4]^T$ represent the element nodal values to be determined for least-squares fit defined using error at four interior points. If $\mathbf{s} = [s_1 \ s_2 \ s_3 \ s_4]^T$ represents the vector of interpolated values at the four interior points, and $\mathbf{a} = [a_1 \ a_2 \ a_3 \ a_4]^T$ represents the actual values of the variable (see Fig. 12.10), the error may be defined as

$$\begin{aligned}\epsilon &= \sum_e (\mathbf{s} - \mathbf{a})^T (\mathbf{s} - \mathbf{a}) \\ &= \sum_e (\mathbf{s}^T \mathbf{s} - 2\mathbf{s}^T \mathbf{a} - \mathbf{a}^T \mathbf{a})\end{aligned}\quad (12.16)$$

The four interior points are generally taken as the Gaussian integration points. The stress values match well at these points. If

$$\mathbf{N} = \begin{bmatrix} N_1^1 & N_2^1 & N_3^1 & N_4^1 \\ N_1^2 & N_2^2 & N_3^2 & N_4^2 \\ N_1^3 & N_2^3 & N_3^3 & N_4^3 \\ N_1^4 & N_2^4 & N_3^4 & N_4^4 \end{bmatrix}\quad (12.17)$$

where N_I^I represents the shape function N_I evaluated at interior point I , then \mathbf{s} can be written as

$$\mathbf{s} = \mathbf{N}\mathbf{q}\quad (12.18)$$

Inserting this into Eq. 12.16, we find that the error becomes

$$\epsilon = \sum_e \mathbf{q}^T \mathbf{N}^T \mathbf{N} \mathbf{q} - 2\mathbf{q}^T \mathbf{N}^T \mathbf{a} + \mathbf{a}^T \mathbf{a}\quad (12.19)$$

Noting that $\mathbf{N}^T \mathbf{N}$ is similar to element stiffness \mathbf{k}^e , and $\mathbf{N}^T \mathbf{a}$ is similar to the element force vector, the stiffness and force-vector assembly can be made. The assembled matrix equations can be put in the form

$$\mathbf{K}\mathbf{Q} = \mathbf{F}\quad (12.20)$$

The solution of this set of equations gives \mathbf{Q} , which is the vector of nodal values of the variable considered for least squares fit of the element values. This least-squares fit is implemented in the program BESTFITQ.

Element quantities such as maximum shear stress, von Mises stress, and temperature gradient can be converted to nodal values and then contour plotting can be done.

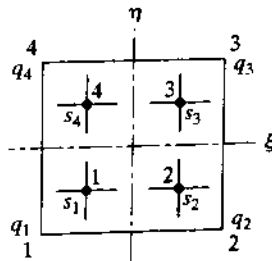


FIGURE 12.10 Least squares fit for a quadrilateral.

The use of computer programs BESTFIT and CONTOUR has already been discussed in Chapter 5 (Example 5.6).

12.4 CONCLUSION

Preprocessing and postprocessing are integral parts of finite element analysis. The general-purpose mesh-generation scheme can model a variety of complex regions. One needs to use some imagination in preparing the block representation of the region. Definition of void blocks and merging of sides enables one to model multiple-connected regions. The node numbering gives sparse matrices and in many cases should give minimum bandwidth by proper block representation. Mesh plotting shows the element layout. The data handling program is a dedicated routine for finite element data preparation and data editing. Ideas for the plotting of deformed configuration and mode shapes can be readily implemented into the programs included here. Contour plottings for triangular and quadrilateral elements have been presented, and programs are included. The computation of nodal values that best fit the element values takes some of the very same steps used in the development of finite elements in earlier chapters.

Finite element analysis involves solution of a wide variety of problems in solid mechanics, fluid mechanics, heat transfer, electrical and magnetic fields, and other areas. Problem solving involves large amounts of data that must be systematically handled and clearly presented. The ideas developed in this chapter should make preparation and handling of input and output data an interesting endeavor rather than a tedious task.

Example 12.1

The quadrant shown in Fig. E12.1 is meshed using program MESHGEN. The input data given are constructed from the display in Fig. E12.1. Connectivity and nodal coordinate data are contained in the output file, and a plot of the mesh can be obtained by running program PLOT2D.

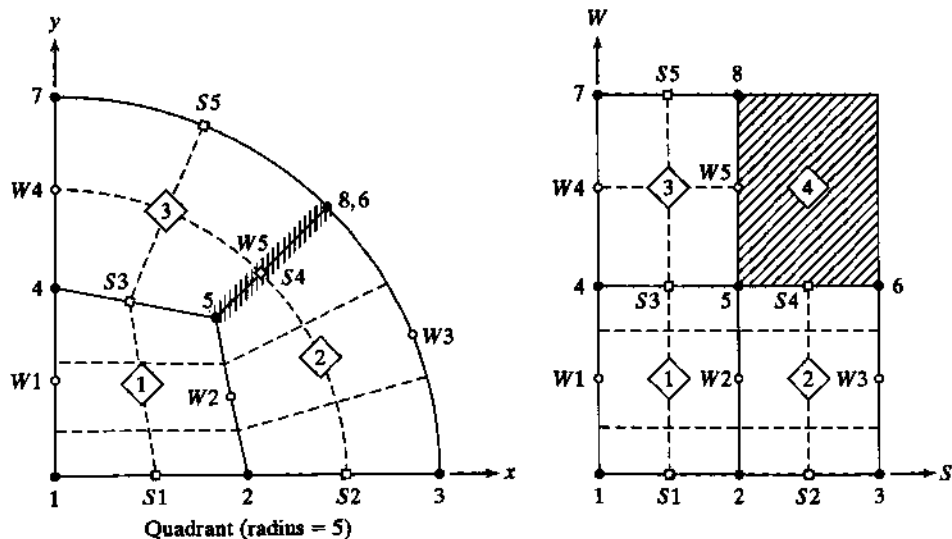


FIGURE E12.1

Input Data File

```

Mesh Generation
Example 12.1
Number of Nodes per Element <3 or 4>
3
BLOCK DATA
#S-Spans (NS)  #W-Spans (NW)  #PairsOfEdgesMergedNSJ)
2              2              1
SPAN DATA
S-Span#  Num-Divisions  (for each S-Span/ Single division = 1)
1        2
2        2
W-Span#  Num-Divisions  (for each W-Span/ Single division = 1)
1        3
2        2
BLOCK MATERIAL DATA (for Material Number other than 1)
Block#  Material  (Void => 0  Block# = 0 completes this data)
4       0
0
BLOCK CORNER DATA
Corner#  X-Coord  Y-Coord (Corner# = 0 completes this data)
1        0        0
2        2.5      0
3        5        0
4        0        2.5
5        1.8      1.8
6        3.536    3.536
7        0        5
8        3.536    3.536
0
MID POINT DATA FOR CURVED OR GRADED SIDES
S-Side#  X-Coord  Y-Coord (Side# = 0 completes this data)
5        1.913    4.619
0
W-Side#  X-Coord  Y-Coord (Side# = 0 completes this data)
3        4.619    1.913
0
MERGING SIDES (Node1 is the lower number)
Pair#  Side1Node1  Side1Node2  Side2Node1  Side2Node2
1      5           6           5           8

```

PROBLEMS

- 12.1. Use program MESHGEN to generate finite element meshes for the regions in Figs. P12.1a and b. Generate meshes using both triangular and quadrilateral elements. For the fillet in P12.1a, use $y = 42.5 - 0.5x + x^2/360$.
- 12.2. Generate a "graded" mesh for the region in Fig. P12.1a so that there are more elements near the left edge of the region. That is, the mesh density reduces along the +x direction. Use MESHGEN with displaced midside nodes.

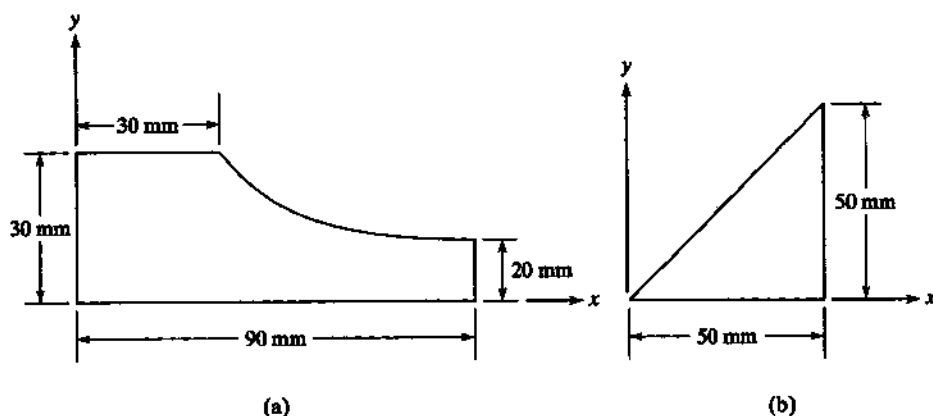


FIGURE P12.1

- 12.3. Use program CONTOUR to draw isotherms for the temperature distribution obtained in Example 10.4.
- 12.4. After solving Problem 5.15 using program CST, complete the following:
- Use program PLOT2D to plot the original and deformed shape. The deformed shape requires selecting a scaling factor and using Eq. 12.3.
 - Use programs BESTFIT and CONTOUR and plot contours of maximum principal stress.
- 12.5. Plot the mode shapes of the beam in Problem 11.4. For this, you will need to modify PLOT2D and interface with INVITR.
- 12.6. This problem illustrates the concept of a dedicated finite element program. Only design related parameters are input to the program, while mesh generation, boundary conditions and loading definition, finite element analysis, and postprocessing are automatically performed. Consider the flywheel in Fig. P12.6. By modifying and interfacing programs MESHGEN, PLOT2D, AXISYM, BESTFIT, and CONTOUR, develop a dedicated program that requires the user to input only the overall dimensions r_h , r_i , r_o , t_h , and t_f and the values of E , ν , ρ , and ω . Your program may consist of independent programs executed through a batch or command file or can consist of one single program. Include the following features:
- a printout of all input data and output displacements and stresses and
 - a plot of original and deformed shapes.
- Solve Problem 6.7. Provide contour plots of stress components.
- 12.7. Plot shearing-stress contours for the torsion problem P10.18.

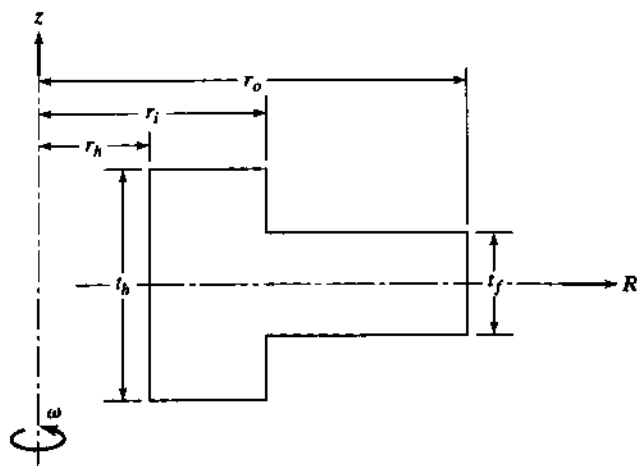


FIGURE P12.6

Program Listings

```

*****
*                PROGRAM MESHGEN                *
* MESH GENERATOR FOR TWO DIMENSIONAL REGIONS *
*      (c) T.R.CHANDRUPATLA & A.D.BELEGUNDU    *
*****
DefInt I-N
DefSng A-H, O-Z
Dim NS, NW, NSJ, NSR, NWR, NNS, NNW, NNT, NGN, NODE
Dim NN, NE, NM, NEN
Dim IDBLK(), NSD(), NWD(), NGCN(), SR(), WR(), SH()
Dim X(), XB(), XP(), NOC(), MAT(), MERG(), NNAR()
Dim Title As String, File1 As String, File2 As String
Dim Dummy As String
Private Sub cmdEnd_Click()
    End
End Sub
'==== MAIN PROGRAM =====
Private Sub cmdStart_Click()
    Call InputData
    Call GlobalNode
    Call CoordConnect
    Call Output
    cmdView.Enabled = True
    cmdStart.Enabled = False
End Sub
'=====

```

```

'==== INPUT DATA FROM FILE =====
Private Sub InputData()
    File1 = InputBox("Input File d:\dir\fileName.ext", "Name of File")
    Open File1 For Input As #1
    '----- READ DATA -----
    Line Input #1, Dummy: Line Input #1, Title
    Line Input #1, Dummy
    Input #1, NEN      ' NEN = 3 for Triangle  4 for Quad
    If NEN < 3 Then NEN = 3
    If NEN > 4 Then NEN = 4
    'Hints: A region is divided into 4-cornered blocks viewed as a
    '        mapping from a Checkerboard pattern of S- and W- Sides
    '        S- Side is one with lower number of final divisions
    '        Blocks, Corners, S- and W- Sides are labeled as shown in Fig. 12.2
    '        Make a sketch and identify void blocks and merging sides
    '---- Block Data ----
    '#S-Spans(NS) #W-Spans(NW) #PairsOfEdgesMerged(NSJ)
    Line Input #1, Dummy: Line Input #1, Dummy
    Input #1, NS, NW, NSJ
    NSW = NS * NW: NGN = (NS + 1) * (NW + 1): NM = 1
    ReDim IDBLK(NSW), NSD(NS), NWD(NW), NGCN(NGN), SH(8)
    '----- Span Divisions -----
    Line Input #1, Dummy
    NNS = 1: NNW = 1
    '--- Number of divisions for each S-Span
    Line Input #1, Dummy

```

continued

```

For KS = 1 To NS
  Input #1, N
  Input #1, NSD(N)
  NNS = NNS + NSD(N)
Next KS
'--- Number of divisions for each W-Span
Line Input #1, Dummy
For KW = 1 To NW
  Input #1, N
  Input #1, NWD(N)
  NNW = NNW + NWD(N)
Next KW

'--- Block Material Data
Input #1, Dummy: Input #1, Dummy
'----- Block Identifier / Material# (Default# is 1) -----
For I = 1 To NSW: IDBLK(I) = 1: Next I
Do
  Input #1, NTMP
  If NTMP = 0 Then Exit Do
  Input #1, IDBLK(NTMP)
  If NM < IDBLK(NTMP) Then NM = IDBLK(NTMP)
Loop

'----- Block Corner Data -----
NSR = NS * (NW + 1): NWR = NW * (NS + 1)
ReDim XB(NGN, 2), SR(NSR, 2), WR(NWR, 2)
Input #1, Dummy: Input #1, Dummy
Do
  Input #1, NTMP
  If NTMP = 0 Then Exit Do
  Input #1, XB(NTMP, 1)
  Input #1, XB(NTMP, 2)
Loop

'----- Evaluate Mid-points of S-Sides -----
For I = 1 To NW + 1
  For J = 1 To NS
    IJ = (I - 1) * NS + J
    SR(IJ, 1) = 0.5 * (XB(IJ + I - 1, 1) + XB(IJ + I, 1))
    SR(IJ, 2) = 0.5 * (XB(IJ + I - 1, 2) + XB(IJ + I, 2))
  Next J
Next I

'----- Evaluate Mid-points of W-Sides -----
For I = 1 To NW
  For J = 1 To NS + 1
    IJ = (I - 1) * (NS + 1) + J
    WR(IJ, 1) = 0.5 * (XB(IJ, 1) + XB(IJ + NS + 1, 1))
    WR(IJ, 2) = 0.5 * (XB(IJ, 2) + XB(IJ + NS + 1, 2))
  Next J
Next I

```

Continued

```

'----- Mid Points for Sides that are curved or graded -----
Line Input #1, Dummy: Line Input #1, Dummy
'---- S-Sides
Do
  Input #1, NTMP
  If NTMP = 0 Then Exit Do
  Input #1, SR(NTMP, 1)
  Input #1, SR(NTMP, 2)
Loop
Line Input #1, Dummy
'---- W-Sides
Do
  Input #1, NTMP
  If NTMP = 0 Then Exit Do
  Input #1, WR(NTMP, 1)
  Input #1, WR(NTMP, 2)
Loop
'----- Merging Sides -----
If NSJ > 0 Then
  Input #1, Dummy: Input #1, Dummy
  ReDim MERG(NSJ, 4)
  For I = 1 To NSJ
    Input #1, N
    Input #1, L1
    Input #1, L2
    Call SideDiv(L1, L2, IDIV1)
    Input #1, L3
    Input #1, L4
    Call SideDiv(L3, L4, IDIV2)
    If IDIV1 <> IDIV2 Then
      picBox.Print "#Div don't match. Check merge data."
    End If
  End If
  MERG(I, 1) = L1: MERG(I, 2) = L2
  MERG(I, 3) = L3: MERG(I, 4) = L4
  Next I
End If
Close #1
End Sub
'=====

```

```

'===== GLOBAL NODE NUMBERS FOR THE MESH =====
Private Sub GlobalNode()
'----- Global Node Locations of Corner Nodes -----
NTMPI = 1
For I = 1 To NW + 1
  If I = 1 Then IINC = 0 Else IINC = NNS * NWD(I - 1)
  NTMPI = NTMPI + IINC: NTMPJ = 0
  For J = 1 To NS + 1
    IJ = (NS + 1) * (I - 1) + J
    If J = 1 Then JINC = 0 Else JINC = NSD(J - 1)
    NTMPJ = NTMPJ + JINC: NGCN(IJ) = NTMPI + NTMPJ
  Next J
Next I

```

continued

```

'----- Node Point Array -----
NNT = NNS * NNW
ReDim NNAR(NNT)
For I = 1 To NNT: NNAR(I) = -1: Next I
'----- Zero Non-Existing Node Locations -----
For KW = 1 To NW
  For KS = 1 To NS
    KSW = NS * (KW - 1) + KS
    If IDBLK(KSW) <= 0 Then
      '----- Operation within an Empty Block -----
      K1 = (KW - 1) * (NS + 1) + KS: N1 = NGCN(K1)
      NS1 = 2: If KS = 1 Then NS1 = 1
      NW1 = 2: If KW = 1 Then NW1 = 1
      NS2 = NSD(KS) + 1
      If KS < NS Then
        If IDBLK(KSW + 1) > 0 Then NS2 = NSD(KS)
      End If
      NW2 = NWD(KW) + 1
      If KW < NW Then
        If IDBLK(KSW + NS) > 0 Then NW2 = NWD(KW)
      End If
      For I = NW1 To NW2
        IN1 = N1 + (I - 1) * NNS
        For J = NS1 To NS2
          IJ = IN1 + J - 1: NNAR(IJ) = 0
        Next J
      Next I
      ICT = 0
      If NS2 = NSD(KS) Or NW2 = NWD(KW) Then ICT = 1
      If KS = NS Or KW = NW Then ICT = 1
      If ICT = 0 Then
        If IDBLK(KSW + NS + 1) > 0 Then NNAR(IJ) = -1
      End If
    End If
  Next KS
Next KW
'----- Node Identification for Side Merging -----
If NSJ > 0 Then
  For I = 1 To NSJ
    I1 = MERG(I, 1): I2 = MERG(I, 2)
    Call SideDiv(I1, I2, IDIV)
    IA1 = NGCN(I1): IA2 = NGCN(I2)
    IASTP = (IA2 - IA1) / IDIV
    I1 = MERG(I, 3): I2 = MERG(I, 4)
    Call SideDiv(I1, I2, IDIV)
    IB1 = NGCN(I1): IB2 = NGCN(I2)
    IBSTP = (IB2 - IB1) / IDIV
    IAA = IA1 - IASTP
    For IBB = IB1 To IB2 Step IBSTP
      IAA = IAA + IASTP
      If IBB = IAA Then NNAR(IAA) = -1 Else NNAR(IBB) = IAA
    Next IBB
  Next I
End If

```

continued

```

'----- Final Node Numbers in the Array -----
NODE = 0
For I = 1 To NNT
  If NNAR(I) > 0 Then
    II = NNAR(I): NNAR(I) = NNAR(II)
  ElseIf NNAR(I) < 0 Then
    NODE = NODE + 1: NNAR(I) = NODE
  End If
Next I
End Sub
Private Sub SideDiv(I1, I2, IDIV)
'----- Number of Divisions for Side I1,I2 -----
IMIN = I1: IMAX = I2
If IMIN > I2 Then
  IMIN = I2
  IMAX = I1
End If
If (IMAX - IMIN) = 1 Then
  IDIV = NGCN(IMAX) - NGCN(IMIN)
Else
  IDIV = (NGCN(IMAX) - NGCN(IMIN)) / NNS
End If
End Sub
'-----

```

```

'===== COORDINATES AND CONNECTIVITY =====
Private Sub CoordConnect()
'----- Nodal Coordinates -----
NN = NODE: NELM = 0
ReDim X(NN, 2), XP(8, 2), NOC(2 * NNT, NEN), MAT(2 * NNT)
For KW = 1 To NW
  For KS = 1 To NS
    KSW = NS * (KW - 1) + KS
    If IDBLK(KSW) <> 0 Then
      '----- Extraction of Block Data -----
      NODW = NGCN(KSW + KW - 1) - NNS - 1
      For JW = 1 To NWD(KW) + 1
        ETA = -1 + 2 * (JW - 1) / NWD(KW)
        NODW = NODW + NNS: NODS = NODW
        For JS = 1 To NSD(KS) + 1
          XI = -1 + 2 * (JS - 1) / NSD(KS)
          NODS = NODS + 1: NODE = NNAR(NODS)
          Call BlockXY(KW, KSW)
          Call Shape(XI, ETA)
          For J = 1 To 2
            C1 = 0
            For I = 1 To 8
              C1 = C1 + SH(I) * XP(I, J)
            Next I
            X(NODE, J) = C1
          Next J
        Next JS
      Next JW
    End If
  Next KS
Next KW

```


continued

```

'----- Connectivity -----
If JS <> NSD(KS) + 1 And JW <> NWD(KW) + 1 Then
  N1 = NODE: N2 = NNAR(NODS + 1)
  N4 = NNAR(NODS + NNS): N3 = NNAR(NODS + NNS + 1)
  NELM = NELM + 1
  If NEN = 3 Then
    '----- Triangular Elements -----
    NOC(NELM, 1) = N1: NOC(NELM, 2) = N2
    NOC(NELM, 3) = N3: MAT(NELM) = IDBLK(KSW)
    NELM = NELM + 1: NOC(NELM, 1) = N3: NOC(NELM, 2) = N4
    NOC(NELM, 3) = N1: MAT(NELM) = IDBLK(KSW)
  Else
    '----- Quadrilateral Elements -----
    NOC(NELM, 1) = N1: NOC(NELM, 2) = N2
    MAT(NELM) = IDBLK(KSW)
    NOC(NELM, 3) = N3: NOC(NELM, 4) = N4
  End If
End If
Next JS
Next JW
End If
Next KS
Next KW
NE = NELM
If NEN = 3 Then
  '----- Readjustment for Triangle Connectivity -----
  NE2 = NE / 2
  For I = 1 To NE2
    I1 = 2 * I - 1: N1 = NOC(I1, 1): N2 = NOC(I1, 2)
    N3 = NOC(I1, 3): N4 = NOC(2 * I, 2)
    X13 = X(N1, 1) - X(N3, 1): Y13 = X(N1, 2) - X(N3, 2)
    X24 = X(N2, 1) - X(N4, 1): Y24 = X(N2, 2) - X(N4, 2)
    If (X13 * X13 + Y13 * Y13) > 1.1 * (X24 * X24 + Y24 * Y24) Then
      NOC(I1, 3) = N4: NOC(2 * I, 3) = N2
    End If
  Next I
End If
End Sub

Private Sub BlockXY(KW, KSW)
  '----- Coordinates of 8-Nodes of the Block -----
  N1 = KSW + KW - 1
  XP(1, 1) = XB(N1, 1): XP(1, 2) = XB(N1, 2)
  XP(3, 1) = XB(N1 + 1, 1): XP(3, 2) = XB(N1 + 1, 2)
  XP(5, 1) = XB(N1 + NS + 2, 1): XP(5, 2) = XB(N1 + NS + 2, 2)
  XP(7, 1) = XB(N1 + NS + 1, 1): XP(7, 2) = XB(N1 + NS + 1, 2)
  XP(2, 1) = SR(KSW, 1): XP(2, 2) = SR(KSW, 2)
  XP(6, 1) = SR(KSW + NS, 1): XP(6, 2) = SR(KSW + NS, 2)
  XP(8, 1) = WR(N1, 1): XP(8, 2) = WR(N1, 2)
  XP(4, 1) = WR(N1 + 1, 1): XP(4, 2) = WR(N1 + 1, 2)
End Sub

```

continued

```

Private Sub Shape(XI, ETA)
'===== Shape Functions =====
SH(1) = -(1 - XI) * (1 - ETA) * (1 + XI + ETA) / 4
SH(2) = (1 - XI * XI) * (1 - ETA) / 2
SH(3) = -(1 + XI) * (1 - ETA) * (1 - XI + ETA) / 4
SH(4) = (1 - ETA * ETA) * (1 + XI) / 2
SH(5) = -(1 + XI) * (1 + ETA) * (1 - XI - ETA) / 4
SH(6) = (1 - XI * XI) * (1 + ETA) / 2
SH(7) = -(1 - XI) * (1 + ETA) * (1 + XI - ETA) / 4
SH(8) = (1 - ETA * ETA) * (1 - XI) / 2
End Sub

```

```

'===== OUTPUT =====
Private Sub Output()
'----- Output from this program is input for FE programs after some changes
File2 = InputBox("Output File d:\dir\fileName.ext", "Name of File")
Open File2 For Output As #2
Print #2, "Program MESHGEN - CHANDRUPATLA & BELEGUNDU"
Print #2, Title
NDIM = 2: NDN = 2
Print #2, "NN NE NM NDIM NEN NDN"
Print #2, NN; NE; NM; NDIM; NEN; NDN
Print #2, "ND NL NMPC"
Print #2, ND; NL; NMPC
Print #2, "Node# X Y"
For I = 1 To NN
    Print #2, I;
    For J = 1 To NDIM
        Print #2, X(I, J);
    Next J
    Print #2,
Next I
Print #2, "Elem# Node1 Node2 Node3";
If NEN = 3 Then Print #2, " Material#"
If NEN = 4 Then Print #2, " Node4 Material#"
For I = 1 To NE
    Print #2, I;
    For J = 1 To NEN
        Print #2, NOC(I, J);
    Next J
    Print #2, MAT(I)
Next I
Close #2
picBox.Print "Data has been stored in the file "; File2
End Sub

```

```

*****
**          PROGRAM PLOT2D          *
**    PLOTS 2D MESHES - TRIANGLES AND QUADS    *
**    (c) T.R.CHANDRUPATLA & A.D.BELEGONDU    *
*****
\----- PROGRAM MAIN -----/
Private Sub cmdPlot_Click()
  Call InputData
  Call DrawLimits(XMIN, YMIN, XMAX, YMAX)
  Call DrawElements
  cmdPlot.Enabled = False
  cmdULeft.Enabled = True
  cmdURight.Enabled = True
  cmdLLeft.Enabled = True
  cmdLRight.Enabled = True
End Sub
\-----

```

```

\----- INPUT DATA FROM FE INPUT FILE -----/
Private Sub InputData()
  File1 = InputBox("Input File d:\dir\fileName", "Name of File")
  Open File1 For Input As #1
  Line Input #1, Dummy: Input #1, Title
  Line Input #1, Dummy: Input #1, NN, NE, NM, NDIM, NEN, NDN
  Line Input #1, Dummy: Input #1, ND, NL, NMPC
  If NDIM <> 2 Then
    picBox.Print "THE PROGRAM SUPPORTS TWO DIMENSIONAL PLOTS ONLY"
    picBox.Print "THE DIMENSION OF THE DATA IS "; NDIM
  End
  End If
  ReDim X(NN, NDIM), NOC(NE, NEN)
  \----- READ DATA -----/
  Line Input #1, Dummy
  For I = 1 To NN: Input #1, N: For J = 1 To NDIM
    Input #1, X(N, J): Next J: Next I
  Line Input #1, Dummy
  For I = 1 To NE: Input #1, N: For J = 1 To NEN
    Input #1, NOC(N, J): Next J: Input #1, NTMP
    For J = 1 To 2: Input #1, C: Next J
  Next I
  Close #1
End Sub
\-----

```

```

\----- DETERMINE DRAW LIMITS -----/
Private Sub DrawLimits(XMIN, YMIN, XMAX, YMAX)
  XMAX = X(1, 1): YMAX = X(1, 2): XMIN = X(1, 1): YMIN = X(1, 2)
  For I = 2 To NN
    If XMAX < X(I, 1) Then XMAX = X(I, 1)
    If YMAX < X(I, 2) Then YMAX = X(I, 2)
    If XMIN > X(I, 1) Then XMIN = X(I, 1)
    If YMIN > X(I, 2) Then YMIN = X(I, 2)
  Next I

```

continued

```

XL = (XMAX - XMIN): YL = (YMAX - YMIN)
A = XL: If A < YL Then A = YL
XB = 0.5 * (XMIN + XMAX)
YB = 0.5 * (YMIN + YMAX)
XMIN = XB - 0.55 * A: XMAX = XB + 0.55 * A
YMIN = YB - 0.55 * A: YMAX = YB + 0.55 * A
XL = XMIN: YL = YMIN: XH = XMAX: YH = YMAX
XOL = XL: YOL = YL: XOH = XH: YOH = YH
End Sub
=====

```

```

=====
DRAW ELEMENTS
=====
Private Sub DrawElements()
'===== Draw Elements =====
picBox.Scale (XL, YH)-(XH, YL)
picBox.Cls
For IE = 1 To NE
For II = 1 To NEN
I2 = II + 1
If II = NEN Then I2 = 1
X1 = X(NOC(IE, II), 1): Y1 = X(NOC(IE, II), 2)
X2 = X(NOC(IE, I2), 1): Y2 = X(NOC(IE, I2), 2)
picBox.Line (X1, Y1)-(X2, Y2), QBColor(1)
If NEN = 2 Then Exit For
Next II
Next IE
cmdNode.Enabled = True
End Sub
=====

```

```

*****
PROGRAM BESTFIT
*****
* BEST FIT PROGRAM *
* FOR 3-NODED TRIANGLES *
* T.R.Chandrupatla and A.D.Belegundu *
*****
'=====
PROGRAM MAIN
=====
Private Sub cmdStart_Click()
Call InputData
Call Bandwidth
Call Stiffness
Call BandSolver
Call Output
cmdView.Enabled = True
cmdStart.Enabled = False
End Sub
=====

```

```

===== STIFFNESS FOR INTERPOLATION =====
Private Sub Stiffness()
  ReDim S(NQ, NBW), F(NQ)
  '--- Global Stiffness Matrix
  For N = 1 To NE
    Call ElemStiff(N)
    For II = 1 To 3
      NR = NOC(N, II): F(NR) = F(NR) + FE(II)
      For JJ = 1 To 3
        NC = NOC(N, JJ) - NR + 1
        If NC > 0 Then
          S(NR, NC) = S(NR, NC) + SE(II, JJ)
        End If
      Next JJ
    Next II
  Next N
  picBox.Print "Stiffness Formation completed..."
End Sub
Private Sub ElemStiff(N)
  '--- Element Stiffness Formation
  I1 = NOC(N, 1): I2 = NOC(N, 2): I3 = NOC(N, 3)
  X1 = X(I1, 1): Y1 = X(I1, 2)
  X2 = X(I2, 1): Y2 = X(I2, 2)
  X3 = X(I3, 1): Y3 = X(I3, 2)
  X21 = X2 - X1: X32 = X3 - X2: X13 = X1 - X3
  Y12 = Y1 - Y2: Y23 = Y2 - Y3: Y31 = Y3 - Y1
  DJ = X13 * Y23 - X32 * Y31      'DETERMINANT OF JACOBIAN
  AE = Abs(DJ) / 24
  SE(1, 1) = 2 * AE: SE(1, 2) = AE: SE(1, 3) = AE
  SE(2, 1) = AE: SE(2, 2) = 2 * AE: SE(2, 3) = AE
  SE(3, 1) = AE: SE(3, 2) = AE: SE(3, 3) = 2 * AE
  A1 = FS(N) * Abs(DJ) / 6
  FE(1) = A1: FE(2) = A1: FE(3) = A1
End Sub
=====

```

```

***** CONTOURA *****
* CONTOUR PLOTTING - CONTOUR LINES *
* FOR 2D TRIANGLES AND QUADRILATERALS *
* T.R.Chandrupatla and A.D.Belegundu *
*****
===== PROGRAM MAIN =====
Private Sub cmdPlot_Click()
  Call InputData
  Call FindBoundary
  Call DrawLimits(XMIN, YMIN, XMAX, YMAX)
  Call DrawBoundary
  Call DrawContours
End Sub
=====

```

```

'===== INPUT DATA FROM FILES =====
Private Sub InputData()
    File1 = InputBox("FE Input File", "d:\dir\Name of File")
    File2 = InputBox("Contour Data File", "d:\dir\Name of File")
    Open File1 For Input As #1
    Line Input #1, DS: Input #1, Title$
    Line Input #1, DS: Input #1, NN, NE, NM, NDIM, NEN, NDN
    Line Input #1, DS: Input #1, ND, NL, NMPC
    If NDIM <> 2 Or NEN < 3 Or NEN > 4 Then
        picBox.Print "This program supports triangular and quadrilateral"
        picBox.Print "Elements only."
    End
    End If
    ReDim X(NN, NDIM), NOC(NE, NEN), FF(NN), NCON(NE, NEN)
    ReDim XX(3), YY(3), U(3), IC(10), ID(10)
    '----- COLOR DATA -----
    IC(1) = 13: IC(2) = 5: IC(3) = 9: IC(4) = 1: IC(5) = 2
    IC(6) = 10: IC(7) = 14: IC(8) = 6: IC(9) = 4: IC(10) = 12
    For I = 1 To 10: ID(I) = 0: Next I
    '----- READ DATA -----
    '----- Coordinates
    Line Input #1, DS
    For I = 1 To NN
        Input #1, n
        For J = 1 To NDIM: Input #1, X(n, J): Next J
    Next I
    '----- Connectivity
    Line Input #1, DS
    For I = 1 To NE
        Input #1, n: For J = 1 To NEN
            Input #1, NOC(n, J): Next J: Input #1, NTMP
        For J = 1 To 2: Input #1, C: Next J: Next I
    Close #1
    Open File2 For Input As #2
    '----- Nodal Values
    Line Input #2, DS
    For I = 1 To NN
        Input #2, FF(I)
    Next I
    Close #2
End Sub

```

```

'===== FIND BOUNDARY LINES =====
Private Sub FindBoundary()
    '----- Find Boundary Lines -----
    'Edges defined by nodes in NOC to nodes in NCON
    For IE = 1 To NE
        For I = 1 To NEN
            I1 = I + 1: If I1 > NEN Then I1 = 1
            NCON(IE, I) = NOC(IE, I1)
        Next I
    Next IE

```

continued

```

For IE = 1 To NE
  For I = 1 To NEN
    I1 = NCON(IE, I): I2 = NOC(IE, I)
    INDX = 0
    For JE = IE + 1 To NE
      For J = 1 To NEN
        If NCON(JE, J) <> 0 Then
          If I1 = NCON(JE, J) Or I1 = NOC(JE, J) Then
            If I2 = NCON(JE, J) Or I2 = NOC(JE, J) Then
              NCON(JE, J) = 0: INDX = INDX + 1
            End If
          End If
        End If
      Next J
    Next JE
    If INDX > 0 Then NCON(IE, I) = 0
  Next I
Next IE
End Sub
=====

```

```

'===== DRAW BOUNDARY =====
Private Sub DrawBoundary()
  picBox.Scale (XL, YH)-(XH, YL)
  picBox.Cls
  '----- Draw Boundary -----
  For IE = 1 To NE
    For I = 1 To NEN
      If NCON(IE, I) > 0 Then
        I1 = NCON(IE, I): I2 = NOC(IE, I)
        picBox.Line (X(I1, 1), X(I1, 2))-X(I2, 1), X(I2, 2))
      End If
    Next I
  Next IE
End Sub

'===== DRAW CONTOUR LINES =====
Private Sub DrawContours()
  '----- Contour Plotting -----
  For IE = 1 To NE
    If NEN = 3 Then
      For IEN = 1 To NEN
        IEE = NOC(IE, IEN)
        U(IEN) = FF(IEE)
        XX(IEN) = X(IEE, 1)
        YY(IEN) = X(IEE, 2)
      Next IEN
      Call ElementPlot
    ElseIf NEN = 4 Then
      XB = 0: YB = 0: UB = 0
      For IT = 1 To NEN
        NIT = NOC(IE, IT)

```

```

XB = XB + 0.25 * X(NIT, 1)
YB = YB + 0.25 * X(NIT, 2)
UB = UB + 0.25 * FF(NIT)
Next IT
For IT = 1 To NEN
  IT1 = IT + 1: If IT1 > 4 Then IT1 = 1
  XX(1) = XB: YY(1) = YB: U(1) = UB
  NIE = NOC(IE, IT)
  XX(2) = X(NIE, 1): YY(2) = X(NIE, 2): U(2) = FF(NIE)
  NIE = NOC(IE, IT1)
  XX(3) = X(NIE, 1): YY(3) = X(NIE, 2): U(3) = FF(NIE)
  Call ElementPlot
Next IT
Else
  Print "NUMBER OF ELEMENT NODES > 4 IS NOT SUPPORTED"
End
End If
Next IE
For I = 1 To 10: ID(I) = 0: Next I
End SubPrivate Sub ElementPlot()
  'THREE POINTS IN ASCENDING ORDER
  For I = 1 To 2
    C = U(I): II = I
    For J = I + 1 To 3
      If C > U(J) Then
        C = U(J): II = J
      End If
    Next J
    U(II) = U(I): U(I) = C
    C1 = XX(II): XX(II) = XX(I): XX(I) = C1
    C1 = YY(II): YY(II) = YY(I): YY(I) = C1
  Next I
  SU = (U(1) - FMIN) / STP
  II = Int(SU)
  If II <= SU Then II = II + 1
  UT = FMIN + II * STP
  Do While UT <= U(3)
    ICO = IC(II)
    X1 = ((U(3) - UT) * XX(1) + (UT - U(1)) * XX(3)) / (U(3) - U(1))
    Y1 = ((U(3) - UT) * YY(1) + (UT - U(1)) * YY(3)) / (U(3) - U(1))
    L = 1: If UT > U(2) Then L = 3
    X2 = ((U(L) - UT) * XX(2) + (UT - U(2)) * XX(L)) / (U(L) - U(2))
    Y2 = ((U(L) - UT) * YY(2) + (UT - U(2)) * YY(L)) / (U(L) - U(2))
    picBox.Line (X1, Y1)-(X2, Y2), QBColor(ICO)
    If ID(II) = 0 Then
      picBox.CurrentX = X1: picBox.CurrentY = Y1
      If (XL < X1 And X1 < XH) And (YL < Y1 And Y1 < YH) Then
        picBox.Print II
        ID(II) = 1
      End If
    End If
  End If
  UT = UT + STP: II = II + 1
Loop
End Sub

```


A P P E N D I X

Proof of $dA = \det \mathbf{J} d\xi d\eta$

Consider a mapping of variables from x, y to u_1, u_2 , given as

$$x = x(u_1, u_2) \quad y = y(u_1, u_2) \quad (\text{A1.1})$$

We assume that these equations can be reversed to express u_1, u_2 , in terms of x, y and that the correspondence is unique.

If a particle moves from a point P in such a way that u_2 is held constant and only u_1 varies, then a curve in the plane is generated. We call this the u_1 curve (Fig. A1.1). Similarly, the u_2 curve is generated by keeping u_1 constant and letting u_2 vary. Let

$$\mathbf{r} = x\mathbf{i} + y\mathbf{j} \quad (\text{A1.2})$$

represent the vector of a point P where \mathbf{i} and \mathbf{j} are unit vectors along x and y , respectively. Consider the vectors

$$\mathbf{T}_1 = \frac{\partial \mathbf{r}}{\partial u_1} \quad \mathbf{T}_2 = \frac{\partial \mathbf{r}}{\partial u_2} \quad (\text{A1.3})$$

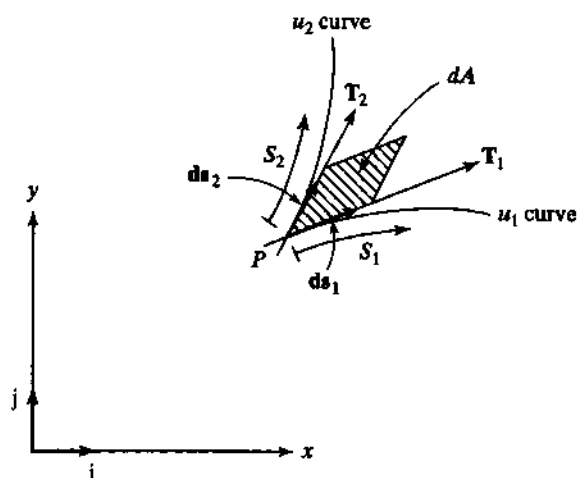


FIGURE A1.1

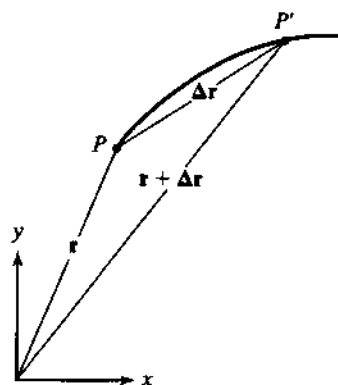


FIGURE A1.2

or, in view of Eq. A1.2,

$$\mathbf{T}_1 = \frac{\partial x}{\partial u_1} \mathbf{i} + \frac{\partial y}{\partial u_1} \mathbf{j} \quad \mathbf{T}_2 = \frac{\partial x}{\partial u_2} \mathbf{i} + \frac{\partial y}{\partial u_2} \mathbf{j} \quad (\text{A1.4})$$

We can show that \mathbf{T}_1 is a vector tangent to the u_1 curve and \mathbf{T}_2 is tangent to the u_2 curve (Fig. A1.1). To see this, we use the definition

$$\frac{\partial \mathbf{r}}{\partial u_1} = \lim_{\Delta u_1 \rightarrow 0} \frac{\Delta \mathbf{r}}{\Delta u_1} \quad (\text{A1.5})$$

where $\Delta \mathbf{r} = \mathbf{r}(u_1 + \Delta u_1) - \mathbf{r}(u_1)$. In the limit, the chord $\Delta \mathbf{r}$ becomes the tangent to the u_1 curve (Fig. A1.2). However, $\partial \mathbf{r} / \partial u_1$ (or $\partial \mathbf{r} / \partial u_2$) is not a unit vector. To determine its magnitude (length), we write

$$\frac{\partial \mathbf{r}}{\partial u_1} = \frac{\partial \mathbf{r}}{\partial s_1} \frac{ds_1}{du_1} \quad (\text{A1.6})$$

where s_1 is the arc length along the u_1 curve and ds_1 is the differential arc length. The magnitude of the vector

$$\frac{\partial \mathbf{r}}{\partial s_1} = \lim_{\Delta s_1 \rightarrow 0} \frac{\Delta \mathbf{r}}{\Delta s_1}$$

is the limiting ratio of the chord length to the arc length, which equals unity. Thus, we conclude that the magnitude of the vector $\partial \mathbf{r} / \partial u_1$ is ds_1 / du_1 . We have

$$\begin{aligned} \mathbf{T}_1 &= \left(\frac{ds_1}{du_1} \right) \mathbf{t}_1 \\ \mathbf{T}_2 &= \left(\frac{ds_2}{du_2} \right) \mathbf{t}_2 \end{aligned} \quad (\text{A1.7})$$

where \mathbf{t}_1 and \mathbf{t}_2 are unit vectors tangent to the u_1 and u_2 curves, respectively. Using Eq. A1.7, we have the following representation of the vectors $d\mathbf{s}_1$ and $d\mathbf{s}_2$, whose lengths are ds_1 and ds_2 (Fig. A1.1):

$$\begin{aligned} d\mathbf{s}_1 &= \mathbf{t}_1 ds_1 = \mathbf{T}_1 du_1 \\ d\mathbf{s}_2 &= \mathbf{t}_2 ds_2 = \mathbf{T}_2 du_2 \end{aligned} \quad (\text{A1.8})$$

The differential area $d\mathbf{A}$ is a vector with magnitude dA and direction normal to the element area, which in this case is \mathbf{k} . The vector $d\mathbf{A}$ in view of Eqs. A1.4 and A1.8 is given by the determinant rule

$$\begin{aligned} d\mathbf{A} &= d\mathbf{s}_1 \times d\mathbf{s}_2 \\ &= \mathbf{T}_1 \times \mathbf{T}_2 du_1 du_2 \\ &= \begin{vmatrix} \mathbf{i} & \mathbf{j} & \mathbf{k} \\ \frac{\partial x}{\partial u_1} & \frac{\partial y}{\partial u_1} & 0 \\ \frac{\partial x}{\partial u_2} & \frac{\partial y}{\partial u_2} & 0 \end{vmatrix} du_1 du_2 \\ &= \left(\frac{\partial x}{\partial u_1} \frac{\partial y}{\partial u_2} - \frac{\partial x}{\partial u_2} \frac{\partial y}{\partial u_1} \right) du_1 du_2 \mathbf{k} \end{aligned} \quad (\text{A1.9})$$

We denote the Jacobian matrix as

$$\mathbf{J} = \begin{bmatrix} \frac{\partial x}{\partial u_1} & \frac{\partial y}{\partial u_1} \\ \frac{\partial x}{\partial u_2} & \frac{\partial y}{\partial u_2} \end{bmatrix} \quad (\text{A1.10})$$

The magnitude dA can now be written as

$$dA = \det \mathbf{J} du_1 du_2 \quad (\text{A1.11})$$

which is the desired result. Note that if we work with ξ - and η -coordinates instead of u_1 - and u_2 -coordinates, as in the text, then

$$dA = \det \mathbf{J} d\xi d\eta$$

This relation generalizes to three dimensions as

$$dV = \det \mathbf{J} d\xi d\eta d\zeta$$

where the Jacobian determinant $\det \mathbf{J}$ expresses the ratio of the volume element $dx dy dz$ to $d\xi d\eta d\zeta$.

Bibliography

There are many excellent published books and articles in various journals on the subject of the finite element method and its applications. A list of books published in the English language is given below. The list includes books dealing with both fundamental and advanced topics. Several of these have been used in the present text without explicit citation. On completing the material from various chapters from this book, the students and users should benefit from referring to other books and articles.

- AKIN, J. E., *Application and Implementation of Finite Element Methods*. London: Academic, 1982.
- AKIN, J. E., *Finite Element Analysis for Undergraduates*. London: Academic, 1986.
- ALLAIRE, P. E., *Basics of the Finite Element Method—Solid Mechanics, Heat Transfer, and Fluid Mechanics*. Dubuque, IA: W. C. Brown, 1985.
- ASKENAZI, A., and V. ADAMS, *Building Better Products with Finite Element Analysis*. On World Press, 1998.
- AXELSSON, O., and V. A. BARKER, *Finite Element Solution of Boundary Value Problems*. Orlando, FL: Academic, 1984.
- BAKER, A. J., *Finite Element Computational Fluid Mechanics*. New York: McGraw-Hill, 1983.
- BAKER, A. J., and D. W. PEPPER, *Finite Elements 1–2–3*. New York: McGraw-Hill, 1991.
- BARAN, N. M., *Finite Element Analysis on Microcomputers*. New York: McGraw-Hill, 1988.
- BATHE, K. J., *Finite Element Procedures in Engineering Analysis*. Englewood Cliffs, NJ: Prentice-Hall, 1981.
- BATHE, K. J., and E. L. WILSON, *Numerical Methods in Finite Element Analysis*. Englewood Cliffs, NJ: Prentice-Hall, 1976.
- BECKER, E. B., G. F. CAREY, and J. T. ODEN, *Finite Elements—An Introduction*, Vol. 1. Englewood Cliffs, NJ: Prentice-Hall, 1981.
- BEYTSCHKO, T., B. MORAN, and W. K. LIU, *Nonlinear Finite Elements for Continua and Structures*. New York: Wiley, 2000.
- BICKFORD, W. M., *A First Course in the Finite Element Method*. Homewood, IL: Richard D. Irwin, 1990.
- BONET, J., and R. D. WOOD, *Nonlinear Continuum Mechanics for Finite Element Analysis*. Cambridge University Press, 1997.
- BOWES, W. H., and L. T. RUSSEL, *Stress Analysis by the Finite Element Method for Practicing Engineers*. Lexington, MA: Lexington Books, 1975.
- BREBBIA, C. A., and J. J. CONNOR, *Fundamentals of Finite Element Techniques for Structural Engineers*. London: Butterworths, 1975.

- BUCHANAN, G. R., *Finite Element Analysis*. New York: McGraw-Hill, 1995.
- BURNETT, D. S., *Finite Element Analysis from Concepts to Applications*. Reading, MA: Addison-Wesley, 1987.
- CAREY, G. F., and J. T. ODEN, *Finite Elements—A Second Course*, Vol. 2. Englewood Cliffs, NJ: Prentice-Hall, 1983.
- CAREY, G. F., and J. T. ODEN, *Finite Elements—Computational Aspects*, Vol. 3. Englewood Cliffs, NJ: Prentice-Hall, 1984.
- CARROLL, W. F., *A Primer for Finite Elements in Elastic Structures*. Wiley, 1999.
- CHARI, M. V. K., and P. P. SILVESTER, *Finite Elements in Electrical and Magnetic Field Problems*. New York: Wiley, 1981.
- CHEUNG, Y. K., and M. F. YEO, *A Practical Introduction to Finite Element Analysis*. London: Pitman, 1979.
- CHUNG, T. J., *Finite Element Analysis in Fluid Dynamics*. New York: McGraw-Hill, 1978.
- CIARLET, P. G., *The Finite Element Method for Elliptic Problems*. Amsterdam: North-Holland, 1978.
- CONNOR, J. C., and C. A. BREBBIA, *Finite Element Techniques for Fluid Flow*. London: Butterworths, 1976.
- COOK, R. D., *Concepts and Applications of Finite Element Analysis*, 2d ed. New York: Wiley, 1981.
- COOK, R. D., *Finite Element Modeling for Stress Analysis*. New York: Wiley, 1995.
- DAVIES, A. J., *The Finite Element Method: A First Approach*. Oxford: Clarendon, 1980.
- DESAI, C. S., *Elementary Finite Element Method*. Englewood Cliffs, NJ: Prentice-Hall, 1979.
- DESAI, C. S., and J. F. ABEL, *Introduction to the Finite Element Method*. New York: Van Nostrand Reinhold, 1972.
- DESAI, C. S., and T. KUNDU, *Introductory Finite Element Method*. CRC Press, 2000.
- FAGAN, M. I. J., *Finite Element Analysis: Theory and Practice*. Addison Wesley Longman, 1996.
- FAIRWEATHER, G., *Finite Element Galerkin Methods for Differential Equations*. New York: Dekker, 1978.
- FENNER, R. T., *Finite Element Methods for Engineers*. London: Macmillan, 1975.
- GALLAGHER, R. H., *Finite Element Analysis—Fundamentals*. Englewood Cliffs, NJ: Prentice-Hall, 1975.
- GRANDIN, H., Jr., *Fundamentals of the Finite Element Method*. New York: Macmillan, 1986.
- HEINRICH, J. C., and D. W. PEPPER, *Intermediate Finite Element Method: Fluid Flow and Heat Transfer Applications*. Taylor & Francis, 1997.
- HINTON, E., and D. R. J. OWEN, *Finite Element Programming*. London: Academic, 1977.
- HINTON, E., and D. R. J. OWEN, *An Introduction to Finite Element Computations*. Swansea, Great Britain: Pineridge Press, 1979.
- HUEBNER, K. H., and E. A. THORNTON, *The Finite Element Method for Engineers*, 2d ed. New York: Wiley-Interscience, 1982.
- HUGHES, T. J. R., *The Finite Element Method—Linear Static and Dynamic Finite Element Analysis*. Englewood Cliffs, NJ: Prentice-Hall, 1987.
- IRONS, B., and S. AHMAD, *Techniques of Finite Elements*. New York: Wiley, 1980.
- IRONS, B., and N. SHRIVE, *Finite Element Primer*. New York: Wiley, 1983.
- JIN, J., *The Finite Element Method in Electromagnetics*. New York: Wiley, 1993.
- KIKUCHI, N., *Finite Element Methods in Mechanics*. Cambridge, Great Britain: Cambridge University Press, 1986.
- KNIGHT, C. E., *The Finite Element Method in Machine Design*. Boston: PWS Kent, 1993.

- KRISHNAMOORTY, C. S., *Finite Element Analysis—Theory and Programming*. New Delhi: Tata McGraw-Hill, 1987.
- LEPI, S. M., *Practical Guide to Finite Elements: A Solid Mechanics Approach*. Marcel Dekker, 1998.
- LIVESLEY, R. K., *Finite Elements: An Introduction for Engineers*. Cambridge, Great Britain: Cambridge University Press, 1983.
- LOGAN, D. L., *A First Course in the Finite Element Method*. Boston: PWS, 1992.
- MARTIN, H. C., and G. F. CAREY, *Introduction to Finite Element Analysis: Theory and Application*. New York: McGraw-Hill, 1972.
- MELOSH, R. J., *Structural Engineering Analysis by Finite Elements*. Englewood Cliffs, NJ: Prentice Hall, 1990.
- MITCHELL, A. R., and R. WAIT, *The Finite Element Method in Partial Differential Equations*. New York: Wiley, 1977.
- MOAVENI, S., *Finite Element Analysis: Theory and Applications with Ansys*. Upper Saddle River: Prentice Hall, 1998.
- NAKAZAWA, S., and D. W. KELLY, *Mathematics of Finite Elements—An Engineering Approach*. Swansea, Great Britain: Pineridge Press, 1983.
- NATH, B., *Fundamentals of Finite Elements for Engineers*. London: Athlone, 1974.
- NAYLOR, D. J., and G. N. PANDE, *Finite Elements in Geotechnical Engineering*. Swansea, Great Britain: Pineridge Press, 1980.
- NORRIE, D. H., and G. DE VRIES, *The Finite Element Method: Fundamentals and Applications*. New York: Academic, 1973.
- NORRIE, D. H., and G. DE VRIES, *An Introduction to Finite Element Analysis*. New York: Academic, 1978.
- ODEN, J. T., *Finite Elements of Nonlinear Continua*. New York: McGraw-Hill, 1972.
- ODEN, J. T., and G. F. CAREY, *Finite Elements: Mathematical Aspects*, Vol. 4. Englewood Cliffs, NJ: Prentice Hall, 1982.
- ODEN, J. T., and J. N. REDDY, *An Introduction to the Mathematical Theory of Finite Elements*. New York: Wiley, 1976.
- OWEN, D. R. J., and E. HINTON, *A Simple Guide to Finite Elements*. Swansea, Great Britain: Pineridge Press, 1980.
- PAO, Y. C., *A First Course in Finite Element Analysis*. Newton, MA: Allyn & Bacon, 1986.
- PINDER, G. F., and W. G. GRAY, *Finite Element Simulation in Surface and Subsurface Hydrology*. New York: Academic, 1977.
- POTTS, J. F., and J. W. OLER, *Finite Element Applications with Microcomputers*. Englewood Cliffs, NJ: Prentice Hall, 1989.
- PRZEMIENIECKI, J. S., *Theory of Matrix Structural Analysis*. New York: McGraw-Hill, 1968.
- RAO, S. S., *The Finite Element Method in Engineering*, 2d ed. Elmsford, NY: Buthe'sworth-Heinemann, 1989.
- REDDY, J. N., *An Introduction to the Finite Element Method*. New York: McGraw-Hill, 1993.
- REDDY, J. N., *Energy and Variational Methods in Applied Mechanics with an Introduction to the Finite Element Method*. New York: Wiley-Interscience, 1984.
- REDDY, J. N., and D. K. GARTLING, *The Finite Element Method in Heat Transfer and Fluid Dynamics*. CRC Press, 2000.
- ROBINSON, J., *An Integrated Theory of Finite Element Methods*. New York: Wiley-Interscience, 1973.
- ROBINSON, J., *Understanding Finite Element Stress Analysis*. Wimborne, Great Britain: Robinson and Associates, 1981.

- ROCKEY, K. C., H. R. EVANS, D. W. GRIFFITHS, and D. A. NETHERCOT, *The Finite Element Method—A Basic Introduction*, 2d ed. New York: Halsted (Wiley), 1980.
- ROSS, C. T. F., *Finite Element Programs for Axisymmetric Problems in Engineering*. Chichester, Great Britain: Ellis Horwood, 1984.
- SEGERLIND, L. J., *Applied Finite Element Analysis*, 2d ed. New York: Wiley, 1984.
- SHAMES, I. H., and C. L. DYM, *Energy and Finite Element Methods in Structural Mechanics*. New York: McGraw-Hill, 1985.
- SILVESTER, P. P., and R. L. FERRARI, *Finite Elements for Electrical Engineers*. Cambridge, Great Britain: Cambridge University Press, 1996.
- SMITH, I. M., *Programming the Finite Element Method*. New York: Wiley, 1982.
- STASA, F. L., *Applied Finite Element Analysis for Engineers*. New York: Holt, Rinehart & Winston, 1985.
- STRANG, G., and G. FIX, *An Analysis of the Finite Element Method*. Englewood Cliffs, NJ: Prentice-Hall, 1973.
- TONG, P., and J. N. ROSSETOS, *Finite Element Method—Basic Techniques and Implementation*. Cambridge, MA: MIT Press, 1977.
- URAL, O., *Finite Element Method: Basic Concepts and Applications*. New York: Intext Educational Publishers, 1973.
- VOLAKIS, J. L., A. CHATTERJEE, and L. C. EMPER, *Finite Element Method for Electromagnetics*. IEEE, 1998.
- WACHSPRESS, E. L., *A Rational Finite Element Basis*. New York: Academic, 1975.
- WAIT, R., and A. R. MITCHELL, *Finite Element Analysis and Applications*. New York: Wiley, 1985.
- WHITE, R. E., *An Introduction to the Finite Element Method with Applications to Non-Linear Problems*. New York: Wiley-Interscience, 1985.
- WILLIAMS, M. M. R., *Finite Element Methods in Radiation Physics*. Elmsford, NY: Pergamon, 1982.
- YANG, T. Y., *Finite Element Structural Analysis*, Englewood Cliffs, NJ: Prentice-Hall, 1986.
- ZAHAVI, E., *The Finite Element Method in Machine Design*, Englewood Cliffs, NJ: Prentice Hall, 1992.
- ZIENKIEWICZ, O. C., *The Finite Element Method*, 3d ed. New York: McGraw-Hill, 1977.
- ZIENKIEWICZ, O. C., and K. MORGAN, *Finite Elements and Approximation*. New York: Wiley-Interscience, 1982.
- ZIENKIEWICZ, O. C., and R. L. TAYLOR, *The Finite Element Method*, Vol. 2. New York: McGraw-Hill, 1991.

Answers to Selected Problems

- (1.2) 3000 psi.
- (1.6) $\sigma_n = 24.29$ MPa.
- (1.10) $q_1 = 1.222$ mm and $q_2 = 1.847$ mm.
- (1.11) $u(x_1) = 0.5$.
- (2.1c) $\lambda_1 = 0.2325$, $\lambda_2 = 5.665$, and $\lambda_3 = 9.103$.
Matrix is positive definite.
 $y_1 = [0.172, 0.668, 0.724]^T$,
 $y_2 = [0.495, 0.577, -0.65]^T$, and
 $y_3 = [0.85, -0.47, 0.232]^T$.
- (2.2b) $\int_{-1}^1 \mathbf{N}^T \mathbf{N} d\xi = \begin{bmatrix} \frac{2}{3} & 0 \\ 0 & \frac{16}{15} \end{bmatrix}$.
- (2.3) $\mathbf{Q} = \begin{bmatrix} 3 & 2.5 \\ 2.5 & 0 \end{bmatrix}$, $\mathbf{c} = \begin{bmatrix} 1 \\ -6 \end{bmatrix}$.
- (2.8) $A_{11,14} \rightarrow B_{11,4}$ and $B_{6,1} \rightarrow A_{6,6}$.
- (3.1) (a) $q = 0.023125$ in. (b) $\epsilon = 0.000625$.
(d) $U_e = 56.25$ lb-in.
- (3.7) $Q_2 = 0.623$ mm and $Q_3 = 0.346$ mm.
- (3.10) Stress in element 1 = 2,691 MPa.
- (3.22) $\mathbf{T}^e = \frac{\ell_e}{30} [4T_1 - T_2 + 2T_3, -T_1 + 4T_2 + 2T_3, 2T_1 + 2T_2 + 16T_3]^T$.
- (4.1) $\ell = 0.8$, $m = 0.6$, $\mathbf{q}' = 10^{-2} [1.80, 4.26]^T$ in.,
 $\sigma = 14,760$ psi, and $U_e = 381.3$ in.-lb.
- (4.3) $K_{1,1} = 4.586 \times 10^5$.
- (4.4) $Q_3 = 219.3 \times 10^{-5}$ in.
- (4.6) Stress in element 1-3 = -100.0 MPa.
- (4.9) Point R moves horizontally by 3.13 mm.

448 Answers to Selected Problems

- (5.1) $\eta = 0.2$ and $y = 4.2$.
- (5.2) Area = 25.5.
- (5.5) $\epsilon_x = 5.897 \times 10^{-4}$.
- (5.9) x -displ. = 0.000195 mm.
- (6.1) Use $\epsilon_\theta = 3.036E6$ psi.
- (6.4) Outer diameter after deformation = 107.8 mm.
- (6.5) Contact pressure = 21,120 psi based on 18-element mesh.
- (6.7) Peak radial stress $\approx 10,000$ psi and peak hoop stress $\approx 54,000$ psi.
- (6.14) Hoop stress reduces from about 990 MPa without a shrink ring to 650 MPa with a ring.
- (7.1) $x = 4.5625$ and $y = 4.375$.
- (7.2) Value of integral = 3253.8.
- (8.1) Deflection under the load point = -0.13335 mm.
- (8.2) Deflection under load = -0.01376 in.
- (8.8) Deflection at midpoint of BC = -0.417 in.
- (8.12) Vertical deflection of point D without tie rod = -11.6 in and with tie rod = -0.87 in.
- (9.7) Max. vertical disp. = -0.0148 in, based on a four-element hexahedral mesh.
- (10.1) $[T_1, T_2, T_3] = [28, 12.6, -2.89]^\circ\text{C}$. (More elements will give better answer.)
- (10.3) Peak Temperature = 120.6°C .
- (10.13) Heat flow out of chimney = 1,190 W/m.
- (10.18) $\alpha = 5.263 \times 10^{-6} T/G$ rad/mm, where T is in N-mm and G is in MPa.
- (10.21) Velocity at waist a - a varies from 345 cm/s to 281 cm/s.
- (10.24) $C = 13.5$.
- (11.1) Lowest natural frequency = 2039 Hz (cps).
- (11.3) Lumped mass results are $\lambda_1 = 1.4684E + 08$ and $\lambda_2 = 6.1395E + 08$.
- (11.7) Stretch mode eigenvalue = 440 Hz.
(Bending mode natural frequency = 331 Hz.)

Index

A

- Acoustics, 343–45, 348
- Area coordinates, 133–34
- Aspect ratio, 154
- Assembly:
 - of global stiffness **K** and load vector **F**, 58–62
 - of global stiffness for banded solution, 116–17
 - of global stiffness for skyline solution, 117–18
 - of global stiffness for frontal solution, 289–91
- Axial vibrations, 345–47
- Axisymmetric elements, 178–207, 354–55

B

- B** matrix, 52, 80, 138, 183, 213, 279, 323
- Back-substitution 30
- Bandwidth, 34, 61, 116–17
- Banded matrix, 34, 61, 116–17
- Beams, 237
- Beams on elastic supports, 247–48
- Bending moment, 245
- Bibliography, 18, 443
- Body forces 3, 54–55, 57, 81, 141–42, 184–85, 213–14, 280
- Boundary Conditions:
 - continuum, 4
 - elimination approach, 63–66

- heat conduction, 308–336
- multipoint constraints, 63, 74–77, 153, 193–94, 287–88
- natural, 315
- penalty approach, 63, 69–74
- scalar field problems, 306–66

C

- Characteristic equation, 27, 376–78
- Cholesky decomposition, 29, 386
- Composite materials (*see* orthotropic materials)
- Computer programs:
 - AXIQUAD, 226
 - AXISYM, 188, 196, 205–07
 - BEAM, 267
 - BEAMKM, 391, 404–06
 - BESTFIT, 158, 422, 435–36
 - BESTFITQ, 423
 - CHOLESKY, 29
 - CONTOURA, 158, 421, 436–39
 - CONTOURB, 158, 421
 - CST, 158, 174–77
 - CSTKM, 391
 - CGSOL 40, 44
 - FEM1D 98–102
 - FRAME2D 268–270
 - FRAME3D 257, 270–74
 - GAUSS, 40, 43
 - GENEIGEN, 391
 - HEAT1D, 361–62
 - HEAT2D, 330, 363–66

Computer programs: *(continued)*

HEXAFRON, 286, 297-305
 INVITR, 381, 406-10
 JACOBI, 385
 MESHGEN, 158, 227, 419, 427-33
 PLOT2D, 158, 419, 434-35
 QUAD, 227, 233-36
 QUADCG, 226
 SKYLINE, 38
 TETRA3D, 284
 TORSION, 355
 TRUSS2D, 117, 128-29
 TRUSSKY, 118

Concentrated force, 3, 52, 58, 59
 Conical (Belleville) Spring, 194-95
 Conjugate gradient method, 39-40, 226
 Constant strain triangle (CST), 133, 174
 Contact, 73
 Contour plotting, 420-24

D

D matrix, 6-8, 157, 180
 Data handling, 419
 Degenerate quadrilaterals, 219
 Degrees of freedom, 47, 105, 114-15, 132, 240, 248, 253-57
 Displacement vector (*see* degrees of freedom)
 Ducts, flow in, 341-43
 Dynamic analysis, 367-410

E

Eigenvalue-eigenvectors, 27-28, 375-76
 Eight-node quadrilateral element, 222-23
 Electric field problems, 339-41

Element:

beam, 237-47
 beam on elastic support, 247-48
 frame:
 planar, 247-53
 3-D, 253-57
 hexahedral, 285-86
 one-dimensional linear, 46-78, 309-20
 one-dimensional quadratic, 78-84
 quadrilateral:
 axisymmetric, 225-26
 four-node, 208-220

 eight-node, 222-23
 nine-node, 220-22
 tetrahedral, 276-85
 triangle, axisymmetric, 181-85
 triangle, heat, 322
 triangle, CST, 130
 triangle, six-node, 223-24
 truss, 103

Element connectivity, 47-48

Element mass matrices:

axisymmetric triangle, 372
 beam element, 374
 constant strain triangle (CST), 372
 frame element, 374
 one-dimensional bar, 370-71
 quadrilateral, four-node, 373
 tetrahedral element, 374-75
 truss, 371

Element matrices for heat conduction, 313-14, 326-28

Element stiffness matrices:

axisymmetric solids, 184
 beam, 243
 beam on elastic supports, 248
 constant strain triangle (CST), 140
 frame, 249-50, 255
 hexahedron, 286
 isoparametric, higher order, 220
 one-dimensional, linear, 54
 one-dimensional, quadratic, 81
 quadrilateral, four-node, 213
 tetrahedron, 279
 trusses, 106, 115

(*see also* element matrices for heat conduction)

Elimination approach for handling boundary conditions, 63-68

Equation solving, 29-40 (*see also* Gaussian elimination,

skyline, conjugate gradient, frontal)

Equilibrium equations, 4, 9

Examples of scalar field problems, table, 307

F

Fins:

1-D, 316-20
 2-D, 329-30

Fixed-end reactions, 245, 257
 Flow, 306, 336–39
 Flywheel, 185, 196, 426
 Forces (*see* body forces, surface traction, concentrated forces)

Fourier's law, 308
 Forward elimination, 36

Frames:

planar, 248–53
 3-D, 253–57

Friction factor in ducts, 341

Frontal method, 289–91

Functional approach, 323

G

Galerkin approach, 13–16:

in elasticity, 14–15, 56–58, 146–48, 187, 243–44

for handling boundary conditions, 65, 70

in scalar field problems, 312–13, 318–19, 323–26, 333–34

Gaussian elimination, 29–36

with column reduction, 36–38 (*see also* skyline)

Gauss points and weights, tables, 216, 224

Gaussian quadrature, 214–17

Generalized eigenvalue problem, 370

Givens rotation, 390

Global stiffness matrix, assembly, 58–59, 61, 116–18

Gram-Schmidt process, 380

Grid point stresses, 421–23

Guyan reduction, 392–94

H

Half-bandwidth, (*see* Bandwidth)

Hamilton's principle, 367

Heat transfer, 306:

one-dimensional fins, 316–20

one-dimensional heat conduction, 309–16

two-dimensional fins, 329–30

two-dimensional heat conduction, 320–29

Helmholtz equation, 306

Hermite shape functions, 241
 Hexahedral element, 285–87

Higher-order elements, 220

Historical background, 1–2, 18

Householder reflection, 387–389

Hydraulic potential, 338

I

Implicit shift, 386

Inclined roller, 153 (*see also* multipoint constraints)

Initial strain (*see* temperature effects)

Input data format:

AXIQUAD, 229

AXISYM, 197

BEAM, 258

BEAMKM, 397

CST, 160–161

FEM1D, 88

FRAME2D, 259

FRAME3D, 259

GENEIGEN, 397

HEAT1D, 349

HEAT2D, 350

HEXAFRON, 292

INVITR, 397

JACOBI, 397

MESHGEN, 161, 330, 425

QUAD, QUADCG, 228

TRUSS2D, TRUSSKY, 119

Integration formula, tetrahedron, 278

Inverse iteration, 379–80

Isoparametric representation:

one-dimensional, 50

quadrilateral, 210

three-dimensional, 277

triangle, 135

Isotherm, 308

J

Jacobi method, 382–86

Jacobian, 137, 211, 278, 440

K

Kinetic energy, 367

L

Lagrangean, 367–68

Lagrange shape function, 49, 78, 285

Lame's constants, 19

- Least square fit, 421–23
 Loads (*see* body forces, surface tractions, concentrated forces)
 LU decomposition, 42
 Lumped (diagonal) mass matrices, 375
- M**
- Magnetic field problems, 339–41
 Mass matrix, derivation, 368–70:
 matrices (*see* element mass matrices)
- Matrices:
 eigenvalue-eigenvectors, 27–28, 375–76
 diagonalization, 381–82, 390–91
 tridiagonalization, 387
 Matrix
 adjoint, 26
 Cholesky decomposition, 29
 cofactor, 26
 determinant, 26
 LU decomposition, 42
 positive definite, 28
 singular, 26
 upper triangular, 26, 32
 Matrix algebra, 21
 Matrix form, quadratic, 27
 Mesh generation, 411–18
 Mesh preparation with tetrahedra, 281–83
 Modeling:
 axisymmetric solids, 191–95
 three-dimensional problems, 287–88
 two-dimensional problems in elasticity, 152–54
 (*see also* boundary conditions)
 Mode shapes (*see* eigenvalue-eigenvectors)
 Multipoint constraints, 74–75, 153, 193–94, 287–88
- N**
- Natural coordinates, 48, 133–35, 208–09, 277, 285–86
 Natural frequencies (*see* eigenvalue-eigenvectors)
 Nine-node quadrilateral element, 220–22

- Nonlinearity, 194–95
 Numerical integration, 214–18

O

- One-dimensional problem:
 elasticity, 45
 fin, 316–20
 heat conduction, 309–16
 Orthogonal space, 380
 Orthotropic materials, 154–57

P

- Penalty approach, 69–75
 summary, 70
 Plane strain, 8
 Plane stress, 7–8
 Plotting, 418
 Potential energy, 52, 139, 179–80, 238
 (*see also* functional approach)
 Potential flow, 336–37
 Preprocessing and
 Postprocessing, 411
 Press fit, 192–94
 Principal stresses, 280–81
 Principles:
 Galerkin, 13
 Hamilton's, 372
 Minimum potential energy, 9
 Saint Venant, 16
 Virtual work, 15

Q

- QR step, 390
 Quadratic shape functions, 79
 Quadratic triangle, 223
 Quadrilateral elements
 (*see* element)

R

- Rayleigh Ritz method, 11–13
 Rayleigh quotient, 379
 Reaction force, 66, 70, 75
 Reynolds number, 342
 Rigid body modes, 394–96
 Row operations, 30

S

- Saint Venant's principle, 16
- Scalar field problems, 306
- Seepage, 338-39
- Serendipity elements, 222-23, 415-16
- Shape functions:
 - axisymmetric, 181
 - beam, 240-41
 - constant strain triangle (CST), 133-35
 - hexahedron, 285
 - linear one-dimensional, 49-50
 - quadratic one-dimensional, 78-79
 - quadrilateral:
 - four-node, 208
 - eight-node, 222
 - nine-node, 220
 - tetrahedron, 277
 - triangle, six-node, 223
- Shear force, 245
- Shifting, 379
- Shrink fit, (*see* Press fit)
- Six-node triangular element, 223-24
- Skyline:
 - stiffness assembly for, 117-18
 - theory (38-39) (*see also* computer programs SKYLINE, TRUSSKY)
- Stiffness matrix (*see* element stiffness matrices, global stiffness matrix)
- Strain-displacement relations, 4
- Stream function, 336-37
- Stress computations, 6-8, 53, 86, 107, 148, 190, 218, 280
- Stress extrapolation, 196
- Stress function, 331
- Stress-strain relation, 6-8 (*see also* **D** matrix)
- Stress tensor, component representation, 3-4

- Sub-parametric element, 222
- Summary of the finite element method, 66-67, 71
- Surface Traction, 3, 55, 81, 142-44, 185-86, 280

T

- Temperature effects
 - axisymmetric solids, 191
 - constant strain triangle, 150-51
 - initial strain, 8
 - one-dimensional problems, 84-88
 - trusses, 111-14
- Tetrahedral element, 275
- Three-dimensional problems, 114, 253, 275
- Torsion, 331-36
- Transformation matrix, 105, 156, 249-50, 256
- Triangular element
 - linear, 130, 178, 322
 - quadratic, 223-24
- Tridiagonalization, 386-389
- Trusses, 103
- Two-dimensional problems:
 - elasticity, 130, 178
 - scalar field problems, 306
 - trusses, 103

V

- Vibration, 367
- Virtual work, principle, 15
- Von Mises stress, 17

W

- Winkler foundations, 247
- Wilkinson shift, 390
- Wood, 154-57

TYPICAL PHYSICAL PROPERTIES OF SOME MATERIALS

| Material | Density kg/m ³ | Ultimate Strength | | Yield strength MPa | Modulus of elasticity E GPa | Poisson's ratio | Coef. of thermal exp. 10 ⁻⁶ /°C | Thermal conductivity W/m °C |
|---|------------------------------|-------------------|--------------|--------------------------|-----------------------------------|--------------------|--|-----------------------------------|
| | | Tension MPa | Comp. MPa | | | | | |
| Aluminum 2014-T6 (alloy) 6061-T6 | 2800 | 470 | | 410 | 72 | 0.33 | 23 | 210 |
| | 2800 | 228 | | 131 | 70 | 0.33 | 23 | 210 |
| Brass cold rolled annealed | 8470 | 540 | | 420 | 105 | 0.35 | 19 | 105 |
| | 8470 | 330 | | 100 | 105 | 0.35 | 19 | 105 |
| Bronze Manganese | 8800 | 450 | | 170 | 100 | 0.34 | 20 | 58 |
| Cast Iron Gray Malleable | 7200 | 170 | 650 | | 95 | 0.25 | 12 | 45 |
| | 7200 | 370 | | 250 | 170 | 0.25 | 12 | 45 |
| Concrete Low strength Medium strength High strength | 2400 | 2 | 20 | | 22 | 0.15 | 11 | 1 |
| | 2400 | 3 | 41 | | 32 | 0.15 | 11 | 1 |
| | 2400 | 4 | 62 | | 40 | 0.15 | 11 | 1 |
| Copper hard-drawn | 8900 | 380 | | 330 | 120 | 0.33 | 17 | 380 |
| Glass Silicon | 2400 | 80 | 400 | | 70 | 0.17 | 8 | 0.8 |
| Magnesium 8.5% Al | 1800 | 350 | | 250 | 45 | 0.35 | 26 | 160 |
| Steel 0.2% C HR 0.2% C CR 0.6% C HR 0.8% C HR quenched | 7850 | 410 | | 250 | 200 | 0.30 | 12 | 42 |
| | 7850 | 550 | | 350 | 200 | 0.30 | 12 | 42 |
| | 7850 | 690 | | 370 | 200 | 0.30 | 12 | 42 |
| | 7850 | 830 | | 700 | 200 | 0.30 | 12 | 42 |
| Stainless 302 CR | 7920 | 860 | | 600 | 194 | 0.30 | 17 | 18 |
| Titanium 6% Al 4% V | 4460 | 900 | | 830 | 110 | 0.34 | 9 | 14 |

Properties vary widely depending on changes in composition, temperature, and treatment conditions.

CR = Cold rolled HR = Hot rolled

| Quantity | Units/Conversion |
|-------------------------------------|--|
| <i>General</i> | |
| Acceleration | 1 in./s ² = 0.0254 m/s ² |
| Area | 1 in. ² = 645.16 mm ² |
| Density (i) | 1 lbm/in. ³ = 27679.905 kg/m ³ |
| (ii) | 1 slug/ft ³ = 515.379 kg/m ³ |
| Force | 1 lb = 4.448 N (N = Newton) |
| Frequency | Hz (hertz = cycle/s) |
| Length | 1 in. = 0.0254 m; 1 ft = 0.3048 m |
| Mass (i) | 1 lbm = 0.45359 kg |
| (ii) | 1 slug = 14.594 kg |
| Moment | 1 in.-lb = 0.1130 N · m |
| Moment of inertia (area) | 1 in. ⁴ = 416231.4 mm ⁴ |
| Moment of inertia (mass) (i) | 1 lbm-in. ² = 2.9264E-4 kg · m ² |
| (ii) | 1 slug-in. ² = 0.009415 kg · m ² |
| Power (i) | 1 in.-lb/s = 0.1130 W (watt = J/s) |
| (ii) | 1 hp = 0.746 kW (1 hp = 550 ft-lb) |
| Pressure | 1 psi = 6894.8 Pa (psi = pounds/in. ² ; Pa = N/m ²) |
| Stiffness | 1 lb/in. = 175.1 N/m |
| Stress (i) | 1 psi = 6894.8 Pa |
| (ii) | 1 ksi = 6.8948 MPa; 1 MPa = 145.04 psi (ksi = 1000 psi; MPa = 10 ⁶ Pa) |
| Time | s (second) |
| Velocity | 1 in./s = 0.0254 m/s |
| Volume | 1 in. ³ = 16.3871E-6 m ³ |
| Work, energy | 1 in.-lb = 0.1130 J (joule = N · m) |
| <i>Heat Transfer</i> | |
| Convection coefficient | 1 Btu/h · ft ² · °F = 5.6783 W/m ² · °C |
| Heat | 1 Btu = 1055.06 J (1 Btu = 778.17 ft-lb) |
| Heat flux | 1 Btu/h · ft ² = 3.1546 W/m ² |
| Specific heat | 1 Btu/°F = 1899.108 J/°C |
| Temperature (i) | T °F = [(9/5)T + 32]°C |
| (ii) | T °K = T °C + 273.15 (K = kelvin) |
| Thermal conductivity | 1 Btu/h · ft · °F = 1.7307 W/m · °C |
| <i>Fluid Flow</i> | |
| Absolute viscosity | 1 lb · s/ft ² = 478.803 P (poise = g/cm · s) |
| Kinematic viscosity | 1 ft ² /s = 929.03 St (stoke = cm ² /s) |
| <i>Electric and Magnetic Fields</i> | |
| Capacitance | F (farad) |
| Charge | C (coulomb) |
| Electric charge density | C/m ³ |
| Electric potential | V (volt) |
| Inductance | H (henry) |
| Permeability | H/m |
| Permittivity | F/m |
| Scalar magnetic potential | A (ampere) |

INTRODUCTION TO FINITE ELEMENTS IN ENGINEERING

THIRD EDITION

Tirupathi R. Chandrupatla • Ashok D. Belegundu

Now in its third edition, *Introduction to Finite Elements in Engineering* provides an integrated approach to finite methodologies through the integration of exercises and examples involving engineering applications. The steps used in the development of the theory are implemented in complete, self-contained computer programs, while retaining the strategies and philosophies of previous editions. It serves as a primary textbook for senior undergraduate and first-year graduate students as well as an invaluable learning resource for practicing engineers.

Hallmark Features:

- Over 250 illustrations integrated throughout the text.
- Problem formulation and modeling emphasized in each chapter.
- Practical examples and problems.
- Pre- and post-processing concepts discussed in the last chapter.

New to the Third Edition:

Additional programs and source code on a companion CD



Includes complete self-contained computer programs with source codes in Visual Basic, Excel-based Visual Basic, MATLAB, QUICKBASIC, FORTRAN, and C.

Tirupathi R. Chandrupatla is a Professor and Program Chair for Mechanical Engineering at Rowan University, Glassboro, New Jersey. His research interests include finite element analysis, design, manufacturing engineering, and optimization.

Ashok D. Belegundu is a Professor of Mechanical Engineering at The Pennsylvania State University, University Park, Pennsylvania. His research interests include finite elements, machine design, and optimization techniques.

Pearson
Education

Prentice Hall
Upper Saddle River, NJ 07458
www.prenhall.com

ISBN 0-13-061591-9



9 780130 615916

90000

